

*Università degli Studi di Verona
Facoltà di Scienze MM.FF.NN.
Dipartimento Scientifico e
Tecnologico*

*Université de la Méditerranée de
Aix en Provence - Marseille II
Faculté des Sciences de Luminy
Département de Biologie*

*Dottorato di Ricerca in
Biotecnologie Industriali e
Ambientali
XVII CICLO*

*Ecole doctorale en sciences de
la vie e de la santé*

LIGHT HARVESTING COMPLEXES IN HIGHER PLANTS: ROLE, ORGANISATION AND REGULATION

Coordinatore :
Ch.mo Prof. Hugo L. Monaco

Directeur école doctorale :
Prof. André Neullion

Supervisore :
Ch.mo Prof. Roberto Bassi

Directeur de thèse:
Prof. Christophe Robaglia

Tomas Morosinotto

TABLE OF CONTENTS	3
Summary – Sommario - Sommaire	7
Introduction	19
<i>Oxygenic photosynthesis</i>	21
<i>The light absorbing complexes: Photosystem I and II</i>	24
<i>Photosynthetic pigments in higher plants</i>	32
<i>Regulation of antenna system properties</i>	36
<i>Experimental Techniques</i>	38
Section A: Biochemical analysis of supramolecular organisation of Photosystem I	47
<i>A.1 Stoichiometry of LHCl antenna polypeptides and characterisation of gap and linker pigments in higher plants Photosystem I</i>	49
<i>A.2 The role of individual Lhca subunits in the stability of higher plant Photosystem I-Light harvesting I supercomplex</i>	57
<i>A.3 PSI adaptation to short and long term light stress</i>	77
Section B: the Antenna complex of Photosystem I: The molecular basis of the low energy absorption forms.	97
<i>B.1 The Lhca antenna complexes of higher plants Photosystem I</i>	99
<i>B.2 Recombinant Lhca2 and Lhca3 Subunits of the Photosystem I Antenna System</i>	113
<i>B.3 Mutation Analysis of Lhca1 antenna complex</i>	123
<i>B.4 The chromophore organization of the Lhca2 subunit of higher plant photosystem I reveals the origin of its 701 nm fluorescence emission form</i>	133
<i>B.5 Pigment-Pigment interactions in the higher plants Photosystem I antenna complex Lhca4. A mutagenesis study</i>	141
<i>B.6 Inside the structure of Lhca3 by mutational analysis</i>	155
<i>B.7 The Nature of a Chlorophyll Ligand in Lhca Proteins determines the Far Red Fluorescence Emission Typical of Photosystem I</i>	169
<i>B.8 LHCl: the antenna complex of Photosystem I in plants and green algae</i>	177

Section C. Supramolecular organisation of higher plants Photosystem II	209
<i>C.1 Structure of a higher plant photosystem II supercomplex retaining chlorophyll b antenna proteins revealed by electron crystallography</i>	211
Section D: Xanthophylls dynamics in higher plants thylakoids	229
<i>D.1 Dynamics of chromophore binding to Lhc proteins “in vivo” and “in vitro” during operation of xanthophyll cycle</i>	231
<i>D.2 Mechanistic aspects of the xanthophyll dynamics in higher plant thylakoids</i>	241
<i>D.3 Occurrence of Lutein Epoxide cycle</i>	251
Appendix I. Spectroscopic characterisation of LHCI	255
Conclusions	259
Acknowledgements	263

Summary

SUMMARY (English)

LIGHT HARVESTING COMPLEXES IN HIGHER PLANTS: ROLE, ORGANISATION AND REGULATION

Photosystems I and II in higher plants are composed of two moieties: (i) a core complex, responsible for the charge separation and (ii) an antenna complex, responsible for the light harvesting. In this PhD work, the supramolecular organisation of antenna systems and their ability to modulate chlorophyll biophysical properties were analysed. Special attention was dedicated to the LHCI antenna and to the understanding of the mechanisms that allows these proteins to modulate chlorophyll absorption and fluorescence properties.

Section A. Biochemical analysis of the Supra-molecular organisation of PSI

In this section, the organisation of antenna system in PSI-LHCI supercomplex is analysed. In the first part (A.1), we¹ measured the stoichiometry of Lhca1-4 polypeptides in PSI-LHCI complex. This was performed by quantifying the different polypeptides from the amount of Coomassie bound upon SDS PAGE separation. We purified PSI-LHCI complex by a method that retains all LHCI polypeptides bound to the Core complex. The results of our analysis showed that one copy of each Lhca1-4 polypeptide is present in PSI-LHCI complex, in full agreement with its structure recently published (Ben Shem et al., Nature 2003). This result imply that in Photosystem I, differently from what observed in PSII, there is no pool of LHCI polypeptides loosely bound to the complex. On the contrary, only four Lhca polypeptides are present per PSI. All previous evaluations of PSI antenna size, based on the chlorophyll content, over-estimated the number of Lhca polypeptides because of the presence of extra chlorophylls, bound at the interface between PSI core and antenna complexes (Ben Shem et al., Nature 2003). In this work, we were able to characterise these chlorophylls as both Chls a and b. The presence of carotenoid molecules at the interfaces was also shown, thus improving the information available from the X-ray analysis. When PSI and PSII supercomplexes were compared, it was shown that “gap pigments” at the interface between protein subunits are a peculiarity of PSI, while they are not present in PSII.

In A.2, Arabidopsis mutants lacking individual Lhca proteins were characterised biochemically. This analysis showed that the absence of one Lhca protein was affecting the binding stability of all

¹ In this work I prefer to use “we” rather than “I” since during my work I had the opportunity of interfacing with many co-workers within and outside my laboratory. Without their contribution, this work would be very different. On the other hand the responsibility for the mistakes that are possibly still present in this text is entirely mine.

the others. These results suggest the presence of strong interactions between Lhca polypeptides, which are contributing to the stability of the whole antenna system. Thus, the binding of Lhca polypeptides to PSI core appears to be strongly cooperative. The gap pigments likely mediate these interactions, since they are coordinated by multiple antenna or core subunits.

Finally, in part A.3, we characterised the adaptation of PSI-LHCI to different environmental conditions. First, we analysed the effect of zeaxanthin, a xanthophyll rapidly synthesised in response to light stresses. These analyses showed that the modification of xanthophyll composition modulates the fluorescence yield of LHCI antenna complexes. Secondly, we analysed PSI in plants grown in different light conditions. Very surprisingly, we found out that the stoichiometry of each Lhca is not affected by environmental conditions, while PSII antenna showed large modifications. The regulation of PSI light harvesting function thus, does not involve the modification of the amount of Lhca1-4 complexes, but other mechanisms, like state transition and regulation of PSII / PSI ratio

Section B: the Antenna complex of Photosystem I: The molecular basis of the low energy absorption forms.

In vascular plants, the antenna complex of Photosystem I is composed by four polypeptides, belonging to Lhc multigenic family and called Lhca1, 2, 3 and 4. The characterisation of individual properties of Lhca proteins isolated from leaves is very difficult, due to the inability of purifying individual polypeptides to homogeneity. In this thesis, a recombinant approach was used to overcome this limitation: individual proteins were characterised individually upon expression in bacteria and reconstitution *in vitro*. In chapters B.1 and B.2, the biochemical and spectroscopic properties of individual Lhca1-4 pigment binding complexes are presented.

The major peculiarity of the antenna system of PSI is the presence of chlorophylls adsorbing at energies lower than the reaction centre P700. These chlorophylls are named “red forms” because they have a characteristic red-shifted fluorescence. It was already known that the red most chlorophylls in PSI-LHCI complex are localised in the antenna system (Mullet et al., Plant Physiol. 1980) and in particular in Lhca4 (Schmid et al., PNAS 1997). The characterisation of individual Lhca polypeptides, however, showed that red shifted chlorophylls are present in all Lhca polypeptides, although their emission energies are different. In particular, Lhca1 and Lhca2 have an emission form at 701 nm, while Lhca3 and Lhca4 emit around 730 nm.

The second part of this section is devoted to the understanding of the molecular basis of these red shifted chlorophylls. This issue was addressed with a mutational analysis: in Lhca1-4, chlorophyll

binding residues were mutated to non polar aminoacids, which are not able to coordinate the magnesium atom of the chlorophylls. The mutant apoproteins were expressed and reconstituted *in vitro*, yielding complexes where specific chlorophylls were absent and allowing the determination of which chromophores are involved in red forms. This work was first done in Lhca1 (B.3), because it is the most stable complex among Lhca proteins. It was then performed also for Lhca2 (limited to three chlorophyll binding sites, B.4), Lhca3 (B.6) and Lhca4 (B.5). This analysis showed that in all Lhca polypeptides red shifted forms are originated from the chlorophylls bound to sites A5/603 and B5/609 (using nomenclature respectively from Kühlbrandt et al., Nature 1994 and Liu et al., Nature 2004). Thus, their origin is conserved in all Lhca complexes, independently from their different absorption energies. During this work, an interesting feature was pointed out: Lhca3 and Lhca4, the complexes showing the red - most fluorescence emission, have an asparagine as ligand for Chl A5/603, while this pigment is instead co-ordinated by a histidine in all other members of Lhc multigenic family. A series of mutants was then built, substituting the asparagine with histidine in Lhca3 and 4 and histidine with asparagine in Lhca1 and 2. The characterisation of these mutants (B.7) showed that the asparagine as ligand for Chl A5/603 is necessary for the red forms: in fact, mutants with histidine had strongly affected red emission without any effect on pigment binding properties. In the case of Lhca1, instead, the presence of asparagine in place of histidine as ligand for Chl A5/603 was also sufficient to induce a red – shift in fluorescence emission.

In B.8, a review that summarises the present knowledge on the antenna complex of PSI is presented.

Section C. Supra-molecular organisation of PSII

In this section, the biochemical and structural characterisation of PSII supercomplexes is presented. This work was performed using a barley mutant, *vir* Zb63, which is depleted in PSI core. This mutant has the peculiarity of forming *in vivo* regular arrays of PSII within the membrane, as shown by early freeze fracture studies (Simpson, Carlsb. Res. Comm. 1980). Stacked membranes were purified from these plants, optimising the conditions in order to obtain membrane patches without disrupting the order of particle arrays. Electronic Cryo-microscopy analysis, performed on this preparation, allowed obtaining of a 2D map of PSII supercomplexes with a 17 Angström resolution. Since it lacks PSI, the Zb63 mutant experiences a severe over-excitation of PSII, as shown by the accumulation of zeaxanthin and decrease of antenna size. The supercomplexes described here should then be considered the elementary unit of PSII, depleted of inducible antenna components. This structure is composed by a LHCII trimer, a CP26 and CP29 per PSII core centre, with two PSII centres in each supercomplex. It was also hypothesised that the formation of regular arrays *in*

vivo is a mechanism for photoprotection: in fact, the delocalisation of adsorbed energy in different PSII units is stabilising the excited states, decreasing the accumulation of Chl triplets.

Section D. Xanthophyll dynamics in higher plants thylakoids

The xanthophyll cycle consists in the conversion of violaxanthin into zeaxanthin with antheraxanthin as an intermediate and it is activated in stress conditions when the light absorbed exceeds the amount usable by photochemistry. The production of zeaxanthin, in fact, enhances the plant ability to survive in these conditions, by participating to a series of photoprotective mechanisms which reduce the amount and the effects of exceeding light (Demmig-Adams and Adams, Nature 2000).

In D.1, the interactions between xanthophyll cycle and antenna proteins were analysed. In fact, both violaxanthin and zeaxanthin, the substrate and the product of the reaction, are generally found bound to Lhc proteins, where they are protected from the converting enzyme, the violaxanthin de-epoxidase (VDE). In this work, we reconstructed in a fully recombinant system the xanthophyll cycle, in order to analyse how antenna-bound violaxanthin is converted to zeaxanthin by VDE. Interestingly, it was found that the conversion of violaxanthin to zeaxanthin was dependent on the liberation of the substrate by Lhc complexes. Moreover, it was found that individual Lhc complexes have a different ability to exchange carotenoids, suggesting a possible specialisation of different members of the multigenic family. In particular, CP24 and CP26 were shown to have the largest ability to exchange violaxanthin with zeaxanthin.

In part D.2, recent results on the xanthophyll dynamics in higher plants thylakoids were reviewed.

In part D.3, extracts from some work performed in collaboration with Dr. Matsubara are presented. Here a second xanthophyll cycle, involving the conversion of lutein epoxide into lutein was characterised. The production of lutein epoxide was shown in peculiar plant species adapted to very low light conditions.

RIASSUNTO (Italian)

LIGHT HARVESTING COMPLEXES NELLE PIANTE SUPERIORI: RUOLO, ORGANIZZAZIONE E REGOLAZIONE

I fotosistemi I e II nelle piante superiori sono formati da due componenti: (i) un centro di reazione, responsabile della separazione di carica e (ii) un complesso antenna, responsabile della raccolta della luce. In questa tesi sono state analizzate l'organizzazione sovramolecolare dei complessi antenna e la loro capacità di modulare le proprietà biofisiche delle clorofille. Un'attenzione particolare è stata dedicata ai meccanismi attraverso i quali le proteine antenna del fotosistema I (LHCI) modulano il loro assorbimento e resa di fluorescenza.

Sezione A. Analisi biochimiche dell'organizzazione sovramolecolare del Fotosistema I

L'oggetto di questa sezione è l'organizzazione del sistema antenna nel supercomplesso PSI-LHCI. Nella prima parte (A.1), abbiamo determinato la stechiometria delle proteine Lhca1-4 nel complesso PSI-LHCI quantificando i diversi polipeptidi dalla quantità di Coomassie legato dopo separazione con SDS PAGE. I risultati di quest'analisi hanno mostrato che una singola copia dei polipeptidi Lhca1-4 è presente nel complesso PSI-LHCI, in pieno accordo con la struttura recentemente pubblicata (Ben Shem et al., Nature 2003). Il metodo di purificazione utilizzato è noto mantenere tutte le proteine antenna legate al centro di reazione, quindi i nostri risultati dimostrano che nel PSI non esiste nessuna frazione di proteine antenna blandamente legate, a differenza di quanto accade nel PSII. Al contrario, sono presenti solo quattro proteine antenna per PSI, almeno nelle condizioni ottimali di crescita delle piante utilizzate per questo esperimento. Tutte le precedenti stime dell'ampiezza dell'antenna del PSI erano basate sul contenuto in pigmenti e avevano sopravvalutato il numero di proteine a causa della presenza di clorofille legate alle interfacce tra core complex e LHCI (Ben Shem et al., Nature 2003). In questo lavoro abbiamo dimostrato che queste clorofille (chiamate "gap" e "linker") sono sia Chl a sia Chl b, ma anche che alcune molecole di carotenoidi sono anch'esse legate alle interfacce. Questo lavoro ha quindi fornito informazioni ulteriori rispetto a quanto ricavato dall'analisi cristallografica. Confrontando i supercomplessi di PSI e PSII è stato dimostrato come la presenza di pigmenti "gap" legati alle

interfacce tra subunità è una caratteristica peculiare del PSI e, al contrario, non sono presenti nel PSII.

In A.2, mutanti di *Arabidopsis* mancanti di singole proteine Lhca sono stati caratterizzati biochimicamente. Questa analisi ha mostrato che l'assenza di una singola proteina Lhca ha un effetto sulla stabilità di legame di tutte le altre. I risultati ottenuti suggeriscono la presenza di forti interazioni tra i polipeptidi Lhca che stabilizzano l'intero sistema antenna. L'associazione dei polipeptidi Lhca al PSI core ha quindi un carattere cooperativo e i pigmenti "gap" sono molto probabilmente i responsabili di queste interazioni, poiché sono legati all'interfaccia tra diverse subunità antenna o del core.

Infine, in A.3, abbiamo caratterizzato l'adattamento del supercomplesso PSI-LHCI alle differenti condizioni ambientali. Prima abbiamo analizzato l'effetto della zeaxantina, una xantofilla che è prodotta rapidamente in risposta a stress luminoso. Questa analisi ha mostrato come il legame di diverse specie di xantofille moduli la resa di fluorescenza del complesso antenna LHCI. Successivamente è stato analizzato il PSI in piante cresciute in diverse condizioni di luce e temperatura. Sorprendentemente, la stechiometria di ogni Lhca non era modificata, a differenza di quanto osservato nel complesso antenna del PSII. La regolazione delle dimensioni dell'antenna del PSI non coinvolge quindi la modifica della quantità di complessi antenna Lhca1-4, ma altri meccanismi, come la transizione di stato e la regolazione del rapporto tra PSII e PSI, sono invece importanti.

Sezione B. Il sistema antenna del Fotosistema I: la base molecolare delle forme rosse.

Nelle piante vascolari il complesso antenna del fotosistema I è composto di quattro polipeptidi, appartenenti alla famiglia multigenica Lhc: Lhca1, 2, 3 e 4. La caratterizzazione delle proprietà individuali di queste proteine isolate da tessuti nativi è molto difficile, a causa dell'incapacità di purificarli all'omogeneità. Per superare questa limitazione, in questa tesi è stato utilizzato un approccio ricombinante: i singoli Lhca sono stati caratterizzati individualmente dopo espressione in batteri e ricostituzione *in vitro*. Nei capitoli B.1 e B.2 sono presentate le proprietà biochimiche e spettroscopiche di Lhca1-4.

Una caratteristica peculiare del complesso antenna del PSI è la presenza di clorofille che assorbono ad energie minori del centro di reazione P700. Queste clorofille sono chiamate "forme rosse" perché hanno una caratteristica emissione nella regione del rosso. Le clorofille più rosse nel complesso PSI-LHCI sono localizzate nel sistema antenna (Mullet et al., *Plant Physiol.* 1980) ed in

particolare in Lhca4 (Schmid et al PNAS 1997). Tuttavia, la caratterizzazione individuale delle proteine Lhca ha dimostrato che clorofille con emissione spostata verso il rosso sono presenti in tutti questi complessi, anche se le energie di emissione sono differenti nelle diverse proteine. In particolare, Lhca1 e Lhca2 hanno un'emissione di fluorescenza a 701 nm, mentre Lhca3 e Lhca4 emettono attorno ai 730 nm.

La seconda parte di questa sezione è stata dedicata alla comprensione della base molecolare della modulazione dell'energia di queste clorofille. Per raggiungere questo scopo è stato utilizzato un approccio mutazionale: i residui leganti le clorofille in Lhca1-4 sono stati sostituiti con amminoacidi apolari, i quali non sono in grado di coordinare il magnesio delle clorofille. Le apoproteine mutate sono state espresse e ricostituite *in vitro*, ottenendo in questo modo dei complessi dove specifiche clorofille erano assenti. Questo lavoro è stato fatto prima per Lhca1 (B.3), scelta poiché questa era la proteina più stabile. Successivamente, è stato fatto anche per Lhca2 (limitato a 3 siti di legame, B.4), Lhca3 (B.6) e Lhca4 (B.5). Questa analisi ha mostrato come in tutte le proteine Lhca le forme rosse sono originate dalle clorofille legate ai siti A5/603 e B5/609 (nomenclatura rispettivamente da Kühlbrandt et al., Nature 1994 and Liu et al., Nature 2004). Quindi, l'origine delle forme rosse è conservata in tutti i complessi Lhca, indipendentemente dalle loro diverse energie di assorbimento. Durante questa analisi è emersa un'interessante caratteristica: Lhca3 e Lhca4, i complessi con le clorofille più rosse, hanno un'asparagina come ligando della clorofilla A5/603, mentre questo pigmento è coordinato da un'istidina in tutti gli altri membri della famiglia Lhc. Per questo motivo sono stati costruiti una serie di mutanti in cui in Lhca3 e 4 era stata sostituita l'asparagina con istidina e all'inverso in Lhca1 e 2. La caratterizzazione di questi mutanti (B.7) ha mostrato che l'asparagina come ligando della clorofilla A5/603 è necessaria per avere le emissioni di fluorescenza più rosse. Nel caso di Lhca1, inoltre, la presenza di asparagina come ligando è anche sufficiente per indurre uno spostamento ad energie minori della emissione di fluorescenza.

In B.8 è presentata una review delle conoscenze attuali sul sistema antenna del Fotosistema I.

Sezione C. Organizzazione sopramolecolare del Fotosistema II

In questa sezione è presentata la caratterizzazione biochimica e strutturale di supercomplessi del PSII. Questo lavoro è stato svolto utilizzando un mutante di orzo privo di PSI, *vir* Zb63. Questo mutante ha la peculiarità di formare *in vivo* cristalli regolari di PSII nella membrana tilacoidale, come mostrato dai precedenti lavori di freeze fracture (Simpson, Carlsb. Res. Comm. 1980). Da questo mutante sono state purificate delle membrane impilate, ottimizzando le condizioni di estrazione in modo da disturbare il meno possibile l'ordine interno dei cristalli. Questa preparazione

è stata poi analizzata mediante criomicroscopia elettronica che ha permesso di ottenere una mappa 2D di supercomplessi del PSII con una risoluzione di 17 Angström. Questo mutante subisce una severa sovraccitazione del PSII a causa dell'assenza del PSI, come dimostrano l'accumulo di zeaxantina e la diminuzione delle dimensioni dell'antenna. Quindi, i supercomplessi descritti devono essere considerati l'unità elementare del PSII, priva di tutti i componenti inducibili del sistema antenna. Questa struttura è composta di un trimero di LHCII, un monomero di CP26 e CP29 per centro di reazione. La formazione di cristalli ordinati *in vivo* potrebbe avere un ruolo nella fotoprotezione: infatti, la delocalizzazione dell'energia assorbita tra diverse unità di PSII stabilizza gli stati eccitati, diminuendo l'accumulo di Chl tripletti.

Sezione D. Dinamica delle xantofille nei tilacoidi delle piante superiori

Il ciclo delle xantofille consiste nella conversione di violaxantina in zeaxantina ed è attivato in condizioni di stress, quando la luce assorbita supera la quantità utilizzabile dalle reazioni fotochimiche. La produzione di zeaxantina, infatti, incrementa la capacità delle piante di resistere in queste condizioni, partecipando a diversi meccanismi di fotoprotezione che riducono la quantità e gli effetti dell'eccesso di energia luminosa (Demmig-Adams and Adams, Nature 2000).

L'oggetto della sezione D.1 era l'interazione tra ciclo delle xantofille e proteine antenna. Infatti, sia la violaxantina sia la zeaxantina, il substrato e il prodotto della reazione, sono generalmente legati alle proteine Lhc, dove sono protette dall'enzima che ne catalizza la conversione, la violaxantina deossidasi (VDE). In questo lavoro, è stato ricostruito il ciclo delle xantofille con un sistema completamente ricombinante, per analizzare come la violaxantina legata alle antenne è convertita in zeaxantina dalla VDE. I risultati ottenuti hanno mostrato che la conversione di violaxantina in zeaxantina è dipendente dalla liberazione del substrato da parte delle proteine antenna. Inoltre, le diverse proteine Lhc hanno mostrato una specifica abilità di scambiare carotenoidi, suggerendo una possibile specializzazione di diversi membri della famiglia multigenica. In particolare, CP24 e CP26 hanno mostrato la maggiore abilità di scambiare violaxantina con zeaxantina.

In D.2 sono stati riassunti le attuali conoscenze sulla dinamica delle xantofille nei tilacoidi delle piante superiori.

Nella parte D.3 è presentato l'estratto di un lavoro svolto in collaborazione con la Dott.ssa Matsubara, che riguarda la caratterizzazione di un secondo ciclo delle xantofille, che coinvolge la conversione di luteina epossido in luteina. La produzione di luteina epossido è stata dimostrata essere tipica di particolari specie di piante, adattate a condizioni di luce particolarmente ridotte.

SOMMAIRE (French)

LIGHT HARVESTING COMPLEXES DANS LE PLANTES SUPERIEURES: ROLE, ORGANISATION ET REGULATION

Dans les photosystèmes I et II des plantes supérieures on peut distinguer deux composants : (i) un centre réactionnel, responsable de la séparation de charge et (ii) un complex antenne, responsable de la récolte de la lumière. Dans ce travail de thèse j'ai analysé l'organisation supramoléculaire des complexes antenne et leur capacité de moduler les propriétés biophysiques des chlorophylles. Une attention particulière a été dédiée aux mécanismes avec lesquels les protéines antenne du photosystème I (LHCI) modulent leur adsorption, ce qui entraîne un changement d'absorption d'une extrême amplitude (40 nm), et leur rendement de fluorescence.

Section A. Analyses biochimiques de l'organisation supramoléculaire du Photosystème I

Dans cette section on a analysé l'organisation du système antenne du supercomplexe PSI-LHCI. Dans la première partie (A.1) on a mesuré la stœchiométrie des protéines Lhca1-4 dans le complexe, obtenu par quantification des polypeptides. Les résultats de cette analyse ont montré que une seule copie de chaque polypeptide Lhca1-4 est présente dans le complexe PSI-LHCI. Ces résultats sont en accord avec la structure récemment publiée (Ben Shem et al., Nature 2003) mais différents des conclusions obtenues par les méthodes de quantification des pigments utilisés dans les travaux précédents, qui avaient donné une valeur de huit polypeptides LHCI par centre réactionnel. Comme la méthode utilisée conserve toutes les protéines antenne liées aux centres réactionnels, ces résultats montrent que le PSI, au contraire du PSII, n'a pas des polypeptides antenne faiblement liés. Cette différence de résultats stœchiométriques est due à la présence d'un groupe importante de chlorophylles liées à l'interface entre les sous-unités du centre réactionnel et les protéines antenne. Dans ce travail on a montré que ces pigments (nommées « Gap » et « linker ») sont Chl a et Chl b et que des caroténoïdes en font partie aussi. La comparaison des supercomplexes du PSI et du PSII, a montré que la présence des pigments « gap » liés à l'interface entre sous-unités est une caractéristique spécifique du PSI, absente chez le PSII.

Dans A.2, des mutants d'*Arabidopsis* déficients dans l'expression de chaque une sous - unité Lhca ont été caractérisés par voie biochimique. Cette analyse a montré que l'absence d'une protéine Lhca a un effet dans la stabilité de toutes les autres. Ces résultats suggèrent qu'il y ait des fortes interactions entre les polypeptides Lhca qui stabilisent l'ensemble du système antenne LHCI. L'association des polypeptides Lhca au PSI core a donc un caractère fortement coopératif. Les pigments « gap » sont très probablement responsables de ces interactions, puisqu'ils sont coordonnés par des différentes sous unités de l'antenne ou du core.

Enfin, dans A.3, on a caractérisé l'adaptation du supercomplexe PSI-LHCI aux différentes conditions environnementales. D'abord, on a analysé l'effet de la zeaxanthine, qui a été montrée être capable de moduler le rendement de fluorescence dans le complexe antenne LHCI. Puis, on a aussi démontré que la quantité de protéines antenne Lhca ne change pas quand les plantes se développent dans des conditions de lumière et de température différentes. La régulation des dimensions de l'antenne du PSI, donc, n'implique pas la modification de la stœchiométrie des complexes Lhca1-4, mais plutôt d'autres mécanismes, comme la transition état I-état II ou la modification du rapport entre PSII et PSI.

Section B : Le système antenne du photosystème I : la base moléculaire des formes d'adsorption à basse énergie.

Dans les plantes vasculaires le complexe antenne du Photosystème I est composé par quatre polypeptides, qui appartiennent à la famille multigénique Lhc : Lhca1, 2, 3 et 4. La caractérisation des propriétés individuelles de ces protéines isolées des tissus foliaires est très difficile, à cause de l'incapacité de les purifier à l'homogénéité. On a donc utilisé une approche d'expression et reconstitution *in vitro* de protéines recombinantes pour franchir cette limitation : les différentes protéines Lhca recombinantes ont donc pu être caractérisées individuellement. Dans les chapitres B.1 et B.2 on a présenté les propriétés biochimiques et spectroscopiques de Lhca1-4.

La caractéristique spectroscopique principale du complexe antenne du PSI est la présence de chlorophylles qui adsorbent la lumière à une énergie plus faible que celle du centre réactionnel (P700). Ces chlorophylles sont appelées « formes rouges » à cause de leur émission déplacée dans le rouge par rapport aux autres chlorophylles. Bien que la localisation des formes rouges dans le LHCI ait été reconnue depuis longtemps (Mullet et al., *Plant Physiol.* 1980), et en particulier dans Lhca4 (Schmid et al., *PNAS* 1997), ici on a montré qu'il y a des chlorophylles avec une émission déplacée vers le rouge dans toutes les protéines Lhca, chacune avec une énergie d'émission

différente. En particulier, Lhca1 et Lhca2 ont une émission à 701 nm tandis que Lhca3 et Lhca4 fluorescent à 730 nm.

La seconde partie de cette section a été dédiée à la compréhension de la base moléculaire de ces chlorophylles rouges. Pour cet objectif on a utilisé une approche de mutagenèse dirigée: les résidus liant les chlorophylles dans Lhca1-4 ont été mutagénisés en résidus apolaires, qui ne sont pas capables de coordonner le magnésium des chlorophylles. Les apoprotéines mutantes ont été exprimées et reconstituées *in vitro*: chaque mutant manquait spécifiquement de certaines chlorophylles. Dans le cas de Lhca1, la protéine la plus stable parmi les quatre (B.3-B.6), et dans les autres sous-unités Lhca, l'analyse a montré que les formes rouges sont produites par les chlorophylles liées aux sites A5/603 et B5/609 (nomenclature d'après respectivement Kuhlbrandt et al., Nature 1994, Liu et al., Nature 2004). Donc, l'origine des formes rouges est conservée dans tous les complexes Lhca, même si leur longueur d'onde d'émission sont différentes. Les résultats suggèrent que les formes rouges soient générées par une interaction excitonique entre deux chlorophylles liées aux sites A5/603 et B5/609. Pendant cette analyse, on a repéré la présence d'une particularité: Lhca3 et Lhca4, les complexes avec les chlorophylles les plus « rouges », ont une asparagine comme ligand de la chlorophylle A5/603, alors que toutes les autres protéines Lhc ont une histidine à la position correspondante. Pour cette raison, on a construit une série de mutants où l'asparagine a été changée en histidine (chez Lhca3 et Lhca4) ou l'inverse (chez Lhca1 et 2). La caractérisation de ces mutants (B.7) a montré que l'asparagine comme ligand de la chlorophylle A5/603 est nécessaire pour obtenir les formes les plus rouges. Dans le cas de Lhca1, en plus, la présence de l'asparagine comme ligand est suffisante pour induire un déplacement vers le rouge de l'émission de fluorescence.

Dans B.8 on présente une révision des connaissances actuelles sur le système antenne du photosystème I.

Section C. Organisation supramoléculaire du photosystème II

Dans cette section, la caractérisation biochimique et structurale des supercomplexes du PSII est présentée. Dans ce travail on a utilisé un mutant d'orge, *vir* Zb63, qui manque du PSI (Simpson, Carlsb. Res. Comm. 1980). Ici, on a purifié des membranes granaires à partir de ce mutant, par une procédure originale qui ne dérange pas l'ordre des cristaux. Cette préparation a été analysée par cryo-microscopie électronique, ce qui a permis d'obtenir une carte 2D de la densité électronique des supercomplexes du PSII avec une résolution de 17 Angström.

Ce mutant subit une sévère photoinhibition, à cause d'une surexcitation du PSII, comme le montre l'accumulation de zeaxanthine et la diminution de la dimension de l'antenne. Les supercomplexes

décrits ici, donc, sont proposés être l'unité élémentaire du PSII, dépourvue de tous les composants inductibles du système antenne. Cette structure est composée par un trimère de LHCII, un monomère de CP26 et de CP29 par centre réactionnel qui est dimérique dans le supercomplexe.

Section D. Dynamique des xanthophylles dans les thylakoïdes des plantes supérieures

Le cycle des xanthophylles est activé dans des conditions de stress, quand la lumière adsorbée est supérieure à la quantité utilisable par la photochimie, et il consiste dans la conversion de violaxanthine en zeaxanthine, par l'intermédiaire de l'anteraxanthine. La production de zeaxanthine, en effet, augmente la capacité des plantes à résister dans ces conditions, en participant à plusieurs mécanismes de photoprotection qui réduisent les effets nocifs de l'excès d'énergie lumineuse (Demming-Adams and Adams, Nature 2000) à travers la modulation vers le bas du temps de vie des chlorophylles dans l'antenne.

Dans la section D.1, j'ai analysé les interactions entre le cycle des xanthophylles et les protéines antenne. En effet, la violaxanthine et la zeaxanthine, le substrat et le produit de la réaction, sont généralement liés aux protéines Lhc, où ils sont protégés de l'action de l'enzyme qui catalyse la conversion: la violaxanthine de-epoxydase. Dans ce travail, on a reconstruit *in vitro* la totalité du cycle des xanthophylles, avec un système complètement recombinant, pour étudier comment la violaxanthine liée aux antennes est convertie en zeaxanthine. Les résultats obtenus ont montré que la production de zeaxanthine est dépendante de la libération du substrat par les protéines antenne. D'ailleurs, les différentes protéines Lhc ont montré une différence de capacité à échanger des caroténoïdes, en suggérant une possible spécialisation des différents membres de la famille multigénique. En particulier, CP24 et CP26 ont montré la plus grande capacité à échanger violaxanthine contre zeaxanthine.

Dans D.2 on a résumé les connaissances actuelles sur la dynamique des xanthophylles dans le thylakoïdes des plantes supérieures.

Dans les parties D.3 on résume un travail développé en collaboration avec le Dr. Matsubara, qui vise à la caractérisation d'un second cycle des xanthophylles, où la lutéine epoxide est convertie en lutéine. La production de lutéine epoxide a été montrée être typique de certaines espèces de plantes adaptées à des conditions de lumière très faible.

Introduction

Oxygenic photosynthesis

Life on earth depends directly or indirectly from the solar energy. Photosynthesis is the process that enables plants, algae and bacteria to harvest light and convert it into chemical energy.

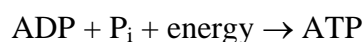
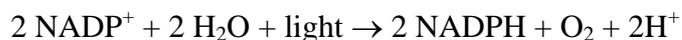
In oxygenic photosynthesis, performed by green plants, algae, and cyanobacteria, water is used as electron donor to reduce CO₂ to carbohydrates, generating molecular oxygen as a secondary product of the reaction.

The overall equation of the reaction is the following:



The whole process can be divided into a light and a dark phase. This classification is based on the dependence from solar energy to occur: the first is strictly dependent from light, while the latter occurs also in the dark occur, provided that ATP and NADPH are available.

The light phase starts with the absorption of sunlight by photosynthetic pigments (chlorophylls and carotenoids) and the transfer of the energy to reaction centre where charge separation occurs. Then, a set of electron transfer processes across the thylakoid membrane leads to the formation of a proton gradient. Finally, free energy and reducing power, in the form of ATP and NADPH + H⁺, are generated. Water is the primary electron donor during this process and O₂ is formed as a by-product upon its oxidation. The light reactions can be summarised with the following equations:



The dark reactions make use of the ATP and NADPH produced during the light reactions to reduce CO₂ to the carbohydrate GAP (Glyceraldehyde-3-Phosphate). GAP is then used for the synthesis of various organic compounds. The process of the dark reactions can be summarised in the following equation:



In photosynthetic eukaryotes, both light and dark reactions take place in a devoted organelle called chloroplast (Fig. 1). In vascular plants, chloroplasts are found especially in leaves mesophyll cells and their number is variable between a few to hundreds per cell, depending on species, growth conditions and developmental stage.

The chloroplast is limited by two membranes (called together *envelope*): the first one is highly permeable, while the second one contains specific transporters which control the flux of metabolites with the cytoplasm. The envelope membranes separate a compartment called *stroma*, which contains all enzymes catalysing the dark reactions as well as the plastidial DNA, RNA and ribosomes.

A third membrane system, the thylakoids, is found in the stroma and it confines a second compartment, the *lumen*. Thylakoid membranes are organised in stacked regions called grana connected by the stroma lamellae. The protein complexes involved in the light reactions of photosynthesis are located in the thylakoid membrane.

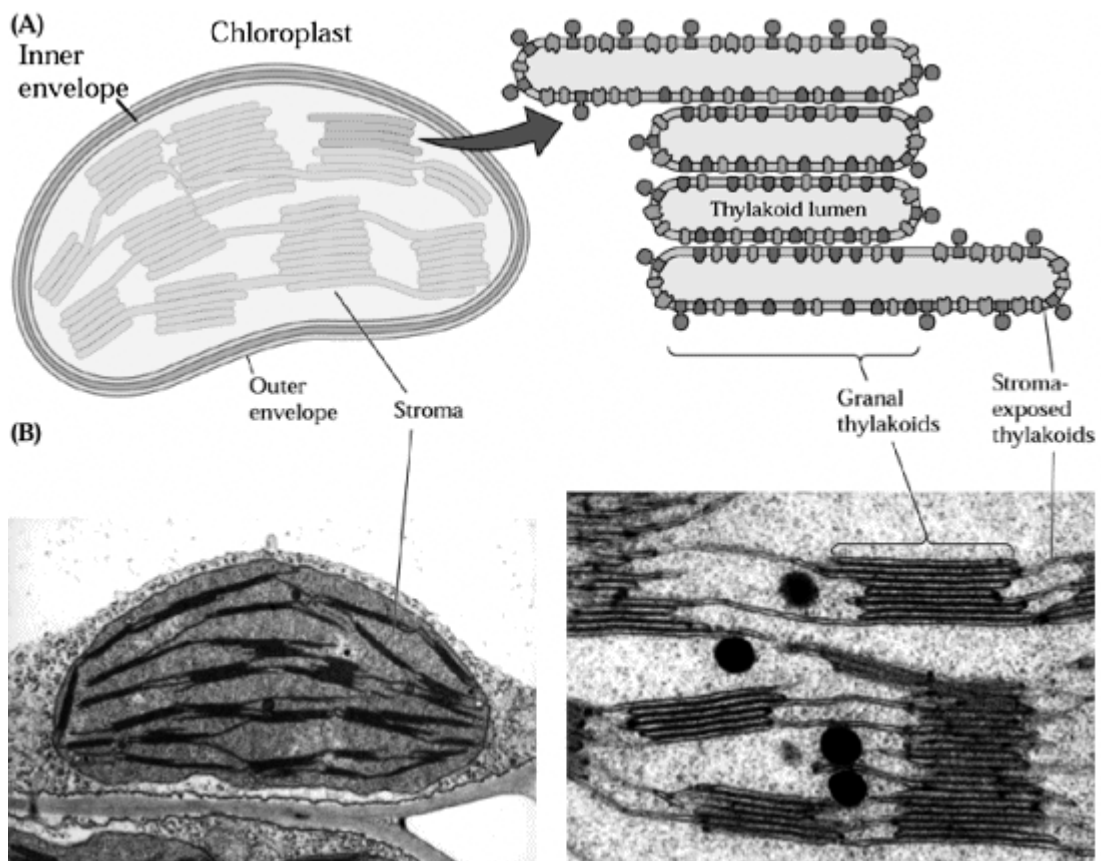


Figure 1. A) Schematic diagram of a plant chloroplast. Thylakoids are distinguished in grana and stromal thylakoids (or stroma lamellae). B) Electronic micrographs of a chloroplast. Images from (Malkin and Niyogi, 2000)

1. The light phase

Four major protein complexes localised in the thylakoids membrane (Photosystem I, cytochrome b_6f complex, Photosystem II and ATP synthase, see Figure 2) catalyse the processes of light harvesting, electron transport and photophosphorylation, leading to the conversion of light energy to chemical free energy (ATP and NADPH).

The pigments bound to PSI and PSII are responsible of the light absorption. Energy harvested is then transferred to the reaction centre, where it is used for charge separation.

Taking account of the efficiency of the system, the energy required for the generation of NADPH cannot be provided by only one photon in the visible range of light. For this reason, two photosystems act in series, as described in the Z-scheme of Bendall and Hill (Hill and Bendall, 1960).

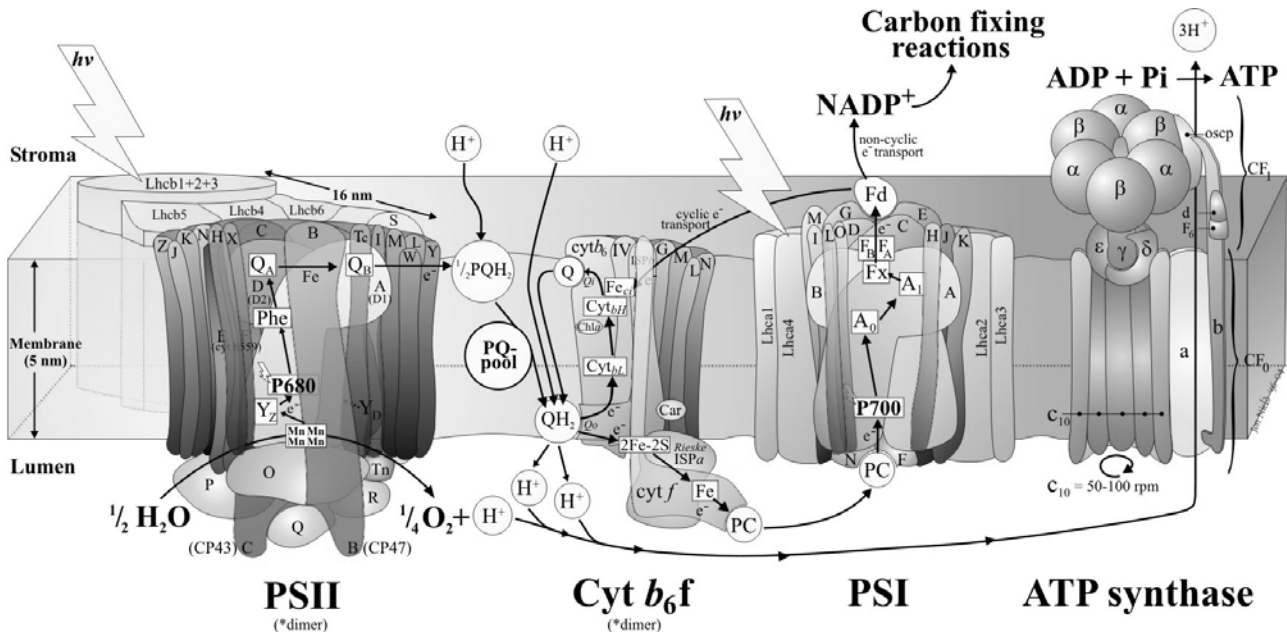


Figure 2. The light phase of photosynthesis. A schematic organisation of the major protein complexes in the thylakoid membrane is shown. Image from Jon Nield <http://www.bio.ic.ac.uk/research/nield/psIIimages/oxygenicphotosynthmodel.html>

Besides converting excited state energy into reducing power in the form of NADPH, the electron transfer reactions of PSII and PSI contribute to the formation of an electrochemical potential across the thylakoid membrane. In fact, the primary charge separation creates an electrical potential and a difference in protons concentration between the stromal and the luminal side of the membrane is built up by several processes (see figure 2):

- During the oxidation of water, 4 protons are released on the luminal side of the thylakoid membrane for each O_2 molecule produced.

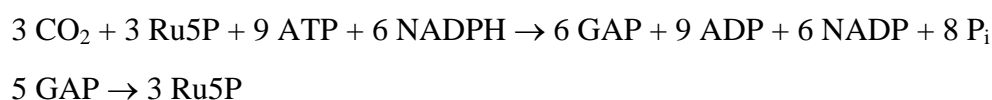
- Protons are used on the stromal side of the thylakoid membrane for the reduction of each NADP⁺ by the FNR.
- Protons are translocated through the thylakoid membrane during the so-called Q-cycle, which describes the reduction and the oxidation of plastoquinone/plastoquinol by the Cyt b₆f complex. The plastoquinol is reduced on the stromal side of the thylakoid membrane whereas the oxidation takes place on the luminal side, thus resulting in a net proton transport. Overall, the Q-cycle oxidises two plastoquinols, reduces one plastoquinone, and translocates 3 H⁺ for every 2 electrons transported to PSI.

The proton gradient generated is utilised by ATP synthase to produce ATP from ADP and P_i, in a process called photophosphorylation.

II. The dark phase

The dark phase of photosynthesis include a series of reactions, called Calvin cycle (Benson and Calvin, 1950), where atmospheric CO₂ is reduced to carbohydrates, using the chemical free energy (ATP and NADPH) produced during the light reactions.

The Calvin cycle consists in the synthesis of one GAP from three CO₂ molecules and in the regeneration of Ru5P to preserve the cyclic character of the process. It can be summarised with the following reactions:



The light absorbing complexes: Photosystem I and II

This work is focused on the light phase of photosynthesis and in particular on the two pigment-binding complexes Photosystem I and II. As mentioned, they are located in the thylakoid membranes, but their distribution is not homogeneous: in fact, PSI is located in the stroma lamellae, while the PSII complex is located in the grana (see Fig. 1).

Although they are structurally different, in both Photosystems two moieties can be identified: (a) a core complex, responsible for charge separation and (b) an antenna complex responsible of increasing the light harvesting and transferring of absorbed energy to the reaction centre.

Core complexes are composed by the products of the genes denominated *Psa* and *Psb* respectively for PSI and PSII. Among them there are both nuclear and chloroplast encoded polypeptides. Their sequences are generally well conserved during evolution and similar polypeptides are found in bacteria and eukaryotic organisms.

The antenna system is instead more variable in different organisms: in higher plants, the organisms subject of this thesis, it is composed by polypeptides belonging to the multigenic family of *light harvesting complexes* (*Lhc*). All these gene products are encoded by the nuclear genome and they are denominated Lhca and Lhcb, respectively for the antenna proteins of PSI and PSII (Jansson, 1999). In vascular plants, up to now, 6 classes of antenna proteins for PSI (Lhca1-6) and 6 for PSII (Lhcb1-6) have been identified. Each group can be composed by one or more genes and their number depend on the species, suggesting that they are the result of gene duplication events occurred quite late in evolution. However, generally Lhcb1 is the largest class: in fact, 5 different Lhcb1 genes have been identified in *Arabidopsis thaliana*, but they are at least 14 in barley (Jansson, 1999, Caffarri et al., 2004).

Lhcb1 and Lhcb2 are not found exclusively associated with photosystem II. In fact, depending on environmental conditions, they can be phosphorylated and migrate from PSII to PSI. This process is called State Transition (for a recent review see Wollman, 2001) and it provides a mechanism for the equilibration of the excitation energy between photosystems, thus increasing the efficiency of the whole process.

In figure 3A the cladogram of Lhca and Lhcb sequences from *Arabidopsis thaliana* is reported. It can be noted that Lhca and Lhcb cluster in two different groups, with Lhcb6 and Lhca1 located in the middle. In fact, evolutionary studies suggested that antenna proteins of PSI and PSII diverged soon, before the separation of individual classes (Durnford et al., 1999). This observation is consistent with some results reported later in this thesis, which showed that Lhca proteins have peculiar biochemical and spectroscopic properties, different from Lhcbs (see *e. g.* chapters B.1 and B.3).

Despite these differences, all these proteins share a common structural organisation, which is represented in figure 3B. They all have 3 transmembrane (A, B and C) and 1 amphipatic (D) helices. In the transmembrane region, Chl and carotenoid molecules are coordinated to the protein. They all have at least 8 conserved chlorophyll binding sites, as deduced by the conservation of nucleophilic residues evidenced in sequence analyses (Jansson, 1994).

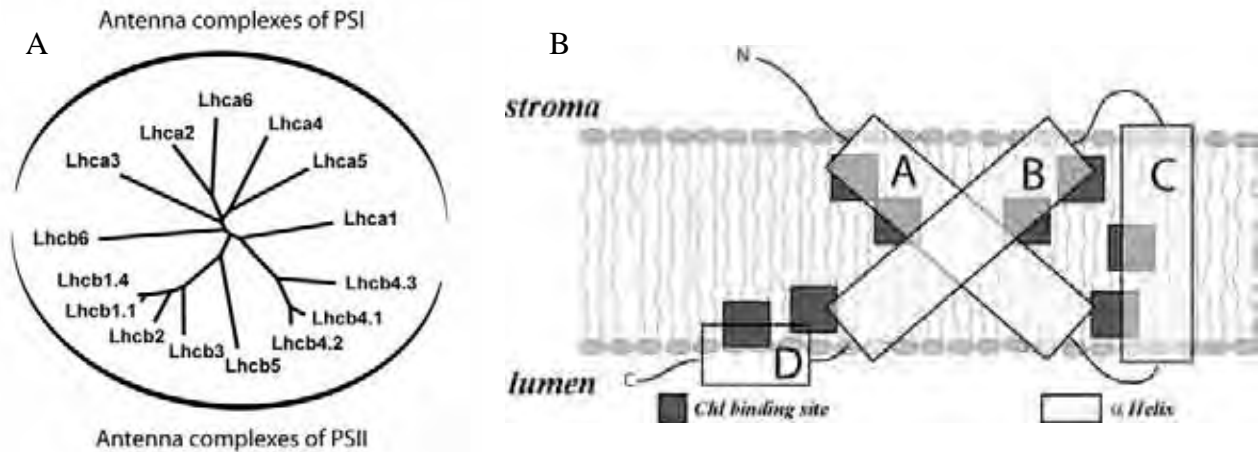


Figure 3. A) Cladogram of Lhc sequences from *Arabidopsis thaliana*. 2 out of the 5 Lhcb1 and one out of 4 Lhcb2 sequences are reported. The association to Photosystem I or II is indicated. B) Schematic representation of the structure of Lhc complexes. α - helices and putative conserved Chl binding residues are indicated

I. Photosystem I

The pigment-binding protein complex photosystem I (Fig. 4) is a light dependent plastocyanin-ferredoxin oxidoreductase. In higher plants it consists of at least 18 polypeptides and it binds about 180 chlorophylls and 35 carotenoid molecules (Boekema et al., 2001, Ben Shem et al., 2003).

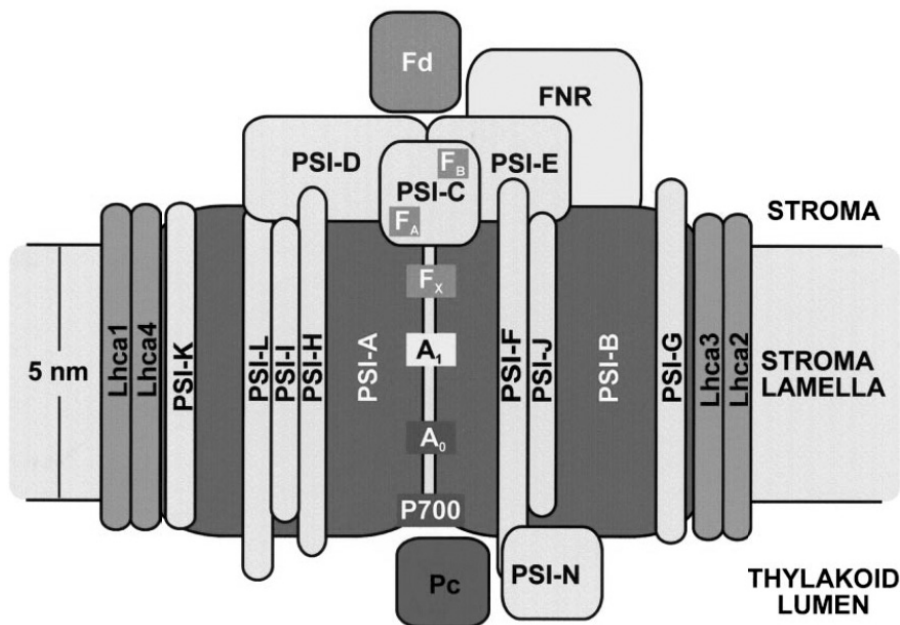


Figure 4. Schematic model of Photosystem I from plants. Image modified from (Scheller et al., 2001)

The PSI core in higher plants is composed by 14 polypeptides (Scheller et al., 2001). Among these, 10 are conserved with respect to bacterial PSI (PsaA-F, PsaI, J, K, L) and 4 are eukaryotic specific polypeptides (PsaG, H, N, O, Scheller et al., 2001).

Two major protein subunits, the products of the plastid genes *psaA* and *psaB*, form a dimer and coordinate the most part of the cofactors. They bind the primary electron donor of PSI (P700), the primary acceptor (A_0 , a Chl molecule), the secondary acceptor (A_1 , a phylloquinone) as well as many Chl *a* and β -carotene molecules (Fromme et al., 2001, fig. 4). The 4Fe-4S centre (F_x) is also bound to the *psaA-psaB* dimer, whereas the two Fe-S centres (F_A and F_B) are bound to PsaC, a stromal subunit.

II. Antenna complex of photosystem I

As mentioned above, 6 different Lhca genes have been identified in Arabidopsis (Jansson, 1999). However, only 4 polypeptides (Lhca1-4) are the major component of PSI antenna complex (LHCI, Croce et al., 2002) and have been identified in the PSI-LHCI structure (Ben Shem et al., 2003). Until last year, only these four polypeptides were detected in PSI-LHCI complexes. Very recently, Lhca5 have been recently identified at the polypeptide level, with both mass spectrometry and specific antibodies (Storf et al., 2004, Ganeteg et al., 2004). However, it was detected only in very low amounts and not tightly associated to PSI and its physiological relevance is still under debate (Ganeteg et al., 2004). Lhca6 gene, instead, it is expressed in very low amounts and the polypeptide has never been detected. Since its sequence is very similar to Lhca2, it could be a pseudogene, without any physiological function, resulting from a recent duplication (Jansson, 1999).

The isolation of LHCI moiety from PSI core was achieved using a detergent treatment, which separates PSI core from antenna without causing protein denaturation (Croce et al., 1998). However, the characterisation of the individual components of LHCI have been difficult, due to the inability to separate different polypeptides in LHCI preparations.

In this thesis, we extensively characterised individual Lhca1-4 complexes following a different method, expressing the apoprotein in *E.coli* and reconstituting the protein *in vitro* (Schmid et al., 1997, see below for a discussion of the method). In chapters B.1 and B.2 biochemical and spectroscopic analyses of Lhca1-4 reconstituted *in vitro* are reported.

Photosystem I from both eukaryotic and prokaryotic organisms has a peculiar spectroscopic feature, the presence of “red forms”, chlorophylls adsorbing at lower energies with respect to the reaction centre P700 (Gobets and van Grondelle, 2001). Red forms are generally found in the PSI core complex, but higher plants are peculiar in this respect: in fact, while they still have red forms in the

core complex, the red-most chlorophylls are found in the antenna complex LHCI (Mullet et al., 1980).

One major topic of this thesis was the analysis of red forms in the antenna complex of Photosystem I of *Arabidopsis thaliana*. First, we were interested in identifying which antenna complexes were responsible of this emission. Interestingly, we found out that all Lhca complexes have low energy absorption forms, although with different energies (see B.1 and B.2). In the case of Lhca1 and Lhca2, strictly they are not red forms, since they absorb light around 695 nm, thus at higher energies with respect to the reaction centre. However, we can include them in a wider definition of red forms because they are red shifted as compared with all other chlorophylls in antenna complexes.

The second step was to characterise which chromophores in these complexes were responsible of the red emission and characterise the molecular basis of the energy shift. This problem was addressed by a mutational approach and results are reported in B.3-B.7.

A wider review on present knowledge on antenna system of PSI and red forms is presented in chapter B.8.

III. Supramolecular organisation of PSI

The structure of PSI-LHCI complex was recently resolved at 4.4 Å resolution by 3D crystallography (Ben Shem et al., 2003, figure 5). Even if its resolution is not yet high enough to provide information on position of all atoms, it furnishes great details on the supramolecular organisation of the complex. In fact, it shows that Lhca1-4 polypeptides are bound to one side of the PSI core complex, as already suggested by electronic microscopy studies (Boekema et al., 2001). Moreover it shows that PsaH is located on the opposite side with respect to LHCI. Since this protein was shown to be necessary for state transition (Lunde et al., 2000), its localisation suggests that LHCI should dock to PSI in this part of the core complex, on the opposite side of LHCI.

An unexpected feature showed in this structure is the presence of only one copy of each Lhca1-4 polypeptides in the structure. In fact, previous estimations, based mainly on pigment evaluations, suggested that around 8 Lhca polypeptides were present in PSI-LHCI complex.

This discrepancy can be clarified considering the presence of chlorophyll molecules bound at the interface between core and LHCI complex. This was again unexpected and in fact these extra pigments explain the reason why the chlorophyll-based estimations were inaccurate. Chapters A.1 and A.2 take advantage of the new pieces of information provided by the structure and provide additional knowledge on the stoichiometry of LHCI polypeptides, the interfaces-bound pigments and the protein-protein interactions in the complex.

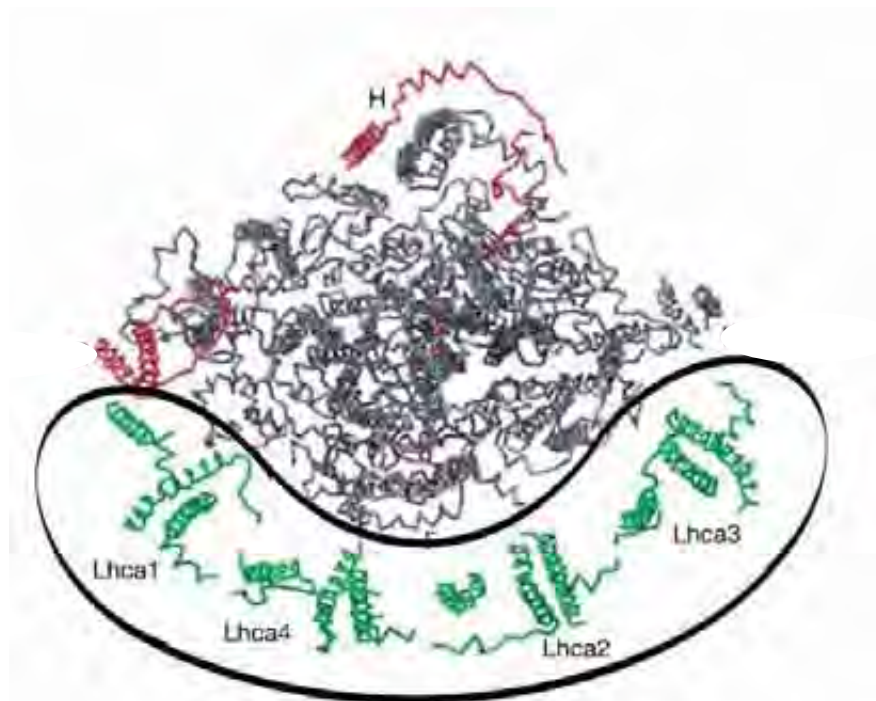


Figure 5. Supramolecular organisation of Photosystem I from *Pisum sativum*. Lhca1-4 and PsaH polypeptides are indicated. Modified from (Ben Shem et al., 2003)

IV. Photosystem II

The PSII complex (Fig. 6) is a multiproteic complex which catalyses the electron transfer from water to plastoquinone.

The core complex contains the reaction centre of PSII where the primary photochemistry takes place. Three subunits, D1, D2 and Cyt b_{559} , coordinate the electron transport cofactors P680 (the reaction centre), pheophytin, Q_A and Q_B . CP43 and CP47, instead, bind respectively 14 and 16 Chl a molecules and compose the inner antenna system (Ferreira et al., 2004). Up to 12 other small subunits are associated with the PSII core; some are involved in the dimerisation or in Chl and carotenoids binding stabilisation, but they do not all have a well clarified function (Ferreira et al., 2004).

On the luminal side of the complex three extrinsic proteins of 33, 23 and 17 KDa (OEC1-3) compose the oxygen evolving complex. They are responsible for the water oxidation and the generation of protons, electrons and molecular oxygen.

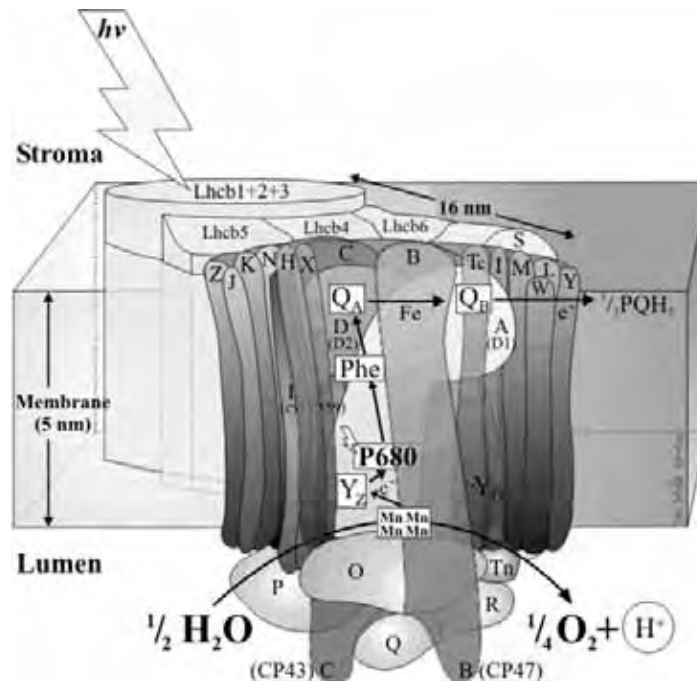


Figure 6. Schematic model of Photosystem II from plants. Picture from Jon Nield <http://www.bio.ic.ac.uk/research/nield/psIIimages/PSII.html>

V. Antenna complex of photosystem II

The antenna complex of Photosystem II is composed by six different classes polypeptides. Differently from what observed for Lhca, members of all 6 classes are found in relevant amounts and are normally associated to PSII.

The major component of PSII antenna complex is called LHCII. This complex is composed by heterotrimers of Lhcb1, 2 and 3. The three polypeptides, however, are not equimolar and Lhcb1 is generally found in bigger amounts (Caffarri et al., 2004). The trimeric LHCII is the only Lhc complex whom structure has been resolved with an high resolution (Liu et al., 2004). This structure showed the presence of 14 chlorophyll (8 Chl a and 6 Chl b) and 4 carotenoid molecules per monomer.

The remaining Lhcb proteins, Lhcb4-6, and are also known as respectively CP29, CP26 and CP24, with an old nomenclature based on their molecular weight. They are altogether classified as minor antennas and they are generally found as monomers. They bind from 8 to 10 Chls and 2 carotenoid molecules per polypeptide (Bassi et al., 1993).

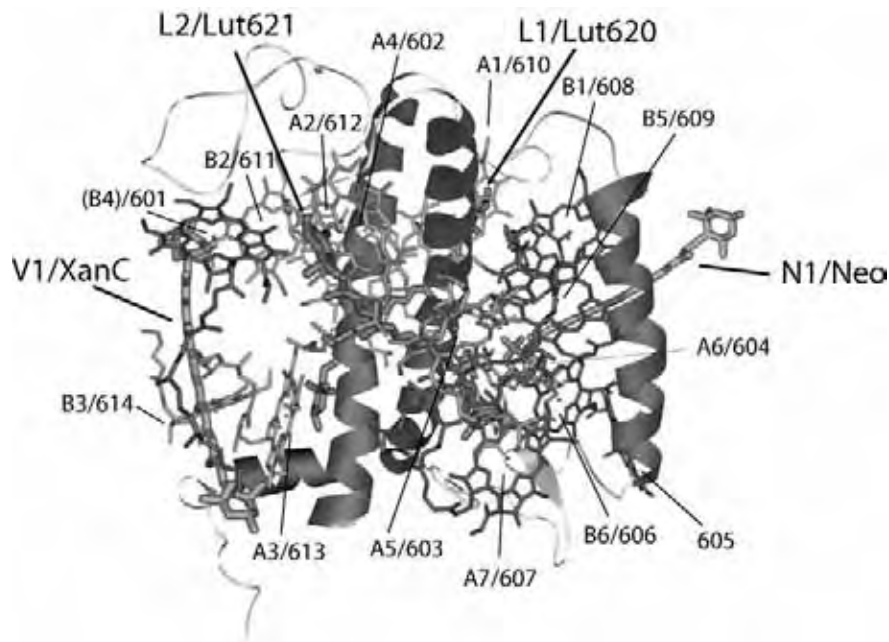


Figure 7. Tridimensional structure of LHCII the major antenna of Photosystem II resolved by (Liu et al., 2004). Chromophores are indicated with the nomenclatures from (Kühlbrandt et al., 1994) and (Liu et al., 2004).

VI. Supramolecular organisation of PSII

Photosystem II forms a supramolecular complex together with its antenna. Unfortunately, we still do not have a structure of this complex with a resolution comparable to the one of PSI. However, electron microscopy measurements provided 2D and 3D structures of PSII supercomplexes at around 2 nm resolution (Boekema et al., 1999, Nield et al., 2000). Two of them, reported in figure 8 clearly show that the organisation of PSII is very different from PSI. PSII, in fact, is dimeric, while PSI in higher plants is a monomer. The association of the antenna proteins is also different: in the basic unit of PSII supercomplexes, five antenna polypeptides are bound per PSII core (one copy of Lhcb4, Lhcb5 and a trimeric LHCII, see chapter C.1). However, binding of other polypeptides were observed, in particular of one Lhcb6 subunit and other trimeric LHCII complexes (see, *e. g.* fig. 8A).

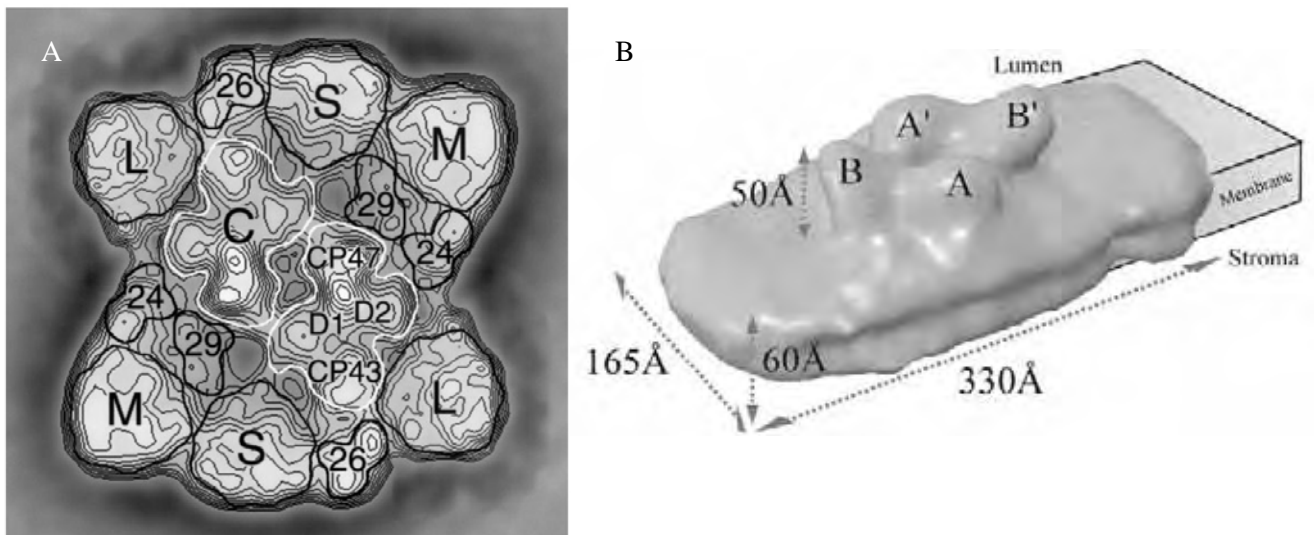


Figure 8. A) Organisation of a dimeric complex of PSII together with its antenna. C, PSII core complex; S, strongly bound LHCII; M, moderately bound LHCII; L, loosely bound LHCII; 29, Lhcb4; 26, Lhcb5; 24, Lhcb6. The right-hand PSII core complex shows the locations of its four largest subunits. Reproduced from (Boekema et al., 1999). B) 3D map of a single dimeric supercomplex the PSII supercomplex at 24 Å. Extrinsic OEC proteins are labelled A/A' (33 kDa OEC protein) and B/B' (23 kDa and 17 kDa OEC proteins). Overall dimensions are also shown. Reproduced from (Nield et al., 2000)

Photosynthetic pigments in higher plants

Two main classes of pigments are responsible for light absorption, charge separation and energy transfer in Photosystems: chlorophylls and carotenoids.

1. Chlorophylls

Chlorophylls are synthesised in a pathway starting from glutamic acid (Malkin and Niyogi, 2000). The basic component of all different types of chlorophylls is a porphyrin (a cyclic tetrapyrrole) in which the four nitrogen atoms of the pyrroles coordinate a magnesium atom. A fifth ring and the phytyl, a chain of 20 carbon atoms responsible for their hydrophobicity, are also present. Different chlorophylls are distinguished from their substitutions: in higher plants, two type of molecules are present, differing in a substituent in the second pyrrole ring, which is a methyl for the Chl *a* and an aldehyde for the Chl *b* (Fig. 9A).

The characteristic ability of Chls to absorb light in the visible region is due to the high number of conjugated double bonds present in these molecules.

The absorption spectra of the chlorophylls present two main bands with an high extinction coefficients (around $10^5 \text{ cm}^{-1} \text{ M}^{-1}$): the Q_y transition in the red part of the spectrum and the Soret transition in the blue part of the spectrum (Fig. 9B).

The Q_y transition corresponds to the transition of an electron from S_0 to S_1 (the first excited state). Another absorption band, called Q_x is visible, even if it is partly masked by the Q_y vibronic transitions. It corresponds to the transition of a ground state (S_0) electron to the second excited state (S_2). The Soret band, on the contrary, corresponds to transitions to higher states.

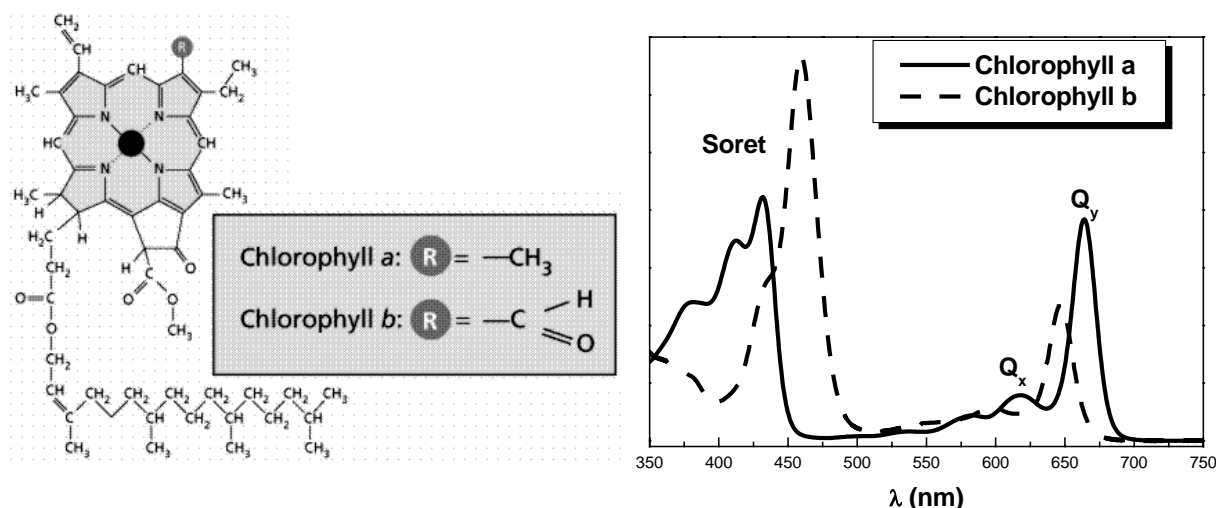


Figure 9. Structure (A) and absorption spectra in acetone 80% (B) of Chl a and b.

In the Chl binding to protein, a key interaction is the coordination of the central Mg. In most cases it is bound by nucleophilic amino acids residues, like histidine (Jordan et al., 2001, Liu et al., 2004). However, the presence of chlorophylls co-ordinated by water or even lipid molecules was also shown (Jordan et al., 2001, Liu et al., 2004). In these cases, where the ligand is not part of the polypeptide chain, other weak interactions, like hydrophobic interactions, play an important role for the stability of the association (Remelli et al., 1999).

II. Carotenoids

Carotenoids are polyisoprene molecules with 40 carbon atoms. Among them, two different classes are distinguished: (i) carotenes (ex. β -carotene), which are hydrocarbures with linear structure and with cyclic groups in one or both extremity, and (ii) xanthophylls (ex. lutein, zeaxanthin), which are oxygenated derivatives of the firsts. They are all synthesised from the terpenoid pathway and they derive from the condensation of 8 IPP (isopentenyl diphosphate) molecules which produces phytoene. Phytoene undergo several reduction steps, introducing four more double bonds and generating lycopene. The following reactions of the pathway are reported in figure 10. At this point the biosynthesis divided in two branches: one drive to the formation of β - carotene, zeaxanthin, violaxanthin and neoxanthin, while the other to α -carotene and lutein. Thank to their system of double conjugated bounds, all these molecules absorb light in the interval between 350 and 550 nm. This spectra are due to the transition from S_0 to S_2 state, since S_1 is forbidden, because of symmetry reasons.

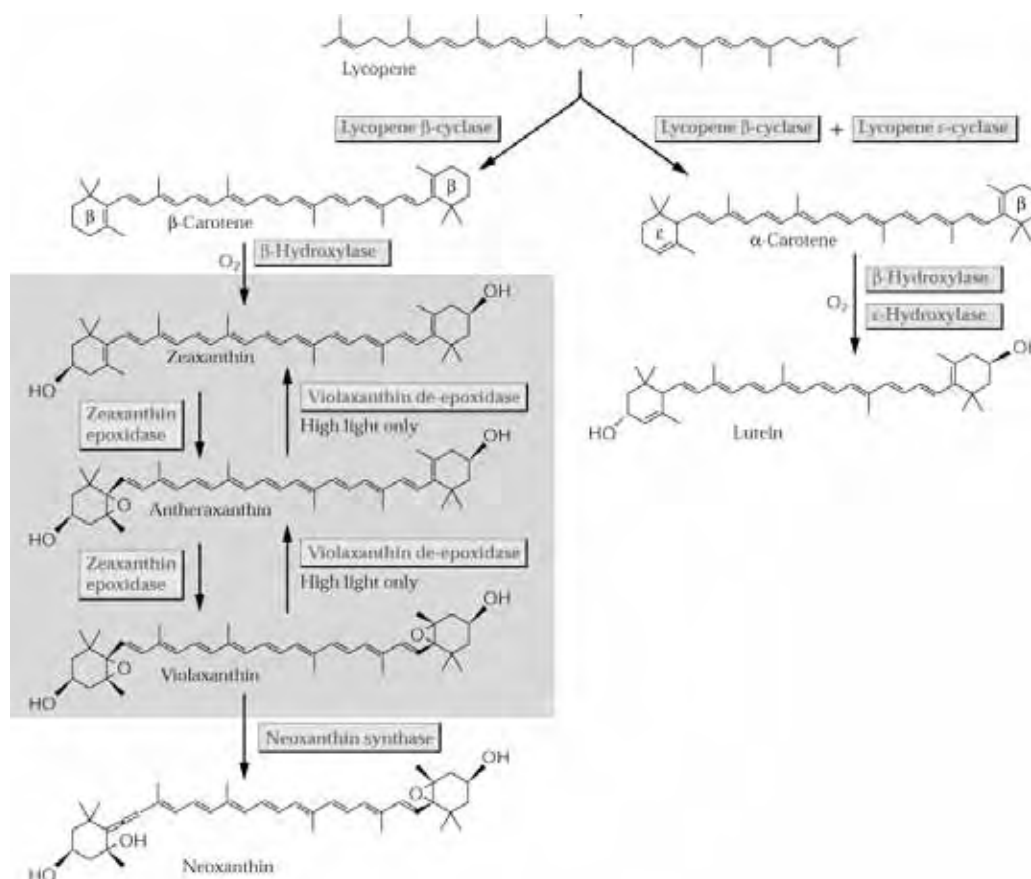


Figure 10. Biosynthetic pathway of carotenoids in higher plants. Enzymes involved in the pathway are indicated. The reactions of xanthophyll cycle (see below) are evidenced. Image from (Malkin and Niyogi, 2000)

In higher plants, the carotenoids normally associated with thylakoid membranes are α and β carotene (bound especially to core complex of both photosystems) and the xanthophylls lutein,

zeaxanthin, violaxanthin and neoxanthin (bound to antenna complexes). However, some species are able to synthesise other peculiar xanthophyll species (Bungard et al., 1999, Matsubara et al., 2001). In chapter D.3 we will focus on one of them, the lutein epoxide, that is synthesised from lutein with a de-epoxidation reaction, catalysed by an enzyme still not identified.

Differently from what observed for the chlorophylls, specific binding motifs for carotenoids have not been identified yet. However, structural and mutational studies suggest that there are not individual residues responsible for the binding as shown for the Chls. On the contrary, a rather large number of weak interactions are important for the association of the protein and the carotenoid (Liu et al., 2004, Gastaldelli et al., 2003).

III. Xanthophyll cycle

The xanthophyll composition in higher plants is not constant but in changes in response to different environmental conditions. In fact, it is known since several years that in high light violaxanthin is converted to zeaxanthin, by the de-epoxidation of two epoxy groups (Yamamoto and Kamite, 1972). Another xanthophyll species, antheraxanthin, is the intermediate of the reaction (fig. 10). The reactions are catalysed by a luminal enzyme, violaxanthin de-epoxidase (VDE), which is activated at low pH. Thus, the enzyme is active in high light conditions, when a big amount of protons is found in the lumen. In low light, instead, luminal pH is higher and a stromal enzyme, the zeaxanthin epoxidase (ZE), catalyses the back conversion of zeaxanthin to violaxanthin. The formation of zeaxanthin lowers the amount and the effect of energy excess, protecting plant from photoinhibition (see below for further details).

Zeaxanthin lowers the light use efficiency by photosynthesis and, if present constitutively, it decreases plants growth (Dall'Osto, Caffarri and Bassi submitted). Thus, the regulation of the xanthophyll cycle has an important physiological influence. It was generally believed that the formation of zeaxanthin is regulated only by the pH dependence of VDE activity (Gilmore and Yamamoto, 1992). However, it should be considered that most part of the substrate of the reaction, the violaxanthin, is bound to antenna proteins of photosystems I and II. In chapter D.1, we analysed the effect of Lhc proteins on the regulation of violaxanthin de-epoxidation.

Xanthophyll dynamics and the effects of zeaxanthin have been reviewed in chapter D.2.

Regulation of antenna systems

Plants experience variable environments during their life and they are often exposed to abiotic stresses, which causes overexcitation of the photosystems. As example, in low temperatures the thylakoid membrane is more rigid and the electron transport inefficient, because the re-oxidation of plastoquinol became a limiting factor. In similar circumstances, even a small light irradiance easily exceeds the photosynthetic capacity of the chloroplast. Similarly, during drought stress, the closure of the stomata, to avoid water loss, results in an inhibition of the Calvin cycle (because of the lacking of substrate, CO₂) and causes overexcitation of the photosystems.

The light excess is very dangerous for cells, because excited Chl molecules can convert into Chl triplets by intersystem crossing. Chl triplets are then stable enough to react with molecular oxygen and generate singlet oxygen and other reactive oxygen species (ROS). These molecules can oxidise and degrade chloroplast components, like proteins, lipids, and pigments.

Plants have evolved several mechanisms to adapt to different light conditions and dissipate the incidental energy in excess. Some of them involve the antenna proteins, which are responsible of the light harvesting. Here they are rapidly exposed, distinguishing between short and long term responses depending on their time scale and if they involve or not *de novo* protein synthesis. In the latter case, antenna proteins are modulated in order to adapt their amount to the energy requirements of photochemistry reactions. In the shorter time scale, instead, the amount of light absorbed can not be regulated. On the contrary, it is the fraction of the energy which is modified by activating quenching mechanisms that safely dissipates energy in excess as heat.

1. Short term responses

Light irradiance in a natural environment may change very rapidly. Plants, thus, need to be able adapt to variable conditions with the same speed, in order to avoid light damages. These short time scales, however, do not allow the modification of light harvesting by the synthesis or degradation of chlorophyll binding proteins. For this reason, plants have evolved the ability to modulate the use efficiency of energy adsorbed. When light in excess, then, the fraction of the energy absorbed which is de-excited thermally is increased, in a process called NPQ (non photochemical quenching).

NPQ is a very complex phenomenon and it involves several processes. Its fastest component is called Q_E (energy dependent quenching) and it is activated very rapidly upon illumination (Muller et al., 2001). Its molecular mechanism is still not completely clear, but it is known to depend from

the presence of a Lhc-like protein, PsbS, that probably acts as a sensor of luminal pH (Li et al., 2000, Li et al., 2002). The physiological relevance of Q_E has been demonstrated by showing that plants affected in Q_E (PsbS depleted plants) have a lower fitness when exposed to rapidly changing light conditions (Kulheim et al., 2002).

The xanthophyll cycle is another mechanism for short term adaptation to light regimes. In fact, as mentioned above, the conversion of violaxanthin to zeaxanthin increase the ability of plants to dissipate the excess energy as heat. The formation of zeaxanthin, however, takes longer than Q_E to be activated (a few minutes) since it involves several enzymatic steps. Several studies suggest that zeaxanthin acts at several distinct levels, as scavenger of Chl triplets or singulet oxygen (Havaux and Niyogi, 1999), as modulator of PsbS activity (Aspinall-O'Dea et al., 2002) and as inductor of fluorescence quenching in antenna complexes (Moya et al., 2001). Moreover, sustained accumulation of zeaxanthin is also involved in the overwinter stress resistance (Gilmore and Ball, 2000). Zeaxanthin, thus, can be considered as a signal molecule of stress since it modulates the activity of photosynthetic machinery in several ways, inducing an adaptation to new conditions. (see chapter D.2 for a wider description of zeaxanthin effects).

The state transition is another mechanism that can be rapidly activated and it has a role in equilibrating the excitation energy absorbed by PSI and PSII (Wollman, 2001). In fact, depending on environmental conditions, LHCII can be phosphorylated by a specific kinase (Depege et al., 2003) and migrate from PSII to PSI. Here LHCII can transfer the energy absorbed to PSI, rather than PSII. The state transition takes several minutes to be activated, since it involves also the migration of LHCII from grana to stroma lamellae.

II. Long term responses

Plants, over the short term responses described above, are also able to adapt on a longer time scale their ability to harvest light in response to the environmental conditions they experience. These adaptations involve several phenomena, for instance the expression or repression of specific proteins, but also chloroplast movements and modification of plants morphology.

For what concerns the photosynthetic machinery, subject of this thesis, one acclimative response particularly interesting is the regulation of the antenna size. It consists in the modification of the number and quality of antenna proteins in response to different light environments. In fact, plants, when grown in light limiting conditions, induce the synthesis of antenna proteins, in order to increase the energy absorption. On the contrary, when light is in excess, the number of antenna

proteins is reduced (Anderson and Andersson, 1988, Lindahl et al., 1995). The presence of this regulation has been well described in the case of PSII, but the regulation of antenna size of PSI is instead poorly studied: this subject was analysed in more details in chapter A.3.

Experimental techniques

In this work, several methods have been used and they are generally described in materials section of each chapter. However, in this paragraph we will analyse in bigger detail the techniques used more extensively or which have been developed during this thesis.

Reconstitution in vitro of Lhc complexes

This method consists in the refolding *in vitro* of Lhc complexes. It exploits the ability of these proteins to self assembly in presence of chlorophylls and carotenoids (Plumley and Schmidt, 1987). During this thesis the procedure has been optimised to obtain better yields and to reconstitute the antenna proteins of PSI.

The method used is schematised in figure 11.

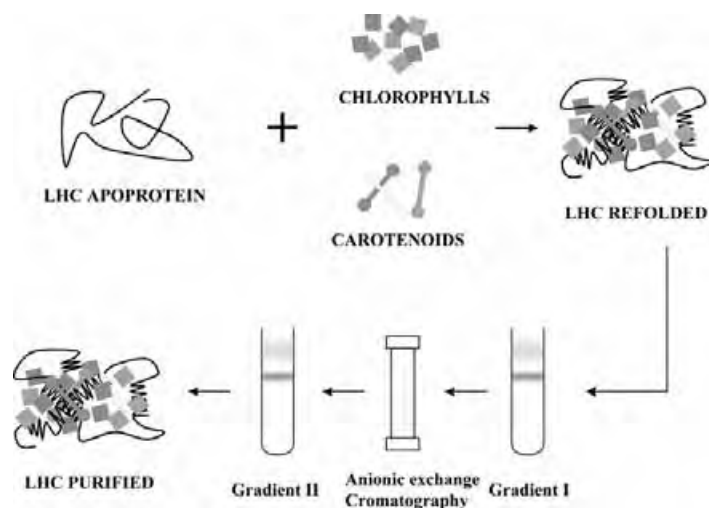


Figure 11. Schematic representation of Lhc reconstitution *in vitro*.

The first step of the procedure is the expression and purification of the unfolded apoprotein. The success of refolding do not depend from the complete pureness of the apoprotein and thus a preparation enriched in the desired Lhc is sufficient. This is achieved by expressing in *E.coli* the cDNA cloned in expression vectors (in this thesis I used a home-modified version of pQE50, from Qiagen). Since Lhc are highly hydrophobic and are not folded without pigments, when expressed in bacteria they are segregated in inclusion bodies. Inclusion bodies are then purified following a method previously described (Nagai and Thøgersen, 1987), which basically consists in several wash

and centrifugation steps of the protein preparation. Washes are done with a solution containing low amounts of detergent, which dissolves all bacterial proteins but the inclusion bodies, since they are highly hydrophobic and precipitate upon centrifugation. At the end of this procedure a preparation enriched in the Lhc apoprotein is obtained, although the most hydrophobic bacterial proteins are present as contaminants. The grade of contamination from bacterial proteins depends mainly on the expression efficiency of the protein. When it is good, contaminants can hardly be detected but, on the other side, when the protein is poorly expressed, inclusion bodies are severely contaminated, as it is in the case of Lhca2 due to the presence of rare codons in its sequence. Inclusion bodies contamination, however, does not prevent the refolding *in vitro*.

The second step is the preparation of a pigment mix. In this thesis, I generally used pigments purified from spinach. In order to obtain a complex as similar as possible of the native ones, the Chl a/b and Chl /car ratios of the pigment mix are adjusted for each protein: in the case of Lhca complexes, they were respectively 4.0 and 2.5.

The third step is the addition of pigments to the protein. The apoprotein at a concentration of 0.4 mg/mg is first boiled to induce a complete denaturation. After cooling to room temperature, the pigment mix, re-suspended in ethanol, is added. In the case of Lhca 0.57 mg of Chl and 0.30 mg of carotenoids are added per mg of apoprotein. During this step it is critical, to avoid inhibition of folding, that the final concentration of ethanol remains under 8%.

The folding of the protein takes only some seconds to occur (Reinsberg et al., 2001). However, the protein was generally treated with cycles of freezing and thawing that increase the specificity of pigment binding sites. In spite of this treatment, the refolding efficiency is below 100% and free pigments and unfolded protein should be removed. Two ultracentrifugation on density gradients and an anionic exchange chromatography were used for this purpose. The chromatography step is particularly important to remove all pigments that are unspecifically bound to Lhc complexes. An alternative method was also developed to increase the overall yield, using apoproteins with an His tail and an affinity chromatography plus a sucrose ultracentrifugation as purification steps. The pigment protein complexes obtained with both methods are substantially identical but for a small difference in Chl a/b ratio.

The reconstitution *in vitro* has several advantages with respect to the purification of pigment protein complexes from leaves. First, in the reconstitution only one polypeptide is present. In fact, Lhc

complexes are very similar the one from the other and they are difficult to separate at homogeneity. In the case of Lhca complexes, deeply analysed in this thesis, it is still impossible to separate individual Lhca complexes without inducing an extensive denaturation of the complexes. In this case then, reconstitution *in vitro* furnishes a unique possibility to gain information on properties of individual gene products.

A second advantage is that it is far easier to perform mutational analyses. To obtain a mutated complex the only need is to express the mutated apoprotein in *E.coli* and use it for reconstitution. This is simpler and faster than introducing mutated apoproteins in transformed plants. This possibility have been widely used here, as reported in section B.

A third advantage is the possibility of modifying the pigment mix and obtain complexes with the desired Chl or carotenoid content. This allows to gain information on the ability of different proteins to bind Chl and carotenoid species and also to characterise the effect of pigment composition on protein properties. These analyses can then be integrated with results from the characterisation of mutated plants, as shown in chapter A.3.

This procedure has, of course, also some limitations. The major one appears to be that, in reconstituted samples, some pigment binding sites appears to be empty, as showed by the comparison of pigment binding stoichiometry obtained from reconstitution studies with the structures of LHCII and LHCI (Remelli et al., 1999, Liu et al., 2004, Ben Shem et al., 2003). This is probably due to the fact that some binding sites are stabilised by protein-protein interactions and they are not found in isolated reconstituted samples.

De-epoxidation in vitro

As mentioned above, the regulation of zeaxanthin formation is a process with a big physiological relevance. In order to study in details this reaction, the xanthophyll cycle was reconstructed *in vitro*, in a full recombinant system (see chapter D.1). The novelty of the approach consists in the fact that the violaxanthin is added bound to recombinant Lhc complexes, as it happens in thylakoid membranes.

A schematic representation of the reaction is shown in figure 12. The components used for the reaction are:

- recombinant VDE from *Arabidopsis thaliana*, expressed in *E.coli*

- recombinant Lhc complexes reconstituted with only violaxanthin as a xanthophyll species.

- MGDG, a lipid that is found in high amounts in thylakoids membrane, which was shown to be necessary for the reaction of VDE (Rockholm and Yamamoto, 1996)
- Ascorbate, that is the source of reducing power for the deepoxydation reaction
- Citrate buffer at pH 5.1, to maintain the low pH, necessary for VDE activity

All components were mixed together and incubated for 30' at 28°C.

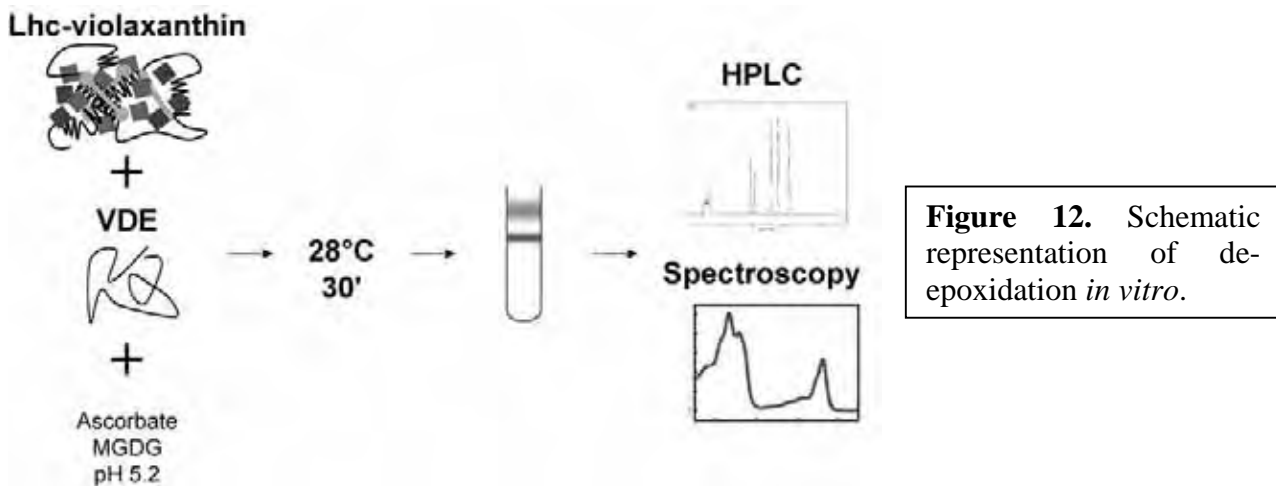


Figure 12. Schematic representation of de-epoxidation *in vitro*.

After the reaction, the mix was concentrated and loaded on a sucrose gradient in order to separate free pigments from Lhc complexes and both fractions were analysed biochemically and spectroscopically.

A set of control experiments was also set up, by removing some of these components or adding free zeaxanthin.

Determination of stoichiometry of Lhca in PSI-LHCI

In chapters A.1, A.2 and A.3 the amount of Lhca polypeptides in the PSI-LHCI complex was determined in WT and mutant plants. For this purpose, it was developed a method for quantification of Lhca proteins by evaluation of the Coomassie bound to polypeptides after SDS PAGE.

In order to perform this measure correctly there are some requirements:

First, the availability of a SDS PAGE separation able to distinguish each Lhca from the others and from all other polypeptides in a PSI-LHCI preparation. The complete separation of Lhc polypeptides is not easily achieved since they are homologous and have similar molecular weight. A method for the separation of Lhca polypeptides from *Zea mays* was already available (Croce et al., 1998), but it was not effective in separating all polypeptides from *Arabidopsis thaliana*, because

the small sequence differences between species modifies the relative mobility enough to impair a good separation. All polypeptides from Arabidopsis PSI were resolved with an SDS-PAGE electrophoresis performed as in (Laemmli, 1970), but using a acrylamide/bis-acrylamide ratio of 75:1 and a total concentration of acrylamide + bis-acrylamide of 4.5 % and 15.5 % respectively for the stacking and running gel. 6 M urea was also incorporated into the running gel.

The second requirement is a good quantification method for the Coomassie stain. In literature there is a method described by (Ball, 1986) that consists in cutting the bands from the gel and then eluting the stain with 3% of SDS and 50% of isopropanol. The Coomassie concentration is then quantified from its absorption at 593 nm. In order to correct the signal for the background staining, slices with the same dimensions are cut in gel regions where any protein is present. Results from Lhca quantifications with this method, however, had a rather large standard deviation, due to the imprecision in hand cutting of the bands. In fact, Lhca polypeptides migrate quite close to the one from the other, especially Lhca2 and Lhca3.

For this reason we developed another method, evaluating the Coomassie bound by densitometry. We used a software (Gel-Pro Analyzer[®]) that is able to measure the Coomassie by integrating the optical density over all band surface. In chapter A.1, this method was verified to be as accurate as the previous one but more precise and therefore it was used alone in chapters A.2 and A.3. Compared to the first procedure, however, there is one extra step for the quantification of the stain: the acquisition of gel image. All results are derived from image analysis and then it is critical to standardise the image acquisition.

In all Coomassie quantifications, moreover, it is very important to verify that the staining is linear with the protein amount. To achieve this purpose we used staining and de-staining solutions which were shown to increase the signal linearity (Ball, 1986). In chapter A.1 it was verified that, in these conditions, the Coomassie signal was linear with protein amount between 0.1-1 and 2-10 μg of Chl loaded respectively for a recombinant Lhca and PSI-LHCI.

The third requirement for the stoichiometry evaluation is the presence of an internal standard. In fact, Coomassie binding depends on the aminoacid composition of the polypeptides and varies significantly even in homologous polypeptides. It is fundamental that standards are loaded in the same gel of the preparation to analyse. In fact, even with the best care in standardising all conditions, quantification from different gels can not be compared with sufficient reliability.

In chapter A.1, as internal standards we used recombinant proteins, reconstituted *in vitro*, that allowed an absolute quantification of Lhca content in PSI-LHCI complex. These standards were

very useful even if they have the disadvantage that, during the cloning of the cDNA sequences, some extra aminoacids are included. This fact was considered during the determination, but it introduced an extra imprecision in the measurement.

Last point is that enough repetitions of the samples have to be loaded in order to have significant results. Depending on the precision required (for an absolute evaluation as in chapter A.1 it was bigger than for the relative one shown in chapter A.2 and A.3), 4 to 8 repetitions were loaded per each sample.

Abbreviations

Car, Carotenoid; Chl, Chlorophyll; Cyt, Cytochrome; Lhc, Light harvesting complex; LHCI, antenna system of Photosystem I; LHCII, Major antenna complex of Photosystem II; Lhca, antenna polypeptides of Photosystem I; Lhcb, antenna polypeptides of Photosystem II; PSI (II), Photosystem I (II); ROS, Reactive oxygen species; VDE, Violaxanthin de-epoxidase; ZE, Zeaxanthin epoxidase

References

- Anderson J M, Andersson B. The dynamic photosynthetic membrane and regulation of solar energy conversion. *Trends Biochem Sci* 1988; (13): 351-355.
- Aspinall-O'Dea M, Wentworth M, Pascal A, Robert B, Ruban A V, Horton P. In vitro reconstitution of the activated zeaxanthin state associated with energy dissipation in plants. *Proc Natl Acad Sci U S A* 2002; (99): 16331-16335.
- Ball E H. Quantitation of proteins by elution of Coomassie Brilliant Blue R from Stained bands after dodecyl sulfate polyacrilamide gel electrophoresis. *Anal Biochem* 1986; (155): 23-27.
- Bassi R, Pineau B, Dainese P, Marquardt J. Carotenoid-Binding Proteins of Photosystem-II. *Eur J Biochem* 1993; (212): 297-303.
- Ben Shem A, Frolow F, Nelson N. Crystal structure of plant photosystem I. *Nature* 2003; (426): 630-635.
- Benson A A, Calvin M. Carbon Dioxide Fixation by Green Plants. *Annual Review of Plant Physiology and Plant Molecular Biology* 1950; (1): 25-42.
- Boekema E J, Jensen P E, Schlodder E, van Breemen J F, van Roon H, Scheller H V, Dekker J P. Green plant photosystem I binds light-harvesting complex I on one side of the complex. *Biochemistry* 2001; (40): 1029-1036.

- Boekema E J, van Roon H, van Breemen J F, Dekker J P. Supramolecular organization of photosystem II and its light-harvesting antenna in partially solubilized photosystem II membranes. *Eur J Biochem* 1999; (266): 444-452.
- Bungard R A, Ruban A V, Hibberd J M, Press M C, Horton P, Scholes J D. Unusual carotenoid composition and a new type of xanthophyll cycle in plants. *Proc Natl Acad Sci USA* 1999; (96): 1135-1139.
- Caffarri S, Croce R, Cattivelli L, Bassi R. A look within LHCII: differential analysis of the Lhcb1-3 complexes building the major trimeric antenna complex of higher-plant photosynthesis. *Biochemistry* 2004; (43): 9467-9476.
- Croce R, Morosinotto T, Castelletti S, Breton J, Bassi R. The Lhca antenna complexes of higher plants photosystem I. *Biochimica et Biophysica Acta-Bioenergetics* 2002; (1556): 29-40.
- Croce R, Zucchelli G, Garlaschi F M, Jennings R C. A thermal broadening study of the antenna chlorophylls in PSI- 200, LHCI, and PSI core. *Biochemistry* 1998; (37): 17255-17360.
- Depege N, Bellafiore S, Rochaix J D. Role of chloroplast protein kinase Stt7 in LHCII phosphorylation and state transition in *Chlamydomonas*. *Science* 2003; (299): 1572-1575.
- Durnford D G, Deane J A, Tan S, McFadden G I, Gantt E, Green B R. A phylogenetic assessment of the eukaryotic light-harvesting antenna proteins, with implications for plastid evolution. *J Mol Evolution* 1999; (48): 59-68.
- Ferreira K N, Iverson T M, Maghlaoui K, Barber J, Iwata S. Architecture of the photosynthetic oxygen-evolving center. *Science* 2004; (303): 1831-1838.
- Fromme P, Jordan P, Krauss N. Structure of photosystem I. *Biochim Biophys Acta* 2001; (1507): 5-31.
- Ganeteg U, Klimmek F, Jansson S. Lhca5 - an LHC-Type Protein Associated with Photosystem I. *Plant Mol Biol* 2004; (54): 641-651.
- Gastaldelli M, Canino G, Croce R, Bassi R. Xanthophyll binding sites of the CP29 (Lhcb4) subunit of higher plant photosystem II investigated by domain swapping and mutation analysis. *Journal of Biological Chemistry* 2003; (278): 19190-19198.
- Gilmore A M, Ball M C. Protection and storage of chlorophyll in overwintering evergreens. *Proc Natl Acad Sci U S A* 2000; (97): 11098-11101.
- Gilmore A M, Yamamoto H Y. Dark induction of zeaxanthin-dependent nonphotochemical fluorescence quenching mediated by ATP. *Proc Natl Acad Sci USA* 1992; (89): 1899-1903.
- Gobets B, van Grondelle R. Energy transfer and trapping in Photosystem I. *Biochim Biophys Acta* 2001; (1057): 80-99.
- Havaux M, Niyogi K K. The violaxanthin cycle protects plants from photooxidative damage by more than one mechanism. *Proc Natl Acad Sci USA* 1999; (96): 8762-8767.
- Hill R, Bendall F. Function of the two cytochrome components in chloroplasts: A working hypothesis. *Nature* 1960; (186): 136-137.

- Jansson S. The light-harvesting chlorophyll a/b-binding proteins. *Biochim Biophys Acta* 1994; (1184): 1-19.
- Jansson S. A guide to the Lhc genes and their relatives in Arabidopsis. *Trends Plant Sci* 1999; (4): 236-240.
- Jordan P, Fromme P, Witt H T, Klukas O, Saenger W, Krauss N. Three-dimensional structure of cyanobacterial photosystem I at 2.5 Å resolution. *Nature* 2001; (411): 909-917.
- Kühlbrandt W, Wang D N, Fujiyoshi Y. Atomic model of plant light-harvesting complex by electron crystallography. *Nature* 1994; (367): 614-621.
- Kulheim C, Agren J, Jansson S. Rapid regulation of light harvesting and plant fitness in the field. *Science* 2002; (297): 91-93.
- Laemmli U K. Cleavage of structural proteins during the assembly of the head of bacteriophage T4. *Nature* 1970; (227): 680-685.
- Li X P, Bjorkman O, Shih C, Grossman A R, Rosenquist M, Jansson S, Niyogi K K. A pigment-binding protein essential for regulation of photosynthetic light harvesting. *Nature* 2000; (403): 391-395.
- Li X P, Phippard A, Pasari J, Niyogi K K. Structure-function analysis of photosystem II subunit S (PsbS) in vivo. *Functional Plant Biology* 2002; (29): 1131-1139.
- Lindahl M, Yang D H, Andersson B. Regulatory proteolysis of the major light-harvesting chlorophyll a/b protein of photosystem II by a light-induced membrane-associated enzymic system. *Eur J Biochem* 1995; (231): 503-509.
- Liu Z, Yan H, Wang K, Kuang T, Zhang J, Gui L, An X, Chang W. Crystal structure of spinach major light-harvesting complex at 2.72 Å resolution. *Nature* 2004; (428): 287-292.
- Lunde C, Jensen P E, Haldrup A, Knoetzel J, Scheller H V. The PSI-H subunit of photosystem I is essential for state transitions in plant photosynthesis. *Nature* 2000; (408): 613-615.
- Malkin R, Niyogi K K. Photosynthesis. In: *Biochemistry and Molecular Biology of Plants*. (Eds. Buchanan BB, Gruissem W, Jones R). American Society of Plant Biologists, 2000; 521-575.
- Matsubara S, Gilmore A M, Osmond C B. Diurnal and acclimatory responses of violaxanthin and lutein epoxide in the Australian mistletoe *Amyema miquelii*. *Australian Journal of Plant Physiology* 2001; (28): 793-800.
- Moya I, Silvestri M, Vallon O, Cinque G, Bassi R. Time-Resolved Fluorescence Analysis of the Photosystem II Antenna Proteins in Detergent Micelles and Liposomes. *Biochemistry* 2001; (40): 12552-12561.
- Muller P, Li X P, Niyogi K K. Non-photochemical quenching. A response to excess light energy. *Plant Physiol* 2001; (125): 1558-1566.
- Mullet J E, Burke J J, Arntzen C J. Chlorophyll proteins of photosystem I. *Plant Physiol* 1980; (65): 814-822.

- Nagai K, Thøgersen HC. Synthesis and sequence-specific proteolysis of hybrid proteins produced in *Escherichia coli*. [153], 461-481. 1987. *Methods in Enzymology*.
- Nield J, Orlova E V, Morris E P, Gowen B, van Heel M, Barber J. 3D map of the plant photosystem II supercomplex obtained by cryoelectron microscopy and single particle analysis. *Nat Struct Biol* 2000; (7): 44-47.
- Plumley F G, Schmidt G W. Reconstitution of chloroform a/b light-harvesting complexes: Xanthophyll-dependent assembly and energy transfer. *Proc Natl Acad Sci USA* 1987; (84): 146-150.
- Reinsberg D, Ottmann K, Booth P J, Paulsen H. Effects of chlorophyll a, chlorophyll b, and xanthophylls on the in vitro assembly kinetics of the major light-harvesting chlorophyll a/b complex, LHCIb. *J Mol Biol* 2001; (308): 59-67.
- Remelli R, Varotto C, Sandona D, Croce R, Bassi R. Chlorophyll binding to monomeric light-harvesting complex. A mutation analysis of chromophore-binding residues. *J Biol Chem* 1999; (274): 33510-33521.
- Rockholm D C, Yamamoto H Y. Violaxanthin de-epoxidase. *Plant Physiol* 1996; (110): 697-703.
- Scheller H V, Jensen P E, Haldrup A, Lunde C, Knoetzel J. Role of subunits in eukaryotic Photosystem I. *Biochim Biophys Acta* 2001; (1507): 41-60.
- Schmid V H R, Cammarata K V, Bruns B U, Schmidt G W. In vitro reconstitution of the photosystem I light-harvesting complex LHCI-730: Heterodimerization is required for antenna pigment organization. *Proceedings of the National Academy of Sciences of the United States of America* 1997; (94): 7667-7672.
- Storf S, Stauber E J, Hippler M, Schmid V H. Proteomic analysis of the photosystem I light-harvesting antenna in tomato (*Lycopersicon esculentum*). *Biochemistry* 2004; (43): 9214-9224.
- Wollman F A. State transitions reveal the dynamics and flexibility of the photosynthetic apparatus. *EMBO J* 2001; (20): 3623-3630.
- Yamamoto H Y, Kamite L. The effects of dithiothreitol on violaxanthin deepoxidation and absorbance changes in the 500nm region. *Biochim Biophys Acta* 1972; (267): 538-543.

Section A:

*Biochemical analysis of supramolecular
organisation of Photosystem I*

A 1

Stoichiometry of LHCI antenna polypeptides and characterisation of gap and linker pigments in higher plants Photosystem I

This chapter is in press on European Journal of Biochemistry,
reproduced with permission.

Matteo Ballottari, Chiara Govoni, Stefano Caffarri and
Tomas Morosinotto

Stoichiometry of LHCI antenna polypeptides and characterization of gap and linker pigments in higher plants Photosystem I

Matteo Ballottari¹, Chiara Govoni¹, Stefano Caffarri^{2,1} and Tomas Morosinotto^{1,2}

¹Dipartimento Scientifico e Tecnologico, Università di Verona, Verona, Italy; ²Université Aix-Marseille II, LGBP- Faculté des Sciences de Luminy, Département de Biologie, Marseille, France

We report on the results obtained by measuring the stoichiometry of antenna polypeptides in Photosystem I (PSI) from *Arabidopsis thaliana*. This analysis was performed by quantification of Coomassie blue binding to individual LHCI polypeptides, fractionation by SDS/PAGE, and by the use of recombinant light harvesting complex of Photosystem I (Lhca) holoproteins as a standard reference. Our results show that a single copy of each Lhca1–4 polypeptide is present in Photosystem I. This is in agreement with the recent structural data on PSI–LHCI complex [Ben Shem, A., Frolow, F. and Nelson, N. (2003) *Nature*, **426**, 630–635]. The discrepancy from earlier estimations based on pigment binding and yielding two copies of each LHCI polypeptide per PSI, is explained by the presence of ‘gap’ and ‘linker’

chlorophylls bound at the interface between PSI core and LHCI. We showed that these chlorophylls are lost when LHCI is detached from the PSI core moiety by detergent treatment and that gap and linker chlorophylls are both Chl *a* and Chl *b*. Carotenoid molecules are also found at this interface between LHCI and PSI core. Similar experiments, performed on PSII supercomplexes, showed that dissociation into individual pigment-proteins did not produce a significant loss of pigments, suggesting that gap and linker chlorophylls are a peculiar feature of Photosystem I.

Keywords: chlorophyll; Coomassie staining; LHCI; photosystem; stoichiometry.

Photosystem I (PSI) is a multisubunit complex, located in thylakoid membranes, acting as a light-dependent plastocyanin–ferredoxin oxidoreductase. The complex from higher plants binds ≈ 180 chlorophylls (Chls) [1,2] and it is composed by two moieties: the core and the antenna complexes. The core complex is composed by 14 polypeptides, it contains the primary donor P700 and it is responsible for the charge separation and the electron transport [3]. It also binds 96 Chl *a* and 22 β -carotene molecules with antenna function, as determined in *Synechococcus elongatus* by X-ray crystallography [4]. In higher plants, biochemical and spectroscopic measurements [5,6], as well as the recent resolved structure of PSI from *Pisum sativum*, suggested values of about 100 chlorophyll molecules [2]. This is consistent with the observed homology between the higher plants and the bacterial complex [1]. The antenna complex of Photosystem I (LHCI) instead, is a peculiar of eukaryotic organisms and in vascular plants it is composed by four polypeptides, namely Lhca1–4, belonging to the Lhc multigene family [7,8]. Each

polypeptide was proposed to bind 10 chlorophyll molecules [9–11] and, based on pigment content, the PSI–LHCI complex was estimated to bind eight light harvesting complex of Photosystem I (Lhca) subunits [1,9]. The recent structure of PSI–LHCI challenged this picture by showing the presence of only one copy of Lhca1–4 polypeptides per core complex [2]. The presence of loosely bound Lhca polypeptides in PSI–LHCI could explain this discrepancy. In this case, the number of Lhca polypeptides would depend on the mildness of solubilization steps, as it has been already observed for Photosystem II (PSII)–LHCII supercomplexes [12,13].

In order to clarify this uncertainty, we measured the stoichiometric ratio between each individual Lhca polypeptide and PSI–LHCI purified in a method known to maintain all antenna polypeptides bound to the PSI core [14]. We determined that a single copy of each Lhca1–4 polypeptide is bound in each PSI–LHCI complex of *Arabidopsis thaliana* as observed in the recently resolved structure [2]. This is true even when using a complex purified with a different method and from a different plant species. The contrasting results with previous stoichiometric estimations can be reconciled by considering that ‘linker’ and ‘gap’ chlorophylls identified in the structure are loosely bound at protein interfaces and are lost upon separation of LHCI from PSI core. In fact, we show that a significant amount of pigment is lost when LHCI is detached from the PSI core moiety. We could then characterize these pigments, showing that they are both Chl *a* and *b*. We also found that a significant amount of carotenoid molecules were lost, suggesting that they are also bound at the interface between LHCI and PSI core. Similar experiments performed on PSII showed that dissociation of

Correspondence to T. Morosinotto, Dipartimento Scientifico e Tecnologico, Università di Verona, Strada le Grazie, 15, 37134 Verona, Italy. Fax: +39 045 8027929, Tel.: +39 045 8027915
E-mail: morosinotto@sci.univr.it

Abbreviations: $\alpha(\beta)$ -DM, *n*-dodecyl- $\alpha(\beta)$ -D-maltoside; Car, carotenoid; Chl, chlorophyll; IOD, integrated optical density; Lhca, light harvesting complex of Photosystem I; PSI (II), Photosystem I (II).
(Received 22 July 2004, revised 28 September 2004, accepted 8 October 2004)

antenna proteins from the core complex did not produce a significant loss of pigments, suggesting that 'gap' chlorophylls are a unique characteristic of PSI.

Materials and methods

Purification of the native and recombinant complexes

PSI-LHCI complex and its PSI core and LHCI moieties were purified from *A. thaliana* as reported previously [14,15]. Plants were grown at $100 \mu\text{E}\cdot\text{m}^{-2}\cdot\text{s}^{-1}$, 19°C , 90% humidity and 8 h of daylight. Thylakoids, prepared as described previously [14] were resuspended at $1 \text{ mg}\cdot\text{mL}^{-1}$ Chl and solubilized with *n*-dodecyl- β -D-maltoside (β -DM) at a final concentration of 1%. The samples were centrifuged at 40 000 *g* for 10 min to eliminate unsolubilized material and then fractionated by ultracentrifugation in a 0.1–1 M sucrose gradient containing 0.06% β -DM and 5 mM Tricine, pH 7.8. After centrifugation for 21 h at 41 000 r.p.m. in an SW41 rotor (Beckman) at 4°C , chlorophyll-containing bands are collected. The lowermost band contained PSI-LHCI and it was pelleted, resuspended at $0.3 \text{ mg Chl}\cdot\text{mL}^{-1}$ in distilled water, and solubilized by 1% β -DM and 0.5% Zwittergent-16. After stirring for 20 min at 4°C the sample was rapidly frozen in liquid nitrogen and slowly thawed to improve the detachment between PSI core and LHCI. Samples were loaded on a 12-mL 0.1–1 M sucrose gradient, containing 5 mM Tricine, pH 7.8 and 0.03% β -DM.

Reconstitution and purification of recombinant Lhca pigment-protein complexes (from *A. thaliana*) were performed as in [9]. PSII supercomplexes were purified upon solubilization of BBY membranes prepared as in [16], but using 0.4% *n*-dodecyl- α -D-maltoside (α -DM). PSII supercomplexes were concentrated and further solubilized with 1% α -DM in order to dissociate the PSII core complex from Lhcb antenna proteins.

SDS/PAGE electrophoresis

SDS/PAGE electrophoresis was performed as [17], but using an acrylamide/bis-acrylamide ratio of 75 : 1 and a total concentration of acrylamide + bis-acrylamide of 4.5% and 15.5%, respectively, for the stacking and running gel. Urea (6 M) was also incorporated into the running gel. The staining for the densitometry was obtained with 0.05% Coomassie R in 25% isopropanol, 10% acetic acid in order to improve linearity with protein amount [18].

Coomassie stain quantification

The protein amount was evaluated after SDS/PAGE by excising each band and eluting the Coomassie stain with 1 mL of 50% isopropanol and 3% SDS. The stain was then quantified by measuring the absorption at 593 nm [18]. Another approach determining the amount of stain bound to each band by colorimetry was also used. We acquired the gel image using a Bio-Rad GS710 scanner. The picture was then analysed with GEL-PRO ANALYZER[®] software (Media Cybernetics Inc., Silver Spring, MD, USA) that quantifies the staining of the bands as IOD (optical density integrated on the area of the band). At least five repetitions of each sample were loaded on the gel to achieve sufficient reproducibility.

Pigment quantification, pigment/protein stoichiometry and Chl : P700 measurement

Pigment composition was determined by a combined approach consisting of HPLC analysis [19] and fitting of the acetone extract with the spectra of the individual pigments [20]. Spectra were recorded using an SLM-Aminco DW 2000 spectrophotometer (SLM Instruments, Inc., Rochester, NY, USA), in 80% acetone. Chl : P700 ratio was determined as described in [5].

Results and discussion

PSI-LHCI stoichiometry

PSI-LHCI complex was purified from *A. thaliana* thylakoids following the method described in [14] which was shown to allow purification of PSI without any loss of Lhca polypeptides during the procedure. The sample purified was also characterized by measuring the Chl : P700 ratio. In our preparation we obtained a value of 176 ± 27 Chls bound per P700 molecule; this was in agreement with previous values [5]. PSI-LHCI polypeptides were then fractionated using a modified SDS/PAGE system based on [17], as described above (Fig. 1). The modification of electrophoretic conditions was necessary to achieve a good separation of Lhca1–4 polypeptides from *A. thaliana*. The correspondence of the bands to Lhca1, 2, 3 and 4 was demonstrated by Western blotting analysis using antibodies directed against oligopeptides of individual Lhca proteins and it is reported in Fig. 1. Another band is visible between Lhca3

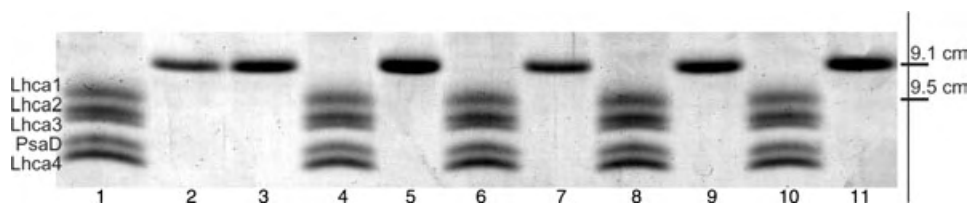


Fig. 1. Example of SDS/PAGE used for stoichiometry determination. Five lanes are loaded with $4.5 \mu\text{g}$ of Chl of PSI-LHCI complex. Lhca1–4 and PsaD bands, as identified by Western blotting, are indicated. Six lanes loaded with different amounts of Lhca1 reconstituted *in vitro* ($0.35 \mu\text{g}$ of Chls loaded in lanes 2 and 7, $0.47 \mu\text{g}$ in lanes 3 and 9, $0.6 \mu\text{g}$ in lanes 5 and 11) are shown. On the right, the mobility of Lhca1 band in recombinant sample and PSI-LHCI complex is reported, expressed as the distance in centimetres from the beginning of running gel. The Coomassie quantification was verified to be linearly dependent on protein amount between 0.1 and $1 \mu\text{g}$ and 2–10 μg of Chls loaded, respectively, for recombinant Lhca and PSI-LHCI samples.

and Lhca4 and it was identified to be a PSI core subunit by comparing the polypeptide composition of PSI-LHCI with isolated PSI core and LHCI. This polypeptide was then identified as PsaD from its molecular mass [3] and from Western blotting with specific antibodies.

As we were able to separate all individual Lhca polypeptides, we could gain information on the quantity of each polypeptide by determining the amount of Coomassie bound to each band. This was performed by excising the bands corresponding to each Lhca protein from stained SDS/PAGE, eluting the Coomassie from excised gel slices with 50% isopropanol and 3% SDS and then quantifying the stain from its absorbance at 593 nm [18]. In Table 1 the amount of Coomassie bound by each Lhca per μg of Chl of PSI-LHCI loaded on the SDS/PAGE is reported.

However, it is well known that the Coomassie staining is not an absolute quantification of the protein amount. In fact, depending on the amino acid composition, different proteins bind the stain with different affinity. For this reason, to correctly quantify the protein amount, an internal standard for each Lhca was needed. For this purpose, we used the recombinant Lhca1–4 from *A. thaliana* reconstituted *in vitro*, where the protein concentration can be easily derived from the absorption spectra [9,11]. These samples were loaded in the same gel and the amount of Coomassie stain per μg of Chl loaded in the SDS/PAGE was measured as well. The results for recombinant samples are also reported in Table 1. From the data presented, it should be noticed that Lhca polypeptides have a different ability to bind Coomassie; this is as expected due to their different amino acid compositions. In particular, Lhca1 appears to bind more stain than Lhca2–4 per μg of Chl loaded in the gel.

In order to achieve a good reproducibility in each gel, eight repetitions of each recombinant Lhca were loaded together with five repetitions of PSI-LHCI. To obtain reliable results, each Lhca band from PSI-LHCI was quantified based on stain binding to the recombinant protein loaded on the same gel. An example of one SDS/PAGE separation used in this measurement for Lhca1 is shown in Fig. 1. It can be noted that recombinant samples have a slightly different mobility with respect to the native samples. This is due to the addition of three to eight amino acid residues at N and C terminal during the cloning of cDNA in expression vectors. As indicated in the Fig. 1, the presence of extra amino acids reduces the mobility of recombinant Lhca1 of about 4%, a value consistent with the number of extra amino acids. Similar modifications of the mobility were observed for Lhca2–4 as well (the decrease in the mobility was of 5, 3 and 3%, respectively). These differences with respect to the native sequence have been taken into account by correcting the Coomassie amount by a factor of 1.09, 1.13, 1.13, 1.18, respectively, for recombinant Lhca1, 2, 3 and 4. These factors are proportional to the number of positively charged residues added by the cloning procedure. It can be appreciated, however, that these factors are small enough and do not affect, to a significant extent, the conclusions drawn regarding stoichiometry.

From Fig. 1 it can also be appreciated that Lhca bands in PSI-LHCI have a similar mobility in the SDS PAGE. In fact, in our gels Lhca1–4 and PsaD bands were all contained

Table 1. Quantification of Coomassie bound to Lhca polypeptides. The amount of Coomassie bound to Lhca1–4 polypeptides per μg of Chl loaded is reported in the case of PSI-LHCI (left) and recombinant complexes (right). The results obtained with the two methods described in the text, the spectrophotometric and colorimetric, are both shown. Values are expressed, respectively, as μg of Coomassie and IOD, the optical density integrated in the whole area of the band. Standard deviation, that approximately correspond to 70% of the confidence interval, is also indicated (SD).

	PSI-LHCI				Recombinant Samples			
	Lhca1	Lhca2	Lhca3	Lhca4	Lhca1	Lhca2	Lhca3	Lhca4
Spectrophotometric analyses (μg Coomassie μg^{-1} Chl \pm SD)	138.1 \pm 11.5	51.3 \pm 12.8	89.3 \pm 22.6	73.5 \pm 6.5	1792.2 \pm 204.8	1118.3 \pm 230.6	1303.0 \pm 318.4	1327.2 \pm 129
Colorimetric analyses (IOD μg^{-1} Chl \pm SD)	35.01 \pm 2.43	23.43 \pm 4.04	37.29 \pm 3.49	39.88 \pm 4.42	524.02 \pm 29.52	371.86 \pm 71.68	521.65 \pm 100.04	790.73 \pm 67.19

in a region 1-cm long. Therefore cutting the bands with accuracy was critical, especially in the case of Lhca2 and Lhca3, which migrate very close to each other.

An alternative method for quantification of the Coomassie stain bound to each band was therefore used in order to increase the accuracy and test the reliability of results. This was performed by analysing digital pictures of the stained gel using a densitometric software that evaluates the amount of stain bound from the intensity of the band. Of course, using this procedure, the acquisition of gel image is critical for the result and for this reason we used a proteomics-dedicated scanner. The quantification of each Lhca band both in PSI-LHCI complex and in recombinant samples is reported in Table 1, expressed as IOD (integrated optical density). The densitometry allows obtaining a better reproducibility than the band excision method used first, as judged from the standard deviation values: spectroscopic quantification yielded values ranging from 10 to 25%, while densitometry within 5 to 20%. As Lhca2 and Lhca3 migrated very close to each other, however, even this second type of analysis yielded a larger deviation in quantification of these bands with respect to Lhca1 or Lhca4.

It should be considered that densitometry does not allow an absolute quantification of the Coomassie bound, like the spectroscopic method does; rather it gives information on the relative amount of stain bound to different bands in the same gel. However, this is sufficient for our purpose of determining the stoichiometry of Lhca polypeptides in PSI-LHCI.

In fact, we can calculate the stoichiometry from values in Table 1, by knowing the molecular mass of Chls and number of chlorophyll molecules bound by each complex. These values are available from previously published work using different techniques. We assumed consensus values for each recombinant Lhca polypeptide of 11 ± 2 Chls molecules [2,10,11]. For the PSI-LHCI complex, a value of 175 ± 15 Chls was considered, taking account both of our Chl : P700 measurement and published data [1,2,5,21].

In Table 2 the results of the Lhca stoichiometry, calculated from these assumptions and values in Table 1, are reported. The stoichiometry was determined first by dividing values in Table 1 per the Chl molecular mass, obtaining the amount of Coomassie bound per chlorophyll mole of PSI or recombinant complex loaded in the SDS/PAGE. The assumption on the number of chlorophyll was then utilized to calculate the amount of Coomassie bound per mole of native PSI-LHCI or recombinant complex. This value represents the Coomassie bound by a mole of the polypeptide per each recombinant sample. In the case of the native complex it represents the amount of Coomassie

bound by each Lhca per mole of PSI-LHCI. Therefore, by dividing the latter by the first figure, we obtain the number of Lhca polypeptides per PSI-LHCI complex. Results obtained from both methods showed that, within the confidence interval, four Lhc polypeptides (one copy of each Lhca1–4) is present in PSI-LHCI complex. The different methods gave slightly different results, suggesting that this procedure is not precise enough to appreciate differences smaller than 0.2 copies. However, these data, derived from two independent determinations, strongly support the idea that one copy per each Lhca1–4 is present in PSI-LHCI complex as recently showed by X-ray crystallography [1]. Considering the total amount of Lhca polypeptides per PSI (Table 2) we can also suggest that the presence of a fifth binding site looks very unlikely. As our PSI preparation derive from plants grown in just one optimal condition, however, there is still the possibility that the stoichiometry is modified in response to different environmental conditions and we are at present performing some experiments in this direction.

In order to test the dependence of our results on data derived from literature, we calculated the stoichiometry results by using a wide range of different assumptions. The results for the case of Lhca1 are reported in Fig. 2. This demonstrates that the accuracy of the assumptions is not critical for our results. In fact, in order to obtain a stoichiometry ratio different than one Lhca per PSI core complex, values very far from any data present in literature must be assumed. As an example, a result of two copies of Lhca1 per PSI can be obtained by assuming values for Chls bound to recombinant Lhca1 and PSI-LHCI complex, of 6 and 180 or 10 and 300, values that are in contrast with all published determinations (1; 2; 5; 10; 11; 19). Similar tables were built for all Lhca1–4, obtaining similar results.

Chlorophyll *a*, *b* and carotenoids are bound at the interface between LHCI and PSI core

Our stoichiometry determination suggests that, in higher plants, one Lhca polypeptide is present per PSI core; this is in agreement with the structure resolved recently [2]. This result, however, is in apparent disagreement with estimations of Lhca polypeptide content based on pigment evaluations [9,22,23]. The presence of loosely bound Lhca polypeptides in PSI-LHCI could explain this discrepancy. In this case, the number of Lhca polypeptides would depend on the mildness of the solubilization steps, as it has been already observed for PSII-LHCII supercomplexes [12,13]. However, the PSI-LHCI we used for our determination was purified with the method described in [9,15] that was shown

Table 2. Lhca vs. PSI stoichiometry. The number of Lhca molecules bound per PSI molecule is determined from Coomassie stain binding using recombinant Lhca complexes as standards. The results obtained by the two methods described in the text, the spectrophotometric and densitometric quantification, are both shown. SD \approx 70% of the confidence interval, is indicated.

	Lhca1	Lhca2	Lhca3	Lhca4	Total
Spectroscopic quantification (polypeptides per PSI \pm SD)	1.23 \pm 0.30	1.37 \pm 0.52	0.92 \pm 0.37	1.13 \pm 0.27	4.65 \pm 0.76
Densitometric quantification (polypeptides per PSI \pm SD)	1.06 \pm 0.23	1.00 \pm 0.33	1.14 \pm 0.33	0.80 \pm 0.20	4.00 \pm 0.56

Lhca1 No Chl per PSI	Number of Chl per polypeptide in Recombinant Sample										
	5	6	7	8	9	10	11	12	13	14	15
100	1.34	1.11	0.95	0.84	0.74	0.67	0.61	0.56	0.51	0.48	0.45
120	1.60	1.34	1.15	1.00	0.89	0.80	0.73	0.67	0.62	0.57	0.53
140	1.87	1.56	1.34	1.17	1.04	0.94	0.85	0.78	0.72	0.67	0.62
160	2.14	1.78	1.53	1.34	1.19	1.07	0.97	0.89	0.82	0.76	0.71
180	2.41	2.00	1.72	1.50	1.34	1.20	1.09	1.00	0.93	0.86	0.80
200	2.67	2.23	1.91	1.67	1.48	1.34	1.21	1.11	1.03	0.95	0.89
220	2.94	2.45	2.10	1.84	1.63	1.47	1.34	1.22	1.13	1.05	0.98
240	3.21	2.67	2.29	2.00	1.78	1.60	1.46	1.34	1.23	1.15	1.07
260	3.47	2.90	2.48	2.17	1.93	1.74	1.58	1.45	1.34	1.24	1.16
280	3.74	3.12	2.67	2.34	2.08	1.87	1.70	1.56	1.44	1.34	1.25
300	4.01	3.34	2.86	2.51	2.23	2.00	1.82	1.67	1.54	1.43	1.34

Fig. 2. Validation of Chl binding assumptions. In this table, different values of Lhca1 stoichiometry, calculated by hypothesizing different numbers of Chl bound to recombinant Lhca1 and to PSI–LHCI complex, are reported. Solid and dashed lines indicate, respectively, values resulting in a stoichiometry of one and two Lhca1 per PSI. The interval of assumptions chosen is indicated in grey.

to maintain all Lhca polypeptides bound to PSI core. In order to elucidate this apparent contradiction, we analysed all fractions from the sucrose gradient fractionation of thylakoids by SDS/PAGE and Western blotting with anti-LHCI Igs, without finding any trace of Lhca polypeptides migrating differently than the PSI–LHCI band. Therefore, we can exclude the possibility of the presence of a loosely bound Lhca pool, at least in plants grown in our conditions. Our stoichiometry determinations also allows the ruling out species-dependent differences between *P. sativum* and *A. thaliana*, as our results obtained with the latter species confirm the structure resolved with PSI from pea.

These apparently contrasting data on LHCI stoichiometry can be explained considering the presence of chlorophyll molecules bound at the interface between LHCI subunits or between LHCI and the PSI core, as suggested from the PSI–LHCI structure and therein defined, respectively, as ‘linker’ and ‘gap’ chlorophylls [2]. These chromophores could be stably bound only in PSI–LHCI and being lost when LHCI is detached from PSI core. This loss of pigments would explain the difference between chlorophyll-based and protein-based estimations.

In order to experimentally verify if the binding of these chlorophylls depends on the interaction between core and antenna complexes, we fractionated the PSI–LHCI into LHCI and PSI core moieties, according to the method previously described by Croce and coworkers [15], and kept trace of the amount of chlorophylls present in each fraction. In Fig. 3A the sucrose gradient fractionation of PSI–LHCI after solubilization with β -DM and zwittergent is shown. The gradient showed four different bands that were characterized by absorption spectroscopy (Fig. 4A) and SDS/PAGE analysis (not shown) and identified as: (i) free pigments; (ii) dimeric LHCI; (iii) PSI-core and (iv) undissociated PSI–LHCI complex. It is interesting to note that Lhca polypeptides were not detected in other gradient fractions different from fraction 2 and 4. In Table 3 the amount of each fraction together with their Chl *a/b* and Chl : Car ratio is reported. The reliability of the preparation was also confirmed by comparing biochemical and spectroscopic data with previous data on similar preparations [9].

The PSI–LHCI preparation we used as starting material was also verified to be equilibrated energetically and devoid of free chlorophylls by fluorescence analysis at 77 K, in agreement with previous determinations [14] (not shown).

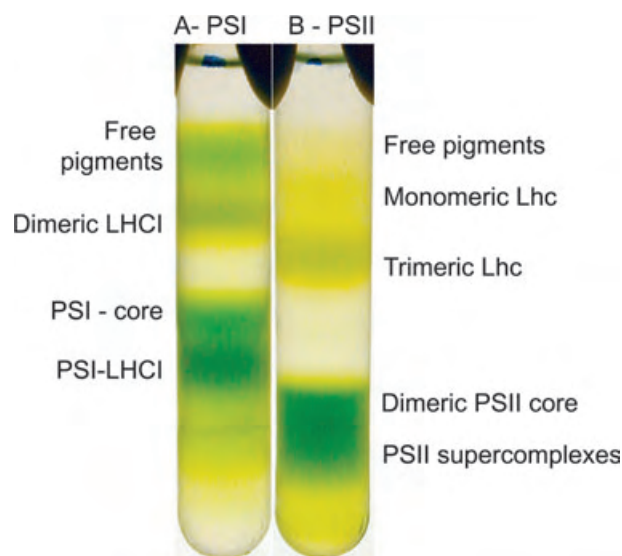


Fig. 3. Sucrose density gradient profile of solubilized PSI and PSII super complexes. Super complexes of (A) PSI–LHCI and (B) PSII–LHCII were loaded on sucrose gradient after solubilization with, respectively, 1% β -DM and 0.5% zwittergent or 1% α -DM.

However, a relevant amount of chlorophyll was found in the free pigment band (11.4% of the total Chl content). We can therefore conclude that these ‘free’ pigments are liberated during the dissociation of the PSI–LHCI complex and therefore they are not tightly bound Lhca proteins nor the PSI-core. We conclude that these chlorophyll molecules are bound to sites stabilized by interactions between LHCI antenna and PSI core complexes and therefore they could be identified bona fide as the ‘gap’ and ‘linker’ chlorophylls found in PSI–LHCI structure [2]. However, we have to be aware that we can not rule out the possibility of a partial denaturation and/or loss of pigments from LHCI or PSI core during purification. For this reason, we have to consider 11.4% as an upper limit and not as a precise quantification of gap and linker chlorophylls.

Even taking into account that the analysis could not be quantitative, the biochemical characterization of the free pigment fraction provided interesting information about the identity of gap and linker chlorophylls (Table 3). In fact,

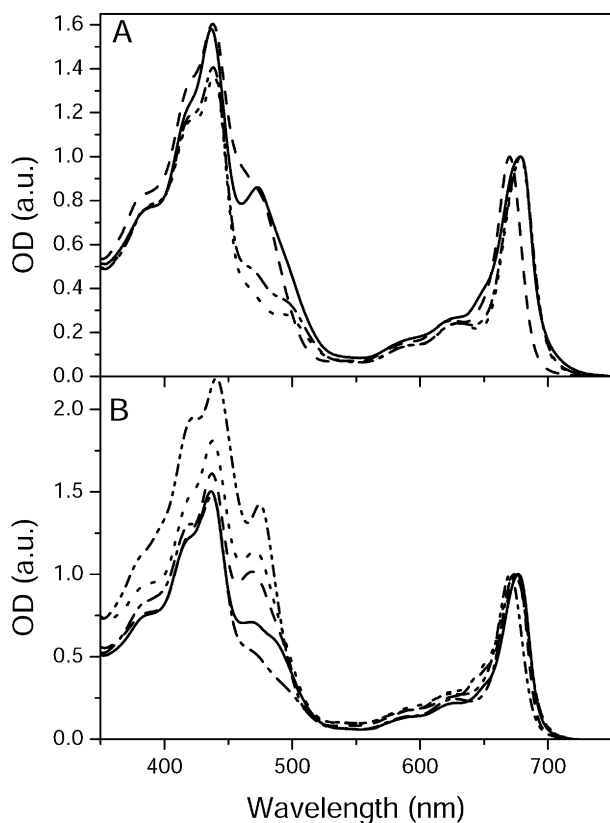


Fig. 4. Absorption spectra of solubilized PSI-LHCI and PSII supercomplexes. Absorption spectra of different bands obtained upon solubilization and sucrose gradient ultracentrifugation of PSI-LHCI (A) and PSII supercomplexes (B) are shown, normalized to the maximum in the Q_y region. In (A) they can be recognized as free pigments (---), LHCI (—), PSI core (····) and PSI-LHCI (-·-·). In (B) they are identified as free pigments (---), monomeric and trimeric Lhc (-·-·), PSII core (-·-·) and PSII supercomplexes (—).

Table 3. Pigment analysis of solubilized PSI-LHCI. Pigment composition of different fractions from sucrose gradients of solubilized PSI-LHCI is reported (Fig. 3A). The chlorophyll content is indicated as the percentage on the total amount of Chl in the gradient. SD \approx 70% of the confidence interval is reported.

	Chl content (%)	SD	Chl <i>a</i> : Chl <i>b</i>	Chl/Car
Free pigments	11.4	3.5	4.9	2.3
LHCI	15.1	4.4	3.4	4.9
PSI- core	26.7	3.8	23.3	7.3
PSI- LHCI	46.8	5.6	10.2	5.3

structural data could not distinguish between Chl *a* and *b* molecules, but, as fraction 1 has a Chl *a* : *b* ratio of 4.93, we can suggest that approximately one sixth of gap and linker chlorophylls are Chl *b*. Therefore these binding sites are not all specific for Chl *a* as the PSI core ones are, but they can also bind Chl *b* as does LHCI.

Data in Table 3 also shows the presence of a significant amount of carotenoids among the pigments released during

the purification: in fact, fraction 1 has a Chl : Car ratio of 3.0. In particular, it contains 47% of lutein, 26% of violaxanthin and 27% of β -carotene. Although we have to consider the possible extra loss of pigments, as mentioned above, this finding strongly suggests that not only chlorophylls, but also carotenoids are bound at the interface between LHCI and PSI core. These carotenoids are most probably important in photoprotection of gap and linker chlorophylls.

Comparison between PSI and PSII

Are the chlorophylls bound at the interface between different subunits also present in Photosystem II or is this a peculiarity of Photosystem I? To address this question, we performed similar experiments on PSII in order to assess if pigments were liberated when PSII-LHCII supercomplexes were dissociated. We purified PSII supercomplexes by a very mild solubilization of BBY membranes (0.4% α -DM) and then separated the core from antenna moieties with a second stronger solubilization step. PSII supercomplexes are more susceptible to detergent treatment and, in order to dissociate antenna from core, we used only 1% α -DM. This treatment was chosen because it left approximately 50% of PSII supercomplexes undissociated, similar to the fraction of intact PSI-LHCI complex left with 1% β -DM and 0.5% zwittergent.

The sucrose gradient ultracentrifugation following solubilization of the PSII supercomplex with 1% α -DM is shown in Fig. 3B. In the case of PSI, we kept traces of pigments in every fraction in order to verify if a substantial amount of chlorophylls were liberated during the dissociation of antenna proteins from core complex. From SDS/PAGE (not shown) and absorption spectra (Fig. 4B) analysis, we identified the different fractions as (i) free pigments; (ii) monomeric Lhc; (iii) trimeric LHCII; (iv) Dimeric PSII core and (v) PSII supercomplexes still intact. Clearly, the fraction of chlorophylls liberated during the separation is far lower than in the case of PSI. In fact, the quantification of chlorophyll amount of each fraction showed that Chl liberated during dissociation was only about 0.5% of the total Chl content, far lower than the 11.4% obtained in the case of PSI-LHCI complex. The absence of free pigment contamination in Lhc fractions was also excluded by measuring the fluorescence emission spectra upon selective excitation of Chl *a* and Chl *b*. The spectra upon different excitations are coincident, demonstrating that all pigments are energetically connected and thus bound to the protein complexes and not free in the membrane (not shown).

These results suggest that the co-ordination of Chl might be in part different in PSI and in PSII; PSI binds Chls both within individual pigment binding proteins and at the interface between subunits. In PSII, Chls are tightly bound to individual proteins. This might be explained if we consider that PSII antenna undergoes important modifications in response to environmental conditions. In fact, the antenna size of PSII is modulated in order to avoid over-excitation of P680 and photoinhibition [24]. Moreover during the state transition, LHCII dissociates from PSII upon phosphorylation and migrates to stroma membranes where it transfers energy to PSI (for review see [25,26]).

These mechanisms would be incompatible with Chl molecules binding at the interface of antenna subunits as it would produce free unprotected Chls very prone to produce harmful oxygen species.

On the contrary, LHCI appears to be firmly bound to its core complex, as also demonstrated by the stronger detergent treatment needed to dissociate the antenna system. Thus, this organization of the antenna appears to be more stable but also less flexible. Most probably therefore at least four Lhca polypeptides are always present in the PSI-LHCI complex. We could therefore hypothesize that the larger part of PSI antenna size regulation is played by the modification of the amount of LHCII associated to the PSI rather by modifying the Lhca content.

Acknowledgements

We thank Roberto Bassi and Roberta Croce for helpful discussions and for critically reading the manuscript. Stefan Jansson and Frank Klimmek are thanked for discussions. This work was founded by 'MIUR' Progetti FIRB N° RBAU01E3CX. S.C. was supported by the European Community's Human Potential Program contract HPRN-CT-2002-00248 (PSICO).

References

- Boekema, E.J., Jensen, P.E., Schlodder, E., van Breemen, J.F., van Roon, H., Scheller, H.V. & Dekker, J.P. (2001) Green plant photosystem I binds light-harvesting complex I on one side of the complex. *Biochemistry* **40**, 1029–1036.
- Ben Shem, A., Frolow, F. & Nelson, N. (2003) Crystal structure of plant photosystem I. *Nature* **426**, 630–635.
- Scheller, H.V., Jensen, P.E., Haldrup, A., Lunde, C. & Knoetzel, J. (2001) Role of subunits in eukaryotic Photosystem I. *Biochim. Biophys. Acta* **1507**, 41–60.
- Jordan, P., Fromme, P., Witt, H.T., Klukas, O., Saenger, W. & Krauss, N. (2001) Three-dimensional structure of cyanobacterial photosystem I at 2.5 Å resolution. *Nature* **411**, 909–917.
- Bassi, R. & Simpson, D. (1987) Chlorophyll–protein complexes of barley photosystem I. *Eur. J. Biochem.* **163**, 221–230.
- Kitmitto, A., Mustafa, A.O., Holzenburg, A. & Ford, R.C. (1998) Three-dimensional structure of higher plant photosystem I determined by electron crystallography. *J. Biol. Chem.* **273**, 29592–29599.
- Jansson, S. (1994) The light-harvesting chlorophyll a/b-binding proteins. *Biochim. Biophys. Acta* **1184**, 1–19.
- Jansson, S. (1999) A guide to the Lhc genes and their relatives in *Arabidopsis*. *Trends Plant Sci.* **4**, 236–240.
- Croce, R., Morosinotto, T., Castelletti, S., Breton, J. & Bassi, R. (2002) The Lhca antenna complexes of higher plants photosystem I. *Biochim. Biophys. Acta* **1556**, 29–40.
- Schmid, V.H.R., Potthast, S., Wiener, M., Bergauer, V., Paulsen, H. & Storf, S. (2002) Pigment binding of photosystem I light-harvesting proteins. *J. Biol. Chem.* **277**, 37307–37314.
- Castelletti, S., Morosinotto, T., Robert, B., Caffarri, S., Bassi, R. & Croce, R. (2003) Recombinant Lhca2 and Lhca3 subunits of the photosystem I antenna system. *Biochemistry* **42**, 4226–4234.
- Boekema, E.J., van Roon, H., van Breemen, J.F. & Dekker, J.P. (1999) Supramolecular organization of photosystem II and its light-harvesting antenna in partially solubilized photosystem II membranes. *Eur. J. Biochem.* **266**, 444–452.
- Yakushevskaya, A.E., Jensen, P.E., Keegstra, W., van Roon, H., Scheller, H.V., Boekema, E.J. & Dekker, J.P. (2001) Supramolecular organization of photosystem II and its associated light-harvesting antenna in *Arabidopsis thaliana*. *Eur. J. Biochem.* **268**, 6020–6028.
- Croce, R., Zucchelli, G., Garlaschi, F.M., Bassi, R. & Jennings, R.C. (1996) Excited state equilibration in the photosystem I–light–harvesting I complex: P700 is almost isoenergetic with its antenna. *Biochemistry* **35**, 8572–8579.
- Croce, R., Zucchelli, G., Garlaschi, F.M. & Jennings, R.C. (1998) A thermal broadening study of the antenna chlorophylls in PSI-200, LHCI, and PSI core. *Biochemistry* **37**, 17255–17360.
- Berthold, D.A., Babcock, G.T. & Yocum, C.F. (1981) A highly resolved, oxygen-evolving photosystem II preparation from spinach thylakoid membranes. EPR and electron-transport properties. *FEBS Lett.* **134**, 231–234.
- Laemmli, U.K. (1970) Cleavage of structural proteins during the assembly of the head of bacteriophage T4. *Nature* **227**, 680–685.
- Ball, E.H. (1986) Quantitation of proteins by elution of Coomassie Brilliant Blue R. from Stained bands after dodecyl sulfate polyacrylamide gel electrophoresis. *Anal. Biochem.* **155**, 23–27.
- Gilmore, A.M. & Yamamoto, H.Y. (1991) Zeaxanthin formation and energy-dependent fluorescence quenching in pea chloroplasts under artificially mediated linear and cyclic electron transport. *Plant Physiol.* **96**, 635–643.
- Croce, R., Canino, G., Ros, F. & Bassi, R. (2002) Chromophores Organization in the Higher Plant Photosystem II Antenna Protein CP26. *Biochemistry* **41**, 7343.
- Malkin, R., Ortiz, W., Lam, E. & Bonnerjea, J. (1985) Structural organization of thylakoid membrane electron transfer complexes: Photosystem I. *Physiol. Veg.* **23**, 619–625.
- Boekema, E.J., Wynn, R.M. & Malkin, R. (1990) The structure of spinach photosystem I studied by electron microscopy. *Biochim. Biophys. Acta* **1017**, 49–56.
- Jansson, S., Andersen, B. & Scheller, H.V. (1996) Nearest-neighbor analysis of higher-plant photosystem I holocomplex. *Plant Physiol.* **112**, 409–420.
- Rintamaki, E., Martinsuo, P., Pursiheimo, S. & Aro, E.M. (2000) Cooperative regulation of light-harvesting complex II phosphorylation via the plastoquinol and ferredoxin–thioredoxin system in chloroplasts. *Proc. Natl Acad. Sci. USA* **97**, 11644–11649.
- Allen, J.F. (1992) Protein phosphorylation in regulation of photosynthesis. *Biochim. Biophys. Acta* **1098**, 275–335.
- Wollman, F.A. (2001) State transitions reveal the dynamics and flexibility of the photosynthetic apparatus. *EMBO J.* **20**, 3623–3630.

A 2

The role of individual Lhca subunits in the stability of higher plant Photosystem I-Light harvesting I supercomplex

Tomas Morosinotto, Matteo Ballottari, Frank Klimmek,
Stefan Jansson and Roberto Bassi

The role of individual Lhca subunits in the stability of higher plant Photosystem I-Light harvesting I supercomplex

Tomas Morosinotto^{1,2}, Matteo Ballottari¹, Frank Klimmek³, Stefan Jansson³ and Roberto Bassi^{1,2}

¹ Dipartimento Scientifico e Tecnologico, Università di Verona. Strada Le Grazie, 15- 37134 Verona, Italy

² Université Aix-Marseille II, LGBP- Faculté des Sciences de Luminy - Département de Biologie - Case 901 - 163, Avenue de Luminy - 13288 Marseille, France

³ Umeå Plant Science Centre, Department of Plant Physiology, Umeå University, S-901 87 Umeå, Sweden

Running title: Antenna binding cooperativity to higher plants Photosystem I

Abbreviations used are: $\alpha(\beta)$ -DM: *n*-dodecyl- $\alpha(\beta)$ -D-maltoside; Car, Carotenoid; Chl, chlorophyll; Lhca (b), light harvesting complex of Photosystem I (II); PSI (II), Photosystem I (II); WT, wild type.

Keywords: Photosystem, LHCI, Lhca, antenna, cooperativity

Abstract

We report on the results obtained by a biochemical analysis of Photosystem I in plants depleted in individual Lhca complexes. Our analysis showed that the lack of one Lhca complex affects the stability of the whole antenna system, demonstrating the cooperative nature of its association to Photosystem I. Strong interactions were shown between Lhca polypeptides and between antenna and core subunits which are important for the stability of the whole supercomplex. These interactions are stronger between respectively Lhca1-4 and Lhca2-3, consistently with their purification as dimers. Gap and linker pigments are proposed to play a fundamental role in mediating the interactions between antenna polypeptides. Differences between in the association of antenna complexes in Photosystem I and II are discussed. Lhca5, a minor component of the antenna system plays a role in the stability of the supercomplex.

Introduction

Photosystem I in higher plants mediates the light driven electron transport from plastocyanin to Ferredoxin. It is composed by two moieties: (i) a core complex, binding chromophores involved in charge separation and electron transport; (ii) an antenna moiety responsible for increasing the absorption cross-section. In higher plants, the core complex is composed by 14 subunits [1; 2] and it also binds about 100 Chl a and 22 β -carotene molecules [3; 4].

The antenna moiety is called LHCI: in higher plants it is composed by 4 major polypeptides encoded by nuclear genes *Lhca1-4* [4; 5]. Two other Lhca gene sequences, *Lhca5* and *Lhca6*, have been identified in *Arabidopsis thaliana*, as well as in other plant species [5]. Lhca5 gene product has been recently detected in thylakoids where it appears to be part of PSI-LHCI supercomplex although in sub-stoichiometric amounts [6; 7]. Lhca6 is highly homologous to Lhca2 and could be a pseudo-gene, but it might be expressed with a physiological role only in particular growth conditions (Klimmek, unpublished)

Recently, the structure of PSI-LHCI complex from *Pisum sativum* has been resolved by X-ray crystallography, showing the presence of one copy each of the Lhca1-4 polypeptide bound to one side of PSI core [4]. A unique feature revealed by this structure is the presence of chlorophyll molecules bound at the interface between LHCI subunits and between LHCI and the PSI core complex, defined respectively as “gap” and “linker” chlorophylls [4]. Biochemical fractionation of LHCI and PSI core showed that, besides Chl a, Chl b and carotenoid molecules are also found in this interfacial pigment pool [8].

In this work, we address the question of how LHCI binds to PSI core by performing a biochemical characterisation of the PSI-LHCI complex from *Arabidopsis thaliana* plants lacking each individual Lhca polypeptides, obtained by either insertion mutagenesis or RNA interference. Our analysis shows that the association of Lhca subunits to PSI core is strongly cooperative: in fact, when one subunit is missing the whole LHCI system is de-stabilised. On this basis, protein - protein interactions, mediated by gap and linker chlorophylls, are suggested to play an important role in LHCI binding to PSI core. These interactions appears to be particularly strong between Lhca1 - Lhca4 and Lhca2 - Lhca3, consistently with their isolation as dimers [9]. The subunit association in *Arabidopsis* PSI-LHCI complex is compared both with Photosystem II and with PSI from *Chlamydomonas reinhardtii*.

Materials and methods

Plant material and thylakoids purification

$\Delta a1-a5$ plants and growing conditions have been previously described in [6; 10]. Thylakoids have been purified from dark adapted plants as in [11].

Non denaturing gels (Deriphat PAGE).

Non-denaturing Deriphat-PAGE was performed following the method developed by Peter and Thornber [12] with the following modifications: the stacking gel had 3.5% (w/v) acrylamide (38:1 acrylamide/ bis-acrylamide). The resolving gel had an acrylamide concentration gradient from 4.5 to 11.5 % (w/v) stabilised by a glycerol gradient from 8% to 16% (w/v). 12 mM Tris and 48 mM Glycine pH 8.5 were also included in the gel. Thylakoids at Chl concentration of 1 mg/ml were solubilised with 0.6 or 1 % of respectively α and β -DM. 30 μ g of chlorophylls were loaded per each lane.

Purification of Photosystem I particles and LHCI

Photosystem I particles were purified from thylakoids by sucrose gradient ultracentrifugation upon solubilisation of thylakoid membranes with 1% β -DM, as described in [13]. To separate Lhc monomers, dimers and trimers Lhc fractions were concentrated, reloaded on a 0.1-1 M sucrose gradient and centrifuged in a SW60 Beckman rotor for 16 hours at 55000 rpm. LHCI and PSI core moieties were purified from PSI as described in [14].

Spectroscopy and pigment analysis.

The absorption spectra were recorded using a SLM-Aminco DK2000 spectrophotometer, in 5 mM Tricine pH 7.8, 0.2 M sucrose and 0.03% β -DM. HPLC analysis was as in [15]. Chlorophyll to carotenoid ratio and Chl a/b ratio was independently measured by fitting the spectrum of acetone extracts with the spectra of individual purified pigments [16].

SDS PAGE Electrophoresis and western blotting analysis

SDS-PAGE electrophoresis was performed as in [17], but using a acrylamide/bis-acrylamide ratio of 75:1 and a total concentration of acrylamide + bis-acrylamide of 4.5 % and 15.5 % respectively for the stacking and running gel. 6 M urea was also incorporated into the running gel. These modifications are optimised for the separation of Lhca1-4 from *Arabidopsis thaliana*. For gel staining, 0.05 % Coomassie R in 25% isopropanol, 10% acetic acid was used, in order to improve linearity with protein amount [18]. In the case of second dimension of non denaturing Deriphat PAGE, before loading gel slices were equilibrated for 30' in 7M Urea, 2% SDS and 100 mM Tris HCl pH 6.8.

Stoichiometry evaluations based on Coomassie stain quantification

The protein amount was evaluated after SDS-PAGE by determining the amount of stain bound to each band by colorimetry. The gel image was acquired by using a Biorad GS710 scanner. The

picture was then analysed with Gel-Pro Analyzer© software, which quantifies the staining of the bands as IOD (Optical density integrated on the area of the band).

Reconstitution in vitro of Lhca1-4 monomeric complexes.

cDNAs of Lhca1-4 from *Arabidopsis thaliana* [9; 19] were expressed and isolated from the SG13009 strain of *E. coli* following a protocol previously described [20; 21]. Reconstitution *in vitro* were performed as described in [9].

Results

Arabidopsis plants depleted in individual Lhca1-5 proteins have been obtained from mutant collections or with an antisense approach. In particular, plants lacking Lhca1, Lhca4 and Lhca5 (respectively $\Delta a1$, $\Delta a4$ and $\Delta a5$) are T-DNA insertion lines, while plants depleted in Lhca2 and Lhca3 ($\Delta a2$ and $\Delta a3$) have been obtained with an antisense RNA inhibition [10; 22].

Non denaturing gels

In order to analyse the effect of the depletion of Lhca polypeptides we compared the composition of thylakoids membranes by separating pigment binding complexes into a non denaturing gel (Deriphat-PAGE) [12]. The result of the electrophoresis of thylakoids solubilised in very mild conditions (0.6 % α -DM) is shown in figure 1. In the picture the identification of each band in WT lane, based on their molecular weight, is also reported.

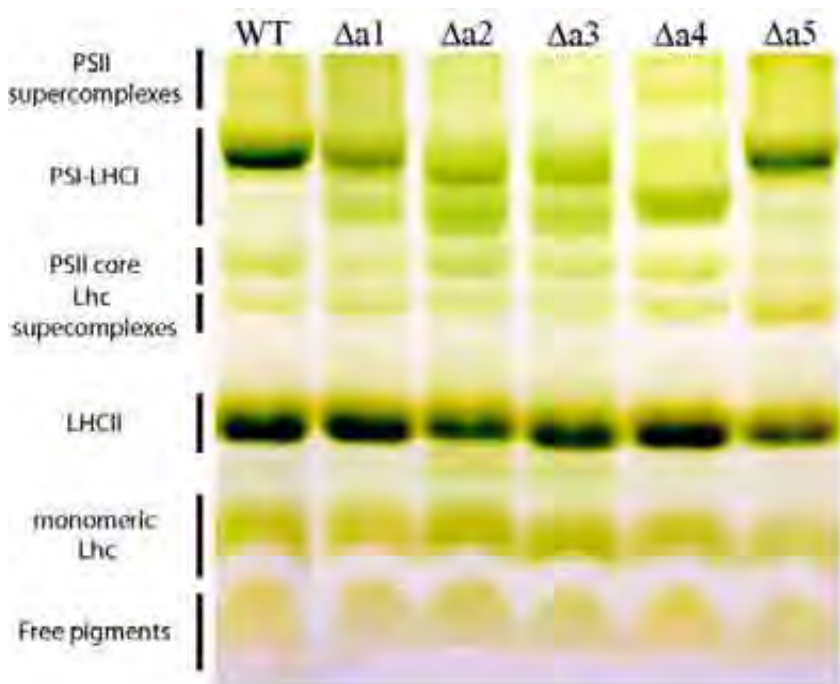


Figure 1. Deriphat PAGE profile of thylakoids from WT and $\Delta a1$ - $a5$ plants. Thylakoids have been solubilised with 0.6 % α -DM before loading. Bands detected in WT have been identified from their mobility and they are indicated on the left. 30 μ g of Chls have been loaded in each lane.

From the picture, it can be seen that the whole profile in Lhca deficient plants is very similar to the WT, with the exception of the region involving PSI-LHCI complex. Thus, the lack of Lhca polypeptides has no detectable effects on Photosystem II subunits, as it was expected. The region of the gel where PSI-LHCI migrated is shown in more detail in figure 2A. In WT plants, one major PSI-LHCI band is present, while in Lhca deficient plants up to three bands can be resolved. In particular, we could recognise three classes of bands, based on their molecular weight. The slowest migrating band corresponds to the PSI-LHCI in WT, while the fastest corresponds to PSI core. The band with intermediate mobility (indicated as PSI-LHCI*), is composed by a Photosystem I with a reduced antenna complement. The identification of the different populations, reported in figure 2, was obtained by running a second dimension on SDS PAGE in denaturing conditions, which separates the component polypeptides from each green bands (as example see below figure 3). Interestingly, the presence of a band corresponding to PSI core is detected in all $\Delta a1$ - $a4$ plants, but not in WT. This finding suggests that, when an individual Lhca polypeptide is lacking, a perturbation is induced in PSI-LHCI supercomplexes that leads to the complete loss of the LHCI moiety in at least a fraction of PSI particles. In $\Delta a4$ plants PSI core is the most represented band, suggesting a wide destabilisation of LHCI in these plants. In $\Delta a1$ plants, instead, the main band corresponds to a PSI-LHCI WT, while in $\Delta a2$ and $\Delta a3$ plants a band of PSI-LHCI* is the most evident. $\Delta a5$ plants are very similar to WT and no major differences could be detected.

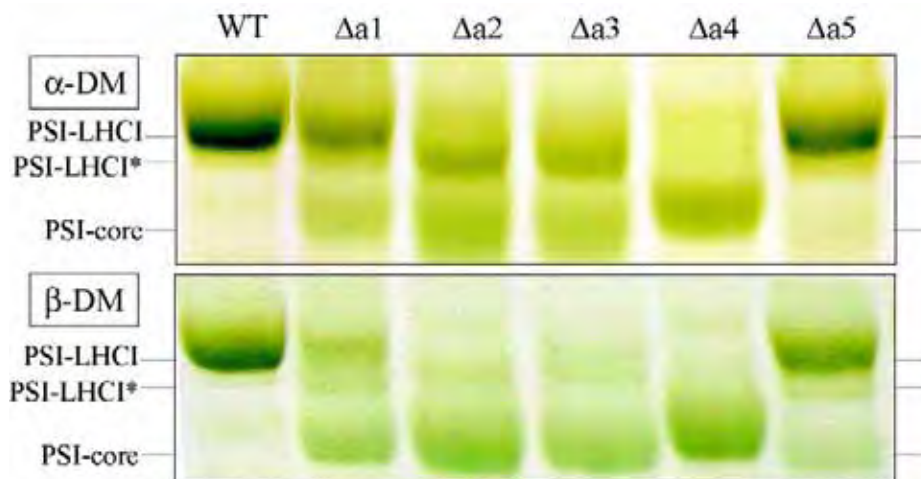


Figure 2. Deriphat PAGE profile of thylakoids purified from WT and $\Delta a1$ - $a5$ plants, particular of Photosystem I region. Thylakoids have been solubilised with (A) 0.6% α -DM or (B) 1% β -DM before loading. Three different PSI bands have been identified by a second denaturing electrophoresis to be respectively PSI with full antenna (PSI-LHCI), PSI with reduced antenna (PSI-LHCI*) and PSI without any antenna polypeptide (PSI-core).

In the figure 2A, some other fainter bands can also be recognised in the different samples. However, we could not identify them unequivocally because, using these very mild solubilisation

conditions, PSII supercomplexes are partially retained and co-migrate with PSI particles. As example, the bands migrating slightly faster or slower than the PSI-LHCI band in the lane loaded with WT membranes have been recognised as PSII particles by 2D analysis (not shown).

In order to have a clearer picture of the mutants pigment-protein pattern, we run a Deriphat PAGE after solubilisation of thylakoids membranes with 1% β -DM; the region involving PSI-LHCI is shown in figure 2B. This is a slightly harsher treatment, which dissociate completely PSII supercomplexes, but do not affect PSI-LHCI WT [13]. In WT lane, in fact, within this molecular weight range there is only one main band of PSI-LHCI, and only traces amount of PSI core are present. Therefore, we can be sure that, also in the case of mutants, all bands shown here derive from PSI. By using this stronger detergent treatment, we recognised bands belonging to the same three classes of mobility mentioned above, but their relative intensities changed with the stronger solubilisation conditions.

In $\Delta a1$ plants all the three bands are visible: one has the same mobility as the WT PSI-LHCI, one of PSI core and one with intermediate mobility containing PSI with reduced antenna content (PSI-LHCI*). The first is due to a fraction of PSI-LHCI WT still present, due to the incomplete phenotype of the mutant that retains a residual level of Lhca1 [10]. In $\Delta a2$ and $\Delta a3$ plants, instead, only bands corresponding to PSI core and PSI with reduced antenna complement are visible. It is interesting to note that the PSI-LHCI* here is clearly less intense with β -DM solubilisation than with α -DM. Since the latter treatment is milder than the first, this finding suggests that PSI-LHCI* is susceptible to detergent treatment and that with β -DM a larger part of the supercomplex dissociates into PSI core and free Lhca components. In $\Delta a4$ plants, the main band is again the PSI core, as shown before also with α -DM solubilisation, but a weak band corresponding to PSI-LHCI* is also visible. $\Delta a5$ plants are again very similar to the WT, even if some faint bands with higher mobility can be recognised (PSI-LHCI* and PSI core), suggesting that the absence of Lhca5 is affecting a small fraction (at maximum 5%) of PSI particles.

Second SDS-PAGE dimension

As mentioned above, we run a second dimension on a denaturing SDS PAGE condition in order to analyse the polypeptide composition of bands from Deriphat PAGE. In figure 3, a particular of the second dimension of PSI region of a non denaturing gel with β -DM solubilisation is shown. From this gel, we could identify the polypeptides contained into the three classes of PSI bands described on Deriphat-PAGE. In the case of PSI-LHCI WT, the spots corresponding to Lhca1-4 are identified based on their mobility in this gel system [8]. In the same region of the gel, also a spot of a PSI core protein, PsaD, can be identified. The presence of this band is useful because it gives an indication of

the PSI core content. Bands of the non denaturing gel corresponding to PSI core can easily be identified because only this spot corresponding to PsaD is visible. As mentioned above, a band corresponding to PSI core is detected in all $\Delta a1$ - $\Delta a4$ plants. The most interesting information provided by this second dimension analysis regarded the PSI-LHCI* band. In fact, we could not only identify this band as a PSI with a reduced Lhca content, but also obtain information on the identity of Lhca polypeptides that are retained in this fraction from the different mutant lines. In fact, PSI-LHCI* from $\Delta a2$ plants contained spots corresponding to Lhca1 and Lhca4, while spots of Lhca2 and Lhca3 were not detectable. The band from $\Delta a3$ had the same composition suggesting that Lhca2 and Lhca3 cannot maintain their interaction with PSI core in the absence of each other. Instead, in PSI-LHCI* from $\Delta a1$, Lhca2 and Lhca3 are retained, while Lhca1 and Lhca4 are not detectable.

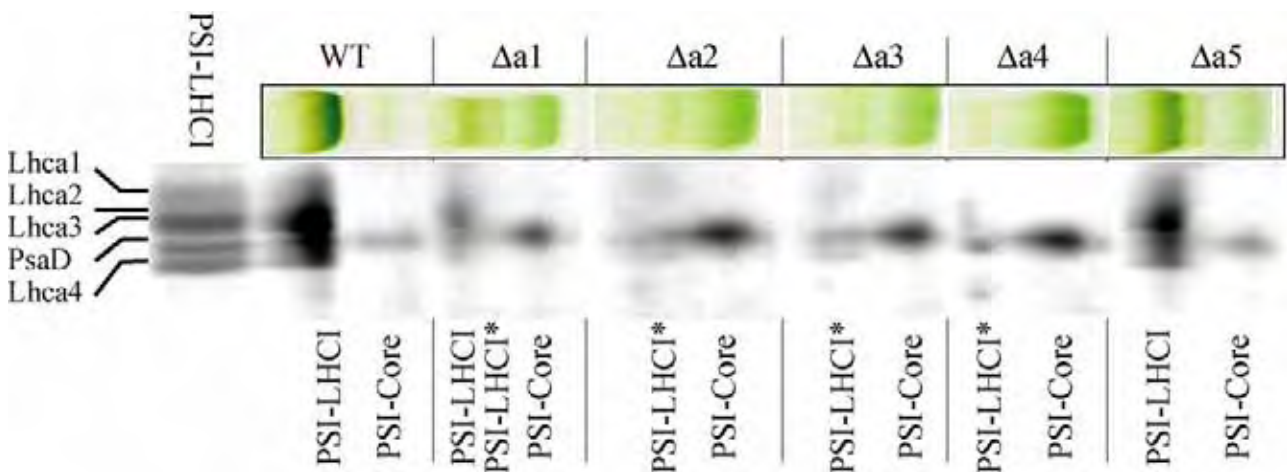


Figure 3. 2D SDS PAGE of PSI bands from WT and $\Delta a1$ - $a5$ plants (particular of region concerning Lhca polypeptides). The region involving PSI from Deriphat PAGE have been loaded in denaturing SDS PAGE. On the top the bands from native gel are reproduced and on the bottom the identification of bands from native gels is reported. PSI-LHCI particles from WT were also loaded on the left. The identification of polypeptides, based on their mobility, is reported.

PSI-Lhca stoichiometry

In order to further characterise these mutants, PSI particles were purified with sucrose gradient centrifugation after 1% β -DM solubilisation. The sucrose gradient ultracentrifugation has a lower resolution power with respect to non denaturing gels: thus, the PSI with reduced antenna complement (PSI-LHCI*) evidenced from gels cannot be fully purified from PSI core (or PSI-LHCI in the case of $\Delta a1$). The lowest part of PSI band was shown to be less contaminated and this was used for the following analyses. In figure 4A, the SDS PAGE profile of purified particles is shown. From a qualitative analysis of the picture, it could be driven that in $\Delta a1$ plants the level of Lhca1 and Lhca4 is reduced with respect to PsaD, Lhca2 and Lhca3. In $\Delta a2$ and $\Delta a3$, instead, both

Lhca2 and Lhca3 could not be detected, with the Coomassie staining. In $\Delta a4$, instead, only small amounts of Lhca2 and Lhca3 are detectable, consistently with the presence of mostly PSI core in the non-denaturing gels. $\Delta a5$ plants have a profile indistinguishable from WT consistent with the results from green-native gels. The same particles were analysed also by western blotting with antibodies against Lhca1-4 (not shown). By using this different detection method, some differences emerged: in fact, in $\Delta a2$ -PSI a residual fraction of Lhca3 was detected and in $\Delta a3$ there was a small amount of Lhca2 left. These results are consistent with a parallel work done on PSI particles purified from the same plants (Klimmek et al submitted). The apparent discrepancy with figure 4A where the same particles are analysed with Coomassie staining is due to the different method of detection: the antibody is more sensitive than the Coomassie staining and it reveals the presence of a traces amount of polypeptides in the particles.

From the Coomassie stained SDS PAGE, we also evaluated quantitatively the stoichiometry of each Lhca by comparing the polypeptide content of mutants with the WT. This was done by measuring the amount of Coomassie blue bound to each band by densitometry, with a method described in [8]. The amount of each Lhca band was then related with the amount of PsaD and PsaF, which were used as internal standards for the quantification of PSI core amount. Knowing that in WT one copy of each Lhca1-4 per PSI core is present, we calculated the amount of Lhca polypeptides per PSI core present in each preparation, [4; 8]. Values resulting from these measurements obtained by this method are reported in figure 4B.

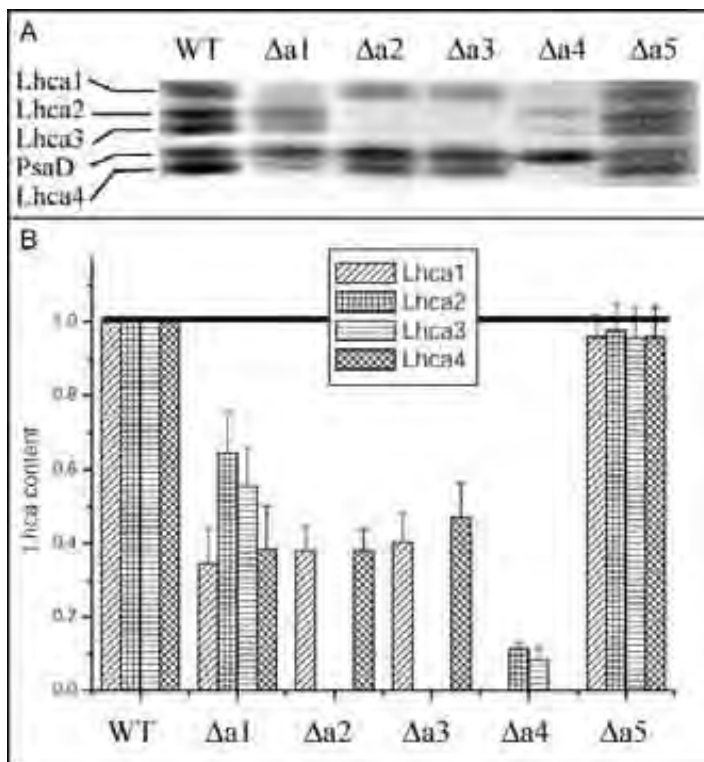


Figure 4. SDS PAGE analysis of PSI particles purified from WT and $\Delta a1$ - $\Delta a5$ plants. (A) Particular of SDS PAGE where Lhca polypeptides migrate. (B) Quantitative evaluation of Lhca1-4 polypeptides per PSI core in all samples. The stoichiometry was obtained by evaluation of Coomassie bound to each Lhca and normalisation to PsaD and PsaF content.

These data confirms the qualitative analysis exposed above, but also gives further interesting information. In fact, in $\Delta a1$ plants, in addition the reduction of Lhca1 and Lhca4 already mentioned, there is a reduction of about the 40% of Lhca2 and Lhca3. In $\Delta a2$ and $\Delta a3$ plants, Lhca2 and Lhca3 are under the Coomassie detection limit and only about 40 % of Lhca1 and Lhca4 is retained. In $\Delta a4$ around 10% of Lhca2 and Lhca3 are retained. In $\Delta a5$ plants, instead, PSI is indistinguishable from WT within the experimental error. This quantification is not fully representative of the PSI particles in thylakoids membranes for two reasons: first, PSI-LHCI* is susceptible to detergent treatment and thus a non well-quantifiable fraction of Lhca are lost upon solubilisation. Second, sucrose gradient centrifugation is not able to fully exclude contamination of PSI-LHCI*. This inability can be remarked in the case of $\Delta a1$ plants, where the residual content of Lhca1 in PSI particles is about 35% of WT, while in thylakoids the residual Lhca1 was estimated to be around 10%. In $\Delta a1$ plants, in fact, PSI particles are enriched in the PSI-LHCI and then Lhca1 content is higher than in thylakoids.

This stoichiometric evaluation, however, is very interesting because it shows which polypeptides are affected by the absence of each polypeptide. Moreover, it shows that we always found Lhca1-4 and Lhca2-3 in similar amounts in all different samples. This strongly suggests the presence of a reciprocal dependence of one member of these two couples from the companion for the association to PSI core. Therefore, when one polypeptide is absent, the other one tend to be lost as well and it is not anymore bound to PSI core, at least stably enough to be co-purified in significant amounts.

LHCI stability is reduced in plants depleted in Lhca1-4 polypeptides

We noted already that the PSI-LHCI* population in $\Delta a2$ and $\Delta a3$ plants is susceptible to detergent treatment and that under stronger solubilisation conditions it is reduced, while the amplitude of the PSI core band is increased. Since the thylakoids used as starting material were the same, this effect must correspond to a release of Lhca from PSI upon β -DM solubilisation. These dissociated proteins should migrate in the upper part of the sucrose gradients, together with the antenna complexes of PSII. In order to verify this hypothesis, we analyse these fractions with western blotting using specific antibodies against Lhca1-4 polypeptides (figure 5A). The presence of Lhca2 and 3 is detected in both $\Delta a1$ and $\Delta a4$ plants, suggesting that in these plants a fraction of these polypeptides is detached from PSI core upon solubilisation. Symmetrically, Lhca1 and 4 are found in the upper band from both $\Delta a2$ and $\Delta a3$ plants. It is worth noting that in WT plants instead, Lhca are stably retained bound to PSI in these solubilisation conditions. Quite surprisingly, instead, $\Delta a5$ plants showed some release of Lhca2 and Lhca4 polypeptides.

It is also interesting to determine if Lhca polypeptides are released from PSI as monomers or dimers. To this aim, we collected the free Lhc fraction (see figure 5B) and run it into an additional sucrose gradient for a longer time in order to increase resolution: as example, the result in the case of $\Delta a4$ plants is also shown in figure 5C. A band with an intermediate mobility between monomeric and trimeric Lhcb was detected. This fraction contained dimeric Lhca complexes as detected by the presence of a red absorption tail due to the typical >700 nm spectral forms in the absorption spectrum (not shown), a spectroscopic fingerprinting of PSI antenna complexes. This finding confirms that a secondary loss of LHCI polypeptides is induced when one Lhca is missing and also suggests that these Lhca polypeptides are lost as dimers, thus confirming their capacity of interacting with each other within Lhca2/3 and Lhca1/4 couples.

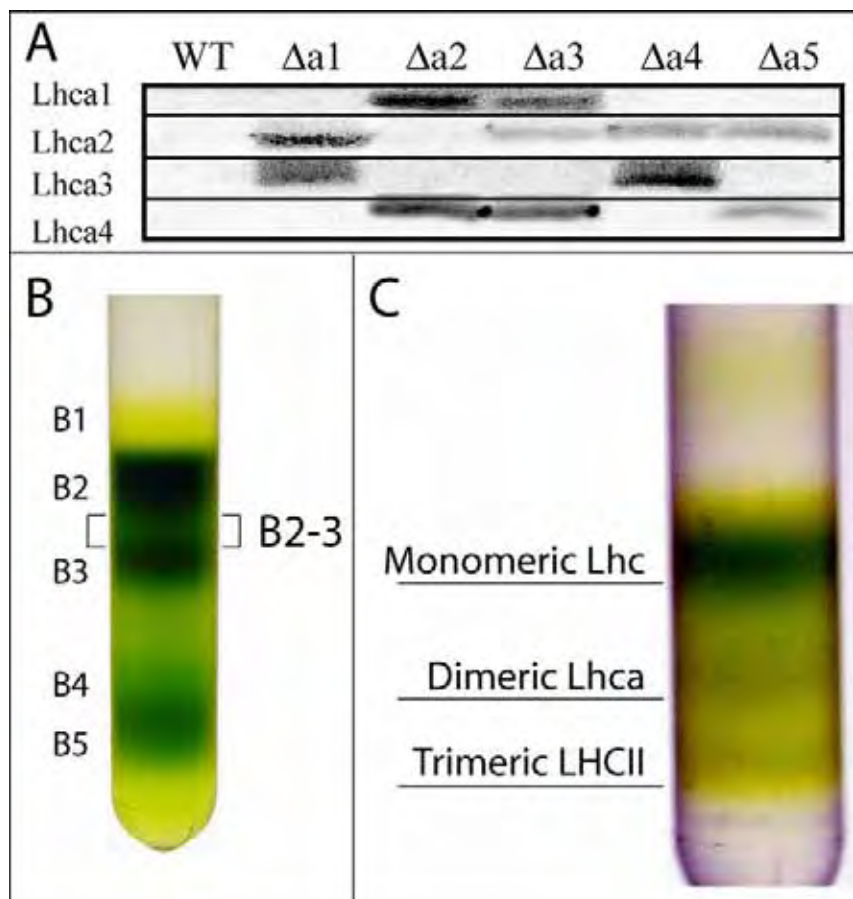


Figure 5. Analysis of Lhca polypeptides released upon thylakoids solubilisation with 1% β -DM. A) Western Blotting analysis of free Lhc complexes fraction after solubilisation of thylakoids membranes. B) Sucrose gradient ultracentrifugation of $\Delta a2$ thylakoid membranes solubilised with 1% β -DM. Five bands are indicated (B1-B5) and have been identified to be respectively: free pigments, monomeric Lhc, trimeric LHCI, PSII core, PSI-LHCI. Note that B4 and B5 are not well resolved. To avoid as much as possible contamination, the lowest part of the band was always used for analyses. The fraction between B2 and B3 (B2-3) is also indicated C) Second sucrose gradient of the B2-3 fraction. Bands corresponding to the different aggregation states are indicated.

Purification of Lhca1-4 dimer

LHCI polypeptides are very difficult to purify the one from the other, due to their biochemical similarity and to the presence of strong interactions between different polypeptides. Up to now, only a partial purification of Lhca1-4 dimer from Lhca2-3 could be achieved [9]. Therefore, most information available on individual properties of Lhca are derived mainly from reconstitutions *in vitro* [19; 23]. However, the recent structure of PSI-LHCI complex [4] recently showed the presence of “gap and “linker” chlorophylls bound at interfaces between PSI core and LHCI and between individual Lhca subunits. These binding sites are most probably not stable in monomeric Lhca reconstituted *in vitro* since protein-protein interactions are missing. For this reason, mutants lacking individual Lhca polypeptides are very useful tools for the characterisation of individual Lhca polypeptides because they could provide information on the extra pigments. A detailed spectroscopic analysis of PSI particles purified from these plants was reported in (Klimmek et al submitted). Here, we isolated LHCI from PSI particles: as expected from the characterisation of PSI-LHCI complexes, SDS PAGE of LHCI isolated from $\Delta a1$ plants was enriched in Lhca2 and Lhca3. Opposite, in LHCI from $\Delta a2$ and $\Delta a3$ plants Lhca2 and Lhca3 polypeptides were not detected and then it contained almost pure Lhca1-4. From $\Delta a4$ plants no LHCI fraction was obtained, since Lhca polypeptides retained in this mutant are too small. Lastly, from $\Delta a5$ plants we obtained a LHCI fraction with a composition indistinguishable from the WT. The LHCI population isolated from all mutant plants (but $\Delta a4$) migrated as dimers in a sucrose density gradient, as it was in the case of the WT. Therefore, this isolation yielded a LHCI preparation with WT composition (WT and $\Delta a5$), one enriched in Lhca2-3 dimers ($\Delta a1$), and one containing Lhca1-4 dimers ($\Delta a2$ and $\Delta a3$). It is then very interesting to analyse their spectroscopic and biochemical properties. In figure 6, absorption spectra of LHCI from $\Delta a1$, $\Delta a2$ and $\Delta a3$ plants are compared with WT. As it can be easily derived from the picture, spectra are all very similar. The only significant difference is detected in the regions corresponding to absorption of Chl b (around 470 and 650 nm). Here, LHCI- $\Delta a3$ showed a slightly larger signal than in WT, while in LHCI- $\Delta a1$ it is smaller. This difference is confirmed by the analysis of pigment binding properties of LHCI populations: LHCI from $\Delta a1$ plants has a slightly higher Chl a/b ratio (4.4 vs. 3.5 of WT).

The purification of LHCI also yielded PSI core preparations from all mutants. As expected, these preparations did not showed any difference depending on the genotype. However, it is interesting to compare the pigment binding properties of PSI core with the one of PSI particles purified from $\Delta a4$ plants. Interestingly, the main difference is in the carotenoid content: in fact, PSI from $\Delta a4$ plants showed the presence of significant amounts of violaxanthin and lutein, while in PSI core

preparation obtained by dissociating PSI-LHCI complex from WT, only β -carotene was found. Recently, it was found that violaxanthin and lutein molecules are bound at interfaces between PSI core and antenna, in addition to gap and linker chlorophylls [8]. Therefore, these xanthophylls found in PSI of $\Delta a4$ plants could be tentatively identified as a fraction of “gap carotenoids” that remains bound even in the absence of Lhc polypeptides.

Discussion

LHCI is co-operatively bound to PSI core

In this work, mutants of *Arabidopsis thaliana* depleted in individual Lhca complexes were biochemically characterised. From this analysis it emerged that in all $\Delta a1$ - $\Delta a4$ plants the binding of LHCI to PSI core was severely affected. In fact, with non denaturing electrophoresis, we always detected important amounts of PSI core without any associated Lhca, even in solubilisation conditions where the PSI-LHCI from WT is fully stable. Therefore, we can conclude that when one Lhca polypeptide is missing, the association of the remaining polypeptides to PSI-core is destabilised. We could still show the presence of PSI with associated antenna polypeptides (PSI-LHCI*), but this was only a fraction of the whole population. This residual population with an associated antenna is also susceptible to detergent treatment: this is evident if we compare the $\Delta a2$ and $\Delta a3$ profiles with α and β -DM solubilisation, the first one being milder than the latter. With α -DM, we detected a relevant amount of PSI with reduced antenna that is strongly reduced using β -DM. In addition, with a western blotting analysis, we found evidences in $\Delta a1$ - $\Delta a4$ plants, that Lhca polypeptides are detached upon solubilisation. We therefore conclude that, in the mutants, some antenna polypeptides are still associated to the PSI core within the thylakoid membranes but they are easily lost upon solubilisation.

This behaviour of mutant PSI-LHCI suggests the presence of strong protein-protein interactions between all Lhca proteins. When one subunit is missing, the binding of all the others to PSI core is weaker. The association of Lhca polypeptides to PSI core therefore appears to be highly cooperative.

Among this network of interactions stabilising the LHCI, Lhca4 appears to play a fundamental role for the interaction with the PSI core. In fact, when this polypeptide is missing, a very few Lhca polypeptides are found associated with PSI core. This effect could be due to its position in the middle of LHCI half moon [4] or to the presence of a critical interaction between Lhca4 and PsaF, the closest subunit of PSI core.

Lhca polypeptides also appear to behave like “couples”, consistently with their isolation as dimers [9]: in fact, Lhca1-4 and Lhca2-3 are not stably bound to PSI in the absence of their own “partner”.

This was shown by 2D SDS-PAGE analysis of the PSI-LHCI* population: in $\Delta a1$ plants, it did not contain Lhca4 while both in $\Delta a2$ and $\Delta a3$ only Lhca1 and Lhca4 were detectable. This hypothesis is confirmed by the evaluation of Lhca stoichiometry in PSI particles (figure 4): Lhca1-4 and Lhca2-3 are always detected in similar amounts, within the experimental deviation.

Recently, the structure of PSI-LHCI was resolved, allowing for the identification of a significant number of chlorophyll molecules in between PSI core and LHCI and between different Lhca, named respectively gap and linker chlorophylls [4]. A biochemical characterisation of these chlorophylls [8] and the pigment analysis of $\Delta a4$ PSI here presented showed that not only Chl a but also Chl b and carotenoid molecules are bound at the interfaces. Therefore, in PSI there is a group of “gap pigments” bound at the interfaces between LHCI and PSI core. Due to their position, they are very likely the responsible in mediating the interactions between antenna and core polypeptides.

Lhca binding flexibility

In all analyses presented so far, no evidence was found for the possible compensatory replacement of some missing Lhca by other Lhca protein (s). In fact, all results here presented suggest that at least Lhca1-4 bind to specific sites that cannot be occupied by other proteins. This is different from what is observed in PSII, where in plants lacking Lhcb1 and Lhcb2, Lhcb5 was over expressed and compensate for their absence. It even maintained the supramolecular structure of PSII supercomplexes by forming trimers with Lhcb3 [24].

These considerations suggest a different organisation of antenna systems in PSI as compared to PSII, even if the polypeptides composing the antenna system share a significant grade of sequence homology. In fact, the PSI antenna system showed stronger interactions between its component polypeptides and stronger interactions with its core complex moiety, since PSI-LHCI complex is stable to detergent treatment while PSII-LHCII complex is only partially retained even in the mildest conditions [8]. This different stability is probably related to the presence of gap and linker pigments that were shown to be present in PSI but not in PSII [8]. The higher stability is accompanied with a smaller flexibility: each polypeptide has a specific binding site that cannot be occupied by other polypeptides to a significant extent.

A rigid organisation of antenna system most probably is also less prone to antenna size regulation, as compared with PSII, where extensive change in antenna content has been described [25]. We can suggest that State I - State II transitions mechanisms is playing a major role in antenna size regulation in PSI, rather than the accumulation of Lhca polypeptides [26].

Comparison with another eukaryotic LHCI: Chlamydomonas reinhardtii

The Photosystem I in eukaryotic organisms has an antenna system composed by polypeptides belonging to Lhc multigenic family. The system here described, composed by Lhca1-4 plus Lhca5, however, is present only in land plants. In another eukaryotic organism, *Chlamydomonas reinhardtii*, it was shown that the PSI has an antenna system considerably larger, containing up to 11 Lhca monomers [27; 28]. In fact, in this algae up to 9 different Lhca polypeptides have been identified both at the sequence and at the polypeptide level and named Lhca1-9¹ [29-31]. It would be very interesting to understand which characteristics described in higher plants LHCI are conserved and which are instead different. For what concerns the subject of this work, the cooperativity of binding of LHCI to PSI core, a work recently published provides interesting information [32]: LHCI has been isolated from *Chlamydomonas* mutants depleted in PSI core. Despite the mutations, the LHCI moiety was shown to be present and to form large supercomplexes, stable to strong detergent treatment (0.8% β -DM). This results suggests that also in LHCI from *Chlamydomonas* strong interactions between Lhca complexes are present and that association of antenna to PSI core is very similar in all eukaryotic organisms [32]. A similar mutant lacking PSI core, *vir zb*⁶³, was isolated also in higher plants (barley). It also retains Lhca polypeptides in the absence of PSI core complex, but they do not form large aggregates but retain their dimeric organisation (data not shown). This difference is possibly due to the larger size of LHCI in *Chlamydomonas* with interactions between LHCI polypeptides extending not only in one direction, as shown in the one layer organisation of plant LHCI, but also radially with respect to PSI core thus accommodating two or more layers of subunits. This extended network of particles could maintain a stable supercomplex even in the absence of the PSI core moiety.

Lhca5:

In all this work, we focused our attention mainly on Lhca1-4 polypeptides. In fact, Δ a1-a4 plants showed the strongest phenotype, while PSI-LHCI from Δ a5 plants was often indistinguishable from WT. However, here PSI-LHCI appeared to be less stable than WT to detergent treatment, as shown by the detection of a PSI core band in non denaturing gels (fig. 2B) and the release of Lhca polypeptides (fig. 5A). These data suggest that the lack of Lhca5 affects a small fraction of the PSI population where the antenna complex is destabilised.

It could be asked if Lhca5 is bound to PSI-LHCI complex in addition to Lhca1-4 polypeptides or replaces of one of them. The first hypothesis seems more likely because Lhca5 did not compensate

¹ the denomination in *Chlamydomonas reinhardtii* is not consistent with the one used for vascular plants.

for the decrease of any other Lhca1-4 polypeptides. Moreover, Lhca5 is partially lost during purification of PSI particles, suggesting a weaker association to the core complex with respect to Lhca1-4 [6].

Since Lhca5 did not show the stability observed for Lhca1-4, it could be also more flexible and its content could depend on regulation from environmental conditions, providing another mechanism for antenna size regulation over the state transition. However, while the increase of the PSI antenna size in response to state transition has been proven by several authors (see [26] for a recent review) the functional effect of Lhca5 is still to be elucidated.

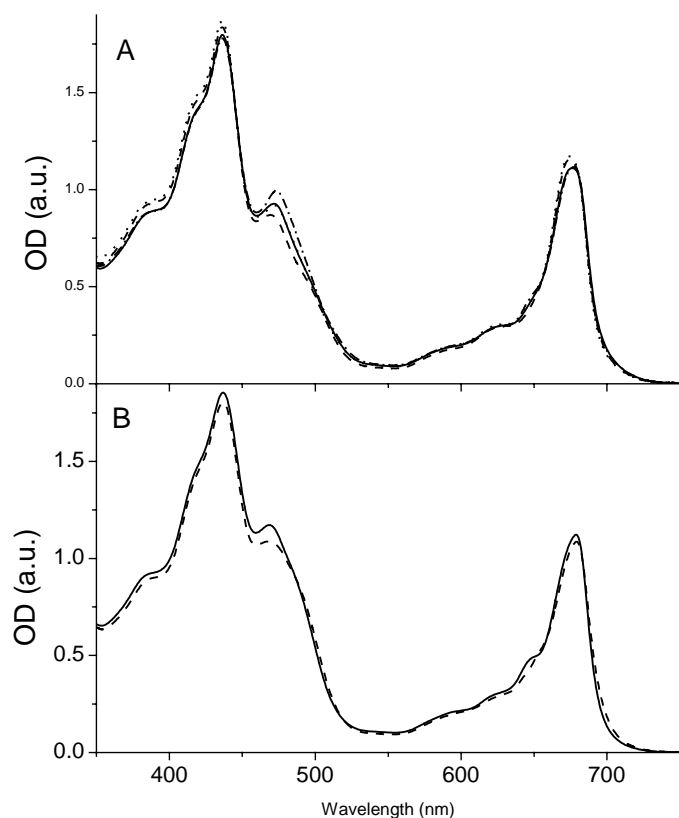


Figure 6. Room temperature absorption spectra of LHCI. A) Absorption spectra of LHCI purified from WT (solid) and $\Delta a1-3$ (respectively dashed, dotted and dash dotted) plants. Spectra are normalised to the total chl content. B) Sum of absorption spectra of Lhca pigment binding complexes reconstituted *in vitro*. Lhca1+4 (solid) and Lhca2+3 (dashed) are shown. Spectra are normalised to the total Chl content.

Individual properties of Lhca polypeptides

By purifying LHCI moieties from plants depleted in individual Lhca, we were able to obtain three different antenna populations with different polypeptide composition. The first, from WT and $\Delta a5$, had with all Lhca1-4, the second, from $\Delta a2$ and $\Delta a3$, had Lhca1 and Lhca4, while the third one, from $\Delta a1$ plants, was enriched in Lhca2-3 but had still significant amounts of Lhca1-4. These three populations, when characterised, did not show any relevant difference from both biochemical and spectroscopic point of view, but a small variation in Chl a/b ratio. This result suggests that, at least in *Arabidopsis thaliana*, Lhca1-4 and Lhca2-3 dimers have very similar properties. This hypothesis is confirmed by data on LHCI populations enriched in Lhca1-4 and Lhca2-3 that also showed small

differences despite individual Lhca [9] holoproteins have distinct properties [19]. However, if we consider that Lhca1-4 and Lhca2-3 are strongly interacting, the dimers properties rather than the individual properties should be considered. In order to have a rough estimation of the dimer properties, we can then compare the aggregate properties of Lhca1-4 and Lhca2-3 reconstituted *in vitro*. In figure 6B, the sum of the individual absorption spectra is shown and it confirms that dimers with similar properties can originate from monomers with different characteristics. We have to be aware that dimers properties are different from the sum of the monomers, since extra pigments are bound at the interfaces between polypeptides and are not stably bound in monomers reconstituted *in vitro* [4; 9]. However, even taking accounts of these limitations, data both from isolated LHCI in mutants and reconstituted Lhca suggested a strong similarity in Lhca1-4 and Lhca2-3 heterodimers. Therefore we suggest that the functional unit of LHCI is an heterodimer composed of two polypeptides of distinct spectral properties. The reasons for this organisation are not clear at present.

Acknowledgements

This work was funded by Ministero dell'Istruzione Università e Ricerca (MIUR) Progetti Fondo per gli Investimenti della Ricerca di Base (FIRB) Grants RBAU01E3CX and RBNE01LACT and by the European Community's Human Potential Program Grant HPRN-CT-2002-00248 (PSICO).

References

- [1] Scheller,H.V., Jensen,P.E., Haldrup,A., Lunde,C., & Knoetzel,J. (2001) Role of subunits in eukaryotic Photosystem I. *Biochim. Biophys. Acta*, **1507**, 41-60.
- [2] Knoetzel,J., Mant,A., Haldrup,A., Jensen,P.E., & Scheller,H.V. (2002) PSI-O, a new 10-kDa subunit of eukaryotic photosystem I. *FEBS Lett.*, **510**, 145-148.
- [3] Jordan,P., Fromme,P., Witt,H.T., Klukas,O., Saenger,W., & Krauss,N. (2001) Three-dimensional structure of cyanobacterial photosystem I at 2.5 Å resolution. *Nature*, **411**, 909-917.
- [4] Ben Shem,A., Frolow,F., & Nelson,N. (2003) Crystal structure of plant photosystem I. *Nature*, **426**, 630-635.
- [5] Jansson,S. (1999) A guide to the Lhc genes and their relatives in Arabidopsis. *Trends Plant Sci.*, **4**, 236-240.
- [6] Ganeteg,U., Klimmek,F., & Jansson,S. (2004) Lhca5 - an LHC-Type Protein Associated with Photosystem I. *Plant Mol. Biol.*, **54**, 641-651.
- [7] Storf,S., Stauber,E.J., Hippler,M., & Schmid,V.H. (2004) Proteomic analysis of the photosystem I light-harvesting antenna in tomato (*Lycopersicon esculentum*). *Biochemistry*, **43**, 9214-9224.
- [8] Ballottari M., Govoni,C., Caffarri,S., & Morosinotto,T. (2004) Stoichiometry of LHCI antenna polypeptides and characterisation of gap and linker pigments in higher plants Photosystem I. *Eur. J. Biochem.*, in press.

- [9] Croce,R., Morosinotto,T., Castelletti,S., Breton,J., & Bassi,R. (2002) The Lhca antenna complexes of higher plants photosystem I. *Biochimica et Biophysica Acta-Bioenergetics*, **1556**, 29-40.
- [10] Ganeteg,U., Kulheim,C., Andersson,J., & Jansson,S. (2004) Is each light-harvesting complex protein important for plant fitness? *Plant Physiol*, **134**, 502-509.
- [11] Haldrup,A., Naver,H., & Scheller,H.V. (1999) The interaction between plastocyanin and photosystem I is inefficient in transgenic Arabidopsis plants lacking the PSI-N subunit of photosystem I. *Plant J.*, **17**, 689-698.
- [12] Peter,G.F. & Thornber,J.P. (1991) Biochemical composition and organization of higher plant photosystem II LIGHT-HARVESTING PIGMENT-PROTEINS. *J. Biol. Chem.*, **266**, 16745-16754.
- [13] Croce,R., Zucchelli,G., Garlaschi,F.M., Bassi,R., & Jennings,R.C. (1996) Excited state equilibration in the photosystem I -light - harvesting I complex: P700 is almost isoenergetic with its antenna. *Biochemistry*, **35**, 8572-8579.
- [14] Croce,R., Zucchelli,G., Garlaschi,F.M., & Jennings,R.C. (1998) A thermal broadening study of the antenna chlorophylls in PSI- 200, LHCI, and PSI core. *Biochemistry*, **37**, 17255-17360.
- [15] Gilmore,A.M. & Yamamoto,H.Y. (1991) Zeaxanthin Formation and Energy-Dependent Fluorescence Quenching in Pea Chloroplasts Under Artificially Mediated Linear and Cyclic Electron Transport. *Plant Physiol.*, **96**, 635-643.
- [16] Croce,R., Canino,g., Ros,F., & Bassi,R. (2002) Chromophores Organization in the Higher Plant Photosystem II Antenna Protein CP26. *Biochemistry*, **41**, 7343.
- [17] Laemmli,U.K. (1970) Cleavage of structural proteins during the assembly of the head of bacteriophage T4. *Nature*, **227**, 680-685.
- [18] Ball, E. H. (1986)) Quantitation of proteins by elution of Coomassie Brilliant Blue R from Stained bands after dodecyl sulfate polyacrilamide gel electrophoresis. *Anal. Biochem.*, **155**, 23-27
- [19] Castelletti,S., Morosinotto,T., Robert,B., Caffarri,S., Bassi,R., & Croce,R. (2003) Recombinant Lhca2 and Lhca3 subunits of the photosystem I antenna system. *Biochemistry*, **42**, 4226-4234.
- [20] Nagai,K. & Thøgersen,H.C. Synthesis and sequence-specific proteolysis of hybrid proteins produced in Esherichia coli. [153], 461-481. 1987. *Methods in Enzimology*.
- [21] Paulsen,H., Finkenzeller,B., & Kuhlein,N. (1993) pigments induce folding of light-harvesting chlorophyll alpha/beta-binding protein. *Eur. J. Biochem.*, **215**, 809-816.
- [22] Ganeteg,U., Strand,A., Gustafsson,P., & Jansson,S. (2001) The Properties of the Chlorophyll a/b-Binding Proteins Lhca2 and Lhca3 Studied in Vivo Using Antisense Inhibition. *Plant Physiol*, **127**, 150-158.
- [23] Schmid,V.H.R., Cammarata,K.V., Bruns,B.U., & Schmidt,G.W. (1997) In vitro reconstitution of the photosystem I light-harvesting complex LHCI-730: Heterodimerization is required for antenna pigment organization. *Proceedings of the National Academy of Sciences of the United States of America*, **94**, 7667-7672.
- [24] Ruban,A.V., Wentworth,M., Yakushevskaya,A.E., Andersson,J., Lee,P.J., Keegstra,W., Dekker,J.P., Boekema,E.J., Jansson,S., & Horton,P. (2003) Plants lacking the main light-harvesting complex retain photosystem II macro-organization. *Nature*, **421**, 648-652.
- [25] Spangfort,M. & Andersson,B. (1989) Subpopulations of the main chlorophyll a/b light-harvesting complex of photosystem II - Isolation and biochemical characterization. *Biochim. Biophys. Acta*, **977**, 163-170.
- [26] Wollman,F.A. (2001) State transitions reveal the dynamics and flexibility of the photosynthetic apparatus. *EMBO J.*, **20**, 3623-3630.

- [27] Germano,M., Yakushevskaya,A.E., Keegstra,W., van Gorkom,H.J., Dekker,J.P., & Boekema,E.J. (2002) Supramolecular organization of photosystem I and light-harvesting complex I in *Chlamydomonas reinhardtii*. *FEBS Letters*, **525**, 121-125.
- [28] Kargul,J., Nield,J., & Barber,J. (2003) Three-dimensional reconstruction of a light-harvesting complex I-photosystem I (LHCI-PSI) supercomplex from the green alga *Chlamydomonas reinhardtii* - Insights into light harvesting for PSI. *Journal of Biological Chemistry*, **278**, 16135-16141.
- [29] Stauber,E.J., Fink,A., Markert,C., Kruse,O., Johanningmeier,U., & Hippler,M. (2003) Proteomics of *Chlamydomonas reinhardtii* light-harvesting proteins. *Eukaryotic Cell*, **2**, 978-994.
- [30] Elrad,D. & Grossman,A.R. (2004) A genome's-eye view of the light-harvesting polypeptides of *Chlamydomonas reinhardtii*. *Curr. Genet.*, **45**, 61-75.
- [31] Tokutsu,R., Teramoto,H., Takahashi,Y., Ono,T.A., & Minagawa,J. (2004) The light-harvesting complex of photosystem I in *Chlamydomonas reinhardtii*: protein composition, gene structures and phylogenetic implications. *Plant Cell Physiol*, **45**, 138-145.
- [32] Takahashi,Y., Yasui,T.A., Stauber,E.J., & Hippler,M. (2004) Comparison of the Subunit Compositions of the PSI-LHCI Supercomplex and the LHCI in the Green Alga *Chlamydomonas reinhardtii*. *Biochemistry*, **43**, 7816-7823.

A 3

Adaptation of Photosystem I antenna system to short and long term light stress

Tomas Morosinotto, Matteo Ballottari, Luca Dall'Osto and
Roberto Bassi

Adaptation of Photosystem I antenna system to short and long term light stress

Abstract

Land plants can often experience light excess and they evolved several mechanisms to adapt their photosynthetic machinery to environmental conditions. The study of this phenomena is generally focused on Photosystem II (PSII) which is believed to be the primary target of photoinhibition. The ability of Photosystem I (PSI) to respond to environmental conditions is instead poorly studied. In this work, we analysed the adaptation of PSI to short and long light stress. In a few minutes upon light stress, PSI exchange violaxanthin with zeaxanthin, as PSII does. In PSI zeaxanthin is effective in reducing its antenna fluorescence yield. Long term adaptation to different light environments, instead, was surprisingly shown to have no effect on Photosystem I antenna size. In all conditions tested, in fact, one copy each of the Lhca1-4 antenna protein was always found associated to PSI core. It is proposed that the key factor for PSI photoprotection is the maintenance of the energy balance with PSII. For this purpose a fundamental role is played by state transition and regulation of PSI/PSII ratio, rather than the modification of antenna size.

Abbreviations

Car, Carotenoid; Chl, Chlorophyll; CHL, Cold High light; CLL, Cold Low Light; Ctr, Control; HL, High light; Lhca (b), Light harvesting complexes of Photosystem I (II); LHCI, Antenna complex of Photosystem I; LL, Low Light; PSI, Photosystem I; Viola, Violaxanthin; Zea, Zeaxanthin

Introduction

Plants are able to convert light in chemical energy thanks to two multi-subunit pigment binding complexes, called photosystems I and II. Although their structural organisation is different, in both Photosystems two moieties can be distinguished: (i) a core complex, where charge separation occurs, and (ii) an antenna complex responsible of light harvesting and transfer of absorbed energy to the reaction centre.

Solar light, harvested by these supercomplexes, provides all the chemical energy necessary for plant life. However, if the adsorbed light exceeds the energy utilisation by photochemistry reactions, it

may cause production of reactive oxygen species and damages to the photosynthetic machinery. This phenomenon, called photoinhibition, is increased if, in combination with high light, other stress factors as chilling, drought or low carbon dioxide are present.

Plants have evolved various mechanisms to avoid light damages and several involve the regulation of the antenna system and its adaptation to environmental conditions. These responses can be distinguished in two classes: (i) short term responses, which are rapidly activated and do not require *de novo* protein synthesis; (ii) long term responses, which consists in the differential accumulation of antenna proteins.

In the first case, the amount of light absorbed cannot be modified. Thus, plants activate specific mechanisms for the safe dissipation of exceeding energy as heat. The fastest response so far identified is called Q_E (energy-dependent quenching of Chls singulets) and it is activated by low luminal pH and a PSII subunit, PsbS (Li et al., 2000). Q_E was shown to be particularly important in rapid light fluctuations, typical of natural environments (Kulheim et al., 2002). Another short term response is the xanthophyll cycle, which consists in the enzymatic conversion of violaxanthin to zeaxanthin, induced in high light conditions (Demmig-Adams and Adams, 1992). Zeaxanthin produced reduces the extent and the effects of light excess by influencing several processes: it increases the scavenging of reactive oxygen species in the membrane (Havaux and Niyogi, 1999) and it modulates both the PsbS activity and the antenna protein fluorescence yield (Aspinall-O'Dea et al., 2002, Moya et al., 2001).

On a longer time scale, instead, the efficiency in energy absorption is adapted to the photochemistry requirements by modulating the number of antenna proteins and, as a consequence, the number of light harvesting pigments (Anderson and Andersson, 1988).

Most studies on adaptation of antenna system to diverse light environments are focused on PSII, because this is generally considered the primary target of photoinhibition (Powles and Bjorkman, 1982, Andersson and Styring, 1991, Barber and Andersson, 1992, Prasil et al., 1992, Aro et al., 1993). However, Photosystem I was also shown to be susceptible of photoinhibition upon illumination of thylakoids membranes (Inoue et al., 1986, Tjus et al., 1998) or of plants at chilling temperatures (Havaux and Devaud, 1994, Sonoike and Terashima, 1994, Ivanov et al., 1998). Moreover, reactive oxygen species produced in PSI were shown to provoke damages in PSII as well, supporting the idea of the necessity of regulation of PSI light harvesting capacity (Tjus et al., 2001).

The aim of this work is to analyse the adaptation of Photosystem I antenna system to different light regimes, in order to clarify which modifications occur in response to environmental conditions. We

analysed both short and long light stresses and the attention was focused on two phenomena: the binding of zeaxanthin to PSI antenna and the regulation of PSI antenna size.

Materials and methods

Plants growing and stress treatments

Arabidopsis WT and mutant plants were grown at $100 \mu\text{E m}^{-2} \text{s}^{-1}$, 19°C , 90% humidity and 8 hours of daylight. For the comparison of different growth conditions, WT *Arabidopsis* plants were treated with the following conditions for 3 weeks: Control: 21°C , $100 \mu\text{E m}^{-2} \text{s}^{-1}$; Low Light: 21°C , $25 \mu\text{E m}^{-2} \text{s}^{-1}$; High Light: 21°C , $1600 \mu\text{E m}^{-2} \text{s}^{-1}$; Cold Low Light: 5°C , $25 \mu\text{E m}^{-2} \text{s}^{-1}$; Cold High Light: 5°C , $600 \mu\text{E m}^{-2} \text{s}^{-1}$.

Purification of the native and recombinant complexes

PSI-LHCI complex and its PSI core and LHCI moieties were purified from *Arabidopsis thaliana* as previously reported (Croce et al., 1996, Croce et al., 1998). Reconstitution and purification of recombinant Lhca pigment-protein complexes (from *Arabidopsis thaliana*) were performed as in (Croce et al., 2002b).

SDS PAGE Electrophoresis and Coomassie stain quantification

SDS-PAGE electrophoresis was performed as (Laemmli, 1970), but using a acrylamide/bis-acrylamide ratio of 75:1 and a total concentration of acrylamide + bis-acrylamide of 4.5 % and 15.5 % respectively for the stacking and running gel. 6 M urea was also incorporated into the running gel. The staining for the densitometry was obtained with 0.05 % Coomassie R in 25% isopropanol, 10% acetic acid in order to improve linearity with protein amount (Ball, 1986).

The protein amount was evaluated after SDS-PAGE by quantifying the stain bound to each band by colorimetry (Ballottari M. et al., 2004). We acquired the gel image using Biorad GS710 scanner and the picture was then analysed with Gel-Pro Analyzer© software, which quantifies the staining of the bands as IOD (Optical density integrated on the area of the band). At least five repetitions of each sample were analysed to achieve sufficient reproducibility.

Spectroscopy and pigment analysis. The absorption spectra at 77 K were recorded using a SLM-Aminco DK2000 spectrophotometer, in 5 mM Tricine pH 7.8, 60% (v/v) glycerol and 0.03% β -DM. HPLC analysis was as in (Gilmore and Yamamoto, 1991). Chlorophyll to carotenoid ratio and Chl a/b ratio were independently measured by fitting the spectrum of acetone extracts with the spectra of individual purified pigments (Croce et al., 2002a). Denaturation temperature measurements were performed by following the decay of the CD signal at 459 nm on a Jasco 600 spectropolarimeter when increasing the temperature from 15 to 75°C with a time slope of 1°C per

min and a resolution of 0.2°C. The thermal stability of the protein was determined by finding the $t_{1/2}$ of the signal decay.

Deriphath PAGE analysis

Non-denaturing Deriphath-PAGE was performed following the method developed by Peter and Thornber (Peter and Thornber, 1991) with the following modifications: the stacking gel had 3.5% (w/v) acrylamide (38:1 acrylamide/ bis-acrylamide). The resolving gel had an acrylamide concentration gradient from 4.5 to 11.5 % (w/v) stabilised by a glycerol gradient from 8% to 16%. 12 mM Tris and 48 mM Glycine pH 8.5 were also included in the gel. 30 µg of chlorophylls were loaded per each lane. Before loading, thylakoids at Chl concentration of 1 mg/ml were solubilised with 0.8 % β-DM. Chl content in each band was quantified from the absorption after pigments extraction with isobutanol (Martinson and Plumley, 1995).

Results

Short term response: Physiological effects of Zeaxanthin on Photosystem I

Plants exposed to high light activate the xanthophylls cycle, the conversion of violaxanthin to zeaxanthin. Zeaxanthin is accumulated free in the membranes and bound to antenna complexes of both Photosystem I and II (Verhoeven et al., 1999, Caffarri et al., 2001). The involvement of both Photosystems in xanthophyll cycle is confirmed by the ability of Lhca to exchange violaxanthin with zeaxanthin. In fact, in de-epoxidation *in vitro* experiments Lhca1 and Lhca4 showed an ability to exchange zeaxanthin comparable to the fastest PSII antenna complex, Lhcb5 (Morosinotto et al., 2002). However, while the physiological effect of zeaxanthin on PSII has been well analysed, its role in PSI, if any, is still not clear. To address this point, we compared PSI-LHCI from Arabidopsis plants mutated in the carotenoid biosynthetic pathway that accumulates constitutively zeaxanthin to different levels. The genotypes used are: Lut2, which is depleted in lutein and accumulates violaxanthin and small amounts of zeaxanthin constitutively (Pogson et al., 1996); Npq2, which is mutated in the zeaxanthin epoxidase, accumulates zeaxanthin and is depleted of violaxanthin and neoxanthin (Niyogi et al., 1998); the double mutant Lut2-Npq2, where zeaxanthin is the only xanthophyll present (Pogson et al., 1998).

PSI particles were purified from these plants and their pigment composition is reported in table 1.

As expected, PSI xanthophyll content is altered in the mutants. In particular, in Lut2 PSI binds violaxanthin and small amounts of zeaxanthin, while in Npq2 it binds lutein and zeaxanthin and it is depleted in violaxanthin. Finally, in the double mutant lut2-npq2 the only xanthophyll found is zeaxanthin. It is interesting to note that there are no significant changes in the total amount of

carotenoid molecules bound. These data show that the absence of one or more xanthophylls species is full compensated by the others. Xanthophyll binding sites in PSI are thus very flexible in binding lutein, violaxanthin or zeaxanthin, while they always exclude neoxanthin. It is also interesting to point out that β -carotene content is poorly affected in all mutants, suggesting that most carotenoid binding sites are specific for carotenes or for xanthophylls.

	Chl a	Chl b	Violaxanthin	Lutein	Zeaxanthin	β -Carotene	Total Car
WT	89.8	10.2	1.5	4.2	0.0	13.6	20.8
LUT2	89.2	10.8	4.6	0.0	0.9	15.3	20.8
NPQ2	88.9	11.1	0.0	2.7	4.0	14.9	21.6
LUT2NPQ2	88.8	11.2	0.0	0.0	7.2	14.4	21.6

Table 1 Pigments bound in Photosystem I in plants with altered xanthophyll content. Chl and carotenoid composition are indicated, normalised to 100 total Chls. Maximum standard deviation is 0.5 in the case of Chl a, Chl b, violaxanthin, lutein and zeaxanthin, 0.8 in the case of β -Carotene and total carotenoids.

Xanthophylls binding sites in Photosystem I are associated with the antenna moiety, while β -carotene is mainly bound to PSI core. In order to analyse the spectroscopic effects of altered carotenoid composition, we isolated LHCI from PSI core complex. Pigment binding data of antenna moiety are reported in table 2. As it was for the PSI-LHCI complex, the total amount of pigments bound to LHCI is not significantly affected by the xanthophylls availability, confirming that PSI antenna polypeptides can bind violaxanthin, lutein and zeaxanthin with similar efficiency.

	Chl a	Chl b	Violaxanthin	Lutein	Zeaxanthin	β -Carotene	Total Car
WT	77.4	22.6	4.4	10.3	0.0	7.2	21.8
LUT2	78.3	21.7	13.2	0.0	1.9	7.2	22.4
NPQ2	77.5	22.5	0.0	5.4	8.3	7.2	20.9
LUT2NPQ2	76.7	23.3	0.0	0.0	14.6	6.2	20.8

Table 2. LHCI pigment binding properties in plants with altered xanthophyll content. Chl and carotenoid composition are indicated, normalised to 100 total Chls. Maximum standard deviation is 0.6 in the case of violaxanthin, lutein and zeaxanthin, 1 in the case of Chl a, Chl b, β -Carotene and total carotenoids.

LHCI absorption spectra are substantially unaffected in all visible region, but in the 480-500 nm interval (figure 1). This is the region where the absorption from carotenoids is dominant and the difference is clearly due to the different absorption characteristics of violaxanthin, lutein and zeaxanthin.

It interesting to analyse carotenoids effect on a Photosystem I peculiar spectroscopic property, the “red forms”, which are chlorophylls absorbing at energies lower than the reaction centre P700. These chlorophylls are located in the antenna complex of PSI and in particular in Lhca4 and Lhca3 complexes (Schmid et al., 1997, Castelletti et al., 2003). The presence of red forms in LHCI is

evidenced in low temperature absorption spectra by a shoulder over 700 nm (figure 1). In samples with altered xanthophyll content, red forms are substantially unaffected, suggesting that the carotenoid content do not have a significant influence on red forms. This was confirmed also by measuring LHCI fluorescence spectra (not shown).

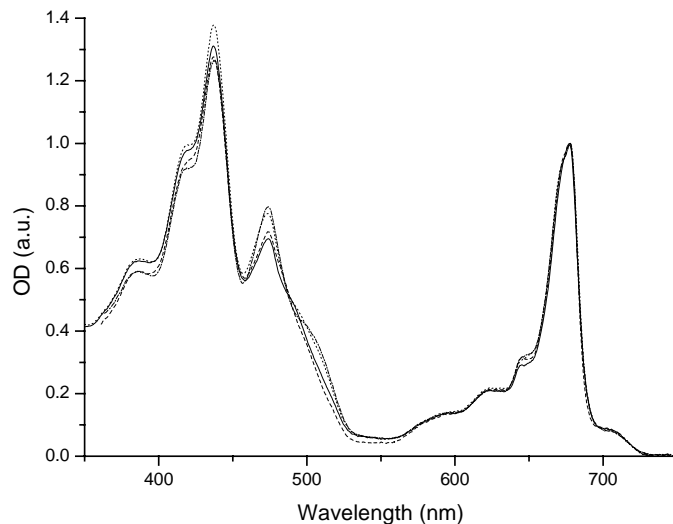


Figure 1. Low temperature absorption spectra of LHCI purified from plants with altered carotenoid composition. Spectra of LHCI from WT (solid), Lut2 (dashed), Npq2 (dotted) and Lut2-Npq2 (dash-dotted) are shown. All spectra are normalised to the maximum

PSII antenna complexes can assume different conformations, which are characterised by a different fluorescence lifetime and fluorescence yield. Interestingly, the carotenoid composition was shown to affect the conformations equilibrium, inducing an increase in the population with shorter fluorescence lifetimes and causing a decrease of the total fluorescence yield (Moya et al., 2001). To verify if this phenomenon is present in LHCI as well, we measured the fluorescence yield of samples purified from the different carotenoid mutants and results are reported in figure 2A. Lut2 sample, binding mainly violaxanthin, has a fluorescence yield indistinguishable from the WT. On the contrary, Npq2 and Lut2-Npq2, binding increasing amounts of zeaxanthin, have a correlated reduction of fluorescence yield. The carotenoid composition is thus influencing the fluorescence yield, which is reduced with the increase of zeaxanthin bound.

In order to confirm that the modulation of fluorescence yield is an effect of carotenoid composition, we evaluated the fluorescence yield in a LHCI component, Lhca4, reconstituted *in vitro* with only violaxanthin, with only zeaxanthin or with a thylakoid carotenoid extract (control). All samples bind carotenoid in similar amounts, confirming that Lhca subunits have a big flexibility in binding carotenoids. The fluorescence yield measurements showed also in this case a reduction upon zeaxanthin binding, even to a bigger extent as compared with LHCI purified from plants (figure

2B). Interestingly, in this case the sample containing violaxanthin only has higher fluorescence yield than the control (containing around 75% lutein and 25% violaxanthin), suggesting that lutein as well induces a decrease in fluorescence yield with respect to violaxanthin, although its effect is smaller than zeaxanthin.

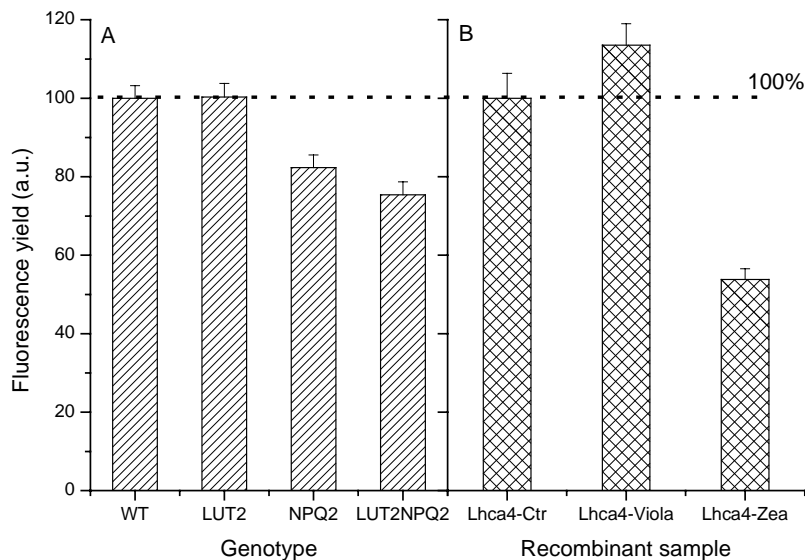


Figure 2. Dependence of LHCI fluorescence yield from carotenoid content. A) Fluorescence yield of LHCI isolated from plants mutated in the xanthophyll biosynthetic pathway. B) Fluorescence yield of Lhca4 reconstituted with different xanthophylls. Values are normalised to 100% respectively to WT and control (CTR) samples.

PSI antenna size modulation by zeaxanthin

Zeaxanthin is known to have several effects on PSII antenna complex. Among them, zeaxanthin was shown to induce a reduction of its antenna size, by decreasing the stability of PSII antenna proteins (Havaux et al., 2004). To verify if the PSI is similarly affected, we evaluated the stoichiometry of each Lhca1-4 polypeptide in PSI particles purified from these mutants following a method described in (Ballottari M. et al., 2004). PSI-LHCI complexes were loaded on a SDS PAGE, which separates all Lhca polypeptides (Figure 3A). To evaluate quantitatively the content of each protein, we quantified the Coomassie stain bound to polypeptides after electrophoresis. The same determination was performed also for two different PSI core polypeptides, PsaD and PsaF, allowing the calculation of the Lhca / core ratio in each sample. Results obtained for the mutants were then compared with WT, where the stoichiometry is known to be of one copy of each Lhca1-4 per PSI core (Ben Shem et al., 2003, Ballottari M. et al., 2004). At the end, thus, we obtained the Lhca stoichiometry in all samples. Final outcome of this analysis is reported in figure 3B: no significant differences between the different genotypes was detected, neither in the content of individual Lhca polypeptide, nor in the total amount of antenna proteins, which are 4 as in the WT

sample. It is worth mention that data have a standard deviation of approx 20% and therefore, we cannot exclude that small changes, under this limit, may occur.

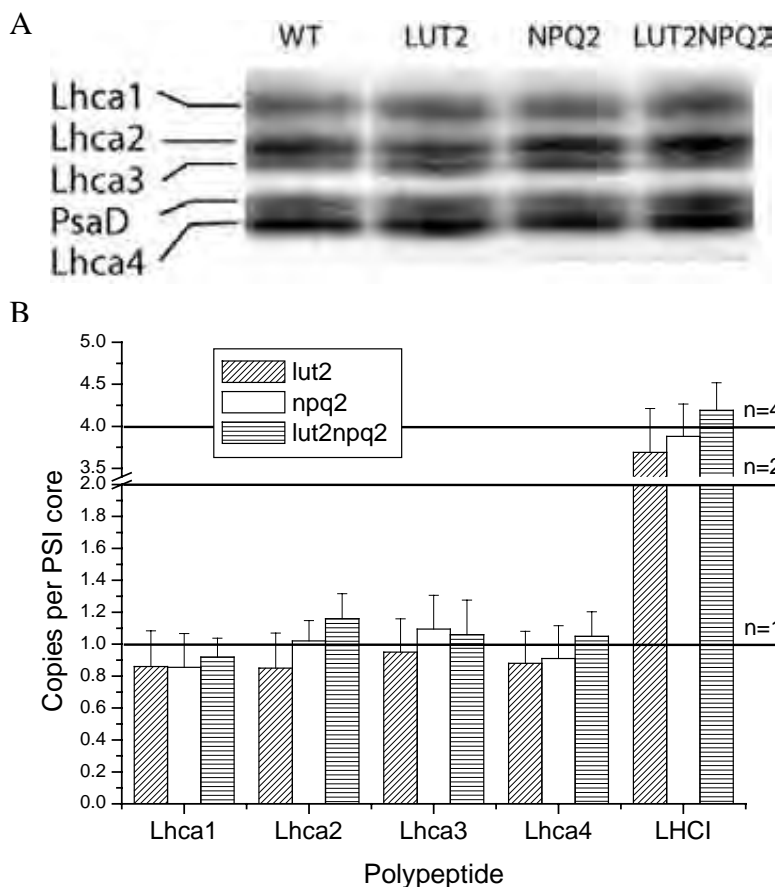


Figure 3. Stoichiometry determination of Lhca polypeptides in PSI with altered carotenoid composition. A) SDS PAGE of PSI particles purified from plants with altered carotenoid content. The region where Lhca polypeptides are migrating is shown. B) Stoichiometry of Lhca polypeptides in different mutants. Also the total Lhca content in each mutant is reported (LHCI).

Nevertheless, results above presented clearly suggest that PSI antenna size is not significantly affected by the zeaxanthin binding to LHCI, differently from what observed for PSII (Havaux et al. 2004). The destabilisation in PSII antenna was explained by a decrease in thermal stability of PSII antenna complexes upon binding of zeaxanthin (Havaux et al., 2004). To verify if this effect is present or not in Lhca polypeptides as well, we measured the thermal stability of LHCI purified from carotenoid mutants and in Lhca4 reconstituted *in vitro* with different xanthophylls (table III). As shown in the table, LHCI and Lhca4 stability is not reduced by zeaxanthin binding but, on the contrary, it is slightly increased. This result, thus, supports the hypothesis that zeaxanthin binding does not affect PSI antenna size.

Purified LHCI	Stability (°C)	SD	% WT	SD
WT	51.7	1.4	100.0	3.8
Lut2	53.6	2.0	103.7	4.8
Npq2	55.5	0.7	107.4	3.2
Lut2Npq2	56.5	2.1	109.4	5.0
Reconstituted samples	Stability (°C)	SD	% Ctr	SD
Lhca4-Ctr	54.1	1.4	100.0	3.7
Lhca4-Viola	53.9	1.9	99.6	4.4
Lhca4-Zea	58.0	1.6	107.2	4.1

Table 3. Thermal stability in LHCI and Lhca4 reconstituted *in vitro* with altered carotenoid composition. Values are reported for LHCI purified from mutant plants and Lhca4 reconstituted *in vitro* with thylakoid extracts (control, Lhca4-Ctr) or only violaxanthin (Lhca4-Viola) or zeaxanthin (Lhca4-Zea). Standard Deviation (SD) is also reported.

Long term adaptation: PSI antenna size modulation

Plants on a long time scale adapt to the average light conditions they are experiencing. In particular, they are able to modulate the number of Lhc polypeptides following the energy requirements of photochemistry. The antenna size of PSII was shown by several authors to be regulated in plants grown in different light regimes, in order to adapt the energy absorbed and transferred to reaction centres to environmental conditions (Anderson and Andersson, 1988). Also in the case of PSI, the antenna content was suggested to be modified in response to different light regimes (Bailey et al., 2001).

As shown above, the carotenoid composition did not affect the PSI antenna size as it did in the case of PSII. However, it is well known that the regulation of antenna size depends on other mechanisms in addition to carotenoid effect, like the regulation of gene transcription and translation. In order to evaluate quantitatively the responses in PSI antenna size, Arabidopsis WT plants were grown for three weeks in different light and temperatures. In particular, the conditions used were 5: control, high, low light and cold plus high or low light, indicated respectively as Ctr, HL, LL, CHL, CLL. Plants exposed to low light conditions did not show any relevant phenotype neither at low temperatures. On the contrary, plants grown in high light showed a reduced growth, the production of anthocyanins and leaves necrosis, especially if plants were treated also with low temperatures.

Thylakoids membranes have been extracted from all plants and used for Photosystem I purification. PSI absorption and fluorescence spectra did not show significant differences as compared with control (not shown).

In order to quantify how PSI antenna complex respond to acclimation to different light regimes, PSI polypeptide composition was analysed on SDS PAGE as described above. We evaluated quantitatively the amount of Lhca1-4 polypeptides from the amounts of Coomassie stain bound to each band after SDS PAGE. The number of each Lhca1-4 per PSI core is reported in figure 4A. Very surprisingly, growth conditions did not show any influence in the amount of each polypeptide and neither in the total number of antenna proteins. Again, we should be aware that the determination is not able to quantify reliably differences below 0.2 polypeptides per core, but this precision is sufficient to conclude that growing plants in different environmental conditions did not have any relevant effect on Lhca1-4 stoichiometry.

To confirm that the PSI particles isolated we analysed were representative of the PSI in thylakoids, we verified that any Lhca polypeptide was lost during the purification. This was done by collecting the bands of isolated antenna complexes from sucrose gradient ultracentrifugation of solubilised thylakoids, which were analysed by western blotting. Antibodies against Lhca1-4 did not detect any significant amount of Lhca polypeptides lost during the purification and thus the PSI particles isolated are fully representative of the thylakoids population.

To verify if the lack of modifications observed was due to a mild light-temperature treatment, we also evaluated PSII antenna size in the same plants. This determination was performed by quantifying the different pigment binding complexes after separation on a non denaturing gel. The amounts of every complex was evaluated by quantifying the Chls in each band upon extraction with isobutanol (Martinson and Plumley, 1995). The ratio between the antenna and PSII core bands is shown in figure 4B. Results clearly show that the PSII antenna size is largely affected in plants here analysed. As expected, antenna size is reduced in high light conditions and increased in low light conditions. This result thus demonstrates that the antenna size stability was not due to a mild treatment of plants, but it is specific behaviour of Photosystem I.

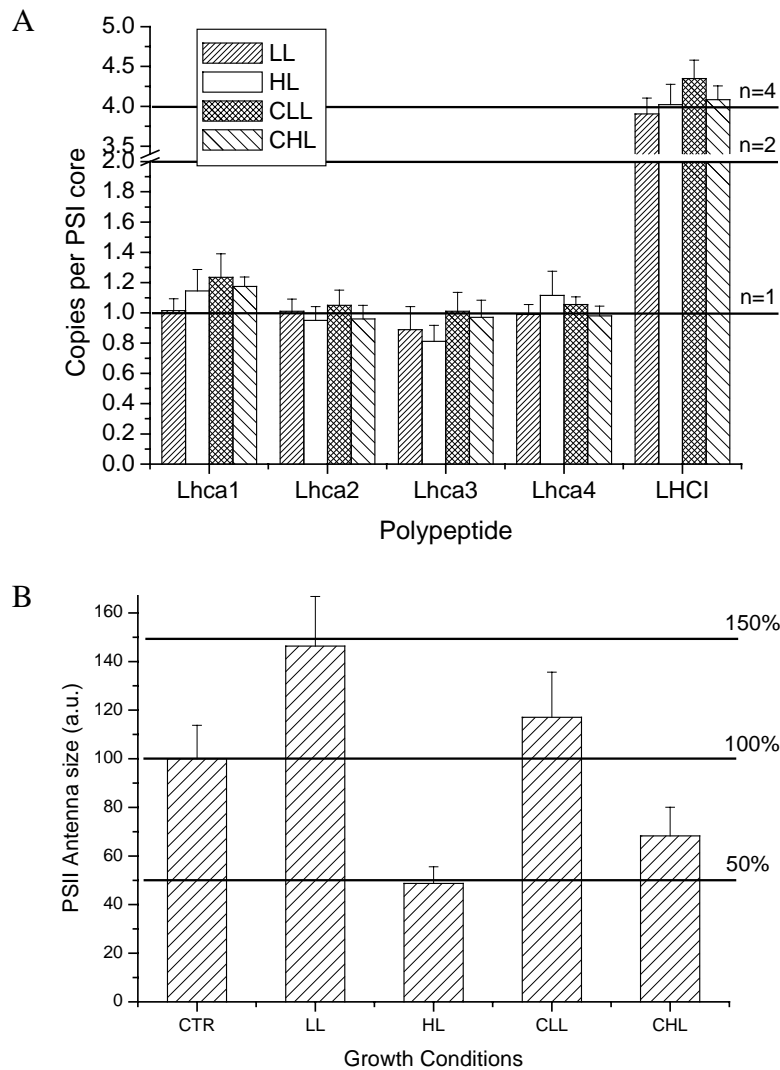


Figure 4. Regulation of PSI and PSII antenna size in response to growth conditions. A) Stoichiometry determination of Lhca polypeptides in PSI from plants grown in different light intensities and temperatures. B) PSII antenna size evaluation in the same plants. Antenna size was normalised to 100% in the case of the control (CTR) sample.

Discussion

In this work, we analysed the adaptation of PSI antenna complex to diverse light conditions. In particular, the attention was focused on two kinds of responses: the zeaxanthin accumulation and the regulation of PSI antenna size.

Physiological role of zeaxanthin in PSI

Zeaxanthin is a xanthophyll accumulated in stressing conditions and it is known to enhance plants stress resistance. This xanthophyll accumulates both in PSI and in PSII, in particular bound to Lhc complexes that constitute their antenna systems (Verhoeven et al., 1999).

The effects of zeaxanthin on PSII are the subject of many studies, while it is still not clear if its binding to PSI is relevant or it is only an evolutionary residue without a physiological relevance. In

this work, we addressed this point by comparing Photosystem I isolated from plants accumulating zeaxanthin to different levels. The modified xanthophyll content did not affect the total amount of chlorophyll and carotenoid molecules bound to PSI. This result indicates that PSI xanthophyll binding sites are very flexible and can all accommodate violaxanthin, lutein or zeaxanthin. Although very flexible, they are not unspecific, since they exclude completely the binding of neoxanthin. Moreover, the amount of β -carotene is substantially conserved in all mutants, suggesting that carotenoid binding sites are specific for carotenes or for xanthophylls. Differently from what observed for PSII, neither the supramolecular organisation of PSI is affected by the carotenoid composition. In fact, the number of antenna polypeptides bound to PSI was unaffected by the accumulation of zeaxanthin. This results is consistent with the observation that zeaxanthin did not reduce the thermal stability in the case of Lhca, differently from what observed for Lhcb polypeptides.

The only significant influence of zeaxanthin binding observed in PSI antenna complex is the reduction of its fluorescence yield. This was observed both in LHCI and in isolated Lhca4 reconstituted *in vitro*, demonstrating that this was a specific consequence of zeaxanthin binding. The same behaviour was evidenced also for PSII antennas (Moya et al., 2001). Thus, when bound to any Lhc complex, zeaxanthin enhance its capacity to dissipate energy non radiatively. The consequence of this difference is that zeaxanthin binding antennas are less efficient in transferring energy to reaction centre, thus reducing the risk of over-excitation.

In addition, it is interesting to note that zeaxanthin effect in Lhca4 is more evident than in whole LHCI complex, which shows the average properties of Lhca1-4 polypeptides. This difference could be tentatively correlated with the fact that Lhca4 is the complex having the red-most chlorophylls in Lhca (Schmid et al., 1997). In fact, it has been shown that red chlorophylls excited states are very efficiently quenched by a nearby carotenoid in Lhca4 (Carbonera et al., Gibasiewicz et al, see appendix I). Zeaxanthin effect, thus, could possibly be enhanced if it is bound in proximity of red chlorophylls.

Antenna size regulation in PSI

Plants acclimate to different light intensities by regulating the amount of PSII antenna polypeptides, thus modifying the number of pigments per reaction centre (Anderson and Andersson, 1988). Here, we evaluated the stoichiometry of Lhca polypeptides in PSI particles isolated from plants grown in different conditions and we obtained surprising results. In fact, the antenna content of PSI was substantially unaffected by environmental conditions and in all samples analysed, one copy of each

Lhca1-4 polypeptide per PSI core was always found. The lack of variations, however, was not due to the mildness of light-temperature treatments: in fact, the same plants showed an effective regulation of PSII antenna size, accordingly with previous reports. This results is in contrast with a previous work where the amount of Lhca polypeptides was shown to be modified by growth conditions (Bailey et al., 2001). The discrepancy is likely due to the different methods used for the quantification: here we evaluate the protein amount from Coomassie staining, verified to be linear in the polypeptide concentration of the experiment (Ballottari M. et al., 2004). Bailey and co-workers, instead, used western blotting analysis, which is more sensitive but less linear, especially when different dilutions of the sample are not quantified. Moreover, here were investigated isolated PSI particles, instead of thylakoids, therefore our results are not affected by the modification of PSII antenna size and PSII/PSI ratio with environmental conditions.

Our results, although unexpected, can be rationalised with the phenotype of Arabidopsis plants depleted in individual Lhca polypeptides (Morosinotto et al., A.2).

In fact, these mutants showed that the absence of single Lhca polypeptides affects the stability of the whole LHCI antenna system. This was explained by the presence of relevant interactions between Lhca polypeptides, due to the presence of pigments at the interfaces between antenna and core polypeptides. This organisation is clearly not suitable for a modification of the number of antenna polypeptides: in fact, if one protein subunit is removed, the whole LHCI moiety of PSI-LHCI complex is destabilised. Moreover, the presence of gap pigments bound at interfaces between protein subunits is also a problem: if one subunit is removed, unprotected free chlorophylls very prone to formation of oxygen reactive species would be exposed and de-stabilized. This figure is also confirmed by the fact that gap pigments were shown to be typical of PSI and not present in PSII (Ballottari M. et al., 2004).

An alternative mechanism for the regulation of PSI antenna size could also be the accumulation of variable amounts of Lhca5, a subunit recently detected in PSI even if in substoichiometric amounts (Ganeteg et al., 2004). This protein could possibly accumulate in different environmental conditions, thus regulating the antenna size of PSI. In favour of this hypothesis there is the fact that Lhca5 is found loosely associated to PSI, suggesting that its binding could be different than the rigid one of Lhca1-4 and more compatible with regulation. On the other side, there is the fact that Lhca5 at the polypeptide level was found in very low amounts, which could be physiologically insignificant. Information available on Lhca5 is still too incomplete to distinguish between the two hypotheses.

Does PSI need regulation of antenna size?

Studies on PSI photoinhibition suggested that Photosystem I is more exposed to light damages when PSII is active and provide a continuous electron flux to reduce P700 (Tjus et al., 1998). On the contrary, when PSII is inactivated, PSI appears to be more stable. In fact, PSI is not affected in thylakoids treated with DCMU, which blocks electron transport from PSII (Sato, 1970). This is due to the fact that, when reduction of PSI by plastocyanine is inhibited, the reaction centre is found in its oxidised form P700⁺, which is very efficient in dissipating excess excitation energy as heat (Nuijs et al., 1986). Moreover, it was shown that the product of PSI activity, NADPH, when accumulated in its reduced form, is able to induce a conformational change and increase PSI energy dissipation as heat (Rajagopal et al., 2003).

These results, taken together, could explain why the modification of the antenna size is not fundamental for PSI acclimation to diverse light environments. On the contrary, the most important factor should be the maintenance of the balance between PSI and PSII. Consistent with this picture, there are mechanisms known to play a role in balancing excitation energy between the Photosystems. With a shorter time scale and without need of *de novo* protein synthesis the state transition are activated, which consists in the movement of LHCII from PSII to PSI (see (Wollman, 2001). On a longer time scale, instead, the PSI/PSII ratio is modified in response to plant needs (Bailey et al., 2001).

PSI vs. PSII: rigidity vs. flexibility

Results presented here allow for a general comparison between PSI and PSII antenna systems with respect to their ability to adapt to different environmental conditions. PSI has a very rigid superstructure: the unit composed by PSI core plus Lhca1-4 is unaffected by the environmental conditions. Results on Lhca depleted plants, moreover, showed that each Lhca has its position in the complex and they cannot be replaced by some other polypeptide (Morosinotto et al., A.2). This is probably due to the presence of strong interactions between Lhca polypeptides and between Lhca polypeptides and core (Ben Shem et al., 2003, Ballottari M. et al., 2004). PSII, instead, shows extensive antenna modifications in different light conditions (Anderson and Andersson, 1988), it has the possibility of forming supercomplexes with different structures (Boekema et al., 1999) and it has the ability to exchange to some extent one subunit with another (Ruban et al., 2003).

In conclusion, the regulation of antenna system in the two photosystems is different. In PSII, the structure is modular and the subunits number can be modulated in response to environmental conditions. In contrast, PSI has a rigid structure and the regulation involves the modification of the number of PSI complexes rather than their modification.

References

- Anderson J M, Andersson B. The dynamic photosynthetic membrane and regulation of solar energy conversion. *Trends Biochem Sci* 1988; (13): 351-355.
- Andersson B, Styring S. Photosystem II: Molecular Organization, Function, and Acclimation. In: *Current Topics Bioenergetics*. 16. (Ed.Lee CP). New York: Academic Press, 1991; 1-81.
- Aro E-M, Virgin I, Andersson B. Photoinhibition of Photosystem-2 - Inactivation, Protein Damage and Turnover. *Biochim Biophys Acta* 1993; (1143): 113-134.
- Aspinall-O'Dea M, Wentworth M, Pascal A, Robert B, Ruban A V, Horton P. In vitro reconstitution of the activated zeaxanthin state associated with energy dissipation in plants. *Proc Natl Acad Sci U S A* 2002; (99): 16331-16335.
- Bailey S, Walters R G, Jansson S, Horton P. Acclimation of *Arabidopsis thaliana* to the light environment: the existence of separate low light and high light responses. *Planta* 2001; (213): 794-801.
- Ball EH. Quantitation of proteins by elution of Coomassie Brilliant Blue R from Stained bands after dodecyl sulfate polyacrilamide gel electrophoresis. *Anal.Biochem.* 155, 23-27. 1986.
- Ballottari M., Govoni C, Caffarri S, Morosinotto T. Stoichiometry of LHCI antenna polypeptides and characterisation of gap and linker pigments in higher plants Photosystem I. *Eur J Biochem* 2004;in press.
- Barber J, Andersson B. Too Much of a Good Thing - Light Can Be Bad for Photosynthesis. *Trends Biochem Sci* 1992; (17): 61-66.
- Ben Shem A, Frolov F, Nelson N. Crystal structure of plant photosystem I. *Nature* 2003; (426): 630-635.
- Boekema E J, van Roon H, Calkoen F, Bassi R, Dekker J P. Multiple types of association of photosystem II and its light- harvesting antenna in partially solubilized photosystem II membranes. *Biochemistry* 1999; (38): 2233-2239.
- Caffarri S, Croce R, Breton J, Bassi R. The major antenna complex of photosystem II has a xanthophyll binding site not involved in light harvesting. *J Biol Chem* 2001; (276): 35924-35933.
- Castelletti S, Morosinotto T, Robert B, Caffarri S, Bassi R, Croce R. Recombinant Lhca2 and Lhca3 subunits of the photosystem I antenna system. *Biochemistry* 2003; (42): 4226-4234.
- Croce R, Canino G, Ros F, Bassi R. Chromophore organization in the higher-plant photosystem II antenna protein CP26. *Biochemistry* 2002a; (41): 7334-7343.
- Croce R, Morosinotto T, Castelletti S, Breton J, Bassi R. The Lhca antenna complexes of higher plants photosystem I. *Biochimica et Biophysica Acta-Bioenergetics* 2002b; (1556): 29-40.

- Croce R, Zucchelli G, Garlaschi F M, Bassi R, Jennings R C. Excited state equilibration in the photosystem I -light - harvesting I complex: P700 is almost isoenergetic with its antenna. *Biochemistry* 1996; (35): 8572-8579.
- Croce R, Zucchelli G, Garlaschi F M, Jennings R C. A thermal broadening study of the antenna chlorophylls in PSI- 200, LHCI, and PSI core. *Biochemistry* 1998; (37): 17255-17360.
- Demmig-Adams B, Adams W W. Photoprotection and other responses of plants to high light stress. *Ann Rev Plant Physiol Plant Mol Biol* 1992; (43): 599-626.
- Ganeteg U, Klimmek F, Jansson S. Lhca5 - an LHC-Type Protein Associated with Photosystem I. *Plant Mol Biol* 2004; (54): 641-651.
- Gilmore A M, Yamamoto H Y. Zeaxanthin Formation and Energy-Dependent Fluorescence Quenching in Pea Chloroplasts Under Artificially Mediated Linear and Cyclic Electron Transport. *Plant Physiol* 1991; (96): 635-643.
- Havaux M, Dall'Osto L, Cuine S, Giuliano G, Bassi R. The effect of zeaxanthin as the only xanthophyll on the structure and function of the photosynthetic apparatus in *Arabidopsis thaliana*. *J Biol Chem* 2004; (279): 13878-13888.
- Havaux M, Devaud A. Photoinhibition of Photosynthesis in Chilled Potato Leaves Is Not Correlated with A Loss of Photosystem-II Activity - Preferential Inactivation of Photosystem-I. *Photosynthesis Research* 1994; (40): 75-92.
- Havaux M, Niyogi K K. The violaxanthin cycle protects plants from photooxidative damage by more than one mechanism. *Proc Natl Acad Sci USA* 1999; (96): 8762-8767.
- Inoue K, Sakurai M, Hiyama T. Photoinactivation sites of photosystem I in isolated chloroplasts. *Plant Cell Physiol* 1986; (27): 961-968.
- Ivanov A G, Morgan R M, Gray G R, Velitchkova M Y, Huner N P A. Temperature/light dependent development of selective resistance to photoinhibition of photosystem I. *FEBS Lett* 1998; (430): 288-292.
- Kulheim C, Agren J, Jansson S. Rapid regulation of light harvesting and plant fitness in the field. *Science* 2002; (297): 91-93.
- Laemmli U K. Cleavage of structural proteins during the assembly of the head of bacteriophage T4. *Nature* 1970; (227): 680-685.
- Li X P, Bjorkman O, Shih C, Grossman A R, Rosenquist M, Jansson S, Niyogi K K. A pigment-binding protein essential for regulation of photosynthetic light harvesting. *Nature* 2000; (403): 391-395.
- Martinson T A, Plumley F G. One-step extraction and concentration of pigments and acyl lipids by sec-butanol from in vitro and in vivo samples. *Anal Biochem* 1995; (228): 123-130.
- Morosinotto T, Baronio R, Bassi R. Dynamics of Chromophore Binding to Lhc Proteins in Vivo and in Vitro during Operation of the Xanthophyll Cycle. *J Biol Chem* 2002; (277): 36913-36920.

- Moya I, Silvestri M, Vallon O, Cinque G, Bassi R. Time-Resolved Fluorescence Analysis of the Photosystem II Antenna Proteins in Detergent Micelles and Liposomes. *Biochemistry* 2001; (40): 12552-12561.
- Niyogi K K, Grossman A R, Björkman O. Arabidopsis mutants define a central role for the xanthophyll cycle in the regulation of photosynthetic energy conversion. *Plant Cell* 1998; (10): 1121-1134.
- Nuijs A M, Shuvalov V A, van Gorkom H J, Plijter J J, Duysens L N M. Picosecond absorbance difference spectroscopy on the primary reactions and the antenna-excited states in photosystem I particles. *Biochim Biophys Acta* 1986; (850): 310-318.
- Peter G F, Thornber J P. Biochemical composition and organization of higher plant photosystem II light-harvesting pigment-proteins. *J Biol Chem* 1991; (266): 16745-16754.
- Pogson B, McDonald K A, Truong M, Britton G, DellaPenna D. Arabidopsis carotenoid mutants demonstrate that lutein is not essential for photosynthesis in higher plants. *Plant Cell* 1996; (8): 1627-1639.
- Pogson B J, Niyogi K K, Björkman O, DellaPenna D. Altered xanthophyll compositions adversely affect chlorophyll accumulation and nonphotochemical quenching in Arabidopsis mutants. *Proc Natl Acad Sci USA* 1998; (95): 13324-13329.
- Powles S B, Bjorkman O. Photoinhibition of photosynthesis: Effect on chlorophyll fluorescence at 77k in intact leaves and in chloroplast membranes of nerium oleander. *Planta* 1982; (156): 97-107.
- Prasil O, Adir N, Ohad I. Dynamics of photosystem II: Mechanism of photoinhibition and recovery processes. In: *The Photosystems: Structure, Function and Molecular Biology*. (Ed.Barber J). Amsterdam: Elsevier, 1992; 295-348.
- Rajagopal S, Bukhov N G, Tajmir-Riahi H A, Carpentier R. Control of energy dissipation and photochemical activity in photosystem I by NADP-dependent reversible conformational changes. *Biochemistry* 2003; (42): 11839-11845.
- Ruban A V, Wentworth M, Yakushevskaya A E, Andersson J, Lee P J, Keegstra W, Dekker J P, Boekema E J, Jansson S, Horton P. Plants lacking the main light-harvesting complex retain photosystem II macro-organization. *Nature* 2003; (421): 648-652.
- Sato K. Mechanism of Photoinactivation in Photosynthetic Systems .2. Occurrence and Properties of 2 Different Types of Photoinactivation. *Plant Cell Physiol* 1970; (11): 29-&.
- Schmid V H R, Cammarata K V, Bruns B U, Schmidt G W. In vitro reconstitution of the photosystem I light-harvesting complex LHCI-730: Heterodimerization is required for antenna pigment organization. *Proceedings of the National Academy of Sciences of the United States of America* 1997; (94): 7667-7672.
- Sonoike K, Terashima I. Mechanism of Photosystem-I Photoinhibition in Leaves of Cucumis-Sativus L. *Planta* 1994; (194): 287-293.
- Tjus S E, Moller B L, Scheller H V. Photosystem I is an early target of photoinhibition in barley illuminated at chilling temperatures. *Plant Physiol* 1998; (116): 755-764.

Tjus S E, Scheller H V, Andersson B, Moller B L. Active oxygen produced during selective excitation of photosystem I is damaging not only to photosystem I, but also to photosystem II. *Plant Physiol* 2001; (125): 2007-2015.

Verhoeven A S, Adams W W, Demmig-Adams B, Croce R, Bassi R. Xanthophyll cycle pigment localization and dynamics during exposure to low temperatures and light stress in *Vinca major*. *Plant Physiology* 1999; (120): 727-737.

Wollman F A. State transitions reveal the dynamics and flexibility of the photosynthetic apparatus. *EMBO J* 2001; (20): 3623-3630.

Section B:

*The antenna complexes of Photosystem I: the
molecular basis of low energy absorption
forms*

B 1

The Lhca antenna complexes of higher plants Photosystem I

This chapter has been published in *Biochimica et Biophysica Acta* 1556 (2002) 29–40, reproduced with permission.

Roberta Croce, Tomas Morosinotto, Simona Castelletti,
Jacques Breton and Roberto Bassi

The Lhca antenna complexes of higher plants photosystem I[☆]

Roberta Croce^{a,1}, Tomas Morosinotto^a, Simona Castelletti^{a,b}, Jacques Breton^c, Roberto Bassi^{a,*}

^a*Dipartimento Scientifico e Tecnologico, Università di Verona, Strada Le Grazie, 15-37234 Verona, Italy*

^b*Departement de Biologie Cellulaire et Moleculaire, CEA-Saclay, France*

^c*Service de Bioénergétique, Bât. 532 CEA-Saclay, 91191, Gif-sur-Yvette, France*

Received 15 April 2002; received in revised form 19 June 2002; accepted 26 July 2002

Abstract

The Lhca antenna complexes of photosystem I (PSI) have been characterized by comparison of native and recombinant preparations. Eight Lhca polypeptides have been found to be all organized as dimers in the PSI–LHCI complex. The red emission fluorescence is associated not only with Lhca1–4 heterodimer, but also with dimers containing Lhca2 and/or Lhca3 complexes. Reconstitution of Lhca1 and Lhca4 monomers as well as of the Lhca1–4 dimer *in vitro* was obtained. The biochemical and spectroscopic features of these three complexes are reported. The monomers Lhca1 and Lhca4 bind 10 Chls each, while the Chl *a/b* ratio is lower in Lhca4 as compared to Lhca1. Three carotenoid binding sites have been found in Lhca1, while only two are present in Lhca4. Both complexes contain lutein and violaxanthin while β -carotene is selectively bound to the Lhca1–4 dimer in substoichiometric amounts upon dimerization. Spectral analysis revealed the presence of low energy absorption forms in Lhca1 previously thought to be exclusively associated with Lhca4. It is shown that the process of dimerization changes the spectroscopic properties of some chromophores and increases the amplitude of the red absorption tail of the complexes. The origin of these spectroscopic features is discussed.

© 2002 Elsevier Science B.V. All rights reserved.

Keywords: Photosynthesis; Chlorophyll-protein; Recombinant Lhc protein

1. Introduction

Photosystem I (PSI), a multi-subunit complex located in the stroma lamellae of thylakoid membranes, is a plastocyanine/ferredoxin oxido-reductase. The complex from higher plants can be divided in two moieties: (i) the core complex, composed of 14 subunits, which contains the primary donor P700 and all the cofactors of the electron transport chain as well as about 100 Chl *a* and 20 β -carotene molecules with antenna function [1–3]; and (ii) the external antenna composed of four polypeptides, belonging to the Lhc family and named Lhca1–4, with molecular weight between 21 and 24 kDa [3,4]. These polypeptides bind to one side of the core complex [5] by interactions with PsaF, PsaG, and PsaK subunits [6,7]. LHCI proteins coordinate

Chl *a*, Chl *b*, lutein, violaxanthin, and small amount of β -carotene [8,9]. On the basis of the high sequence homology of these polypeptides with the major LHCI antenna complex, it has been proposed that Lhca proteins share a high degree of structural similarity with the LHCI proteins [10]. Currently, little information is available on individual Lhca, mainly due to difficulties in purification. Most of the data on Lhca complexes have been obtained by studying a fraction containing all of the complexes [11,12] or two sub fractions, namely LHCI-730 and LHCI-680, which were suggested to consist of dimeric Lhca1–4 and monomeric Lhca2-(3) complexes, respectively [13,14]. More recently, Lhca1 and Lhca4 were reconstituted *in vitro* in both monomeric and heterodimeric forms [15], allowing time-resolved studies on homogeneous preparations [16,17].

The absorption spectrum of the PSI–LHCI supramolecular complex is characterized by the presence of chlorophyll forms that absorb at lower energy than the reaction center. It has been shown that at RT more than 80% of the energy is present in these forms and has to be transferred energetically uphill to be used for photosynthesis [18]. The “red forms” have been extensively analyzed both in bacteria and higher

[☆] A part of the experiments included in this paper has been previously published in the Proceedings of the XI International Conference on Photosynthesis (ed. G. Garab).

* Corresponding author. Tel.: +39-45-8027916; fax: +39-45-8027929

E-mail address: bassi@sci.univr.it (R. Bassi).

¹ Present address: Istituto di Biofisica, CNR Milano, Via Celoria 26, 20133, Milano, Italy.

plants. However, information about their function and localization are still controversial (for a review see Ref. [19] and references therein). In higher plants it has been proposed that most of the red forms are associated with the external antenna, particularly Lhca4 [15,20,21]. It has also been suggested that Lhca2 and Lhca3 are responsible for the 680-nm emission and therefore do not bind “red Chls”. More recently, the analysis of a fraction containing all of the Lhca proteins indicated that some of the red forms can also be associated with these Lhca2 and/or Lhca3 [11]. Analysis of anti-sense plants depleted on these proteins supports this suggestion [22].

In this work, we analyzed LHCI complexes either purified from higher plants or reconstituted *in vitro*, in order to study the biochemical and spectroscopic properties of Lhca proteins.

2. Material and methods

2.1. Purification and analysis of the native complexes

Native complexes were purified from *Zea mays* and *Arabidopsis thaliana* as already reported [23]. The sample buffer was 10 mM tricine pH 7.8, 0.3 M sucrose, and 0.03% β -DM, and samples were frozen until use. Size-exclusion chromatography was performed using a Bio Select, SEC-125-5 (300 \times 7.8 mm) Bio-Rad column. The elution buffer was 50 mM NaHPO₃, 150 mM NaCl, and 0.025% DM, and the flow rate was 0.8 ml/min.

Cross-linking experiments were performed using different concentrations of glutaraldehyde (0.5%, 1%, 2%). The sample concentration was 10 μ g/ml of Chl. The solutions were left in ice for 20 min and then blocked with 1/40 vol of NaBH₄ (in 2 M NaOH).

2.2. Electrophoresis and nondenaturing iso-electro-focalization

SDS-PAGE tris–sulfate was performed as reported in Ref. [24]. Nondenaturing electrophoresis was performed as in Ref. [25], but using 0.05% of SDS in the superior buffer, in the dark at 4 °C.

Nondenaturing IEF was performed as reported in Ref. [26]. Green fractions were identified in the 3.9–4.55 pH range.

2.3. DNA constructions

Plasmids were constructed using standard molecular cloning procedures [27]. Bacterial hosts were *Escherichia coli* DH5 α strain [28] and SG13009 strain [29]. cDNA of Lhca1 and Lhca4 from *A. thaliana* were supplied by Arabidopsis Biological Resource Center (ABRC) at the Ohio State University. The sequences codifying for the mature proteins were subcloned in pQE 50 by Qiagen.

2.4. Isolation of overexpressed Lhca apoproteins from bacteria

Lhca apoproteins were isolated from the SG13009 strain transformed with Lhca1 and Lhca4 constructs following a protocol previously described [30,31].

2.5. Reconstitution and purification of Lhca–pigment complexes

These procedures were performed as described in Ref. [32] with the following modifications: in the reconstitution mix we always add 420 μ g of apoprotein, 240 μ g of chlorophyll and 60 μ g of carotenoid. The Chl *a/b* ratio in the pigment mixture was 4 for all reconstitutions and the carotenoid composition in the mixture was reflecting the composition in the thylakoid membrane (lutein, neoxanthin, violaxanthin, and b-carotene, respectively 4:3:2:1). The pigments used were purified from spinach thylakoids.

2.6. Pigment analysis and pigment/protein stoichiometry

The pigment complement of the holoprotein was analyzed by HPLC [33] and fitting of the acetone extract with the spectra of the individual pigments [34]. The protein was quantified by ninhydrin method [35] and by SDS-PAGE analysis [36].

2.7. Spectroscopy

The absorption spectra at RT were recorded by SLM-Aminco DK2000 spectrophotometer, in 10 mM Hepes pH 7.5, 20% glycerol, and 0.06% β -DM; 0.4-nm step was used. The fluorescence emission spectra were measured on Jasco FP-777 fluorimeter at RT and 77 K and corrected for the instrumental response. The samples were excited at 440, 475, and 500 nm. The band widths were 5 nm in excitation and 3 nm in emission. For the excitation spectra the emission were recorded at 685 and 720 nm. All fluorescence spectra were measured at 0.02 OD at the maximum of Q_y transition.

LD spectra were obtained as described in Refs. [37,38] using samples oriented by the polyacrylamide gel squeezing technique.

The CD spectra were measured at 10 °C on a Jasco 600 spectropolarimeter. The samples were in the same solution described for the absorption. All the spectra presented were normalized to the same polypeptide concentration, based on the Chl binding stoichiometry [39].

Denaturation temperature measurements were performed by following the decay of the CD signal at 459 nm when increasing the temperature from 20 to 80 °C with a time slope of 1 °C per min and a resolution of 0.2 °C. The thermal stability of the protein was determined by finding the $t_{1/2}$ of the signal decay.

2.8. Analysis of the Q_y region of the spectra

Spectral forms of Chlorophyll *a* and *b* in pigment–protein complexes between 630 and 720 nm was determined by Cinque et al. [40]. These forms were utilized for a fitting of the absorption spectrum of Lhca1 in this interval [34].

3. Results

Both PSI and PSII have an antenna moiety constituted by Lhc polypeptides binding Chl *a*, Chl *b*, and xanthophylls. While the components of the PSII antenna have been characterized in detail leading to an overall knowledge of several aspects of the PSII–LHCII organization including supramolecular organization of subunits [41,42], stoichiometry of protein, pigment components [43] and distribution of different pigment species into individual binding sites within Lhc gene products [44,45], the knowledge of PSI antenna system components is still insufficient due to the difficulty in the purification of individual Lhca gene products. In this study we have integrated the study of native complexes isolated from thylakoids with that of recombinant Lhca1 and -4 pigment proteins and obtained an improved picture of PSI–LHCI organization.

3.1. Native LHCI

LHCI complexes were purified from *A. thaliana* and *Z. mays* as reported previously [23]. Fig. 1A shows the SDS-

PAGE analysis of the LHCI fraction as compared to that of the PSI–LHCI original preparation, while Fig. 1B shows the densitometric analysis. The polypeptide patterns of the LHCI and PSI core were complementary in yielding the PSI–LHCI pattern in both composition and relative amounts, thus ensuring that no polypeptides have been lost during purification. This was further confirmed by immunoblot analysis with anti-Lhca1–4 antibodies (not shown).

The pigment content of the LHCI fractions was analyzed by HPLC and fitting of the spectrum of the acetone extract was performed with the spectra of the individual pigments in this solvent. The data are reported in Table 1. The Chl *a/b* ratio of the preparations was 3.8 for *Z. mays* and 3.3 for *A. thaliana*, while the Chl/Car ratio was 4.6 in both cases. Only three carotenoid species were found in the complexes, namely lutein, violaxanthin, and β -carotene. Neoxanthin was not present, in agreement with previous results [9].

The pigment-to-protein stoichiometry was calculated for LHCI from *Z. mays* by independent determination of Chl and protein concentrations. A value of 10 Chls per polypeptide was obtained. Due to the presence of four polypeptides in the preparation, this value represents the average number of Chls bound to Lhca polypeptides. The pigment–protein ratio of LHCI in *A. thaliana* was the same as in *Z. mays*, suggesting that although the relative amount of Chl *a* and *b* can differ between the two species, the overall number of chromophores per polypeptide is conserved.

The aggregation state of Lhca complexes was tested in the *Z. mays* preparation by four different methods: size exclusion chromatography, nondenaturing gel electrophore-

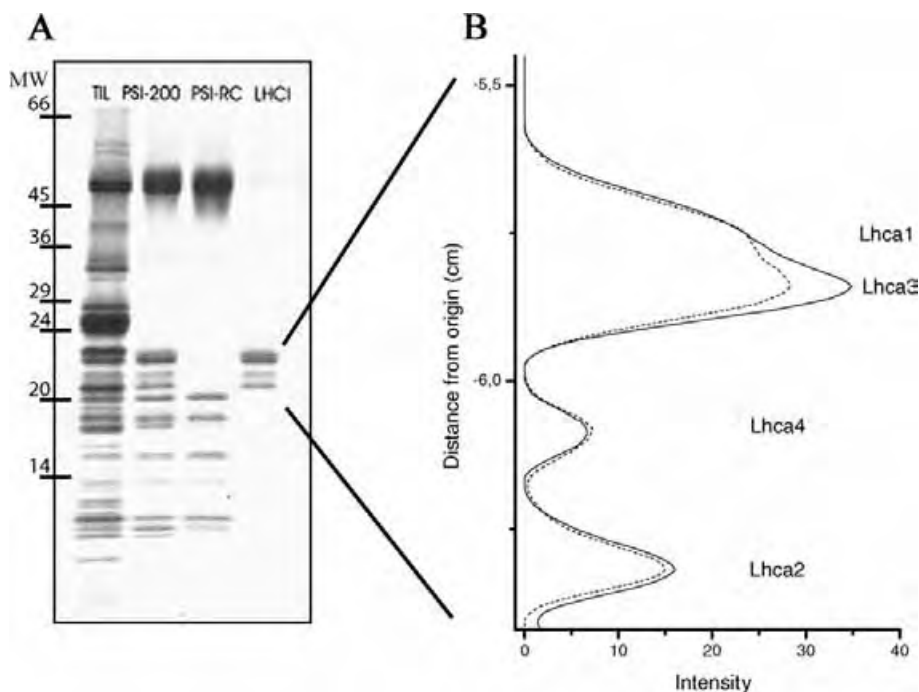


Fig. 1. LHCI purification. (A) SDS-PAGE of the LHCI purification steps: line 1: thylakoids; line 2: PSI-200; line 3: PSI-core; line 4: LHCI. (B) Densitometric analysis of the LHCI region (about 20–24 kDa) of lines 2 (solid) and 4 (dotted). The distance from the origin is measured from the protein gel.

Table 1
Pigment composition of reconstituted complexes

Sample	Chl <i>a/b</i>	Chl/car	Neo	Viola	Lute	β -Carotene	Denaturation temperature ($^{\circ}$ C)
nLHCI Zm	3.8 ± 0.2	4.6 ± 0.1	–	0.55	1.2	0.4	nd
nLHCI Ar	3.3 ± 0.1	4.6 ± 0.1	–	0.6	1.1	0.45	57
rLhca1	4.0 ± 0.1	3.3 ± 0.1	0.12	1.05	1.81	–	54
rLhca4	2.3 ± 0.2	4.9 ± 0.2	–	0.5	1.5	–	45
rLhca1–4	3.0 ± 0.2	4.0 ± 0.1	0.08	0.8	1.2	0.4	56

All complexes have been reconstituted with Chl *a/b* ratio of 4.0 in the pigment mix and in the presence of the full car complement.

sis, sucrose gradient ultracentrifugation, and cross-linking (Fig. 2A–D). In the first three experiments, LHCII monomers and trimers were used as a standard. In size exclusion chromatography, the retention time of LHCI was intermediate between monomeric and trimeric LHCII (Fig. 2A). The same results were obtained in sucrose gradient ultracentrifugation, where LHCI proteins were found in band 2 (Fig. 2B), with a sedimentation factor value in between the two aggregation states of LHCII. The presence of a band at approximately 44 kDa (Fig. 2D) in the cross-linking experiments confirms that the aggregation state is dimeric. This

was also corroborated further by nondenaturing gel electrophoresis (Fig. 2C). In addition, the latter experiment clearly indicates that no monomers were present in the preparation. The same results were obtained for the *Arabidopsis* preparation, where all Lhca complexes were found in a single sucrose gradient band that exhibited the characteristics of the dimer. We can therefore conclude that Lhca proteins are organized as dimers in vivo.

In order to purify different dimers, the LHCI fraction was subjected to nondenaturing IEF followed by sucrose gradient ultracentrifugation. Although it was not possible to

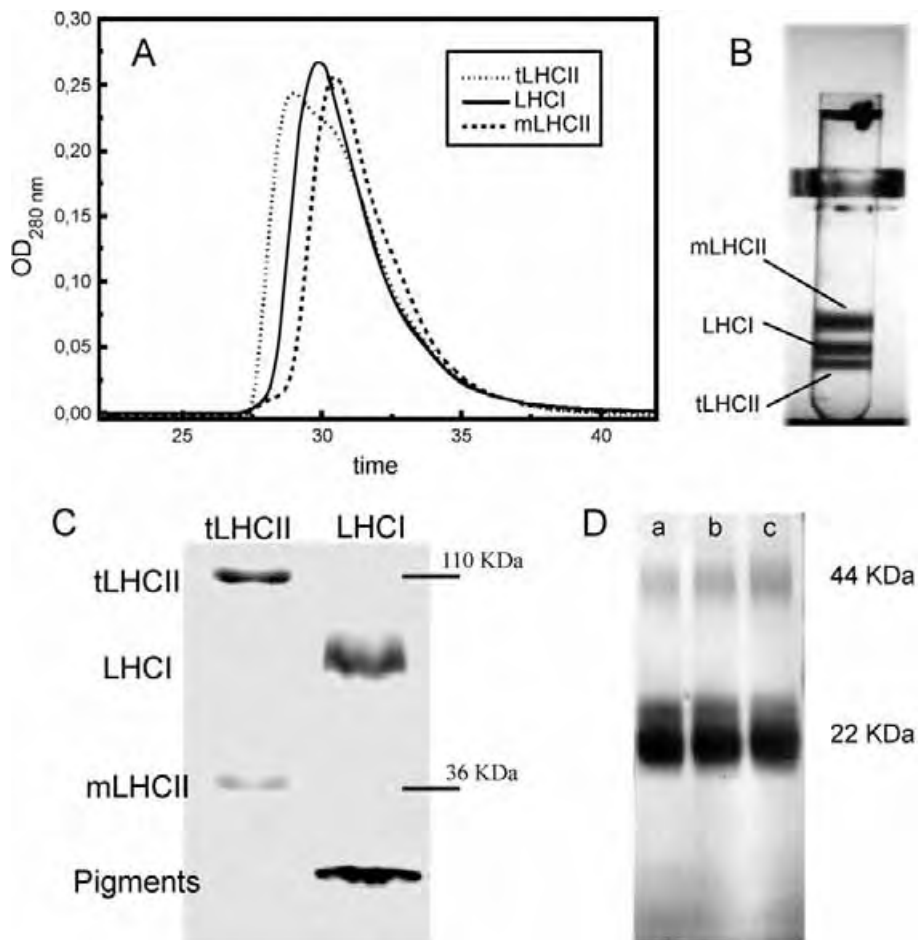


Fig. 2. Determination of the aggregation state of Lhca complexes. (A) Size exclusion chromatography. The retention time of LHCI fraction (solid) is compared with the retention times of LHCII trimers (dotted) and monomers (dashed). (B) Sucrose gradient. The mobility of Lhca complexes is compared with LHCII trimers and monomers. (C) Nondenaturing gel electrophoresis. Line 1: LHCII trimer and monomer; line 2: LHCI fraction. (D) Cross-linking experiments in which LHCI fraction was treated with different amounts of glutaraldehyde: line a, 0.5%; line b, 1%; line c, 2%.

purify the dimers to homogeneity, fractions enriched in individual polypeptides were obtained, as detected by SDS-PAGE (Fig. 3A). In Fig. 3B, the absorption spectra of two fractions, called LHCI-A and LHCI-B, containing 80% of Lhca1/4 and 70% of Lhca2/3, respectively, are shown. The absorption maxima of the two fractions were 680.0 and 681.5 nm, respectively. The red absorption tail is present in both spectra and displays very similar intensity. The fluorescence spectra at RT of the two fractions are reported in Fig. 3C, together with the fluorescence spectrum of the starting material (LHCI). The spectrum maxima are at 685.0 nm and have a broad shoulder at higher wavelengths, typical of PSI antenna complexes [3]. Although LHCI-A

(containing Lhca1–4) showed enhanced red emission as compared to the starting material, the LHCI-B spectrum also has a substantial contribution from the red-shifted emission band.

3.2. PSI core to LHCI stoichiometry

We have used SDS-PAGE and densitometry to study the distribution of pigments between PSI core and LHCI. To this end, the Chl concentration of both the PSI–LHCI and LHCI preparation was carefully determined and aliquots were loaded on a SDS-PAGE in four replicates (not shown). After running, gel was stained with Coomassie blue and destained [46]. Densitometry was then performed with the aim of determining the amount of Chl associated with LHCI proteins that had to be loaded in to the gel in order to obtain a level of Coomassie staining of the LHCI associated bands equal to that of the corresponding bands in PSI–LHCI complex. This ratio was 0.43, thus showing that approximately 43% of PSI–LHCI total Chl was associated with LHCI polypeptides. Similar results were obtained using *A. thaliana* and *Z. mays* preparations.

3.3. Reconstituted complexes

The present data clearly indicate that it is not possible to purify the individual Lhca complexes to homogeneity while maintaining the in vivo characteristics. To overcome this problem, Lhca1, Lhca4, and their heterodimeric complex were obtained by in vitro reconstitution using the apoproteins expressed in *E. coli* and reconstituted with pigments and lipids [15]. The reconstituted complexes were purified by sucrose gradient ultracentrifugation and ion exchange chromatography. The reconstitution yield of Lhca4 was lower than for Lhca1, implying a lower stability for this complex. The thermal stability of these pigment–proteins was investigated by the decay of the CD signal at 459 nm with increasing temperature. The denaturation temperature of Lhca1 was 54 °C, while the value dropped to 45 °C for Lhca4, which is the lowest stability of all Lhc complexes so far analyzed [47]. The Lhca1–4 heterodimer is more stable, with a denaturation temperature of 56 °C, similar to the value obtained for the native preparation (57 °C), thus indicating that protein–protein interactions play a role in complex stabilization.

The pigment composition of the three samples was analyzed as reported above. The data are shown in Table 1. Whereas the Chl *a/b* ratio in the pigment mix used for reconstitution was the same, the Chl *a/b* of refolded Lhca1 was larger than in Lhca4, indicating that Lhca4 has a higher affinity for Chl *b*. The heterodimer has a Chl *a/b* ratio intermediate between the two monomers. The Chl/*car* ratio of the complexes was also very different (3.5 in Lhca1, 5 for Lhca4, and 4.0 for the dimer) as well as the carotenoid composition: β -carotene is not bound to the monomers, while it is bound to the heterodimer.

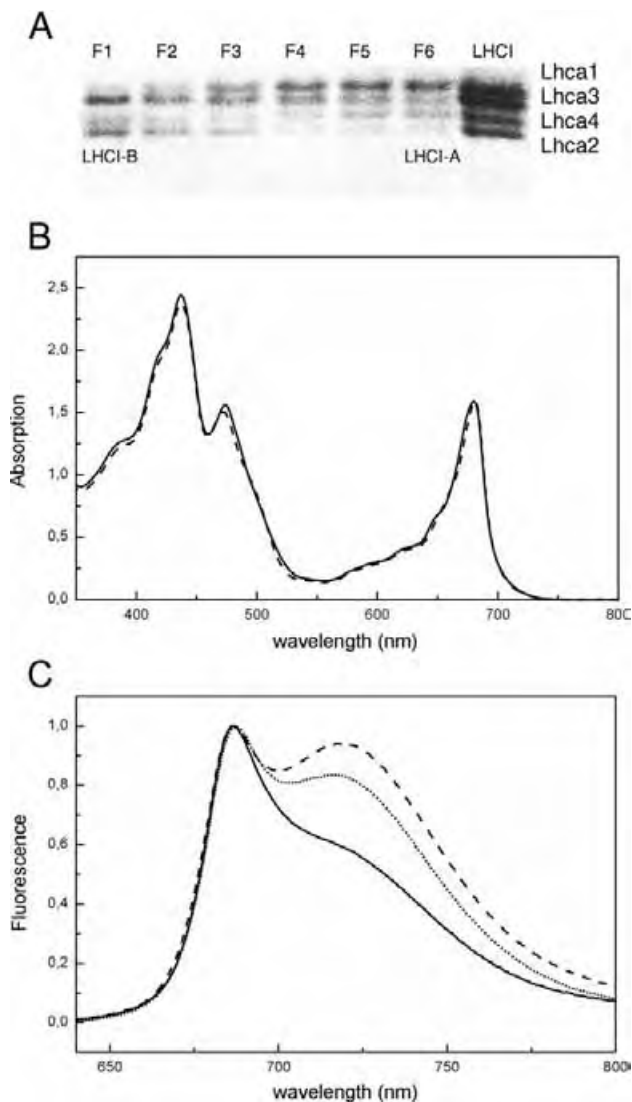


Fig. 3. Analysis of IEF fractions enriched in individual polypeptides. (A) SDS-PAGE of the fractions obtained by IEF on LHCI preparation. The acidity is decreasing from fraction 1 to 6. (B) Absorption spectra at RT of LHCI-A (dashed) and LHCI-B (solid). (C) Fluorescence emission spectra at RT upon excitation at 475 nm of LHCI-A (dashed), LHCI-B (solid) and LHCI fraction before IEF (dotted). All the spectra are normalized to the maximum.

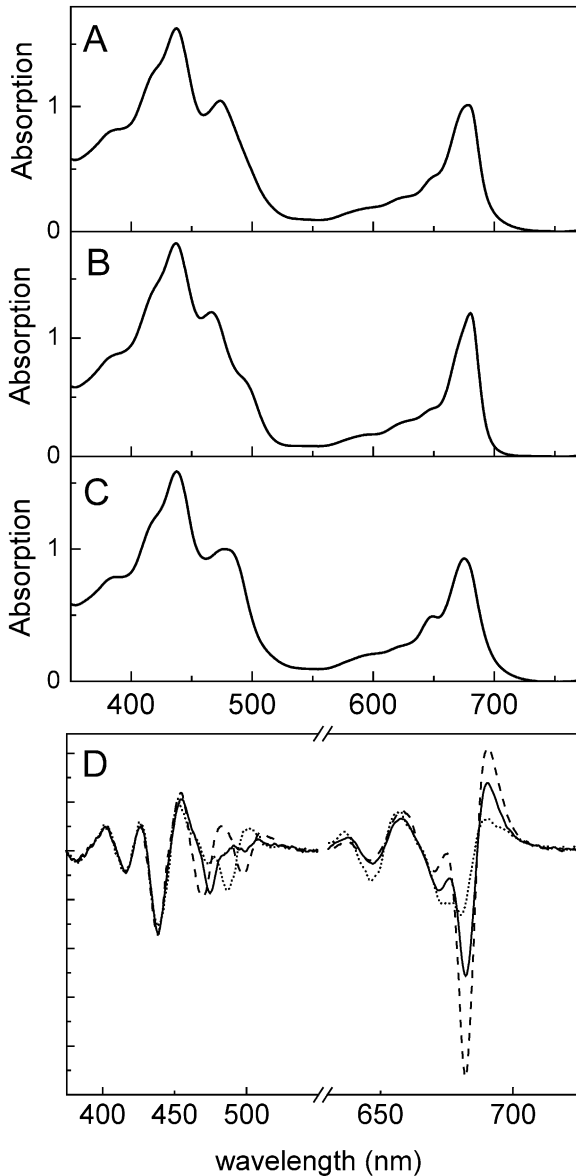


Fig. 4. Absorption spectra at RT of Lhca1-4 dimer (A), Lhca1 (B) and Lhca4 (C). In panel D the second derivatives of the three spectra are reported: Lhca1-4 (solid), Lhca1 (dashed) and Lhca4 (dotted).

The absorption spectra at RT of the complexes are reported in Fig. 4A–C. The absorption maxima of Lhca1, Lhca4, and Lhca1-4 are at 680.5, 675.5 and 679.0 nm, respectively. Absorption tails were also observed at wavelengths longer than 700 nm, particularly in the latter two samples, in agreement with previous measurements [17]. The second derivative analysis of the three spectra is reported in Fig. 4D. In the Q_y region, three main components were observed in all spectra at 646, 672, and 682 nm, although differing in relative amplitude. Major differences were observed in the 480–500-nm interval where the signal can tentatively be associated with the lowest vibrational level of the carotenoid S_2 state. Peaks were detected at 498

and 486 nm for Lhca1 and Lhca4, respectively, while both these components were present in the dimer.

3.4. Linear dichroism (LD) spectra

LD spectra of the three reconstituted samples are shown in Fig. 5. The spectra differ, particularly in the ratio between the amplitude of the Q_y and the Soret signals. In the case of Lhca4, the intensity is almost identical in the two regions, while for both the Lhca1 protein and the Lhca1-4 heterodimer the signal in the red has higher amplitude than that in the blue, similar to the case all PSII antenna complexes [34]. Unfortunately, it is not possible to normalize the LD spectra and thus specifically attribute these features to either a change in carotenoid or Chls orientation. The LD spectra of Lhca1 and Lhca4 peak at 680.0 and 681.5 nm, respectively. In the red absorption tail, a positive contribution is observed in both Lhca4 and Lhca1-4 dimer, indicating that the dipole moment of the Q_y transition forms an angle larger than 54.7° with respect to the normal to the membrane plane. This in agreement with previous measurements on the native preparation [11]. In Lhca1, the red most peak in the Soret region is at 499 nm, while the main signal peaks at 490 nm in Lhca4. In addition, Lhca4 also shows a signal above 500 nm, in agreement with the absorption spectra.

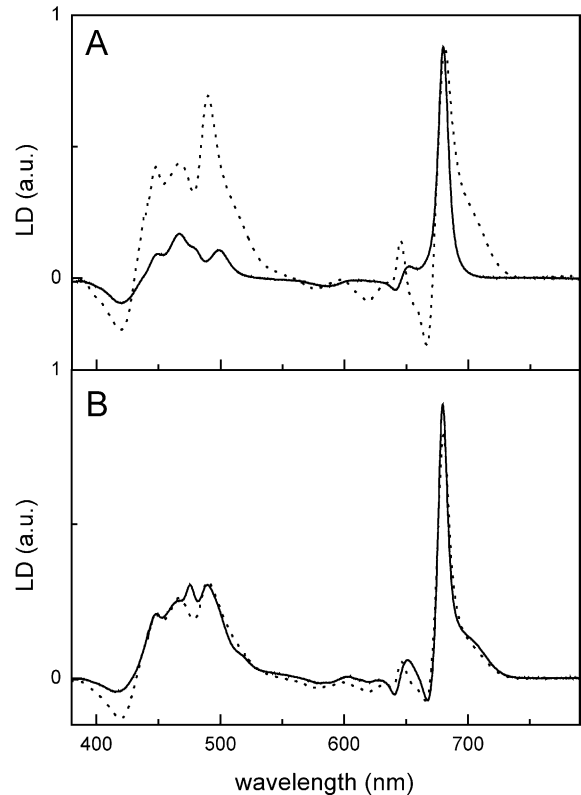


Fig. 5. LD spectra at 100 K. (A) Lhca1 (solid) and Lhca4 (dotted) normalized to the maximum. (B) Lhca1-4 (solid) and sum of Lhca1 and Lhca4 (dotted) normalized as explained in the text (see Results).

In order to analyze the spectral changes that possibly accompany dimerization, we attempted a comparison between the LD spectra of the two monomers with the spectrum of the dimer. To this end, it was necessary to establish the relative contributions of Lhca1 and Lhca4, which was tentatively accomplished by varying their relative ratio and comparing the sum to the spectrum of the heterodimer. The best match was obtained by a 5:7 ratio between the two spectra, as shown in Fig. 5B. The two spectra display similar characteristics in most of the analyzed spectral range. However, there were differences in the 650–660-nm range and in the Soret region where a new signal appears, peaking at 475 nm. These differences can be attributed to Chl *b* molecules on the basis of the peak wavelength, suggesting that Chl *b* chromophores undergo reorganization or coupling to other chromophores upon establishment of monomer–monomer interactions.

3.5. CD spectra

The CD spectra of the three reconstituted samples are presented in Fig. 6. In the Q_y region Lhca1 and Lhca4 are rather different, the former showing three components at 684 (–) nm, 669 (–) nm and 647 (–) nm. Lhca4 shows negative components at 689 (–) nm and 647 (–) nm, where the 647 nm is more intense than in Lhca1. The major difference in this spectral region was the presence of a strong positive signal peaking at 674 nm with a shoulder at approximately 663 nm while the 669 nm (–) was absent. The spectrum of the heterodimer was more similar to Lhca4 than to Lhca1. In the Soret region, the differences are even more pronounced: Lhca4 exhibits strong signal with components at 492 nm (–), 470 nm (–) and 442 nm (+). Lhca1 shows a small, red-shifted signal with respect to the one in the same region of Lhca4 at approximately 504 (–) nm and a more intense negative component at 459 nm.

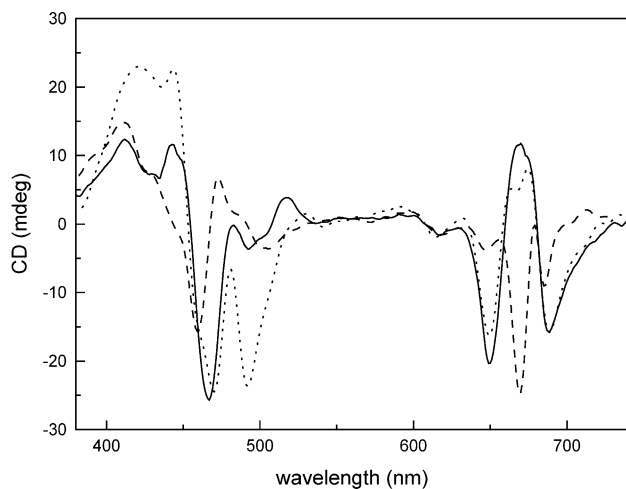


Fig. 6. Circular dichroism spectra at 10 °C of Lhca1–4 (solid), Lhca1 (dashed) and Lhca4 (dotted). The spectra are normalized to the same protein concentration.

The spectrum of the dimer is characterized by an intense signal at 467 nm (–), similar to Lhca4, while the intensity of the 492 nm (–) component is much smaller. From these spectra, it is apparent that dimerization induces conformational changes that are reflected by the chromophore interactions. In particular, the negative contribution at 669 nm of Lhca1 disappears in the dimer, where a positive signal is observed at the same wavelength. This suggests that the Chls, which are responsible for this signal in Lhca1, change their orientation or coupling to other pigments.

In the Soret region, the most interesting feature is associated with the negative 492 nm signal of Lhca4, which disappears almost completely upon dimerization. A similar effect is observed for the positive component at approximately 430 nm. These signals can be tentatively attributed to Chl *a*–carotenoid interaction, which is lost in the dimer, suggesting an environmental change of one carotenoid binding site of Lhca4 upon dimerization.

3.6. Fluorescence spectra

The fluorescence spectra at RT of recombinant Lhca1, Lhca4, and their heterodimeric complex are reported in Fig. 7A. In all cases, the maximum peaks are at 684–686 nm. However, Lhca4 and the Lhca1–4 dimer exhibit a strong shoulder at approximately 720 nm. This red-shifted signal is further displaced to lower energies (732 nm) upon decreasing the temperature 77 K (data not shown) in agreement with previous reports [15]. The excitation energy transfer among chlorophylls was equilibrated as determined by the identical spectral shape obtained upon excitation at different wavelengths, namely 440, 475, and 500 nm (not shown). A minor deviation from this pattern was observed in the Lhca4 complex, consisting in the presence of a new emission at 677 nm upon excitation at 440 nm, and was attributed to a small amount of free Chl *a*. This effect is to be ascribed to the lower stability of this holoprotein rather than to differences in the rate of equilibration between chromophores, as can be judged from its increase in amplitude with the time of incubation.

3.7. Energy transfer efficiency from Car and Chl *b* to Chl *a*

The excitation spectra (Fig. 7B) show a major peak at 440 nm and minor contributions from Chl *b* and carotenoids superimposing in a broad shoulder with decreasing amplitude extending to 510 nm. Identical spectra were obtained for both the 685- and 720-nm emission in agreement with the Boltzmann's equilibration of the complexes (see above). Excitation of Lhca1, Lhca4, and Lhca1–4 heterodimer at different wavelengths produced emission spectra with the same shape, implying thermal equilibration among chlorophyll ligands. This result is in contrast to previous reports showing higher contribution by Chl *b* and carotenoids, with respect to Chl *a*, to the red-most emission in both Lhca4 and Lhca1–4 [15]. In the earlier study, this result may have

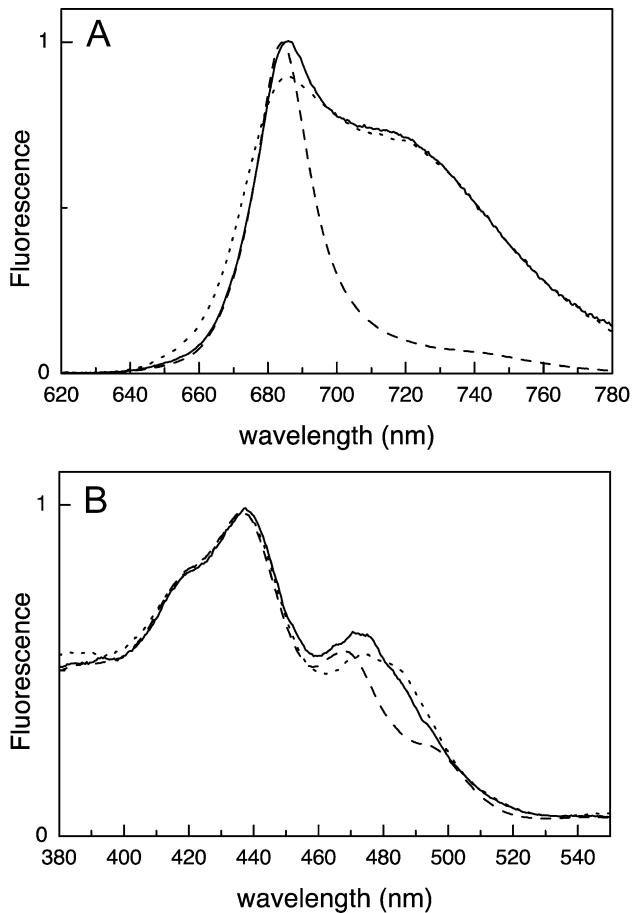


Fig. 7. Fluorescence emission spectra (A) and excitation (B) for Lhca1–4 (solid), Lhca1 (dashed) and Lhca4 (dotted). The spectra are registered at RT and normalized to the maximum. The excitation wavelength was 500 nm for all complexes, while in the excitation spectra the emission was 685 nm for Lhca1 and 720 for Lhca4 and Lhca1–4 complexes.

been due to the presence of uncoupled Chl *a* molecules, which, upon direct excitation at 440 nm, would have led to an artefactual increased amplitude of the Chl *a* emission band.

The spectra were further analysed in order to verify the ability of Chl *b* and carotenoids bound to Lhca proteins in transferring excitation energy to Chl *a*. To this end, the Soret region of the absorption spectra was analysed in terms of the contributions of individual pigments. This was performed by using the deconvolution procedure and the spectral absorption forms of Chl *a*, Chl *b*, and xanthophylls in Lhc protein environment as previously reported [48]. The same description was then used for fitting the fluorescence excitation spectra, and the relative intensity of the individual spectral contributions, after normalisation to 100% transfer efficiency for the Chl *a* contribution, was used to calculate the transfer efficiency from individual pigments [49]. The results show a carotenoid-to-Chl transfer efficiency very close to 65% in the three samples. This figure is lower than in Lhcb proteins for which a value close to 75% were previously reported by using the same procedure [47].

4. Discussion

4.1. Pigment-to-protein stoichiometry

Analysis of pigment-to-protein stoichiometry on the native LHCI fraction (which contains all four Lhca complexes) yields 10 ± 0.5 bound Chls and around 2.3 carotenoids per polypeptide in both *Z. mays* and *A. thaliana* [9].

Lhcb proteins bind either three (LHCII, [45]) or two (CP29, CP26, CP24, [44]) xanthophylls per polypeptide while strong homology suggests a similar figure for Lhca proteins. The Chl-to-Car ratio of Lhca1 and Lhca4 was 3.35 and 4.90, respectively. These values are consistent with Lhca1 and Lhca4 binding 10 Chls each plus three and two xanthophylls per polypeptide, respectively. Different figures would yield non-integer values for the number of xanthophyll binding sites in contrast with previous determinations in recombinant Lhc proteins. This is consistent with the report of 10 Chl per polypeptide in CP24, the only Lhcb protein clustering with Lhca in sequence analysis [50]. A value as low as 5 was previously suggested for the number of Chls bound to Lhca1 and Lhca4 [15]. However, the value of 5 Chls per polypeptide would be inconsistent with the conservation of 8 Chl binding residues [50], which have been experimentally shown to bind Chls in both LHCII and CP29 [44,45]. Our stoichiometric determinations of 10 Chls per polypeptide in nLHCI would imply 15 Chls per polypeptide for both Lhca2 and Lhca3, which seems improbable. Based on the above considerations and on stoichiometry of 2.3 cars per 10 Chl in the native complex containing the four Lhca polypeptides, we conclude that only one of the four Lhca proteins, i.e. Lhca1, binds three xanthophylls. Lhca4, -2, and -3 bind two xanthophyll molecules per polypeptide each while all of them bind 10 Chls. Small deviations from these values cannot be excluded for Lhca3 and Lhca2 but seem unlikely due to the strong homology with CP24 [51].

4.2. PSI core to Lhca stoichiometry

Densitometric analysis of SDS-PAGE gels loaded with PSI–LHCI and LHCI preparations showed that 43% of total Chl was associated with LHCI. Since the number of Chls associated with PSI core in barley was determined to be 111 ± 4 [2] the total number of Chls in the PSI–LHCI complex can be calculated as 195 ± 6 and the LHCI moiety should bind 84 ± 3 Chls. Since we have determined a value of 10 Chls per LHCI polypeptide, it follows that there are approximately 8 Lhca polypeptides per PSI core complex.

4.3. Lhca4

The recombinant Lhca4 complex is the least stable of all the Lhc proteins, its melting temperature being at 45 °C, well below that of Lhca1 (54 °C) and of the other Lhc proteins (64–77 °C). It should be noted, however, that the Lhca1/Lhca4 has essentially the same melting temperature

as that of Lhca1 (56 vs. 54 °C), thus suggesting that upon dimerization Lhca4 assumes a more stable conformation. The Lhca4 complex binds 7 Chl *a*, 3 Chl *b*, and 2 carotenoid molecules: 0.5 violaxanthin and 1.5 luteins. This xanthophyll complement is similar to what was observed for the two central sites, L1 and L2, of LHCII complex. By analogy with other Lhc proteins binding two xanthophylls per polypeptide, i.e. CP29, CP26, and CP24, we suggest that the xanthophyll binding sites conserved in Lhca4 correspond to L1 and L2 sites of LHCII. The absorption spectrum of Lhca4 is characterized by a red absorption tail at wavelengths longer than 700 nm. This band is featureless even at low temperature (not shown), indicating a very large FWHM. The fluorescence emission at RT shows a maximum at 686 nm and a shoulder at 720 nm, which originates from the red absorption in agreement with previous results [23,11]. At low temperature the maximum is red-shifted to 732 nm as shown in previous reports [15] (data not shown). The LD spectrum is quite peculiar when compared to the LD spectra of all other antenna complexes, not only for the presence of a positive contribution associated with the red forms, but also because the amplitude of the spectrum in the Q_y range is similar to that in the Soret region. A more quantitative evaluation is possible upon normalization of Lhca4 and Lhca1 spectra (Fig. 5A) based on fitting the dimer LD spectrum to obtain a spectral sum similar to the dimer (Fig. 5B). Whereas we need to be cautious about this normalization procedure, the good match between the two spectra in Fig. 5B suggests the 5:7 ratio between the amplitude of Lhca4 and Lhca1, respectively, is reasonable. The comparison shows marked differences in the intensity of the LD signal in the carotenoid absorption region (430–520 nm). This suggests that at least one xanthophyll in Lhca4 is differently oriented and its transition moment, lying close to the polyene chain [52], forms a larger angle with the normal to the membrane plane. The main signal in Q_y region is associated with a Chl *a* form absorbing at 681.5 nm, while the signal is very low around 675 nm, at the maximum of the absorption. This suggests that the positive LD spectrum of this complex is mostly associated with a Chl *a* absorbing at 681 nm. A similar behavior was observed in LHCII, where the LD positive signal was attributed to the Chl *a* in site A2 also absorbing at 681 nm [34].

4.4. Lhca1

The Lhca1 complex binds Chl *a* and Chl *b* with a ratio of 4.0 and the total Chl (*a* + *b*) to Car is 3.35 corresponding to a Chl complement of 8 Chl *a*, 2 Chl *b*. Moreover, 2 luteins and 1 violaxanthin per polypeptide are probably located in sites L1, L2, and N1 in agreement with previous results with Lhc proteins [10,53,54]. Lhca1 shows higher reconstitution yield and stability as compared to Lhca4.

The Q_y absorption peak of Lhca1 is localized at 680.5 nm at RT while the fluorescence emission is located at 684 nm and a contribution at 701 nm is also visible at LT,

indication of the presence of low energy forms [15]. While it is well established that Lhca4 contains red-shifted Chl *a* absorption forms [15], it was previously reported that Lhca1 has none. This does not seem to be completely true: in fact, contributions at wavelengths as long as 690 nm and low amplitude contributions at 700 nm are also apparent. Further support to the presence of low energy absorption forms is provided by the comparison with the fluorescence emission spectra of recombinant Lhca1 reconstituted with Chl *a* only (Fig. 8). A detailed analysis of this pigment–protein complex is outside the scope of this manuscript and will be presented in a forthcoming paper; however, it is clear that the red side broadening of the Lhca1 spectrum depends on the presence of Chl *b*. Similar results have been shown for Lhca4 [55] in which the intense red-shifted (732 nm) emission peak was completely abolished by the lack of Chl *b*. These results both confirm the presence of low energy absorption forms in Lhca1 and strongly suggest they originate from the same protein domains as the 720-nm emission peak of Lhca4.

To investigate the distribution of Chl electronic transitions in Lhca1, the absorption spectrum in the Q_y transition was fitted with the spectra of Chl *a* and Chl *b* in protein environment (Fig. 9, as in Ref. [34]). Two Chl *b* forms and six Chl *a* forms were needed in order to fit the spectrum. The two Chl *b* show maxima at 644 and 652 nm, each accounting in amplitude for one Chl. The six Chl *a* forms peak at 663, 669, 676, 682.4, 689, and 700 nm, respectively. The 689-nm form accounts for 0.75 Chl *a* molecule, while the intensity of the 700-nm form represents only 1% of the absorption. It is reasonable to suppose that these are the absorption forms responsible for the emission contribution at 702 nm. While the low energy absorption forms of Lhca1 are less red-shifted than in Lhca4, it is clear that

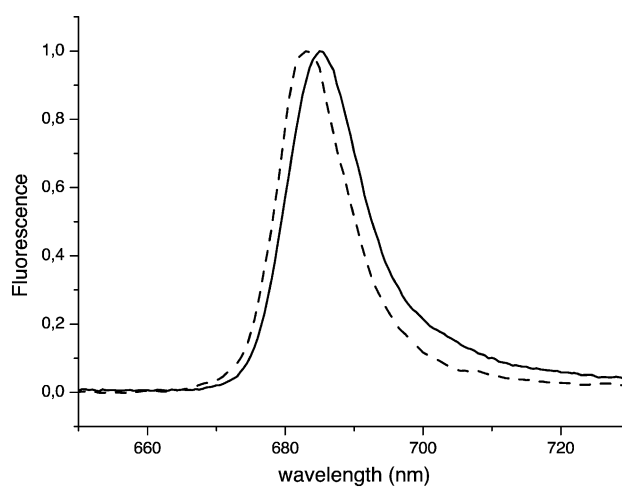


Fig. 8. Comparison of the emission spectra at 77 K of Lhca1 (solid) and Lhca1–Chl *a* (dashed) excited at 475 nm. The spectra are normalized to the maximum.

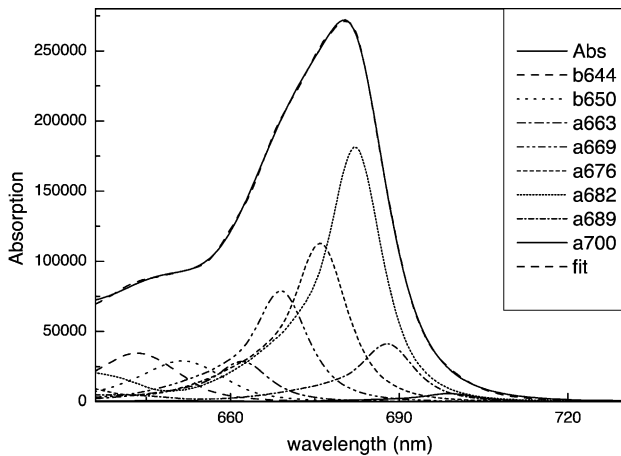


Fig. 9. Fitting of the absorption spectrum of Lhca1 at RT with the spectra of Chl *a* and Chl *b* in protein environment [34].

the protein scaffold is modulating the spectroscopic characteristics of the individual Chls in Lhca1 differently compared to PSII antenna system, shifting most of the Chl transitions to lower energy. In fact, the amplitude of the 682.4-nm form in Lhca1 accounts for three Chl *a* molecules while in LHCII, CP29, and CP26, the red-most Chl *a* form, absorbing at 681 nm, was associated with only one Chl located in site A2 [44,45]. The red-shift effect on Lhca1 chromophores also extends to at least one xanthophyll molecule, whose red-most peak was at 499 nm (Fig. 4D), 4–7 nm with respect to the absorption of violaxanthin or lutein in LHCII [54].

4.5. Lhca1–Lhca4 dimer

Lhca1 and Lhca4 assemble *in vitro* to form heterodimers according to a previous report [15]. The biochemical properties of the dimer are intermediate between the two monomers. In addition, the dimer bound small amounts of β -carotene, which is not present in the monomers. Since there is no increase of xanthophyll content in the dimer with respect to the sum of monomers, we suggest that folding in the presence of the partner protein changes the affinity of one carotenoid binding site which can now accommodate β -carotene.

Several lines of evidence indicate that dimerization affects the chromophore organization: CD and fluorescence spectra of the dimer are different as compared to the sum of the monomers, and the LD analysis indicates a change in the orientation of Chl *b* as compared to the sum of monomers. In order to investigate if the dimerization process also affects the red-shifted absorption, we compared the spectrum of the dimer with the sum of the spectra of Lhca1 and Lhca4 upon normalization to the protein content. The result is presented in Fig. 10. The two spectra are quite similar but an increase by 30% is observed in the amplitude of the red tail. This is compensated by a decreased absorption at 678 nm. This suggests

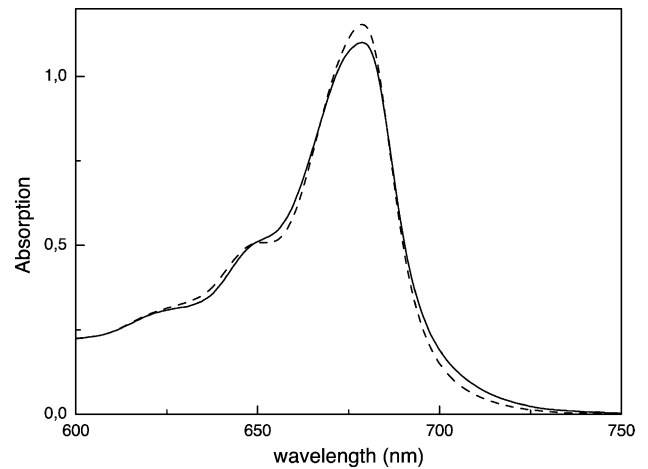


Fig. 10. Comparison of the absorption spectra of Lhca1–4 dimer (solid) with the sum of the spectra of (Lhca1 and Lhca4)/2 (dashed). The spectra are normalized to the protein concentration.

that the protein–protein interactions play a role in the red absorption similar to the case of the bacterial reaction center [56].

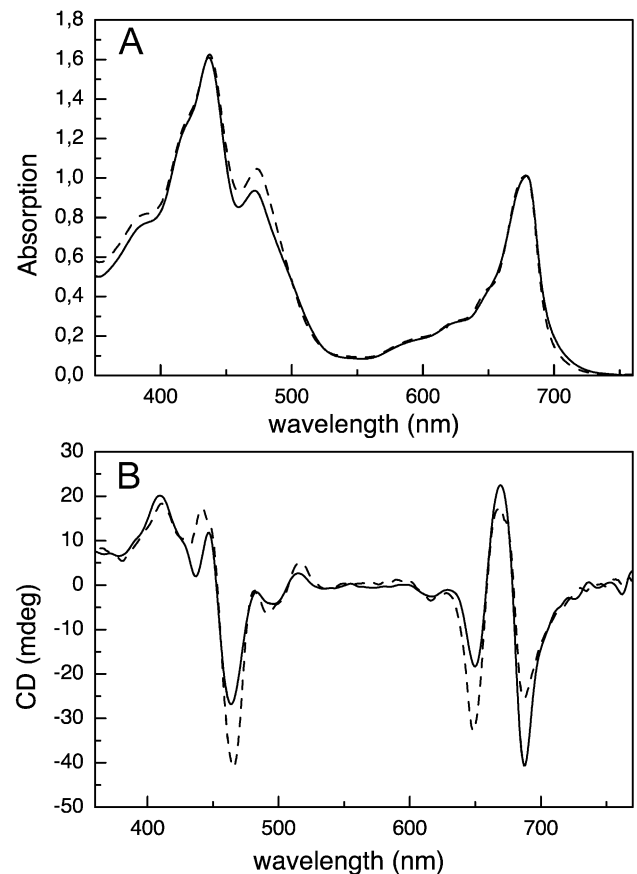


Fig. 11. Comparison between the spectroscopic characteristics of the LHCI native fraction (solid) and Lhca1–4 reconstituted dimer (dashed). (A) Absorption spectra at RT normalized to the maximum; (B) CD spectra at 10 °C normalized to the absorption.

4.6. Lhca2 and Lhca3

In most of the reports present in the literature, purification of LHCI complexes by sucrose gradient ultracentrifugation yielded two bands: the upper was named LHCI-680 from the peak in fluorescence emission spectrum and contained Lhca2+Lhca3. The lower band (LHCI-730) contained Lhca1+Lhca4 [3]. On this basis it was argued that Lhca2 and Lhca3 do not contain “red” Chls. However, spectroscopic analysis of the LHCI preparation [11] and anti-sense experiments, where the absence of Lhca2 or Lhca3 was correlated to a blue shift of the red fluorescence peak [22], suggested “red” Chls might be associated to Lhca2 and Lhca3. The LHCI-680 fraction was not present in our experiments, suggesting that mild procedures were effective in maintaining all Lhca polypeptides in their dimeric form. A monomeric LHCI band showing a 690-nm emission was only obtained upon harsh treatment of the LHCI fraction with detergent (data not shown). The analysis of this fraction, which was indeed enriched in Lhca3 and Lhca2 polypeptides, reveals that these complexes were present in monomeric form and were showing a lower Chl *a/b* ratio [9]. We conclude that the LHCI-680 (or 690) fraction is the product of artefactual monomerization while native Lhca2 and -3 are, in fact, dimers. Whereas it was not possible to purify to homogeneity Lhca2 and Lhca3 in dimeric state, fractions enriched in these two complexes were obtained. The Lhca2/3-enriched fraction showed a red tail in the absorption spectra, whose amplitude was similar to that of fractions enriched in Lhca1–4. This was associated to red-shifted fluorescence emission. An additional evidence for the association of “red” absorption and emission forms to Lhca2 and Lhca3 is obtained by comparing absorption and fluorescence emission spectra of the recombinant Lhca1–4 heterodimeric complex with the native LHCI preparation: they have similar amplitude of “red” forms in both fluorescence and absorption spectra (Fig. 11A), thus implying that Lhca2/3 dimers have similar content in red forms as Lhca1–4. The two types of dimers are likely to have similar pigment organization as indicated (Fig. 11) by the very similar absorption and CD spectra of the native LHCI and the recombinant heterodimer.

Acknowledgements

This work was founded by CNR “agenzia 2000” and by “MIUR” Progetto FIRBn.RBAU01ECX.

References

- [1] P. Jordan, P. Fromme, H.T. Witt, O. Klukas, W. Saenger, N. Krauss, *Nature* 411 (21-6-2001) 909–917.
- [2] J. Knoetzel, A. Mant, A. Haldrup, P.E. Jensen, H.V. Scheller, *FEBS Lett.* 510 (16-1-2002) 145–148.
- [3] R. Bassi, D. Simpson, *Eur. J. Biochem.* 163 (1987) 221–230.
- [4] S. Jansson, *Biochim. Biophys. Acta* 1184 (1994) 1–19.
- [5] E.J. Boekema, P.E. Jensen, E. Schlodder, J.F. van Breemen, H. van Roon, H.V. Scheller, J.P. Dekker, *Biochemistry* 40 (2001) 1029–1036.
- [6] P.E. Jensen, M. Gilpin, J. Knoetzel, H.V. Scheller, *J. Biol. Chem.* 275 (2000) 24701–24708.
- [7] H.V. Scheller, P.E. Jensen, A. Haldrup, C. Lunde, J. Knoetzel, *Biochim. Biophys. Acta* 1507 (2001) 41–60.
- [8] I. Damm, D. Steinmetz, L.H. Grimme, in: M. Baltscheffsky (Ed.), *Current Research in Photosynthesis*, vol. II, 1989, pp. 607–610.
- [9] R. Croce, R. Bassi, in: G. Garab (Ed.), *Photosynthesis. Mechanisms and Effects*, vol. I, 1998, pp. 421–424.
- [10] W. Kühlbrandt, D.N. Wang, Y. Fujiyoshi, *Nature* 367 (1994) 614–621.
- [11] J.A. Ihalainen, B. Gobets, K. Sznee, M. Brazzoli, R. Croce, R. Bassi, R. van Grondelle, J.E.I. Korppi-Tommola, J.P. Dekker, *Biochemistry* 39 (2000) 8625–8631.
- [12] B. Gobets, J.T.M. Kennis, M. Brazzoli, R. Croce, I.H. van Stokkum, R. Bassi, J.P. Dekker, H. Van Amerongen, G.R. Fleming, R. van Grondelle, *J. Phys. Chem., B* 105 (2001) 10132–10139.
- [13] J. Knoetzel, I. Svendsen, D.J. Simpson, *Eur. J. Biochem.* 206 (1992) 209–215.
- [14] S.E. Tjus, M. Roobol-Boza, L.-O. Palsson, B. Andersson, *Photosynth. Res.* 45 (1995) 41–49.
- [15] V.H.R. Schmid, K.V. Cammarata, B.U. Bruns, G.W. Schmidt, *Proc. Natl. Acad. Sci. U. S. A.* 94 (1997) 7667–7672.
- [16] A.N. Melkozernov, S. Lin, V.H.R. Schmid, H. Paulsen, G.W. Schmidt, R.E. Blankenship, *FEBS Lett.* 471 (2000) 89–92.
- [17] A.N. Melkozernov, V.H.R. Schmid, G.W. Schmidt, R.E. Blankenship, *J. Phys. Chem., B* 102 (1998) 8183–8189.
- [18] R. Croce, G. Zucchelli, F.M. Garlaschi, R. Bassi, R.C. Jennings, *Biochemistry* 35 (1996) 8572–8579.
- [19] B. Gobets, R. van Grondelle, *Biochim. Biophys. Acta* 1057 (2001) 80–99.
- [20] H. Zhang, H.M. Goodman, S. Jansson, *Plant Physiol.* 115 (1997) 1525–1531.
- [21] J. Knoetzel, B. Bossmann, L.H. Grimme, *FEBS Lett.* 436 (1998) 339–342.
- [22] U. Ganeteg, A. Strand, P. Gustafsson, S. Jansson, *Plant Physiol.* 127 (2001) 150–158.
- [23] R. Croce, G. Zucchelli, F.M. Garlaschi, R.C. Jennings, *Biochemistry* 37 (1998) 17255–17360.
- [24] R. Bassi, U. Hinz, R. Barbato, *Carlsberg Res. Commun.* 50 (1985) 347–367.
- [25] U.K. Laemmli, *Nature* 227 (1970) 680–685.
- [26] P. Dainese, G. Hoyer-hansen, R. Bassi, *Photochem. Photobiol.* 51 (1990) 693–703.
- [27] J. Sambrook, E.F. Fritsch, T. Maniatis, *Molecular Cloning. A Laboratory Manual*, 2nd ed., Cold Spring Harbor Laboratory Press, USA, 1989.
- [28] T.J. Gibson (1984). Thèse.
- [29] S. Gottesman, E. Halpern, P. Trisler, *J. Bacteriol.* 148 (1981) 263–265.
- [30] K. Nagai, H.C. Thøgersen, *Methods Enzymol.* 153 (1987) 461–481.
- [31] H. Paulsen, S. Hobe, *Eur. J. Biochem.* 205 (1992) 71–76.
- [32] E. Giuffra, D. Cugini, R. Croce, R. Bassi, *Eur. J. Biochem.* 238 (1996) 112–120.
- [33] A.M. Gilmore, H.Y. Yamamoto, *Plant Physiol.* 96 (1991) 635–643.
- [34] R. Croce, G. Canino, F. Ros, R. Bassi, *Biochemistry* 41 (2002) 7334–7343.
- [35] C.H.W. Hirs, *Methods Enzymol.* 11 (1967) 325–329.
- [36] A. Pagano, G. Cinque, R. Bassi, *J. Biol. Chem.* 273 (1998) 17154–17165.
- [37] P. Haworth, C.J. Arntzen, P. Tapie, J. Breton, *Biochim. Biophys. Acta* 679 (1982) 428–435.
- [38] P. Haworth, P. Tapie, C.J. Arntzen, J. Breton, *Biochim. Biophys. Acta* 682 (1982) 152–159.

- [39] E. Giuffra, G. Zucchelli, D. Sandona, R. Croce, D. Cugini, F.M. Garlaschi, R. Bassi, R.C. Jennings, *Biochemistry* 36 (1997) 12984–12993.
- [40] G. Cinque, R. Croce, R. Bassi, *Photosynth. Res.* 64 (2000) 233–242.
- [41] E.J. Boekema, H. van Roon, F. Calkoen, R. Bassi, J.P. Dekker, *Biochemistry* 38 (1999) 2233–2239.
- [42] R. Harrer, R. Bassi, M.G. Testi, C. Schäfer, *Eur. J. Biochem.* 255 (1998) 196–205.
- [43] P. Dainese, R. Bassi, *J. Biol. Chem.* 266 (1991) 8136–8142.
- [44] R. Bassi, R. Croce, D. Cugini, D. Sandona, *Proc. Natl. Acad. Sci. U. S. A.* 96 (1999) 10056–10061.
- [45] R. Remelli, C. Varotto, D. Sandona, R. Croce, R. Bassi, *J. Biol. Chem.* 274 (1999) 33510–33521.
- [46] E.H. Ball, *Anal. Biochem.* 155 (1986) 23–27.
- [47] E. Formaggio, G. Cinque, R. Bassi, *J. Mol. Biol.* 314 (2001) 1157–1166.
- [48] R. Croce, G. Cinque, A.R. Holzwarth, R. Bassi, *Photosynth. Res.* 64 (2000) 221–231.
- [49] R. Croce, M.G. Muller, R. Bassi, A.R. Holzwarth, *Biophys. J.* 80 (2001) 901.
- [50] E. Pichersky, S. Jansson, in: D.R. Ort, C.F. Yocum (Eds.), *Oxygenic Photosynthesis: The Light Reactions*. Dordrecht 1996, pp. 507–521.
- [51] R. Bassi, E. Giuffra, R. Croce, P. Dainese, E. Bergantino, in: R.C. Jennings, G. Zucchelli, F. Ghetti, G. Colombetti (Eds.), *Light as an Energy Source and Information Carrier in Plant Physiology* NATO ASI Series. Series A: Life Sciences, vol. 287, Plenum, New York, 1996, pp. 41–63.
- [52] P.M. Dolan, D. Miller, R.J. Cogdell, R.R. Birge, H.A. Frank, *J. Phys. Chem., B* 105 (2001) 12134–12142.
- [53] R. Croce, R. Remelli, C. Varotto, J. Breton, R. Bassi, *FEBS Lett.* 456 (1999) 1–6.
- [54] R. Croce, S. Weiss, R. Bassi, *J. Biol. Chem.* 274 (1999) 29613–29623.
- [55] V.H.R. Schmid, P. Thome, W. Ruhle, M.D. Paulsen, W. Kuhlbrandt, H. Rogl, *FEBS Lett.* 499 (2001) 27–31.
- [56] N.V. Karapetyan, D. Dorra, A.R. Holzwarth, J. Kruip, M. Rögner, in: G. Garab (Ed.), *Photosynthesis: Mechanisms and Effects*, vol. I, 1998, pp. 583–586.

B 2

Recombinant Lhca2 and Lhca3 Subunits of the Photosystem I Antenna System

This chapter has been published in *Biochemistry*
42 (2003), pp 4226 - 4234, reproduced with permission.

Simona Castelletti*, Tomas Morosinotto*, Bruno Robert,
Stefano Caffarri, Roberto Bassi and Roberta Croce

*Equal contribution

Recombinant Lhca2 and Lhca3 Subunits of the Photosystem I Antenna System

Simona Castelletti,^{‡,§,||} Tomas Morosinotto,^{‡,||} Bruno Robert,[§] Stefano Caffarri,^{‡,⊥} Roberto Bassi,^{‡,⊥} and Roberta Croce^{*,#}

Dipartimento Scientifico e Tecnologico, Università di Verona, Strada Le Grazie, 15- 37234 Verona, Italy, Service de Bioénergétique, Bât. 532 CEA-Saclay, 91191 Gif-sur-Yvette, France, Université Aix-Marseille II, LGBP (Laboratoire de Genétique et Biophysique des Plantes) Faculté des Sciences de Luminy, Département de Biologie, Case 901-163, Avenue de Luminy-13288 Marseille, France, and Istituto di Biofisica, CNR sezione di Milano, c/o Dipartimento di Biologia, Via Celoria 26, 20133 Milano, Italy

Received December 20, 2002; Revised Manuscript Received February 14, 2003

ABSTRACT: In this study, two gene products (Lhca2 and Lhca3), encoding higher plants (*Arabidopsis thaliana*) Photosystem I antenna complexes, were overexpressed in bacteria and reconstituted in vitro with purified chloroplast pigments. The chlorophyll-xanthophyll proteins thus obtained were characterized by biochemical and spectroscopic methods. Both complexes were shown to bind 10 chlorophyll (*a* and *b*) molecules per polypeptide, Lhca2 having higher chlorophyll *b* content as compared to Lhca3. The two proteins differed for the number of carotenoid binding sites: two and three for Lhca2 and Lhca3, respectively. β -carotene was specifically bound to Lhca3 in addition to the xanthophylls violaxanthin and lutein, indicating a peculiar structure of carotenoid binding sites in this protein since it is the only one so far identified with the ability of binding β -carotene. Analysis of the spectroscopic properties of the two pigment proteins showed the presence of low energy absorption forms (red forms) in both complexes, albeit with different energies and amplitudes. The fluorescence emission maximum at 77 K of Lhca2 was found at 701 nm, while in Lhca3 the major emission was at 725 nm. Reconstitution of Lhca3 without Chl *b* reveals that Chl *b* is not involved in originating the low energy absorption forms of this complex. The present data are discussed in comparison to the properties of the recombinant Lhca1 and Lhca4 complexes and of the native LHCI preparation, previously analyzed, thus showing a comprehensive description of the gene products composing the Photosystem I light harvesting system of *A. thaliana*.

The outer antenna system of higher plant Photosystem I, LHCI,¹ is composed of four proteins (*I*–*3*), the products of the genes Lhca1–4 (*4*), which coordinate Chl *a*, Chl *b*, lutein, violaxanthin, and β -carotene (*5*, *6*). These complexes are present in dimeric form in vivo (*7*), and they are located on one side of the PSI core complex (*8*), in connection with PsaF, PsaG, and PsaK subunits (*9*, *10*). The sequence homology with Lhcb proteins suggests that they share structure similarity with LHCII complex (*11*, *12*). Thus, their structure is proposed to include three membrane spanning helices and one amphipatic helix on the luminal side of the membrane.

The purification of each Lhca gene product to homogeneity has proven problematic because of strong interactions between subunits in the heterodimers, which require harsh detergent treatments to be broken, yielding into denaturation.

Most of the studies on the complexes purified from thylakoids membrane have therefore been achieved on heterogeneous preparations containing several polypeptides (*3*, *7*, *13*–*16*) leading to determination of the average properties of the complexes. A possible solution to this problem has been offered by overexpression of the genes in bacterial systems and reconstitution in vitro of the apoproteins with pigments (*17*). Biochemical and spectroscopic data are now available for Lhca1 and Lhca4 subunits (*7*, *18*–*22*).

The major characteristic of LHCI is the presence of significant absorption in the low energy side of the spectrum because of Chl spectral forms red-shifted at energies lower than the Photosystem I primary donor, P700. These forms were found to be associated to a LHCI subfraction named LHCI-730, which contains Lhca1 and Lhca4 (*3*, *13*, *14*, *23*). In vivo and in vitro analyses have demonstrated that the red absorption originates mainly from Chls associated to the Lhca4 subunit (*18*, *24*). The presence of low energy forms in Lhca2 and Lhca3 complexes is more controversial. In the early purifications of LHCI antenna, these two complexes were found in a fraction showing a low-temperature emission peak at 680–690 nm (named LHCI-680) (*3*, *13*, *14*, *23*). It was argued that no red-shifted Chl forms were associated to these two subunits. More recently, analysis of a LHCI preparation containing all four Lhca proteins revealed the presence of a 702 nm fluorescence emission component that was attributed to Lhca2 and/or Lhca3 dimers (*15*, *16*).

* Author to whom correspondence should be addressed. E-mail: roberta.croce@unimi.it. Tel +39 0250314856. Fax +39 0250314815.

[‡] Università di Verona.

[§] Service de Bioénergétique.

^{||} These authors contributed equally to this work.

[⊥] Université Aix-Marseille II.

[#] Istituto di Biofisica.

¹ Abbreviations: AA, amino acid; b-car, β -carotene; CD, circular dichroism; Car, carotenoid; Chl, chlorophyll; HPLC, high-performance liquid chromatography; Lhc, light harvesting complex; LHCI and LHCII, light harvesting complex of Photosystem I and II; LT, low temperature (77 K); lute, lutein; neo, neoxanthin; PSI, Photosystem I; RT, room temperature; viola, violaxanthin.

Purification of a dimeric fraction enriched in Lhca2 and Lhca3 also suggested that red forms could be associated to these complexes (6, 7). A similar proposal came from the analysis of antisense plants depleted in Lhca2 and Lhca3 subunits (25). In fact, these plants showed a blue-shifted 77 K fluorescence emission spectrum as compared to WT plants and decreased absorption at 695 and 715 nm. The *in vitro* reconstitution of monomeric Lhca2 and Lhca3 appears to confirm the presence of low energy forms in these two subunits (22).

The aim of this work is to provide information on Lhca2 and Lhca3 complexes, which are at present the lesser known antenna proteins of higher plants. In this study, Lhca2 and Lhca3 apoproteins of *Arabidopsis thaliana* overexpressed in *Escherichia coli* were reconstituted *in vitro* with pigments, and the refolded complexes were characterized by biochemical and spectroscopic methods to give a complete picture of their properties. The results are discussed in comparison with the data previously obtained for Lhca1 and Lhca4 and for the native LHCI dimeric preparation (7) with major emphasis on the low energy spectral forms.

MATERIALS AND METHODS

DNA Constructions. Plasmids were constructed using standard molecular cloning procedures (26). cDNA of Lhca2 and Lhca3 from *A. thaliana* were supplied by Arabidopsis Biological Resource Center (ABRC) at the Ohio State University. The coding regions for the putative mature polypeptides were amplified by PCR (Lhca2: forward primer, GGGGTCGACCAGTCGCAGCTGATCCAG, reverse primer, GGGAAGCTTCTTGGGTGTGAAAGC; Lhca3: forward primer, CGAGGATCCGCTGCAGCTCACCTGTC, reverse primer, CGGAAGCTTGTGGAACCTGAGGCTGGTC). The amplified regions were cloned in the pQE-50 (Qiagen) expression vector.

Isolation of Overexpressed Lhca Apoproteins from Bacteria. Lhca apoproteins were expressed and purified from *E. coli*, using BL21 and SG13009 strains respectively for Lhca2 and Lhca3 constructs, following a protocol previously described (27, 28).

Reconstitution and Purification of Lhca–Pigment Complexes. These procedures were performed as described in (29) with the following modifications: 420 μ g of apoprotein, 240 μ g of chlorophylls, and 35 μ g of carotenoids were used in the reconstitution. The Chl *a/b* ratio in the pigment mixture used for the reconstitution of the control samples was 4. To obtain complexes enriched in Chl *b*, a Chl *a/b* ratio of 0.2 was used. The reconstitution in the absence of Chl *b* was performed with purified Chl *a* from Sigma. All reconstitutions were performed in the presence of all carotenoids of the thylakoid membrane. The pigments used were purified from spinach.

Pigment Analysis. The pigment complement of the holoprotein was analyzed by HPLC (30) and fitting of the absorption spectra of the acetone extracts with the spectra of the individual pigments (31).

Spectroscopy. The absorption spectra at RT were recorded by SLM-Aminco DK2000 spectrophotometer, in 10 mM HEPES pH 7.5, 20% (v/v) glycerol (70% for LT), and 0.06% β -DM, using a step of 0.45 nm. The fluorescence emission spectra were measured on a Jasco FP-777 fluorimeter and

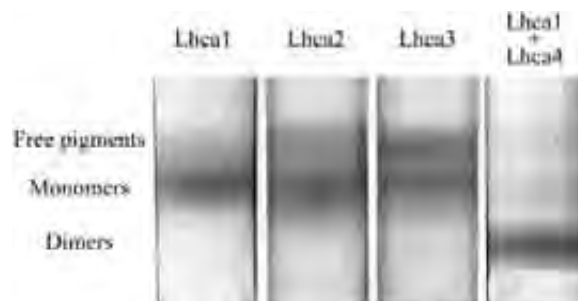


FIGURE 1: Aggregation state of Lhca2 and Lhca3. The mobility of the two complexes upon ultracentrifugation in glycerol density gradient is compared to the mobility of Lhca1 monomer and Lhca1-4 dimer.

corrected for the instrumental response. The samples were excited at 440, 475, and 500 nm. The bandwidths were 5 nm in excitation and 3 nm in emission. For the excitation spectra, the emission was at 700 nm. All fluorescence spectra were measured at 0.02 OD at the maximum of Q_y transition. For the low-temperature measurements, the samples were in 70% glycerol, 10 mM HEPES pH 7.5, 0.03% β -DM.

The CD spectra were measured at 10 °C on a Jasco 600 spectropolarimeter. The samples were in the same solution described for the absorption. All the spectra presented were normalized to the same polypeptide concentration, based on the Chl binding stoichiometry (32).

Denaturation temperature measurements were performed by following the decay of the CD signal at 470 nm when increasing the temperature from 20 to 75 °C with a time slope of 1 °C/min and resolution of 0.2 °C. The thermal stability of the protein was determined by finding the $T_{1/2}$ of the signal decay.

RESULTS

Lhca2 and Lhca3 apoproteins were overexpressed in *E. coli*, and the complexes were reconstituted *in vitro* by refolding in the presence of the full pigment complement extracted from chloroplasts. Both proteins yielded a green band upon sucrose gradient ultracentrifugation. The reconstituted products were then purified from unfolded polypeptides and unspecifically bound pigments by anionic exchange chromatography. The aggregation state of the complexes was investigated by glycerol density gradient ultracentrifugation, a method previously shown to be effective in separating monomers from dimers and free pigments (21). As compared with Lhca1 monomer and Lhca1-4 dimer, Lhca2 and Lhca3 were shown to be obtained in monomeric state (Figure 1).

Pigment Composition. The pigment composition of Lhca2 and Lhca3 was determined by HPLC analysis and fitting of the absorption spectrum of the acetone extracts with the spectra of individual pigments in the same solvent. The results are presented in Table 1. Although the reconstitution of both proteins was performed with the same pigment mixture, the Chl *a/b* ratio was lower in Lhca2 with respect to Lhca3 (1.84 vs 6.0), indicating higher affinity for Chl *b* of the former complex. The Chl/car ratio was also different in the complexes, being 5.0 for Lhca2 and 3.4 for Lhca3. Lutein and violaxanthin were found associated to both proteins, while β -carotene was specifically bound to Lhca3. The neoxanthin, although present in the recon-

Table 1: Pigment Composition of Reconstituted Complexes^a

sample	Chl <i>a/b</i> ratio	Chl/car	Chl <i>b</i>	viola	lute	b-car	Den T (°C)
Lhca2	1.85 ± 0.15	5.0 ± 0.2	54.3 ± 2.9	7.2 ± 1.4	23.5 ± 1.6		53.3 ± 1.9
Lhca3	6.0 ± 0.8	3.5 ± 0.2	16.8 ± 2.0	7.8 ± 0.6	18.9 ± 0.5	6.7 ± 2.3	45.6 ± 1.4

^a The data are the average of four reconstitutions. The values are considered for 100 molecules of Chl *a*.

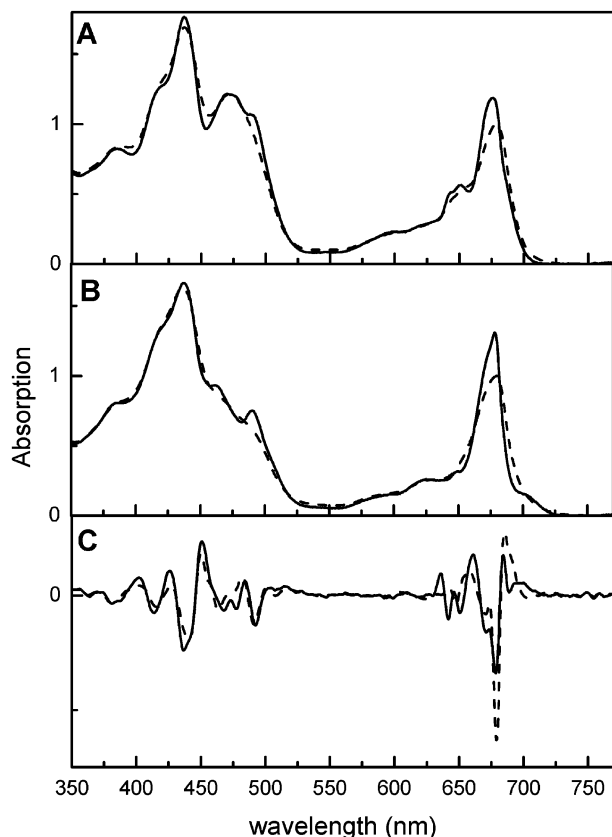


FIGURE 2: Absorption spectra at RT (dashed) and LT (solid) of reconstituted Lhca2 (A) and Lhca3 (B). The spectra are normalized to the total area. In panel C, the second derivative of the spectra at LT is presented: Lhca2 (solid) and Lhca3 (dashed).

stitution mixture, was absent from both complexes in agreement with the composition of native LHCI preparation (7) thus confirming the specificity of the *in vitro* refolding procedure.

Absorption Spectra. The absorption spectra at room temperature (RT) and at 77 K (LT) of the complexes are reported in Figure 2 along with the second derivatives of the LT spectra. The absorption maximum of Lhca2 in the Q_y region was at 676.5 nm (679.0 at RT). The second derivative analysis of Lhca2 showed minima at 678.5 nm (682.1 nm at RT), 671 nm (673 nm) in the Q_y region of Chl *a*, and at 651 nm (652.4 nm) and 642 nm (643 nm) in the Chl *b* region. In the blue region of the spectrum, the minimum at 495 nm (492 nm) is related to the carotenoids red most transition and the two minima at 477 and 468 nm to the S_0-S_3 transitions of Chls *b*. In the case of Lhca3, the absorption maximum was at 678.5 nm (679.4 nm at RT), and in the second derivative the values found for the components in Q_y range were of 679 nm (682.1 nm at RT) and 672 nm (671 nm) for Chl *a*, while in the Chl *b* absorption range a small signal was observed at 648 nm (651 nm). In the blue range, Lhca3 showed two signals, at 507 and 491 nm, which can be attributed to carotenoid transitions, while

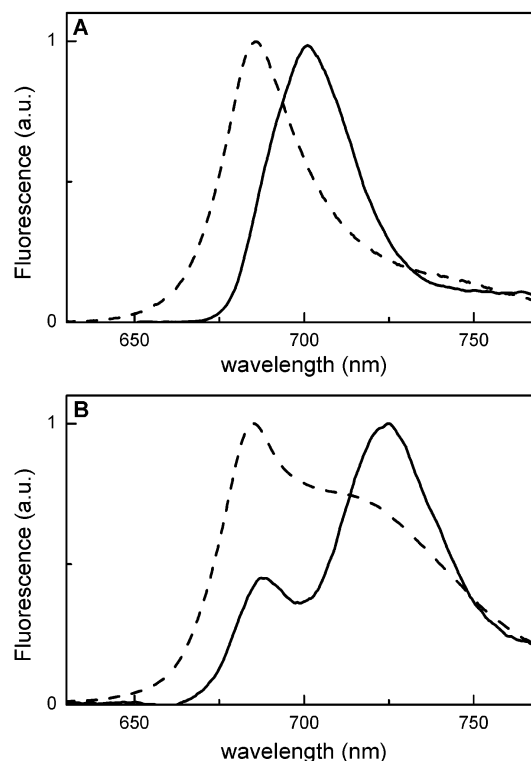


FIGURE 3: Fluorescence emission spectra at RT (dashed) and 77 K (solid) of Lhca2 (A) and Lhca3 (B). The spectra are normalized to the maximum.

components at 475 and 465 nm could be tentatively attributed to different forms of Chl *b* S_0-S_3 transitions. Besides that, the second derivative analysis of the Lhca3 spectrum also showed a 704.6 nm signal, which could not be resolved in the case of Lhca2.

The most interesting feature is the presence of absorption at wavelengths longer than 700 nm, clear indication for red forms in both complexes, albeit with different intensities: the absorption above 700 nm represents at RT the 2.7% (1.1% at LT) of the Q_y absorption in Lhca2 and 5% (5.4% at LT) in Lhca3.

Fluorescence Spectra. The fluorescence emission spectra of the two samples, recorded at RT and 77 K, are shown in Figure 3. At room temperature, Lhca2 fluoresced with a single peak at 688 nm, and the band was asymmetrically broadened, showing contributions at lower energy (Figure 3A). At 77 K, the peak shifted to 701 nm, but a contribution at 688 nm was still present in the high-energy side of this band (Figure 3A). Lhca3 at RT exhibited the emission maximum at 685 nm and strong red emission at wavelengths longer than 705 nm. At low temperature, the spectrum was dominated by a broad signal at 725 nm, while a 688 nm peak was still detectable (Figure 3B). These data are in perfect agreement with the absorption spectra and confirm that both complexes have Chl forms absorbing at

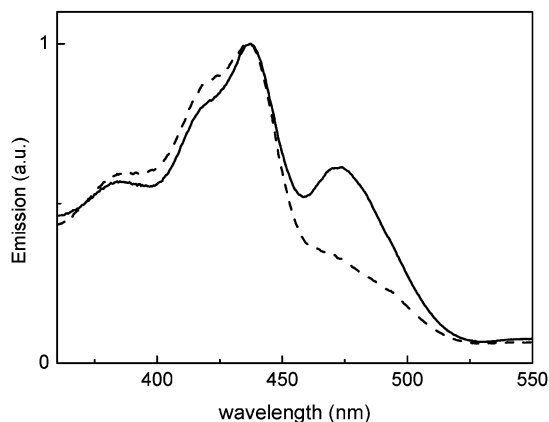


FIGURE 4: Fluorescence excitation spectra of Lhca2 (solid) and Lhca3 (dashed). The spectra are normalized to the maximum.

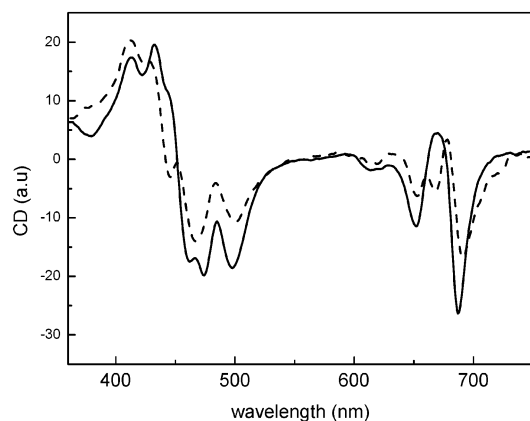


FIGURE 5: CD spectra at RT of Lhca2 (solid) and Lhca3 (dashed). The spectra are normalized to the Chl concentration.

The excitation spectra of the complexes at RT are shown in Figure 4. Comparison between the Soret region of the absorption and the excitation spectrum allowed calculating the carotenoid to chlorophyll energy transfer efficiency in the complexes (31). To this end, the absorption spectra of Lhca2 and Lhca3 were described in terms of sum of absorptions of individual pigments, using the spectra of pigments in protein environment (33). The same description was applied to the excitation spectra: the position of the maxima of the pigments obtained by the analysis of the absorption spectrum was fixed, and only the amplitudes were used as free parameters. The comparison of the areas of the individual pigments in the absorption and excitation spectra yielded the transfer efficiency for each species. The results for Lhca2 indicated an overall carotenoid to Chl energy transfer yield of 75%, a value similar to other Lhc proteins. The error is around 5% assuming for Chl *a* 100% transfer efficiency.

Surprisingly, in Lhca3 the transfer efficiency from carotenoid to Chl was as low as 55%. From the comparison of the absorption and excitation spectra it was observed that a carotenoid absorbing at higher energy (red most peak at 485–489 nm) does not transfer energy to Chl *a*.

CD Spectra. The CD spectra of the two complexes are reported in Figure 5. Lhca2 showed negative components in the Q_y region at 687 and 652 nm and a positive one at 669–670 nm. In the spectrum of Lhca3 complex, three negative signals were present in this range at 691, 668, and 653 nm and a positive one at 678 nm. In this case, a negative

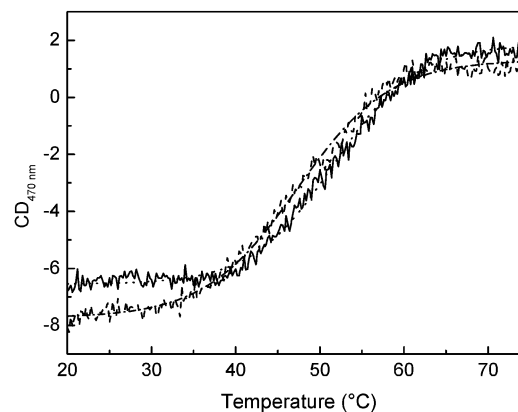


FIGURE 6: CD signal at 470 nm of Lhca2 (solid) and Lhca3 (dotted) vs temperature. The experimental data were fitted with a sigmoidal curve, and the denaturation temperature determinate as $T_{1/2}$.

component at wavelengths longer than 700 nm was also observed, reflecting at least part of the red forms absorption.

In the blue region, a strong and broad negative band, with three minima of similar intensity at 498, 474, and 462 nm, characterizes Lhca2. The Lhca3 spectrum in the blue showed two contributions at 467 nm (–) and 500 nm (–).

Protein Complex Stability. The stability of the complexes was measured following the CD signal decay with increasing temperature. The sigmoidal fit of the curves (Figure 6) indicated that the denaturation temperatures for Lhca2 and Lhca3 were of 53.3 ± 1.9 and 45.6 ± 1.4 °C, respectively.

Reconstitution with Different Chl Species. Chlorophyll *b* has been proposed to be involved in the red-shifted spectral forms of LHCI (34). This finding was supported by the loss of red forms upon reconstitution of Lhca4 (35) and Lhca1 (7) with Chl *a* plus xanthophylls but without Chl *b*. It is interesting to assess whether the red forms found in Lhca3, which are quite similar to the ones of Lhca4, are also dependent on the presence of Chl *b*. A positive answer would support a similar origin for red forms in all Lhca gene products. To assess the dependence of the spectral properties of Lhca complexes on Chl *b*, in vitro reconstitution of the Lhca3 complex was performed either in the absence of Chl *b* or in the presence of a Chl *b* excess with respect to the control conditions above-described. Beside, we have reconstituted Lhca4 in the same conditions to obtain comparative results. In the absence of Chl *b*, both proteins yielded a stabile monomer (Lhca3-a; Lhca4-a), which did not contain Chl *b* as assessed by HPLC analysis, but still coordinates Chl *a* and carotenoids. The reconstitution in the presence of excess of Chl *b* also gave a stable product for Lhca4 (Lhca4-b, Chl *a/b* 0.18), while Lhca3 was unstable in these conditions, confirming that this protein requires high Chl *a* occupancy. The absorption and the emission spectra at low temperature of the three holoproteins obtained are presented in Figure 7. The spectra of Lhca3-a were very similar to the spectra of the control Lhca3, with respect to the amplitude of the red forms. The Q_y transition showed a peak at 679 nm, and strong absorption at wavelengths longer than 700 nm was detected. The presence of the red forms was confirmed by the emission spectrum, which showed the maximum at 725 nm (Figure 7A) and a second peak at 685 nm, reproducing the spectrum of the control (see Figure 3B for comparison). In the case of Lhca4-a the situation was different: both absorption and

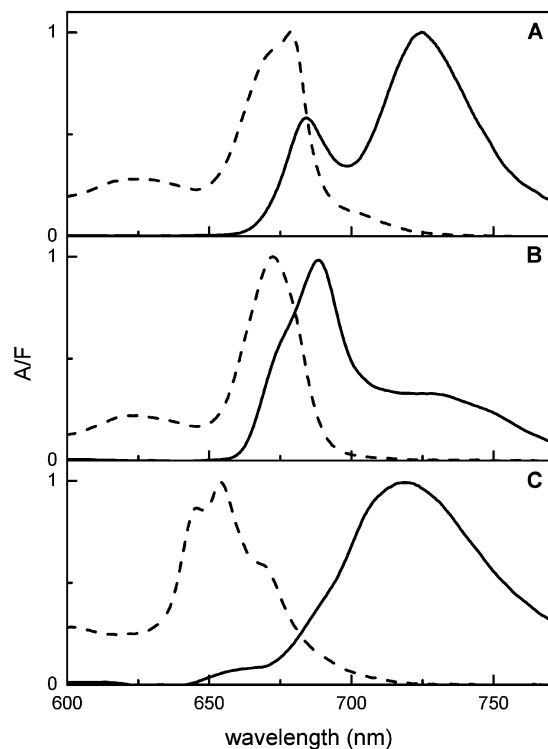


FIGURE 7: Absorption (dashed) and fluorescence emission (solid) spectra at 77 K of Lhca3-a (A), Lhca4-a (B), and Lhca4-b (C).

spectral forms. The fluorescence spectrum showed a 690 nm peak, although a residual weak emission at around 730 nm was still detectable. Moreover, this complex also showed emission contribution around 675 nm, indicating the presence of Chls that do not transfer energy efficiently, and then suggesting that this sample is less stable than the control. The Lhca4-b complex had different spectroscopic properties as compared to both the control and the sample reconstituted with Chl *a* only: its absorption spectrum was characterized by three main bands at 646, 654, and 670 nm, reflecting the high content in Chl *b* (8.5 Chls *b* vs 1.5 Chls *a*), but absorption above 700 nm was still present. The fluorescence emission spectrum showed that most of the energy in this sample is emitted from red-shifted forms, peaking at 719 nm, thus shifted by 11 nm to the blue as compared to the control Lhca4.

DISCUSSION

Lhca2 and Lhca3 are two pigment-protein complex components of the Photosystem I antenna system of higher plants, together with Lhca1 and Lhca4. The predicted size of the Lhca2 polypeptide is of 212 amino acids for a molecular mass of 23 kDa, while Lhca3 is longer (232 AA) and has a molecular mass of 25 kDa (4). Little is at present known about these complexes because of difficulties in purification. The possibility to overexpress the apoproteins in *E. coli* and to reconstitute the complexes in vitro with pigments represents at the moment a unique tool to study the properties of these LHCI subunits. In the following, we discuss the major biochemical and spectroscopic features of Lhca2 and Lhca3 as compared to those of Lhca1 and Lhca4, the two LHCI subunits previously described in detail (7, 18).

Pigment Composition. Pigment/protein stoichiometry measurements on the native LHCI preparation, containing all four

Table 2: Comparison between the Pigment Complements of the Four Lhca Recombinant Complexes^a

sample	Chl <i>a</i>	Chl <i>b</i>	viola	lute	b-car	refs
Lhca1	8 ± 0.04	2 ± 0.04	1.05	1.81		7
Lhca2	6.5 ± 0.2	3.5 ± 0.2	0.47	1.52		this paper
Lhca3	8.6 ± 0.2	1.4 ± 0.2	0.66	1.62	0.57	this paper
Lhca4	7.0 ± 0.2	3 ± 0.2	0.5	1.5		7

^a The number of Chls was determined on the basis of the Chl/Car ratio (see text). The values reported indicate the number of pigments per polypeptide.

Lhca complexes, have shown that 10 Chls are bound in average to each Lhca protein. The analysis of Lhca1 and Lhca4 monomers reconstituted in vitro actually indicated that both complexes coordinate 10 Chls (7) (Table 2). Therefore, a similar stoichiometry is expected for Lhca2 and Lhca3. In all antenna complexes analyzed so far, an integer number of tightly bound carotenoids has always been observed, either two or three depending on the protein (36). The Chl/Car ratio of Lhca2 is 5.0, then assuming a Chl to polypeptide stoichiometry of 10, the complex would accommodate exactly two xanthophylls. In Lhca3, the Chl/Car ratio is 3.4, which would be consistent with the binding of three carotenoids per polypeptide. On the basis of these observations, we propose that each Lhca2 and Lhca3 monomeric complex binds 10 Chls and respectively two and three xanthophyll molecules.

A similar study on the pigment complement of Lhca complexes was recently performed on tomato Lhca complexes (22). Although the results are consistent, differences between the data presented here and the ones by Schmidt and co-workers can be appreciated, especially in the complement of carotenoid binding to each gene product. Discrepancies may be due to species-specific differences as we clearly show in the case of *Zea mays* versus *A. thaliana* LHCI preparations (7). Another source of variability can be the different methods used for the purification of the reconstituted complex from unspecifically bound pigments following reconstitution (cfr. refs 22 and 7).

The primary structure analysis indicates that all the residues, which have been proven to be Chl binding ligands in Lhcb1, are conserved in the Lhca2 and Lhca3 proteins. The only difference is the substitution of glutamine with glutamate as a ligand for Chl B6. This is likely to be a conservative substitution since it was previously shown that Glu can coordinate Chl in both CP29 and Lhca1 (21, 37). In the case of Lhca3, an additional substitution is found at the putative Chl A5 binding site whose binding residue is asparagine, while histidine is found at this position in all Lhc complexes but Lhca4. The Asn versus His substitution was previously reported to be a conservative change for site A2 in Lhcb1 versus Lhcb4 since both amino acid residues were found to be active in the coordination of Chl *a* chromophores. We conclude that Chl binding sites A1, A2, A3, A4, A5, B3, B5, and B6 are present in both Lhca2 and Lhca3. On the basis of sequence analysis, we also suggest that a ninth Chl is accommodated in site B2. In fact, mutation analysis of LHCI has shown that Chl B2 is coordinated via the Chl ligand in site A2 (11, 38) when asparagine is the ligand of Chl A2 (as in Lhcb1, Lhcb5, and Lhca1), while site B2 is empty when histidine is the A2 ligand as in the case of Lhcb4 (21, 37, 38). It was suggested that Chl A2

may assume different orientations, which allows (Asn) or inhibits (His) in the coordination of the additional Chl in site B2 (32). Identification of the location for the tenth Chl ligand can only be tentative. In Lhca1, a Chl binding site has been proposed to be located near Chl A4 (21). Because of the high homology between Lhca proteins, it is possible that this Chl is present in all Lhca complexes.

The carotenoid composition of Lhca2 and Lhca3 is similar except for the presence of β -carotene in Lhca3 (0.5 molecules per polypeptide). The main xanthophyll is lutein, accounting for 1.5 and 1.65 molecules per polypeptide in Lhca2 and Lhca3, respectively, while 0.5 molecules of violaxanthin per monomer were found in Lhca2 versus 0.7 in Lhca3 (Table 2).

The analysis of the Lhcb antenna complexes has identified four carotenoid binding sites. Two of these sites, namely L1 and L2, are located in the center of the molecule and are occupied in all Lhc complexes analyzed so far (11, 36). The third site, N1, located in the C-helix domain, is available only in LHCII and possibly in Lhca1 complex (21, 39), while the loosely binding fourth site, V1, was so far only found in LHCII (40, 41). It seems thus likely that Lhca2 accommodates its two xanthophylls in sites L1 and L2. Site L1 has been shown to be occupied by lutein in all Lhc proteins so far analyzed. The high amount of lutein detected in Lhca2 is consistent with lutein occupancy of site L1 in this protein.

Three carotenoids are coordinated to Lhca3. While it is likely that two of them are accommodated in the L1 and L2 sites, the localization of the third xanthophyll can be discussed. Two sites are the possible candidates: location in site N1 would yield a strong red-shift of the ligand spectrum and an efficient energy transfer to Chl (42), while location in site V1 (40, 41, 43) would induce a smaller spectral shift without energy transfer to Chl *a*. The analysis of the excitation spectrum of Lhca3 revealed that one xanthophyll molecule, absorbing around 485–489 nm, does not transfer energy to Chls. This picture fits the characteristics for site V1 described in LHCII (41) thus suggesting this is the site occupied in the Lhca3 monomer. Although this third carotenoid is not active in light-harvesting, its binding to the complex appears to be rather specific: in fact, this site is able to exclude neoxanthin, which was present in the reconstitution mixture, from binding.

Recombinant versus Native. The Chl *a/b* ratio of the native LHCI preparation from *A. thaliana*, which contains all four Lhca complexes, is 3.3 (30.7 Chls *a* and 9.3 Chls *b* in a minimal unit including one polypeptide for each of the four Lhca) (7). Lhca1 and Lhca4 have been previously reconstituted in vitro using the same procedure here applied to Lhca2 and Lhca3. This led to recombinant proteins with a Chl *a/b* ratio of 4 and 2.3, respectively (see Table 2 for a summary of the pigment complement of the Lhca complexes) (7). Allowing for the presence of an identical number of individual Lhca per P700, we can calculate an averaged Chl *a/b* ratio for the reconstituted complexes of 3.04 (30.1 Chls *a* and 9.9 Chls *b*), which closely reproduces the value obtained on the native LHCI purified from chloroplasts (7).

Similar calculation for carotenoids shows that the four recombinant complexes bind together 10 carotenoid molecules, while nine were found to be associated to the native LHCI preparation. Possible explanations for this discrepancy include: (i) the native complexes are present in dimeric form,

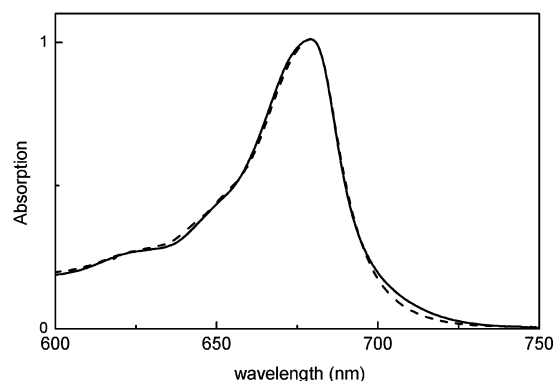


FIGURE 8: Comparison between absorption spectrum of the LHCI native fraction (solid) and the sum of Lhca2 and Lhca3 reconstituted monomers (dashed). The spectra of Lhca2 and Lhca3 normalized to the protein content before performing the sum.

while calculation is based on recombinant monomers. It is thus possible that the third xanthophyll-binding site of Lhca3 is occupied in monomers but not in the native dimers. (ii) Alternatively, we note that detergent treatment removes the xanthophyll in the site V1 of LHCII. Considering that the purification of native LHCI antennas requires harsh detergent treatment (0.5% zwittergent + 1% DM) and repeated freezing–thawing, it is likely that this site can be emptied in the purification of the native complex.

Previous comparison of the native LHCI preparation with the recombinant Lhca1-4 dimer has suggested that the sum of the spectroscopic properties of Lhca2 and Lhca3 has to be similar to that observed for the native LHCI preparation (7). The comparison of the absorption spectra is presented in Figure 8, where the sum of Lhca2 and Lhca3 spectra, obtained upon normalization to the protein concentration, is compared to the spectrum of the native preparation from *A. thaliana* (7). The two spectra are practically identical except for the range above 700 nm, where the native complex shows higher amplitude in the red tail. This difference can be ascribed to the fact that here we are analyzing monomers, while in the native preparation all complexes are in dimeric form. This is consistent with the previous finding that dimerization of Lhca1 and Lhca4 seems to increase the amplitude of the red-shifted spectral forms (7).

Red Forms. The absorption spectra of Lhca2 and Lhca3 are characterized by significant amplitude in the low energy tail, indicating the presence of red spectral Chl forms. This red tail is more pronounced in Lhca3 as compared to Lhca2, suggesting that the energy levels and/or the amplitude of the red forms in the two complexes are different. A similar difference was observed in the case of Lhca1 and Lhca4 proteins, the latter complex exhibiting more intense absorption at lower energy (18). In Figure 9, the absorption spectra at 77 K of the four Lhca complexes are presented. Lhca3 and Lhca4 show an intense red tail, while with different shapes. In Lhca1, the absorption at wavelengths longer than 700 nm is very small, and in Lhca2 a strong absorption component can be detected around 690 nm. Unfortunately, the absorption is structureless in this low energy region and does not allow determining with certainty the properties of each red absorption band. However, information about the energy levels can be obtained from the analysis of the fluorescence emission spectra, in which the contribution at low energy is strongly enhanced. In Figure 10, a comparison

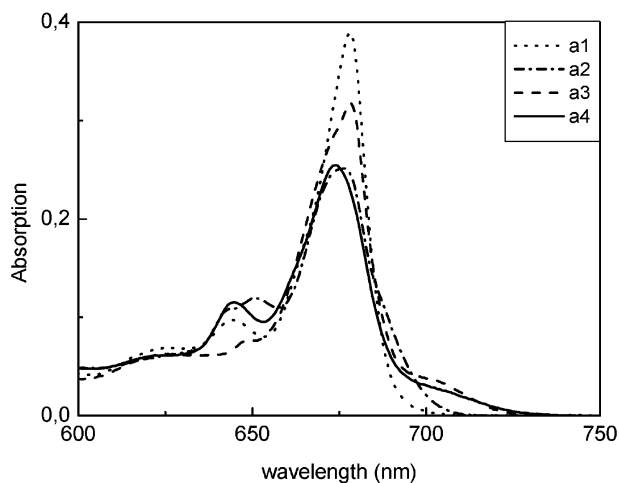


FIGURE 9: Comparison between the absorption spectra at 77 K of Lhca1 (dotted), Lhca2 (dash-dot), Lhca3 (dashed), and Lhca4 (solid). The spectra are normalized to the protein concentration.

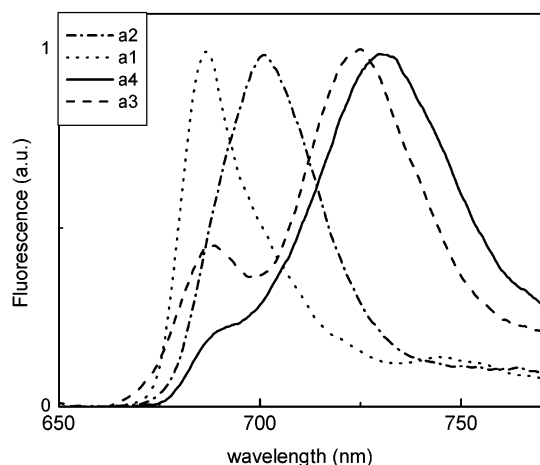


FIGURE 10: Comparison between the fluorescence emission spectra at 77 K of Lhca1 (dotted), Lhca2 (dash-dot), Lhca3 (dashed), and Lhca4 (solid). The spectra are normalized to the maximum.

of the fluorescence emission spectra at low temperature of the four Lhca complexes is presented. The emission peaks at 77 K of Lhca complexes are 686 nm for Lhca1, 701 nm for Lhca2, 725 nm for Lhca3, and 730 nm for Lhca4. Contributions at 701 nm for Lhca1, at 688 nm for Lhca2, and at 685–690 nm for both Lhca3 and Lhca4 can also be detected. It is thus clear that, although red forms are a common characteristic of the Lhca branch of Lhc family, their energy levels and their intensities differ in each complex. This heterogeneity may derive from different mechanisms: (i) the low energy absorptions originate in all complexes from the same pigment pool, and the differences in transition energies and/or intensities of the red forms in each complex are modulated by small changes in the protein/chromophore environment; (ii) two pigment pools, located in different protein environments, are responsible for the red emissions at 701–702 and 725–730 nm, and while in Lhca1 and Lhca2 only the higher energy form is present, in Lhca3 and Lhca4 both are present. Mutational analysis of Lhca1 indicates that the low energy forms of this complex originate from interactions between Chls in the domain formed by sites A5, B5, and B6 (21). The decrease of red forms upon mutation at site B5 and deletion of the N-terminal in Lhca4 suggest that the same domain is responsible for the low

energy absorption in Lhca4 (44, 45). While these results seem to indicate that the Chls absorbing at low energies are accommodated in the same sites in all Lhca complexes, more detailed analysis is required to support this hypothesis.

Role of Chl b in the Red Forms. It has been proposed that the large bathochromic spectral shifts of red forms may be due to strong Coulombic interactions between Chl molecules, leading to excitonic band splitting, with the red forms representing the low energy excitonic band of a Chl dimer (46–48). In the case of Lhca4, it has been shown that reconstitution in the absence of Chl *b* yields a complex that does not contain red forms, and it was proposed that Chl *b* can be one of the terms of the interaction leading the low energy absorption (35). Here we have performed the same experiment for Lhca3, which shows an intense red emission and used Lhca4 as control. Besides, we have also obtained a Lhca4 complex binding excess of Chl *b*. The choice of using a low Chl *a/b* ratio instead of reconstituting with only Chl *b* is based on preliminary experiments that have shown that reconstitution in the total absence of Chl *a* does not yield stable complexes for Lhca3 and Lhca4 (22, 35). In the case of Lhca3, neither the reconstitution with Chl *b* only (22) nor the complex in which Chl *b* is in strong excess (Chl *a* is still present in limiting amounts) yielded a folded protein. This indicates that several Chl binding sites need to be occupied by Chl *a* to obtain a stabilization of the complex. Reconstitution with only Chl *a* gives a stable product, which has properties similar to the control sample, in particular with respect to energy and amplitude of the red forms thus showing that Chl *b* does not play any role in determining the red absorption of Lhca3.

The situation appears different in the case of Lhca4. The sample reconstituted with only Chl *a* shows the emission maximum at 690 nm, but red emission at 730 nm is still detectable, although less intense than in the control sample. The presence of the 730 nm emission in Lhca4-a indicates that this form originates from Chl *a* molecules. The ratio between the emissions from the bulk and the red forms suggests that the preparation of Lhca4-a is heterogeneous. In fact, because of the high energetic difference between the bulk and the low energy forms, it is expected, for an equilibrated system, that the energy is emitted from the red forms. This is not the case at 77 or at 4 K (35), clearly indicating that there are at least two populations in the sample, one containing red forms, and the other depleted of this property. The presence of at least two conformations, having different fluorescence lifetimes, was previously described in the case of Lhc complexes (49). In Lhca4-a, the changes in the bound chromophores may have affected the equilibrium between the two conformations thus stabilizing the conformation with lower wavelength emission.

When Lhca4 is reconstituted with an excess of Chl *b* (Lhca4-b), the emission is still red, although the maximum is shifted 11 nm to the blue as compared to the control. This difference can be easily explained by hypothesizing that one of the two Chls *a* chromophores interacting in the control complex is substituted by a Chl *b* in Lhca4-b. Even in the case that the two Chls maintain the same relative distance, the same geometry, and the other partner of the interaction (a Chl *a*) has the same monomeric absorption as in the control sample, the presence of the Chl *b* as a second member of the interaction would reduce the excitonic shift in the

absorption because of two factors: (i) the value for the transition moment for Chl *b* is smaller than for Chl *a*, and this would reduce the value of the interaction strength (*J*); (ii) because of the larger energetic distance between the two monomers, the shift of each forms would be smaller. Another possible explanation is that the 719 nm emission form is already present in the control Lhca4 complex and that in the Lhca4-b the red most shifted forms, originating the 730 nm emission, is lost. This seems unlikely since the 719 nm emission was never detected in previous work (15, 19). However, this possibility cannot be ruled out at present.

The maintaining of the Chl–Chl interactions responsible for red-shifted forms in Lhca4-b despite major changes in the sites occupancy, while in the Lhca4-a complex these are strongly reduced and the complex destabilized, suggests that the role of Chl *b* is structural. The presence of a Chl *b* in one of the sites (possibly B6 according to the mutational analysis of Lhca1 (21)) is needed to keep the complex in the right conformation leading to the red forms. It is interesting to note that the stability of Lhca3 and Lhca4 proteins exhibiting strong red-shifted fluorescence emission is substantially lower (by approximately 10°) with respect to Lhca1 and Lhca2, while this effect does not depend on the number of carotenoids bound to each holoprotein. It thus appears that the maintaining of the special pigment–pigment interactions requires the adoption of a less stable conformation.

Do Lhca2 and Lhca3 Form Homo- or Heterodimers? It has been shown that all Lhca complexes are dimers in vivo (7). While in vitro reconstitution has shown that Lhca1 and Lhca4 forms heterodimers and that the energy is efficiently transferred from one subunit to the other (18, 20), it is at present not known whether Lhca2 and Lhca3 form homo- or heterodimers. Reconstitution of Lhca2 and Lhca3, in the same conditions leading to the formation of Lhca1-4 heterodimer, does not induce dimerization of these complexes (22), probably indicating that an unknown component is needed to stabilize the dimer but leaving the question open. Ihalainen et al. (15) showed that two low energy emitters at 702 and 730 nm, respectively, were present in the LHCI preparation containing all four complexes. The 730 nm emission was assigned to the Lhca1-4 heterodimer, in agreement with previous data, while the 702 nm was assigned to Lhca2 and/or Lhca3 homo/heterodimer(s).

The data in the present work show that the 701 nm emission originates from Lhca2 complex, while Lhca3 shows emission at 725 nm. If a heterodimer would be formed between these two complexes, then only the 725 nm emission is expected in the native preparation because of effective energy transfer between the two subunits as observed for the Lhca1-4 complex. The fact that the 702 nm component is detectable in the LHCI native preparation, where all complexes are in dimeric form, suggests that at least part of the Lhca2 and Lhca3 population forms a homodimer. This hypothesis is supported by the analysis of the lifetime decay of the LHCI native preparation (16) that suggests the presence of three different types of dimers.

CONCLUSIONS

In this work, we have obtained recombinant Lhca2 and Lhca3 holoprotein by refolding apoproteins overexpressed in *E. coli* with purified pigments. The pigment–protein

complexes were characterized for their biochemical and spectroscopic properties allowing a comparative study of the four gene product components of LHCI. These proteins are able to modulate the absorption/emission properties of specific Chls and to produce red-shifted spectral forms. While this seems to be a characteristic of all Lhca, it appears that the amplitude and the transition energy of these forms are different in the four complexes. Reconstitution of Lhca3 and Lhca4 with different Chl complements led to the conclusion that the red absorption originates from interaction between Chl *a* molecules and that any direct or indirect involvement of Chl *b* can be excluded for Lhca3. In Lhca4, Chl *b* may contribute to stabilization of a protein conformation allowing for the right geometry between Chl *a* molecules involved in the excitonic interaction yielding to red forms.

REFERENCES

- Mullet, J. E., Burke, J. J., and Arntzen, C. J. (1980) *Plant Physiol.* 65, 814–822.
- Bassi, R., Machold, O., and Simpson, D. (1985) *Carlsberg Res. Commun.* 50, 145–162.
- Bassi, R., and Simpson, D. (1987) *Eur. J. Biochem.* 163, 221–230.
- Jansson, S. (1999) *Trends Plant Sci.* 4, 236–240.
- Damm, I., Steinmetz, D., and Grimme, L. H. (1990) in *Current research in photosynthesis* (Baltscheffsky, M., Ed.) pp 607–610, Kluwer Academic Publishers, Dordrecht, The Netherlands.
- Croce, R., and Bassi, R. (1998) in *Photosynthesis: Mechanisms and Effects* (Garab, G., Ed.) pp 421–424, Kluwer Academic Publishers, Dordrecht, The Netherlands.
- Croce, R., Morosinotto, T., Castelletti, S., Breton, J., and Bassi, R. (2002) *Biochim. Biophys. Acta* 1556, 29–40.
- Boekema, E. J., Jensen, P. E., Schlodder, E., van Breemen, J. F., van Roon, H., Scheller, H. V., and Dekker, J. P. (2001) *Biochemistry* 40, 1029–1036.
- Jensen, P. E., Gilpin, M., Knoetzel, J., and Scheller, H. V. (2000) *J. Biol. Chem.* 275, 24701–24708.
- Scheller, H. V., Jensen, P. E., Haldrup, A., Lunde, C., and Knoetzel, J. (2001) *Biochim. Biophys. Acta* 1507, 41–60.
- Kühlbrandt, W., Wang, D. N., and Fujiyoshi, Y. (1994) *Nature* 367, 614–621.
- Green, B. R., and Pichersky, E. (1994) *Photosynth. Res.* 39, 149–162.
- Lam, E., Ortiz, W., and Malkin, R. (1984) *FEBS Lett.* 168, 10–14.
- Tjus, S. E., Roobol-Boza, M., Palsson, L.-O., and Andersson, B. (1995) *Photosynth. Res.* 45, 41–49.
- Ihalainen, J. A., Gobets, B., Sznee, K., Brazzoli, M., Croce, R., Bassi, R., van Grondelle, R., Korppi-Tommola, J. E. I., and Dekker, J. P. (2000) *Biochemistry* 39, 8625–8631.
- Gobets, B., Kennis, J. T. M., Brazzoli, M., Croce, R., van Stokkum, I. H., Bassi, R., Dekker, J. P., Van Amerongen, H., Fleming, G. R., and van Grondelle, R. (2001) *J. Phys. Chem. B* 105, 10132–10139.
- Plumley, F. G., and Schmidt, G. W. (1987) *Proc. Natl. Acad. Sci. U.S.A.* 84, 146–150.
- Schmid, V. H. R., Cammarata, K. V., Bruns, B. U., and Schmidt, G. W. (1997) *Proc. Natl. Acad. Sci. U.S.A.* 94, 7667–7672.
- Melkozernov, A. N., Schmid, V. H. R., Schmidt, G. W., and Blankenship, R. E. (1998) *J. Phys. Chem. B* 102, 8183–8189.
- Melkozernov, A. N., Lin, S., Schmid, V. H. R., Paulsen, H., Schmidt, G. W., and Blankenship, R. E. (2000) *FEBS Lett.* 471, 89–92.
- Morosinotto, T., Castelletti, S., Breton, J., Bassi, R., and Croce, R. (2002) *J. Biol. Chem.* 277, 36253–36261.
- Schmid, V. H. R., Potthast, S., Wiener, M., Bergauer, V., Paulsen, H., and Storf, S. (2002) *J. Biol. Chem.* 277, 37307–37314.
- Knoetzel, J., Svendsen, I., and Simpson, D. J. (1992) *Eur. J. Biochem.* 206, 209–215.
- Zhang, H., Goodman, H. M., and Jansson, S. (1997) *Plant Physiol.* 115, 1525–1531.
- Ganeteg, U., Strand, A., Gustafsson, P., and Jansson, S. (2001) *Plant Physiol.* 127, 150–158.

26. Sambrook, J., Fritsch, E. F., and Maniatis, T. (1989) *Molecular cloning. A laboratory manual*, Cold Spring Harbor Laboratory Press, Woodbury, NY.
27. Nagai, K., and Thøgersen, H. C. (1987) *Methods Enzymol.* 153, 461–481.
28. Paulsen, H., and Hobe, S. (1992) *Eur. J. Biochem.* 205, 71–76.
29. Giuffra, E., Cugini, D., Croce, R., and Bassi, R. (1996) *Eur. J. Biochem.* 238, 112–120.
30. Gilmore, A. M., and Yamamoto, H. Y. (1991) *Plant Physiol.* 96, 635–643.
31. Croce, R., Canino, G., Ros, F., and Bassi, R. (2002) *Biochemistry* 41, 7343.
32. Giuffra, E., Zucchelli, G., Sandona, D., Croce, R., Cugini, D., Garlaschi, F. M., Bassi, R., and Jennings, R. C. (1997) *Biochemistry* 36, 12984–12993.
33. Croce, R., Cinque, G., Holzwarth, A. R., and Bassi, R. (2000) *Photosynth. Res.* 62, 221–231.
34. Mukerji, I., and Sauer, K. (1990) *Curr. Res. Photosynth.* 2, 321–324.
35. Schmid, V. H., Thome, P., Ruhle, W., Paulsen, H., Kuhlbrandt, W., and Rogl, H. (2001) *FEBS Lett.* 499, 27–31.
36. Sandona, D., Croce, R., Pagano, A., Crimi, M., and Bassi, R. (1998) *Biochim. Biophys. Acta* 1365, 207–214.
37. Bassi, R., Croce, R., Cugini, D., and Sandona, D. (1999) *Proc. Natl. Acad. Sci. U.S.A.* 96, 10056–10061.
38. Remelli, R., Varotto, C., Sandona, D., Croce, R., and Bassi, R. (1999) *J. Biol. Chem.* 274, 33510–33521.
39. Croce, R., Remelli, R., Varotto, C., Breton, J., and Bassi, R. (1999) *FEBS Lett.* 456, 1–6.
40. Ruban, A. V., Lee, P. J., Wentworth, M., Young, A. J., and Horton, P. (1999) *J. Biol. Chem.* 274, 10458–10465.
41. Caffarri, S., Croce, R., Breton, J., and Bassi, R. (2001) *J. Biol. Chem.* 276, 35924–35933.
42. Croce, R., Muller, M. G., Bassi, R., and Holzwarth, A. R. (2001) *Biophys. J.* 80, 901–915.
43. Croce, R., Weiss, S., and Bassi, R. (1999) *J. Biol. Chem.* 274, 29613–29623.
44. Schmid, V. H. R., Paulsen, H., and Rupprecht, J. (2002) *Biochemistry* 41, 9126–9131.
45. Rupprecht, J., Paulsen, H., and Schmid, V. H. R. (2001) *Photosynth. Res.* 63, 217–224.
46. Gobets, B., Van Amerongen, H., Monshouwer, R., Kruip, J., Rögner, M., van Grondelle, R., and Dekker, J. P. (1994) *Biochim. Biophys. Acta* 1188, 75–85.
47. Savikhin, S., Xu, W., Soukoulis, V., Chitnis, P. R., and Struve, W. S. (1999) *Biophys. J.* 76, 3278–3288.
48. Engelmann, E., Tagliabue, T., Karapetyan, N. V., Garlaschi, F. M., Zucchelli, G., and Jennings, R. C. (2001) *FEBS Lett.* 499, 112–115.
49. Moya, I., Silvestri, M., Vallon, O., Cinque, G., and Bassi, R. (2001) *Biochemistry* 40, 12552–12561.

BI027398R

B 3

*Mutation Analysis of Lhca1 antenna
complex*

This chapter has been published in Journal of Biological Chemistry
277 (2002) pp. 36253 - 36261, reproduced with permission.

Tomas Morosinotto, Simona Castelletti, Jacques Breton,
Roberto Bassi and Roberta Croce

Mutation Analysis of Lhca1 Antenna Complex

LOW ENERGY ABSORPTION FORMS ORIGINATE FROM PIGMENT-PIGMENT INTERACTIONS*

Received for publication, May 23, 2002, and in revised form, June 13, 2002
Published, JBC Papers in Press, July 2, 2002, DOI 10.1074/jbc.M205062200

Tomas Morosinotto[‡], Simona Castelletti^{‡§}, Jacques Breton[§], Roberto Bassi^{‡¶},
and Roberta Croce^{‡||}

From the [‡]Dipartimento Scientifico e Tecnologico, Università di Verona. Strada Le Grazie, 15-37234 Verona, Italy and the [§]Service de Bioénergétique, Bâtiment 532 CEA-Saclay, 91191 Gif-sur-Yvette, France

The light harvesting complex Lhca1, one of the four gene products comprising the photosystem I antenna system, has been analyzed by site-directed mutagenesis with the aim of determining the chromophore(s) responsible for its long wavelength chlorophyll spectral form, a specific characteristic of the LHCI antenna complex. A family of mutant proteins, each carrying a mutation at a single chlorophyll-binding residue, was obtained and characterized by biochemical and spectroscopic methods. A map of the chromophores bound to each of the 10 chlorophyll-binding sites was drawn, and the energy levels of the Q_y transition were determined in most cases. When compared with Lhcb proteins previously analyzed, Lhca1 is characterized by stronger interactions between individual chromophores as detected by both biochemical and spectroscopic methods; most mutations, although targeted to a single residue, lead to the loss of more than one chromophore and of conservative CD signals typical of chlorophyll-chlorophyll interactions. The lower energy absorption form (686 nm at 100K, 688 nm at room temperature), which is responsible for the red-shifted emission components at 690 and 701 nm, typical of Lhca1, is associated with a chlorophyll a/chlorophyll a excitonic interaction originating from a pigment cluster localized in the protein domain situated between helix C and the helix A/helix B cross. This cluster includes chlorophylls bound to sites A5-B5-B6 and a xanthophyll bound to site L2.

The light-harvesting system of higher plant photosynthesis is composed of pigment-binding proteins belonging to the Lhc multigenic family (1). Lhc polypeptides are able to bind Chl¹ a, Chl b, and xanthophyll molecules in a suitable structural and dynamic mutual arrangement, ensuring high efficiency of energy transfer processes involved in light-harvesting and photo-protection (2, 3). Among Lhc proteins, only the structure of LHCI, the main antenna complex of photosystem II, has been determined at near atomic resolution, revealing the presence of three transmembrane helices, 12 Chls, two carotenoids, and

eight Chl-binding residues (4). Based on sequence comparison, it has been proposed that all Lhc proteins have a similar fold (5), characterized by a cross between helices A and B, stabilized by ionic pairs buried in the lipid bilayer, and stabilized by an helix C domain perpendicular to the membrane plane. Helix D is parallel to the luminal surface because of its amphiphilic nature. The first (A) and third (B) transmembrane helices and the putative Chl-binding ligands are highly conserved in all family members (6). Despite high homology, each complex has specific biochemical and spectroscopic properties that, although not yet fully understood, are thought to be the basis for the physiological role of each Lhc proteins. LHCI is characterized by low energy absorption forms that are responsible for the emission at wavelengths as long as 700 nm or more (7–9). Whereas it has been proposed that the amplitude of these “red” spectral forms is maximal in the Lhca4 complex (10), this seems to be a property of all Lhca proteins, thus exhibiting absorption and fluorescence emission spectra red-shifted as compared with the Lhcb proteins (12).² Lhca1 has two spectral forms absorbing at 688 and 700 nm and fluorescing with components at 690 and 701 nm, respectively, whose amplitude accounts for nearly one Chl molecule per holoprotein. Each polypeptide binds eight Chls a, two Chls b, and three xanthophylls molecules.² This is the most stable Lhca member so far expressed and reconstituted *in vitro* (10),² thus making it best suitable for an analysis of the origin of red spectral forms based on mutation studies. In this work, Lhca1 has been analyzed by site-selected mutagenesis at the putative Chl-binding sites and *in vitro* reconstitution. Comparison with the available data on CP29 and LHCI (13, 14) allows detection of multiple pigment-pigment interactions and the identification of a pigment-protein domain responsible for the peculiar low energy spectral forms of this pigment protein.

EXPERIMENTAL PROCEDURES

DNA Constructions—Mutation analysis on Lhca1 from *Arabidopsis thaliana*² was performed as previously reported (14).

Isolation of Overexpressed Lhca1 Apoproteins from Bacteria—Lhca1 WT and mutants apoproteins were isolated from the SG13009 strain of *Escherichia coli* transformed with constructs following a protocol described previously (15, 16).

Reconstitution and Purification of Lhca1-Pigment Complexes—These procedures were performed as described in Ref. 17 with the following modifications. The reconstitution mixture contained 420 μg of apoprotein, 240 μg of chlorophylls, and 60 μg of carotenoids in total 1.1 ml. The Chl a/b ratio of the pigment mixture was 4.0. The pigments used were purified from spinach thylakoids.

Protein and Pigment Concentration—HPLC analysis was as in Ref. 18. The chlorophyll to carotenoid ratio and the Chl a/b ratio were independently measured by fitting the spectrum of acetone extracts

* This work was funded by CNR “agenzia 2000” and by “MIUR” Progetto FIRB n.RBAU01ECX. The costs of publication of this article were defrayed in part by the payment of page charges. This article must therefore be hereby marked “advertisement” in accordance with 18 U.S.C. Section 1734 solely to indicate this fact.

¶ To whom correspondence should be addressed. Tel.: 390458027916; Fax: 390458027929; E-mail: bassi@sci.univr.it.

|| Present address: Istituto di biofisica, CNR Milano, c/o Dipartimento di Biologia, Via Celoria 26, 20133 Milano, Italy.

¹ The abbreviations used are: Chl, chlorophyll; HPLC, high performance liquid chromatography; LD, linear dichroism; Lhc, light-harvesting complex; LHCI and LHCI, light-harvesting complexes of photosystems I and II; Lu, lutein; WT, wild type.

² Croce, R., Morosinotto, T., Castelletti, S., Breton, J., and Bassi, R. (2002) *Biochim. Biophys. Acta*, in press.

with the spectra of individual purified pigments. For determination of pigment stoichiometry of different mutants, the Chl/apoprotein ratio of each mutant was determined using WT protein as reference. Chl concentration was determined as in Ref. 19, and the apoprotein content of every mutant was determined as previously reported (20).

Spectroscopy—The absorption spectra at room temperature and 100 K were recorded using a SLM-Aminco DK2000 spectrophotometer, in 10 mM Hepes, pH 7.5, 20% glycerol (60% at low temperature (LT)), and 0.06% *n*-dodecyl- β -D-maltopyranoside. The wavelength sampling step was 0.4 nm. Fluorescence emission spectra were measured using a Jasco FP-777 spectrofluorimeter and corrected for the instrumental response. The samples were excited at 440, 475, and 500 nm. The spectral bandwidth was 5 nm (excitation) and 3 nm (emission). Chlorophyll concentration was about 0.02 μ g/ml. LD spectra were obtained as described in Refs. 21 and 22 using samples oriented by the polyacrylamide gel squeezing technique.

The CD spectra were measured at 10 °C on a Jasco 600 spectropolarimeter. The optical density of the samples was 1 at the maximum in the Q_y transition for all complexes, and the samples were in the same solution described for absorption measurements. All of the spectra presented were normalized to the polypeptide concentration based on the Chl binding stoichiometry (23). The denaturation temperature measurements were performed by following the decay of the CD signal at 459 nm while increasing the temperature from 20 to 80 °C with a time slope of 1 °C/min and a resolution of 0.2 °C. The thermal stability of the protein was determined by finding the $t_{1/2}$ of the signal decay.

Photobleaching—The kinetics of Lhca1 WT and mutant photobleaching was measured as described (24) with a light intensity of about 6000 μ E m⁻² s⁻¹, and a sample temperature of 10 °C. The data were normalized at 100% at time 0 (initial and maximal absorbance = 0.6).

RESULTS

Sequence comparison shows that all amino acid residues that have been proven to bind Chl in Lhcb1 (14) are conserved in the Lhca1 sequence. The only difference detected was the substitution of the glutamine ligand of Chl in site B6 by a glutamate (1). Glutamate has been reported as Chl ligand in site B6 of CP29, whereas substitution of Gln with Glu in Lhcb1 did not prevent Chl binding (13).

In this work, each putative Chl-binding ligand was mutated to an apolar residue, as reported in Table I, to prevent Chl coordination in each individual site. In the case of sites A1 and A4, in which Chl is coordinated by a glutamate residue charge compensated by an arginine residue, both amino acids were mutated on the basis of previous experience with CP29, showing that noncompensated charges in transmembrane helices decreased complex stability and prevented protein folding (13). In the case of site B5, whose ligand is coordinated by an intrahelix ionic pair, both the single (E110V) and the double (E110V/R113L) mutations were performed. We only report on the results obtained by using the single mutant, essentially identical to those from the mutant carrying the double mutation.

The apoproteins were expressed in *E. coli* and then reconstituted *in vitro* with pigments. All of the mutant proteins yielded a folded complex upon reconstitution, as shown by the appearance of a green band upon sucrose gradient ultracentrifugation, but mutant A1, an indication that the Glu¹⁴⁸ (helix A)-Arg⁴⁹ (helix B) ionic bridge is essential for stabilization of Lhca1, as previously observed in CP29 (13). The green bands were harvested with a syringe and submitted to anion exchange chromatography to remove unspecifically bound pigments. The eluate was concentrated, and the aggregation state of Lhca1 WT and mutant proteins was investigated by ultracentrifugation into a density gradient that was shown to be effective in separating monomers from dimers and free pigments (10). As a reference we used WT Lhca1/Lhca4 heterodimer produced by co-refolding the two apoproteins with pigments in the presence of lipids (10).² In agreement with previous work (10), recombinant WT Lhca1 was monomeric and did not form homodimers or higher order aggregates. Fig. 1 shows the result of glycerol

TABLE I
Mutation at the putative Chl binding sites
For each putative Chl-binding site the target AA residue and the substituting residue are reported.

Site	A1	A2	A3	A4	A5	B3	B5	B6
Ligand	R49 E148	N151	Q165	E44 R153	H47	H181	E110 R113	E 102

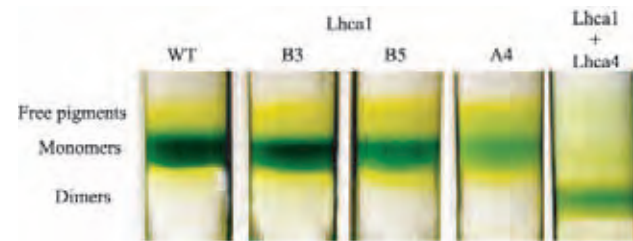


FIG. 1. Aggregation state of Lhca1 mutants. The mobility of WT Lhca1 and selected mutants (B3, B5, and A4) upon ultracentrifugation into a density gradient is compared with that of (monomeric) Lhca1 WT and the (dimeric) Lhca1-Lhca4 complex.

gradient ultracentrifugation of WT and three representative Lhca1 mutants, showing that they all have a sedimentation rate corresponding to monomeric aggregation state as was the case for the all mutant proteins not shown in the figure. The yield of reconstitution was differentially affected by each mutation, ranging from 90% of WT yield in the case of mutant B3 to 20% of WT yield in the case mutant A3 (A2, 55%; A4, 25%; A5, 75%; B5, 50%; and B6, 75%). Irrespective of the yield, the complex obtained showed the same mobility in the glycerol gradient, suggesting that no important changes were produced by the mutation in the overall structure of the complex. When native LHCI from *Arabidopsis* was ultracentrifuged in the same conditions, it exhibited the same sedimentation rate as the recombinant Lhca1/Lhca4 heterodimer (not shown) (25).²

The stability of the reconstituted holoproteins, as studied by the kinetic of CD signal decay with increasing temperature, is reported in Table II. Mutant at the site B3 ligand did not show a significant decrease in stability with respect to WT. The remaining mutations all produced a decrease in stability in the range of 20–30% as compared with WT.

Pigment Composition—The pigment composition of the mutant holoproteins was analyzed by HPLC and fitting of the spectra of the acetone extracts with the spectra of the individual pigments. The results are summarized in Table II. Interestingly, most of the mutants showed an increase of the Chl a/b ratio compared with WT. This was surprising; an opposite effect was expected because Lhca1 binds eight Chls a and two Chls b, and therefore the majority of the mutations should affect Chl a-binding sites and thus lead to a decrease in Chl a/b ratio. Nevertheless, a clear loss of Chl a was only observed in case of mutations at sites A3 and B3, whereas the mutations at sites A4, A5, B5, and B6 showed a loss of Chl b. It is interesting to note that most of the complexes were also affected in xanthophyll binding as shown by an increase of the Chl/carotenoid ratio in five mutants of seven. The violaxanthin/Lu ratio also changed in most cases, with a preferential loss of violaxanthin in mutants A5, B5, and B6 and of lutein in mutant A3, indicating at least partial selectivity of the carotenoid-binding sites.

The above results imply that both Chls and carotenoids were lost as a consequence of the mutations at most of the Chl-binding residues. To support this finding, pigment/protein stoichiometry was measured for each mutant protein.

TABLE II
Pigment composition of the Lhca1 mutants

The stability values are the averages of three measurements. The different mutants were reconstituted four times, and the pigment determination is the average of fitting of two acetone extract and two HPLC analysis for each reconstitution. Chl tot represents the Chl to protein stoichiometry.

Sample	Site	Stability °C	Chl a/b	Chl/car	Pigments per 100 Chl a ^a				V _x / Lu	Chl tot
					Chl b	N _x	V _x	Lu		
WT		54.1 ± 1.9	3.97 ± 0.13	3.35 ± 0.18	25.2	1.8	13.0	22.7	0.57	10
N151V	A2	45.3 ± 2.4	4.07 ± 0.15	3.43 ± 0.10	24.5	1.5	12.4	22.4	0.56	7.9 ± 0.6
Q165L	A3	46.1 ± 1.5	3.51 ± 0.03	3.31 ± 0.17	28.5	2.4	17.7	18.7	0.94	7.3 ± 0.9
E44V/R153L	A4	48.8 ± 0.4	5.62 ± 0.19	3.74 ± 0.15	17.8	1.4	10.3	19.7	0.52	7.7 ± 0.6
H47F	A5	39.2 ± 4.6	5.71 ± 0.27	3.48 ± 0.10	17.5	1.5	7.9	24.5	0.32	8.2 ± 0.8
H181F	B3	53.7 ± 2.1	3.79 ± 0.16	3.14 ± 0.09	26.4	0.9	15.2	24.1	0.63	9.0 ± 0.6
E110V	B5	38.7 ± 3	7.82 ± 0.06	3.79 ± 0.08	12.8	0.6	6.9	22.6	0.30	7.9 ± 0.5
E102V	B6	42.9 ± 2.9	5.66 ± 0.30	4.09 ± 0.23	17.7	0.2	6.5	22.0	0.30	9.4 ± 0.5

^a Average error, 5%.

The results are summarized in Table II. It clearly appears that only in two mutant proteins, namely B3 and B6, a single chlorophyll was lost, whereas mutations at sites A2, A3, A4, A5, and B5 brought the loss of two or three Chls. It was also confirmed that all of the mutants except for the one in site B3 lost part of their xanthophyll complement together with Chls ligands (Table II).

Absorption Spectra—Binding to individual sites has been shown to tune transition energy of each chromophore to different levels that determine pathway of energy equilibration within Lhc proteins. Further complexity is added to the system by pigment/pigment interactions producing additional energy levels. To determine the absorption properties of Chls in individual binding sites, the absorption spectra of WT and mutant Lhca proteins were recorded at 100 K (Fig. 2) and at room temperature (not shown). At least five Chl a (662, 669, 676, 682, and 688 nm) and two Chls b (644 and 651 nm) absorption forms have been reported as components of Lhca1 spectrum.² The main absorption peak was found at 680.5 and 678.5 nm at room temperature and 100 K, respectively, whereas a shoulder from Chl b absorption was detected at around 645 nm. Mutant proteins showed a blue shift of the major peak, thus implying that most of the mutations affected the environment of Chl a chromophores. In particular, WT minus mutant difference spectra (e.g. Figs. 6, 7, and 8A) indicated that spectral forms at 680 nm were associated to both sites A2 and A3, whereas a 663-nm form was clearly lacking in the mutant at site B3. A special feature of LHCI proteins is the presence of low amplitude, red-shifted, absorption forms. These are responsible for long wavelength fluorescence emission and can be detected at the long wavelength edge of the spectrum. Mutations at sites A5, B5, and B6 clearly showed a reduction in this red tail. These mutants also showed a decreased absorption at 644 nm, indicating a loss of Chl b.

Linear Dichroism—Absorption spectral components of Lhca1 are not readily associated to individual binding sites as previously obtained with Lhcb4 (13). This is due to the loss of more than one Chl upon mutation of a single Chl-binding ligand. An additional source of complexity is that pigments bound to mutant proteins may undergo frequency shift with respect to their absorption in the WT protein because of the loss of interacting neighbor pigments. In this case, two spectral effects combine: (i) the loss of forms originating from pigment-pigment interactions and (ii) the appearance of shifted absorption(s) from the residual noninteracting partner of a disrupted pair. In an attempt to gather more detailed information on the spectroscopic effects of mutations, we have analyzed LD spectra of WT *versus* mutant Lhca1 proteins. LD signals depend not only on absorption wavelength but also on the orientation of the dipole tran-

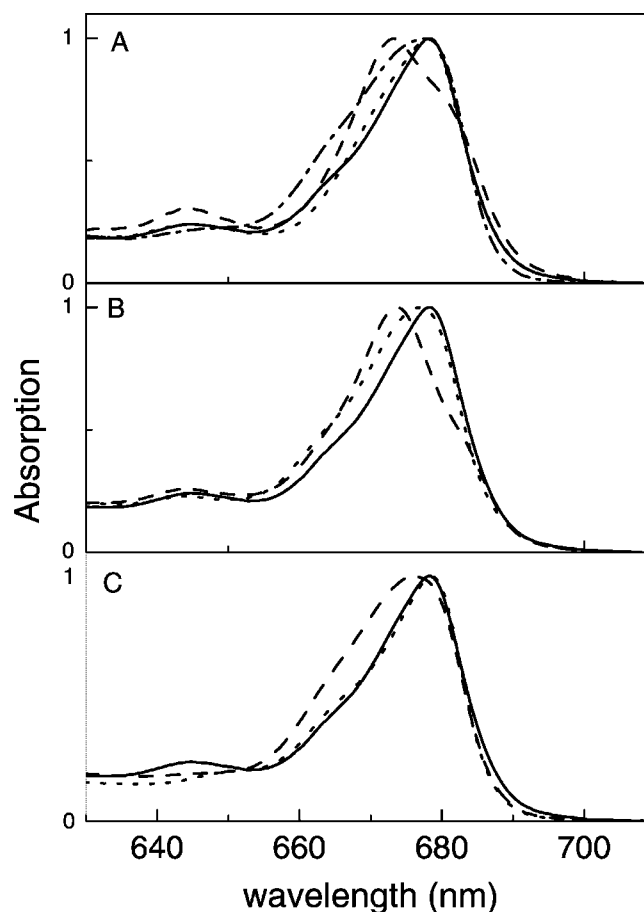


FIG. 2. Absorption spectra at 100 K of all reconstituted complexes. All the spectra are normalized to the maximum. In all of the panels the spectrum of the WT is reported (solid lines). A, dashed line, A3; dotted line, B3; dashed and dotted line, A5. B, dashed line, A2; dotted line, A4. C, dashed line, B5; dotted line, B6.

chromophores with similar transition energy but different orientations. The LD spectra of WT and mutants at 100 K are reported in Fig. 3 as normalized to the Chl a Q_y peak. The LD spectrum of WT Lhca1 holoprotein is characterized by a negative signal at 642 nm and two positive components at 652 and 679.8 nm. Only mutants B5 and B6 are affected in the amplitude of the 642 nm signal. The positive 680-nm signal from the Chl a Q_y transition was essentially unaffected by most mutations, showing at the most a minor red shift, except in the case of the A2 mutant whose spectrum was shifted to 677 nm. This indicates that a Chl a ligand in site A2 is responsible for most of the 680-nm LD signal. Mutants A4 and A5 lost positive LD

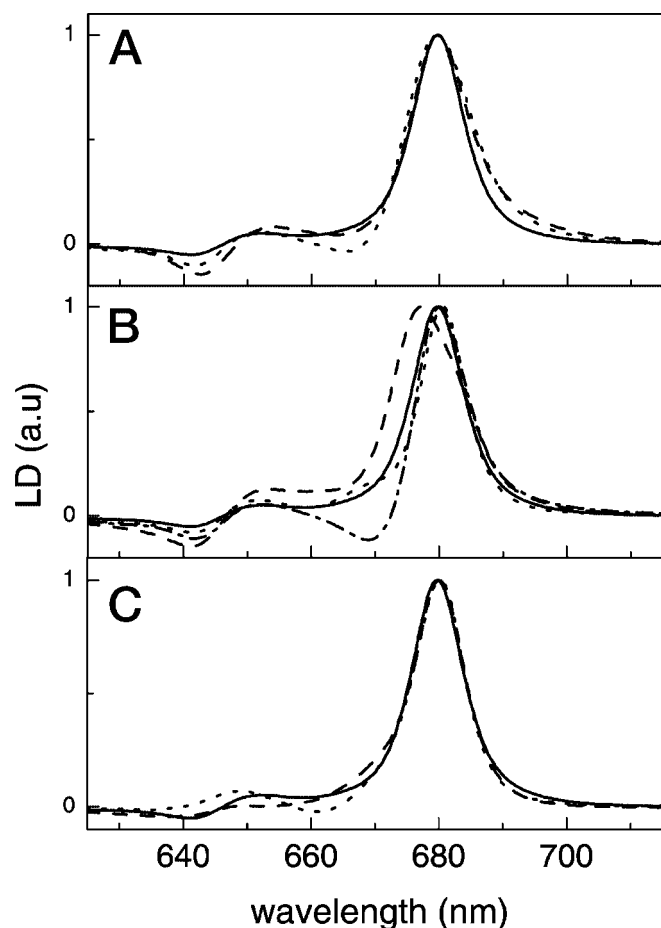


FIG. 3. Linear dichroism spectra at 100 K of Lhca1 complexes. All the spectra are normalized to the Chl *a* peak. In all of the panels the spectrum of the WT is reported (solid line). A, dashed line, A3; dotted line, B3. B, dashed line, A2; dotted line, A4; dashed and dotted line, A5. C, dashed line, B5; dotted line, B6.

around 677 nm, and their peaks are slightly red-shifted (by 0.8 and 0.4 nm, respectively), suggesting that the missing chromophores contribute to the blue edge of the main Chl *a* LD peak. Changes were observed in the 660–670-nm region for all of the mutant proteins. In particular, mutant A5 showed a strong negative contribution at 670 nm, whereas a negative contribution around 665 nm can be detected in mutants A3 and B3.

CD Spectra—The above results strongly suggest closer packing of pigments in Lhca1 with respect to Lhcb proteins. This should yield excitonic interactions that can be studied by circular dichroism. To test the presence of pigment/pigment interactions, CD spectra of all complexes were measured and are reported in Fig. 4. On the basis of the CD pattern in the 600–750-nm range, the mutants can be classified in two categories: (i) mutants A2, A3, and A4 showed the loss of a 683-nm (–) contribution and an increase of signal at 672 nm (+) (Fig. 4A) and (ii) mutants A5, B5, and B6 showed an increased amplitude of a 685 nm (–) signal and the disappearance of a contribution at 668 nm (–) (Fig. 4B). In the Soret region, changes in the CD spectrum were also detected; mutants A5 and B5 lost the major positive signal at 412 nm. They also lost a negative contribution at 501 nm, probably associated to a carotenoid molecule. This signal is possibly correlated to a contribution (+) at 430 nm, which decreases in the same mutants, suggesting the presence of a xanthophyll/Chl *a* interaction. An opposite effect was detected in the CD spectrum of the A2 mutant, where an increase of both signals was observed

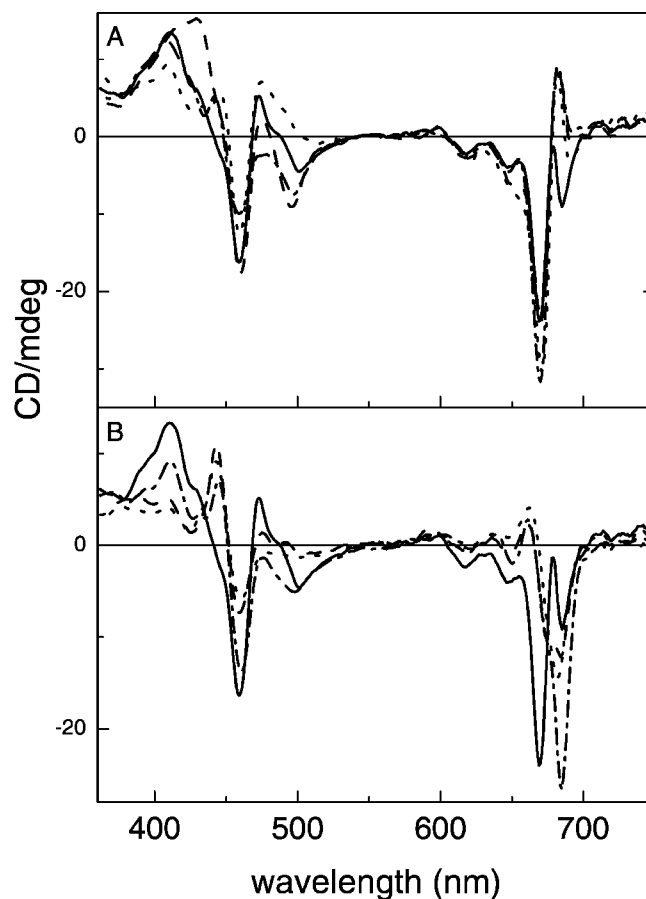


FIG. 4. Circular dichroism spectra at 10 °C of Lhca1 complexes. The spectra are normalized to the polypeptide concentration. In both panels the WT spectrum is presented (solid line). A, dashed line, A2; dotted line, A3; dashed and dotted line, A4. B, dashed line, A5; dotted line, B5; dashed and dotted line, B6.

along with a shift to the blue of the 497 nm (–) contribution. The signal in the 470–520-nm region is possibly the result of different effects; in the A3 mutant, the new positive contribution at 490 nm is probably related to the absence of a negative signal at this wavelength. Based on the biochemical data, which indicated loss of lutein in the A3 mutant, the negative signal at 490 nm can be attributed to this xanthophyll species. Also in this case, a decrease of the 430 nm (+) contribution can be observed, thus suggesting a lutein/Chl *a* interaction.

Fluorescence Emission Spectra—The fluorescence emission spectrum of WT Lhca1 shows a major peak at 685 nm, whereas two components at 690 and 701 nm are detectable toward longer wavelengths (10).² Mutants A2, A3, A4, and B3 show emission peak wavelengths identical to that of WT. The red-shifted component, however, has a higher amplitude in mutants A3 and A4, thus suggesting the loss of bulk Chl *a* without affecting the pigment-binding domain responsible for the low energy forms. The second group of mutants, namely A5, B5, and B6, showed a blue shift of the major peak by 2–3 nm and a decreased amplitude of low energy emission. The emission spectra of selected mutants, *i.e.* A4 and A5, at 100 K are presented in Fig. 5, together with the spectrum of WT Lhca1.

Photobleaching—The effect of mutations on photoprotection by quenching of triplet chlorophyll states was assessed by studying the kinetics of photobleaching (24). The kinetic of Q_y and absorption decay, upon strong illumination in the presence of O_2 , showed two kind of different behavior; mutants A2,

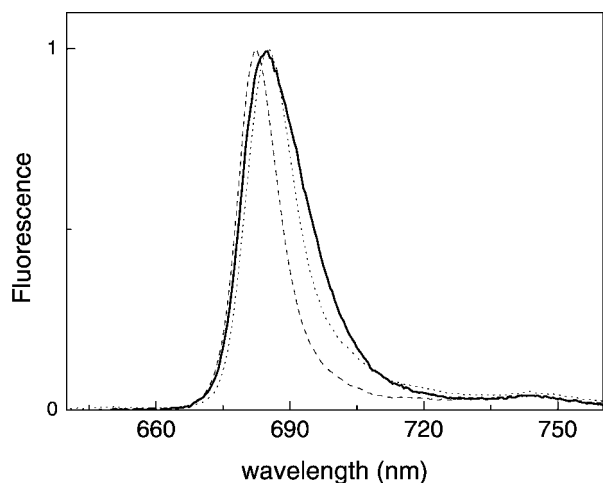


FIG. 5. **Fluorescence emission spectra at 100 K.** Lhca1 WT (dotted line), A4 (solid line), and A5 (dashed line) are shown. The spectra were recorded at 0.01 optical density. The spectra are normalized to the maximum.

A3, and B3 were similar to WT, whereas mutants A5, B5, and B6 were more sensitive to photobleaching (Fig. 6). Mutant A4 showed a somehow intermediate behavior; although the initial rate (0–5 min) of decay was as fast as those of the most sensitive mutants, longer times of exposure yielded a slow bleaching similar to that of WT.

DISCUSSION

Energy transfer within Lhc proteins is defined by the distance between chromophores, by their transition energy, and by the mutual orientation of transition vectors (26, 27). Determination of these major parameters has been difficult to obtain in higher plant antenna proteins by spectroscopic methods because of the high number of bound chromophores having their spectra overlapping the Q_y band. Recently, introduction of mutation analysis of Chl-binding residues allowed the interchange of individual amino acid residues, coordinating Chls through their central Mg^{2+} atom, and determination of individual chromophore spectra by difference spectroscopy. The case of CP29 (Lhcb4) was the simplest. This protein binds eight Chls and two xanthophylls, which have, if any, very weak excitonic interactions between each other (23). Each mutation led to the removal of a single Chl, and an individual spectral form was detected in the absorption difference spectrum (13, 28). A somewhat more complex situation was found in the major antenna protein LHCI (Lhcb1) that binds 12 Chl/polypeptide and shows excitonic interactions between a subset of its chromophores. Some Lhcb1 mutations caused removal of single Chls from the protein and of individual spectral forms. Other mutations led to the loss of multiple Chls and of excitonic interactions as detected by both absorption band shifts and by the disappearance of conservative CD signals (14). In the present study, mutation analysis was applied to Lhca1, a protein binding ten Chls and three xanthophylls.² This pigment protein was stable upon reconstitution *in vitro* from the apoprotein overexpressed in *E. coli* and purified pigments. Moreover, the recombinant protein showed characteristics corresponding to those of the native protein as judged by its capacity of forming heterodimers with Lhca4, which exhibited spectral features typical of native LHCI (10).² All of the Lhca1 mutants could refold in the presence of pigment with the exception of mutant A1, and the mutant proteins showed the same (monomeric) aggregation state as WT Lhca1 (10). Much of the data obtained with Lhca1 indicate an higher level of pigment/pigment interactions: (i) only two mutations (B3 and B6) caused the loss of a

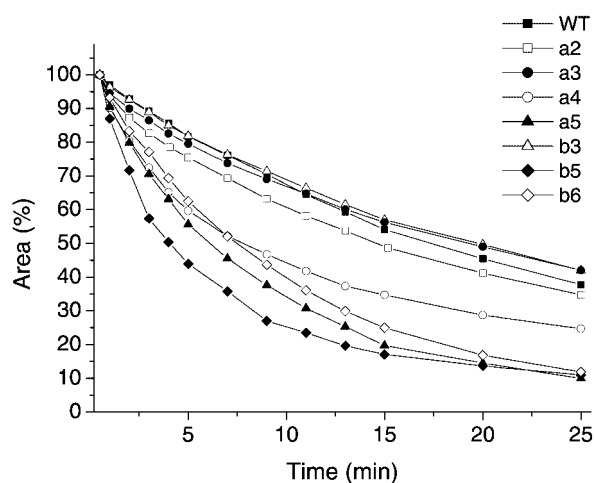


FIG. 6. **Photobleaching of Lhca1 mutants.** The decay curves show the total Q_y absorption relative to a 100% initial value. Points refer to experimental data.

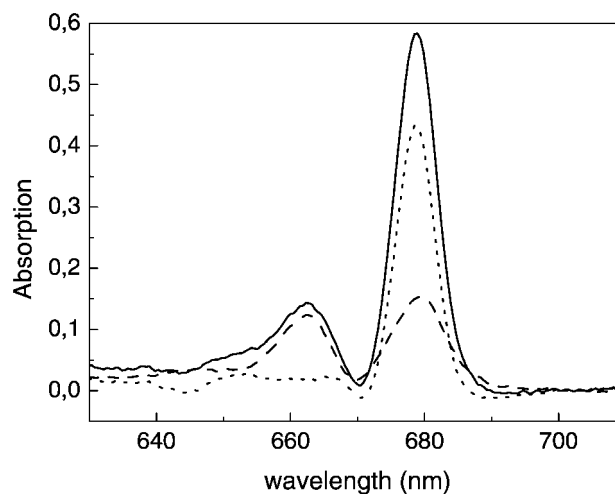


FIG. 7. **Spectroscopic analysis of A3 and B3 mutants.** Absorption difference spectra at 100 K of WT minus A3 (solid line), WT-B3 (dashed line), and B3-A3 (dotted line). The spectra were normalized to the Chl concentration before subtraction.

single Chl, whereas two Chls were lost in most cases. (ii) All of the mutations, except for the one in site B3, caused loss of xanthophylls, whereas in CP29 and LHCI this effect was found only for few specific mutations. (iii) WT minus mutant difference CD spectra showed the loss of conservative signals with the typical shape of an excitonic interaction in all mutants (e.g. Fig. 10B).

The involvement of most Lhca1 pigments into tight interactions is evidenced by the unexpected effect of mutations on the protein stability as assessed by thermal denaturation. In CP29 and LHCI, having a low level of pigment/pigment interactions, each mutation affected protein stability to a different extent, because of specific roles of each protein domain in maintaining protein folding (13, 24). The opposite was found in Lhca1; all of the mutations, except for A1, which prevented the formation of a stable pigment-protein complex, and B3, which has the same stability as WT, led to a similar decrease of protein stability. However, the effect was rather small and of similar amplitude for mutations in different structural domains, suggesting a more crucial role for interacting pigments in maintaining fold-

129 Lhca1 exhibits two major spectroscopic differences with respect to CP29 and LHCI: (i) a red-shifted "bulk" absorption of

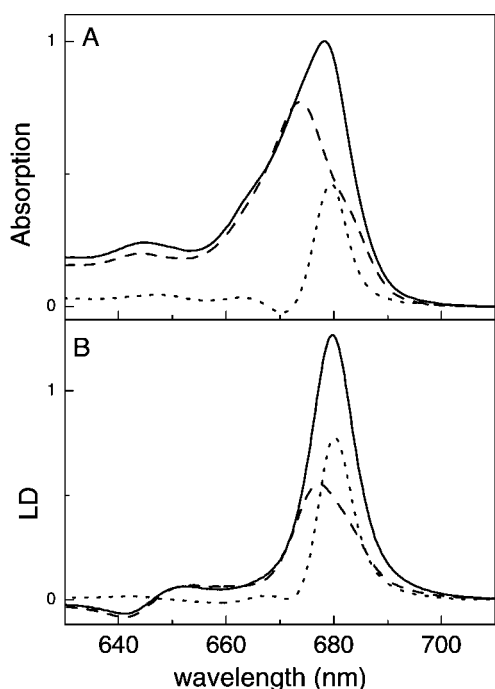


FIG. 8. **Spectroscopic analysis of A2 mutant.** Absorption (A) and LD (B) spectra at 100K of Lhca1-WT (solid lines) and A2 mutant (dashed lines) along with the difference spectrum (dotted lines). The absorption spectra are normalized to the polypeptide concentration before subtraction, whereas the linear dichroism spectra are normalized as reported in Ref. 27.

the Q_y transition as shown by the 680.5-nm peak and (ii) the presence of “minor” spectral forms further shifted to lower energies. It is interesting to discuss how pigment/pigment interactions contribute to each of these two effects.

In the following, we summarize the effects of individual mutations with the aim of identifying the chromophore bound to each individual site, its spectroscopic characteristics, and the interactions with neighbor pigments. In doing so we first analyze chromophores that only contribute to the bulk absorption band (sites A3, B3, A2, and A4) followed by those which also contribute to the low energy absorption forms (sites A5, B5, and B6).

Mutants Specifically Affecting Bulk Absorption

Mutants A3 and B3—The mutation on Chl B3 ligand has the smallest influence on the properties of the pigment-protein complex. Biochemical analysis clearly indicated the loss of one Chl a (0.9 Chl a and 0.1 Chl b). Nevertheless, two peaks with similar intensity, at 663 and 679 nm, were present in the WT minus B3 difference absorption spectrum (LT) (Fig. 7).

The mutation on Chl A3 ligand influences the binding of at least two Chls ligands. Again the LT (RT) difference spectrum shows two peaks at 663 (663.6) and 679 (681.6) nm, with a relative intensity of 1:3 (Fig. 7).

The above data strongly suggest the presence of an interaction between two Chls a bound to these two sites, in agreement with their close location in LHCI (4, 29). According to this figure, the WT minus A3 difference spectrum shows the absorption contribution of the two interacting Chls. Because the B3 mutant does not lose Chl A3 but loses the interaction, the B3 minus A3 difference spectrum reveals the contribution of the Chl A3 monomer. As shown in Fig. 7, this corresponds to a single band peaking at 678.5 nm. This absorption band is blue-shifted by 0.5–1 nm with respect to the low energy band of the interaction. The absorption of B3 monomer is thus expected to peak around 663 nm, similar to what is observed in LHCI

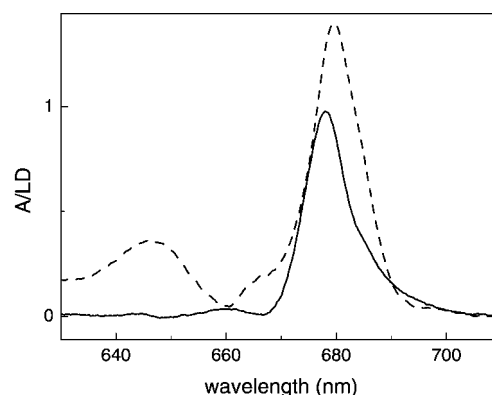


FIG. 9. **Spectroscopic analysis of A4 mutant.** The absorption (dashed lines) and LD (solid lines) difference spectra at 100 K of A4 mutant are shown. The spectra are normalized to the polypeptide concentration before subtraction, whereas the linear dichroism spectra are normalized as reported in Ref. 27.

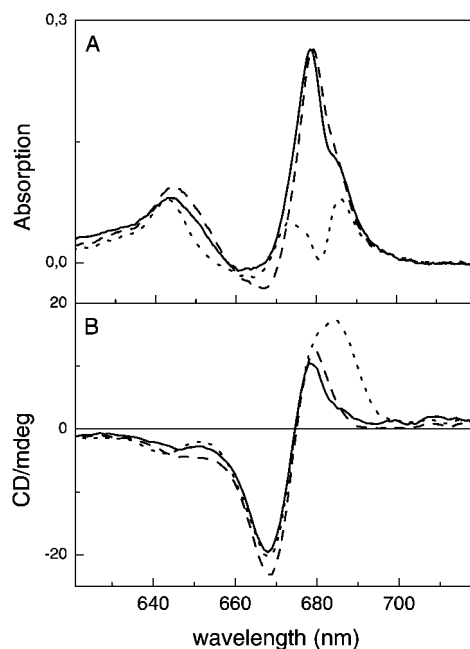
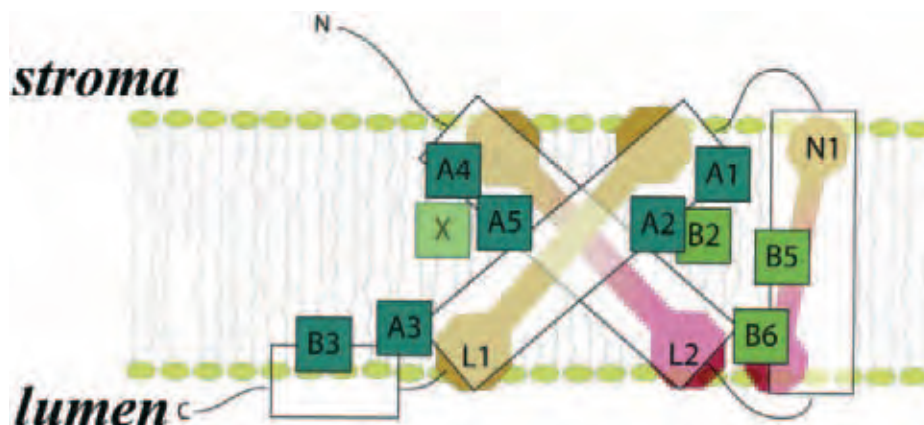


FIG. 10. **Spectroscopic analysis of A5, B5 and B6 mutants.** The absorption difference spectra at 100 K (A) and circular dichroism difference spectra (B) of WT-A5 (solid lines), WT-B5 (dashed lines), and WT-B6 (dotted lines) are shown. The spectra before subtraction are normalized to the polypeptide concentration.

(14). The small red shift of Chl A3 in the dimer is as expected for an interaction between two Chls rather distant in energy (around 350 cm^{-1}), because of the small value of the overlap integral between these two chromophores (23). The redistribution of the oscillating strength between the two monomers is rather strong, depending only on the angle between the dipole moments of the two pigments (30). A further result, highlighting a stronger pigment-pigment interaction in Lhca1 with respect to CP29 and LHCI, is the loss of one lutein molecule as an effect of mutation in site A3, whereas xanthophylls were not affected by the homologous mutation in LHCI and CP29. This is likely to be the lutein in site L1. In fact, site L1 has been found to be specific for lutein in all Lhc proteins so far analyzed (31–33) and is the only xanthophyll site located in close contact to Chl A3 (4). The loss of lutein in L1 can explain the high similarity of CD and LD spectra of mutants A3 and A2, suggesting that the loss of this xanthophyll may affect the organization of the A2-B2 domain, which is responsible

FIG. 11. Model of Lhca1 structure. Chl and carotenoid binding site occupancy were modified from Ref. 4. Chl a and mixed sites are indicated in blue and green, respectively; lutein and violaxanthin are in orange and purple, respectively. The wavelengths of absorption peak for individual chlorophylls are indicated in Table III.



for both the strong positive LD signal at 681 nm and the 684–672 nm excitonic interaction visible in the CD spectrum (see below).

Mutant A2—The mutation at the Chl A2 ligand induces the loss of two Chl molecules: 1.5 Chl a and 0.5 Chl b. The second lost Chl is here suggested to be Chl B2, because in the homologous protein LHCII B2 is the nearest neighbor to A2 (4) and has been shown to be bound through Chl A2 (14). WT minus A2 difference spectrum at LT (RT), shows a major Chl a peak at 679.5 (682) nm (Fig. 8A), whereas the Chl b contribution at LT (RT) is found at 649 (651) nm. A negative component in this difference spectrum is also observed at 670 nm and is attributed either to a shift induced by the mutation in the absorption of a neighbor Chl or to the absorption of a monomeric Chl upon disruption of an excitonic interaction (with Chl A4, see below). The presence of an excitonic interaction between Chls A2 and B2 is supported by the WT – mutant difference CD spectrum showing a conservative signal (Fig. 4), with contributions at 672 (+) and at 685 nm (–). The same signal disappears in the A4 mutant. The organization of the A2/B2/A4 domain in Lhca1 is thus homologous to that in LHCII, as suggested by the very similar effect of the mutations in sites A2 and A4. The only difference is that although site B2 was specific for Chl b in LHCII (14), it has a mixed Chl a/Chl b occupancy in Lhca1. The presence of a Chl ligand in site B2 is also supported by the ligation of Chl A2 by Asn (like in LHCII and CP26) rather than by His (as in CP29). This is consistent with the large amplitude of the LD signal of Chl A2 (Fig. 8B), characteristic of the specific orientation assumed by Chl A2 when binding Chl B2 (33). On the basis of difference spectra and of Chl a binding to site A2 in CP29 and LHCII (14), we assign the 679.5 nm (682 nm at room temperature) absorption to Chl A2, whereas in site B2 Chl b absorbs at 650 nm and Chl a absorbs at 682 nm.

In both CP29 and LHCII, Chl A2 was the red-most absorbing pigment (680 and 681 nm, respectively) and thus the principal fluorescence emitter. This is not the case in Lhca1; although the absorption properties of Chl A2 seem to be conserved across the family, the fluorescence spectrum of A2 mutant peaks at 685 nm as in the WT, and the low energy emission tail is still present, thus indicating that the red-most absorption in Lhca1 is not associated to this Chl.

Mutant A4—Mutant A4 loses two Chl molecules: 1.2 Chl a and 0.8 Chl b. The WT minus mutant difference spectrum shows two major peaks at 679 and 646 nm representing the absorption of Chl a and Chl b, respectively, but minor contributions at 684 (+), 674 (+), and around 660–670 nm were also detected (Fig. 9). These features clearly indicate that the mutations do not influence only the target site but also the spectroscopic characteristics of neighbor pigments. The difference LD spectrum shows a positive contribution at 678 nm, whereas

TABLE III
Properties of the Chl-binding sites in Lhca1 as derived from mutational analysis
The maximum value of the Q_y absorption band of Lhca1 chlorophylls at each binding site was determined at 100 K.

Site	Occupancy	Absorption
A1	A	ND ^a
A2	A	682
A3	A	680 (663–681)
A4	A	678–679
A5	A	675–679 (668–686)
B2	A/B	650/682
X	A/B	644/ND
B3	A	663 (663–681)
B5	A/B	644/(668–686)
B6	A/B	644/(668–686)

^a ND, not determined.

no changes were observed in the Chl b absorption region (Fig. 9). The CD spectrum of A4 mutant is identical to the spectrum of A2 mutant, in agreement with the results on LHCII (see the A2 mutant discussion), thus indicating the loss of the same excitonic interaction. On the basis of the homology with LHCII, we suggest that site A4 is occupied by a Chl a molecule peaking at 678 nm, whereas the second lost Chl is probably accommodated in B2 site, which shows mixed occupancy.

Mutants Affecting the Low Energy Absorption Forms

Mutant A5—This mutant loses 1.2 Chl a and 0.8 Chl b with respect to WT Lhca1. It is interesting to consider that only one Chl a was lost upon mutation on A5 ligand in both CP29 and LHCII, suggesting that one additional Chl, held in place by interactions with other Chls rather than with a specific amino acid residue, is present in Lhca1. The difference absorption spectrum (Fig. 10A) shows several contributions: a major 679-nm signal and a shoulder at 686 nm in Chl a region, whereas a Chl b contribution is observed at 644 nm. In agreement with previous finding in CP29 and LHCII, we suggest that site A5 binds Chl a and that a Chl b site is also affected by the mutation. Based on the LHCII structure, the only site located in close proximity to Chl A5 is site B5. However, it is quite unlikely that mutant A5 loses also Chl in site B5, which is bound in a different protein domain and has a defined ligand on the protein. Moreover, pigment analysis and LD spectra clearly show that A5 and B5 mutants do not lose the same Chls; the 642 nm (–) signal disappears in mutant B5, whereas it is conserved in the LD spectrum of mutant A5. On this basis we propose the presence of a new site in Lhca1. This site should have mixed Chl a/Chl b occupancy but higher affinity for Chl b (0.8 versus 0.2). The bound Chl should be located in the proximity of Chl A5 and should be oriented close to the magic angle as suggested by the absence of a detectable LD signal. We

cannot exclude that this site corresponds to site B1 in LHCII. Nevertheless, the distance (13.4 Å) appears to be too large for a proximity effect similar to that described for the loss of Chl B2 in the mutant A2. The determination of the energy transition of Chl a in site A5 is not straightforward; the WT minus A5 difference absorption spectrum shows a major contribution at 679 nm, whereas the LD spectrum shows changes in shape at around 675 nm (Fig. 3). The WT minus A5 difference CD spectrum shows the presence of excitonic interactions adding uncertainty to the attribution (see below). At the moment, we cannot explain this discrepancy and are thus forced to leave this question open.

Mutants B5—The ligand of site B5 is constituted by a ionic pair that has the double function of coordinating Chl B5 and providing end-capping of helix C. In Lhca1, the B5 mutant loses two Chls (0.9 Chl a and 1.1 Chl b) with respect to WT. It is interesting to observe that in LHCII, the double mutation induced the loss of additional Chls (namely A6 and A7), whereas in Lhca1, the E110V/R113L double mutation yields a complex with the same biochemical and spectroscopic characteristics as the single (E110V) mutant. This suggests that sites A6 and A7 are not present in the Lhca1 structure. The absorption difference spectrum is almost identical to the one of A5 mutant in which positive contributions at 644, 678.5, and 686 nm were detected (Fig. 10A). In the LD spectrum, the negative signal associated to a 643-nm Chl b disappears. Among all mutants, only B5 and B6 lose the Chl b LD signal (Fig. 3), thus implying that the second Chl lost upon mutation in site B5 is Chl B6. On the basis of the pigment analysis, which indicates that site B6 is a mixed site with 65% Chl b occupancy (see below), we can conclude that site B5 also shows mixed occupancy (1:1, Chl a:Chl b).

Mutant B6—The pigment analysis of B6 mutant indicates the loss of one Chl: 0.35 Chl a and 0.65 Chl b, thus attributing mixed occupancy to the B6 site. This is consistent with previous results with CP29. In fact, glutamate as ligand for Chl in B6 confers mixed occupancy to this site (13). On the contrary, the spectroscopic effects are strikingly different with respect to CP29; the absorption difference spectrum shows at least three positive contributions peaking at 643, 673, and 686 nm and two negatives at 665 and 680 nm (Fig. 10A), suggesting that the B6 ligand is involved in tight interactions with neighbor pigments. The nearest neighbors are sites A5 and B5 and mutations at these three sites lead to the loss of the 686-nm absorption form and of the red-shifted emission contributions at 690 and 701 nm. The difference CD spectrum supports this view: an excitonic signal (685 nm (+)/668 nm (-)) is lost in the B6 mutant, similar to what is observed for A5 and B5 complexes (Fig. 10B). We conclude that interactions between Chls bound to the protein domain in between helix C and the helix A-helix B crossing are responsible for the low energy absorption forms in Lhca1. However, a detailed interpretation is not straightforward. A possible explanation considers the presence of an excitonic interaction between two of the Chls in sites A5, B5, and B6. Excitonic interactions have been so far detected between Chl A2/B2 (14) and Chl A3/B3 (this work) having edge to edge distances below 5 Å. The distances between the components of the A5/B5/B6 cluster are of 4.8, 7.4, and 10.5 Å for the A5/B5, B5/B6, and A5/B6 pairs, respectively, based on LHCII structure (4). Our best hypothesis is that the Chl a/Chl a excitonic interaction originates from interactions between Chl A5 and the Chl a component in site B5. Yet mutation at site B6 disrupts the interaction. The influence of Chl B6 on the putative Chl A5/Chl B5 interaction may well be mediated by the xanthophyll in site L2, which is lost upon mutation in site B6. Chl A5 is in close contact with the xanthophyll in site L2, and its

absence could change the orientation/distance of Chl A5 with respect to Chl B5. This scheme is similar to that described above for the effect of the A3 mutation on the orientation of Chl A2 through the loss of lutein in site L1. The violaxanthin in site L2 is somewhat special, having its S_0 - $S_{2,0}$ transition at 501 nm, thus red-shifted by 28 nm with respect to its absorption in acetone. Because violaxanthin bound to sites L1, L2, and V1 of LHCII is shifted by 19, 19, and 12 nm, respectively (31, 34), it appears that in Lhca1, violaxanthin undergoes a special interaction that yields into the red-most absorption observed for a violaxanthin molecule in a protein environment. This violaxanthin spectral form is lost in all three mutants.

Whereas the details are not completely clear, we propose that the red-most absorption of the Lhca1 complex originates from an excitonic interaction leading to a high energy band around 668 nm and a low energy contribution at 686 nm, which involves the domain composed by Chls A5, B5, and B6 and carotenoid L2. The absorption wavelength of the band indicates that two Chls a and possibly a carotenoid molecule are involved in the interaction. We suggest that red forms originate in Lhca4 from a similar chromophore organization. The requisite for Chl b to generate the red emission in Lhca4 (35) may thus consist of the occupancy of site B6 by Chl b.

Mutant A1—The mutant affected at site A1 does not fold *in vitro*, confirming the primary role of the Glu¹⁴⁸-Arg⁴⁹ ionic bridge, not only as a ligand for Chl A1 but also in the stabilization of protein folding. The same effect was previously observed in both CP29 and LHCII (13, 14). By computation of the Chl a *versus* Chl b occupancy in the other sites, it clearly appears that site A1 accommodates a Chl a molecule as was the case in CP29 and LHCII. A description of site occupancy in Lhca1 and of the wavelength absorption peak for individual Chls is given in Fig. 11 and Table III.

Lhca1 in the Lhca1-4 Heterodimer

The comparison between the CD spectra of Lhca1 and Lhca4 monomers with Lhca1-4 heterodimer showed that, in the dimer, the negative contribution at 669 nm, typical of Lhca1, is lost.² This suggests that the pigment(s) responsible for this signal in Lhca1 are involved in the dimerization process. Because this signal is clearly associated with Chls A5, B5, and B6, we suggest that the C helix domain is involved in dimerization.

Carotenoid-binding Sites in Lhca1

Lhca1 has three xanthophyll-binding sites that can accommodate both violaxanthin and lutein when refolded *in vitro*.² Most mutants are affected in the carotenoid binding, thus allowing localization into individual sites. Mutation A3 shows that lutein is preferentially bound to L1 site and has an $S_{2,0,0}$ transition at 492 nm, as detected by absorption difference spectra (not shown). The remaining two xanthophylls, 1.2 violaxanthin and 0.8 lutein, are located in sites L2 and N1. From the analysis of the mutant A5 (located in close proximity of L2) and B5 (close to site N1), it can be concluded that both sites bind lutein and violaxanthin. We thus propose that the affinity of the three xanthophyll-binding sites is as follows: Lu in L1, Lu + violaxanthin in L2 in agreement with results with Lhcb1, and Lu + violaxanthin + neoxanthin traces in N1 (Fig. 11). An important issue derives from the photobleaching experiments; removal of lutein from site L1 did not lead to a substantial increase of photobleaching. This is in contrast with previous results with LHCII (24) showing that lutein in site L1 was essential for Chl triplet quenching. We suggest that L2 rather than L1 is the primary ³Chl* quencher in Lhca1. This might be due to a different conformation of Lhca *versus* Lhcb protein as discussed below.

Lhca versus Lhcb

A major difference between Lhca and Lhcb proteins consists of their different fluorescence yield, which is lower in Lhca. Fluorescence decay kinetic shows three lifetime components in Lhca1: 0.35, 1.7, and 3.6 ns that account, respectively, for 27, 53, and 20% of the total decay (36). The same lifetime components have been found in Lhcb proteins, although with different relative amplitudes, the 3.6-ns lifetime having the highest amplitude (37, 38). Lhcb proteins may undergo conformational changes to a low fluorescence conformation in excess light conditions upon triggering of NPQ (37) and/or incorporation of zeaxanthin into the L2 site (11, 24). Lhca proteins appear to assume a constitutive “dissipative” conformation, thus suggesting that the “quenched” conformation of Lhcb proteins is similar to that of Lhca proteins. The study of Lhca proteins may therefore be important not only for the understanding of their role as antenna for photosystem I but also as models for the mechanism of nonradiative dissipation in photoprotection.

REFERENCES

- Jansson, S. (1999) *Trends Plant Sci.* **4**, 236–240
- Van Amerongen, H., and van Grondelle, R. (2001) *J. Phys. Chem. B* **105**, 604–617
- Bassi, R., and Caffarri, S. (2000) *Photosynthesis Res.* **64**, 243–256
- Kühlbrandt, W., Wang, D. N., and Fujiyoshi, Y. (1994) *Nature* **367**, 614–621
- Green, B. R., Pichersky, E., and Kloppstech, K. (1991) *Trends Biochem. Sci.* **16**, 181–186
- Pichersky, E., and Jansson, S. (1996) in *Oxygenic Photosynthesis: The Light Reactions* (Ort, D. R., and Yocum, C. F., eds) pp. 507–521, Kluwer Academic Publishers, Norwell, MA
- Mullet, J. E., Burke, J. J., and Arntzen, C. J. (1980) *Plant Physiol.* **65**, 814–822
- Wollman, F.-A., and Bennoun, P. (1982) *Biochim. Biophys. Acta* **680**, 352–360
- Bassi, R., and Simpson, D. (1987) *Eur. J. Biochem.* **163**, 221–230
- Schmid, V. H. R., Cammarata, K. V., Bruns, B. U., and Schmidt, G. W. (1997) *Proc. Natl. Acad. Sci. U. S. A.* **94**, 7667–7672
- Crimi, M., Dorra, D., Bosinger, C. S., Giuffra, E., Holzwarth, A. R., and Bassi, R. (2001) *Eur. J. Biochem.* **268**, 260–267
- Ihalainen, J. A., Gobets, B., Sznee, K., Brazzoli, M., Croce, R., Bassi, R., van Grondelle, R., Korppi-Tommola, J. E. I., and Dekker, J. P. (2000) *Biochemistry* **39**, 8625–8631
- Bassi, R., Croce, R., Cugini, D., and Sandona, D. (1999) *Proc. Natl. Acad. Sci. U. S. A.* **96**, 10056–10061
- Remelli, R., Varotto, C., Sandona, D., Croce, R., and Bassi, R. (1999) *J. Biol. Chem.* **274**, 33510–33521
- Nagai, K., and Thøgersen, H. C. (1987) *Methods Enzymol.* **153**, 461–481
- Paulsen, H., Finkenzeller, B., and Kuhllein, N. (1993) *Eur. J. Biochem.* **215**, 809–816
- Giuffra, E., Cugini, D., Croce, R., and Bassi, R. (1996) *Eur. J. Biochem.* **238**, 112–120
- Gilmore, A. M., and Yamamoto, H. Y. (1991) *Plant Physiol.* **96**, 635–643
- Porra, R. J., Thompson, W. A., and Kriedemann, P. E. (1989) *Biochim. Biophys. Acta* **975**, 384–394
- Pagano, A., Cinque, G., and Bassi, R. (1998) *J. Biol. Chem.* **273**, 17154–17165
- Haworth, P., Arntzen, C. J., Tapie, P., and Breton, J. (1982) *Biochim. Biophys. Acta* **679**, 428–435
- Haworth, P., Tapie, P., Arntzen, C. J., and Breton, J. (1982) *Biochim. Biophys. Acta* **682**, 152–159
- Giuffra, E., Zucchelli, G., Sandona, D., Croce, R., Cugini, D., Garlaschi, F. M., Bassi, R., and Jennings, R. C. (1997) *Biochemistry* **36**, 12984–12993
- Formaggio, E., Cinque, G., and Bassi, R. (2001) *J. Mol. Biol.* **314**, 1157–1166
- Croce, R., and Bassi, R. (1998). in *Photosynthesis: Mechanisms and Effects* (Garab, G., ed) pp. 421–424, Kluwer Academic Publishers, Norwell, MA
- Forster, T. (1965) in *Modern Quantum Chemistry: Action of Light and Organic Crystals* (Sinanoglu, O., ed) pp. 93–137, Academic Press, New York
- Knox, R. S. (1975) in *Bioenergetics of Photosynthesis: Cell Biology* (Govindjee, ed) pp. 183–221, Academic Press, New York
- Simonetto, R., Crimi, M., Sandona, D., Croce, R., Cinque, G., Breton, J., and Bassi, R. (1999) *Biochemistry* **38**, 12974–12983
- Trinkunas, G., Connelly, J. P., Müller, M. G., Valkunas, L., and Holzwarth, A. R. (1997) *J. Phys. Chem. B* **101**, 7313–7320
- Cantor, C. R., and Schimmel, P. R. (1980) *Biophysical Chemistry*, Vol. II, pp. 390–398, W. H. Freeman and Company, New York
- Croce, R., Weiss, S., and Bassi, R. (1999) *J. Biol. Chem.* **274**, 29613–29623
- Hobe, S., Niemeier, H., Bender, A., and Paulsen, H. (2000) *Eur. J. Biochem.* **267**, 616–624
- Croce, R., Canino, G., Ros, F., and Bassi, R. (2002) *Biochemistry* **41**, 7334–7343
- Caffarri, S., Croce, R., Breton, J., and Bassi, R. (2001) *J. Biol. Chem.* **276**, 35924–35933
- Schmid, V. H., Thome, P., Ruhle, W., Paulsen, H., Kuhlbrandt, W., and Rogl, H. (2001) *FEBS Lett.* **499**, 27–31
- Melkozernov, A. N., Schmid, V. H. R., Schmidt, G. W., and Blankenship, R. E. (1998) *J. Phys. Chem. B* **102**, 8183–8189
- Moya, I., Silvestri, M., Vallon, O., Cinque, G., and Bassi, R. (2001) *Biochemistry* **40**, 12552–12561
- Polivka, T., Zigmantas, D., Sundstrom, V., Formaggio, E., Cinque, G., and Bassi, R. (2002) *Biochemistry* **41**, 439–450

B 4

The chromophore organization of the Lhca2 subunit of higher plant photosystem I reveals the origin of its 701 nm fluorescence emission form

This chapter has been published in Journal of Biological Chemistry 279 (2004) pp 48543 - 48549, reproduced with permission.

Roberta Croce, Tomas Morosinotto, Janne A. Ihalainen, Agnieszka Chojnicka, Jacques Breton, Jan P. Dekker, Rienk van Grondelle and Roberto Bassi

Origin of the 701-nm Fluorescence Emission of the Lhca2 Subunit of Higher Plant Photosystem I*

Received for publication, August 4, 2004, and in revised form, August 24, 2004
Published, JBC Papers in Press, August 24, 2004, DOI 10.1074/jbc.M408908200

Roberta Croce^{‡§}, Tomas Morosinotto^{¶||}, Janne A. Ihalainen^{**}, Agnieszka Chojnicka^{**},
Jacques Breton^{‡‡}, Jan P. Dekker^{**}, Rienk van Grondelle^{**}, and Roberto Bassi^{¶||}

From the [‡]Istituto di Biofisica, CNR, Trento, *clo ITC via Sommarive 18, Povo, Trento 38100, Italy*,
[¶]Dipartimento Scientifico e Tecnologico, Università di Verona, *15 Strada Le Grazie, Verona 37134, Italy*,
^{||}Université Aix-Marseille II, LGBP- Faculté des Sciences de Luminy, Département de Biologie, Case 901,
163 Avenue de Luminy, Marseille 13288, France, ^{**}Faculty of Science, Division of Physics and Astronomy,
Vrije Universiteit, De Boelelaan 1081, 1081 HV Amsterdam, The Netherlands, and ^{‡‡}Service de Bioenergetique,
Bat. 532, Commissariat a l'Energie Atomique, Saclay, Gif-sur-Yvette Cedex 91191, France

Photosystem I of higher plants is characterized by red-shifted spectral forms deriving from chlorophyll chromophores. Each of the four Lhca1 to -4 subunits exhibits a specific fluorescence emission spectrum, peaking at 688, 701, 725, and 733 nm, respectively. Recent analysis revealed the role of chlorophyll-chlorophyll interactions of the red forms in Lhca3 and Lhca4, whereas the basis for the fluorescence emission at 701 nm in Lhca2 is not yet clear. We report a detailed characterization of the Lhca2 subunit using molecular biology, biochemistry, and spectroscopy and show that the 701-nm emission form originates from a broad absorption band at 690 nm. Spectroscopy on recombinant mutant proteins assesses that this band represents the low energy form of an excitonic interaction involving two chlorophyll *a* molecules bound to sites A5 and B5, the same protein domains previously identified for Lhca3 and Lhca4. The resulting emission is, however, substantially shifted to higher energies. These results are discussed on the basis of the structural information that recently became available from x-ray crystallography (Ben Shem, A., Frolow, F., and Nelson, N. (2003) *Nature* 426, 630–635). We suggest that, within the Lhca subfamily, spectroscopic properties of chromophores are modulated by the strength of the excitonic coupling between the chromophores A5 and B5, thus yielding fluorescence emission spanning a large wavelength interval. It is concluded that the interchromophore distance rather than the transition energy of the individual chromophores or the orientation of transition vectors represents the critical factor in determining the excitonic coupling in Lhca pigment-protein complexes.

Photosystems I and II have a common general organization including a core complex moiety, binding Chl¹ *a* and β -caro-

tene, and an outer antenna moiety, binding Chl *a*, Chl *b*, and xanthophylls. Nonetheless, their spectroscopic properties are substantially different. Both compartments of the PSI super-complex are enriched in red-shifted chlorophyll absorption forms, whereas those of PSII are not. This property of PSI results in a preferential light harvesting in the near infrared spectral region (>700 nm) and causes the so-called "Emerson effect" that opened the way to the discovery of the two photosystems (1). In green plants, LHCI, the outer antenna of PSI, is the most red form-enriched compartment and is composed of four different complexes, the products of the genes *lhca1* to -4 (2). These complexes are located on one side of the core complex (3, 4) and can be isolated as dimers (5). The Lhca proteins belong to the Lhc multigenic family, and they share high sequence homology with the antenna complexes of PSII (6). Despite these strong similarities, the spectroscopic properties of Lhca and Lhcb complexes are very different. In particular, the emission spectrum of LHCI peaks at 733 nm, more than 50 nm red-shifted as compared with the emission spectra of the antenna system of PSII (LHCII) (7). *In vitro* reconstitution has shown that the red-shifted Chls are a common characteristic of Lhca complexes, although their energies differ strongly in different subunits. Emission forms at 701–702 nm have been found associated with Lhca1 and Lhca2, whereas 725- and 733-nm emissions were reported for Lhca3 and Lhca4, respectively (5, 8–11). It has been shown that the red emission of Lhca3 and Lhca4 originates from the low energy absorption band of an excitonic interaction involving Chl *a* in sites A5 and, probably, B5 (12), whereas the difference in energy is associated with the nature of the Chl A5 ligand, since the substitution of Asn in Lhca3 and Lhca4 by His, the usual ligand for Chl A5 in Lhc complexes, leads to the loss of the red spectral forms (12). In the present work, we analyze in detail Lhca2 with the aim of understanding the origin of the 701-nm emission that dominates the fluorescence spectrum at low temperature. It should be noticed that Lhca bears His as a ligand for Chl A5, yet its fluorescence emission is red-shifted by 20 nm with respect to the highly homologous subunit Lhcb6 (CP24) and other Lhcb proteins, thus opening the question of whether a different mechanism of modulation for the physico-chemical properties of chromophores is at work in Lhca2. By performing a detailed analysis by biochemical and spectroscopic methods on WT and mutant Lhca recombinant proteins, we conclude that the fluorescence emission band at 701 nm derives from excitonic coupling between chromophores A5 and B5, despite the presence of a His ligand for Chl A5. These results are discussed on the basis of the structural information that re-

* This work was supported by Ministero dell'Istruzione Università e Ricerca Progetti Fondo per gli Investimenti della Ricerca di Base Grants RBAU01E3CX and RBNE01LACT and by European Community Human Potential Program Grant HPRN-CT-2002-00248. The costs of publication of this article were defrayed in part by the payment of page charges. This article must therefore be hereby marked "advertisement" in accordance with 18 U.S.C. Section 1734 solely to indicate this fact.

§ To whom correspondence should be addressed. Tel.: 390461405360; Fax: 390461405372; E-mail: croce@itc.it.

¹ The abbreviations used are: Chl, chlorophyll; FWHM, full-width half-maximum; LD, linear dichroism; LHCI and LHCII, light-harvesting complex I and II, respectively; PSI and PSII, photosystem I and II, respectively; WT, wild type.

cently became available from x-ray crystallography (1, 13). We suggest that in green plant LHCI, differences in interchromophore distances rather than in transition energies of the individual chromophores of the interacting pair or in the orientation of their transition vectors represent the critical factor in determining excitonic coupling.

EXPERIMENTAL PROCEDURES

DNA Constructions and Isolation of Overexpressed Lhca Apoproteins from Bacteria—cDNAs of Lhca2 from *Arabidopsis thaliana* (11) were mutated with the QuikChange® site-directed mutagenesis kit, by Stratagene. WT and mutant apoproteins were isolated from the BL21 strain of *Escherichia coli* transformed with these constructs following a protocol previously described (14, 15).

Reconstitution and Purification of Protein-Pigment Complexes—Reconstitution and purification were performed as described in Ref. 16 with the following modifications. The reconstitution mixture contained 420 μg of apoprotein, 240 μg of chlorophylls, and 60 μg of carotenoids in a total of 1.1 ml. The Chl *a/b* ratio of the pigment mixture was 4.0. The pigments used were purified from spinach thylakoids.

Protein and Pigment Concentration—High pressure liquid chromatography analysis was as in Ref. 17. The chlorophyll to carotenoid ratio and Chl *a/b* ratios were independently measured by fitting the spectrum of acetone extracts with the spectra of individual purified pigments in 80% acetone (18).

Spectroscopy—The absorption spectra at room temperature and 77 K were recorded using an SLM-Aminco DK2000 spectrophotometer, in 10 mM Hepes, pH 7.5, 20% glycerol (60% at low temperature) and 0.06% β -dodecylglucosylmaltoside. Wavelength sampling step was 0.4 nm, scan rate was 100 nm/min, and optical path length was 1 cm.

The absorption spectra at 4 K were measured using a home-built spectrophotometer at OD 0.5 in the same buffer as described above, but with 67% glycerol.

Fluorescence emission spectra at 77 K were measured using a Jasco FP-777 spectrofluorimeter and corrected for the instrumental response. The samples were excited at 440, 475, and 500 nm. The spectral bandwidth was 5 nm (excitation) and 3 nm (emission). The chlorophyll concentration was about 0.02 $\mu\text{g}/\text{ml}$ in 60% glycerol and 0.03% β -dodecylglucosylmaltoside. The spectra between 130 and 4 K of the WT were measured with a 0.5-m imaging spectrograph (Chromex 500IS) and a CCD camera (Chromex Chromcam I). For broad band excitation, a tungsten halogen lamp (Oriol) was used with band pass filters transmitting at 420, 475, and 506 nm. For narrow band excitation, a dye laser (Coherent CR599) was used, which was pumped by an argon ion laser (Coherent Inova 310). The optical bandwidth of the laser was 0.6 nm, and the power was kept at 0.15 milliwatts/cm². The spectra were corrected for the wavelength dependence of the detection system.

CD spectra were measured at 10 °C on a Jasco 600 spectropolarimeter. The wavelength sampling step was 0.5 nm, the scan rate 100 nm/min, and spectra were recorded with eight accumulations. The OD of the samples was 1 at the maximum in the Qy transition for all complexes, and the samples were in the same solution as described for the absorption measurements. All spectra presented were normalized to the polypeptide concentration based on the Chl binding stoichiometry.

LD spectra were measured as described in Ref. 19 using samples oriented by the polyacrylamide gel squeezing technique.

RESULTS

Analysis of Lhca2-WT Complex—Lhca2 WT was obtained by overexpression of the apoprotein in *E. coli* and reconstitution *in vitro* with pigments. The complex was purified from excess pigment and unfolded apoprotein by sucrose gradient ultracentrifugation, anion exchange chromatography, and glycerol gradient ultracentrifugation and was obtained in monomeric form, as previously described (11).

Absorption—The absorption spectrum of Lhca2 at 4 K shows its maximum in the Chl Qy region at 679.5 nm, whereas in the Chl *b* region two local maxima can be detected at 644 and 652 nm (Fig. 1). The second derivative analysis allows resolution of several absorption forms: three Chl *b* at 643, 651, and 653 nm and four Chl *a* at 661, 672, 680.5, and 688.5 nm. In the blue region, the minimum at 497 nm is associated to the redmost peak ($S_0 > S_{2,0}$ transition) of the carotenoids, whereas those at

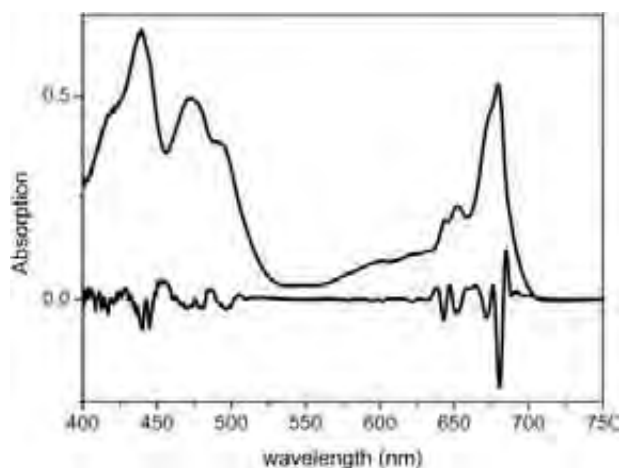


FIG. 1. Absorption spectrum at 4 K of Lhca2-WT. The spectrum is presented together with its second derivative.

480 and 471 nm may represent the Soret bands of two Chl *b* spectral forms.

Fluorescence Measurements—Fluorescence emission spectra of Lhca2 were measured at different temperatures upon excitation in the blue spectral region (Fig. 2). Two emission forms at 688 and 701 nm can be detected. The latter dominates the spectrum at 4 K, but the 688-nm form is still present, indicating that the energy transfer between these two forms is not complete, thus suggesting some kind of heterogeneity in the sample.

In order to obtain information on the origin of the two fluorescence emissions, fluorescence emission spectra upon selective excitation in the Qy band of the complex were measured. A selection of spectra is presented in Fig. 3A. The relative contribution of the 688- and 701-nm forms changed as a function of the excitation wavelength. In particular, the 688-nm emission reached its maximum for excitations in the 680–683-nm range, indicating that it originates from the red part of the bulk absorption. For excitation above 685 nm, the amplitude of the 688-nm emission band drops considerably, and the spectrum is dominated by the low energy emission form.

In Fig. 3B, the excitation wavelength is plotted *versus* the maximum of the emission (squares). By increasing the excitation wavelength from 680 to 685 nm, a blue shift of the emission maximum of the redmost form to 697 nm (excitation at 685 nm) is observed. This blue shift is due to the contribution to the emission of a larger fraction of “red” pigments absorbing in the blue wing of the inhomogeneous distribution, which are selectively excited at this wavelength (20, 21). Above 685 nm, the emission maximum undergoes a red shift, exhibiting a linear relation with the excitation wavelength, thus reaching a value of 701 nm for excitation at 690 nm. By exciting in the redmost part of the absorption spectrum, a further red shift of the emission maximum was observed. For excitations within the red tail of the absorption spectrum (around 710 nm), the emission maximum is still broad (340 cm^{-1}), indicating large homogeneous broadening. Moreover, for excitation above 700 nm, site selection does not have a strong influence on the shape and the width of the emission, thus suggesting that the spectrum is dominated by inhomogeneous broadening.

The site-selected fluorescence data allow also determining the peak wavelength of the absorption form responsible for the 701-nm emission. This value corresponds to the excitation wavelength at which the emission peak coincides with that in spectra obtained from nonselective excitation (see Ref. 20 for more details). By following this procedure, the absorption maximum of the red band is calculated to be approximately at 690 nm, in agreement with the second derivative analysis of the

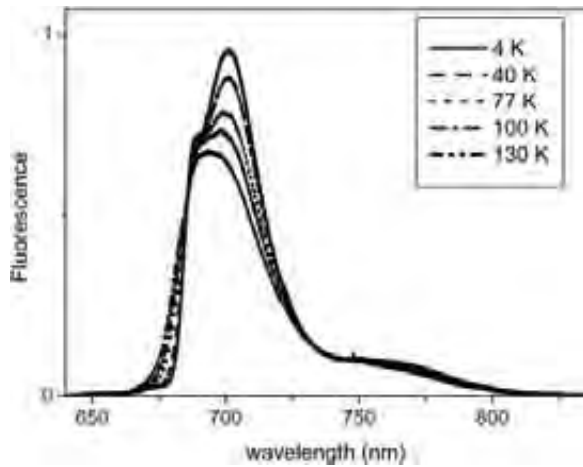


FIG. 2. **Temperature dependence of the fluorescence emission spectrum.** Fluorescence emission spectra of Lhca2-WT measured at 4, 40, 77, 100, and 130 K. The sample was excited at 506 nm.

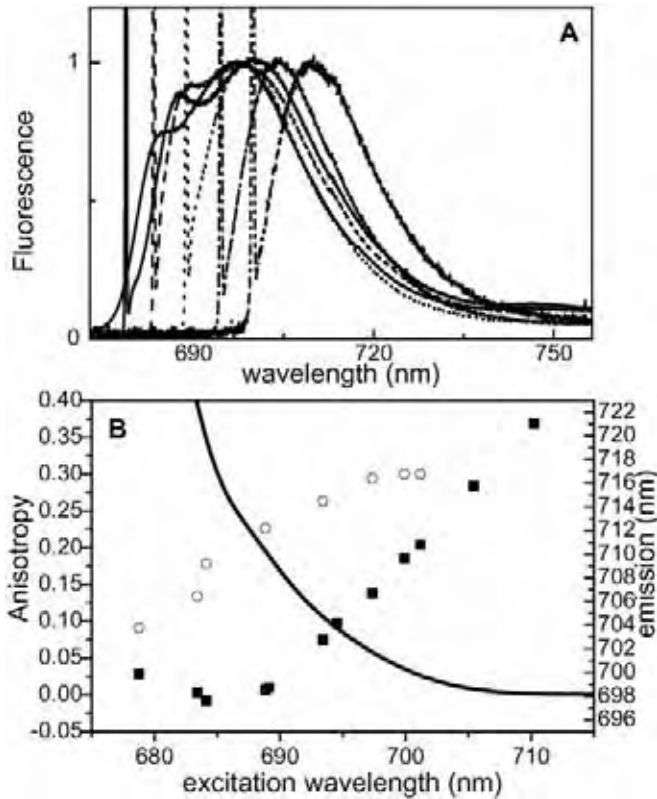


FIG. 3. **Site-selected fluorescence.** A, selection of emission spectra of Lhca2 at 4 K, laser excitation at 679, 683, 689, 694, and 700 nm. The spectra were normalized to the maximum of the emission. The sharp peak is largely due to elastic scattering of the laser excitation light. B, emission and absorption characteristics of Lhca2-WT complex at 4 K. Closed squares, dependence of the emission maximum as a function of the excitation wavelength. Open circles, value of the anisotropy of the emission detected at 701 nm. Line, tail of the absorption spectrum.

absorption spectrum, which showed the redmost absorption form at 688.5 nm (see Fig. 1).

Additional information on the characteristics of the red absorption tail can be obtained by fluorescence anisotropy measurements, which gives an indication of the orientation of the absorbing and emitting dipoles. In Fig. 3B (circles), the values of the fluorescence anisotropy detected at 701 nm are reported as a function of the excitation wavelength. It is clear that the values of the anisotropy also depend on the excitation wavelength. Upon excitation around 680 nm, the anisotropy value is

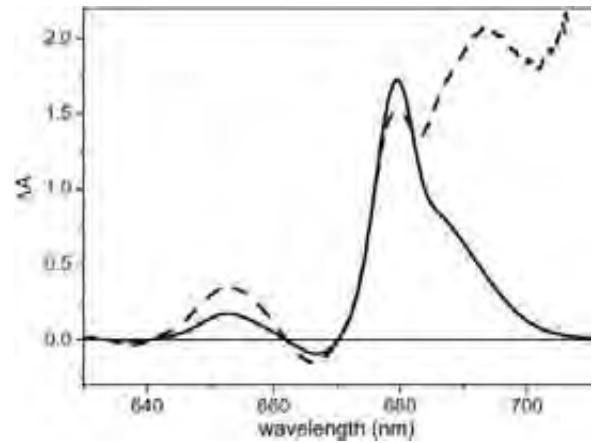


FIG. 4. **Linear dichroism.** LD (solid line) and LD/3OD (dashed line) spectra of Lhca2-WT at 10 K. The scale is in arbitrary units.

low, and it rises to a maximum of 0.32 for excitation wavelength above 697 nm, a value very similar to that obtained in the analysis of the 702-nm emission form in a native LHCI preparation (7). This result indicates that above this wavelength, no depolarization due to energy transfer takes place, thus suggesting that the same band is responsible for the absorption and the emission. The alternative hypothesis of energy transfer between pigments having the same dipole transition orientation is extremely unlikely.

LD Spectra—The LD spectrum of Lhca2 shows strong positive contribution in the Chl *a* Q_y absorption region, with a maximum at 679.5 nm and a shoulder around 690 nm (Fig. 4). The signal becomes slightly negative at 667 nm. In the Chl *b* absorption region, a positive contribution is observed at 653 nm. The reduced LD spectrum (*LD/3A*) shows the largest value around 690 nm, indicating that the Chl(s) responsible for this absorption forms is oriented with the largest angle with respect to the normal to the membrane plane. A second positive LD value corresponds to the maximum of the absorption spectrum (679.4 nm), whereas a local minimum is present at 683 nm.

Localization of the Low Energy Absorbing Form(s) into the Lhca2 Structure—The above measurements strongly indicate that the red-shifted fluorescence signal at 701 nm is associated with an absorption form peaking at 690 nm. In order to identify which chromophore is responsible for this absorption, mutation analysis at selected Chl-binding residues was performed. Based on previous analysis with Lhca3 and Lhca4 (12), residues coordinating Chl A5, B5, and B6, involved in the low energy absorption forms, were mutated to nonbinding residues (*i.e.* which cannot coordinate the central magnesium of the Chls) (see Table I for details). The apoprotein was expressed in *E. coli*, and the complex was reconstituted *in vitro* with pigments. In all cases, stable monomeric complexes were obtained. The pigment content of the complexes is shown in Table I.

The decreased Chl/Car ratio observed in all mutants indicates loss of Chls in the Chl binding site mutants, and the higher Chl *a/b* ratio as compared with the WT complex implies that Chl *b* molecules are preferentially lost. Normalization to the carotenoid content would indicate loss of one Chl in the A5 mutant, two Chls in B5, and one Chl in B6. However, this stoichiometry may not be correct in the case of mutants A5 and B5, since the corresponding mutants in all other Lhca complexes showed a loss of carotenoid molecules. Moreover, loss of one Chl in A5 would indicate that this site has mixed occupancy, which is very unlikely, because the A5 site has been found to accommodate one Chl *a* molecule in all complexes analyzed so far (22–24). We thus suggest that the A5 mutant loses two Chls molecules, one Chl *a* and one Chl *b*, as was the

TABLE I
Pigment composition of the complexes

The amount of carotenoids is calculated for the given Chl stoichiometry. The error in the data is less than 0.1.

Sample	Mutation	Chl <i>a/b</i>	Chl/Carotenoid	Chl total	Lutein	Violaxanthin
RLhca2-WT		2.1	5.0	10	1.68	0.32
RLhca2-A5	H52F	2.2	4.5	8	1.41	0.35
RLhca2-B5	E108V/R111L	4.7	4	7	1.44	0.3
RLhca2-B6	E100V	3.1	4.4	9	1.57	0.25

case in Lhca1, whereas a small loss of carotenoids accounts for the change in Chl/Car ratio. The B5 mutant loses most probably three Chl molecules, two Chls *b* and one Chl *a*. The loss of Chl *a* is consistent with the analysis of the absorption spectrum (see below), which is strongly affected in the Chl *a* Qy absorption region.

To check the influence of the mutation on the 701-nm emission form of the complex, fluorescence emission spectra at 77 K were measured (Fig. 5). Mutant A5 and B5 showed emission maximum at 686 nm, thus shifted by 15 nm to the blue as compared with the WT peak, indicating that both mutations affect the low energy emission form. The fluorescence emission of the B6 mutant was, instead, very similar to that of the WT, showing that mutation at this Chl binding site does not influence the chromophore(s) responsible for the 701-nm emission.

The absorption spectra of the three mutants and the WT at 77 K are presented in Fig. 6A and the second derivative of the spectra are shown in Fig. 6B.

Mutant A5 was mainly affected in the Chl *a* region, where the absorption form at 690 nm disappeared. A decrease in the amplitude of the spectrum in the Chl *b* region could also be observed, in agreement with the Chl *b* loss (see Table I). Mutant B5 showed dramatic changes in the absorption spectrum as compared with the WT; not only two Chl *b* forms (at 642 and 651 nm) were lost, but also a 688-nm absorbing Chl *a* form. Absorption at 680 nm was also decreased and was partially compensated by the increased signal at 670 nm, possibly due to the presence of unconnected Chls. Mutant B6 was affected mainly in the Chl *b* region, where the absorption at 642 nm disappeared, an indication that the Chl *b* accommodated in the B6 site absorbs at this wavelength. Minor changes could also be detected in the Chl *a* absorption region. Interestingly, the effect of the mutation at site B6 on the red-shifted absorption forms is different in Lhca2 as compared with Lhca1 (24) and Lhca4.² In these homologous proteins, loss of Chl B6 significantly affected the red-shifted emission forms. This difference may be related to the observation that the B6 mutants of Lhca1 and Lhca4 lose xanthophylls, whereas Lhca2 did not. The loss of red forms in Lhca1 and Lhca4 upon mutation at site B6 was interpreted as an indirect effect mediated by the carotenoid molecule (24). The different results obtained for the B6 mutant in Lhca2 seem to indicate that the carotenoid organization in the Lhca complexes is different with respect to others Lhca subunits.

The CD spectra at room temperature of WT and mutants are reported in Fig. 7. Mutant A5 is identical in the Chl *b* region to the WT but shows strong differences in the Chl *a* region. Comparison with the WT spectrum indicates that this mutant loses a negative CD signal at 687 nm and a positive one at 672 nm, thus suggesting loss of an excitonic interaction. A strong decrease in the intensity of the CD signal in the Chl *b* region is observed for both B6 and B5 mutants, thus implying that the Chl *b* molecules lost in the B5 and B6 mutants participate in pigment-pigment interactions. In particular, the comparison of the spectra of the WT with the one of mutant B6 shows that, in

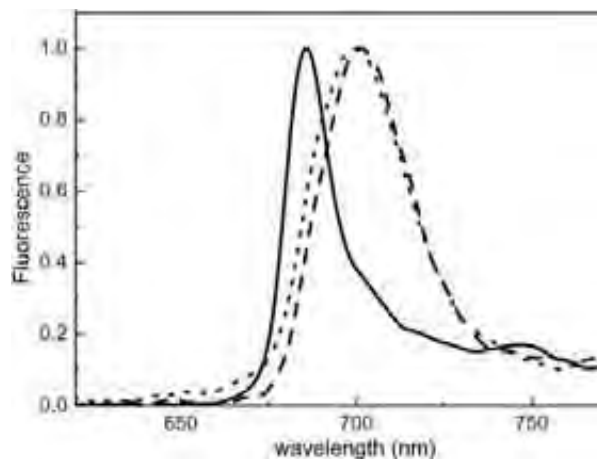


FIG. 5. Fluorescence emission spectra at 77 K of Lhca2 WT and mutants Lhca2-WT (dashed line), Lhca2-A5 mutant (solid line), and Lhca2-B6 mutant (dotted line) upon excitation at 500 nm. The spectra were normalized to the maximum of the emission.

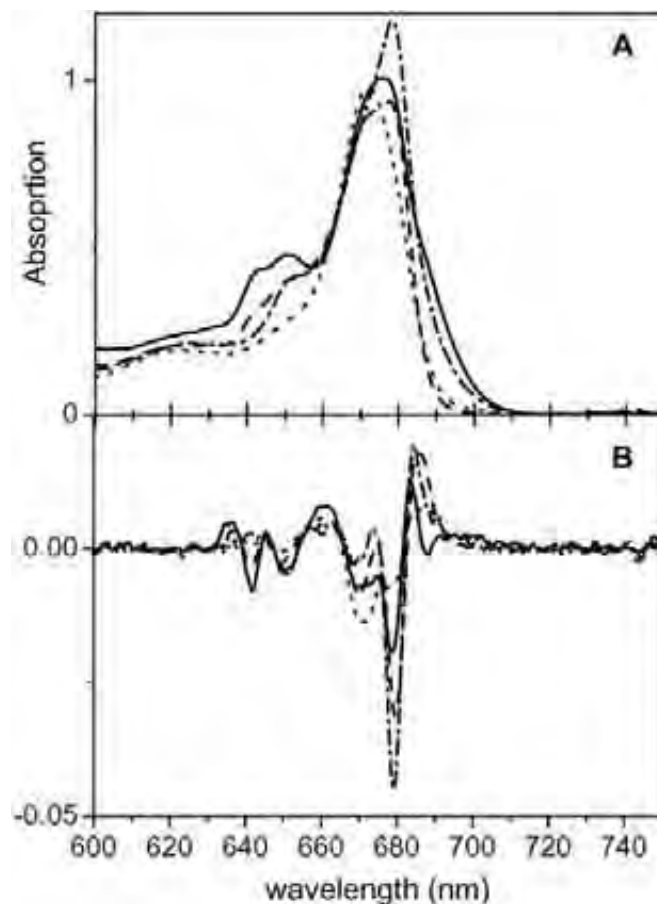


FIG. 6. Absorption spectra at 77 K of Lhca2-WT and mutants. A, absorption spectra of Lhca2-WT (solid line), Lhca2-A5 (dashed line), Lhca2-B5 (dotted line), and Lhca2-B6 (dash-dotted line). The spectra are normalized to the Chl content. B, second derivative of the spectra reported in A.

² T. Morosinotto, R. Bassi, and R. Croce unpublished results.

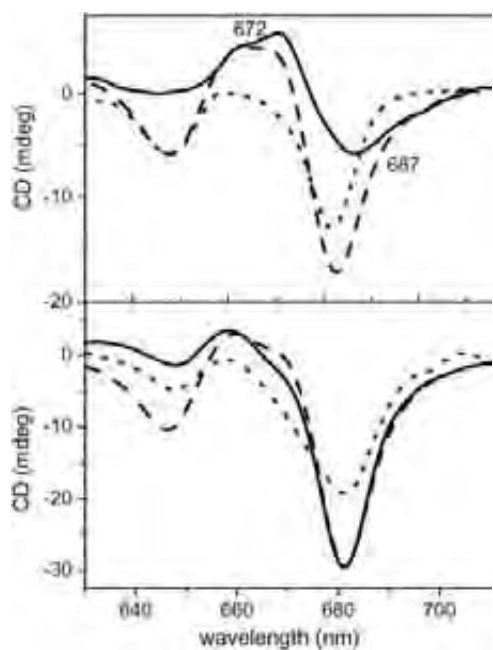


FIG. 7. Circular dichroism spectra of Lhca2-WT and mutants at 10 °C. All of the spectra are normalized to the absorption (A): Lhca2-WT (dashed line), Lhca2-A5 (dotted line), and difference WT-A5 (solid line). B, Lhca2-WT (dashed line), Lhca2-B5 (dotted line), Lhca2-B6 (solid line).

the latter, the loss of the negative signal in the Chl *b* region is connected with the loss of a positive contribution in the Chl *a* region (around 670 nm), thus suggesting the presence of a Chl *b*-Chl *a* interaction.

DISCUSSION

The current results show that Lhca2 takes a unique position within the LHCI proteins. Unlike Lhca3 and Lhca4, it does not show strong absorption above 700 nm, but nevertheless its emission is still 22-nm red-shifted as compared with the emission maxima of all Lhcb complexes. In the case of Lhca3 and Lhca4, it was shown that the red absorption is associated with the presence of an Asn as ligand for Chl A5 (12). This is not the case of Lhca2, which has a His in this position, a feature shared with all Lhcb proteins that do not show red-shifted Chl forms. We thus proceeded with the analysis of the chromophore organization in Lhca2 and identified the absorption band responsible for the 701-nm emission band, with the aim of understanding the mechanism that allows modulation of the physico-chemical properties of chlorophyll ligands.

Lhca2 has been shown to have the emission maximum at 701 nm (at 4 K). A second emission form was also detected at 688 nm in the 4 K spectrum, thus suggesting heterogeneity in the sample. Several sources of spectroscopic heterogeneity have been reported for Lhc proteins, including phosphorylation-induced spectral changes in CP29 (25), the presence of multiple gene products in the LHCI preparations with different spectral features (26), and conformational changes induced by zeaxanthin binding to site L2 (27, 28). In the present work, a recombinant Lhca2 preparation was analyzed, which was the product of a single gene, did not contain zeaxanthin, was monomeric as detected by sucrose gradient ultracentrifugation, and was not phosphorylated. We conclude that the persistence of the two fluorescence emission bands is the product of a previously unrecognized source of molecular heterogeneity, which is reflected in the establishment or not of the molecular feature responsible for the 701-nm emission. Two hypotheses can be proposed for explanation of these data; either the Lhca2

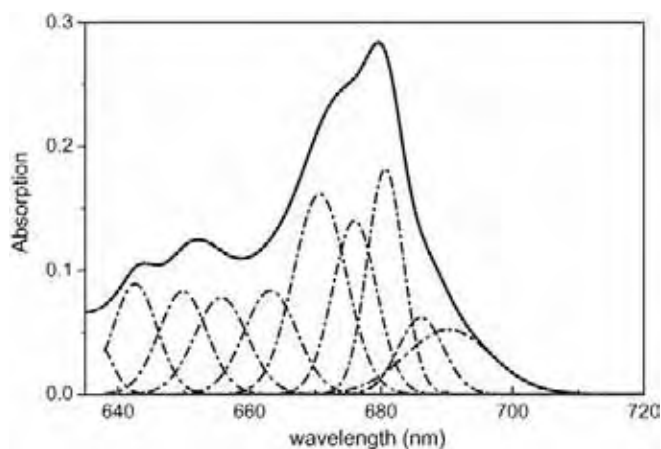


FIG. 8. Gaussian description of the absorption spectrum of Lhca2-WT at 4 K. 10 Gaussians are used to describe the spectrum.

protein is present into two conformations in which the two interacting chromophores are set at different distances and/or different orientations with respect to each other, or one of the two sites can be occupied by either Chl *a* or Chl *b*. The difference in transition energies between Chl *a* and Chl *b* and the difference in the orientation of the transition vectors (29) would make the observable spectral shift of a Chl *a*/Chl *b* interaction much smaller with respect to that of a Chl *a*/Chl *a* interaction. The likelihood of these hypotheses will be discussed below.

Site-selected fluorescence measurements indicate that the 689-nm emission originates from bulk Chls absorbing around 682 nm, whereas the 701-nm emission form is associated with a Chl absorption form at 690 nm. This result is confirmed by the mutation analysis, which showed that both mutants losing the 701-nm emission also lack the 690-nm absorption form.

Spectral Characteristics of the 690-nm Absorption Form—In order to get more details on the 690-nm absorption form of Lhca2, the absorption spectrum of the WT complex was described in terms of Gaussian forms, using the values obtained by second derivative analysis as starting parameters (Fig. 8). Three Chl *b* bands were needed to describe the region between 640 and 660 nm, namely at 642, 649, and 655 nm. The red part of the Q_y Chl *a* absorption region was described with two Gaussians at 686 and 690 nm, with the latter showing a broadened spectrum. An oscillation strength corresponding to the absorption of 0.85 Chl *a* molecules is associated with this band.

This description is in good agreement with the fluorescence data; the redmost band, which is responsible for the 701-nm emission, absorbs at 690 nm, as suggested by the site-selected fluorescence measurements, and a second band, peaking at 686 nm, is needed for description of the red absorption tail. The absorption of this second band fades to zero at around 697 nm, in agreement with the anisotropy measurements, which suggest that only above 697 nm, excitation energy is exclusively absorbed by the redmost pigment, whereas the 686-nm band is less broadened (8-nm FWHM), thus suggesting that this absorption derives from a monomeric pigment.

The energetic separation between the absorption maximum and the emission peak represents the Stokes shift. For the 690-nm absorption form, which emits at 701 nm, the Stokes shift is 11 nm (240 cm⁻¹). This is larger than observed in Lhcb complexes (where it is around 2 nm). From the Stokes shift, a value of the optical reorganization energy ($S\nu$) can be obtained, which corresponds to 120 cm⁻¹ (Stokes shift $\approx 2S\nu$).

The characteristics of the absorption band broadening can yield important information on the chromophore protein environment. The analysis of the WT minus mutant difference spectra indicates that at 77 K the FWHM of the band is around

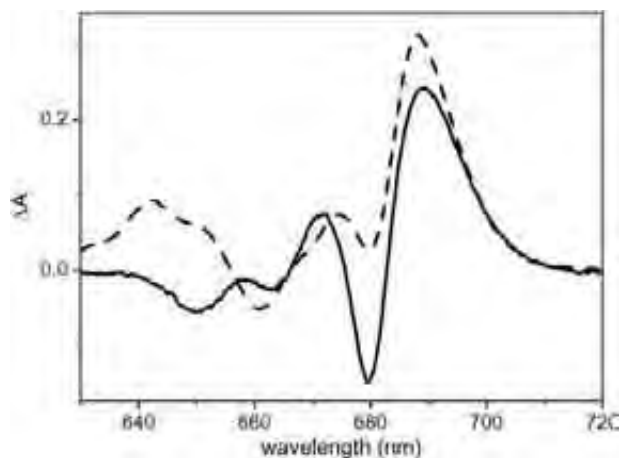


FIG. 9. Comparison of the absorption (dashed line) and linear dichroism (solid line) difference spectra of WT and A5 mutants.

400 cm^{-1} . At this temperature, the homogeneous broadening of the band can be described as follows,

$$\text{FWHM}_{\text{hom}}^2 = 7.7S\nu T \text{ with } \text{FWHM}^2 = \text{FWHM}_{\text{hom}}^2 + \text{FWHM}_{\text{inh}}^2 \quad (\text{Eq. 1})$$

where $\text{FWHM}^2 = \text{FWHM}_{\text{hom}}^2 + \text{FWHM}_{\text{inh}}^2$. Using the value of $S\nu$ obtained from the Stokes shift, the value for the FWHM_{hom} is 270 cm^{-1} , which gives a value of the inhomogeneous broadening of around 300 cm^{-1} . Such a large value for the inhomogeneous broadening is consistent with data from site-selected fluorescence measurements, since the excitation in the red tail did not affect the shape and width of the emission band.

The 690-nm absorption form of Lhca2 is thus characterized by a larger value of both homogeneous and inhomogeneous broadening as compared with the bulk Chl absorption form, for which these two values are both around 100 cm^{-1} (30). In this respect, the 690-nm band of Lhca2 shows characteristics very similar to the red absorption forms observed in several organisms (20), although its energy is significantly higher.

The Origin of the 701-nm Emission—Large values of optical reorganization energy are usually associated with the presence of pigment-pigment interactions. It has already been suggested that the red forms of Lhca3 and Lhca4 are the low energy term of an interaction between two Chl *a* molecules. Mutational analysis shows that these two chromophores are bound to sites Chl A5 and Chl B5, since mutation at these sites completely abolishes the red emission forms. This conclusion is in agreement with the finding that site A5 binds Chl *a* in Lhca as well as in any other Lhc protein (22–24), whereas site B5 either binds Chl *a* or has a mixed Chl *a*-Chl *b* occupancy as derived from pigment analysis of WT and mutant protein as well as their spectroscopic analysis. We conclude that the low energy spectral forms originate from the same protein domain in all Lhca complexes and involve Chls A5 and B5. Nevertheless, the energy level of these red-shifted transitions is modulated to a different extent in each Lhca subunit.

The presence of pigment-pigment interaction inducing the absorption at 688–690 nm of Lhca2 is supported by the comparison of the CD spectra of WT and A5 mutant, which lack a negative contribution around 687 nm and a positive one at 672 nm (values at room temperature). Similar components can be detected in the WT minus A5 absorption and LD difference spectra (Fig. 9). In both cases, two absorptions, at 688–689 nm and at 672–674 nm, can be detected, representing Chl forms lost by the effect of the mutation at site A5 and having positive LD spectra. These data can be interpreted as the loss of an excitonic interaction having the low energy band at 688–690 nm and the high energy band at 672–674 nm, as the effect of

A5 mutation. To describe both difference spectra, a negative band peaking at 679 nm is required. This band is present in the mutant but not in the WT and shows a positive LD signal (Fig. 6). Considering that all spectroscopic techniques consistently indicate that the interaction leading to the 690-nm absorption involves two Chl *a* molecules and that in the A5 mutant only one Chl *a* molecule is lost, the gain in the absorption can be interpreted as the contribution of the noninteracting monomer, which is left alone in the A5 mutant. Based on the mutation analysis, which suggested that the two interacting Chls are accommodated in sites A5 and B5, we conclude that the “new” 679-nm form detected in WT minus A5 difference spectra represents the absorption of the monomeric Chl *a* in site B5. This is in agreement with the analysis of the homologous protein CP29 (22), showing that a noninteracting Chl *a* absorbing at 679 nm is bound to site B5.

From the energetic distance between the two bands in the CD spectrum and considering the two monomers as isoenergetic, a value of 150 cm^{-1} for the interaction energy can be calculated (notice that a very similar value is obtained considering the absorption of monomeric A5 at 675 nm as was the case in all Lhc complexes analyzed so far (22, 23)). This value is half of the value observed for the interaction energy in Lhca3 and Lhca4.³

Once it is concluded that in all Lhca complexes the red forms originate from interaction between Chls *a* in sites A5 and B5, it is interesting to investigate the origin of the large difference in interaction energy between the complexes, which is reflected in a difference of around 30 nm between the emission maxima of Lhca2 and Lhca4. Two major factors control the amplitude of the interaction energy: the distance between the chromophores and the relative orientation of their dipole moment transition (the geometric factor k). ($V_{1,2} = 5.5k\mu_1\mu_2/R^3$, where R is the center to center distance between the chromophores and μ represents the dipole moment of the Chls). The analysis of the LD spectra of the complexes indicates that the redmost absorption form of both Lhca4 and Lhca2 forms the largest angle with the normal to the membrane plane (12) (this work). Although small differences in the orientation between the Chls in the two complexes cannot be excluded, we can assume, in a first approximation, a similar geometric factor in the two complexes. On this basis, the difference in interaction energy can be explained by considering that the distance between the two interacting Chls is around 2 Å larger in Lhca2 compared with Lhca4 by applying the equation, $V = 90k/R^3$. Recently, the structure of the PSI-LHCI complex has been elucidated at 4.4-Å resolution, and the position of the bound Chl has been defined. The center to center distance between Chl A5 and B5 in Lhca4 has been shown to be 7.9 Å, whereas in Lhca2 the value is 10.4 Å (3). This is consistent with the proposal that in Lhca4, the presence of the Asn as a ligand for Chl A5 allows a shorter distance between the two interacting Chls as compared with the complexes that have His for Chl A5 ligation (12).

Comparison with LHCII—Previous work with Lhca3 and Lhca4 has highlighted the importance of the presence of an Asn as ligand for Chl A5 for the generation of the red-shifted 730-nm fluorescence in Lhca3 and Lhca4, the only members of the Lhc superfamily holding Asn as a Chl A5 ligand. The present work shows that a significant, although lower, level of excitonic interaction can be obtained without the intervention of Asn ligation, and yet this interaction is sufficient for yielding the 701-nm emission form of Lhca2. This finding implies that additional structural signatures differentiate the Lhca from

³ R. Croce, T. Morosinotto, J. A. Ihalainen, A. Chojnicka, J. P. Dekker, R. van Grondelle, and R. Bassi, manuscript in preparation.

the Lhcb subfamily as a requirement for the chromophore-chromophore interactions in the helix C domain. This problem can be addressed thanks to the recent elucidation of LHCII structure at high resolution, since in Lhcb 1–3, the components of trimeric LHCII, the ligand of Chl A5 is His, as in Lhca2, and yet no 701-nm fluorescence emission can be detected. Moreover, the two structures in this domain are also very similar (3, 13), thus allowing detailed comparison. Why does LHCII not have red forms? Both x-ray structure (13) and mutation analysis (23, 31) consistently identify the ligand at site B5 as Chl *b*. Although the distance and mutual orientation between Chl *a* A5 and Chl *b* B5 allow for interaction in LHCII (13), the large energy gap between Chl *a* and Chl *b* makes the shift induced in the absorption form very small. In the case of Lhca2, biochemical and spectral analysis are consistent with site B5 having low selectivity and thus allowing for binding of both Chl *a* and Chl *b*. This mixed occupancy is crucial to explain the presence of two emission forms in the emission spectrum of Lhca2. We suggest that the blue form (emission at 689 nm) originates from the population of the ensemble having Chl *b* in site B5, whereas the 701-nm emission is originating from the population in which site B5 accommodates a Chl *a* molecule. The crucial question is thus how the selectivity of each Chl binding site is determined in Lhca proteins. The structure of LHCII shows that all but one Chl *b* present have the formyl group hydrogen-bonded with protein residues of water molecules. It can thus be speculated that the possibility to form this hydrogen bond affects the affinity of a site for Chl *b* versus Chl *a*, through an energy minimization effect. In LHCII, Chl *b* in site B5 is stabilized by hydrogen bond with the NH of Gln¹³¹ (13). In the Lhca2 complex, as well as in all Lhca complexes, this Gln is substituted by a Glu residue. The Glu cannot act as hydrogen donor, and it can be expected that in this case Chl B5 loses its high affinity for Chl *b* and thus can also accommodate Chl *a*.

REFERENCES

- Evans, J. R. (1986) *Photobiochem. Photobiophys.* **10**, 135–147
- Haworth, P., Watson, J. L., and Arntzen, C. J. (1983) *Biochim. Biophys. Acta* **724**, 151–158
- Ben Shem, A., Frolow, F., and Nelson, N. (2003) *Nature* **426**, 630–635
- Boekema, E. J., Jensen, P. E., Schlodder, E., van Breemen, J. F., van Roon, H., Scheller, H. V., and Dekker, J. P. (2001) *Biochemistry* **40**, 1029–1036
- Croce, R., Morosinotto, T., Castelletti, S., Breton, J., and Bassi, R. (2002) *Biochim. Biophys. Acta* **1556**, 29–40
- Jansson, S. (1994) *Biochim. Biophys. Acta* **1184**, 1–19
- Ihalainen, J. A., Gobets, B., Sznee, K., Brazzoli, M., Croce, R., Bassi, R., van Grondelle, R., Korppi-Tommola, J. E. I., and Dekker, J. P. (2000) *Biochemistry* **39**, 8625–8631
- Schmid, V. H. R., Cammarata, K. V., Bruns, B. U., and Schmidt, G. W. (1997) *Proc. Natl. Acad. Sci. U. S. A.* **94**, 7667–7672
- Zhang, H., Goodman, H. M., and Jansson, S. (1997) *Plant Physiol.* **115**, 1525–1531
- Schmid, V. H. R., Potthast, S., Wiener, M., Bergauer, V., Paulsen, H., and Storf, S. (2002) *J. Biol. Chem.* **277**, 37307–37314
- Castelletti, S., Morosinotto, T., Robert, B., Caffarri, S., Bassi, R., and Croce, R. (2003) *Biochemistry* **42**, 4226–4234
- Morosinotto, T., Breton, J., Bassi, R., and Croce, R. (2003) *J. Biol. Chem.* **278**, 49223–49229
- Liu, Z., Yan, H., Wang, K., Kuang, T., Zhang, J., Gui, L., An, X., and Chang, W. (2004) *Nature* **428**, 287–292
- Nagai, K., and Thøgersen, H. C. (1987) *Methods Enzymol.* **153**, 461–481
- Paulsen, H., Finkenzeller, B., and Kuhllein, N. (1993) *Eur. J. Biochem.* **215**, 809–816
- Giuffra, E., Cugini, D., Croce, R., and Bassi, R. (1996) *Eur. J. Biochem.* **238**, 112–120
- Gilmore, A. M., and Yamamoto, H. Y. (1991) *Plant Physiol.* **96**, 635–643
- Croce, R., Canino, G., Ros, F., and Bassi, R. (2002) *Biochemistry* **41**, 7343
- Haworth, P., Tapie, P., Arntzen, C. J., and Breton, J. (1982) *Biochim. Biophys. Acta* **682**, 152–159
- Gobets, B., Van Amerongen, H., Monshouwer, R., Kruip, J., Rögner, M., van Grondelle, R., and Dekker, J. P. (1994) *Biochim. Biophys. Acta* **1188**, 75–85
- den Hartog, F. T. H., Dekker, J. P., van Grondelle, R., and Völker, S. (1998) *J. Phys. Chem. B* **102**, 11007–11016
- Bassi, R., Croce, R., Cugini, D., and Sandona, D. (1999) *Proc. Natl. Acad. Sci. U. S. A.* **96**, 10056–10061
- Remelli, R., Varotto, C., Sandona, D., Croce, R., and Bassi, R. (1999) *J. Biol. Chem.* **274**, 33510–33521
- Morosinotto, T., Castelletti, S., Breton, J., Bassi, R., and Croce, R. (2002) *J. Biol. Chem.* **277**, 36253–36261
- Croce, R., Breton, J., and Bassi, R. (1996) *Biochemistry* **35**, 11142–11148
- Caffarri, S., Croce, R., Cattivelli, L., and Bassi, R. (2004) *Biochemistry* **43**, 9467–9476
- Moya, I., Silvestri, M., Vallon, O., Cinque, G., and Bassi, R. (2001) *Biochemistry* **40**, 12552–12561
- Formaggio, E., Cinque, G., and Bassi, R. (2001) *J. Mol. Biol.* **314**, 1157–1166
- Van Amerongen, H., and van Grondelle, R. (2001) *J. Phys. Chem. B* **105**, 604–617
- Hayes, J. M., Gillie, J. K., Tang, D., and Small, G. J. (1988) *Biochim. Biophys. Acta* **932**, 287–305
- Rogl, H., and Kuhlbrandt, W. (1999) *Biochemistry* **38**, 16214–16222

Section B:

*The antenna complexes of Photosystem I: the
molecular basis of low energy absorption
forms*

B 1

The Lhca antenna complexes of higher plants Photosystem I

This chapter has been published in *Biochimica et Biophysica Acta* 1556 (2002) 29–40, reproduced with permission.

Roberta Croce, Tomas Morosinotto, Simona Castelletti,
Jacques Breton and Roberto Bassi

B 2

Recombinant Lhca2 and Lhca3 Subunits of the Photosystem I Antenna System

This chapter has been published in *Biochemistry*
42 (2003), pp 4226 - 4234, reproduced with permission.

Simona Castelletti*, Tomas Morosinotto*, Bruno Robert,
Stefano Caffarri, Roberto Bassi and Roberta Croce

*Equal contribution

B 3

*Mutation Analysis of Lhca1 antenna
complex*

This chapter has been published in Journal of Biological Chemistry
277 (2002) pp. 36253 - 36261, reproduced with permission.

Tomas Morosinotto, Simona Castelletti, Jacques Breton,
Roberto Bassi and Roberta Croce

B 4

The chromophore organization of the Lhca2 subunit of higher plant photosystem I reveals the origin of its 701 nm fluorescence emission form

This chapter has been published in Journal of Biological Chemistry
279 (2004) pp 48543 - 48549, reproduced with permission.

Roberta Croce, Tomas Morosinotto, Janne A. Ihalainen,
Agnieszka Chojnicka, Jacques Breton, Jan P. Dekker,
Rienk van Grondelle and Roberto Bassi

B 5

Pigment-Pigment interactions in the higher plants Photosystem I antenna complex Lhca4. A mutagenesis study

Tomas Morosinotto, Milena Mozzo, Roberto Bassi and
Roberta Croce

B 6

*Inside the structure of Lhca3 by
mutational analysis*

Milena Mozzo, Tomas Morosinotto, Roberto Bassi and
Roberta Croce

B 7

*The Nature of a Chlorophyll ligand in Lhca
Proteins determines
the Far Red Fluorescence emission typical
of Photosystem I*

This chapter has been published in Journal of Biological Chemistry
278 (2003), pp 49223 - 49229, reproduced with permission.

Tomas Morosinotto, Jacques Breton, Roberto Bassi and
Roberta Croce

B 8

*LHCI: the antenna complex of
Photosystem I in plants and green algae*

This chapter is in press in the book: 'Photosystem I: The Plastocyanin: Ferredoxin Oxidoreductase in Photosynthesis' J.H. Goldbeck ed. in the series 'Advances in Photosynthesis in Respiration' by Kluwer Academic Publishers, B.V.

Roberta Croce, Tomas Morosinotto and Roberto Bassi

Pigment-pigment interactions in the higher plants Photosystem I antenna complex Lhca4. A mutagenesis study

Abstract

Lhca4 is the Photosystem I subunit to which is associated the most red emission (733 nm at 4K) typical of PSI. It has been proposed that this spectral property originates from an absorption band representing the low energy term of an interaction involving two Chl a molecules (1). In this study we have analyzed the pigment-pigment interactions between nearest neighboring chromophores in the Lhca4 complex by using site direct mutagenesis in order to identify the chromophores responsible for the red-most absorption forms. The red-shifted fluorescence peak was lost upon mutation affecting sites A4, A5 and B5. Based on shorter distance between Chls A5 and B5 (7.9 Å) vs. Chls A4 and A5 (12.2 Å) in Lhca4 (2), we suggest that the low energy emission originates from an interaction involving pigments in sites A5 and B5. Mutation at site B6 maintains a red-shifted emission form, implying that chromophores responsible for the interaction are maintained, but the peak is blue-shifted by 15 nm, suggesting a modification in the chromophores organization. The evidences for pigment-pigment interactions between Chls in sites B3-A3 and B6-A6 are also discussed.

Introduction

The fluorescence emission spectrum of leaves shows two major peaks, one at 685 nm and the second at 735 nm. Fractionation of the thylakoid membranes showed that the former emission is associated to Photosystem II and the latter to Photosystem I, which are respectively located in the granal and stromal lamellar components. In each photosystem, light is absorbed by antenna Chls and efficiently transferred to the reaction center where charge separation takes place. In the Photosystem II, the reaction center absorbs around 680 nm and it is isoenergetic with its antenna (3). In the Photosystem I, instead, a significant Chl pool, responsible for the 735 nm emission, absorbs at wavelengths longer than 700 nm, the absorption of the special pair. This causes most of the energy to be stored at energy lower than the reaction center, implying counter gradient energy transfer prior to charge separation (4).

The presence of Chls absorbing at energy lower than the primary donor is the fingerprinting of the Photosystem I in all organisms (5). In higher plants, however, Photosystem I is enriched in low-energy absorption forms which extend the light absorption in the far-red region of the spectrum, probably providing evolutionary advantage in shade leaves (6). These spectral forms are

concentrated in the LHCI complex, a 4 subunit, half-moon shaped structure which is located on one side of the PSI-core complex (2). The four subunits, called Lhca1, 2, 3 and 4, are present as dimers in vivo, they all have red shifted emission, although at different energies. Lhca1 and Lhca2 emits at 701 nm, Lhca3 at 725 nm and Lhca4 at 733 nm, as revealed from the analysis of recombinant proteins (7-10) and reverse genetic (11;12). It has been shown that an excitonic interaction between Chl a molecules is responsible for the large shift in absorption (1) and that this is promoted by the presence of an asparagine residue as a ligand for Chl A5 (1), suggesting that this Chl is directly involved in the interaction.

One of the main requisites for strong pigment-pigment coupling is a short distance between the interacting chromophores. In this work we have used the recent structural data on the Lhca4 protein (2) as a guidance for mutation analysis: the Chl binding sites which accommodate the nearest-neighbor pigments were mutated in order to analyze the presence of pigment-pigment interactions.

Material and Methods

DNA constructions and isolation of overexpressed Lhca apoproteins from bacteria. cDNAs of Lhca4 from *Arabidopsis thaliana* (9) were mutated with QuickChange© Site directed Mutagenesis Kit, by Stratagene©. WT and mutants apoproteins were isolated from the SG13009 strain of *E. coli* transformed with constructs following a protocol previously described (13;14).

Reconstitution and purification of protein-pigment complexes. They were performed as described in (15) with the following modifications: the reconstitution mixture contained 420 µg of apoprotein, 240 µg of chlorophylls and 60 µg of carotenoids in total 1.1 ml. The Chl a/b ratio of the pigment mixture was 4.0. The pigments used were purified from spinach thylakoids.

Protein and pigment concentration. HPLC analysis was as in (16). Chlorophyll to carotenoid ratio and Chl a/b ratio was independently measured by fitting the spectrum of acetone extracts with the spectra of individual purified pigments (17).

Spectroscopy. The absorption spectra at RT and 77K (LT) were recorded using a SLM-Aminco DK2000 spectrophotometer, in 10 mM Hepes pH 7.5, 20% glycerol (60% at LT) and 0.06% β-DM. Wavelength sampling step was 0.4 nm, scan rate 100 nm/min, optical pathlength 1 cm. Fluorescence emission spectra were measured using a Jasco FP-777 spectrofluorimeter and corrected for the instrumental response. The samples were excited at 440, 475 and 500 nm. The spectral bandwidth was 5 nm (excitation) and 3 nm (emission). Chlorophyll concentration was about 0.02 µg/ml in 60% glycerol and 0.03% β-DM.

The CD spectra were measured at 10°C on a Jasco 600 spectropolarimeter. Wavelength sampling step was 0.5 nm, scan rate 100 nm/min and spectra were recorded with eight accumulations. The

OD of the samples was 1 at the maximum in the Q_y transition for all complexes and the samples were in the same solution described for absorption measurements. All spectra presented were normalized to the polypeptide concentration based on the Chl binding stoichiometry.

Results

Mutation analysis was performed on Lhca4 complex. The putative binding ligands of Chls A3, A4, A5, B3, B5 and B6 were substituted with aminoacids, which could not coordinate the central Mg of the Chls (see table I). The reconstituted complexes were thus purified from the excess of pigments used in the reconstitution by sucrose gradient ultracentrifugation and anionic exchange chromatography.

All mutants yielding stable reconstituted monomeric complexes as can be inferred by their mobility in glycerol gradient, but mutant A3 (data not shown). In this case, in fact, any stable pigment-protein complex could be isolated. Most probably the mutation is affecting the stability of L1 site, as shown in Lhca1 (18) thus preventing the correct folding of the complex. The relative pigment content of the reconstituted complexes is reported in table I.

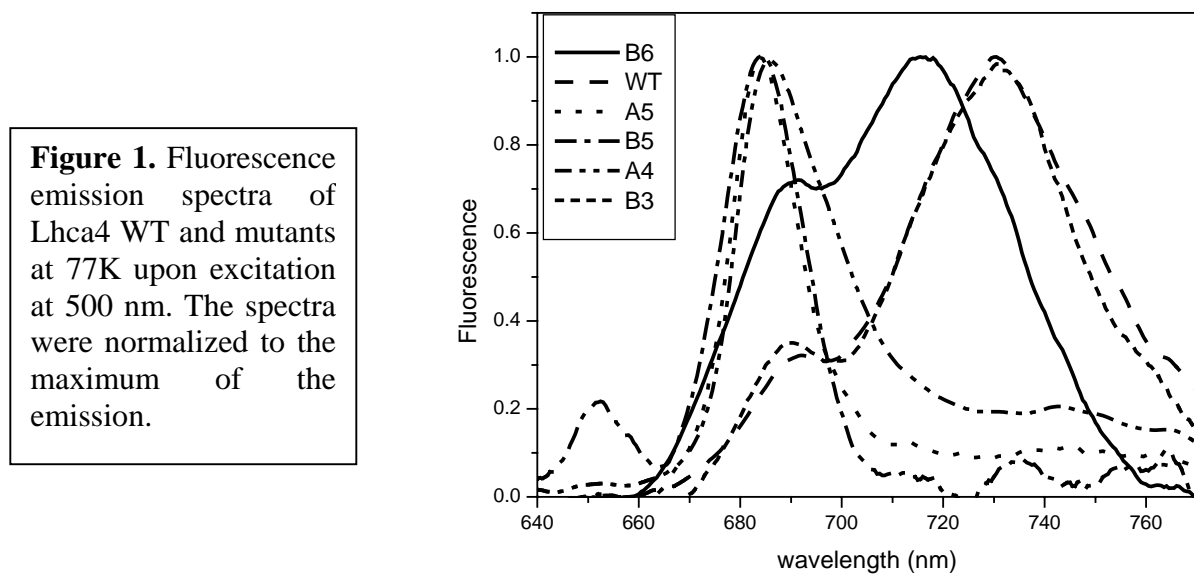
Sample	Residue	Chl a/b	Δ Chla	Δ Chlb	Viola	Lutein	Binding site from (2)
Lhca4-WT	-	2.5	-	-			
Lhca4-A4	E44V/R158L	2.1	-1	-	-0.1	-0.1	A4 -11014
Lhca4-A5	N47F	3.7	-1	-1	-0.1	-0.25	A5 -11015
Lhca4-B3	H185F	2.1	-1				B3 -11023
Lhca4-B5	E102V/R105L	5.2	-1.5	- 1.5	-0.2	-0.2	B5 -11025
Lhca4-B6	E94V	3.9		-1	-0.1	-0.3	B6 -11026

Table I. Pigment content of Lhca4 WT and mutated complexes.

Mutants A4 and B3 exhibit lower Chl *a/b* ratio as compared to the WT. Normalizing to the carotenoid content it can be concluded that both mutations affect the binding of one Chl *a* molecule. The other three mutants showed Chl *a/b* higher than the WT, suggesting loss of Chl *b* molecules. Based on the similarity with the same mutants in other complexes, it can be suggested that mutant A5 loose two Chls molecules, one Chl *a* and one Chl *b*. The normalization to the carotenoid content would suggests the loss of only one Chl molecule and mixed occupancy for this Chl binding site, in contrast with the finding that in all complexes analyzed so far site A5 is selective for Chl *a* (18-20). This hypothesis is also in contrast with the loss of carotenoids observed upon mutation at site A5 in

Lhca1, Lhca2 and Lhca3 (18), Croce et al 2004, unpublished results. We thus suggest that mutation at site A5 induces partial loss of the xanthophyll in site L2 together with loss of 1 Chl *a* and 1 Chl *b*. Loss of cars can be observed also in the B6 mutant, again in agreement with the data on other complexes (18-20). This mutant is affected in the binding of one Chl *b* molecule. The effect of mutation at site B5 is larger, as can be inferred from the lower stability of the mutant complex when compared to the WT (data not shown). We suggest that this mutant loses at least three Chls molecule, 1.5 Chl *a* and 1.5 Chl *b*.

The effect of each mutation on the red forms of Lhca4 was assessed from fluorescence emission spectra of the complexes, measured at 77K, which are reported in figure 1.



The emission spectrum of the B3 mutant is identical to WT, implying this chlorophyll is not involved in red emission. On the contrary, complete depletion of the red emission was observed in mutants A5 and B5. Mutant A4 also lost the 733 nm emission, but retains emission around 700 nm, as detectable from asymmetric broadening of the low energy side of the 685 nm peak. Finally, in mutant B6 red forms are still present, but the peak is blue shifted by 15 nm as compared to WT.

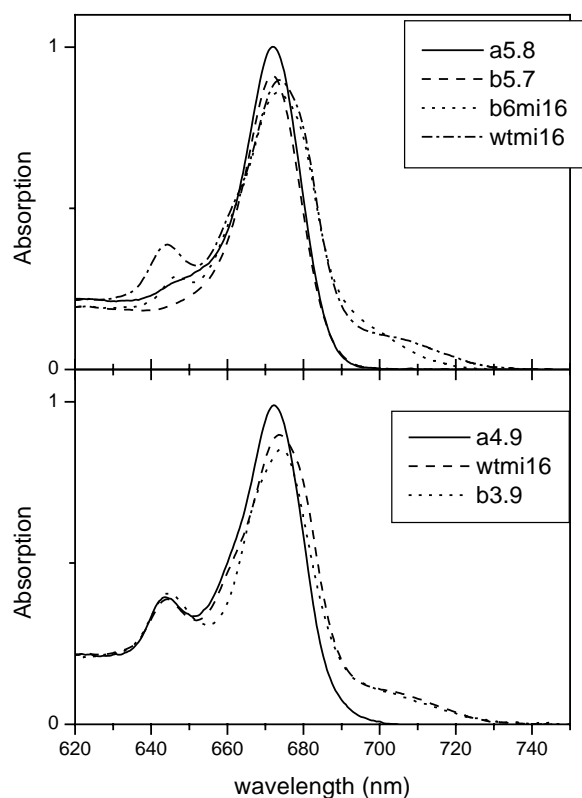


Figure 2. Absorption spectra at 77K of Lhca4-WT and mutants. The spectra were normalized to the Chl content. (A) A5, B5, B6 and WT; (B) A4, B3 and WT.

In order to get information about the spectral characteristics of the Chls affected by the mutations, the absorption spectra of all complexes were measured at 77K and they are shown in figure 2. In agreement with pigment analysis, mutants A4 and B3 do not show differences in the Chl *b* absorption region as compared to the WT (fig 2B), while differences were observed for mutants A5, B5 and B6 (Fig 2A). In particular, Lhca4-B5 loses most of the absorption in this region. Mutations at sites A5, A4 and B5 completely abolish the red absorption tail typical of the WT. The B3 mutant is identical to WT in this region, while B6 mutant still exhibits absorption above 700 nm. However, the peak of the red most band is clearly shifted to a shorter wavelength, consistently with the observed blue shift in fluorescence emission.

In order to detect pigment-pigment interactions, the CD spectra of all complexes were measured and they are presented in figure 3. Mutants B3 and A4 do not show any difference in the Chl *b* absorption region (630-655 nm), in line with the results of pigment composition and absorption spectra. The A5 mutant, despite losing a Chl *b* molecule, shows in the Chl *b* region a signal identical to WT, indicating that the Chl *b* lost upon mutation at this site is probably not involved in interaction with other chromophores or that the interaction is CD silent.

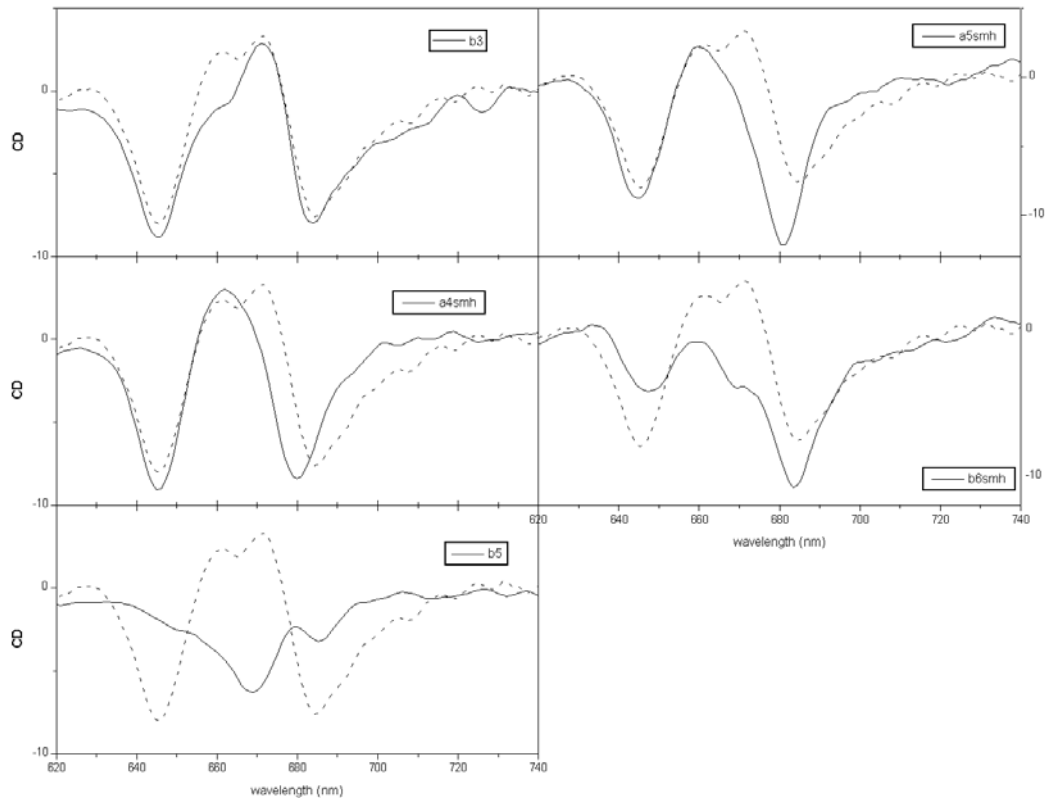


Figure 3. CD spectra of all Lhca mutants (solid) compared to Lhca4-WT (dashed). The spectra were normalized to the Chl content. (A) B3; (B) A4; (C) B5; (D) A5; (E) B6.

Mutants B5 and B6 exhibit strong differences in the Chl *b* absorption region. B6 loses half of the negative signal and mutation at B5 leads to the complete loss of the Chl *b* signal.

In the Chl *a* region a shift of the main negative band to shorter wavelengths is observed for mutants A5 and A4, this shift has been reported to be associated to the loss of the pigment-pigment interaction responsible of the red forms (*I*). The main difference in the Chl *a* absorption region of mutant B6 was detected in the 670-675 nm range, where the spectrum of the mutant shows negative component, opposite to the WT. The CD spectrum of the B3 mutant is identical to the WT but for the absence of a positive contribution at 660 nm.

Discussion

It has been previously suggested that the red absorption typical of Lhca complexes represents the low energy band of an excitonic interaction having the high energy term at 683 nm (*I*). Site selected fluorescence measurements indicate that the red most absorption band of Lhca4 peaks at 708 nm at 4K (Croce et al. unpublished results), thus yielding a value of 280 cm^{-1} for the interaction energy. On these basis, calculation of the distance between the interacting Chls, assuming the best

possible geometric arrangement, yields to a value of 8.6 Å or below. From the structure of Lhca4 (2), four pairs of Chls comply with this requirement: A5-B5, which center to center distance is 7.9 Å, A3-B3 at 8.13 Å, B6-A6 at 8.35 Å and A4-B4 (1031) at 8.334 Å (see table II with the center-center distance of all Chls are calculated from the structure). The analysis of mutant proteins here described is meant to verify which, among these chromophores are involved in the origin of red forms.

The fluorescence emission spectra of the complexes shows that Chl in site B3 is not involved in the interaction leading to the red forms, being the emission spectrum at LT of this mutant identical to the WT. All other mutants have an effect, although of different extent, on the red emission. In the following, we discuss the properties of the individual chromophores of Lhca4 and the effects of the mutation, at the corresponding sites.

Chlorophyll B3

The mutant loses one Chl a molecule thus suggesting that a Chl a is accommodated in this site in the Lhca4 complex, as it was the case in Lhca1 (18).

In the CD spectrum the main difference with respect to WT is observed in the positive signal at 660 nm, which disappears in the mutant. This feature suggests that Chl a in site B3 is interacting with a neighbor pigment. Unfortunately, no clear changes can be observed in other regions of the spectrum, possibly the negative component of the interaction is hidden by other signals. The nearest neighbor of Chl B3 is Chl A3 (8.13Å) and then we proposed that the observed loss of the 660 nm CD positive band is the signature of the interaction between Chls A3 and B3.

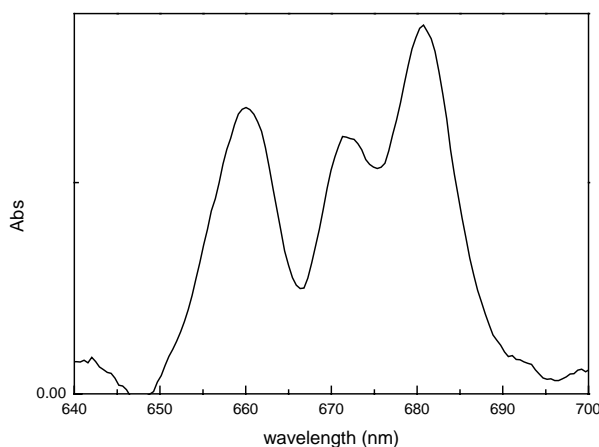


Figure 4. Difference absorption spectrum between Lhca4-WT and Lhca4-B3 mutant. Before subtraction, the spectra were normalized at the Chl content.

The difference absorption spectrum shows three positive bands with maxima at 660 nm, 672 nm and 680 nm (Fig 4). The first band corresponds to the signal lost in the CD spectrum and possibly represents the high energy band of the interacting dimer. The other two peaks are probably a

combination of the low energy band of the interaction, which is lost in the mutant, and of the absorption of the monomeric Chl, still present in the mutant. The absence of negative component in the spectrum can be attributed to the fact that there is energy redistribution between the two interacting Chls which favors the form at low energy (as it was the case in Lhca1 (18)). This is supported by the observation that the amplitude of the 660 nm absorption band corresponds to the absorption of less than one Chl molecule. The feature observed in the absorption difference spectrum can be explained considering that the shift induced by the interaction should not be very large and the negative monomeric absorption can be hidden by the low energy term of the dimer. Gaussian description of the difference spectrum (data not shown) suggests that the low energy absorption form peaks at 677 nm, while the monomer absorption is blue shifted of 1-2 nm. Although the impossibility to reconstituted mutant A3 does not allow obtaining more details, it is clear that the two interacting monomers are not isoenergetic and that the Chl monomer in site A3 absorbs at energy lower than B3. Moreover, the data clearly indicates that Chl B3 is not involved in the red emission of Lhca4 complex.

Mutant B6

Mutant B6 loses one Chl *b* molecule, suggesting that a Chl *b* is accommodated in this site. The fluorescence emission spectrum of the mutant is 15 nm blue shifted as compared to the WT, implying a change in the red Chl environment. Although loss of Chl *a* molecules was not detected in the complex, the absorption spectrum of the mutant differs from the absorption spectrum of the WT in the Qy Chl *a* absorption region (Fig. 5). A decrease in intensity above 700 nm (max 712 nm) is observed in absorption together with a gain around 693-694 nm. This difference explains the observed fluorescence shift: the red-most absorption in the mutant is blue-shifted and this new spectral form is the responsible for the 716 nm emission observed.

To get information on the “new” band present in the mutant, the absorption spectrum at low temperature of Lhca4-B6 complex was described in terms of Gaussians (Fig 5B). In order to fit the spectrum a large band peaking around 694 nm is required (FWHM 26 nm), while in the WT the red most band was detected at 708 nm (Croce et al. in preparation). However, the 694 band in B6 mutant has width similar to the absorption band of the red pigments, suggesting similar origin. We thus propose that mutation at site B6 induces a shift of 14 nm in the absorption of the low energy form, thus implying that the chromophores involved in the interaction are still in place, although somehow disturbed in their organization. Moreover, the data clearly indicate that the Chl located in site B6 is not directly responsible for the low energy emission, while its role seems to be important

in maintaining the right geometry between the interacting Chls as was already suggested in the case of Lhca1 complex (18).

The Chl *b* in site B6 absorbs at 642/483 nm as can be judged by the absorption difference spectrum (Fig 5A). Loss of negative amplitude in the CD spectrum at the same wavelength (fig 3 E) suggests that this Chl is involved in pigment-pigment interaction. The positive term of the interaction is not present in the Chl *b* region of the CD spectrum, thus suggesting that it should be searched for in the Chl *a* region, where loss of positive signal around 672 nm can be detected. Although changes with different origin in this region cannot be excluded, due to the effect on the interaction leading to the red-most form, it is likely that the 672 nm component represents the signal of the second term of the interaction involving Chl B6. The structure of Lhca4 shows that the nearest neighbor of Chl B6 is Chl A6 (2). We thus suggest that A6 site accommodates a Chl *a* molecule in Lhca4 and that this Chl interacts with Chl B6. The oscillator strength associated to the 642 nm absorption band in the WT-B6 difference spectrum corresponds to a bit less than one Chl. This implies that the energy distribution favors the low energy band of the interaction. In the difference spectrum, a slightly negative signal is observed around 668 nm and a positive one at 673 nm (Fig 5A). These two signals possibly represent a combination between the loss of absorption of the dimer and the gain of the absorption of monomeric A6, which is still present in the mutated B6 complex.

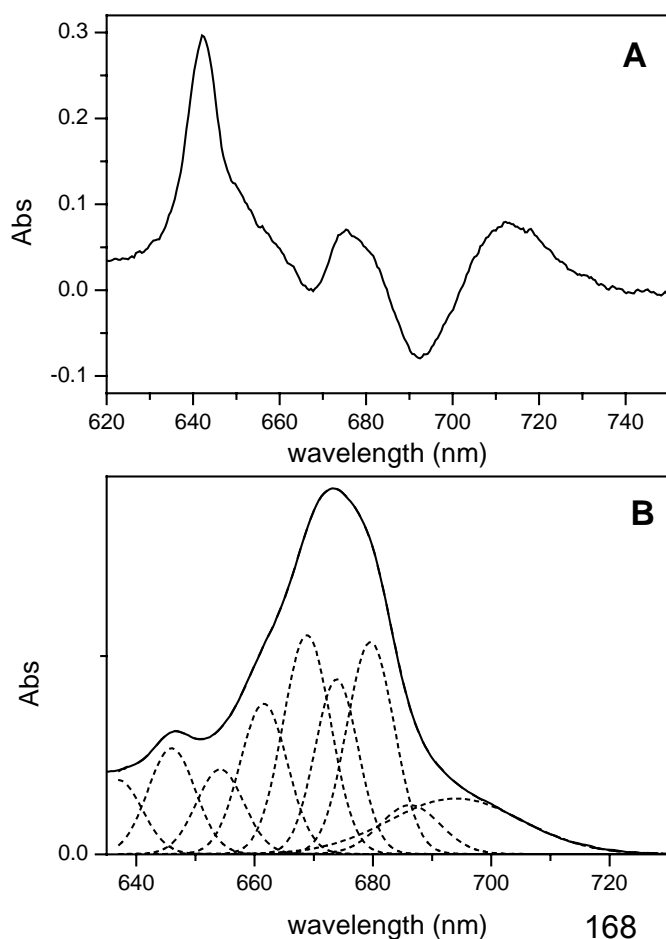


Figure 5. (A) Difference absorption spectrum between Lhca4-WT and Lhca4-B6 mutant. Before subtraction, the spectra were normalized at the Chl content. (B) Gaussian deconvolution of the absorption spectrum at 77K of Lhca4-B6 mutant.

In conclusion, it appears clear that Chl B6 is not the direct responsible for the low energy absorption in Lhca4. The Chl coordinated to this site absorbs at 642 nm and it seems to interact with a neighbor Chl A6. We propose that Chl B6 plays a role in keeping the conformation of the protein which yields to the red forms, as it was already suggested in Lhca1 (18). This effect is possibly mediated by the carotenoid in L2 site, which is partially lost in the mutant.

Mutant A4

Mutant A4 loses one Chl a molecule, thus suggesting that A4 site accommodates a Chl a, as was the case in all Lhc complexes analyzed so far (19) (18;20). The fluorescence emission spectrum of A4 mutant does not show the 733 nm component, but still conserved emission around 700 nm (see in figure 1 the comparison with A5 and B5 mutants).

The loss of red forms upon mutation at the A4 site can have at least two different origins:

- 1) A4 Chls is directly involved in the red absorption and the mutation has a direct effect on the low energy absorption
- 2) Mutation at this site changes the conformation of the protein, thus having an indirect effect on the red forms.

Tree mutants shows loss of the red emission in Lhca4: A4, A5 and B5. The substitution of the natural ligand for Chl A5 (Asn) with an His showed clearly the direct involvement of Chl A5 in the low energy forms. From the structure, it is clear that the distance between Chl A4 and Chl A5 is too large to allow the strong interaction responsible of the red forms. The other possibility is that the red forms originates from interaction involving all three Chls, namely A4, A5 and B5. But in this case mutation at sites A4 and B5 would have left at least part of the interaction in the mutants, while this does not seem the case, even though in the A4 mutant part of the fluorescence at 700 nm is still present.

On the other hand we should consider that mutation at site A4 affects the ionic bridge between E44 and R158, which stabilizes the structure of Lhc proteins (21). The absence of the ionic pair can have an effect on the transmembrane helices packing and thus on the position of the Chls coordinated to these helices. This hypothesis is consistent with the fact that the mutated complex is obtained with a low yield and is unstable. Based on these consideration we thus propose that the lack of red emission in the A4 mutant is mainly due to a different conformation assumed by the mutated complex than to a direct involvement of Chl A4 in the red forms.

Mutant A5

The mutation at site A5 induces the loss of two Chls molecules, one Chl *a* and one Chl *b*. Lhca4-A5 complex does not show the 733 nm emission form typical of Lhca4-WT, suggesting that the A5 site is involved in the interaction leading to the red form, in agreement with previous experiments where the loss of red forms was observed upon substitution of the Asn ligand of Chl A5 with an His (Lhca4-NH mutant)(1).

The absorption difference spectrum WT-A5 mutant is reported in fig. 6. In the red region of the Qy Chl *a* absorption, at least two forms can be detected at 683 and above 700 nm.

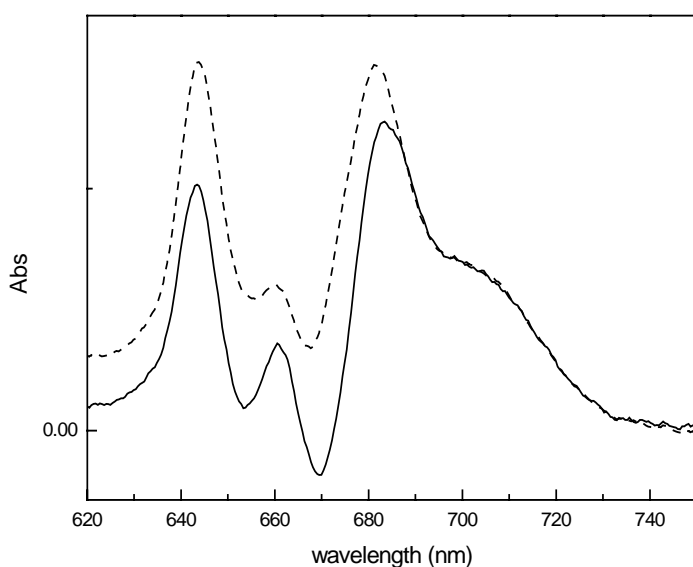


Figure 6. Difference absorption spectrum between Lhca4-WT and Lhca4-A5 mutant (solid) and Lhca4-B5 mutant (dashed). Before subtraction, the spectra were normalized at the Chl content.

The same two features were already observed in the WT-NH difference spectrum (1) and are the “markers” of the lost interaction yielding to the red forms. A negative contribution in the absorption spectrum is detected around 670 nm. This component probably represents at least in part the absorption of the monomer of the Chl(s) which in the WT interacts with Chl A5 and which is (are) still present in the complex. However, considering the low stability of the complex this signal is probably the sum of several contributions including the absorption of disconnected Chls, which are present in the sample, as judged by fluorescence emission spectra.

In the Chl *b* region the absorption difference spectrum shows a band at 645/473 nm (468/470 nm at RT), which can be associated to the Chl *b* lost in this sample. The CD spectrum is identical to the WT in the Chl *b* region, indication that this Chls does not interact with other pigments or the interaction is CD silent. Whatever the reason for the absence of the CD signal is, it is clear that this Chl *b* does not participate to the interaction leading to the red forms, having the red most forms a clear negative CD signal. Moreover, this Chl *b* form peaks at 645 nm, a typical wavelength for monomeric Chl *b* in a protein environment.

Mutant B5

Mutation at site B5 induced loss of at least three Chl molecules: 1.5 Chl *a* and 1.5 Chl *b*, indication that the substitution of the ER bridge on the C-helix strongly affects the complex.

The fluorescence emission spectrum shows that this mutation completely abolished the red emission forms, thus suggesting that Chls loss upon mutation at this site are involved in the low energy absorption. In absorption, the lack of the red most band and of the 683 nm component is also clear (fig.6). However, the main peak in the absorption difference spectrum is more intense than in the case of the A5 mutant and blue shifted of 2 nm, suggesting loss of a second Chl *a* form absorbing more in the blue (Fig 6). The intensity of the absorption in the Chl *b* region is reduced in agreement with the pigment analysis. The CD signal is very different from the one of the WT, indication that the mutation at this site strongly perturbed the pigment organization.

Out of the three Chls lost in this mutant, one seems to be Chl B6 due to the lack in both absorption and CD spectra of the same components observed in the B6 mutant. The other two sites affected by mutation E102/R105 accommodate in total 1.5 Chl *a* and 0.5 Chl *b*. This indicates that site B5 coordinates Chl *a* or has mixed occupancy. The Chl *b* peaks at 647 nm.

Conclusions

From the mutation analysis of Lhca4, it can be concluded that the red forms originate from an interaction between Chls in sites A5 and B5. Loss of red emission upon mutation at site A4 is possibly due to a different folding of the mutant which is induced by the loss of the ionic pair E44 R158 which stabilizes the WT structure, rather than to a direct involvement of Chl A4 in the interaction, although this possibility can not be completely ruled out.

	A1	A2	A3	A4	A5	A6	A7	B1	B2	B3	B5	B6
A1	-	13,8	24,9	16,1	17,6	16,4	23,9	8,93	18,9	28,4	15,9	19,7
A2	13,8	-	14,9	17,6	21,3	18,3	25,6	21,2	9,26	15,5	24,5	25,3
A3	24,9	14,9	-	19,9	20,3	22,5	22,9	28,9	16,1	8,13	26,9	28,3
A4	16,1	17,6	19,9	-	12,2	25,3	25,9	18,8	15,7	24,9	16,3	27,7
A5	17,6	21,3	20,3	12,2	-	18,9	15,1	15,2	24,0	27,7	7,9	18,5
A6	16,4	18,3	22,5	25,3	18,9	-	12,3	15,8	26,8	27,2	18,5	8,35
A7	23,9	25,6	22,9	25,9	15,1	12,3	-	20,3	32,0	30,0	16,3	10,1
B1	8,93	21,2	28,9	18,8	15,2	15,8	20,3	-	26,5	34,2	9,9	14,9
B2	18,9	9,26	16,1	15,7	24,0	26,8	32,0	26,5	-	15,3	28,3	33,0
B3	28,4	15,5	8,13	24,9	27,7	27,2	30,0	34,2	15,3	-	33,8	34,2
B5	15,9	24,5	26,9	16,3	7,9	18,5	16,3	9,9	28,3	33,8	-	15,7
B6	19,7	25,3	28,3	27,7	18,5	8,35	10,1	14,9	33,0	34,2	15,7	-

Table II. Center to center distance between Lhca4 Chls as calculated from the structure (2).

References

1. Morosinotto, T., Breton, J., Bassi, R., and Croce, R. (2003) *J. Biol. Chem.* 278, 49223-49229.
2. Ben Shem, A., Frolov, F., and Nelson, N. (2003) *Nature* 426, 630-635.
3. Jennings, R. C., Bassi, R., Garlaschi, F. M., Dainese, P., and Zucchelli, G. (1993) *Biochemistry* 32, 3203-3210.
4. Croce, R., Zucchelli, G., Garlaschi, F. M., Bassi, R., and Jennings, R. C. (1996) *Biochemistry* 35, 8572-8579.
5. Gobets, B. and van Grondelle, R. (2001) *Biochim. Biophys. Acta* 1057, 80-99.
6. Rivadossi, A., Zucchelli, G., Garlaschi, F. M., and Jennings, R. C. (2003) *Photosynt. Res.* 60, 209-215.
7. Schmid, V. H. R., Cammarata, K. V., Bruns, B. U., and Schmidt, G. W. (1997) *Proceedings of the National Academy of Sciences of the United States of America* 94, 7667-7672.
8. Schmid, V. H. R., Potthast, S., Wiener, M., Bergauer, V., Paulsen, H., and Storf, S. (2002) *Journal of Biological Chemistry* 277, 37307-37314.
9. Croce, R., Morosinotto, T., Castelletti, S., Breton, J., and Bassi, R. (2002) *Biochimica et Biophysica Acta-Bioenergetics* 1556, 29-40.
10. Castelletti, S., Morosinotto, T., Robert, B., Caffarri, S., Bassi, R., and Croce, R. (2003) *Biochemistry* 42, 4226-4234.
11. Zhang, H., Goodman, H. M., and Jansson, S. (1997) *Plant Physiol* 115, 1525-1531.
12. Ganeteg, U., Strand, A., Gustafsson, P., and Jansson, S. (2001) *Plant Physiol* 127, 150-158.
13. Nagai, K. and Thøgersen, H. C. [153], 461-481. 1987. *Methods in Enzymology*.
14. Paulsen, H., Finkenzeller, B., and Kuhlein, N. (1993) *Eur. J. Biochem.* 215, 809-816.
15. Giuffra, E., Cugini, D., Croce, R., and Bassi, R. (1996) *Eur. J. Biochem.* 238, 112-120.
16. Gilmore, A. M. and Yamamoto, H. Y. (1991) *Plant Physiol.* 96, 635-643.
17. Croce, R., Canino, g., Ros, F., and Bassi, R. (2002) *Biochemistry* 41, 7343.
18. Morosinotto, T., Castelletti, S., Breton, J., Bassi, R., and Croce, R. (2002) *J. Biol. Chem.* 277, 36253-36261.
19. Bassi, R., Croce, R., Cugini, D., and Sandona, D. (1999) *Proc. Natl. Acad. Sci. USA* 96, 10056-10061.
20. Remelli, R., Varotto, C., Sandona, D., Croce, R., and Bassi, R. (1999) *J. Biol. Chem.* 274, 33510-33521.
21. Kühlbrandt, W., Wang, D. N., and Fujiyoshi, Y. (1994) *Nature* 367, 614-621.

B 6

*Inside the structure of Lhca3 by
mutational analysis*

Milena Mozzo, Tomas Morosinotto, Roberto Bassi and
Roberta Croce

Inside the structure of Lhca3 by mutation analysis

Abstract

In this work, we analysed with a mutational approach the structure of Lhca3, one component of the antenna system of higher plants Photosystem I. Based on the recent structure of PSI-LHCI (Ben Shem et al., Nature 2003) it has been suggested that Lhca3 has a different folding with respect to all other members of the Lhc family. In particular, it was proposed that the two central helices are swooped and Chls in sites A3 and B3 are not present. This different folding would imply that the Chls coordinated to the two central helices have different ligands in Lhca3 with respect to the other Lhc complexes. This suggestion was tested by mutation analysis, by substituting the putative binding residues with aminoacids not able to coordinate Chls. Data obtained indicate that the mutations in Lhca3 have a similar effect similar to what observed in the other Lhca complexes. Moreover, also in Lhca3 the red emission forms originate from interaction between Chls in site A5 and B5, as demonstrated for other PSI antenna subunits. This strongly suggests that Lhca3 folding is very similar to the one of the other antenna proteins. Evidences for the presence of Chls in sites A3 and B3 are also presented.

Introduction

Higher plants Photosystem I, the plastocyanin/ferredoxin oxido-reductase, is composed by a core complex and by an outer antenna system, consisting of four major polypeptides, the products of the genes Lhca1-4 (1;2). Recently, the structure of PSI-LHCI supercomplex has been resolved at 4.4 Å (3), providing information about the organisation of the complexes and the localisation of most Chl molecules. It showed that Lhca1-4 are bound on one side of the core, as previously suggested (4), and that only one copy of each polypeptide is present per P700. Moreover, the structure and following biochemical analyses showed that several Chl and carotenoid molecules are bound at the interface between the reaction centre and the antenna system, stabilising their binding and possibly favouring the energy transfer to P700 (3;5).

The Chl organisation of the four Lhca complexes is very similar to the one of LHCII (3;6), consistently with the conservation in Lhca of all residues which are Chl ligands in LHCII (2). Only in the case of Lhca3, the structure shows some peculiarity. In fact, it has been hypothesised that Lhca3 may have a different folding as respect to the other Lhc complexes and the two central helices could be swooped (3). In Lhca3 structure, moreover, the Chls in sites A3 and B3¹ are missing and are substituted by a new Chl in an intermediate position (1041- nomenclature from (3)). Although structurally similar to Lhcb, Lhca proteins are characterised by the presence of Chls emitting below 700 nm that are not present in antenna complexes of Photosystem II (1). In particular, Lhca1 and Lhca2 show emission at 701 nm, while Lhca3 and Lhca4 emit at low temperature respectively at 725 and 733 nm (8-12). It has been shown that part of the large shift in absorption is due to excitonic interactions involving Chl A5. The interaction is facilitated by the presence of an asparagine as ligand for Chl A5 in Lhca3 and Lhca4: the substitution of N with H in this position was abolishing the red emission in both Lhca3 and Lhca4 (13). It was demonstrated that, in Lhca1, Lhca2 and Lhca4, the interaction leading to the red forms involves Chls in site A5 and B5 (14-16).

In this work, we verified by mutation analysis the validity of this hypothesis in the case of Lhca3. Data obtained indicate that also in this complex red forms originate from the interaction between A5 and B5 Chls. Moreover, we found evidences supporting that Lhca3 folding is similar to the one of the other Lhc complexes and suggesting the presence in this complex of Chls A3 and B3.

Material and Methods

DNA constructions and isolation of overexpressed Lhca apoproteins from bacteria. cDNA of Lhca3 from *Arabidopsis thaliana* (12) was mutated with QuickChange© Site directed Mutagenesis Kit, by

¹ For the nomenclature of Chl binding sites, the one from (7) was generally used. The correspondence to nomenclature from (3) is reported in table I and II.

Stratagene©. WT and mutants apoproteins were isolated from the SG13009 strain of *E. coli* transformed with constructs following a protocol previously described (17) (18;18).

Reconstitution and purification of protein-pigment complexes. They were performed as described in (19) with the following modifications: the reconstitution mixture contained 420 µg of apoprotein, 240 µg of chlorophylls and 60 µg of carotenoids in total 1.1 ml. The Chl a/b ratio of the pigment mixture was 4.0. The pigments used were purified from spinach thylakoids.

Protein and pigment concentration. HPLC analysis was as in (20). Chlorophyll to carotenoid ratio and Chl a/b ratio was independently measured by fitting the spectrum of acetone extracts with the spectra of individual purified pigments (21).

Spectroscopy. The absorption spectra at RT and 100K were recorded using a SLM-Aminco DK2000 spectrophotometer, in 10 mM Hepes pH 7.5, 60% glycerol and 0.06% β-DM. Wavelength sampling step was 0.4 nm, scan rate 100 nm/min, optical pathlength 1 cm. Fluorescence emission spectra were measured using a Jasco FP-777 spectrofluorimeter and corrected for the instrumental response. The samples were excited at 440, 475 and 500 nm. The spectral bandwidth was 5 nm (excitation) and 3 nm (emission). Chlorophyll concentration was about 0.02 µg/ml in 60% glycerol and 0.03% β-DM.

The CD spectra were measured at 10°C on a Jasco 600 spectropolarimeter. Wavelength sampling step was 0.5 nm, scan rate 100 nm/min and spectra were recorded with 8 accumulations. The OD of the samples was 1 at the maximum in the Qy transition for all complexes and the samples were in the same solution described for absorption measurements.

Results

The gene of Lhca3 was mutated at the putative Chl binding sites by substituting nucleophilic residues with apolar aminoacids, which could not coordinate the central Mg of the Chls. The mutations performed are reported in table I. The Chl binding sites nomenclature from Kühlbrandt et al. (7) and Ben Shem et al. (3) are reported. WT and mutant apoproteins were overexpressed in *E.coli* and reconstituted *in vitro* by adding pigments. The refolded complexes were purified from the excess of pigments used in the reconstitution by sucrose gradient ultracentrifugation and ionic exchange chromatography.

All mutants were yielding stable reconstituted products but in the case of R57L/E177V and E52V/R182L. The reconstitution yield of Q194L was far lower than the one of the WT and of the other mutants, indication that this site plays an important role in protein stabilisation. This is consistent with what observed in the case of Lhca4, where it was not possible to obtain a stable complex carrying a mutation at this site (16).

The pigment content of the complexes were analysed by HPLC and fitting of the absorption spectra of acetone extracts with the spectra of individual pigments. The results are reported in table I.

All reconstituted mutants were affected in the pigment binding. As expected, seen the high Chl *a/b* ratio of this complex, most mutations affect Chl *a* binding sites, as inferred by the fact that most mutants have a lower Chl *a/b* ratio as compared to the WT. Only two mutants have Chl *a/b* ratio higher than the WT, namely E119V/R122L and N55F.

Sample	Putative chl Binding site	Chl tot	Chl a/b	Chl a	Chl b	Violax	Lutein	β -Car
WT		10	6.0	8.6	1.4	0.6	1.7	0.5
R57L/E177V	A1 –11011	-	-	-	-	-	-	-
N180V	A2 –11012	8	4.7	6.6	1.4	0.5	1.4	0.4
Q194L	A3 –11013	7	4.3	5.7	1.3	0.6	1.9	-
E52V/R182L	A4 –11014	-	-	-	-	-	-	-
N55F	A5 –11015	8	7.3	7	1	0.3	1.7	-
H209F	B3 –11023	9	5.3	7.6	1.4	0.6	1.7	0.5
E119V/R122L	B5 –11025	8	9.2	6.3	0.7	0.3	1.5	-
E111V	B6 –11026	9	5.9	7.7	1.3	0.4	1.9	0.1

Table I. Pigment composition of Lhca3 WT and mutated in different chlorophyll binding sites. The putative Chl binding sites affected by the mutation are indicated, as identified from sequence homologies. Nomenclature from (7) and (3) are reported. The standard deviations on pigments binding data reported in the table are at maximum 0.2.

The number of the Chls lost was estimated considering constant the amount of Chl *b* in all mutants but E119V/R122L and N55F. This hypothesis is supported by the analyses of the absorption spectra, which, for most mutants, showed no changes in Chl *b* region compared with the WT (see below). In this view, Lhca3-N180V loses two Chls *a*, mutants H209F and E111V one and mutant Q194L three, although this last value should be taken with some caution due to the high instability of the complex and the presence of unconnected Chls. In the case of mutants E119V/R122L and N55F the loss of 1.5 Chl *a* and 0.5 Chl *b* was estimated based on previous results of Lhca mutational studies (14-16).

For what concerns carotenoids, a specific loss of β -carotene was observed in A5, B5 and B6 mutants.

Fluorescence emission spectra

The low temperature emission spectrum of Lhca3 is dominated by the emission at 724 nm. This fluorescence originates from a broad absorption band peaking at 704 nm (13). To detect the mutations effect on the low energy forms, the emission spectra of all complexes were recorded at 77K (Figure 1.). The emission spectrum of the WT is characterised by maximum at 724 nm and a second component at 689 nm. Three of the mutants, namely E119V/R122L, N55F and Q194L, loose the red emission at 724 nm. Their fluorescence spectra are similar and show maxima at 682.5 nm. Mutant E111V still show 724 nm emission although the ratio between the red and blue fluorescence is modified as compared to the WT, with the blue emission dominating the spectrum. The complex does not contain “disconnected” Chls, as judged from emission spectra at different excitation wavelengths, therefore the modification observed has different origin. Mutants H209F and N180V show emission spectra very similar to the WT, with maxima at 724 nm. In the case of Lhca3-N180V complex, a difference can be observed in the 680-690 nm region where the mutant shows reduced intensity as respect to the WT, suggesting that this mutation is affecting a Chl, which participates to the 690 nm emission.

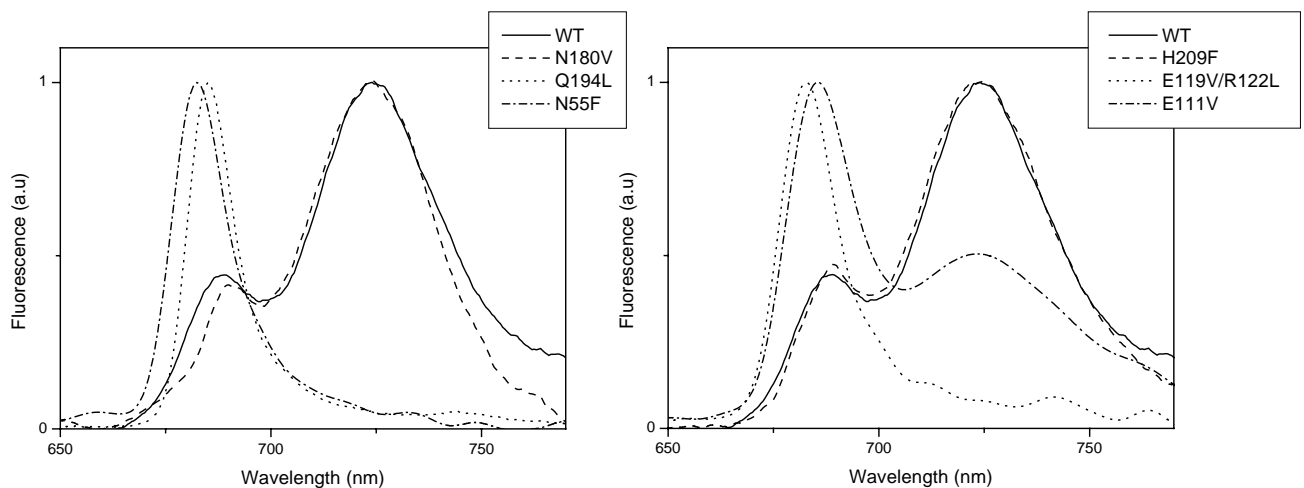


Figure 1. Fluorescence emission spectra at 77 K of Lhca3 WT and mutant. A) Emission spectra of Lhca3 WT and mutants N180V, Q194L, N55F. B) Emission spectra of Lhca3 WT and mutant H209F, E119V/R122L, E111V. All spectra are normalised to 1 at the maximum.

Absorption

The absorption spectra of all complexes were measured at 77K and they are reported in figure 2.

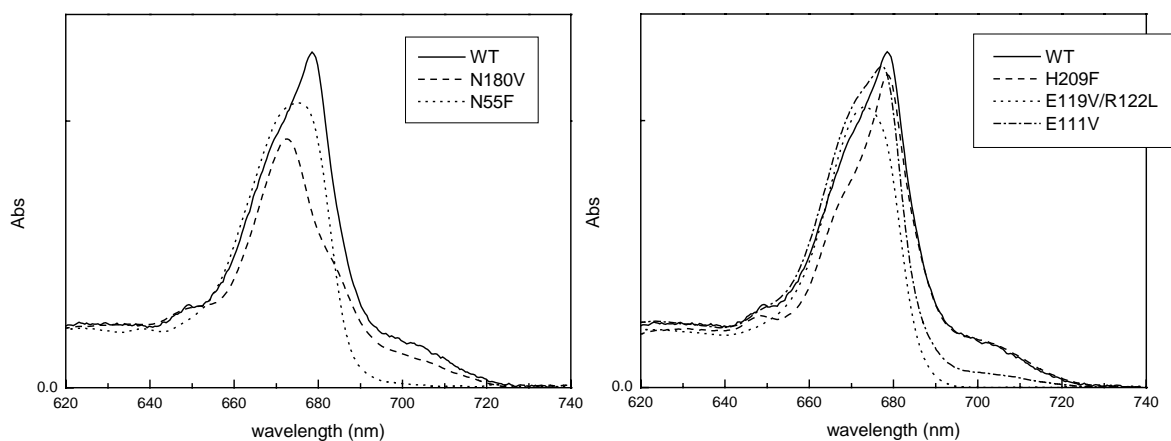


Figure 2. Absorption spectra at 100 K of Lhca3 WT and mutants. A) Absorption spectra of Lhca3 WT and mutants N180V, Q194L, N55F. B) Absorption of Lhca3 WT and mutant H209F, E119V/R122L, E111V. All spectra are normalised to the Chl content.

The spectra show that mutants E119V/R122L, N55F and Q194L lose completely the red absorption tail, confirming the fluorescence data. All other complexes exhibit absorption above 700 nm, although in the case of Lhca3-E111V complex its intensity is strongly reduced as compared to the WT. In agreement with the pigment analysis, the only two mutations affecting the Chl b absorption region are E119V/R122L and N55F. Clear loss of absorption around 660 and 670 nm is observed upon mutation H209V, while Lhca3-N180V complex is strongly depleted in the absorption forms at 680 nm.

Discussion

From the analysis of the structure of PSI-LHCI complex, it has been suggested that Lhca3 may fold differently as compared with the other Lhc complexes. In particular, it was suggested that the helix closest to helix C is not the first helix, but the third one. In this case, the numbering of residues should be changed and the Chls (labelled as in (7) and (3)) would have different ligands. For clarity the ligand for the Chls in the two possible conformations of Lhca3 are reported in table II.

If the suggestion is correct we can expect that the ligand for the Chls coordinated to residues of the A and B helices, namely Chls A1, A2, A3, A4 and A5 are opposite with respect to the ligands in all other Lhc complexes. Moreover, from the structural data it is proposed that Lhca3 lacks Chls in site A3 and B3. In their place, a new Chl (1041), located in an intermediate position, is present.

Ligands	“alignment-based” conformation	“reverse” conformation
R57L/E177V	A1-11011	A4-11014
N180V	A2-11012	A5-11015
Q194L	A3-11013	-
E52V/R182L	A4-11014	A1-11011
N55F	A5-11015	A2-11012
H209F	B3-11023	-
E119V/R122L	B5-11025	B5-11025
E111V	B6-11026	B6-11026

Table II. Correspondence of chlorophyll ligands and binding sites. In the “alignment-based” conformation, the binding sites identified in LHCII structures (7) and (6) have been located in Lhca3 by sequence alignment. The “reverse” conformation, instead, indicates the correspondence follows the hypothesis that helix A and B are swooped in Lhca3 (3).

In order to check these suggestions, mutation analysis at the putative Chl binding sites was performed. It was already shown that several domains are highly conserved through the Lhc family: A2 Chls was always found to absorb at 680-681 nm in all complexes analysed so far and it was also shown to be involved in pigment-pigment interaction with Chl B2 when the ligand was N (14;21;22). Moreover, in Lhca1, 2 and 4 complexes, it was shown that Chl A5 is involved in pigment-pigment interaction, yielding to the red emission forms (13;15;16). If the folding of Lhca3 is different from the other Lhc complexes, we can expect that mutation at the N180 residue does not affect Chl in site A2, but instead Chl in site A5, while mutation at N55 would influence Chl in site A2. Considering that the Chl organisation is very similar in the Lhc complexes we can thus expect to see the “signature” of Chl A2 upon mutation at N55 and the “signature” of Chl A5 upon mutation at N180. The analysis of results from mutation analysis and their comparison with analogous studies on other Lhc complexes, thus, will allow to establish if Lhca3 has, or not, a different folding as respect to the other Lhc complexes.

The two ER bridges – R57/E177 and E52/R182 (mutations at sites A1 and A4).

From the structure of LHCII (7) it was proposed that the folding of this complex was stabilised by two ionic pairs between helices A and B. Moreover, these residues are also the direct ligands for Chls A1 and A4. These residues are conserved in all Lhc family members, and in relatives with lower homology, like PsbS (23). By mutation analysis it has been demonstrated that in the case of

Lhcb1 it was possible to obtain stable reconstituted complexes in the absence of these ionic pairs, but with the difference that the mutation at the ligand of Chl A1 was destabilising the structure of the complex much more than the mutation at the ER ligand for Chl A4 (22). It was concluded that the E (helix A) R (helix B) ionic pair play the major role in the structure stabilisation as respect to E (helix B) R (Helix A). This results was confirmed by mutation analysis on Lhcb4 and Lhca1: in both cases a stable complex was obtained when the ER pair responsible for the coordination of Chl A4 was removed, while mutation at the other pair was inhibiting the folding of the complex (14;24). The results in the case of Lhca3 are different: both mutations are lethal for the protein, suggesting that in this complex all four residues play a fundamental role in protein stabilisation. It should be noted that Lhca4 showed similar behaviour to Lhca3 upon this mutation: in fact, although the A4 mutant was still stable enough to be purified, it was extensively destabilised (16).

Mutation N180

In Lhc complexes, Chl A2 is usually coordinated to the N (or H) in the third helix. Substitution of the ligand for this Chls was giving similar results in all Lhc complexes analysed so far: Chl in A2 position is the most red pigment of the bulk with absorption around 680-681 nm (22;25) and it is interacting with a neighbour Chl, B2 (21;22). This result was confirmed by the recent structure of LHCII where it was shown that the A2-B2 interaction is the strongest present in the complex (6).

In Lhca3, the mutation N180V leads to the loss of 2 Chl a molecules, as already observed in Lhca1 (14). In the absorption difference spectrum at low temperature, two bands are present at 666 nm and 679.5 nm (figure 3). Most of the oscillator strength is in the lower energy band (ratio 1:10). The same components can be observed in the CD spectrum (data not shown) thus suggesting that these

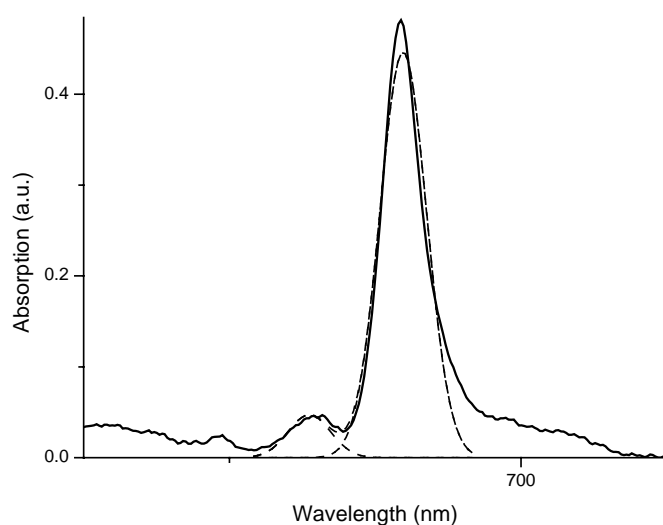


Figure 3. Difference absorption spectra between Lhca3 WT and N180V mutant (solid). Gaussian fitting of the absorption spectra is also reported (dashed).

are the two bands of an excitonic interaction. Considering isoenergetic monomers, the interaction

energy would be 149 cm^{-1} and the angle between the two transition dipoles 145° . These values are very similar to the values calculated from the structure of LHCII for the interaction between A2 and B2 (6).

This result suggests that also in Lhca3 N180 coordinates Chl A2 and it confirms that this domain is strongly conserved in all Lhc complexes. The possibility that in Lhca3 N180V coordinates Chl A5 and that this pigment has the same properties of Chl A2 in LHCII is very unlikely, specially considering that Chl A5 is located on the other side of the complex and it should interact with Chls in the C helix domain (see below). The second Chl lost is most probably accommodated in site B2, which is located in close proximity of Chl A2. We can conclude that in Lhca3 sites A2 and B2 both coordinates a Chl a molecule, which are responsible for the 663/680 nm absorption. This mutant also shows a decreased amount of lutein, while violaxanthin and β -carotene were almost unaffected. This specific loss of lutein upon mutation suggests that the chl site is located near L1, which was shown to bind lutein in all members of Lhc multigenic family (26). Data on carotenoid occupancy thus confirm the identification of this binding site as the A2.

Mutations at Q194 and H209 (A3 and B3)

The structure of PSI-LHCI suggests that Chls A3 and B3 are not present in Lhca3: in their place a "new" Chl in intermediate position (11041) was modelled. (3). However, the putative ligands for these two Chls are conserved in Lhca3 as in all other Lhc proteins but Lhcb6, which misses Chl B3 (2). We performed a mutation at both residues and obtained reconstituted complexes, which show biochemical and spectroscopic properties clearly different from the WT. The Q194L mutant is strongly affected in the Chl binding and it loses at least three Chl molecules. Two are the possible explanations: Chl A3 is present in Lhca3 and it is lost by the direct effect of the mutation or the mutation Q194L influences the binding of a carotenoid molecule and thus change the folding and the stability of the complex inducing loss of Chls which are not in A3 site. Mutation analysis at the same ligand in Lhca1 complex has shown that both these hypothesis are correct: here, in fact, the mutant is losing the Chl in A3 site, but it is also losing the carotenoid in L1 site and this loss destabilises the binding of other Chls which are in contact with lutein in L1 (14). Results presented here suggest a similar effect in Lhca3 as well.

A clearer indication of the presence of Chl A3 and B3 in Lhca3 comes from the analysis of the H209F mutant. In all complexes analysed so far the mutation at this site has a localised effect and does not influence the folding of the protein, in agreement with the location of this Chl at the periphery of the complex (22;24;25). However, Chl B3 is located near by Chl A3 in all complexes

and seems to interact with it, as suggested by the LHCII structure (6) and by the mutation analysis in Lhca1 (14). The H209F mutation in Lhca3 induces the loss of only one Chl a molecule, thus suggesting that H209 is coordinating a Chl molecule in Lhca3. Moreover, the absorption difference spectrum has shown different contributions as it was in the case of Lhca1 and Lhca4 (14;16). This suggests that the Chl a lost by effect of the mutation H209F is interacting with a second Chl a. In the structure there are no chlorophylls located in the proximity of Chl 1041 and thus the interacting chlorophylls can be proposed to be Chl A3. We conclude that Chl organisation in the D helix domain is conserved in Lhca3 and Chl molecules are present in sites A3 and B3.

Mutation N55 and E119V/R122L

It has been shown that in Lhca1, Lhca2 and Lhca4 the red forms originate from pigment-pigment interaction involving Chls in sites A5 and B5. Substitution of the ligand for these two Chls with residues which can not coordinate Chl leads to the loss of the red most emission in all complexes (14-16). In the case of Lhca3 it was demonstrated that the substitution of N55 with H was not leading to the loss of Chls, but was completely abolishing the red forms, as it was the case in Lhca4 (13). If the folding of Lhca3 is different from the one of the other Lhc complexes, the N55H mutation should have affected not Chl in site A5, as suggested, but Chl in site A2. This would imply that the second Chl participating to the interaction leading to the red forms could not be, in Lhca3, Chl B5, which is 24.7 Å distant from Chl A2 (3), but should be Chl B2, which is far 9.3 Angstroms. If this is correct, mutation at site B5 should then not influence the red forms.

The data show that this is not the case: mutation at site B5 completely abolished the red forms, as well as mutation at site N55, thus suggesting that the Chls coordinated by these residues are located nearby. We can conclude that N55 in Lhca3 is coordinating Chl A5 and not Chl A2 and that in Lhca3 the red emission originates from an interaction between Chls A5 and B5. Thus, red forms have a common origin in all Lhca complexes, even if they have different energies in the different complexes.

Are other chlorophylls involved in red forms?

Two other Lhca3 mutants were shown to have an effect on red forms: E111V and Q194L, identified as B6 and A3, seen that Lhca3 has a conserved Chl organisation.

Mutant E111V loses one Chl a molecule. In fluorescence, B6 mutant still shows the 724 nm emission typical of Lhca3, albeit its intensity is strongly reduced and the maximum of the emission is at 686 nm. This finding is in line with the role of Chl B6 in stabilising the conformation yielding to the red forms, already suggested in the case of Lhca1 (14). In its absence, the equilibrium

between the conformations is shifted toward the conformation yielding the 685 nm emission. However, the 724 nm emission is clearly still present and thus B6 is not directly involved in the red most forms of Lhca3, although it has a strong indirect influence.

For what concerns Q194L, instead, the explanation is less straightforward. In fact, A3 mutant induce a strong depletion of red forms. On the other side, Chl A5 and B5 were shown to be directly involved in red forms in Lhca3 and these chlorophylls are located around 20 Angstrom away from A3². The phenotype of Chl A3 can be explained as an indirect effect, due to the perturbation of the structure. In fact, as discussed above, the mutation induces a large destabilisation of the complex.

Carotenoids organisation

From the analysis of the pigment content on the mutants, it is possible to get information about the carotenoid organisation in Lhca3. β -carotene is specifically lost upon mutations at sites A5, B5 and B6, thus indicating that it is accommodated in the L2 site. In the same mutants also a reduction of violaxanthin was observed, which suggests that L2 has mixed occupancy. Loss of lutein was observed upon mutation at site A2, thus confirming that in Lhca3, as in all Lhc complexes analysed so far, L1 site is occupied by lutein. From these data it can also be concluded that the third carotenoid binding site accommodate lutein and violaxanthin. Although it is at present difficult to localise the binding site for the third xanthophylls, the occupancy is very similar to the V1 site of LHCII, thus suggesting a similar organisation in Lhca3. This hypothesis is supported by the analysis of the excitation spectrum of Lhca3 which shows that the energy transfer yield from cars to Chls in this complex is 55% vs. values of 75% in Lhca2, which contains only two cars per polypeptide, accommodated in sites L1 and L2 (12). This difference in energy transfer efficiency can be explained considering the third car is accommodated in V1 site, which has been shown do not be poorly efficient in energy transfer (27).

Conclusions

Data presented here show that the Lhca3 has a folding very similar to the one of all other members of the Lhc family and that the same residues are responsible for the coordination of the Chls. Mutational analysis also suggests that both Chls A3 and B3, although not visible in the structure, are present in the complex. However, it should be noticed that Lhca3 is the only protein where the mutations at both ionic bridges between helices A and B inhibit the folding, suggesting that it might have some structural peculiarity as compared with the other Lhc complexes. On the same line are

² Chl A3 is not present in Lhca3 structure and this distance was estimated from Lhca1, 2 and 4.

the results on A3 mutant, which was yielding a stable complex in all Lhc analysed so far, but which in Lhca3 shows high instability.

However, if we compare the phenotype of A3 and A4 mutants in Lhca3 with the same mutations in Lhca4 (16) we can observe some similarities. In fact, in both complexes one mutant was strongly destabilised and the other completely unstable. Moreover, the unstable complex (A4 in Lhca4 and A3 in Lhca3) showed a strong perturbation of red forms, effect which was not shown by A3 and A4 mutants of Lhca1 (14). Thus, in both Lhca3 and Lhca4 Chl A5 and B5 play a major role in red forms, but other chromophores could have a role, direct or indirect, in the establishment of the strong red shift observed.

References

1. Haworth, P., Watson, J. L., and Arntzen, C. J. (1983) *Biochim. Biophys. Acta* 724, 151-158.
2. Jansson, S. (1994) *Biochim. Biophys. Acta* 1184, 1-19.
3. Ben Shem, A., Frolov, F., and Nelson, N. (2003) *Nature* 426, 630-635.
4. Boekema, E. J., Jensen, P. E., Schlodder, E., van Breemen, J. F., van Roon, H., Scheller, H. V., and Dekker, J. P. (2001) *Biochemistry* 40, 1029-1036.
5. Ballottari M., Govoni, C., Caffarri, S., and Morosinotto, T. (2004) *Eur. J. Biochem.* in press.
6. Liu, Z., Yan, H., Wang, K., Kuang, T., Zhang, J., Gui, L., An, X., and Chang, W. (2004) *Nature* 428, 287-292.
7. Kühlbrandt, W., Wang, D. N., and Fujiyoshi, Y. (1994) *Nature* 367, 614-621.
8. Schmid, V. H. R., Cammarata, K. V., Bruns, B. U., and Schmidt, G. W. (1997) *Proceedings of the National Academy of Sciences of the United States of America* 94, 7667-7672.
9. Zhang, H., Goodman, H. M., and Jansson, S. (1997) *Plant Physiol* 115, 1525-1531.
10. Ganeteg, U., Strand, A., Gustafsson, P., and Jansson, S. (2001) *Plant Physiol* 127, 150-158.
11. Schmid, V. H. R., Potthast, S., Wiener, M., Bergauer, V., Paulsen, H., and Storf, S. (2002) *Journal of Biological Chemistry* 277, 37307-37314.
12. Castelletti, S., Morosinotto, T., Robert, B., Caffarri, S., Bassi, R., and Croce, R. (2003) *Biochemistry* 42, 4226-4234.
13. Morosinotto, T., Breton, J., Bassi, R., and Croce, R. (2003) *J. Biol. Chem.* 278, 49223-49229.
14. Morosinotto, T., Castelletti, S., Breton, J., Bassi, R., and Croce, R. (2002) *J. Biol. Chem.* 277, 36253-36261.
15. Croce, R., Morosinotto, T., Ihalainen, J. A., Chojnicka, A., Breton, J., Dekker, J. P., van Grondelle, R., and Bassi, R. (2004) *J. Biol. Chem.*
16. Morosinotto, T., Mozzo, M., Bassi, R., and Croce, R. (2004) *submitted*.
17. Nagai, K. and Thøgersen, H. C. (1987), *Methods in Enzimology*.461-481.

18. Paulsen, H., Finkenzeller, B., and Kuhlein, N. (1993) *Eur. J. Biochem.* 215, 809-816.
19. Giuffra, E., Cugini, D., Croce, R., and Bassi, R. (1996) *Eur. J. Biochem.* 238, 112-120.
20. Gilmore, A. M. and Yamamoto, H. Y. (1991) *Plant Physiol.* 96, 635-643.
21. Croce, R., Canino, g., Ros, F., and Bassi, R. (2002) *Biochemistry* 41, 7343.
22. Remelli, R., Varotto, C., Sandona, D., Croce, R., and Bassi, R. (1999) *J. Biol. Chem.* 274, 33510-33521.
23. Dominici, P., Caffarri, S., Armenante, F., Ceoldo, S., Crimi, M., and Bassi, R. (2002) *J. Biol. Chem.* 277, 22750-22758.
24. Bassi, R., Croce, R., Cugini, D., and Sandona, D. (1999) *Proc. Natl. Acad. Sci. USA* 96, 10056-10061.
25. Rogl, H. and Kuhlbrandt, W. (1999) *Biochemistry* 38, 16214-16222.
26. Morosinotto, T., Caffarri, S., Dall'Osto, L., and Bassi, R. (2003) *Physiologia Plantarum* 119, 347-354.
27. Caffarri, S., Croce, R., Breton, J., and Bassi, R. (2001) *J. Biol. Chem.* 276, 35924-35933.

B 7

*The Nature of a Chlorophyll ligand in Lhca
Proteins determines
the Far Red Fluorescence emission typical
of Photosystem I*

This chapter has been published in Journal of Biological Chemistry
278 (2003), pp 49223 - 49229, reproduced with permission.

Tomas Morosinotto, Jacques Breton, Roberto Bassi and
Roberta Croce

The Nature of a Chlorophyll Ligand in Lhca Proteins Determines the Far Red Fluorescence Emission Typical of Photosystem I*

Received for publication, August 19, 2003, and in revised form, September 21, 2003
Published, JBC Papers in Press, September 22, 2003, DOI 10.1074/jbc.M309203200

Tomas Morosinotto^{‡§}, Jacques Breton[¶], Roberto Bassi^{‡§||}, and Roberta Croce^{**}

From the [‡]Dipartimento Scientifico e Tecnologico, Università di Verona, Strada Le Grazie, 15-37134 Verona, Italy, the [§]Université Aix-Marseille II, Laboratoire de Genétique et Biophysique des Plantes, Faculté des Sciences de Luminy, Département de Biologie, Case 901-163, Avenue de Luminy, 13288 Marseille, France, the [¶]Service de Bioénergétique, Bât. 532, Commissariat à l'Énergie Atomique, Saclay, 91191 Gif-sur-Yvette Cedex, France, and the ^{**}Consiglio Nazionale delle Ricerche, Istituto di Biofisica, Via Sommarive 18, 38050 Povo (Trento), Italy

Photosystem I of higher plants is characterized by a typically long wavelength fluorescence emission associated to its light-harvesting complex I moiety. The origin of these low energy chlorophyll spectral forms was investigated by using site-directed mutagenesis of *Lhca1–4* genes and *in vitro* reconstitution into recombinant pigment-protein complexes. We showed that the red-shifted absorption originates from chlorophyll-chlorophyll (Chl) excitonic interactions involving Chl A5 in each of the four Lhca antenna complexes. An essential requirement for the presence of the red-shifted absorption/fluorescence spectral forms was the presence of asparagine as a ligand for the Chl *a* chromophore in the binding site A5 of Lhca complexes. In Lhca3 and Lhca4, which exhibit the most red-shifted red forms, its substitution by histidine maintains the pigment binding and, yet, the red spectral forms are abolished. Conversely, in Lhca1, having very low amplitude of red forms, the substitution of Asn for His produces a red shift of the fluorescence emission, thus confirming that the nature of the Chl A5 ligand determines the correct organization of chromophores leading to the excitonic interaction responsible for the red-most forms. The red-shifted fluorescence emission at 730 nm is here proposed to originate from an absorption band at ~700 nm, which represents the low energy contribution of an excitonic interaction having the high energy band at 683 nm. Because the mutation does not affect Chl A5 orientation, we suggest that coordination by Asn of Chl A5 holds it at the correct distance with Chl B5.

Photosystem I is a multisubunit pigment-protein complex of the chloroplast membrane acting as a plastocyanin/ferredoxin oxidoreductase in oxygenic photosynthesis. One important spectroscopic feature of PSI¹ is the presence of Chls absorbing at energy lower than the PSI primary electron donor, P700.

* This work was funded by Ministero dell'Istruzione Università e Ricerca (MIUR) Progetti Fondo per gli Investimenti della Ricerca di Base (FIRB) Grants RBAU01E3CX and RBNE01LACT and by the European Community's Human Potential Program Grant HPRN-CT-2002-00248 (PSICO). The costs of publication of this article were defrayed in part by the payment of page charges. This article must therefore be hereby marked "advertisement" in accordance with 18 U.S.C. Section 1734 solely to indicate this fact.

|| To whom correspondence should be addressed. Tel.: 39-0458027916; Fax: 39-0458027929; E-mail: bassi@sci.univr.it.

¹ The abbreviations used are: PSI/II, Photosystem I/II; CD, circular dichroism; Chl, chlorophyll; FWHM, full-width half-maximum; HN, His → Asn mutation; LD, linear dichroism; LHCI, light-harvesting complex of PSI; LHCI, light-harvesting complex of PSII; NH, Asn → His mutation; WT, wild type.

Although these spectral forms account for only a small percentage of the total absorption, their effect in the energy transfer and trapping of PSI is very prominent (1), with at least 80% of excitation in the complex transiting through them on their way to P700 (2). It has been widely proposed that these forms represent the low energy contributions of excitonic interactions, which involve two or more Chl molecules (3–5); however, the identity of the chromophores involved and the details of the interaction are still unknown.

Although the presence of low energy-absorbing Chls is ubiquitous in the PSI of different organisms, their amounts and energies appear to be highly species-dependent (1). In the PSI of higher plants, the red forms are associated with the outer antenna, LHCI (6, 7). LHCI is composed by four pigment-binding proteins, namely Lhca1–4 (6, 8). These complexes, localized on one side of the core complex (9, 10), are organized in dimers with 10 Chl molecules per subunit (11).

As for their properties, Lhca2 and Lhca4 differ from Lhca1 and Lhca3 in many respects. The first two have higher Chl *b* content with respect to Lhca1 and Lhca3 and bind two carotenoid molecules per polypeptide rather than three (12). For their folding, Lhca2 and Lhca4 require both Chl *a* and Chl *b*, whereas Lhca1 and Lhca3 are stable with Chl *a* only (12, 13). Circular dichroism spectra, yielding information of pigment organization within the complex, also show strong similarities between Lhca2 and Lhca4 on one hand and Lhca3 and Lhca1 on the other (12). The close relation between Lhca2 and Lhca4 is confirmed by sequence analysis, which shows 55% identity and 75% homology (14). Surprisingly, the distribution of red forms does not fit into the picture, because these are associated mainly with Lhca3 and Lhca4 (fluorescence emission at 725–730 nm), whereas Lhca1 and Lhca2 have emission at higher energy (702 nm) (12, 13, 15). Based on high homology between proteins with different content in red forms, a sequence motif associated with the presence of lowest absorption band, common to Lhca3 and Lhca4 and not present in Lhca1 and Lhca2, should possibly be detected. In fact, Lhca3 and Lhca4 have Asn as the ligand for Chl A5 instead of His (Fig. 1), which is in this position in all other components of Lhc family, including Lhca1 and Lhca2 (14), which show no or a low amount of red-shifted spectral forms. It should be noted that Chl A5 has been involved in red forms together with Chl B5 (16). In this work, the effect of the presence of Asn as ligand for Chl A5 in Lhca complexes was analyzed in relation to the appearance of the red emission, which characterizes the antenna complexes of Photosystem I. We show that an essential requirement for the presence of the red-shifted absorption/fluorescence spectral forms was the presence of Asn as ligand for the Chl *a* in the binding site A5 of Lhca complexes. Conversely, substitution of

Lhca1 RYKESELIHCRWAMLAVPGILVPEALGYGNWV
Lhca2 WFVQAEVLVHGRWAMLVAGILIPExLGKIGII
Lhca3 WLAYGEIINGRFAMLGAAAGIAPEILGKAGLI
Lhca4 WFVQAEVLNGRWAMLVAGMLLPEVFTKIGII
 . * : : * : * * . . . * : * * : . . :

FIG. 1. Sequence comparison between the B helices of the four Lhca complexes. The bold characters indicate the ligand for Chl A5. An asterisk (*) stands for identity, a colon (:) indicates strong homology, and a period (.) stands for weak homology.

the His ligand with Asn produces a shift of Lhca1 fluorescence emission to lower energy. We conclude that His *versus* Asn binding of Chl A5 controls the strength of the interaction with Chl B5 by changing the interchromophore distance.

EXPERIMENTAL PROCEDURES

DNA Constructions and Isolation of Overexpressed Lhca Apoproteins from Bacteria—cDNAs of Lhca1–4 from *Arabidopsis thaliana* (11, 12) were mutated with QuikChange© site-directed mutagenesis kit, Stratagene. WT and mutant apoproteins were isolated from the SG13009 strain of *Escherichia coli* transformed with constructs following a protocol described previously (17, 21–23). Reconstitution and purification of protein-pigment complexes were performed as described (11, 12).

Protein and Pigment Concentration—High performance liquid chromatography analysis was as described (18). The chlorophyll-to-carotenoid ratio and the Chl *a/b* ratio was measured independently by fitting the spectrum of acetone extracts with the spectra of individual purified pigments (19).

Spectroscopy—The absorption spectra at room temperature and 100 K were recorded using an SLM-Aminco DK2000 spectrophotometer in 10 mM Hepes, pH 7.5, 20% glycerol (60% at low temperature) and 0.06% *n*-dodecyl- β -D-maltopyranoside. The wavelength sampling step was 0.4 nm, the scan rate was 100 nm/min, and the optical pathlength was 1 cm. Chlorophyll concentration was \sim 10 μ g/ml. Fluorescence emission spectra were measured using a Jasco FP-777 spectrofluorometer and corrected for the instrumental response. The samples were excited at 440, 475, and 500 nm. The spectral bandwidth was 5 nm (excitation) and 3 nm (emission). Chlorophyll concentration was \sim 0.02 μ g/ml in 60 and 80% (Lhca1 only) glycerol and 0.03% *n*-dodecyl- β -D-maltopyranoside. LD spectra were obtained as described by using samples oriented uniaxially by the polyacrylamide gel-squeezing technique (20).

The CD spectra and denaturation temperature measurements were measured at 10 °C on a Jasco 600 spectropolarimeter. The wavelength sampling step was 0.5 nm, the scan rate was 100 nm/min, and spectra were recorded with eight accumulations. The OD of the samples was 1 at the maximum in the Q_y transition for all complexes, and the samples were in the same solution described for absorption measurements. All spectra presented were normalized to the polypeptide concentration based on the Chl binding stoichiometry as described (16).

Denaturation temperature measurements were performed by following the decay of the CD signal at 459 nm while increasing the temperature from 20 to 80 °C with a time slope of 1 °C per min and a resolution of 0.2 °C. The thermal stability of the protein was determined by finding the $t_{1/2}$ of the signal decay.

RESULTS

Mutation Asn-His in Lhca3 and Lhca4—Lhca proteins are strongly conserved, and residues coordinating Chl ligands are identical in the four members of the sub-family. The only exception is the ligand of Chl A5, a His in Lhca1 and Lhca2, which is substituted by Asn in Lhca3 and Lhca4. Because this difference correlates with the presence of a strong red-shifted fluorescence emission band at \sim 730 nm, we proceeded to mutate residues Asn-62 (Lhca3) and Asn-47 (Lhca4) into His. After overexpression in bacteria and reconstitution *in vitro* with purified pigments, mutant Lhca3 and 4 complexes were obtained having a monomeric aggregation state as determined by gradient ultracentrifugation (not shown).

The pigment composition of the Asn \rightarrow His (NH) mutant (Lhca3-N62H and Lhca4-N47H), as compared with the WT complexes reconstituted in the same conditions, is reported in Table I. It is worth noting that the conservative mutation 189 leaves the number and relative ratio of the chromophores in the

complexes unchanged with respect to their WT counterparts. Nevertheless, spectroscopic analysis shows that Lhca3-N62H and Lhca4-N47H have lost their low energy absorption features present in WTs (Fig. 2). This is confirmed by low temperature fluorescence emission spectra (Fig. 3). In Lhca3, the emission peak is shifted from 725 nm in the WT to 686 nm in the mutant. In WT Lhca4 the emission maximum is at 730 nm, whereas the mutation yields a complex with a 686-nm peak, although an additional emission is present at around 702 nm. The difference between WT and mutant absorption spectra showed that the loss of absorption in the red tail of the Q_y transition was compensated by an increase at around 675 nm (676 in Lhca3 and 674 in Lhca4). A second positive contribution in the difference absorption spectrum was visible at 683 nm. No significant difference is observed in Chl *b* and carotenoid absorption regions, thus indicating that the mutation does not affect the energy levels of these pigments. It has been suggested that the red forms are the result of strong excitonic interactions between antenna Chls (3, 16). To analyze this aspect, the CD spectra of the four samples were recorded (Fig. 4). Both Lhca3 and Lhca4 WT were characterized by the presence of a large negative contribution at wavelength longer than 700 nm. Upon mutation, this signal disappeared, together with a positive contribution at 680–681 nm. The shape of the signal in the CD difference spectra (Fig. 4, dash-dot lines) suggests the loss in the mutants of an excitonic interaction with the low energy contribution at 700–705 nm and the high energy band around 682–683 nm, in complete agreement with the absorption spectra in which two positive contributions at these wavelengths were lost upon mutation.

The strength of a Chl-Chl interaction depends on both the distance between the chromophores and the orientation of their dipole moments. To check whether the Asn *versus* His exchange had affected the orientation of the Chls, linear dichroism spectra of the complexes were measured (Fig. 5).

The spectra of WTs are identical to those of the corresponding mutant proteins in the 460–520 nm region, an indication that no changes occur in the carotenoid orientation. In the mutants, the positive contribution at long wavelengths is substituted by a new absorption around 676 nm, which still exhibited positive LD. The comparison of the difference absorption and LD spectra (Figs. 2 and 5) suggests that Chl A5, although changing its ligand residue, maintains the same orientation as in the WT. We therefore exclude the proposal that the loss of the excitonic interaction might be due to a change in the orientation of Chls as a consequence of the mutation.

Mutation His \rightarrow Asn in Lhca1 and Lhca2—The above results clearly demonstrate that the presence of Asn as a ligand for Chl A5 is a requirement for the presence of the red-most forms. To test the hypothesis that this feature is also sufficient for the presence of this spectroscopic property, Lhca1 and Lhca2, which have His ligand at their A5 site (H47 and H52, respectively) and show emission at 702 nm (13), were mutated to Asn-47 and Asn-52. Both mutant proteins yielded a refolded monomeric product. In the case of Lhca2, the recombinant complex was unstable as judged from heat denaturation data (Table I). This suggests that the His \rightarrow Asn exchange is affecting the folding of Lhca2, thus preventing a selective evaluation of the effect of ligand exchange. On this basis, this sample will not be analyzed any further in this work.

In the case of Lhca1, a stable mutant complex was obtained. The fluorescence spectra was shifted by 11 nm toward the red compared with the WT (Fig. 6A). Consistently, the absorption and LD spectra showed an increase in the red-most absorption region of Lhca1-H47N as compared with WT.

Additional features are the loss of the 684 nm (positive LD)

TABLE I
Pigment composition of reconstituted complexes

Abbreviations used in this table include the following: Car, carotenoids; Car_T, carotenoid total; Chl_T, chlorophyll total; Viola, violaxanthin; Lute, lutein; β -Car, β -carotene (Lhca3); Neo, neoxanthin (Lhca1); and DT, denaturation temperature.

Sample	Chl <i>a/b</i>	Chl/Car	Chl _T	Car _T	Chl <i>b</i>	Viola	Lute	β -Car/Neo	DT
Lhca1-WT	4.02 \pm 0.13	3.45 \pm 0.14	10	2.90 \pm 0.13	1.99 \pm 0.07	1.09	1.52	0.28	54.2 \pm 1.5
Lhca1-NH	4.1 \pm 0.06	3.2 \pm 0.16	9.5	2.96 \pm 0.07	2.04 \pm 0.07	1.08	1.63	0.26	51.2 \pm 1.8
Lhca2-WT	1.85 \pm 0.15	5.02 \pm 0.18	10	1.99 \pm 0.07	3.52 \pm 0.19	0.47	1.50		53.3 \pm 1.9
Lhca2-NH	2.43 \pm 0.05	4.60 \pm 0.11	9	1.96 \pm 0.05	2.63 \pm 0.03	0.48	1.48		43.2 \pm 1.6
Lhca3-WT	5.50 \pm 0.13	3.70 \pm 0.09	10	2.70 \pm 0.06	1.54 \pm 0.03	0.63	1.70	0.37	45.6 \pm 1.4
Lhca3-NH	5.60 \pm 0.29	3.68 \pm 0.19	10	2.72 \pm 0.14	1.52 \pm 0.07	0.65	1.74	0.33	39.5 \pm 1.5
Lhca4-WT	2.38 \pm 0.11	4.83 \pm 0.20	10	2.07 \pm 0.09	2.96 \pm 0.09	0.36	1.72		47.2 \pm 0.8
Lhca4-NH	2.36 \pm 0.09	4.91 \pm 0.08	10	2.04 \pm 0.09	2.97 \pm 0.12	0.35	1.68	0.08	49.5 \pm 1.9

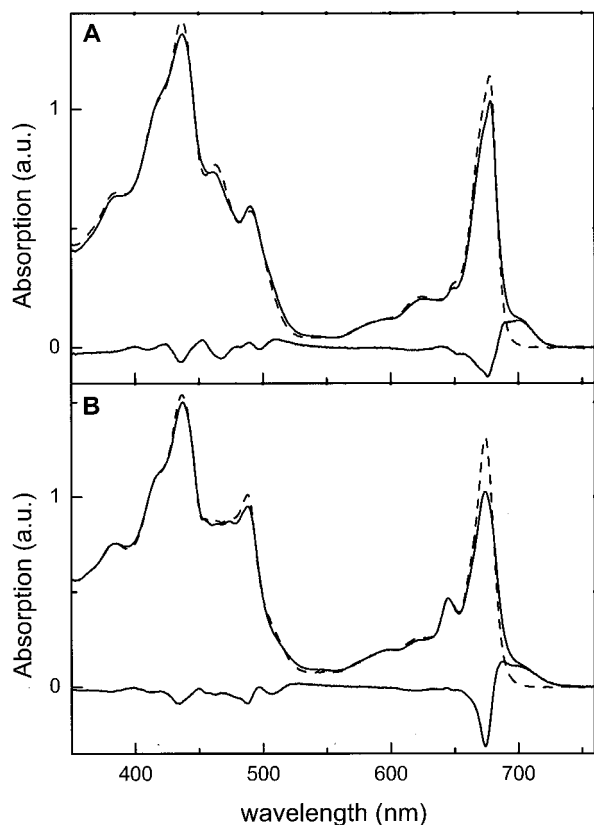


FIG. 2. Absorption spectra at 100 K of Lhca3 and Lhca4 WT and NH mutant. WT (upper solid line), NH mutant (dashed line), and difference (lower solid line) spectra of Lhca3 (A) and Lhca4 (B) are shown. All the spectra are normalized to the total absorption (see "Experimental Procedures"). a.u., arbitrary units.

and of the 678 nm (negative LD) absorption bands (Fig. 5, B and D), probably due to small differences in pigment content. Moreover, the CD spectrum of the mutant is red-shifted and shows increased negative signal above 700 nm (Fig. 5C). We can therefore conclude that the substitution of His with Asn as ligand for Chl A5 in Lhca1 allows the interactions that yield the red forms to be established.

DISCUSSION

Chlorophyll *a* is essential for plant photosynthesis. This single molecular species catalyzes a number of functions including light harvesting, excitation energy transfer, charge separation, and electron transport. Such a unique performance depends largely on the modulation of its physico-chemical properties by the environment provided by specific binding proteins. In reaction centers, the presence of dimers of the Chl molecule confers the "special" nature of a primary donor. In antenna proteins, energy levels of each individual chlorophyll chromophore are modulated by interactions with amino acid groups

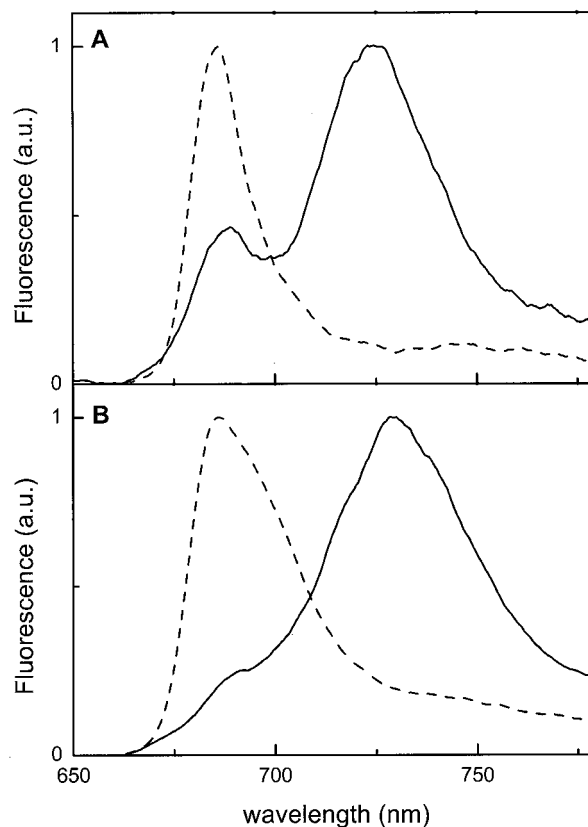


FIG. 3. Fluorescence emission at 77 K of Lhca3 and Lhca4 WT and NH mutant. Spectra of WT (solid line) and NH mutant (dashed line) of Lhca3 (A) and Lhca4 (B) are shown. The spectra are normalized to the maximum (see "Experimental Procedures"). a.u., arbitrary units.

and carotenoid molecules to optimize both energy transfer and photoprotection (21–23). In Photosystem II, the protein environment also provides modulation of chlorophyll fluorescence lifetime and, thus, of the efficiency of energy transfer to P680 by undergoing conformational changes induced by the binding of violaxanthin *versus* zeaxanthin to an allosteric site called L2 (24). The most dramatic example of modulation of the spectroscopic properties of Chl is found in PSI with the presence of long wavelength absorption forms extending light harvesting to the low energy region of the spectrum not absorbed by PSII pigments of the shading canopy (25). Although PSII fluoresces in the 675–695 nm range, PSI exhibits fluorescence emission at \sim 735 nm, thus implying a 60 nm shift with respect to fluorescence emission of Chl *a* in solution. These characteristics have been attributed to the LHCI complex and, more recently, associated with the two *Lhca* gene products Lhca3 and Lhca4 (12). Nevertheless, the structural features responsible for the origin of red forms are still unknown, although mutation analysis of Lhca1 has suggested Chls A5 and possibly B5 to be involved in

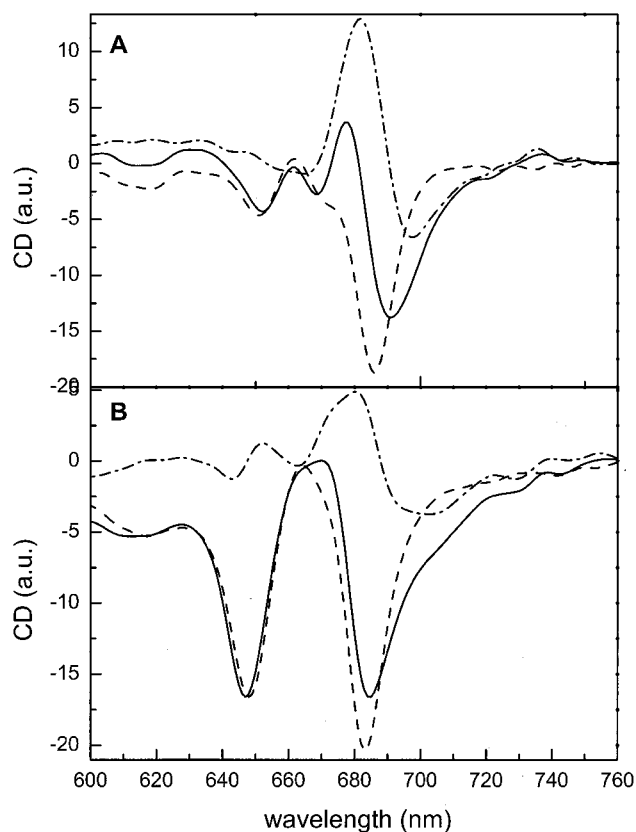


FIG. 4. Circular dichroism spectra at room temperature of Lhca3 and Lhca4 WT and NH mutant. WT (solid line), NH mutant (dashed line), and difference (dash-dot line) spectra of Lhca3 (A) and Lhca4 (B) are shown. The spectra are normalized to the same absorption (see "Experimental Procedures"). *a.u.*, arbitrary units.

the low energy absorption band (16). The involvement of Chl A5 was also suggested in the case of Lhca4, because the deletion of the N-terminal protein domain abolished the red emission (26). Analysis of the protein sequences has identified a difference in the ligand for Chl A5 in Lhca3/4 as compared with Lhca1/2. In the first two complexes, an Asn is present in this position, whereas His is the ligand in the other two, as it is in all other higher plant antenna complexes, which do not exhibit red-shifted emission. To determine the role of the ligand, this residue was mutated in all four Lhca proteins, substituting His for Asn in Lhca1 and Lhca2 and Asn for His in Lhca3 and Lhca4.

Is Asn, as Ligand for Chl A5, Necessary to Yield to the Low Energy Absorption Forms?—Although Lhc proteins differ in the number of Chl ligands, site A5 belongs to the highly conserved core domain formed by transmembrane helices A and B. The His residue in the A5 ligand position was shown to bind a Chl *a* molecule in all of the Lhc proteins analyzed to date (*i.e.* Lhcb1, Lhcb4, and Lhca1) by the loss of a Chl upon mutation of the ligand residue to a non-binding Phe residue. It is important to note that, in both Lhca3 and Lhca4, the substitution of Asn with His did not influence either the number or the composition of pigments bound to the complex.

Nevertheless, the mutation led to the loss of the red forms in both Lhca3 and 4, proving that Asn has a major role, as ligand of Chl A5, in effecting their presence. Moreover, only very specific spectral changes were obtained as a result of the mutation, whereas the spectra were unaffected at most wavelengths. Thus, the Asn to His substitution has a very specific effect, whereas it does not influence the overall properties of the pigment-protein complexes. We conclude that coordination

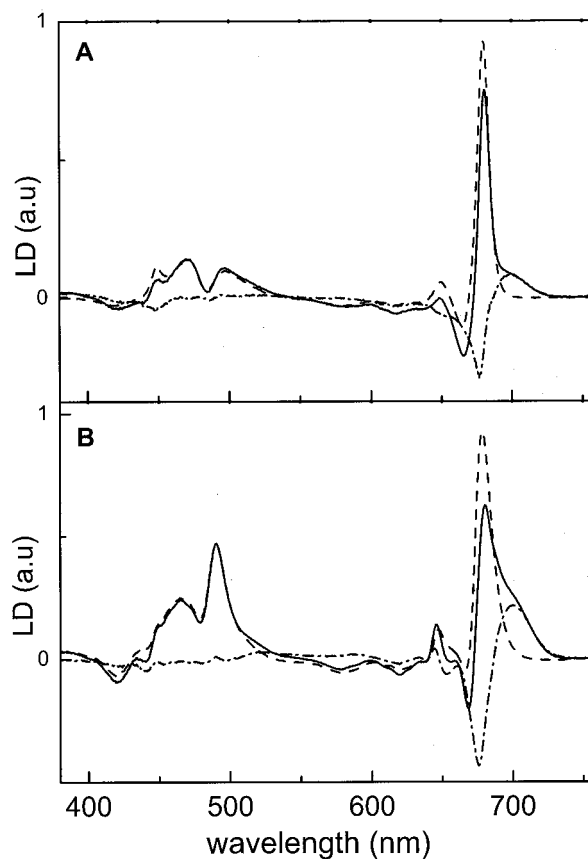


FIG. 5. Linear dichroism spectra at 100 K of Lhca3 and Lhca4 WT and NH mutant. Linear dichroism spectra at 100 K of WT (solid line), NH mutant (dashed line), and the difference (dash-dot line) spectra of Lhca3 (A) and Lhca4 (B) are shown. The spectra are normalized in the blue region (see "Experimental Procedures"). *a.u.*, arbitrary units.

through His induces a re-organization of chromophores involved in the interaction(s) responsible for the red-most spectral feature in the WT complexes.

Orientation and distance are the major determinants in excitonic interactions. In this case, LD analysis shows that the orientation of the Chls is not affected by the mutation. On this basis, we suggest that the main effect of the mutation is to increase the distance between the two interacting Chls. This is realistic considering the structure of the two residues, with Asn having smaller steric hindrance as compared with His (Fig. 8). It has to be considered that the His *versus* Asn substitution appears to be a usual tool for modulation of Chl-Chl interactions in Lhc proteins; Chl A2, when coordinated by Asn in Lhcb1, establishes excitonic interactions with neighbor pigments, namely Chl B2 and Chl A4. This interaction is absent in Lhcb4 (CP29) in which His is the ligand for Chl A2 (21, 22) and again present in the Asn-bearing Lhcb5 (CP26), whose overall biochemical and spectral characteristics are very close to those of CP29 (19).

Is the Presence of Asn as Ligand for Chl A5 Sufficient to Lead to the Red Forms?—A complete mutation analysis of Lhca1 complex showed that the red-most spectral form in this complex, emitting at 702 nm, originates by an interaction between Chls in sites A5 and B5 (16). Upon mutation of the His ligand for Chl A5 in Lhca1, the fluorescence emission of Lhca1-H47N showed a 11-nm red shift as compared with the WT, a clear indication of the formation of a new red spectral form. The absorption and LD spectra display a small but clearly detectable increase in the absorption at wavelengths of >700 nm. Gaussian analysis of the difference LD spectra, where the

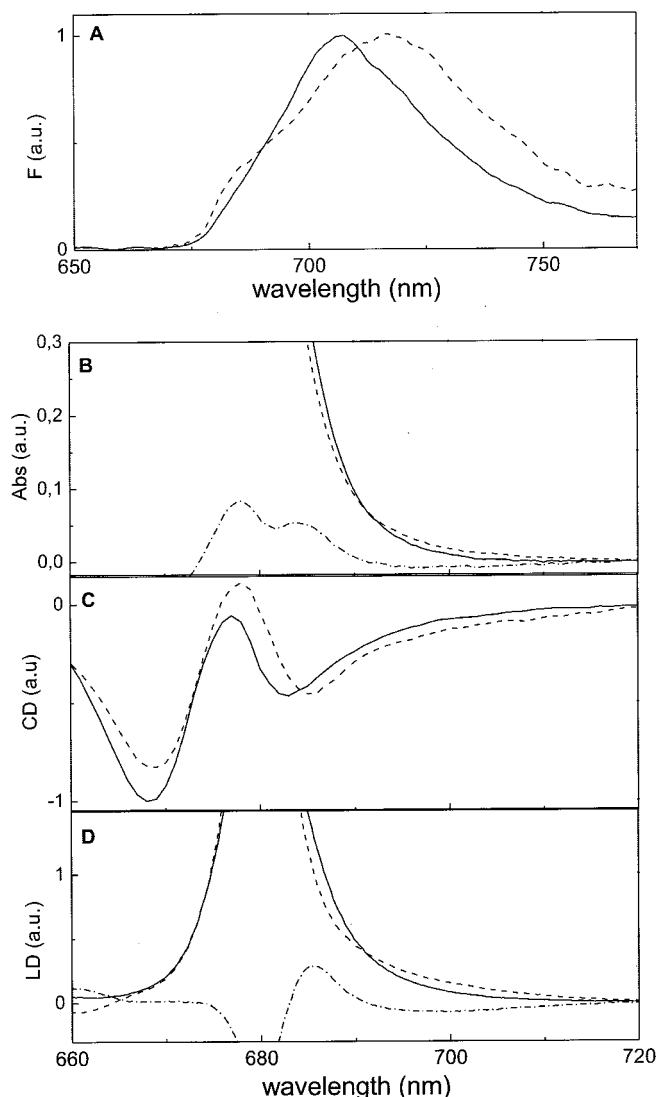


FIG. 6. **Spectroscopic analysis of Lhca1.** Spectroscopic analysis of Lhca1 WT (solid line) and Lhca1-HN mutant (dashed line) is shown. A, fluorescence (F) emission spectra upon excitation at 440 nm at 77 K. B, absorption (Abs) spectra at 100 K. C, CD spectra at 10 °C. D, LD spectra at 100 K. The difference spectra are also presented in most cases (dash-dot line). a.u., arbitrary units.

signal is more clearly detectable, indicates that the newly formed band absorbs with a maximum at 700 nm. The pigment complement of Lhca1-HN is similar to that of the WT, although not identical, as was the case for Lhca3-NH and Lhca4-NH. By normalizing the number of Chls to the carotenoid content, a value of 9.5 Chls in the mutant *versus* 10 in the WT is obtained. It therefore appears that the Asn introduced in Lhca1 as Chl A5 ligand, although able to coordinate Chl, cannot produce 100% occupancy of the site as is the case in the WT. We conclude that the Lhca1 H47N mutant yields a mixed population in which $\sim 50\%$ of the complexes lose the Chl A5 ligand. This is confirmed by preliminary results showing incomplete energy equilibration among Chl *a* chromophores, although Chl *b* to Chl *a* energy transfer is complete. Nevertheless, this experiment shows that the presence of Asn is sufficient to generate the red forms in Lhca1. Our failure to obtain a similar result with Lhca2 suggests, however, that the overall structure of the complex must be suited to host the Chl A5 in the new location. The Lhca2-HN mutant, in fact, loses pigments and does not exhibit red-shifted fluorescence.

Energy Levels of the Interacting Chls—To determine the

energy levels of the interacting Chls, the difference absorption spectra (WT minus mutant) of Lhca3 and Lhca4 were analyzed in terms of Gaussian bands.

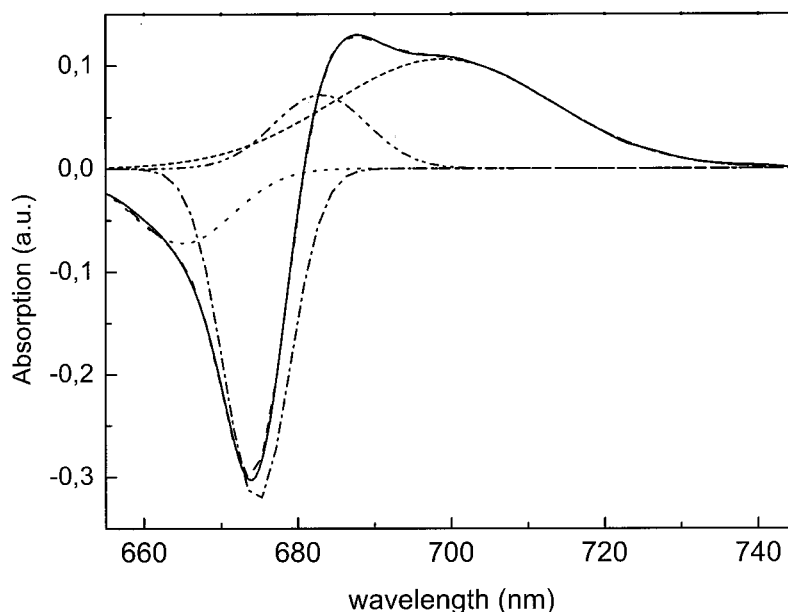
The data, for Lhca4 only, are reported in Fig. 7 and are fully consistent with the data for Lhca3. Three Gaussian components are required for a satisfactory description of the difference spectrum, *i.e.* two positives at 683 nm (FWHM = 15.4 nm) and 700 nm (FWHM = 31.8 nm) and one negative at 675 nm (FWHM = 9.3 nm). The two positive bands are likely to represent the high and the low energy bands of the excitonic interaction, respectively. This proposal is supported by the analysis of the CD spectra; the mutation led to the loss of one negative component at around 703–705 nm and of a positive component at 680 nm. The negative band represents the absorption of the monomers in the absence of the interaction. Considering that the 675-nm band is the only negative contribution observed in the spectra, it can be concluded that the monomers are isoenergetic. Similar values for the absorption of monomeric Chl A5 were found in LHCI and CP29 (21, 22), thus supporting the present conclusion. We have to highlight the fact that the bandwidth of the red-most transition is very large, as is expected in the case of a Chl dimer because of strong electron-phonon coupling, whereas the absorption at 675 nm has the FWHM typical of a Chl monomer.

The low energy transition responsible for the fluorescence emission at 730 nm in a native LHCI preparation composed of Lhca heterodimers was proposed to be lying at 711 nm and to be associated with Lhca4 (27). Such a 711-nm band is not detectable in our difference spectra. We notice, however, that in order to describe the red absorption tail of both Lhca4 and Lhca3 with a form peaking at 709–711 nm having an FWHM of ~ 30 nm (as the fluorescence line narrowing data suggest; Ref. 28) a second Gaussian band with maximum around 697 nm and FWHM of 25 nm would be required. This model with two red-shifted forms, however, would imply an oscillator strength of <1 Chl per Lhca4 monomer associated with the 711-nm form in both Lhca3 and Lhca4 (data not shown). Although a scenario implying more than one red-shifted form in Lhca proteins cannot be discarded without complementary experiments, at present we favor the simpler hypothesis that the 730-nm fluorescence emission band originates from a single absorption form with the maximum of ~ 700 nm on the basis of the following considerations.

First, the values of the Huang-Rhys factors and the mean frequencies of the phonon distribution for the red band of LHCI, as calculated from fluorescence line narrowing measurements, are 2.7 and 0.2 and 110 cm^{-1} and 190 cm^{-1} , respectively (28). Thus, a value of 670 cm^{-1} for the Stokes shift ($2S_{1v_1} + 2S_{2v_2}$) can be proposed, localizing the absorption band responsible for the 730-nm fluorescence emission in Lhca4 (735 nm in LHCI) at 700–705 nm. Second, the band shape of the red-most part of the absorption and LD spectra are identical, implying that if two components are present, then they must have the same dipole orientation of their Q_y transition, which seems unlikely. Third, the CD spectra show the red-most minimum at 703–705 nm, in agreement with the data obtained in the native LHCI preparation (minimum at 706 nm) (27). The absorption maximum associated to this CD signal is thus expected to be shorter than 705 nm.

It has also been proposed that Chl *b* participates in the interaction yielding the red forms in Lhca4 (29). The absorption difference spectra for Lhca3 and Lhca4 do not show any contribution in the Chl *b* region. If a Chl *b* was directly involved in the interaction, a shift of this band upon loss of the interaction is expected. On the basis of the present data we can then exclude a direct involvement of Chl *b* molecules in the red emission forms. This conclusion is in agreement with the pre-

FIG. 7. **Gaussian description of the difference absorption spectra.** Difference absorption spectra of Lhca4-WT and Lhca4-N47H (solid line) and its Gaussian description is shown. *a.u.*, arbitrary units.



vious suggestion that Chl *b* involvement was indirect and due to a structural role for Chl B6 (12, 16).

Based on the above considerations, we conclude that the two bands of the excitonic interaction lie at 683 and 700 nm and a value of 180 cm^{-1} can thus be obtained for the resonance interaction energy, V_{12} . The red shift observed for the two excitonic bands, as compared with the absorption of the monomers, is due to the displacement energy as was already observed for dimers of Chl in solution (30, 31).

An oscillator strength of 1.17 Chl molecules per monomer is associated with the 700-nm absorption band in Lhca4. From this value, the angle between the dipole transition moments of the interacting monomers can be calculated to be $\sim 80^\circ$. A model for the organization of the two interacting Chls in WT and the mutants Lhca3 and Lhca4 is proposed in Fig. 8, which is based on the structure of LHCI (32).

In the LD spectra, the 700-nm band shows a positive contribution, which indicates that the angle between the dipole transition moment and the normal to the membrane plane is $>54.7^\circ$. As for the 683-nm contribution, it does not appear in the LD spectrum, thus suggesting that the Chl responsible for this absorption has a dipole transition moment oriented at the magic angle.

Conclusion—In this work, we have identified the primary role for an Asn residue as a ligand for Chl A5 in determining the chromophore organization yielding the most red-shifted spectral forms of Lhca3 and Lhca4, from which originates the far red fluorescence emission band typical of PSI. The presence of Asn in that position is necessary for the formation of the red-shifted band. It also appears to be sufficient in complexes where Chl binding to site A5 by an Asn residue is allowed. Its role is to keep the two Chls close enough for excitonic interaction. We also suggest that the differences in transition energy and amplitude of red-most bands in the individual Lhca1–4 antenna complexes depends on the strength of the interaction most probably between the same Chl pair, namely Chl A5 and B5. The finding that the fluorescence emission spectrum of Lhca4, upon mutation of Asn-47 to His, closely resembles that of Lhca2-WT supports this conclusion. Our analysis also strongly suggests that the 730-nm emission band originates from a broad absorption around 700 nm. This transition represents the low energy contribution of an excitonic interaction, the high-energy band of which was found at 683 nm. The

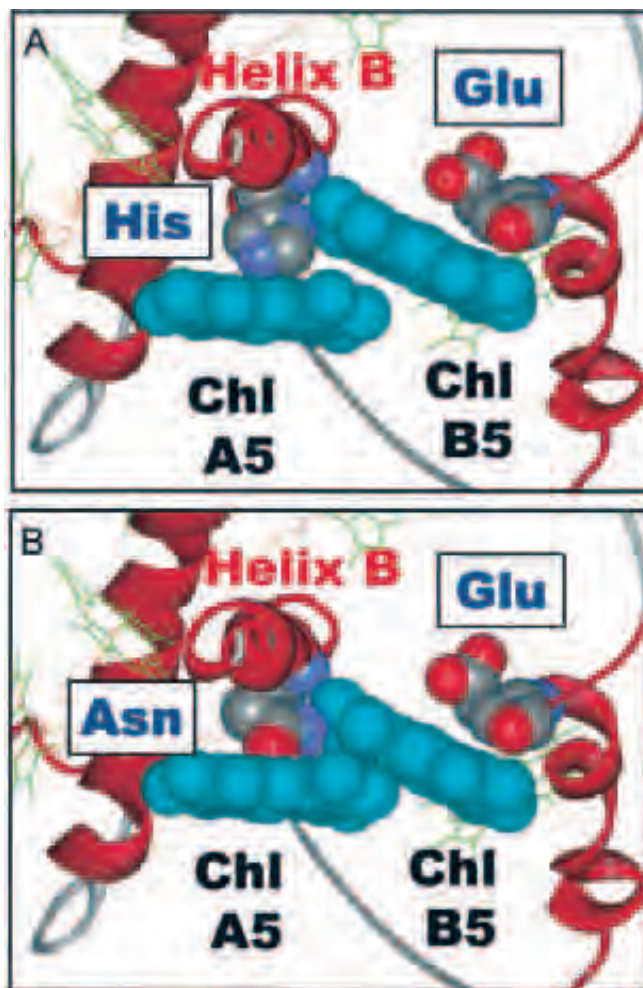


FIG. 8. **Model of Lhca3 and Lhca4 structure.** Suggested geometrical organization of the two interacting Chls responsible for the low energy absorption in Lhca3 and Lhca4. *A*, organization in the mutants in which Asn is substituted by His. *B*, organization in the WT.

possibility that the 700-nm absorption contains more than a single contribution cannot be completely discarded, and this point needs to be analyzed further.

REFERENCES

1. Gobets, B. & van Grondelle, R. (2001) *Biochim. Biophys. Acta* **1057**, 80–99
2. Croce, R., Zucchelli, G., Garlaschi, F. M., Bassi, R. & Jennings, R. C. (1996) *Biochemistry* **35**, 8572–8579
3. Gobets, B., Van Amerongen, H., Monshouwer, R., Kruij, J., Rögner, M., van Grondelle, R. & Dekker, J. P. (1994) *Biochim. Biophys. Acta* **1188**, 75–85
4. Ratsep, M., Johnson, T. W., Chitnis, P. R. & Small, G. J. (2003) *J. Phys. Chem. B* **104**, 836–847
5. Savikhin, S., Xu, W., Soukoulis, V., Chitnis, P. R. & Struve, W. S. (1999) *Biophys. J.* **76**, 3278–3288
6. Bassi, R. & Simpson, D. (1987) *Eur. J. Biochem.* **163**, 221–230
7. Mukerji, I. & Sauer, K. (1990) in *Current Research in Photosynthesis* (Baltshoeffsky, M., ed) Vol. 2, pp. 321–324, Kluwer Academic Publishers, Amsterdam
8. Mullet, J. E., Burke, J. J. & Arntzen, C. J. (1980) *Plant Physiol.* **65**, 814–822
9. Boekema, E. J., Jensen, P. E., Schlodder, E., van Breemen, J. F., van Roon, H., Scheller, H. V. & Dekker, J. P. (2001) *Biochemistry* **40**, 1029–1036
10. Scheller, H. V., Jensen, P. E., Haldrup, A., Lunde, C. & Knoetzel, J. (2001) *Biochim. Biophys. Acta* **1507**, 41–60
11. Croce, R., Morosinotto, T., Castelletti, S., Breton, J. & Bassi, R. (2002) *Biochim. Biophys. Acta* **1556**, 29–40
12. Castelletti, S., Morosinotto, T., Robert, B., Caffarri, S., Bassi, R. & Croce, R. (2003) *Biochemistry* **42**, 4226–4234
13. Schmid, V. H. R., Potthast, S., Wiener, M., Bergauer, V., Paulsen, H. & Storf, S. (2002) *J. Biol. Chem.* **277**, 37307–37314
14. Jansson, S. (1999) *Trends Plant Sci.* **4**, 236–240
15. Schmid, V. H. R., Cammarata, K. V., Bruns, B. U. & Schmidt, G. W. (1997) *Proc. Natl. Acad. Sci. U. S. A.* **94**, 7667–7672
16. Morosinotto, T., Castelletti, S., Breton, J., Bassi, R. & Croce, R. (2002) *J. Biol. Chem.* **277**, 36253–36261
17. Paulsen, H., Finkenzeller, B. & Kuhlein, N. (1993) *Eur. J. Biochem.* **215**, 809–816
18. Gilmore, A. M. & Yamamoto, H. Y. (1991) *Plant Physiol.* **96**, 635–643
19. Croce, R., Canino, G., Ros, F. & Bassi, R. (2002) *Biochemistry* **41**, 7343
20. Haworth, P., Arntzen, C. J., Tapie, P. & Breton, J. (1982) *Biochim. Biophys. Acta* **679**, 428–435
21. Bassi, R., Croce, R., Cugini, D. & Sandona, D. (1999) *Proc. Natl. Acad. Sci. U. S. A.* **96**, 10056–10061
22. Remelli, R., Varotto, C., Sandona, D., Croce, R. & Bassi, R. (1999) *J. Biol. Chem.* **274**, 33510–33521
23. Formaggio, E., Cinque, G. & Bassi, R. (2001) *J. Mol. Biol.* **314**, 1157–1166
24. Morosinotto, T., Caffarri, S., Dall'Osto, L. & Bassi, R. (2003) *Physiol. Plant.*, in press
25. Rivadossi, A., Zucchelli, G., Garlaschi, F. M. & Jennings, R. C. (2003) *Photosynth. Res.* **60**, 209–215
26. Schmid, V. H., Paulsen, H. & Rupprecht, J. (2002) *Biochemistry* **41**, 9126–9131
27. Ihalainen, J. A., Gobets, B., Sznee, K., Brazzoli, M., Croce, R., Bassi, R., van Grondelle, R., Korppi-Tommola, J. E. I. & Dekker, J. P. (2000) *Biochemistry* **39**, 8625–8631
28. Ihalainen, J. A., Rätsep, M., Jensen, P. E., Scheller, H. V., Croce, R., Bassi, R., Korppi-Tommola, J. E. I. & Freiberg, A. (2003) *J. Phys. Chem. B* **107**, 9086–9093
29. Schmid, V. H., Thome, P., Ruhle, W., Paulsen, H., Kuhlbrandt, W. & Rogl, H. (2001) *FEBS Lett.* **499**, 27–31
30. Sauer, K., Lindsay, J. G. & Schultz, A. (1966) *J. Am. Chem. Soc.* **88**, 2681–2689
31. Van Amerongen, H., Valkunas, L. & van Grondelle, R. (2000) *Photosynthetic Excitons*, p. 52, World Scientific Publishing Co., Singapore
32. Kuhlbrandt, W., Wang, D. N. & Fujiyoshi, Y. (1994) *Nature* **367**, 614–621

B 8

*LHCI: the antenna complex of
Photosystem I in plants and green algae*

This chapter is in press in the book: 'Photosystem I: The Plastocyanin: Ferredoxin Oxidoreductase in Photosynthesis' J.H. Goldbeck ed. in the series 'Advances in Photosynthesis in Respiration' by Kluwer Academic Publishers, B.V.

Roberta Croce, Tomas Morosinotto and Roberto Bassi

LHCI: the antenna complex of Photosystem I in plants and green algae.

Roberta Croce, Tomas Morosinotto and Roberto Bassi

Table of Contents

Summary

I. Introduction: LHCI within the PSI supercomplex

II. Characterization of LHCI

- A. Identification of Lhca genes with their gene products
- B. Differential characterization of individual Lhca gene products
 - 1. Fractionation of LHCI – native LHCI
 - a. Purifications
 - b. Pigment content
 - 2. Reverse genetics and chlorina mutants
 - 3. Recombinant proteins

III: Models of LHCI polypeptides

- A. Polypeptide structure
- B. Chlorophyll binding
 - 1. How many chlorophylls are bound to Lhca complexes?
 - 2. Chlorophyll organization
- C. Carotenoid binding

IV. Dimerization of Lhca proteins

V. PSI-LHCI stoichiometry

VI. Energy transfer

VII. On the origin of red absorption forms

- A. Which complexes coordinate the red Chl
- B. Which are the absorption characteristics of the red forms?
- C. How many Chls absorb in the red?
- D. Which Chl specie(s) is involved in red-forms?
- E. Where are the “red Chls” located in the Lhca architecture?
- F. Which is the role of the polypeptide chain in modulating the absorption of the red Chls in the four Lhca complexes?
- G. Which is the mechanism responsible for the large absorption shift of the red forms compared to the bulk Chls?

VIII: Lhca proteins of *Chlamydomonas reinhardtii*

Acknowledgements

References

Summary

In this chapter we summarize the results of many reports, since 1979, on the chlorophyll a/b binding light harvesting complex of Photosystem I. In the first part of this chapter we review results which led to the present knowledge of the biochemical properties of the individual gene products constituting LHCI: in particular, the presence and distribution of red-shifted spectral forms and the idea that LHCI, different from LHCII, is organized into hetero-dimeric complexes. Recent developments based on EM and X-ray crystallography are reported that lead to the understanding that LHCI is bound to a side only of the PSI-LHCI supramolecular complex rather than surrounding the reaction center as recently found in bacterial photosynthesis. The evidence that each Lhca subunit is present in a single copy per reaction center is also reported as compared with the data leading to a previous model with two copies of Lhca polypeptides. In the second part of the chapter, we focused on the origin of the peculiar characteristic of LHCI: the red-shifted chlorophyll spectral forms. First, the evidence for their origin from Chl-Chl interactions is reviewed; second, the different models for the organization of the chromophores involved in these interactions, which have been recently proposed, are discussed. We conclude that present evidence favors the origin of red-forms from Chl a-Chl a excitonic interaction between chromophores localized in binding sites A5 and possibly B5 of Lhca proteins while the evidence for involvement of additional chromophores such as chlorophyll b are consistent with an indirect structural role of the ligand in site B6.

Abbreviations:

α (β)-DM	<i>n</i> -dodecyl- α (β)-D-maltoside
β -car	β -carotene
Car	carotenoid
CD	circular dichroism
Chl	chlorophyll
FWHM	full width half maximum
LD	linear dichroism
Lhc	light harvesting complex
OGP	<i>n</i> -Octyl- β -D-Glucopyranoside
PSI(II)	Photosystem I(II)
Viola	Violaxanthin
WT	wild type

I. Introduction: LHCI within the PSI supercomplex.

Photosystem I is a multisubunit complex located in the stroma lamellae of thylakoid membranes, which function as light-dependent plastocyanine/ferredoxin oxido-reductase. In higher plants and green algae, this supramolecular complex is composed by two chlorophyll binding moieties: (i) the core complex and (ii) the external antenna, encoded by either chloroplast and nuclear genes, respectively. The core is composed by 14 subunits, among which PsaA and PsaB, binding the primary donor P700 and cofactors of the electron transport chain as well as the greatest portion of 96-103 Chl a and 22 β -carotene molecules. In fact, only a few Chls are bound to the minor subunits of the core complex (Ben Shem et al., 2003; Jordan et al., 2001; Scheller et al., 2001), see also book chapter 3 and 5. Besides the inner antenna chlorophylls bound to the core moiety, plant PSI is equipped of a peripheral antenna system binding Chl a, Chl b and carotenoid molecules to four polypeptides, namely Lhca1-4, with molecular weight between 21 and 24 kDa (Haworth et al., 1983; Bassi and Simpson, 1987; Jansson, 1994). The polypeptide composition of PSI-LHCI, PSI-core and LHCI is reported in figure 1.

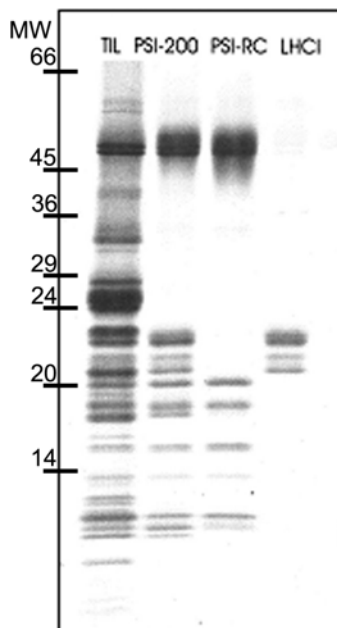


Figure 1. Polypeptide composition of the PSI-LHCI supercomplex and its two moieties: the PSI core complex binding Chl a and β -carotene and the LHCI moiety binding also Chl b and the xanthophylls lutein and violaxanthin. The separation was performed by SDS-urea PAGE.

The topological organization of the LHCI moiety within the PSI supercomplex remained obscure till the recent EM work by single particle analysis (Boekema et al., 2001b) showing that Lhca subunits are located asymmetrically, on one side only of a monomeric core complex (fig. 2). This organization is contrasting with respect to that of PSII where a dimeric core complex is symmetrically surrounded by peripheral antenna proteins binding at multiple sites (Boekema et al., 1999). Nearest-neighbor analysis was performed either by covalent cross-linking or by observing the loss of Lhca components upon knock out or antisense depletion of individual core complex

subunits. On these basis it was proposed that Lhca3 may interacts with PsaK, Lhca2 with PsaG and Lhca1/Lhca4 with PsaF and PsaJ (Jansson et al., 1996; Jensen et al., 2000; Scheller et al., 2001). Moreover, it was also suggested that each Lhca component is in contact with two others (Jansson et al., 1996).

An somehow alternative model has been recently proposed from the crystal structure of PSI-LHCI complex from pea, resolved at 4.4 Å (Ben Shem et al., 2003). Lhca complexes were localized asymmetrically on one side of the core complex moiety, aligned in a crescent-like structure. The only clear interaction could be observed between the helix C of Lhca1 and PsaG while Lhca 2,3 and 4 subunits are proposed to interact with the core components trough small binding surfaces at their stroma exposed regions. Both structural and biochemical data support the view of a LHCI antenna moiety arranged on a side only of the PSI core complex. The reason for this topological organization rather unusual among photosynthetic systems, generally characterized by a circular or symmetrical arrangement of antenna subunits around the reaction center complex (Roszak et al., 2003; Boekema et al., 2001a; Bibby et al., 2001) appears to be a structural adaptation to the functioning of State I-State II transitions (Allen, 1992). This mechanism provides a balance in energy transfer to PSII versus PSI by transfer of phosphorylated LHCII subunits to stroma lamellae where they serve in increasing the antenna size for PSI. The docking of LHCII to the PSI core complex has been reported to be mediated by the PsaH subunit (Lunde et al., 2000) which is located on the LHCI-free side of the PSI core thus being accessible for binding phosphorylated LHCII.



Figure 2. Localization of LHCI polypeptides within the PSI-LHCI complex resolved by X-ray diffraction. Top (stromal) view of the PSI-LHCI complex is shown. The four Lhca subunits are aligned into a crescent-like structure on the lower part of the figure. Subunits exclusive of eukaryotic PSI complex are also indicated. Figure was reproduced from (Ben Shem et al., 2003) with permission of the authors.

From the spectroscopic point of view, the most striking feature of Photosystem I is the presence of Chls which absorb at energy lower than P700, the reaction center (Butler and Norris, 1963). This is clearly visible in the fluorescence emission spectra of the PSI-LHCI complex peaking at approximately 740 nm. The absorption and emission spectra of PSI-LHCI, PSI-core and LHCI are reported in fig. 3. The absorption spectra show that the Chl b, responsible for the absorption at 475 and 650 nm, is associated with LHCI proteins, together with the absorption forms at wavelength > 700 nm, which form the red-most tail in the spectra.

The fluorescence emission spectra of the PSI-LHCI supercomplex and of its two moieties reflect the distribution of red-most absorption forms. Thus, PSI-LHCI, PSI-core and LHCI exhibits their fluorescence emission peaks at respectively 740, 720 and 735 nm (Mullet et al., 1980b).

It has been demonstrated that, at physiological temperature, 80-90% of the excited states in the system reside in the red-shifted forms (Croce et al., 1996). This implies that, in order to be used for charge separation, most of the excitation energy in PSI has to be transferred uphill from red absorption forms to P700, the reaction center.

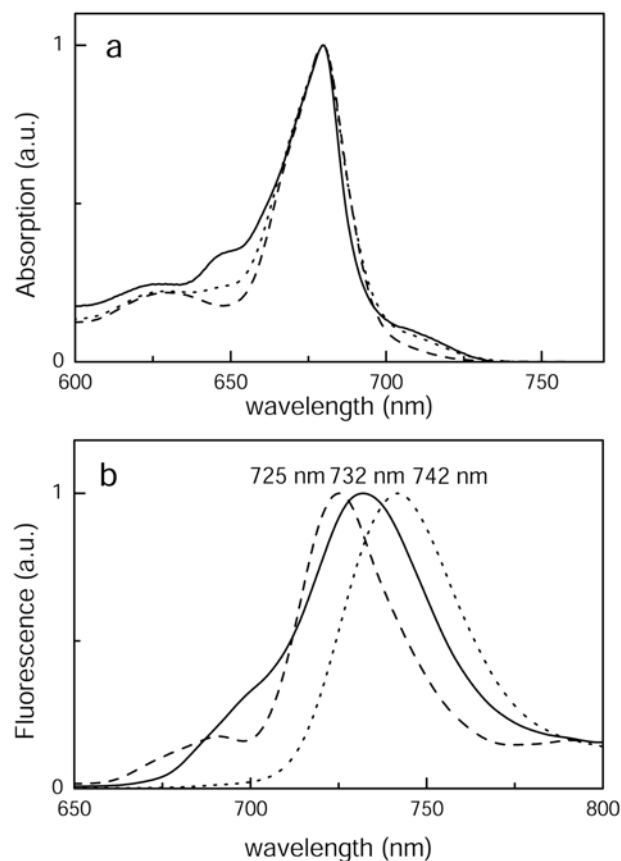


Figure 3. Spectroscopic properties of LHCI (solid), PSI core (dash), PSI-LHCI (dot). (a) Absorption spectra at 77 K (b) Fluorescence spectra at 77 K, emission maxima are also reported.

II. Characterization of LHCI

A. Identification of Lhca genes with their gene products.

Lhca proteins are encoded by the nuclear genome, synthesized by cytoplasmic ribosomes, imported across the two membranes of the chloroplast envelope and finally inserted into the thylakoid membrane (Lubben et al., 1988). Lhca gene sequences are now available from different organisms, thanks to the work of sequencing projects (e.g. see TIGR web site, <http://www.tigr.org/tdb/tgi/plant.shtml>).

In vascular plants, 6 classes of Lhca genes have been identified, namely *Lhca1-6*. Moreover, several copies of the same gene can be found, depending on the species considered (see, e.g. (Jansson, 1994) and references therein). In figure 4a the alignment of protein sequences of Lhca from *Arabidopsis thaliana* is reported (Jansson, 1994). Biochemical studies on *Arabidopsis* as well as on other plants have shown that only the proteins encoded by genes *Lhca1-4* are expressed in the different experimental conditions investigated (see par. II B and references therein). No information is at present available for the products of the genes *Lhca5* and *6* except that they are transcribed at very low level (Jansson, 1999). However, the possibility that *Lhca5* and *Lhca6* are expressed in special environmental conditions or developmental states cannot be ruled out yet. *Lhca6*, highly homologous to *Lhca2*, was proposed to be a pseudogene (Jansson, 1999).

Lhca genes belong to the Lhc multigenic family, which also includes the genes for the outer antenna of Photosystem II, namely *Lhcb1-6* (Jansson, 1999). In figure 4b an unrooted cladogram created by ClustalX of all Lhc deduced protein sequences from *Arabidopsis thaliana* is shown. Antenna proteins of Photosystem I cluster together, being more homologous to each other than to the Lhcb Photosystem II components. Interesting exceptions from this general trend are *Lhca1*, which is more related to *Lhcb4* than to the *Lhca 2-4*, and *Lhcb6* which is intermediate between the two clusters. Evolutionary studies on Lhc multigenic family confirmed a separation between Lhca and Lhcb proteins: in fact, Durnford et al (1999) proposed that Lhca and Lhcb proteins diverged before the separation of different Lhca and Lhcb complexes. Thus, Lhca and Lhcb proteins as separate groups within the Lhc family, suggesting they have specific properties and functions, probably adapted to the characteristics of the Photosystems they are each serving.

```

Lhca1 -----MASNSLMSCGIAAVYPS-----LLSSS-----K-SKFVSA
Lhca2 -----MASSLCASSAIAAIISS---PSFLGGKK---LRLKKKLTVPVAV
Lhca3 ---MAAQALVSSSLTSSVQTARQIFGSKP---VASAS-----QKSSSFVVK
Lhca4 -----MATVTTTHASASIFRPCTSKPRFLTGSS---GRLNRDLSFTSI
Lhca5 -----MAVVLRRGGITGGFLHHR-R----DASS-----VITRRISSVKA
Lhca6 MAFATIASALTSTLTLSTSRVQNPTQRRRPHVVASTSSTGGRLMRERLVVVV
      :
      :
      :
Lhca1  GVPLPNAGNVGRIRMAAHWMPGEP RPAYLDGSAPGDFGFDPLGLGEVPA-
Lhca2  SRPDASVRAVAADPDRPIWFPGSTPPEWLDGSLPGDFGFDPLGLSSDPD-
Lhca3  A---AAAPPVKQGANRPLWVASSQSLSYLDGSLPGDYGFDPGLGLS-DPEG
Lhca4  G-SSAKTSSFKVEAKKGEWLPGLASPDYLTGSLAGDNGFDPLGLAEDPE-
Lhca5  A---GGGINPTVAVERATWLPGLNPPYLDGNLAGDYGFDPGLGLGEDPE-
Lhca6  AGKEVSSVCEPLPPDRPYGSLVALHLNWLGDGSLPGDFGFDPLGLSDPD-
      .
      : * . . ** ***** : * . *
      :
Lhca1  -----NLERYKESELIHCRWAMLA VPGILVPEALGYGNVVKQAQ---EWAA
Lhca2  -----SLKWNVQAEIVHCRWAMLGAAGIFIP EFLTKIGILNTP---SWY-
Lhca3  TGGFIEPRWLAYGEI INGRFAMLGAAGAI APEILGKAGLI PAETALPWFQ
Lhca4  -----NLKWFVQAEILVNGRWAMLG VAGMLLPEVFTKIGI INVP---EWY-
Lhca5  -----SLKWVYQAEIVHSRFAMLG VAGILFTDLLRRTTGIRNLP---VWY-
Lhca6  -----TLKWFAQAEIIHSRWAMLA VTGII IPECLERLGF IENF---SWY-
      .
      : . * : : : * : * : * : : :
      :
Lhca1  ----LPGGQATYLG NVPVWGTLP TILAIEFLAIAFVEHQRSMEK-DP---
Lhca2  ----TAGEQEY-----FTDKTTLFVVELLIGWAEGRRWADI I KPGSV
Lhca3  TGVI PPAGTYTY-----WADNYTLFVLEMALMGFAEHRR LQDWNYPGSM
Lhca4  ----DAGKEQY-----FASSTLFVIEFI LPHVVEIRRWQDIKNPGSV
Lhca5  ----EAGAVKFD-----FACTKTLIVVQFLLMGFAETKRYMDFVSPGSQ
Lhca6  ----DAGSREY-----FADSTTLFVAQVMLMGWAEGRRWADLIKPGSV
      .
      : * : : : * : : : * : : : *
      :
Lhca1  EKK-----K-----YPGG-AFDPLGYSK-DPKKLEELKVKKEIK
Lhca2  NTD-PVFP--NNKLTG-TDVGYPGGWFDPLGWGSGSPAKLKELRTKEIK
Lhca3  GKQ--YFLGLEKGLAGSGNPAYPGGPFNPLGFGK-DEKSLKELKLKEVK
Lhca4  NQD-PIFK--QYSLPK-GEVGYPGG-IFNPLNF----APTQEAKEKEILA
Lhca5  AKEGSFFFGLEAALEG-LEPGYPGGPLLNLPLGLAK-DVQNAHDWKLKEIK
Lhca6  DIE-PKYP--HKVNPK-PDAGYPGGWFDPMWGRGSPPEPVMVLRTKEIK
      .
      : **** : : : : :
      :
Lhca1  NGRLLALLAFVGFVCVQQSAYPGTGPLENLATHLADPWHNNIGDIVIPFN-
Lhca2  NGRLLAMLA VMGAWFQH-IYTGTPIDNLFAHLADPGHATIFAAFTPK--
Lhca3  NGRLLAMLA I LGYFIQG-LVTGVGYPQLLDHLADPVNNVLTSLKFH--
Lhca4  NGRLLAMLA FLGFVVQH-NVTGKGFENLLQHLSDPWHNTIVQTFN----
Lhca5  NGRLLAMMAMLGFFVQA-SVTHTGPIDNLVEHLSNPWHKTIIQTLFTSTS
Lhca6  NGRLLAMLA FLGFCFQA-TYTSQDPIENMAHLADPGHCNVFSAFTSH--
      .
      : ***** : : * . . * : * * : * : :
      :

```

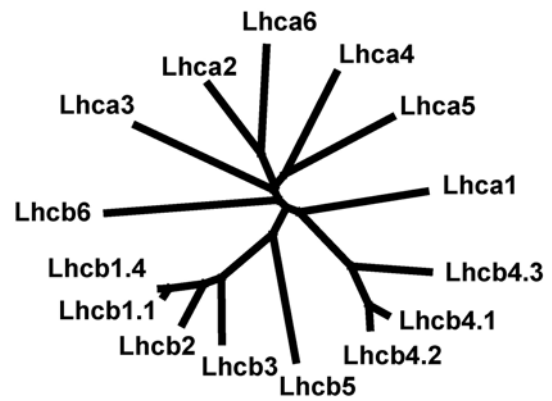


Figure 4. (a) Alignment of protein sequences of Lhca1-6 from *Arabidopsis thaliana*. Chl binding residues are indicated in bold. (b) An unrooted cladogram of deduced protein sequences of Lhc proteins of *Arabidopsis thaliana*.

B. Differential characterization of individual Lhca gene products

The first evidence for the presence of a Chl a/b antenna in higher plants PSI came from the work of Mullet et al. (1980b), who purified PSI complexes differing for their antenna size and for the presence of four polypeptides with molecular mass between 20 and 24 kDa, thereafter identified as the outer antenna system of PSI.

In order to purify the individual Lhca complexes and to determine their biochemical and spectroscopic characteristics, different approaches have been used: purification of LHCI from plants, reverse genetics and refolding in vitro. In the following, the main steps to the determination of the properties of individual Lhca complexes are summarized.

1. Fractionation of LHCI – native LHCI

a. Purifications

LHCI complexes were first purified from pea by Haworth et al. (1983) by sucrose gradient centrifugation. The authors isolated a fraction containing 4 polypeptides with molecular weight

between 20 and 24 kDa, having a Chl a/b ratio of 3.7. In the following years several attempts to further purify LHCI complexes were performed using different methods including sucrose gradient ultracentrifugation (Lam et al., 1984b; Kuang et al., 1984; Bassi and Simpson, 1987; Ikeuchi et al., 1991a; Schmid et al., 2002b), non-denaturing electrophoresis (Lam et al., 1984a; Kuang et al., 1984; Dunahay and Staeheli, 1985; Bassi et al., 1985; Vainstein et al., 1989; Knoetzel et al., 1992; Preiss et al., 1993) and perfusion chromatography (Tjus et al., 1995).

In 1984 Lam et al. (1984a) purified two Lhca fractions from spinach by sucrose gradient ultracentrifugation. The upper band contained the 22 and 23 kDa polypeptides (Lhca2 and Lhca3), while the lower was enriched in the 20 kDa polypeptides (Lhca1 and Lhca4). The fractions showed similar Chl a/b ratio (3.5 ± 0.5), but differed substantially in their spectroscopic properties, with the upper band emitting at 680 nm and the lower at 730 nm. Based on these results, LHCI fractions were named according to their emission peaks at low temperature: LHCI-730 and LHCI-680 (Bassi et al., 1985) and this nomenclature was used in most of the following papers. From these early experiments it was concluded that the red forms were associated to the 20 and 21 kDa polypeptides (Lhca1 and Lhca4), rather than to the heavier subunits (Lhca2 and Lhca3). The polypeptide composition of LHCI-680 and LHCI-730 varied, however, in the different preparations. LHCI-730 in some preparations contained only Lhca1 and Lhca4 (Knoetzel et al., 1992; Tjus et al., 1995; Schmid et al., 2002b), while in others all four Lhca polypeptides were present (Bassi et al., 1985; Bassi and Simpson, 1987; Ikeuchi et al., 1991b). Typically, the LHCI-730 fraction had by a Q_y band Chl a absorption peak at 670-676 and by a 77K fluorescence emission peak at 730 nm. LHCI-680 was found to be enriched in Lhca2 and Lhca3 polypeptides, it showed lower sedimentation rate in sucrose gradient and higher mobility in non denaturing electrophoresis (green gels) as compared to LHCI-730, indicating a lower aggregation state. LHCI-680 had an absorption peak in the Q_y region at 668-670 nm and a fluorescence emission peak at 678-680 nm (Lam et al., 1984a; Knoetzel et al., 1992; Tjus et al., 1995). Exceptions to this pattern suggested a further grade of heterogeneity among the individual gene products: the "LHCI-680" isolated by Bassi and Simpson (1987) from barley contained a single polypeptide, Lhca2, had a Chl a/b ratio of 2.0. Its absorption peak was at 674 and the fluorescence emission peaked at 690 nm. The LHCI-680 preparation described by Ikeuchi et al. (1991b), was enriched in Lhca2 and Lhca3. Whereas showing the maximum of fluorescence emission at 680 nm, had a prominent shoulder above 700 nm suggesting the presence of red-shifted spectral forms in either Lhca2 or 3. In other reports, fractionation of PSI-LHCI complex did not yield a LHCI-680 fraction. The Haworth's preparation (1983), showed emission at 730 nm and contained all four Lhca polypeptides. Also the LHCI preparation by Croce et al. (1998), did not contain a LHCI-680 fraction but only a LHCI-730 with a dimeric aggregation state. From

the latter preparation, two emissions were resolved, peaking at 702 and 730 nm (Ihalainen et al., 2000). It was suggested that the LHCI-680 fraction contains complexes that are not in their fully native state. This is consistent with the blue-shifted absorption peaks (668-670 nm) and the fluorescence emission from partially disconnected Chls (Palsson et al., 1995) with longer fluorescence lifetimes with respect to LHCI-730. Thus, it appears that Lhca2 and Lhca3 can migrate either as monomers, in the LHCI-680 fraction, or dimers, in the LHCI 730 fraction, exhibiting spectroscopic data different depending on aggregation state: longer lifetime emission and blue-shifted absorption in LHCI-680 with respect to LHCI-730. This might be due to higher sensitivity to detergent treatment of Lhca2 and 3 with respect to Lhca1 and 4, as suggested by Lam et al. (1984a).

An attempt to purify Lhca2 and Lhca3 in native state was made by Croce et al. (Croce and Bassi, 1998; Croce et al., 2002) by non-denaturing IEF. In this work fractions containing dimeric complexes were purified either enriched in Lhca2/Lhca3 or Lhca1/Lhca4. Red emission forms were retained not only in Lhca4 containing fractions but also in those in which Lhca2/Lhca3 were predominant, thus suggesting that one or both of these two subunits also accommodate red-shifted Chl forms.

b. Pigment content

The purification of individual Lhca complexes in their native state by classical biochemical methods was very difficult, due to the strong association between the external antenna and the core complex. This property of the complex requires harsh detergent treatment for dissociation. Nevertheless, information about the average biochemical and spectroscopic characteristics of the LHCI complexes was obtained in several plant species.

A summary of LHCI preparations is presented in table 1. Pigment composition of the complexes is also reported.

The Chl a/b ratio values obtained from the different preparations vary considerably, with tomato and barley showing the lowest values (2.5) and maize and pea the highest (4). Both the methods of preparation and intrinsic differences in the Chl b content of LHCI from different species might be the cause for these differences as judged by the finding that the same procedures applied to maize and Arabidopsis, yielded a/b ratios of 3.8 and 3.3 respectively (Croce et al., 2002). Preparations involving the use of Triton X-100 appear to undergo partial Chl loss. More consistent are the data on the carotenoid composition: Lhca complexes bind violaxanthin and lutein, similar to Lhcb proteins (Bassi et al., 1993). However, they do not bind neoxanthin. β -carotene, instead, which is not bound to Lhcb proteins, appears as a minor but genuine chromophore for Lhca proteins.

Thus, biochemical fractionation, although not yielding purification of individual, undenatured, Lhca gene products, provided a characterization of the overall properties of LHCI. Moreover, evidence for heterogeneity of the four Lhca components with respect to both pigment composition and enrichment in red-shifted absorption forms was provided.

Plant material	Fraction	Chl a/b	Chl tot	Viola	Lutein	β -car	Reference
Pea	LHCI	3.7					(Haworth et al., 1983)
	680/730	3.5					(Lam et al., 1984a)
Spinach	680	3.1					(Palsson et al., 1995)
	730	3.2					(Palsson et al., 1995)
Barley	680 ^a	2.0					(Bassi and Simpson, 1987)
	730	2.2					(Bassi and Simpson, 1987)
Tomato	680	2.5	8.99	0.43	0.92	0.4	(Schmid et al., 2002b)
	730	2.57	7.17	0.39	0.84	0.18	(Schmid et al., 1997)
		2.48	11.41	0.54	0.99	0.42	(Schmid et al., 2002b)
LHCI	LHCI	3.8	10	0.55	1.2	0.4	(Croce and Bassi, 1998)
	680	4-5					(Vainstein et al., 1989)
Maize	730	2-2.5					(Vainstein et al., 1989)
	Lhca2/Lhca3	3.8	10	0.5-0.6	1.1-1.2	0.6	(Croce, 1997)
	Lhca1/Lhca4	3.6-3.8	10	0.6-0.7	1.3-1.4	0.4	(Croce, 1997)
Arabidopsis	LHCI	3.3	10	0.6	1.1	0.45	(Croce et al., 2002)
Spinach ^b		3.0	92	7	12	8	(Damm et al., 1990)

Table 1. Pigment composition of LHCI. Data shown were obtained with different purification methods and from different plant species (see par. II B). ^a this preparation contained only Lhca2. ^b data were obtained by difference between the pigment composition of PSI-200 and PSI-core

2. Reverse genetic and *Chlorina* mutants

An alternative approach on the way to clarify the properties of Lhca complexes has been the analysis of plants lacking one or more Lhca gene products. The barley *Chlorina* mutant collection (Simpson et al., 1985) has first been used, followed by knock out mutants or antisense plants.

The *Chlorina f2* mutant lacking Chl b was analyzed by Mullet et al. to support Chl b binding to LHCI complexes and their content in red emission forms (1980a). The preferential failure of *Clo-f2*

to accumulate Lhca4 led to the conclusion that the red-forms are associated to this subunit (Bossmann et al., 1997; Knoetzel et al., 1998). This suggestion was supported by Zhang et al. (1997), who produced antisense *Arabidopsis* plants lacking Lhca4, showing a 6 nm blue shift in the fluorescence emission peak. Antisense plants lacking Lhca2 and Lhca3 (Ganeteg et al., 2001) led the authors conclude that absorption forms at 695 and 715 nm, connected to emissions at 702 and 735 respectively, were associated to Lhca2 and Lhca3. Thus the use of mutant plants lacking one or more Lhca proteins showed to be valuable in establishing the relation between gene products and the associated absorption and fluorescence forms overcoming the problems due to the partial denaturation of pigment-proteins during purification.

3. Recombinant proteins

A third approach to the study of PSI antenna system has been the *in vitro* production of Lhca holoproteins by overexpression of the apoproteins in bacteria and reconstitution *in vitro* with purified pigments. This approach, first introduced by Plumley and Schmidt (1987), exploits the ability of Lhc proteins to fold *in vitro* in the presence of chlorophylls and carotenoids. This procedure was first applied to Lhcb proteins, which can be purified more easily than Lhca subunits from thylakoids. Comparison of native and recombinant proteins showed that reconstitution *in vitro* yielded complexes indistinguishable by biochemical and spectroscopic analysis (Giuffra et al., 1996; Pascal et al., 2001; Croce et al., 2003).

In 1997 Schmid et al. (1997) reconstituted Lhca1 and Lhca4 from tomato genes and showed that the two complexes, although homologous, had distinct properties, with Lhca4 emitting at 730 nm and Lhca1 at 686 nm. These experiments provided a direct demonstration that the red-most forms were associated to Lhca4. The same procedure was later applied to Lhca2 and Lhca3 from tomato (Schmid et al., 2002b) and to the four Lhca gene products from *Arabidopsis* (Croce et al., 2002; Castelletti et al., 2003). It was shown that red-shifted forms are a common characteristic of Lhca proteins, their amplitude and wavelength of emission increasing in the order Lhca1 > 2 > 3 and 4 (Castelletti et al., 2003).

The pigment content of the four Lhca complexes from *Arabidopsis* is reported in table 2. All Lhca were estimated to coordinate 10 Chls per polypeptide, while differing sensibly in their Chl a to Chl b ratio. In particular, the higher Chl b content was found in Lhca2 (Chl a/b=1.8), the lowest in Lhca3 (Chl a/b= 6). The carotenoid content was found to be either 2 (in Lhca2 and 4) or 3 (in Lhca1 and 3). Reconstitution *in vitro* confirmed that neoxanthin is not a component of the antenna system of PSI. In fact, although present in the reconstitution mixture during refolding, it was never bound in the complexes. Lhca3 has the peculiar feature of binding β -carotene in its monomeric state

(Croce et al., 2002; Castelletti et al., 2003). While the results on tomato Lhca differ slightly, the trend in both Chl a/b and carotenoids binding (Schmid et al., 2002b) is consistent with the data found using *Arabidopsis* genes. Reconstitution in the absence of individual pigment species revealed that Lhca1 and Lhca3 need Chl a only for folding, while Chl b is, in addition, essential for the stability of Lhca2 and Lhca4 (Schmid et al., 2002b), consistent with the different affinity of the complexes for the two Chl species.

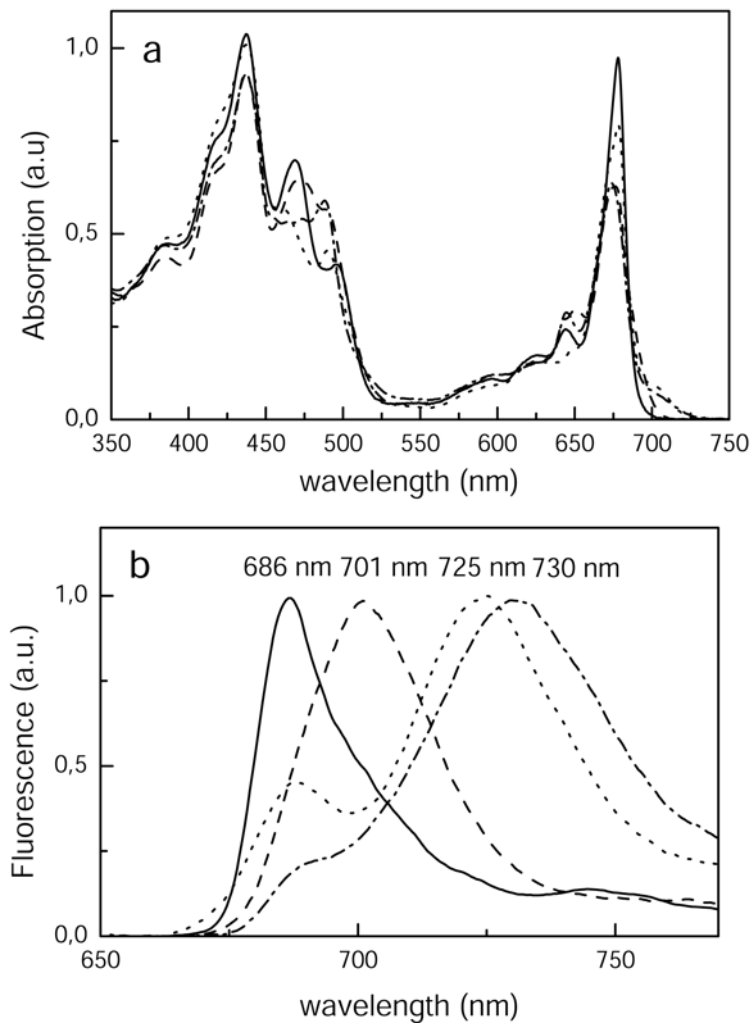


Figure 5. (a) Absorption and (b) fluorescence emission spectra at 77K of recombinant Lhca complexes: Lhca1 (solid), Lhca2 (dash), Lhca3 (dot), Lhca4 (dash-dot). All genes are from *Arabidopsis thaliana*. Emission maxima are also reported.

The possibility to have homogeneous preparations of each Lhca complex allowed determining their spectroscopic properties. The analysis of the emission spectra at low temperature showed that all Lhca complexes contained emission forms at wavelength longer than 700 nm. In particular Lhca4 showed emission maximum at 733 nm, Lhca3 at 725 nm, Lhca2 at 702 nm. Lhca1 emission peak was at 690 nm but a shoulder was also present at 701 nm (Fig. 5b). The absorption spectra of individual Lhca (Fig. 5a) demonstrated that each of them has peculiar characteristics and different distribution of the absorption forms. The Qy absorption peaks of Lhca1, Lhca2 and Lhca3 are

determined at around 680 nm, strongly red shifted with respect to Lhcb complexes. This is not the case for Lhca4 whose Qy absorption peak was found at 676 nm (fig. 5a).

A comparison between the pigment organization in Lhca and Lhcb complexes can be done by analyzing the CD and LD spectra of the complexes. A red shift in both CD and LD is observed for Lhca complexes as compared to Lhcb, which indicates that the red forms contribute to the dichroic spectra. Interestingly, in the carotenoids absorption region, the spectra showed larger differences, thus supporting the hypothesis that the xanthophylls in Lhca complexes are differently organized/oriented as compared to Lhcb complexes. (Croce et al., 2002; Castelletti et al., 2003; Morosinotto et al., 2003).

In vitro reconstitution yielded a major contribution to the detailed knowledge of the biochemical and spectroscopic characteristics of individual Lhca complexes. It clearly appeared that the four Lhca complexes, despite high sequence homology, strongly differ in the pigment binding affinity and in the distribution of the absorption forms. Strongly shifted fluorescence emissions were associated to both Lhca4 and Lhca3 monomers while Lhca1 and 2 had a limited shift of their red-most spectral forms.

Sample	Chl a	Chl b	Viola	Lutein	β -car
Lhca1	8 \pm 0.04	2 \pm 0.04	1.05	1.81	-
Lhca2	6.5 \pm 0.2	3.5 \pm 0.2	0.47	1.52	-
Lhca3	8.6 \pm 0.2	1.4 \pm 0.2	0.66	1.62	0.57
Lhca4	7.0 \pm 0.2	3 \pm 0.2	0.5	1.5	-

Table 2. Pigment composition of reconstituted Lhca complexes from *Arabidopsis thaliana*. Data shown are from (Castelletti et al., 2003).

III. Models of LHCI polypeptides

A. Polypeptide structure

The structure of one member of Lhc family, the main antenna complex of Photosystem II LHCII, has been resolved from 2D crystals by electron crystallography (Kühlbrandt et al., 1994). The high sequence homology between the members of the Lhc multifamily (Durnford et al., 1999) suggested that they share the same structural organization (Green and Durnford, 1996). This was confirmed by the structure of PSI-LHCI complex, where the 3D organization of Lhca polypeptides was resolved.

Superimposition of the structure of the transmembrane domain of Lhca complexes with LHCII showed almost perfect match with three transmembrane helices and one amphipatic helix exposed on the luminal side of the membrane (Ben Shem et al., 2003). The N-terminal is exposed to the stroma and the C-terminus to the thylakoid lumen (Kühlbrandt et al., 1994; Ben Shem et al., 2003) (Figure 6).

Less information is at present available about the organization of loops connecting α -helices which is not resolved from 2D crystals of LHCII. The analysis of the primary structure reveals differences between the Lhc proteins in the length of the loops connecting the transmembrane helices. In this respect Lhca1 is similar to Lhcb4 having the stromal and the luminal loops with the same length (23-25 aa). Lhca2, 3 and 5 have longer stromal loops of 41 residues (Lhca2), 43 (Lhca3) and 36 (Lhca4), and shorter luminal loops (of 17, 26 and 17 residues, respectively), making these complexes more similar to Lhcb6. Structural data suggest these differences do not influence the packing of the transmembrane domain, but might be involved in the interactions with core complex subunits (Ben Shem et al., 2003).

B. Chlorophyll binding

1. How many Chls are bound to each Lhca complex?

The pigment determination on purified LHCI fraction containing all four Lhca complexes showed that there are in average 10 Chls per polypeptide (Croce and Bassi, 1998). This value was consistently found by analyzing fractions enriched in Lhca2-Lhca3 or Lhca1-Lhca4. In the PSI-LHCI structure (Ben Shem et al., 2003) the authors observed 56 Chls associated to the external antenna, 14 Chls per each Lhca complex. However, Lhca proteins appears to be embedded into a sort of “pigment bed” composed of chlorophylls either tightly bound to Lhca proteins or bound at the interface between two neighbor Lhca polypeptides or filling the gap between the LHCI crescent-like structure and PSI core complex. Part of Chls loosely associated to LHCI thus appears to be prone to be freed during solubilization thus leaving 10 Chls bound to each Lhca polypeptide as determined from both the Chl to polypeptide ratio and carotenoid to Chl ratio. Particularly the latter parameter appears to be reliable due to the inner location of three carotenoid binding sites in Lhc proteins (Croce et al., 2002; Castelletti et al., 2003).

2. Chlorophyll organization

From the structure of LHCII complex eight aminoacid residues were indicated as Chl ligands, while the mode of binding of the remaining 4 Chl molecules remained unclear. Mutation analysis confirmed that all the eight Chl binding residues were indeed able to coordinate the central Mg^{2+} of

the Chls in LHCII. It was suggested that the additional 4 Chls were brought in place by interaction with other chromophores, although the involvement of residues in the intra-helices loops could not be excluded (Kühlbrandt et al. 1994; Remelli et al., 1999). Primary structure comparison between LHCII and the Lhca complexes showed that all the Chl binding residues present in LHCII are conserved in Lhca proteins, with few substitutions: (i) Chl B6 is coordinated by a Gln in LHCII, while this position is occupied by a Glu in all Lhca proteins; (ii) an Asn residue is present at site A5 in Lhca3 and Lhca4, while in LHCII as well as in all other antenna complexes the ligand for Chl A5 is an His. Mutation analysis confirmed that these residues coordinate Chls as well as all other conserved aminoacids (Morosinotto et al., 2002; Morosinotto et al., 2003).

A detailed study of the pigment organization, in order to assign the Chl occupancy to the individual sites and to determine the spectroscopic properties of each Chl was performed by mutation analysis on Lhca1 (Morosinotto et al., 2002). The results are summarized in table 3 where the attribution of chromophores to different sites in Lhca1 is compared to that in Lhcb1.

Site	Lhcb1	Lhca1
A1	Chl a (679 nm)	Chl a (nd)
A2	Chl a (681 nm)	Chl a (682 nm)
A3	Chl a/Chl b (662/650nm)	Chl a (+traces Chl b) 663-681
A4	Chl a (674)	Chl a (678-9)
A5	Chl a (674)	Chl a (675-679nm)
B3	Chl a/ Chl b (665/650)	Chl a (traces Chl b) 663
B5	Chl b (652)	Chl a/Chl b 644/(668-686)
B6	Chl b (652)	Chl a/Chl b 644/(668-686)
B1	Chl a 679.4	-
B2	Chl b 644	Chl a/Chl b 650/682
A6/A7	0.5 Chl a/1.5 Chl b 679/652	-
X ^a	-	Chl a/Chl b 644/ND

Table 3. Biochemical and spectroscopic properties of the Chls in each binding site for Lhcb1 and Lhca1. Data shown are from respectively (Remelli et al., 1999) and (Morosinotto et al., 2002). The site nomenclature used here is derived from the LHCII nomenclature proposed by Kühlbrandt et al. (1994). It indicates the position of the chlorophyll in the structure. The A and B prefix is not meant here as indication of the Chl a/ Chl b occupancy of the site. ^a this site seems do not be present in Lhcb1 complex. In Lhca this Chl is lost together with Chl A5.

The results indicate that the occupancy of most of the sites in Lhca1 is similar to Lhcb1, the major differences being due to the increased affinity for Chl a vs. Chl b of the sites showing mixed Chl a and Chl b occupancy. Interestingly, in Lhca1 most of the mutations caused the loss of more than one pigment differently from what observed in Lhcb1 and Lhcb4 while several interactions between chromophores were spectroscopically detected in LHCI (Remelli et al., 1999; Bassi et al., 1999). This different pattern of response suggests that pigment-pigment interactions are stronger in Lhca proteins as compared to Lhcb proteins. Crystal structure showed that the plane of the tetrapyrrole is differently oriented in at least three Chls within Lhca complexes as compared to LHCII, namely Chls in sites B5 (or A5), A7 and A3 (Ben Shem et al., 2003).

C. Carotenoid binding

The carotenoid organization in Lhca1 was not resolved in crystal structure thus information is restricted to data from mutation analysis. Most of the mutations at Chl binding residues also yielded loss of carotenoid molecules. This was useful for the localization of xanthophyll binding sites within Lhca1 and determination of their affinity for ligands. Three carotenoids are tightly bound to Lhca1 as well as to Lhcb1 and they are likely to be located at the same three binding sites, namely L1 and L2, nearby helices A and B, and N1 near helix C. The affinity of each site for the individual xanthophyll species is not the same: neoxanthin, which is accommodated in the site N1 of Lhcb1 (Croce et al., 1999) is absent in Lhca1 and substituted by violaxanthin and lutein. Lutein is conserved as ligand for site L1 in all Lhc complexes analyzed so far. However, while the occupancy of site L1 is essential for Lhcb protein folding, in Lhca1 Lutein is lost upon mutation at site A3 without destabilization of the complex (Remelli et al., 1999; Bassi et al., 1999). Site L2 accommodates both lutein and violaxanthin with similar affinity.

Based on the results of the mutation analysis a model for the chromophore organization in Lhca1 can be drawn (fig. 6).

Preliminary results on the mutation analysis of Lhca2, Lhca3 and Lhca4 suggest that all Lhca share similar pigment organization, with the exception of the number of bound xanthophylls: two in Lhca2 and Lhca4, three in Lhca 1 and 3. Lutein is in site L1, while site L2 is occupied by both lutein and violaxanthin. Lhca3 was shown to coordinate also β -carotene (Schmid et al., 2002b; Castelletti et al., 2003) but its binding site is not yet clear.

The structure of Lhca complexes is similar to LHCII with respect to both apoprotein and chromophores organization. However, differences can be observed in the affinity of the pigment binding sites for the individual chromophores. Small differences in the pigment organization can be detected both by mutation analysis and by X ray diffraction, suggesting that the peculiar

spectroscopic characteristics of Lhca complexes might be due to small changes in interchromophore distance and orientation, particularly in the domain including the stromal side of helices A and C.

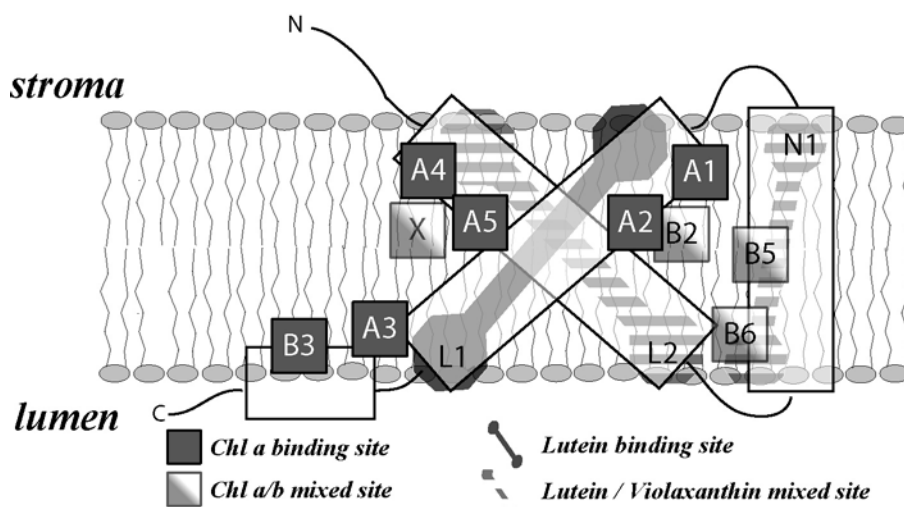


Figure 6. Schematic 2D representation of Lhca structure, based on reconstitution experiments. Conserved Chl and xanthophyll binding sites are indicated, using the nomenclature proposed by (Kühlbrandt et al., 1994). Residues directly co-ordinating chlorophylls are also indicated.

IV Dimerization of Lhca proteins

It is now accepted that all Lhca complexes are present in dimeric form *in vivo* (Croce and Bassi, 1998; Croce et al., 2002). This suggestion was first made by Kuang et al. (1984) and by Bassi (1985) from their apparent mobility as a 40 kDa band in non denaturing electrophoresis. Similar suggestion was also made based on sucrose gradient ultracentrifugation (Ikeuchi et al., 1991a) and by nearest-neighbor analysis (Jansson et al., 1996) yielding cross-linking products between 40 and 45 kDa.

The suggestion that Lhca1 and Lhca4 form heterodimers (Knoetzel et al., 1992), was later confirmed by *in vitro* reconstitution (Schmid et al., 1997). In the Lhca1-Lhca4 heterodimer there is complete energy transfer between Lhca1 and Lhca4, as demonstrated by the single 733 nm emission peak in the spectrum of the dimer. The CD and the LD spectra of the dimer also showed that the dimerization influenced the pigment organization, especially of Chls b (Schmid et al., 1997; Croce et al., 2002). Moreover, the heterodimer was more stable to heat denaturation than the two monomers. Dimerization also involved binding of β -carotene, probably at the subunit interface (Croce et al., 2002).

Consistent with the data *in vitro*, analysis of chlorina mutants (Knoetzel et al., 1998) and of Lhca4 antisense plants (Zhang et al., 1997) showed that, although Lhca1 is maintained in the absence of Lhca4, its stoichiometry with respect to PSI RC is decreased, suggesting they form dimers *in vivo*.

The results on Lhca2 and Lhca3 are less clear: they did not dimerize *in vitro* (Schmid et al., 2002b) but antisense plants lacking either Lhca2 or Lhca3 showed relevant reduction of Lhca3 and Lhca2 respectively, thus suggesting that the two subunits are connected (Ganeteg et al., 2001). Moreover, partial purification of LHCI by preparative IEF gives both dimers enriched in Lhca1-4 and in Lhca2-3, suggesting their association (Croce et al., 2002). Evidence for Lhca2 homodimers was obtained by analyzing a native LHCI preparation containing all Lhca complexes: two different emissions, at 702 and 733 nm were detected (Ihalainen et al., 2000), which is predictable only if dimers of Lhca2 cannot transfer to Lhca3, whose red-most transition is at far lower energy (Castelletti et al., 2003).

The dimerization of Lhca1 and Lhca4 has been studied *in vitro* producing proteins modified by deletions or point mutagenesis. It has been shown that the Trp residue at position 4 of Lhca1 is involved in dimerization together with an additional Trp residue localized at the C-terminus of the same protein. Lhca4 C and N termini are not involved in strong interactions with Lhca1 since Lhca1-4 dimerization was broken only after complete deletion of the N and C-terminal sequences (Schmid et al., 2002a). This is consistent with the X-ray data showing that Lhca1 bind to the C helix and to the luminal loop of Lhca4.

We can conclude that Lhca complexes are present as heterodimers *in vivo* with the Lhca1-Lhca4 pair being more stable than the Lhca2-Lhca3 dimer. More experiments are needed to elucidate the interaction between Lhca2 and Lhca3 and to determine the spectroscopic characteristics of this heterodimer.

V. PSI-LHCI stoichiometry

The number of antenna proteins bound to PSI has not been for long time a matter of debate. It was believed that there were eight Lhca per P700. This figure was derived from E.M. analysis (Boekema et al., 1990) and it was in good agreement with the pigment stoichiometry data, attributing 80 Chls to the LHCI moiety and 10 Chl to each polypeptide (see above). However, a more detailed electron microscopy analysis suggested that the surface occupied by LHCI in projection PSI-LHCI complex could accommodate 4-5 Lhca per reaction center (Boekema et al., 2001b). The 3D structure of PSI-LHCI complex supports the 4 Lhca per PSI stoichiometry. The structure allowed also explanation of the discrepancy between the pigment stoichiometry and the structural data. In fact, linker Chls are present in between the Lhca complexes and the core and in between the individual Lhca subunits. These Chls could be lost upon separation of LHCI from the core, thus impairing stoichiometry estimations based on pigment content of individual polypeptides.

Thus, four Lhca complexes are present in the PSI-LHCI supercomplex, connected to the core by linker Chls that are lost upon dissociation of the LHCI fraction from the core moiety.

VI. Energy transfer

Analysis of the excitation spectra of Lhca complexes reveals that the carotenoid transfer energy to Chl with 65% efficiency, lower than in Lhcb complexes (70-80%, Croce et al., 2002; Castelletti et al., 2003). The energy transfer pathways in Lhca complexes are reviewed in cap. 9, where the reader is addressed for more details. Here we stress the point that the figure obtained from time resolved data indicate that the energy transfer within LHCI complexes is very similar to that observed for Lhcb complexes. The only difference is represented by the energy transfer component to the red absorbing forms, which takes place in approximately 5 ps. We have to note that a similar lifetime has been associated to the Chl a-Chl a equilibration in LHCII and CP29 (Van Amerongen and van Grondelle, 2001; Croce et al., 2003). The energy transfer between monomers within the dimeric complex is slower than the energy transfer between individual subunits in LHCII trimers (30 ps vs. 12 ps, Kleima et al., 1997). These results suggests that the pigment organization in Lhca complexes is not very different compared to Lhcb with the exception of the presence of the red forms, while the monomers in the dimer seems to be less strongly associated respect to the trimer of LHCII.

VII. On the origin of Red absorption forms

Following characterization of individual LHCI components, the elucidation of the structural features responsible for the huge shift in the Chl fluorescence emission has been the target of research on LHCI. In higher plants photosynthetic complexes the Chls Q_y absorption band is located within the 640-660 nm range for Chl b and between 660 and 682 nm for Chl a. In the case of the red forms the Chls involved are expected to absorb above 700 nm, thus energetically far apart from the bulk Chls. It has been widely proposed that the red forms represent the low energy band of an excitonic interaction between two or more Chl molecules (Gobets et al., 1994). In the following we will address some detailed questions about red forms:

- A. Which complex(es) coordinate the red Chls?
- B. Which are the absorption characteristics of the red forms?
- C. How many Chls absorb in the red?
- D. Which are the Chls involved?
- E. Where are the red Chls located within the Lhca complexes?

- F. Which is the role played by the protein in modulating the absorption of the red Chls in the four Lhca complexes?
- G. Which mechanism is responsible for the large absorption shift of the red forms as compared to the bulk Chls?

A. Which complexes coordinate the red Chls.

The solubilization of PSI-200 in PSI-core and LHCI complexes yielded to the conclusion that the most red forms are associated with the outer antenna system in higher plants in contrast with other organism, where the red emission originates from chlorophylls associated to the PSI-core (see (Gobets and van Grondelle, 2001) for a review).

In vitro reconstitution of individual Lhca complexes yielded the emission spectra of individual Lhca complexes, showing that emissions at 4K for Lhca4, Lhca3, Lhca2 and Lhca1 were at 733 nm, 725, 702 and 690 nm respectively (Castelletti et al., 2003). The Lhca1-4 heterodimer showed the same fluorescence emission as the Lhca4 monomer, indicating complete energy transfer from Lhca1 to the red forms of Lhca4 (Schmid et al., 1997).

B. Which are the absorption characteristics of the red forms?

While in fluorescence the red forms can be easily detected, especially at low temperature, the determination of the absorption forms responsible for the red emission is not straight forward since the red pigments represent at most the 5% of the total absorption in the Qy region (Ihalainen et al., 2000). Although these forms are expected to be energetically distant from the bulk Chls, it was not possible to detect a clear band even at 4K, due to lack of structure in the spectra. This suggests that these forms are largely inhomogeneously broadened. From the early analysis of the 735 nm emission on chloroplasts (Butler et al., 1979) it was proposed that the origin of the red emission was an absorption band at 705 nm (Boardman et al., 1978). Site-selected fluorescence measurements on a PSI-200 preparation indicated 716 nm as the upper limit for the maximum of the band responsible for the long wavelength emission (Gobets et al., 1994). Similar work on purified dimeric LHCI fraction shifted this estimation to 711 nm (Ihalainen et al., 2000). The bandwidth of the 711 nm absorption was suggested to be 356 cm⁻¹ by Gaussian deconvolution of the red tail of LHCI absorption spectra while site-selected fluorescence analysis showed that the contribution of the homogeneous and inhomogeneous broadening to the bandwidth were respectively of 210 cm⁻¹ and 290 cm⁻¹. Consistently, an electron-phonon coupling value of 2.7 was derived from fluorescence line narrowing experiments (Ihalainen et al., 2003): the stronger coupling found in photosynthetic

antenna complexes. From these values the FWHM of the red band in LHCI being 30 nm and the Stokes shift 35 nm could be calculated.

Analysis of the reconstituted Lhca complexes at 77K, by Gaussian deconvolution of difference absorption spectra (see below), suggested that the absorption is located between 700 and 705 nm for both Lhca3 and Lhca4 (Morosinotto et al., 2003). The origin band for the 702 nm emission of Lhca1 and Lhca2 complexes was located at 686-688 nm by comparison of the spectra of WT and point mutant proteins (Morosinotto et al., 2002; Morosinotto, Bassi and Croce, unpublished).

C. How many Chls absorb in the red?

In LHCI preparation it was estimated that the red absorption represent the 5% of the total absorption in the Qy band, meaning 0.5 Chls per complex, or 1 Chl molecule per dimer. Analysis of the absorption spectra of reconstituted complexes at low temperature suggested that in both Lhca3 and Lhca4 the red tail represents roughly the absorption of 1 Chl molecule (Morosinotto et al., 2003) in agreement with the analysis on the native complex. Due to the difficulties associated to the determination of the actual band shape of the low energy absorption forms, this value has to be taken as a rough estimation. However, the value found suggests that the Chls involved in the excitonic interaction yielding to the red forms are not in the head-to-tail arrangement, but their dipole transition vectors are organized almost perpendicular to each other.

D. Which Chl specie(s) is involved in red-forms?

Mukerji and Sauer (1990) observed that excitation of Chl b increased the amplitude of red emission as compared to excitation of Chl a, thus concluding that Chl b is closely connected to red – shifted chromophores. Suggestion of a direct involvement of Chl b in the red forms was also made by Schmid et al. (2001) based on the observation that reconstitution of Lhca4 in the absence of Chl b caused loss of red forms. However, Chl a only Lhca3 (Castelletti et al., 2003), retained the red-shifted emission while Chl a only Lhca4 although reducing the amplitude of red emission, still retained in part this spectral feature. It was shown that by increasing Chl b content in Lhca4 above the control level, a progressive blue shift in the emission peak from 733 to 722. This result was interpreted as evidence that a Chl a-Chl a interaction was substituted by a Chl b-Chl a interaction, thus yielding a smaller emission shift due to the larger difference in the transition energy level of interacting monomers (see below). These results show that the interacting Chls responsible for red forms are in fact Chl a molecules, while suggest that Chl b is possibly needed in order to maintain the chromophore conformation responsible for red- forms.

E. Where are the “red Chls” located in the Lhca architecture?

Mutation of Chl binding residues in Lhca complexes allows determination of the binding sites responsible for red forms. Mutation analysis of Lhca1 (see par. III B) revealed that the 702 nm fluorescence emission component is lost upon mutations at site A5, B5 and B6. On the basis of the occupancy of these sites (Chl a for A5, mixed site for B5 and Chl b for B6), it was proposed that the red emission originates from a Chl a-Chl a interaction between Chls located in sites A5 and B5, while the presence of a Chl in site B6 stabilized the conformation leading to the red forms. The mixed occupancy of site B5 allows explaining the presence of the 690 nm fluorescence component: when Chl b is accommodated in site B5 the Chl a-Chl a interaction yielding to the red form is lost, yielding instead the 690 nm bulk emission (Morosinotto et al., 2002).

The involvement of the A5 B5 domain in the origin of red forms was confirmed in all Lhca complex by building mutants at the Chl binding site A5, B5 and B6 (Morosinotto, Bassi and Croce, unpublished). In all complexes the absence of Chl A5 and B5 lead to the complete disappearance of red emission. B6 mutants, instead, have a slightly different phenotype, especially in Lhca3 and Lhca4: red emission is strongly reduced but not abolished.

From the analysis of the Lhca mutants two conclusions have been drawn: (i) the red forms originate from the same chromophores in all Lhca complexes; (ii) the model proposed for the origin of red forms by excitonic interactions of two Chl a molecules in the sites A5 and B5, proposed after the analysis of mutations in Lhca1, is probably maintained in all Lhca proteins.

An alternative hypothesis was recently proposed suggesting that a new Chl binding site whose ligand residue would be a His belonging to helix C is responsible of red forms by establishing excitonic interactions with both Chl A5 and Chl B5 (Melkozernov and Blankenship, 2003). This hypothesis is not consistent with the previous report that Lhca3 has strong red-shifted emission (Schmid et al., 2002b; Castelletti et al., 2003) and yet lacks the putative Chl binding His residue. Moreover, the recent structure of Lhca4 did not show the presence of an additional Chl coordinated to this particular residue (Ben Shem et al., 2003).

F. Which is the role of the polypeptide chain in modulating the absorption of the red Chls in the four Lhca complexes?

Primary sequence analysis shows a strong homology between Lhca2 and Lhca4. Also Lhca1 and Lhca3 are closely related. This clustering extends to the Chl a/b ratio and to the number of xanthophylls per polypeptide. However, the distribution of red forms is not consistent with the pattern being associated mainly to Lhca3 and Lhca4 and rather correlating to a specific substitution in the ligand of Chl A5: an Asparagine in Lhca1 and 3 versus Histidine in Lhca1-2 and in the rest of

Lhcb proteins, depleted in red forms. Mutation at the A5 ligand (Asn > His) in Lhca3 and Lhca4 led to loss of red form without affecting the pigment composition. The importance of the presence of Asn as ligand for site A5 for the formation of red forms was confirmed by the reverse mutation on Lhca1: the His >Asn mutant gained red shifted emission (Morosinotto et al., 2003).

G. Which is the mechanism responsible for the large absorption shift of the red forms compared to the bulk Chls?

The type of interaction between chromophores responsible for the large absorption shift of the red forms has been investigated (Morosinotto et al., 2003) by comparing the absorption spectra of mutants lacking the red forms with the spectra of the WT complexes. It was shown that in the His 97 mutant of Lhca4, two absorption forms at 682 nm and 703 nm were lost, while absorption at 675 nm was gained. This spectrum was interpreted as the loss of an excitonic interaction having its high energy term at 682 nm and the low energy contribution at 703 nm, while the 675 nm was representing the absorption of the non-interacting monomers. This was consistent with the analysis of the CD spectra (Morosinotto et al., 2003).

On this basis it was proposed that part of the large shift of the red absorption band could be associated to the interaction energy (around 200 cm⁻¹). However, the energy associated to this interaction does not fully account for the large red shift of the absorption. Possibly, the presence of the Asn in this position directly influences the properties of the Chl ligand by changing the geometry of the tetrapyrrole or otherwise leading to a different folding of the protein domain which favors the red absorption.

The absence of the red emission in the Asn>His mutants of Lhca4 and Lhca3 was thus interpreted as the loss of the excitonic interaction between Chl A5 and Chl B5. Two parameters influence the interaction, the distance between the chromophores and the orientation of their dipole moments. LD spectra showed no changes in the chromophores orientation, thus suggesting that the substitution of Asn with His increased the distance between the two interacting Chls, thus lowering the interaction energy (Morosinotto et al., 2003).

VIII. Lhca proteins in *Chlamydomonas reinhardtii*.

The first evidence for the presence of a Chl b containing antenna in LHCI has been obtained in *Chlamydomonas reinhardtii* (Wollman and Bennoun, 1982). Evolutionary studies on Lhc complexes led to the conclusion that Lhca proteins diverged more than Lhcb during evolution (Durnford et al., 1999). Antenna complex of *Chlamydomonas reinhardtii* has recently been the object of two electro-microscopy studies (Germano et al., 2002; Kargul et al., 2003). In these

studies the authors analyzed the structure of PSI-LHCI by single particle analysis leading to the conclusion that in Photosystem I between 11 and 14 Lhca subunits are bound to the core complex (Germano et al., 2002; Kargul et al., 2003). These data are consistent with the larger surface occupied by LHCI in *Chlamydomonas* as compared to spinach (Germano et al., 2002). Consistently, *Chlamydomonas reinhardtii* LHCI was shown to contain 7 distinct polypeptides (Bassi et al., 1992) or 9 (Stauber et al., 2003). These data, integrated with the sequence available in databases, allowed the identification of at least 9 distinct polypeptides composing LHCI complex of Photosystem I in *Chlamydomonas*. These polypeptides have been named Lhca1-9, but these names do not exactly reflect homology to higher plants genes. In particular, five different groups have been identified based on homology with vascular plants Lhca. This is summarized in table 4 (Stauber et al., 2003).

Clamydomonas reinhardtii Protein	Homologous in plants	in vascular plants	Nomenclature from (Bassi et al., 1992)
Lhca1	Lhca1		p22.1
Lhca2	Lhca2		p19
Lhca3	Lhca3		p14.1
Lhca4	Lhca2 or Lhca4		p14
Lhca5	Lhca2 or Lhca4		p15.1
Lhca6	Lhca2 or Lhca4		p18.1
Lhca7	Lhca5		p15
Lhca8	Lhca5		p18
Lhca9	Lhca2		p22.2

Table 4. Lhca polypeptides identified in *Clamydomonas* and their homologous in vascular plants. The correspondence is derived from (Stauber et al., 2003). The older nomenclature, used in previous works on *Clamydomonas* (Bassi et al., 1992) is also reported.

Biochemical and spectroscopic properties of LHCI of *Chlamydomonas reinhardtii* are known in less detail than in vascular plants. Bassi et al (Bassi et al., 1992) identified two LHCI populations, one emitting at 680 nm and the other at 705 nm. Similar purifications of LHCI from higher plants yielded the LHCI-680 and LHCI-730 described above (par II B) Thus, red forms in LHCI are not red shifted to the same extent as in vascular plants (Wollman and Bennoun, 1982).

Recently, Kargul et al (2003) isolated *Chlamydomonas* PSI-LHCI complex showing fluorescence emission maximum at 715 nm. Unfortunately it's not clear if this red emission originated from the antenna or from the core complex.

Pigment binding properties of LHCI of *Chlamydomonas* have not been analyzed in detail yet. The recent availability of all protein sequences, however, allow determining that all 8 Chl binding residues present in higher plants Lhc are conserved in *Chlamydomonas* proteins, strongly suggesting that these complexes bind at least 8 chlorophylls each. Xanthophyll binding properties have not been identified yet. Indirect evidences suggest that xanthophyll binding properties of LHCI in *Chlamydomonas* are similar to those in vascular plants as deduced from the observation that *Chlamydomonas* mutants depleted in lutein, violaxanthin and neoxanthin, thus leaving only zeaxanthin and beta carotene as carotenoid species available, were shown to retain a stable LHCI. In these conditions Lhcb proteins were severely affected (Polle et al., 2001). The same phenotype was observed the *Arabidopsis* npq2-lut2mutant (Havaux et al. 2004).

From the comparison of Lhca sequences from *Arabidopsis* and *Chlamydomonas*, some interesting observations could be made. Lhca1 and Lhca3 from *Arabidopsis* and the corresponding genes from *Chlamydomonas* are highly homologous while Lhca2 and Lhca4 from higher plants do not have closely related genes in *Chlamydomonas*. Moreover, it is interesting to note that in *Chlamydomonas* there are two genes homologous to Lhca5 and that one of them is expressed at high level (Lhca8, Stauber et al., 2003). This suggests that Lhca8 have a physiological function in *Chlamydomonas reinhardtii* that could possibly be maintained by Lhca5 gene in *Arabidopsis thaliana*.

It has been observed that LHCI from *Chlamydomonas* showed reduced red forms as compared with higher plants. A possible explanation for these characteristics of algal HCI can be found in the observation that genes highly homologous to higher plants Lhca4 and Lhca3, in fact have His as the Chl A5 ligand. Asn however, is present at site A5 in three Lhca polypeptides of *Chlamydomonas* (Lhca2, Lhca4, Lhca9) thus suggesting they may be responsible for the 705-715 nm fluorescence emission.

Acknowledgements

We want to thank Prof. Nelson from the Tel Aviv University for the reproduction of the picture in figure 2.

References

- Allen JF (1992) How does protein phosphorylation regulate photosynthesis? *Trends Biochem Sci* 17: 12--17
- Bassi R (1985) Spectral properties and polypeptide composition of the chlorophyll-proteins from thylakoids of granal and agranal chloroplasts of maize (*zea mays* L.). *Carlsberg Res Commun* 50: 127--143
- Bassi R, Croce R, Cugini D, and Sandona D (1999) Mutational analysis of a higher plant antenna protein provides identification of chromophores bound into multiple sites. *Proc Natl Acad Sci USA* 96: 10056--10061
- Bassi R, Machold O, and Simpson D (1985) Chlorophyll-proteins of two photosystem I preparations from maize. *Carlsberg Res Commun* 50: 145--162
- Bassi R, Pineau B, Dainese P, and Marquardt J (1993) Carotenoid--Binding Proteins of Photosystem-II. *Eur J Biochem* 212: 297--303
- Bassi R and Simpson D (1987) Chlorophyll-protein complexes of barley photosystem I. *Eur J Biochem* 163: 221--230
- Bassi R, Soen SY, Frank G, Zuber H, and Rochaix JD (1992) Characterization of Chlorophyll-a/b Proteins of Photosystem-I from *Chlamydomonas-Reinhardtii*. *J Biol Chem* 267: 25714--25721
- Ben Shem A, Frolov F, and Nelson N (2003) Crystal structure of plant photosystem I. *Nature* 426: 630--635
- Bibby TS, Nield J, and Barber J (2001) Iron deficiency induces the formation of an antenna ring around trimeric photosystem I in cyanobacteria. *Nature* 412: 743--745
- Boardman NK, Anderson JM, and Goodchild DJ (1978) Chlorophyll-protein complexes and structure of mature and developing chloroplast. In: Sanadi DR and Vernon LP (ed) *Curr. Top. Bioenerg.* 8, pp 35--109
- Boekema EJ, Hifney A, Yakushevskaya AE, Piotrowski M, Keegstra W, Berry S, Michel KP, Pistorius EK, and Kruijff J (2001a) A giant chlorophyll-protein complex induced by iron deficiency in cyanobacteria. *Nature* 412: 745--748
- Boekema EJ, Jensen PE, Schlodder E, van Breemen JF, van Roon H, Scheller HV, and Dekker JP (2001b) Green plant photosystem I binds light-harvesting complex I on one side of the complex. *Biochemistry* 40: 1029--1036
- Boekema EJ, van Roon H, Calkoen F, Bassi R, and Dekker JP (1999) Multiple types of association of photosystem II and its light-harvesting antenna in partially solubilized photosystem II membranes. *Biochemistry* 38: 2233--2239
- Boekema EJ, Wynn RM, and Malkin R (1990) The structure of spinach photosystem I studied by electron microscopy. *Biochim Biophys Acta* 1017: 49--56
- Bossmann B, Knoetzel J, and Jansson S (1997) Screening of chlorina mutants of barley (*Hordeum vulgare* L.) with antibodies against light-harvesting proteins of PS I and PS II: Absence of specific antenna proteins. *Photosynthesis Research* 52: 127--136

- Butler WL and Norris KH (1963) Lifetime of the long-wavelength chlorophyll fluorescence. *Biochim Biophys Acta* 66: 72--77
- Butler WL, Tredwell CJ, Malkin R, and Barber J (1979) The relationship between the lifetime and yield of the 735nm fluorescence of chloroplasts at low temperatures. *Biochim Biophys Acta* 545: 309--315
- Castelletti S, Morosinotto T, Robert B, Caffarri S, Bassi R, and Croce R (2003) Recombinant Lhca2 and Lhca3 subunits of the photosystem I antenna system. *Biochemistry* 42: 4226--4234
- Croce R. Il fotosistema I delle piante superiori: studi biochimici e spettroscopici. 1997.
- Croce R and Bassi R (1998) The light-harvesting complex of photosystem I: pigment composition and stoichiometry. In: Garab G (ed) *Photosynthesis: Mechanisms and Effects*, 1 pp 421--424 Kluwer Academic Publisher,
- Croce R, Morosinotto T, Castelletti S, Breton J, and Bassi R (2002) The Lhca antenna complexes of higher plants photosystem I. *Biochim Biophys Acta* 1556: 29--40
- Croce R, Muller MG, Bassi R, and Holzwarth AR (2003) Chlorophyll b to chlorophyll a energy transfer kinetics in the CP29 antenna complex: A comparative femtosecond absorption study between native and reconstituted proteins. *Biophysical Journal* 84: 2508--2516
- Croce R, Remelli R, Varotto C, Breton J, and Bassi R (1999) The neoxanthin binding site of the major light harvesting complex (LHC II) from higher plants. *FEBS Lett* 456: 1--6
- Croce R, Zucchelli G, Garlaschi FM, Bassi R, and Jennings RC (1996) Excited state equilibration in the photosystem I -light - harvesting I complex: P700 is almost isoenergetic with its antenna. *Biochemistry* 35: 8572--8579
- Croce R, Zucchelli G, Garlaschi FM, and Jennings RC (1998) A thermal broadening study of the antenna chlorophylls in PSI- 200, LHCI, and PSI core. *Biochemistry* 37: 17255--17360
- Damm I, Steinmetz D, and Grimme LH (1990) Multiple functions of b-carotene in Photosystem I. In: Baltscheffsky M (ed) *Current research in photosynthesis*, pp 607--610
- Dunahay TG and Staeheli A (1985) Isolation of photosystem I complexes from octyl glucoside/sodium dodecyl sulfate solubilized spinach thylakoids. Characterization and reconstitution into liposomes. *Plant Physiol* 78: 606--613
- Durnford DG, Deane JA, Tan S, McFadden GI, Gantt E, and Green BR (1999) A phylogenetic assessment of the eukaryotic light-harvesting antenna proteins, with implications for plastid evolution. *J Mol Evolution* 48: 59--68
- Ganeteg U, Strand A, Gustafsson P, and Jansson S (2001) The Properties of the Chlorophyll a/b-Binding Proteins Lhca2 and Lhca3 Studied in Vivo Using Antisense Inhibition. *Plant Physiol* 127: 150--158
- Germano M, Yakushevska AE, Keegstra W, van Gorkom HJ, Dekker JP, and Boekema EJ (2002) Supramolecular organization of photosystem I and light- harvesting complex I in *Chlamydomonas reinhardtii*. *FEBS Letters* 525: 121--125

- Giuffra E, Cugini D, Croce R, and Bassi R (1996) Reconstitution and pigment-binding properties of recombinant CP29. *Eur J Biochem* 238: 112--120
- Gobets B, Kennis JTM, Ihalainen JA, Brazzoli M, Croce R, van Stokkum LHM, Bassi R, Dekker JP, Van Amerongen H, Fleming GR, and van Grondelle R (2001) Excitation energy transfer in dimeric light harvesting complex I: A combined streak-camera/fluorescence upconversion study. *J Phys Chem B* 105: 10132--10139
- Gobets B, Van Amerongen H, Monshouwer R, Kruip J, Rögner M, van Grondelle R, and Dekker JP (1994) Polarized site-selected fluorescence spectroscopy of isolated Photosystem I particles. *Biochim Biophys Acta* 1188: 75--85
- Gobets B and van Grondelle R (2001) Energy transfer and trapping in Photosystem I. *Biochim Biophys Acta* 1057: 80--99
- Green BR and Durnford DG (1996) The Chlorophyll-carotenoid proteins of oxygenic photosynthesis. *Annu Rev Plant Physiol Plant Mol Biol* 47: 685--714
- Havaux M, Dall'Osto L, Cuiné S, Giuliano G and Bassi R (2004) The effect of zeaxanthin as the only xanthophyll on the structure and function of the photosynthetic apparatus in *Arabidopsis thaliana* *J Biol Chem* in press.
- Haworth P, Watson JL, and Arntzen CJ (1983) The detection, isolation and characterisation of a light-harvesting complex which is specifically associated with Photosystem I. *Biochim Biophys Acta* 724: 151--158
- Ihalainen JA, Gobets B, Sznee K, Brazzoli M, Croce R, Bassi R, van Grondelle R, Korppi-Tommola JEI, and Dekker JP (2000) Evidence for two spectroscopically different dimers of light-harvesting complex I from green plants. *Biochemistry* 39: 8625--8631
- Ihalainen JA, Rätsep M, Jensen PE, Scheller HV, Croce R, Bassi R, Korppi-Tommola JEI, and Freiberg A (2003) Red Spectral Fractions of Chlorophylls in green Plant PSI - A Site-Selective and High-Pressure Spectroscopy Study. *J Phys Chem B* 107: 9086--9093
- Ikeuchi M, Hirano A, and Inoue Y (1991a) Correspondence of Apoproteins of Light-Harvesting Chlorophyll-A/B Complexes Associated with Photosystem-I to Cab Genes - Evidence for A Novel Type-Iv Apoprotein. *Plant Cell Physiol* 32: 103--112
- Ikeuchi M, Nyhus KJ, Inoue Y, and Pakrasi HB (1991b) Identities of four low-molecular-mass subunits of the photosystem I complex from *Anabaena variabilis* ATCC 29413. Evidence for the presence of the *psaI* gene product in a cyanobacterial complex. *FEBS Lett* 287: 5--9
- Jansson S (1994) The light-harvesting chlorophyll a/b-binding proteins. *Biochim Biophys Acta* 1184: 1--19
- Jansson S (1999) A guide to the Lhc genes and their relatives in *Arabidopsis*. *Trends Plant Sci* 4: 236--240
- Jansson S, Andersen B, and Scheller HV (1996) Nearest-neighbor analysis of higher-plant photosystem I holocomplex. *Plant Physiol* 112: 409--420

- Jensen PE, Gilpin M, Knoetzel J, and Scheller HV (2000) The PSI-K subunit of photosystem I is involved in the interaction between light-harvesting complex I and the photosystem I reaction center core. *J Biol Chem* 275: 24701--24708
- Jordan P, Fromme P, Witt HT, Klukas O, Saenger W, and Krauss N (2001) Three-dimensional structure of cyanobacterial photosystem I at 2.5 Å resolution. *Nature* 411: 909--917
- Kargul J, Nield J, and Barber J (2003) Three-dimensional reconstruction of a light-harvesting complex I-photosystem I (LHCI-PSI) supercomplex from the green alga *Chlamydomonas reinhardtii* - Insights into light harvesting for PSI. *J Biol Chem* 278: 16135--16141
- Kleima FJ, Gradinaru CC, Calkoen F, van Stokkum IHM, van Grondelle R, and Van Amerongen H (1997) Energy transfer in LHCII monomers at 77K studied by sub- picosecond transient absorption spectroscopy. *Biochemistry* 36: 15262--15268
- Knoetzel J, Bossmann B, and Grimme LH (1998) Chlorina and viridis mutants of barley (*Hordeum vulgare* L.) allow assignment of long-wavelength chlorophyll forms to individual Lhca proteins of photosystem I in vivo. *FEBS Lett* 436: 339--342
- Knoetzel J, Svendsen I, and Simpson DJ (1992) Identification of the Photosystem-I Antenna Polypeptides in Barley - Isolation of 3 Pigment-Binding Antenna Complexes. *European Journal of Biochemistry* 206: 209--215
- Kuang T-Y, Argyroudi-Akoyunoglou JH, Nakatani HY, Watson J, and Arntzen CJ (1984) The origin of the long-wavelength fluorescence emission band (77- degrees-k) from photosystem I. *Arch Biochem* 235: 618--627
- Kühlbrandt W, Wang DN, and Fujiyoshi Y (1994) Atomic model of plant light-harvesting complex by electron crystallography. *Nature* 367: 614--621
- Lam E, Ortiz W, and Malkin R (1984a) Chlorophyll a/b proteins of photosystem I. *FEBS Lett* 168: 10--14
- Lam E, Ortiz W, Mayfield S, and Malkin R (1984b) Isolation and characterization of a light-harvesting chlorophyll a/b protein complex associated with photosystem I. *Plant Physiol* 74: 650--655
- Lubben TH, Theg SM, and Keegstra K (1988) Transport of Proteins Into Chloroplasts. *Photosynthesis Research* 17: 173--194
- Lunde C, Jensen PE, Haldrup A, Knoetzel J, and Scheller HV (2000) The PSI-H subunit of photosystem I is essential for state transitions in plant photosynthesis. *Nature* 408: 613--615
- Melkozernov AN and Blankenship RE (2003) Structural modeling of the Lhca4 Subunit of LHCI-730 peripheral antenna in photosystem I based on similarity with LHCII. *J Biol Chem* 278: 44542--44551
- Morosinotto T, Breton J, Bassi R, and Croce R (2003) The nature of a chlorophyll ligand in Lhca proteins determines the far red fluorescence emission typical of photosystem I. *J Biol Chem* 278: 49223--49229

- Morosinotto T, Castelletti S, Breton J, Bassi R, and Croce R (2002) Mutation analysis of Lhca1 antenna complex. Low energy absorption forms originate from pigment-pigment interactions. *J Biol Chem* 277: 36253--36261
- Mukerji I and Sauer K (1990) A spectroscopic study of a photosystem I antenna complex. *Curr Res Photosynth* 321--324
- Mullet JE, Burke JJ, and Arntzen CJ (1980a) A Developmental study of Photosystem I peripheral Chlorophyll Proteins. *Plant Physiol* 65: 823--827
- Mullet JE, Burke JJ, and Arntzen CJ (1980b) Chlorophyll proteins of photosystem I. *Plant Physiol* 65: 814--822
- Palsson LO, Tjus SE, Andersson B, and Gillbro T (1995) Ultrafast Energy-Transfer Dynamics Resolved in Isolated Spinach Light-Harvesting Complex-I and the Lhc-I-730 Subpopulation. *Biochim Biophys Acta* 1230: 1--9
- Pascal A, Gastaldelli M, Ceoldo S, Bassi R, and Robert B (2001) Pigment conformation and pigment-protein interactions in the reconstituted Lhcb4 antenna protein. *FEBS Lett* 492: 54--57
- Plumley FG and Schmidt GW (1987) Reconstitution of chloroform a/b light-harvesting complexes: Xanthophyll-dependent assembly and energy transfer. *Proc Natl Acad Sci USA* 84: 146--150
- Polle JEW, Niyogi KK, and Melis A (2001) Absence of lutein, violaxanthin and neoxanthin affects the functional chlorophyll antenna size of photosystem-II but not that of photosystem-I in the green alga *Chlamydomonas reinhardtii*. *Plant Cell Physiol* 42: 482--491
- Preiss S, Peter GF, Anandan S, and Thornber JP (1993) The Multiple Pigment-Proteins of the Photosystem-I Antenna. *Photochem Photobiol* 57: 152--157
- Remelli R, Varotto C, Sandona D, Croce R, and Bassi R (1999) Chlorophyll binding to monomeric light-harvesting complex. A mutation analysis of chromophore-binding residues. *J Biol Chem* 274: 33510--33521
- Rozsak AW, Howard TD, Southall J, Gardiner AT, Law CJ, Isaacs NW, and Cogdell RJ (2003) Crystal structure of the RC-LH1 core complex from *Rhodospseudomonas palustris*. *Science* 302: 1969--1972
- Scheller HV, Jensen PE, Haldrup A, Lunde C, and Knoetzel J (2001) Role of subunits in eukaryotic Photosystem I. *Biochim Biophys Acta* 1507: 41--60
- Schmid VH, Thome P, Ruhle W, Paulsen H, Kuhlbrandt W, and Rogl H (2001) Chlorophyll b is involved in long-wavelength spectral properties of light-harvesting complexes LHC I and LHC II. *FEBS Lett* 499: 27--31
- Schmid VHR, Cammarata KV, Bruns BU, and Schmidt GW (1997) In vitro reconstitution of the photosystem I light-harvesting complex LHCI-730: Heterodimerization is required for antenna pigment organization. *Proc Nat Acad Sci* 7667--7672
- Schmid VHR, Paulsen H, and Rupprecht J (2002a) Identification of N- and C-terminal Amino Acids of Lhca1 and Lhca4 Required for Formation of the Heterodimeric Peripheral Photosystem I Antenna LHCI-730. *Biochemistry* 41: 9126--9131

- Schmid VHR, Potthast S, Wiener M, Bergauer V, Paulsen H, and Storf S (2002b) Pigment binding of photosystem I light-harvesting proteins. *J of Biol Chem* 277: 37307--37314
- Simpson DJ, Machold O, Hoyer-hansen G, and von Wettstein D (1985) Chlorina mutants of barley (*Hordeum vulgare* L.). *Carlsberg Res Commun* 50: 223--238
- Stauber EJ, Fink A, Markert C, Kruse O, Johanningmeier U, and Hippler M (2003) Proteomics of *Chlamydomonas reinhardtii* light-harvesting proteins. *Eukaryotic Cell* 2: 978--994
- Tjus SE, Roobolboza M, Palsson LO, and Andersson B (1995) Rapid Isolation of Photosystem-I Chlorophyll-Binding Proteins by Anion-Exchange Perfusion Chromatography. *Photosynthesis Research* 45: 41--49
- Vainstein A, Peterson CC, and Thornber JP (1989) Light-harvesting pigment-proteins of photosystem I in maize. Subunit composition and biogenesis. *J Biol Chem* 264: 4058--4063
- Van Amerongen H and van Grondelle R (2001) Understanding the energy transfer function of LHCII, the major light-harvesting complex of green plants. *J Phys Chem B* 105: 604--617
- Wollman F-A and Bennoun P (1982) A new chlorophyll-protein complex related to photosystem I in *Chlamydomonas reinhardtii*. *Biochim Biophys Acta* 680: 352--360
- Zhang H, Goodman HM, and Jansson S (1997) Antisense inhibition of the photosystem I antenna protein Lhca4 in *Arabidopsis thaliana*. *Plant Physiol* 115: 1525--1531

Section C:

Supramolecular organisation of higher plants

Photosystem II

C 1

Structure of a higher plant photosystem II supercomplex retaining chlorophyll b antenna proteins revealed by electron crystallography

Tomas Morosinotto, Roberto Bassi, Edward Morris and Jim Barber

This chapter is has been submitted

Structure of a higher plant photosystem II supercomplex retaining chlorophyll *b* antenna proteins revealed by electron crystallography[#]

Tomas Morosinotto[‡], Roberto Bassi[‡], Edward Morris[°], and James Barber^{°*}

[‡] *Dipartimento Scientifico e Tecnologico, Università di Verona, Strada Le Grazie 15, I-37134 Verona, Italy.* [§] *Université Aix-Marseille II, - Département de Biologie UMR 6191 - LGBP - Case 901 - 163, Avenue de Luminy - 13288 Marseille, France.* [°] *Wolfson Laboratories, Department of Biological Sciences, South Kensington Campus, Imperial College London, London, SW7 2AZ, UK*

* Corresponding author. Tel: +44 20 75945266. Fax: +44 20 75945267. E-mail: j.barber@imperial.ac.uk.

Running Title: Structure of a higher plant photosystem II supercomplex

¹Abbreviations used are: α -DM, n-dodecyl- α -D-maltopyranoside Chl, Chlorophyll; EM, Electron microscopy; Lhc, Light harvesting complex; OEC, oxygen evolving complex; PS Photosystem

[#]This work was supported by Ministero dell'Istruzione dell'Università e della Ricerca Progetto Fondo Investimenti Ricerca di Base (no. RBAU01E3CX and n°RBNE01LACT.) and Biotechnology and Biological Research Council (BBSRC) (J. B., E.M.). We would like to thank Prof. Diter von Wettstein (Washington State University, Pullman) and Dr. David Simpson (Carlsberg Research Laboratory, Copenhagen) for kindly supplying barley WT and mutant seeds.

ABSTRACT: Photosystem II of higher plants is a multisubunit transmembrane complex composed of a core moiety and an extensive peripheral antenna system. The core contains subunits catalysing electron transport reactions and the chlorophyll *a* antenna proteins, CP43 and CP47, while the peripheral antenna is composed of trimeric and monomeric light harvesting proteins of the Lhc family which bind both chlorophyll *a* and *b*. Although high resolution structural data have been obtained for the core complex of PSII and for the major trimeric Lhc component as isolated entities, the overall organisation of the complete

supramolecular complex has only been described at relatively low resolution by single particle analysis of electron microscope images. In this work, we analyse the structure of a Lhc-containing PSII supercomplex which crystallises *in situ* in grana membranes of a barley mutant (*Hordeum vulgare viridis zb63*). Isolation of the granal membrane fraction by a newly developed gentle method allowed preparation of ordered arrays for analysis by low temperature electron microscopy (EM). This analysis has provided a 2D projection map of the supercomplex revealing a dimeric PSII core surrounded by monomeric and trimeric Lhc antenna proteins. Based on previous identification of molecular masses by nearest-neighbour analysis and on published crystallographic structures, we assign the monomeric antennae as CP26 (Lhcb5) and CP29 (Lhcb4) and the trimeric component as the tightly bound light harvesting complex II (LHCII). Biochemical fractionation and analyses of the grana membrane preparation confirmed this composition. Our results suggest that the PSII-LHCII supercomplex described here is the basic unit of PSII in plants.

INTRODUCTION

Energy of solar radiation required for plant photosynthesis is trapped by chlorophyll (Chl)¹ and carotenoids bound to thylakoid membrane proteins which are organised into two supramolecular complexes: Photosystem (PS) I and II. Each photosystem is composed of two components with different function and biogenesis: the core complex and the peripheral antenna system. In the case of PSII, the core complex contains the D1 and D2 subunits catalysing electron transport reactions plus the chlorophyll *a* and β -carotene binding proteins, CP43 and CP47, all of which are encoded by chloroplast genes. The peripheral antenna system of plant PSII is composed of multiple subunits of homologous proteins belonging to the Lhc family which are encoded by nuclear *cab* genes and imported into the chloroplast. These bind Chl *a* and *b* as well as xanthophylls. This peripheral antenna system is composed of inner and outer Lhc proteins where the level of the latter varies with growth conditions (1). The structure of PSII has been the subject of intense research in the past few years yielding high resolution maps of the core complex isolated from cyanobacteria (2-4) and from higher plants (5, 6). Nevertheless the organisation of the peripheral antenna system is only known at low resolution, derived from a combination of electron microscopy (EM), single particle analyses (7-10) and nearest neighbour analyses (11).

PSII has been shown to form regular arrays in grana membranes upon detergent treatment (12, 13) or *in vivo* (14, 15) which have been used for structural analysis at low

resolution. However, isolation procedures usually resulted in the dissociation of Lhc subunits from the PSII core (12) or introduced disorder into the regular arrays. For meaningful analysis it is desirable to study 2D crystals of PSII which have formed naturally in thylakoids, so that the structure retains all features of the fully functional complex. Large 2D crystals have been described in the thylakoid membranes of the barley mutant *viridis zb63* (16), a mutant lacking PSI but with normal PSII activity (17, 18). Freeze-etching analyses on these 2D crystals has been performed (16, 19) but the method is limited in resolution due to metal replication of the particle surface. In this study we describe an isolation procedure for 2D crystals of PSII from the *viridis-zb63* barley mutant, with a similar lattice to that observed by freeze-etching in intact chloroplasts. Analysis by electron cryomicroscopy (cryo-EM) yielded a projection map at $\sim 20 \text{ \AA}$ resolution which reveals the organisation of a dimeric PSII core complex surrounded by peripheral Lhc antenna proteins, both monomeric and trimeric. These results are discussed in terms of proposed models of the LHCII-PSII supercomplex which seems to be a basic PSII structural unit binding the inner peripheral Lhc antenna system.

MATERIALS AND METHODS

Biochemistry. Plants of barley WT and *zb63* mutant plants were grown at $100 \mu\text{E m}^{-2} \text{ s}^{-1}$, 19°C , 90% humidity and 8 hours of daylight for 8-10 days. Thylakoids were isolated as in (20), with the addition of 15 mM NaCl and 5 mM MgCl_2 in order to maintain the granal stacking (21). Thylakoids (0.5 mg Chl/ml) were solubilised with different amounts of α -DM ranging from 0.05 to 0.75 %, always in the presence of 15 mM NaCl and 5 mM MgCl_2 . Unsolubilised thylakoids were pelleted at $3500 \times g$, while partially solubilised grana membranes were pelleted at $40000 \times g$. In order to remove the oxygen evolving complex (OEC) proteins, grana particles were washed with 0.8 M Tris HCl pH 8.0 as in (22).

Extensive thylakoid solubilisation and separation of isolated complexes with centrifugation on a sucrose gradient was performed as in (23), after washing the membranes with 5 mM EDTA in order to remove Mg^{2+} . SDS-PAGE analyses were performed with a Tris-Tricine buffer system as in (24) with an acrylamide concentration gradient of 12 to 18%. Pigment composition was determined by HPLC analysis (25) and by fitting the acetone extract absorption spectra with those of the individual pigments (23). Spectra were recorded using an SLM-Aminco DW 2000 spectrophotometer, in 80 % acetone or in 0.5 M sucrose, 10 mM Hepes and 0.06 % α -DM.

Electron microscopy. Electron microscopy (EM) was conducted using an FEI CM200 FEG electron microscope operated at 200 kV accelerating voltage in low dose mode. Images were recorded on Kodak S0163 film at a calibrated magnification of 48,600x. Samples were applied to glow-discharged carbon coated grids: either stained with 2% uranyl acetate or rapidly frozen by plunging into liquid ethane.

Image analysis. Electron micrographs were digitised using a Leafscan film scanner at a step size of 10 microns. MRC image programs (26) were used for Fourier space analysis of the 2D crystals and Imagic programs (27) were used in the real space analysis of crystal patches.

Molecular modelling. Molecular models of the spinach core complex (6) and LHCII (28) were superimposed onto the cryo-EM projection map using the program O (29).

RESULTS

Sample preparation and identification of crystalline arrays. Freeze-fracture EM analysis of the *viridis-zb63* barley mutant which lacks PSI showed that particles containing PSII, known as EFs particles, were ordered into regular 2D arrays (16). Since the mutation is lethal the seedlings must be maintained in heterozygous state and homozygous mutants can be distinguished from the WT by their paler green colour. These can survive for up to two weeks on seed reserves allowing for chloroplast isolation. In order to make arrays accessible to transmission EM, a fractionation treatment is required for selective isolation of ordered grana membranes. Detergent treatment, however, may disrupt the regular arrays or modify the crystal spacing with respect to that observed in freeze-fractured membranes (16). Isolation of grana membranes has been previously performed by fractionation of thylakoids with limited amount of Triton-X-1000 (30) thus yielding 2D crystals of PSII core complexes by selective extraction of peripheral antenna components. More recently, alkyl-glucoside detergents have been employed to isolate PSII supercomplexes containing peripheral antenna systems (7, 9-11, 31).

Here we performed a novel separation of grana membranes of *vir-zb63* by using different amounts of α -DM in the presence of 5 mM Mg^{2+} to maintain granal stacking (21). This procedure yields a membranous fraction that can be pelleted at 40,000 x g and appears to be depleted in ATPase polypeptides when analysed by SDS-PAGE (Figure 1a). The absence of this complex indicates that the treatment achieved the purification of grana membranes free from stroma lamellae. Among a range of detergent concentrations used, 0.1% α -DM allowed isolation of a pelletable fraction that upon negative staining showed roughly circular membranes patches about 0.8 μ m in diameter (Figure 2a). The size of these patches is

consistent with their derivation from grana partitions. SDS-PAGE and immunoblotting analyses of the membranes containing the arrays showed that no detectable modification of PSII composition was introduced by the membrane fractionation procedure other than a reduction of the PsbS subunit (Figure 1b).

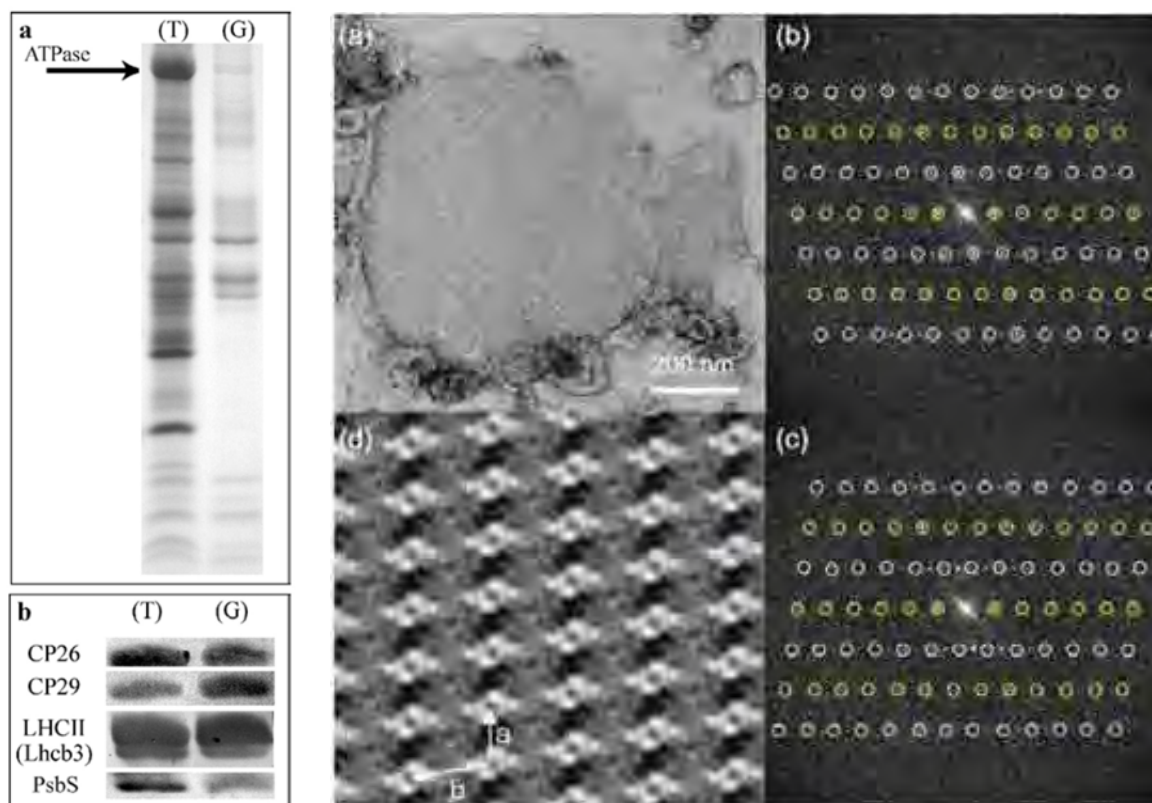


FIGURE 1 (Left): Comparison of (a) SDS-PAGE and (b) immunoblotting analyses of the granal membrane preparation (G) isolated from the barley mutant *vir-zb63* used for EM studies with its thylakoid membranes (T).

FIGURE 2 (right): Characterization of the PSII supercomplex 2D crystals by negatively stained EM and image analysis. (a) Electron micrograph of negatively stained 2D crystal. (b & c) Fourier transform derived from (a) displayed as amplitudes. Two reciprocal lattices are identified arising from oppositely orientated PSII supercomplex arrays viewed from the luminal (b) and stromal (c) sides. Reflections marked with yellow circles are common to each reciprocal lattice while those marked with white circles derive from a single layer. (d) Fourier filtered image corresponding to the layer viewed from the luminal side.

A number of PSII-rich patches contained clearly visible, stain-excluding particles arranged in regular rows (Figure 2a, d). Indexation of Fourier transforms of such images reveal two lattices (Figure 2b, c). The lattices, which are mirror images of each other, have cell dimensions of 16.5 x 25 nm and lattice angles of 100° or 80°. Images derived by Fourier

filtration of each such lattice after appropriate corrections for long-range disorder are characterized by strongly stain excluding particles (Figure 2d) consistent with the projection appearance of negatively stained dimeric PSII core arrays (5, 12, 13, 30, 32). The arrangement of the particles within the array is such that they are substantially separated from each other and connected by material which excludes stain much more weakly. This appearance may be explained by the presence of additional protein subunits which do not substantially protrude from the lipid bilayer and are thus only weakly contrasted by negative stain. The spacing of these lattices is consistent with that observed by freeze-fracture of thylakoids (16). The presence of two mirror related lattices suggests that the membrane patches consist of two stacked lipid bilayers containing PSII arrays back-to-back.

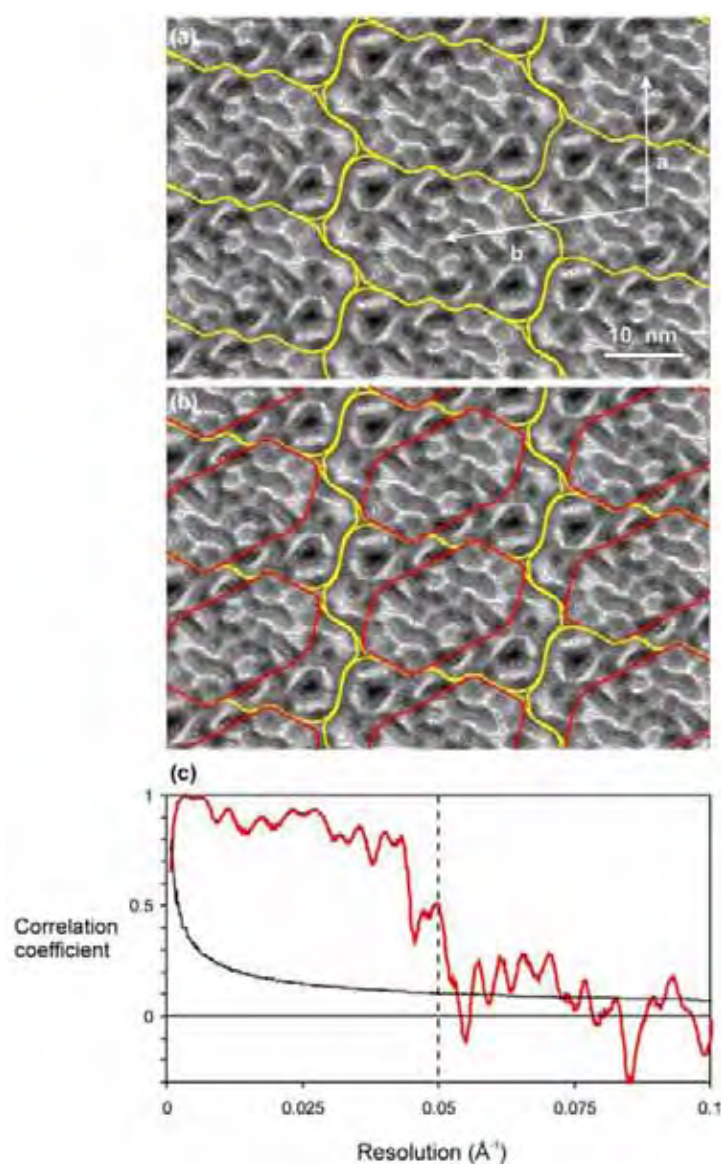


FIGURE 3: Projection structure of the PSII supercomplex array determined by cryo-EM and image analysis. (a) Projection map shown as gray scale overlaid with contours. (b) Projection map as in (a) with the location of the PSII dimeric core outlined in red and the PSII supercomplex outlined in yellow. (c) Resolution assessment of the projection map by Fourier ring correlation. Correlation coefficient (red line) and 3σ threshold (yellow) are plotted as a function of resolution. The approximate resolution of the projection map 20 \AA is shown by vertical dashed line.

Electron cryomicroscopy and image analysis of the 2D arrays. Preparations identified by negative stain, as being rich in well ordered lattices, were subjected to cryo-EM. Patches

containing lattices could be recognised with a reasonable success rate at low magnification (4000x) from their size, shape and density. Low dose images of these patches were recorded at a defocus level of about 0.7 μm . Favourably imaged areas with well developed crystalline lattices were identified for image analysis. From these regions Fourier filtered images were obtained for each of the two component lattices. The filtered images were used as references to obtain the locations of the individual unit cells by cross-correlation. Patches of crystal corresponding approximately to four unit cells were extracted and processed by single particle analysis methods. A total of 372 patches were aligned and averaged together to produce a projection map (Figure 3a). The resolution of the map as estimated by the Fourier ring correlation coefficient is about 20 Å (see Figure 3c). Compared to the projection map derived from negatively stained 2D crystals (Figure 2d) the cryo-EM equivalent shows substantially enhanced structural detail. The central core complex regions contain densities characteristic of projection structures of individual subunits of the PSII core (Figure 3b) and are connected together by strong densities. The particles that make up the array are of a size and shape reminiscent of that of the LHCII-PSII supercomplex studied by single particle analyses (7, 9, 10). To investigate this possibility and establish a comparison between thylakoids isolated from wild type (WT) barley plants and from the *vir-zb63* mutant, a series of biochemical analyses were conducted.

	Chl b	Neoxanthin	Violaxanthin	Antheraxanthin	Lutein	Zeaxanthin	Beta-carotene
WT Thylakoids	31.6	5.4	5.4	0.0	14.6	0.0	7.8
zb63 Thylakoids (T)	14.7	5.3	3.3	3.5	19.3	7.7	6.9
zb63 Grana (G)	16.4	4.7	3.2	3.0	17.9	6.4	6.5

Table I: Pigment composition of WT and *vir-zb63* thylakoids and grana preparation from mutant. Data are normalized to 100 Chl a molecules.

Biochemical analysis of *vir-zb63* thylakoids. Thylakoid (T) and granal (G) preparations from homozygous mutant plants were analysed for pigment and polypeptide composition. As compared to WT, dark adapted *vir-zb63* thylakoids and grana contained, on a Chl a basis, lower Chl b and violaxanthin (V). Lutein content, instead, was higher while neoxanthin and β -carotene were substantially unaffected (Table I). It is worth noting that, while in WT antheraxanthin (A) and zeaxanthin (Z) were only present in traces, in mutant thylakoids V, A

and Z were present in similar amounts, their total amount being three times higher than in WT.

Polypeptide compositions of WT and *vir-zb63* thylakoids are shown in Figure 4a while immunoblotting analysis with antibodies specific for PSI and PSII proteins is shown in Figure 4b. As expected, PSI core polypeptides (PsaC, PsaE and PsaH) were not detected in the mutant although the Lhc polypeptides (Lhca1-4) comprising the LHCI antenna system of PSI were retained. The subunit composition of PSII appears not to be significantly affected by the mutation in *vir-zb63* apart from the absence of the peripheral Lhcb6 antenna component, CP24.

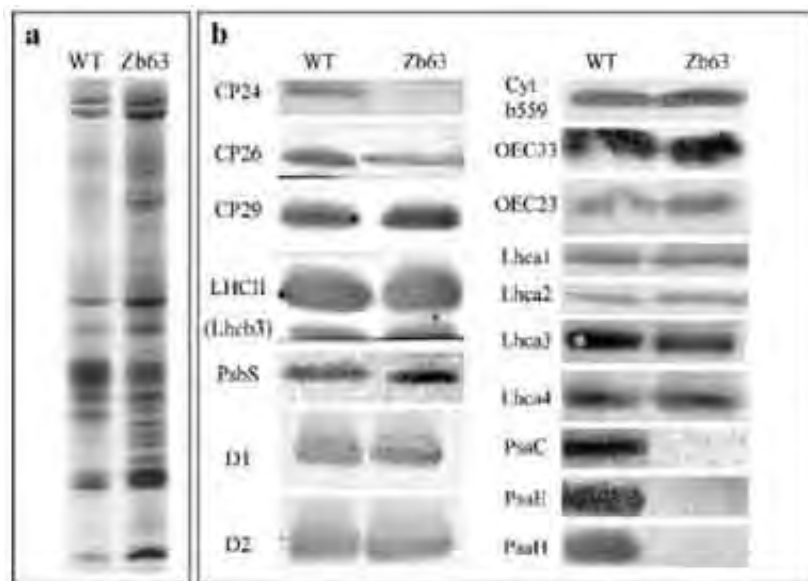


FIGURE 4: Comparison of protein composition of thylakoid membranes from WT barley and barley mutant *vir-zb63* (zb). (a) SDS-PAGE and (b) immunoblotting analyses.

In order to characterise the pigment-protein holocomplexes in the mutant and compare them with those of the WT, thylakoids were solubilised with α -DM and fractionated by sucrose gradient ultracentrifugation (Figure 5). In each case seven green bands were resolved, albeit in different amounts, which were characterised by pigment analysis, absorption spectroscopy and SDS-PAGE (data not shown). For the mutant the respective bands contained: (B1) free pigments, (B2) monomeric and (B3) trimeric Lhc proteins; (B4) monomeric and (B5) dimeric PSII cores. Bands 6 and 7 contained supramolecular complexes of PSII with Lhcb proteins. For the solubilised WT thylakoids, the PSI-LHCI holocomplex, absent in *vir-zb63*, migrated in band 5 together with dimeric PSII cores and in bands 6-7 together with PSII supercomplexes. In Table II the distribution of chlorophyll among the different green bands in the sucrose gradient is compared, in order to assess the relative quantities of the various complexes. Significant differences in mutant pattern compared with WT are evidenced, in particular a lower content of trimeric LHCII by a factor of six. These

results suggest that PSII in *vir-zb63* differs from WT PSII in having a smaller antenna size due to a lower content of trimeric LHCII, possibly as a consequence of the absence of CP24.

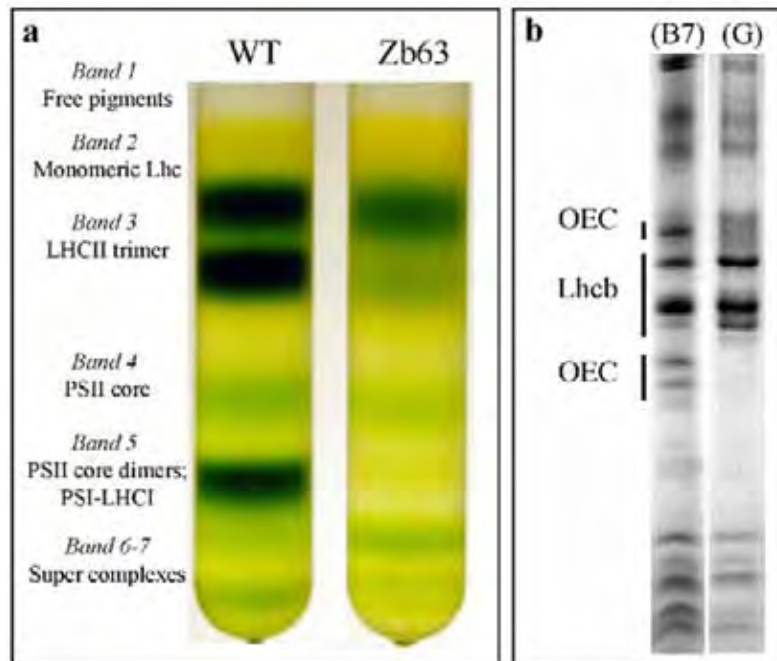


FIGURE 5: (a) Sucrose gradient ultracentrifugation of WT with *vir-zb63* thylakoids after solubilisation with 0.6% α -DM. (b) Comparison of SDS-PAGE of the granal membrane preparation (G) isolated from the barley mutant *vir-zb63* used for EM studies with band 7 from the sucrose density gradient (B7) in Figure 5a. Bands corresponding to Oxygen Evolving Complex and to Lhc polypeptides are indicated.

	A -% Total		B - % PSII core	
	WT	zb63	WT	zb63
Band 1	1.8	5.8	37.4	50.5
Band 2	29.9	55.5	611.4	484.5
Band 3	42.3	15.2	864.9	133.0
Band 4	4.9	11.5	100.0	100.0
Band 5	20.1	1.6	412.2	14.3
Band 6+7	1.0	10.3	20.9	89.9
Total	100.0	100.0	2046.7	872.2

Table II: Quantification of bands in the two gradients, normalized respectively to the total Chl content (A) or to the PSII core band (B)

Nevertheless, distinct bands corresponding to LHCII-PSII supercomplexes (bands 6 and 7) are more abundant in the *vir-zb63* as compared to WT. This difference is even more striking

taking into account that the corresponding bands derived from WT thylakoids contain significant amounts of LHCI-PSI complex as judged by SDS-PAGE analysis (not shown). Bands 6 and 7 from *vir-zb63* contained two different supercomplexes: band 7 contained the PSII core, CP26, CP29 and LHCII giving a SDS-PAGE profile similar to that of the granal membranes used for EM analysis, except for the presence of OEC proteins, which were removed during grana isolation (Figure 5b). This similarity is confirmed by comparison of Chl a/b ratio (6.1 for grana vs. 6.8 for band 7). In contrast, the SDS-PAGE profile of band 6 showed a reduction of CP26 and LHCII content (not shown), giving rise to a higher Chl a/b ratio in this fraction, a clear indication of a smaller antenna content (16.4). This band therefore contained LHCII-PSII supercomplexes which had been stripped of some of their Lhcb antenna system.

DISCUSSION

The barley mutant *vir-zb63* studied here does not contain PSI but has normal PSII activity except that its antenna size is significantly smaller than WT (17, 18). The smaller antenna size is confirmed by our analysis of its thylakoid membranes showing that CP24, a component of the PSII antenna, is lacking and the level of the major trimeric LHCII complexes is strongly decreased. When observed by freeze-fracture EM, thylakoids of this mutant show large EFs particle arrays in the grana partition region while WT plants do not (16). In WT plants, supramolecular complexes of PSII supercomplexes form a variety of particle sizes (33) due to binding of LHCII trimers at multiple sites although in some cases arrays similar to those that dominate in *vir-zb63* are also observed. However in the *vir-zb63* mutant, lack of CP24 and the concomitant decrease in the LHCII level induces an organisation of PSII particles of the same size into regular arrays. The molecular basis for the down regulation of Lhcb proteins in this mutant is not known in detail. However, it is well known that PSII antenna size is regulated by the plastoquinone pool which links electron flow between PSII and PSI. In excess light the over reduction of the plastoquinone pool triggers LHCII degradation (34) and decreases the expression of *cab* genes that encode them (35, 36). The lack of PSI in *vir-zb63* inevitably means that the plastoquinone pool is over reduced, an expectation shown by Bergantino and co-workers (37) and confirmed by accumulation of the stress induced xanthophylls, zeaxanthin and antheraxanthin, in the thylakoids (Table I). Moreover, accumulation of zeaxanthin in the membrane might facilitate protein-protein interaction as previously shown in an *in vitro* system, thus favouring self-organisation of PSII into arrays (38).

The PSII arrays detected in the grana partitions of *vir-zb63* thylakoids are highly ordered and cover most of the grana membrane surface (18). Isolation of these particles by Triton X-100 leads to the preparation of paired membranes with opposite orientation which undergo reorganisation and loss of order (30, 39). We have used an alternative method of membrane isolation by employing limited solubilisation of stacked thylakoids with the mild detergent α -DM. This procedure produced membrane patches with a diameter of about 0.8 μ m, a value comparable to grana dimension *in vivo* (16). This correspondence in size suggests that at least some grana remain intact after solubilisation. Moreover, this method also yields crystalline patches of paired membranes that do not appear to undergo severe reorganisation and can be conserved in a frozen state before structural analysis. The unit cell of these arrays, as identified by negative staining and cryo-EM was 16.5 x 25 nm, equivalent to that reported from freeze-etching experiments (18) supporting our view that no major changes were introduced in the organisation of the PSII array by the isolation procedure. Since PSII in *vir-zb63* has normal activity (17) it is likely that the structural data inferred from this provides a meaningful representation of functional PSII *in vivo* even though the extrinsic OEC proteins were absent.

The structures derived from cryo-EM analysis and negative stain clearly show twofold symmetry (Figures 2d, 3a). The central domain of this dimeric structure, corresponding to the most clearly defined feature in images of negatively stained crystals (Figure 2d), can be assigned to the dimeric PSII core. This assignment is reinforced by the appearance of this domain in the projection map of these crystals derived from cryo-EM. Here densities can be attributed to secondary structure components within the various subunits of the core complex as modelled in Figure 6, consistent with earlier structures of this dimeric core complex of higher plants (6, 32) and with the recent X-ray structure of the PSII core dimer of cyanobacteria (2-4). Six other masses can be clearly resolved in the structure, symmetrically arranged, three on each side of the dimeric PSII core domain. Their size and shape correspond to either the trimeric LHCII complex (28) or to its monomeric components. The monomeric Lhc proteins thus can be identified with CP29 (Lhcb4) and CP26 (Lhcb5), due to the absence of CP24 (Lhcb6) in *vir-zb63*. The presence of these monomeric Lhc proteins and the absence of CP24 were also found for the isolated LHCII-PSII supercomplex of spinach (32). Comparison of molecular structures of PSII core complex (40) with that of the smaller complex lacking the CP43 subunit (41) allowed identification of the CP43 subunit. This earlier assignment has now been confirmed by X-ray crystallography (2-4). Since CP26 forms cross linking products with CP43 (11) the monomeric Lhc protein located in between the

CP43 subunit of PSII core complex and the trimeric LHCII can be identified as CP26. The remaining mass can therefore be attributed to CP29 which also agrees with cross-linking studies (11) and is supported by EM analysis on single particles (7, 9, 10, 33).

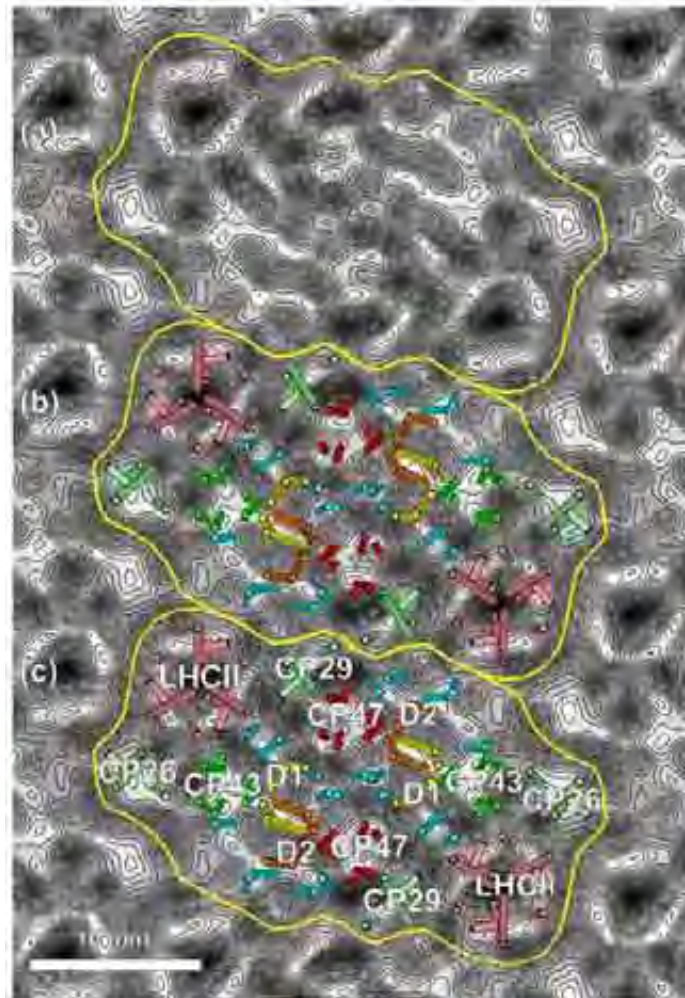


FIGURE 6: Interpretation of the PSII supercomplex projection map. (a) Projection map represented as gray scale with overlaid contours, with PSII supercomplex regions outlined in yellow. (b) Projection map is overlaid with cylinders representing the transmembrane helices of the plant PSII dimeric core subunits (6) and LHC subunits (28). (c) As in (b) with labeled subunits

The above assignments of density to specific subunits within the particle which makes up the array in the granal thylakoids of the barley *vir-zb63* mutant is consistent with the assignments previously made for LHCII-PSII supercomplexes isolated from spinach (see (42)). Indeed, detergent solubilisation of the *vir-zb63* thylakoid membranes and the analyses of one of the resulting sucrose density fractions (band 7), confirmed the presence of the LHCII-PSII supercomplex. This LHCII-PSII supercomplex with one trimeric LHCII per monomer tightly bound to each side of the core dimer through interactions with CP26 and

CP29, seems to be a minimal fundamental unit containing the inner peripheral Lhc antenna. In fact, since in this mutant PSI is absent and PQ is over-reduced (37), we can hypothesise that these plants are down regulating the PSII antenna size to the minimal level possible. It is to this basic unit that other LHCII trimers and CP24 can attach to form larger supramolecular organisations as visualised by Boekema and colleagues (33). The formation and adjustment of the outer peripheral LHCII system regulates the absorption cross section of PSII in response to different growth conditions. The calculated antenna size of the LHCII-PSII supercomplex is about 100 Chls per PSII reaction centre and the binding of the additional LHCII trimers to form the outer peripheral system, will increase the antenna size to about 200 Chls per PSII, typically found in WT plants growing under normal conditions. Indeed, it is probably the presence of the outer LHCII peripheral system in WT thylakoids that prevents the formation of extensive arrays of PSII complexes of the type observed in the grana of *vis-zb63*.

The down regulation of *cab* genes encoding Lhcb proteins and the formation of 2D arrays of LHCII-PSII supercomplexes in response to the over reduction of the plastoquinone pool is likely to be physiologically important. Within arrays there should be efficient energy transfer among LHCII-PSII supercomplexes such that light energy not trapped by a reaction centre can be transferred to neighbouring complexes. In this way the energy would be delocalised in the whole array and have a higher probability of encountering a protective quenching centre composed of zeaxanthin and/or PsbS. Formation of arrays of PSII supercomplexes in thylakoid membranes has been reported in several conditions (8, 15) and is extreme in the *vir-zb63* mutant studied here. We therefore suggest that changing the interactions between different PSII units is an additional mechanism of regulation of the photosynthetic apparatus in response to changes in the light environment and that this regulation is controlled by the redox state of plastoquinone which couples electron flow from PSII to PSI .

Although single particle analysis has provided a 3D structure of the LHCII-PSII supercomplex the 2D crystals of the supercomplex studied here offer the possibility of obtaining a more detailed structure of this basic PSII unit. The task at hand will be to improve the order of the 2D crystals by adjusting detergent treatments and collect data from tilted samples. Thus the work presented here not only establishes the LHCII-PSII supercomplex as an *in vivo* basic unit of PSII but also represents the starting point for obtaining its 3D structure at a resolution better than that currently available.

References

1. Spangfort, M., and Andersson, B. (1989) *Biochim. Biophys. Acta* 977, 163-170.
2. Zouni, A., Witt, H. T., Kern, J., Fromme, P., Krauss, N., Saenger, W., and Orth, P. (2001) *Nature* 409, 739-743.
3. Kamiya, N. and Shen, J. R. (2003) *Proc. Natl. Acad. Sci. U. S. A* 100, 98-103.
4. Ferreira, K. N., Iverson, T. M., Maghlaoui, K., Barber, J., and Iwata, S. (2004) *Science* 303, 1831-1838.
5. Morris, E. P., Hankamer, B., Zheleva, D., Friso, G., and Barber, J. (1997) *Structure* 5, 837-849.
6. Hankamer, B., Morris, E., Nield, J., Gerle, C., and Barber, J. (2001) *J. Struct. Biol.* 135, 262-269.
7. Boekema, E. J., Hankamer, B., Bald, D., Kruip, J., Nield, J., Boonstra, A. F., Barber, J., and Rögner, M. (1995) *Proc. Natl. Acad. Sci. USA* 92, 175-179.
8. Boekema, E. J., van Breemen, J. F., van Roon, H., and Dekker, J. P. (2000) *J. Mol. Biol.* 301, 1123-1133.
9. Nield, J., Orlova, E. V., Morris, E. P., Gowen, B., van Heel, M., and Barber, J. (2000) *Nat. Struct. Biol.* 7, 44-47.
10. Nield, J., Funk, C., & Barber, J. (2000) *Philos. Trans. R. Soc. Lond B Biol. Sci.* 355, 1337-1344.
11. Harrer, R., Bassi, R., Testi, M. G., and Schäfer, C. (1998) *Eur. J. Biochem.* 255, 196-205.
12. Bassi, R., Ghiretti, M. A., Tognon, G., Giacometti, G. M., and Miller, K. R. (1989) *Eur. J. Cell Biol.* 50, 84-93.
13. Santini, C., Tidu, V., Tognon, G., Ghiretti, M. A., and Bassi, R. (1994). *Eur. J. Biochem.* 221, 307-315.
14. Seibert, M., DeWit, M., and Staehelin, L. A. (1987) *J. Cell Biol.* 105, 2257-2265.
15. Ruban, A. V., Wentworth, M., Yakushevskaya, A. E., Andersson, J., Lee, P. J., Keegstra, W., Dekker, J. P., Boekema, E. J., Jansson, S., and Horton, P. (2003) *Nature* 421, 648-652.
16. Simpson, D. J. (1983) *Eur. J. Cell Biol.* 31, 305-314.
17. Hiller, R. G., Moller, B. L., and Hoyerhansen, C. (1980) *Carlsberg Res. Commun.* 45, 315-328.
18. Simpson, D. J., and Vonwettstein, D. (1980) *Carlsberg Res. Commun.* 45, 283-314.

19. Miller, K. R., and Jacob J.S. (1991) in Proc. EMSA Meet., 49th (Bailey G.W., and Hall, E.L., Eds), pp. 196-197, San Francisco Press, San Francisco, U. S. A.
20. Bassi, R., Rigoni, F., Barbato, R., and Giacometti, G. M. (1988) *Biochim. Biophys. Acta* 936, 29-38.
21. Berthold, D. A., Babcock, G. T., and Yocum, C. F. (1981) *FEBS Lett.* 134, 231-234.
22. Ljungberg, U., Akerlund, H.-E., Larsson, C., and Andersson, B. (1984) *Biochim. Biophys. Acta* 767, 145-152.
23. Caffarri, S., Croce, R., Breton, J., and Bassi, R. (2001) *J. Biol. Chem.* 276, 35924-35933.
24. Schägger, H., and von Jagow, G. (1987) *Anal. Biochem.* 166, 368-379.
25. Gilmore, A. M., and Yamamoto, H. Y. (1991) *Plant Physiol.* 96, 635-643.
26. Crowther, R. A., Henderson, R., and Smith, J. M. (1996) *J. Struct. Biol.* 116, 9-16.
27. van Heel, M., Harauz, G., Orlova, E. V., Schmidt, R., and Schatz, M. (1996) *J. Struct. Biol.* 116, 17-24.
28. Kühlbrandt, W., Wang, D. N., and Fujiyoshi, Y. (1994) *Nature* 367, 614-621.
29. Jones, T. A., Zou, J.-Y., and Cowan, S. W. (1991) *Acta Cryst. A* 47, 110-119.
30. Marr, K. M., McFeeters, R. L., and Lyon, M. K. (1996) *J. Struct. Biol.* 117, 86-98.
31. Dominici, P., Caffarri, S., Armenante, F., Ceoldo, S., Crimi, M., and Bassi, R. (2002) *J. Biol. Chem.* 277, 22750-22758.
32. Hankamer, B., Morris, E. P., and Barber, J. (1999) *Nat. Struct. Biol.* 6, 560-564.
33. Boekema, E. J., van Roon, H., Calkoen, F., Bassi, R., and Dekker, J. P. (1999). *Biochemistry* 38, 2233-2239.
34. Lindahl, M., Yang, D. H., and Andersson, B. (1995) *Eur. J. Biochem.* 231, 503-509.
35. Escoubas, J. M., Lomas, M., LaRoche, J., & Falkowski, P. G. (1995) *Proc. Natl. Acad. Sci. U. S. A.* 92, 10237-10241.
36. Teramoto, H., Nakamori, A., Minagawa, J., & Ono, T. A. (2002) *Plant Physiol* 130, 325-333.
37. Bergantino, E., Sandona, D., Cugini, D., and Bassi, R. (1998) *Plant Mol. Biol.* 36, 11-22.
38. Ruban, A. V., and Horton, P. (1999) *Plant Physiol.* 119, 531-542.
39. Ford, R. C., Stoylova, S. S., and Holzenburg, A. (2002) *Eur. J. Biochem.* 269, 326-336.

40. Barber, J., Nield, J., Morris, E. P., Zheleva, D., and Hankamer, B. (1997) *Physiol. Plant.* 100, 817-827.
41. Rhee, K. H., Morris, E. P., Barber, J., and Kühlbrandt, W. (1998) *Nature* 396, 283-286.
42. Barber, J., Nield, J., Morris, E. P., and Hankamer, B. (1999) *Trends Biochem. Sci.* 24, 43-45.

Section D:

*Xanthophylls dynamics in higher plants
thylakoids*

D 1

Dynamics of chromophore binding to Lhc proteins “in vivo” and “in vitro” during operation of xanthophyll cycle

This chapter is in press on Journal of Biological Chemistry, (2002) 277, pp. 36913-36920. reproduced with permission.

Tomas Morosinotto, Roberta Baronio and Roberto Bassi

Dynamics of Chromophore Binding to Lhc Proteins *in Vivo* and *in Vitro* during Operation of the Xanthophyll Cycle*

Received for publication, May 30, 2002, and in revised form, July 10, 2002
Published, JBC Papers in Press, July 11, 2002, DOI 10.1074/jbc.M205339200

Tomas Morosinotto, Roberta Baronio, and Roberto Bassi‡

From the Dipartimento Scientifico e Tecnologico, Università di Verona, Strada Le Grazie, 37134 Verona, Italy

Three plant xanthophylls are components of the xanthophyll cycle in which, upon exposure of leaves to high light, the enzyme violaxanthin de-epoxidase (VDE) transforms violaxanthin into zeaxanthin via the intermediate antheraxanthin. Previous work (1) showed that xanthophylls are bound to Lhc proteins and that substitution of violaxanthin with zeaxanthin induces conformational changes and fluorescence quenching by thermal dissipation. We have analyzed the efficiency of different Lhc proteins to exchange violaxanthin with zeaxanthin both *in vivo* and *in vitro*. Light stress of *Zea mays* leaves activates VDE, and the newly formed zeaxanthin is found primarily in CP26 and CP24, whereas other Lhc proteins show a lower exchange capacity. The de-epoxidation system has been reconstituted *in vitro* by using recombinant Lhc proteins, recombinant VDE, and monogalactosyl diacylglycerol (MGDG) to determine the intrinsic capacity for violaxanthin-to-zeaxanthin exchange of individual Lhc gene products. Again, CP26 was the most efficient in xanthophyll exchange. Biochemical and spectroscopic analysis of individual Lhc proteins after de-epoxidation *in vitro* showed that xanthophyll exchange occurs at the L2-binding site. Xanthophyll exchange depends on low pH, implying that access to the binding site is controlled by a conformational change via luminal pH. These findings suggest that the xanthophyll cycle participates in a signal transduction system acting in the modulation of light harvesting *versus* thermal dissipation in the antenna system of higher plants.

Supramolecular complexes of the thylakoid membrane called photosystems catalyze higher plant photosynthesis. Each photosystem is composed of a core moiety containing electron transport components and binding Chl¹ *a* and β -carotene (2, 3) and by an antenna moiety containing, as light harvesting pigments, Chl *a*, Chl *b*, and a number of xanthophylls, bound to proteins belonging to the Lhc family (4). When light intensity

exceeds the capacity for electron transport from water to NADP⁺, excess energy can be diverted to molecular oxygen with the formation of reactive species harmful for the chloroplast, thus leading to photoinhibition of photosystems (5). In these conditions photoprotection mechanisms are activated leading to the thermal dissipation of excess chlorophyll singlet states (6). At the same time, the pigment composition of thylakoid membranes is modified by the operation of the xanthophyll cycle, consisting of the de-epoxidation of violaxanthin to antheraxanthin and zeaxanthin by the luminal enzyme VDE, which binds to thylakoids upon activation by low luminal pH. During operation of the xanthophyll cycle, violaxanthin bound to a low affinity site of LHCII (7) is released into the membrane lipids where it is de-epoxidized. Newly synthesized zeaxanthin has been reported to act freely in the membrane together with tocopherol in the scavenging of reactive oxygen species (8). Moreover, zeaxanthin can be exchanged for violaxanthin in high affinity binding sites of Lhc proteins where it induces a conformational change leading to increased thermal dissipation (1, 9, 10). Knowledge of the xanthophyll exchange in different Lhc proteins is limited, and the understanding of the mechanisms is very low. In this study we analyzed the extent of the xanthophyll exchange in the different Lhc proteins *in vivo* upon activation of the xanthophyll cycle by strong illumination. We compared these results with those obtained *in vitro* by using a reconstituted system composed of recombinant Lhc proteins and the recombinant VDE enzyme. The extent of zeaxanthin binding to Lhc proteins strongly differed among members of the Lhc protein family. The results obtained by the simple *in vitro* system closely reproduce those obtained *in vivo*, thus suggesting that differences in protein structure are the major determinants for the regulation of xanthophyll exchange. Biochemical and spectroscopic analysis of Lhc proteins upon *in vitro* de-epoxidation showed that xanthophyll exchange occurs specifically at the L2-binding site. This site was previously shown (10) to act as an allosteric regulator of thermal dissipation activity in Lhc proteins by controlling the transition between two conformations of Lhc proteins (1). These data suggest that the xanthophyll cycle is part of a signal transduction system acting in the modulation of light harvesting *versus* thermal dissipation in the photosystems of higher plants.

EXPERIMENTAL PROCEDURES

Plant Material and Treatments—*Z. mays* (cv. Dekalb DK300) plants were grown for 2 weeks at 23 °C at low light intensities (~80 μ E, 14 h light/10 h dark). One set of plants was light-stressed at ~1000 μ E m⁻² s⁻¹ for 30 min at 20 °C, whereas control plants were maintained at growth conditions. After treatment leaves were rapidly harvested, cooled in ice, and chloroplast membranes were isolated as previously reported (11). Thylakoids were solubilized with 1% DM and fractionated by flatted preparative isoelectric focusing as previously described (12). Fractions from IEF were further fractionated by sucrose gradient ultracentrifugation to eliminate co-migrating pigments. Free pigment formed a yellow band in the upper part of the gradient, whereas Lhc proteins formed multiple green bands migrating at higher sucrose den-

* This work was supported in part by Consiglio Nazionale delle Ricerche Agenzia 2000 and by MIUR Progetto FIRB n. RBAU01ECX. The costs of publication of this article were defrayed in part by the payment of page charges. This article must therefore be hereby marked "advertisement" in accordance with 18 U.S.C. Section 1734 solely to indicate this fact.

‡ To whom correspondence should be addressed. Tel.: 39-045-802-7916; Fax: 39-045-802-7929; E-mail: bassi@sci.univr.it.

¹ The abbreviations used are: Chl, chlorophyll; β -DM: *n*-dodecyl- β -D-maltoside; CP, chlorophyll protein; HPLC, high performance liquid chromatography; Lhc, light harvesting protein; Lhca, light harvesting complex of PSI; Lhcb, light harvesting complex of PSII; LHCII, major light harvesting complex of PSII; PS, photosystem; VDE, violaxanthin de-epoxidase; Tricine, *N*-[2-hydroxy-1,1-bis(hydroxymethyl)ethyl]glycine; IPTG, isopropyl-1-thio- β -D-galactopyranoside; MGDG, monogalactosyl diacylglycerol; NPQ, excitation energy.

sities. The green fractions from each tube were pooled for further analysis.

Pigment Analysis—The pigment content was determined by HPLC (13) and fitting of the acetone extract with the spectra of the individual pigments (14).

Gel Electrophoresis—SDS-PAGE was performed with the Tris-Tricine buffer system as previously reported (15).

Expression of Recombinant VDE—The construct QAV expressing VDE was a kind gift of Prof. Yamamoto (16). For the VDE expression, *Escherichia coli* cultures (SG13009 strain) (17) with a 600-nm absorbance of 0.6 were induced with 1 mM IPTG for 3 h and purified on a Ni²⁺ affinity column. The protein was denatured in 6 M guanidine-HCl, 20 mM HEPES, pH 8, 0.2 M NaCl and then refolded with a slow dilution of the denaturant with the renaturation buffer (10% glycerol, 0.25% *n*-octyl- β -D-glucoside, 20 mM HEPES, pH 7.5, 100 mM NaCl) (16).

Isolation of Overexpressed Lhc Apoproteins from Bacteria—Lhc were expressed and isolated from *E. coli* following a protocol as previously described (11, 18).

Reconstitution and Purification of Lhc-pigment Complexes—Lhca1 and Lhca4 from *Arabidopsis thaliana*, Lhcb4 (CP29) and Lhcb5 (CP26) from *Z. mays*, and Lhcb1, Lhcb2, and Lhcb3 from *Hordeum vulgare* were reconstituted as described (19) with the following modifications. The reconstitution mixture contained 420 μ g of Lhc apoprotein and 240 μ g of chlorophyll *a* plus *b*. The Chl *a/b* ratio in the pigment mixture varied from 2.3 to 4.5 as optimized for the different Lhc proteins: Lhcb1–3, 2.3; CP26, 3.0; CP29, 4.5; and Lhca1/4, 4.0. Xanthophyll content was 90 μ g of violaxanthin for Lhcb1, Lhcb2, and Lhcb3 and 60 μ g for CP26, CP29, and Lhca1, 4.

Spectroscopy—The absorption spectra at room temperature were recorded by a SLM-Aminco DK2000 spectrophotometer and a 0.4-nm step was used. The CD spectra were measured at 10 °C on a Jasco 600 spectropolarimeter. Samples were in 10 mM HEPES, pH 7.5, 20% glycerol, and 0.06% β -DM.

Deconvolution of Spectra into Absorption Forms—Absorption spectra were analyzed in terms of the contribution of individual pigments by using the absorption spectra of pigments in Lhc proteins as previously reported (20).

De-epoxidation Reaction in Vitro—Lhc proteins (3 μ g of chlorophyll) were mixed with 60 μ g/ml monogalactosyl diacylglycerol (MGDG) and added to the reaction mixture containing 250 mM citrate buffer, pH 5.1, and 0.02% β -DM and 1.5×10^{-3} units of the VDE enzyme preparation. The de-epoxidation was performed at 28 °C for 30' and started by adding 30 mM of ascorbate as described in Ref. 21. The reaction was stopped by the addition of 250 μ l of Tris-HCl 3 M, pH 8.45. Following the reaction, proteins were concentrated in Centricon tubes (10 kDa cut-off) and purified from free pigments by ultracentrifugation in 15–40% glycerol gradient containing 0.06% β -DM and 10 mM HEPES-KOH, pH 7.5.

RESULTS

De-epoxidation in Vivo—Maize plants were exposed to high light intensity to induce de-epoxidation. Thylakoids from light stressed plants were isolated and fractionated into different Lhc complexes by preparative IEF (12). Fig. 1 shows the polypeptide composition of the different fractions as determined by SDS-PAGE. We obtained 12 different fractions ranging from a pI of 3.9–6.5. Although IEF did not allow purification of individual pigment-binding proteins, the distribution of each Lhc polypeptide among different fractions was determined by immunoblotting with specific antibodies. The reactions obtained with α -CP24, α -CP26, α -CP29, α -LHCI, and α -LHCII antibodies are also indicated in Fig. 1. The pigment composition of individual fractions was determined by HPLC analysis upon separation of free pigments from pigment-protein complexes by sucrose gradient ultracentrifugation (12). The violaxanthin and zeaxanthin levels in each fraction are shown in Fig. 2.

Fractions 1–4 contain only LHCII and have a low level of zeaxanthin (0.4–0.6 mol/100 mol of Chl *a*). It is interesting to observe that fractions enriched in Lhcb3 (fraction 1) have the highest level of zeaxanthin. These data suggest that Lhcb3 can bind zeaxanthin more efficiently than other LHCII components, although to a low level.

The fractions with the highest zeaxanthin content (0.9–1.3 mol/100 mol Chl *a*) were those with pI ranging from 4.2 to 4.5

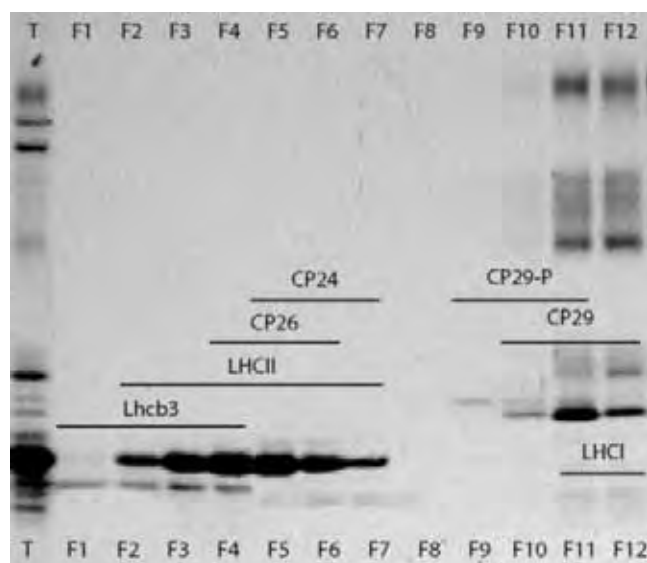


FIG. 1. SDS-PAGE of fractions obtained from the IEF separation of *Z. mays* thylakoids. Lanes are as follows: T, thylakoids; F1–F12, fractions 1–12. The black lines indicate the polypeptide presence as detected by reactions with specific antibodies.

and numbered from 5 to 7. These fractions contained LHCII, CP26, and CP24. Because fractions 1–4 contained only LHCII and showed a very low zeaxanthin content, we conclude that zeaxanthin is mostly bound to CP26 and CP24. Their enhanced zeaxanthin level is even more significant if we consider that LHCII is the most abundant component in these fractions. In fact, densitometric analysis of SDS-PAGE showed that CP26 and CP24 content in these fractions is in the range of 5–10% of the total protein.

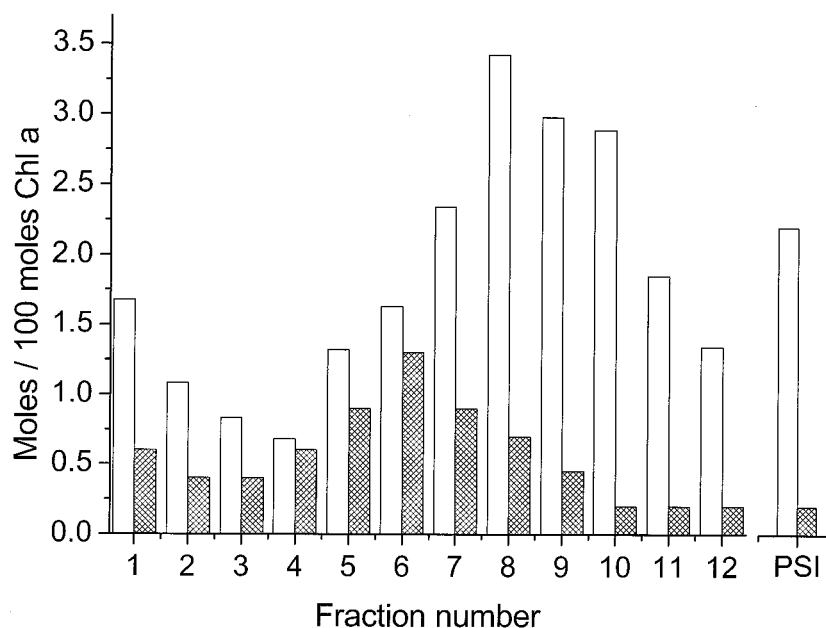
Fraction 8 did not contain any polypeptide, and even immunoblotting with α -Lhc proteins could not detect any specific reaction, suggesting no Lhc proteins were present in this fraction. CP29 in its phosphorylated form is the only protein present in fraction 9 (22, 23). Zeaxanthin is present in this fraction at the level of 0.45 mol/100 mol of Chl *a*, similar to fractions 1–4 containing LHCII.

The remaining fractions (10–12) contained CP29 in its non-phosphorylated form and the PSI-LHCI complex. The level of zeaxanthin in these fractions was low (0.2 mol/100 mol of Chl *a*).

To obtain a better estimation of the zeaxanthin content of LHCI, we have purified the PSI-LHCI complex from CP29 by sucrose gradient. The zeaxanthin content of this preparation was 0.2 mol/100 mol of Chl *a*. Due to the presence of LHCI together with PSI core (see Fig. 1), which binds high amounts of Chl *a*, the actual content of zeaxanthin in LHCI proteins is probably underestimated.

Reconstituted in Vitro System to Examine Exchange of Violaxanthin for Zeaxanthin—Although the determination of the zeaxanthin content of individual Lhc proteins upon de-epoxidation *in vivo* is physiologically relevant, little information can be obtained on the biochemical factors controlling xanthophyll exchange. In fact, zeaxanthin is exchanged for violaxanthin, whose content in individual Lhc proteins ranges from 0.2 mol/poly peptide in Lhcb1 to 1.2 mol/poly peptide in Lhca1. Moreover, the accessibility of zeaxanthin-binding sites to newly formed zeaxanthin can be different depending on the aggregation state of individual Lhc proteins in the thylakoid supramolecular assemblies. To determine the intrinsic capacity of individual Lhc proteins to exchange violaxanthin for zeaxanthin, we have used a simplified reconstituted system (21) in which de-epoxidation is performed *in vitro* using a recombinant VDE

FIG. 2. Violaxanthin and zeaxanthin content of fractions from IEF separation. Violaxanthin (empty bars) and zeaxanthin (filled bars) content in different fractions is expressed in mol/100 mol of Chl *a*.



enzyme (16) expressed in *E. coli* and purified by affinity chromatography. As substrate we used recombinant Lhc proteins reconstituted *in vitro* from the apoprotein expressed in bacteria and purified pigments. To overcome the problem of a different content of violaxanthin and evaluate their specific exchange capacity, we have reconstituted the different Lhc proteins with violaxanthin as the only xanthophyll (24–26), thus obtaining recombinant proteins with a comparable xanthophyll composition.

Expression of Recombinant VDE in *E. coli*—Violaxanthin de-epoxidase from *A. thaliana* (16) was expressed in *E. coli* and purified by affinity chromatography. To increase the specific activity, this preparation was subjected to a denaturation/renaturation cycle by first treating with 6 M guanidine-HCl and, upon binding to a Ni²⁺ column, slowly diluting the guanidine-HCl with renaturation buffer. VDE obtained by this procedure showed 12 times higher activity (350 nmol of violaxanthin de-epoxidized min⁻¹ mg protein⁻¹) with respect to the protein purified in the native state, suggesting that an inefficient folding had occurred in the bacterial host.

Reconstitution of Different Lhc Proteins with Violaxanthin—Seven different Lhc polypeptides were expressed in *E. coli* and reconstituted with violaxanthin as the only carotenoid: Lhcb1, Lhcb2, Lhcb3, Lhcb4 (CP29), Lhcb5 (CP26), Lhca1, and Lhca4. The pigment complement of different polypeptides, as obtained by HPLC and fitting of acetone extracts, is summarized in Table I. The xanthophyll content of different Lhc proteins ranged between 2 and 3 per polypeptide. The lower value was obtained in the case of CP29 (1.9 mol/mol of polypeptide), whereas Lhca1 yielded a value near 3 (2.8 mol/polypeptide). Lhcb3 protein bound ~2.4 violaxanthin/polypeptide. This latter value is clearly different from previous results obtained with Lhcb1 from *Z. mays* showing a value of 2.0 (24). The reason for this difference must be ascribed to the different gene product and strongly suggests that the affinity of individual binding sites for different xanthophyll species can vary between individual Lhcb gene products.

We then analyzed recombinant proteins reconstituted with violaxanthin as the only xanthophyll to assess whether the modification in xanthophyll composition did actually modify Lhc protein conformation. To this aim we compared the absorption and CD spectra of Lhc proteins reconstituted with the whole set of xanthophylls to those of the same complexes re-

TABLE I
Pigment composition of Lhc complexes reconstituted with violaxanthin

Pigment composition of Lhcb1, Lhcb2, Lhcb3, CP26, CP29, Lhca1, and Lhca4 reconstituted *in vitro* with violaxanthin as the unique carotenoid. All values are indicated as moles per polypeptide. The number of chlorophylls used for normalization was in Refs. 35, 41, 42, and 51. For Lhcb2 the same value of Lhcb1 was used.

	Lhcb1	Lhcb2	Lhcb3	CP26	CP29	Lhca1	Lhca4
Chl <i>a</i> /Chl <i>b</i>	1.5	1.4	1.9	2.3	2.9	4.2	2.6
Chl <i>a</i>	7.1	7.0	7.2	6.2	5.9	8.1	7.2
Chl <i>b</i>	4.9	5.0	3.8	2.8	2.1	1.9	2.8
Violaxanthin	2.5	2.1	2.7	2.2	1.9	2.8	2.2
Chl tot	12	12	11	9	8	10	10

constituted with violaxanthin only. Differences were detected in the Soret range due to the direct absorption of xanthophylls; however, in the Qy range the absorption and CD spectra of Lhc proteins with violaxanthin only were essentially identical to those of the corresponding control Lhc protein (see CP26 and Lhca1, Fig. 3, A–D). The Qy absorption and CD spectra are an excellent probe of protein conformation because Chl absorption is modulated by each binding site to distinct energy levels and responds to conformational changes (23, 27). The observation that only very minor changes could be detected in this spectral region clearly shows that Lhc proteins reconstituted with violaxanthin only are representative of their control forms also binding lutein and neoxanthin. This is consistent with previous work with Lhcb1 and CP26 (24, 25).

De-epoxidation *in Vitro*—A reconstituted *in vitro* system for Lhc xanthophyll de-epoxidation was accomplished by mixing recombinant Lhc proteins with recombinant VDE plus MGDG and ascorbate, previously shown to be essential for VDE activity (28). Preliminary experiments were run at different temperatures and pH values by using the activity assay previously reported (29) with purified violaxanthin as a substrate rather than Lhc proteins. The de-epoxidation activity was strongly dependent on temperature with a 5-fold increase between 20 and 28 °C and also a sharp pH optimum at 5.2. The assay conditions were therefore set at 28 °C and pH 5.2 for 30 min when using Lhc-bound violaxanthin as a substrate with 60 μg/ml MGDG and 30 mM ascorbate as co-factors. These assay conditions were successful for all Lhc proteins except CP24, which was denatured by prolonged incubation at 28 °C, consistent with a previous report (30) of low stability of this

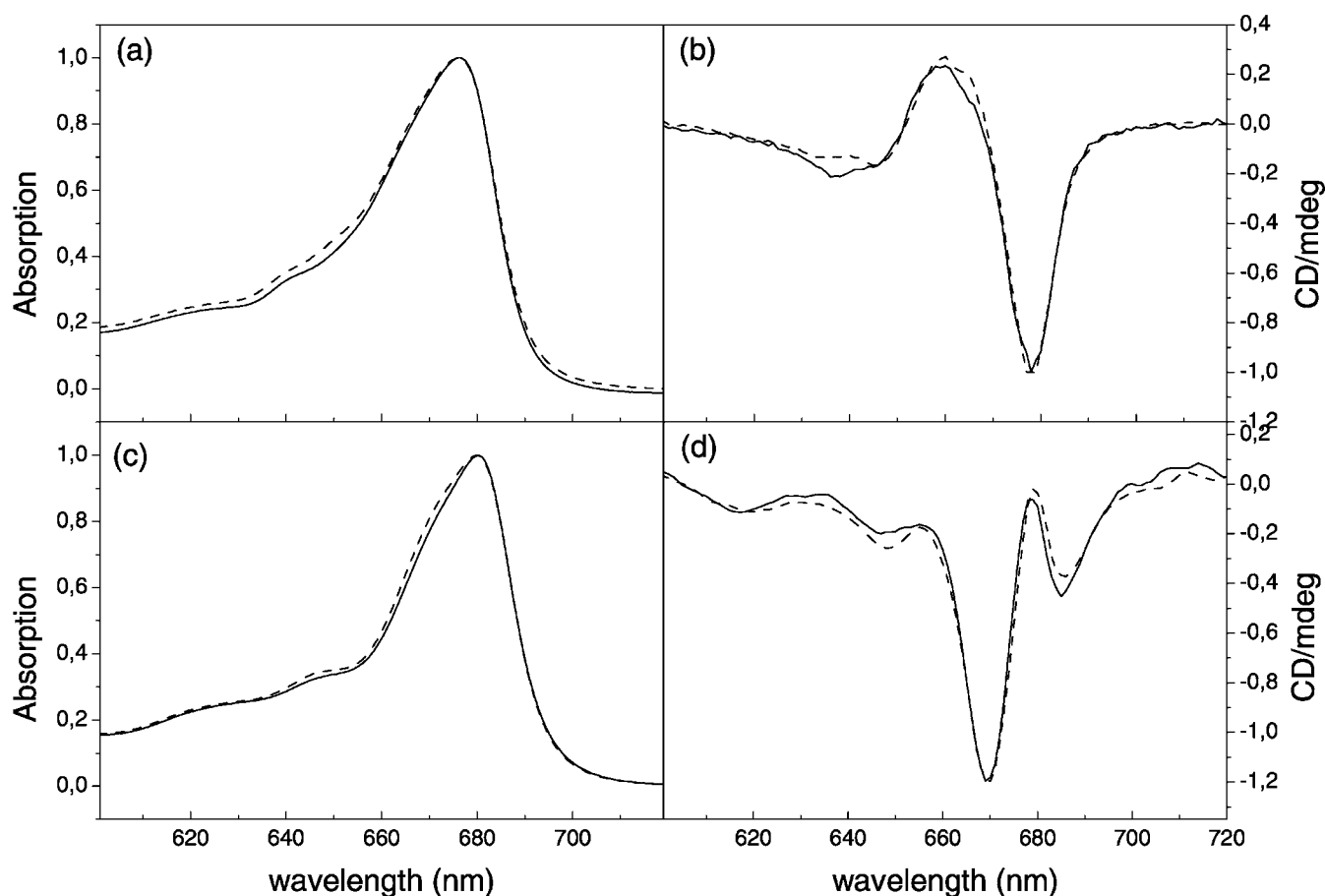


FIG. 3. **Spectral comparison of Lhc reconstituted with only violaxanthin and with a control carotenoid content.** Absorption and CD spectra of CP26 (a and b, respectively) and Lhca1 (c and d, respectively), control (solid line), and reconstituted with violaxanthin as the unique xanthophyll (dashed line) are shown.

pigment-protein complex both recombinant or purified from thylakoids.

Following incubation, Lhc complexes were re-purified by a glycerol gradient to separate pigments freed during the incubation from pigment-protein complexes. The pigment content of the two fractions was analyzed by HPLC and fitted to acetone extracts. In all cases, the free pigment fractions, obtained as a yellow-green band on the upper region of the gradient, showed the highest level of de-epoxidated xanthophylls, in particular antheraxanthin, implying the favored substrate for de-epoxidation was the freed xanthophyll in MGDG rather than the protein-bound form. Only traces of antheraxanthin were found to be protein-bound, suggesting that the affinity of the protein-binding sites was higher for either violaxanthin or zeaxanthin than antheraxanthin. The results in Fig. 3 show that all proteins are able to exchange violaxanthin with zeaxanthin, although the amplitude of the effect was very different depending on the gene product.

Among Lhc complexes, CP26 showed the highest level of zeaxanthin after 30' of de-epoxidation (7.7 mol/100 mol of Chl *a*) as compared with the rest of the Lhcb proteins. In fact, CP29, Lhcb1, Lhcb2, and Lhcb3 had reduced levels of zeaxanthin after incubation under the same conditions (0.8–2.2 mol zeaxanthin/100 mol of Chl *a*). Longer periods of incubation led to a decrease in differences between the individual Lhc proteins when the reaction approached saturation (90'–120'). An interesting result was obtained with Lhca1 and Lhca4 proteins, which showed a violaxanthin-to-zeaxanthin exchange efficiency comparable with CP26 (4.1 and 6.0 mol zeaxanthin/100 mol of Chl *a*, respectively).

The control samples were incubated in the same conditions but without the enzyme. In Fig. 4 we show the CP26 results because it was the most efficient protein in violaxanthin exchange. After 30' incubation at 28 °C, pH 5.2, without VDE, the complex was purified by gradient ultracentrifugation. Even in the absence of the enzyme, the content in violaxanthin was reduced, although to a lower extent with respect to the sample incubated with VDE (6.3 mol/100 mol of Chl *a* versus 8.7 mol/100 mol of Chl *a*). If zeaxanthin was added in excess (1 μ g/ml) to the mixture at the beginning of the incubation, the total xanthophyll content did not decrease; however, part of the violaxanthin was substituted by zeaxanthin. These data indicate that xanthophyll exchange at low pH does not depend on the presence of the VDE enzyme but only on the xanthophylls present in the reaction mixture. Similar results were obtained with Lhca4. In this case when zeaxanthin was supplied in the reaction mixture in the absence of VDE enzyme, it was bound by the protein to a level of 18 mol/100 mol of Chl *a*.

In a second experiment, Lhca4 was incubated with an excess of zeaxanthin at neutral pH (7.5). In this case, the exchange level was \sim 3 times lower than at pH 5.2 (5.5 versus 18 mol of zeaxanthin bound/100 mol of Chl *a*). Consistently, the level of violaxanthin that remained bound to the Lhca4 protein after incubation with zeaxanthin was 16 and 27 mol/100 mol of Chl *a*, at pH 5.2 and pH 7.5, respectively.

A further observation on the effect of the incubation of Lhc proteins was that the Chl *a/b* ratio decreased upon incubation in the reaction medium (Table II). Either a loss of chlorophyll *a* or the gain of chlorophyll *b* can explain this effect. The latter hypothesis seems unlikely in this *in vitro* system in which

FIG. 4. Violaxanthin and zeaxanthin content of different Lhc complexes after the de-epoxidation *in vitro*. Violaxanthin (empty bars) and zeaxanthin (filled bars) content in different Lhc proteins is expressed in mol/100 mol of Chl *a*.

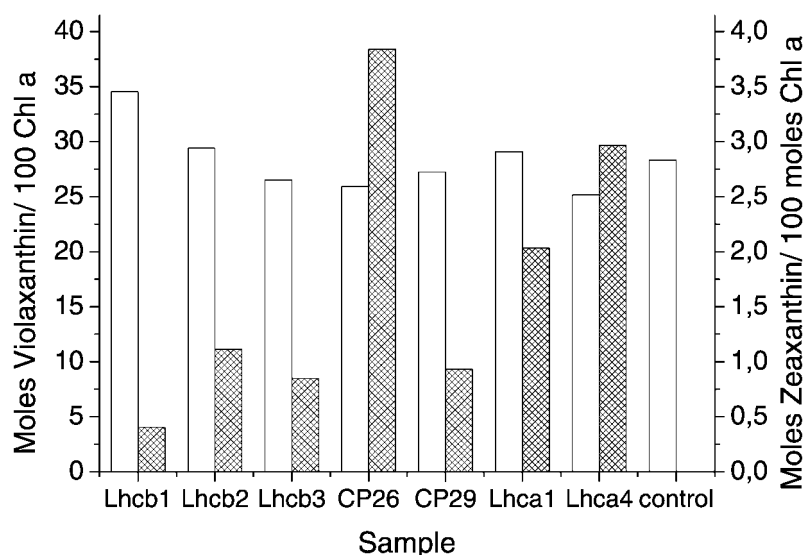


TABLE II

Pigment composition of Lhc complexes after de-epoxidation *in vitro*

Values are normalized following the hypothesis of one Chl *a* is lost during the reaction. Difference values are obtained from normalized pigment binding data of Lhc complex before (Lhc-Vx, Table I) and after the reaction (Lhc-Depox). All values are indicated as moles per polypeptide.

	Lhc complexes after de-epoxidation							Control
	Lhcb1	Lhcb2	Lhcb3	CP26	CP29	Lhca1	Lhca4	
Chl <i>a</i> /Chl <i>b</i>	1.3	1.3	1.9	1.7	2.5	4.2	2.0	1.8
Chl <i>a</i>	6.2	6.3	6.5	5.0	5.0	7.3	6.0	5.2
Chl <i>b</i>	4.8	4.7	3.5	3.0	2.0	1.7	3.0	2.8
Violaxanthin	2.1	1.8	1.7	1.3	1.4	2.1	1.5	1.5
Zeaxanthin	0.0	0.1	0.1	0.4	0.1	0.3	0.4	0.0
Chl tot	11	11	10	8	7	9	9	8
	Difference: (Lhc-Vx) - (Lhc-Depox)							
Chl <i>a</i>	0.9	0.7	0.7	1.2	0.9	0.8	1.2	1.1
Chl <i>b</i>	0.1	0.3	0.3	-0.2	0.1	0.2	-0.2	-0.1
Violaxanthin	0.4	0.2	1.0	0.9	0.5	0.7	0.7	0.7

excess Chl *b* is not available, and the alternative hypothesis of a loss of Chl *a* is also supported by an increase of the Chl *a/b* ratio in the free pigment fraction after the de-epoxidation (not shown). Because the Chl *a/b* ratio did not change upon incubation at pH 7.5, we suggest that the low pH treatment was necessary not only for xanthophyll exchange but also for the loss of Chl *a*. When normalized to the Chl-to-protein stoichiometry of the individual Lhc proteins, the amplitude of Chl *a* release corresponded to one mol/mol of polypeptide (1.0 ± 0.1 Chl *a*/Lhc polypeptide, Table II).

DISCUSSION

In this work we analyzed the de-epoxidation of violaxanthin to zeaxanthin and its binding to Lhc proteins *in vivo* and *in vitro*. The integration between these two approaches should allow both to identify the relative level of involvement of the different Lhc proteins into the xanthophyll cycle mechanism and to determine to what extent this is determined by the structure of individual gene products *versus* other factors such as the accessibility of Lhc to the enzyme. The first approach consisted of the exposure of maize seedlings to excess light, a condition that activates VDE and induces accumulation of zeaxanthin in the thylakoid membrane (31, 32). The treatment was for 30' to obtain sufficient levels of de-epoxidation. Moreover, 30 min of illumination with saturating light allows the saturation of excitation energy (NPQ) (not shown). Shorter treatments yielded essentially the same results, although the extent of de-epoxidation and the level of accumulation in indi-

vidual Lhc proteins was lower. Nevertheless, the distribution of zeaxanthin was essentially the same as detected following illumination for 30'. De-epoxidation *in vitro* was also carried out for 30'. Previous work (21) showed that saturation of zeaxanthin incorporation into Lhcb1 protein is attained at ~70 min of reaction at 28 °C. From preliminary experiments, we chose 30' incubation to efficiently detect the differences between individual Lhc proteins and at the same time obtain significant levels of de-epoxidation.

The major physiological mechanism in which the xanthophyll cycle has been involved so far is the thermal dissipation of NPQ, which is thought to be devoted mainly to protection of PSII from photoinhibition (8).

The Minor Antenna Complexes—Data from de-epoxidation *in vivo* showed that zeaxanthin binds mainly to CP26 and CP24. This is confirmed also by *in vitro* experiments where CP26 is the Lhc protein that shows the highest rate of violaxanthin exchange with zeaxanthin. In the case of CP24, we only have data from *in vivo* experiments because recombinant CP24 showed to be unstable at assay conditions in agreement with previous reports (30) with both the native and recombinant proteins. Nevertheless, the finding of high zeaxanthin in fraction 7 of the IEF separation, where there is no CP26 (as detected by specific antibodies), suggests that CP24 can exchange violaxanthin with zeaxanthin at a similar rate to CP26. It is possible that longer treatments may induce even higher zeaxanthin content in CP24 due to the fact that in CP24 neoxanthin is absent and is substituted by corresponding amounts of violaxanthin (30, 33). It is worth noting that selective depletion of CP26 (34) in transgenic tobacco led to the alteration of the xanthophyll cycle and inhibition of energy dissipation under stress conditions.

CP29 was well separated by the IEF procedure. In fraction 9 we only find phosphorylated CP29, which binds little zeaxanthin. It has been previously shown that phosphorylation does not affect the pigment binding properties of CP29 (23). Data from *in vivo* and *in vitro* experiments consistently show that CP29 has a low capacity for zeaxanthin binding, similar to Lhcb2 and Lhcb3, at least in the present experimental conditions. This result is somewhat surprising because of the high similarity between CP29 and CP26. These two proteins bind a similarly low number of chlorophylls (35), show a similar distribution of xanthophylls among binding sites with lutein in L1 and violaxanthin/neoxanthin in L2 (36), and can both be refolded *in vitro* with zeaxanthin inducing fluorescence quenching (9, 25). These characteristics of CP26 and CP29 suggest

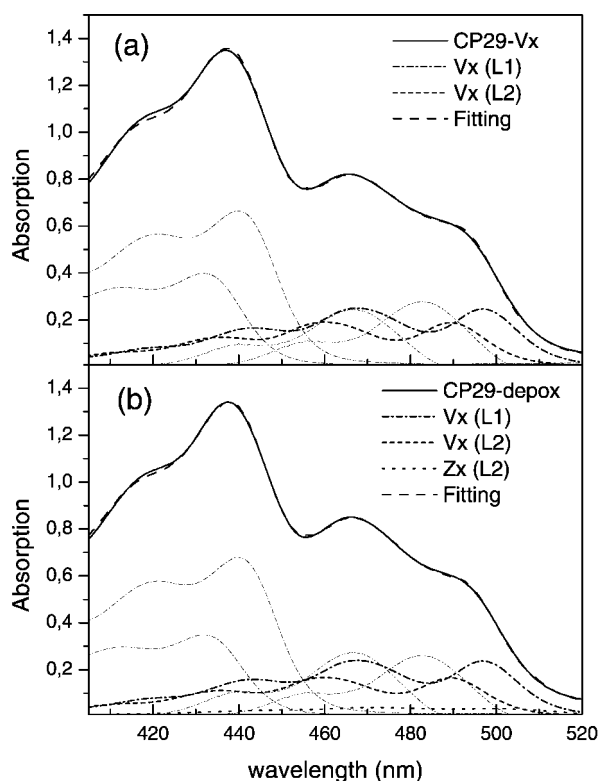


FIG. 5. Spectral reconstruction of CP29 before and after the de-epoxidation *in vitro*. Spectral deconvolution of CP29-Vx (a) and CP29-depox (b) is shown. Also, Chl *a* (dash dotted) and Chl *b* (dash dot dotted) forms are indicated.

that the major difference between the two proteins is the capacity of exchanging violaxanthin *versus* zeaxanthin in site L2. A possible physiological significance of this difference is that CP26 and CP29 might be involved in short *versus* long-term acclimation to excess light. Protonable residues have been detected as dicyclohexylcarbodiimide-binding sites in both CP29 and CP26 although in different domains of the protein (37, 38). Because violaxanthin-to-zeaxanthin exchange occurs in conditions of low luminal pH *in vivo* and *in vitro*, it might be that the distribution of DCCD-binding sites exposed to the luminal surface of Lhc proteins controls the xanthophyll exchange rate. DCCD binding has been recently reported for PsbS (39), a Lhc-like protein whose deletion in *Arabidopsis* strongly decreased the capacity for light-induced thermal dissipation (40). Because PsbS was shown to be unable to bind pigments in a stable manner, the function of protonable residues in this protein might induce a conformational change. Such conformational change could then be transferred to neighbor Lhc proteins, inducing transition to the quenched conformation (1).

The Major LHCII Antenna Complex—Analysis of pigment binding data of the IEF fractions containing LHCII only show that this trimeric complex can exchange violaxanthin for zeaxanthin, although to a lower extent with respect to CP26 and CP24. The study of recombinant Lhcb1, Lhcb2, and Lhcb3 gene products *in vitro*, however, indicates that the three components of LHCII differ in their capacity for binding zeaxanthin, Lhcb2 and Lhcb3 scoring better with respect to Lhcb1. This is consistent with the high zeaxanthin level in IEF fraction 1, containing almost pure Lhcb3. Lhcb3 was shown to contain a low energy Chl *a* ligand (Chl *a*, 686 nm), which is absent in Lhcb1, making it a local sink for excitation energy in a trimeric LHCII complex (41). The higher zeaxanthin exchange rate in Lhcb3 might be strategic for the control of the lifetime of excited states in the whole trimeric LHCII complex.

The PSI-LHCI Complex—Analysis *in vivo* shows that zeaxanthin is bound to the PSI-LHCI complex at a level of 0.2 mol/100 mol of Chl *a*. Xanthophylls are only bound to the LHCI moiety, which accounts for 34% of Chl *a* in the PSI-LHCI complex.² We can thus estimate a zeaxanthin content of ~0.6 mol/100 mol of Chl *a* in LHCI. This is consistent with the high level of zeaxanthin binding by Lhca1 and Lhca4 *in vitro*, considering we have assayed monomeric Lhca complexes, whereas LHCI is dimeric *in vivo* (43, 44). Oligomerization has been suggested to decrease the capacity for xanthophyll exchange in trimeric LHCII (21), but the finding of zeaxanthin in LHCI upon both *in vivo* and *in vitro* experiments suggests that xanthophyll exchange involves both PSI and PSII, confirming previous results with *Vinca major* (45).

Mechanism of De-epoxidation—The *in vitro* analysis of de-epoxidation also provides useful information about the mechanism of de-epoxidation of violaxanthin bound to Lhc proteins. It can be asked whether de-epoxidation occurs on violaxanthin still bound to Lhc proteins or in a free xanthophyll pool. The control samples incubated in the absence of VDE underwent the loss of a fraction of its bound violaxanthin, which might be the actual substrate for the reaction. This hypothesis is supported by two findings: first, the incubation of violaxanthin containing complexes with free zeaxanthin in the absence of VDE yielded incorporation of zeaxanthin into Lhc proteins and second, the capacity of individual Lhc proteins to release violaxanthin in the medium when incubated in the absence of VDE is related to the violaxanthin-to-zeaxanthin exchange capacity during VDE reaction.

We conclude that de-epoxidation occurs in a free-pigment pool dissolved in MGDG. This can explain the early finding that in the *Chlorina f2* mutant of barley (lacking Lhc proteins) de-epoxidation in high light occurs faster and to a higher final level than in wild type (46). The limiting steps of the reaction of violaxanthin-to-zeaxanthin exchange in Lhc proteins, therefore, are the liberation of violaxanthin from and the rebinding of zeaxanthin to their binding sites.

It is worthwhile to emphasize the pH-dependence of the xanthophyll exchange process. Excess light conditions lead to low luminal pH, which is known to activate VDE. Our findings suggest that Lhc proteins might be the targets of an independent effect of luminal pH, thus regulating their xanthophyll exchange capacity. Further studies are needed to assess the details of pH-dependence for individual Lhc proteins and also to verify the role of individual protonable residues in mediating the pH effect. However, it appears that pH-dependence might reflect conformational changes whose immediate effect is detected here as the efficiency of xanthophyll exchange but might also affect other properties of Lhc proteins such as their fluorescence yield. Such a hypothesis would be consistent with the residual level of NPQ detected in *npq1* and *npq2* mutants in which the xanthophyll cycle is disrupted (47).

Carotenoid Exchange Involves the Violaxanthin in One Site—Only a fraction of the Lhc-bound xanthophyll could be exchanged, in agreement with previous results with Lhcb1 (21) and with the previously described (48) limited availability of the violaxanthin substrate for de-epoxidation. We have further analyzed the changes in the spectral properties of Lhc proteins upon de-epoxidation *in vitro* to assess the role played by individual xanthophyll-binding sites in the exchange. This is possible because of the different tuning of xanthophyll optical transition energy by the binding to different sites (20, 49). In the simple case of CP29, for example, it was possible to assess

² Croce, R., Morosinotto, T., Castelletti, S., Breton, J., and Bassi, R. (2002) *Biochim. Biophys. Acta* 1556/1, 29–40.

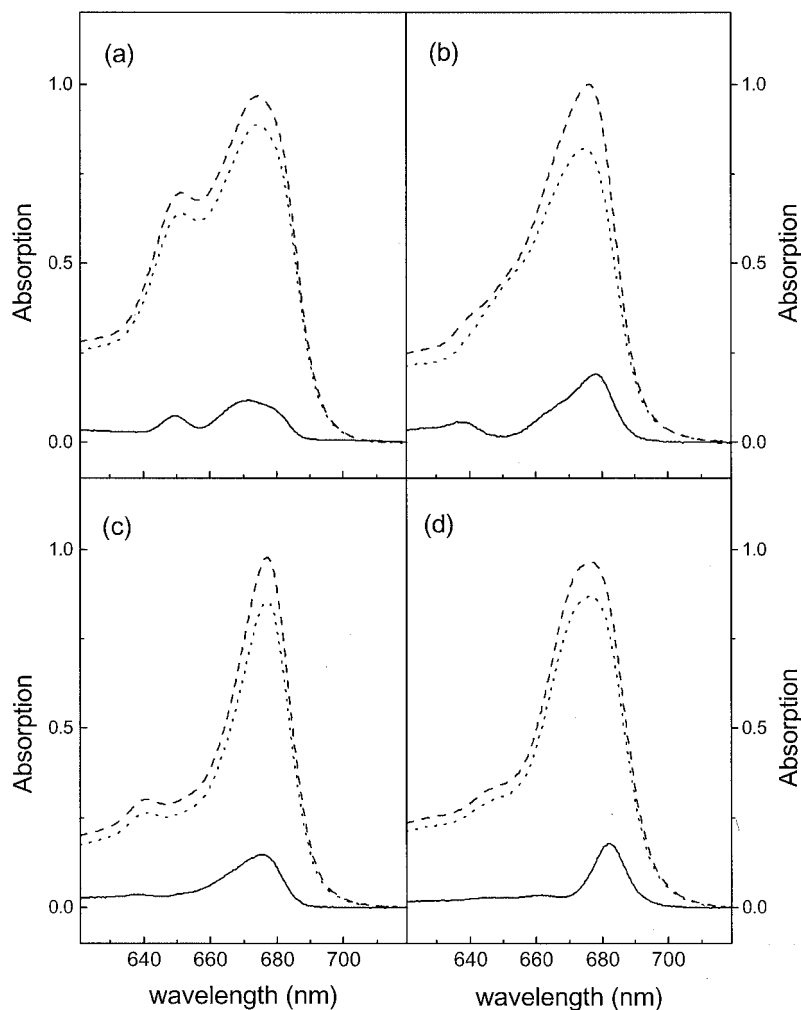
TABLE III

Carotenoid spectral forms identified in CP29 before (CP29-Vx) and after (CP29-depox) the de-epoxidation

Amplitude and shift of the spectral forms of xanthophylls bound in different sites, as identified by spectral deconvolution, is shown.

	Violaxanthin (L1)		Violaxanthin (L2)		Zeaxanthin (L2)		Total Amplitude
	Amplitude	Shift	Amplitude	Shift	Amplitude	Shift	
CP29-Vx	0.93	24	0.97	17			1.9
CP29-depox	0.82	24	0.54	17	0.1	17	1.46

FIG. 6. Spectroscopic differences upon de-epoxidation *in vitro*. Difference spectra (solid line) of Lhcb1 (a), CP26 (b), CP29 (c), and Lhca1 (d) before (dashed line) and after (dotted line) the de-epoxidation are shown. Spectra were normalized to the number of chlorophylls as in Ref. 42.



that binding of violaxanthin to site L1 or site L2 yielded a red-shift of 24 or 17 nm, respectively, with respect to the absorption of the pigment in 80% acetone (20).² Fig. 5A shows such a deconvolution. It is worth noting that the spectral contributions closely fit the chromophore stoichiometry determined biochemically; in particular, two different spectral forms of violaxanthin with similar amplitude corresponding to the pigment bound to either site L1 or L2 (Table III). After de-epoxidation *in vitro*, the absorption spectrum was analyzed by the same method, but the spectral form of zeaxanthin was also included (Fig. 5B). Table III shows the amplitude of carotenoid absorption forms resulting from the analysis of CP29 spectra before and after the de-epoxidation. The amplitude of violaxanthin adsorbing at 489.8 nm was reduced with respect to the 497-nm form, suggesting the former is the species preferentially replaced by zeaxanthin. Consistently, a zeaxanthin form with a 17-nm red-shift was obtained, implying the newly incorporated zeaxanthin is located in site L2.³ Similar results were

obtained with other Lhc proteins, showing that one violaxanthin spectral form with characteristics consistent with binding to site L2 was preferentially reduced with respect to the others. These data strongly suggest that violaxanthin *versus* zeaxanthin exchange occurs in site L2 in all Lhc proteins analyzed. Our hypothesis is also supported by previous data on Lhcb1 showing that site L1 occupancy is fundamental for protein stability (10), whereas Lhc proteins with an empty L2 site maintain their folding (27).

Xanthophyll Exchange Involves the Chl a in Site a4—One additional issue emerging from experiments *in vitro* is the involvement of Chls in xanthophyll exchange. In fact, all complexes show the loss of a Chl *a* chromophore upon de-epoxidation. To verify whether or not the lost chromophore was derived from a particular binding site, we calculated difference spectra in the Qy band where Chl chromophores exhibit fine tuning of their S0-S1 transition energies depending on the particular binding site (27, 50). Examples of the difference spectra obtained in the case of Lhcb1, CP29, CP26, and Lhca1 are shown in Fig. 6. For all seven Lhc proteins analyzed, the lost chromophore absorbed at wavelengths between 675 and 682 nm.

³ R. Croce, M. Gastaldelli, G. Canino, and R. Bassi, unpublished observations.

These results can be compared with the results obtained by mutation analysis of Lhcb1 and CP29 in which the absorption of individual chromophores was determined (27, 50) to identify the binding site made empty during the process of xanthophyll exchange. Results are consistent with the loss of Chl *a* in site a4, whose absorption is tuned at 676 and 673/681 nm, respectively, in CP29 and Lhcb1 (27, 50). Structural data from LHCI (51) shows that the Chl in site a4 is in close vicinity with the xanthophyll in site L2, thus allowing the hypothesis that occupancy of site a4 might affect the rate of xanthophyll exchange in site L2. The ligand of Chl a4 is a conserved glutamate in all Lhc complexes (4), and this acidic group has a pK of 4.28, so it is possible that in acidic conditions it can be protonated and lose the ability to coordinate the Mg^{2+} of chlorophyll. Proton flow through Lhc proteins was previously proposed to be activated in conditions of low luminal pH that also lead to de-epoxidation (52). We do not think that Chl is actually freed in the membrane during operation of the xanthophyll cycle; however, a transient/partial disconnection of Chl a4 from its binding site cannot be excluded and might be involved in the mechanism of xanthophyll exchange.

CONCLUSION

In this study we have analyzed the phenomenon of the exchange of xanthophyll chromophores bound to Lhc proteins during the operation of the xanthophyll cycle *in vivo* and *in vitro*. The results show that CP26 and CP24 are the components of the PSII supercomplex that exhibit the highest rate of xanthophyll exchange. We found that xanthophyll are specifically exchanged in the L2 site, one of the 2/3 tight xanthophyll-binding sites found in Lhc proteins. This site was previously found not to be essential for Lhc protein folding but rather to be an allosteric binding site affecting the fluorescence yield of Lhc proteins (10) by controlling the equilibrium between conformations characterized by different fluorescence yield and thus having conservative *versus* dissipative characteristics with respect to the excitation energy (1). Analysis *in vitro* shows that the xanthophyll exchange occurs through the intermediate release of violaxanthin and rebinding of newly formed zeaxanthin in agreement with previous results (21). The exchange rate is thus determined by the characteristics of individual Lhc proteins that is, in turn, determined by the effect of low pH on protein structure. This determines a dynamic distribution of violaxanthin *versus* zeaxanthin in different subunits of photosystem II complexes that might regulate the excitation energy flow in PSII antenna to prevent over-excitation of reaction centers and photoinhibition. The present findings are consistent with recent results (7) showing the presence of a loosely bound violaxanthin pool in the major LHCI antenna protein, which is available for de-epoxidation. The xanthophyll cycle thus appears to have the characteristics of a signal transduction pathway for the light stress signal, constituted by low luminal pH, activating VDE, and synthesizing a messenger molecule, zeaxanthin, which diffuses in the thylakoid membrane and affects the functional characteristics of Lhc proteins, CP26 and CP24, mediating excitation energy transfer from the major LHCI antenna to the PSII reaction center.

Acknowledgments—We thank Prof. H. Yamamoto and Dr. A. D. Hieber for the kind gift of the VDE expressing enzyme and for critically reading the manuscript. We also thank Drs. Roberta Croce for sharing unpublished results and Stefano Caffarri for sharing clones of barley Lhcb1, Lhcb2, and Lhcb3 before publication and for the Curve fitting program.

REFERENCES

- Moya, I., Silvestri, M., Vallon, O., Cinque, G., and Bassi, R. (2001) *Biochemistry* **40**, 12552–12561

- Bassi, R., Hoyer-hansen, G., Barbato, R., Giacometti, G. M., and Simpson, D. J. (1987) *J. Biol. Chem.* **262**, 13333–13341
- Fromme, P., Jordan, P., and Krauss, N. (2001) *Biochim. Biophys. Acta* **1507**, 5–31
- Jansson, S. (1999) *Trends Plant Sci.* **4**, 236–240
- Kok, B., Gassner, E. B., and Rurainski, H. J. (1966) *Photochem. Photobiol.* **4**, 215–227
- Niyogi, K. K. (1999) *Annu. Rev. Plant Physiol. Plant Mol. Biol.* **50**, 333–359
- Caffarri, S., Croce, R., Breton, J., and Bassi, R. (2001) *J. Biol. Chem.* **276**, 35924–35933
- Havaux, M., and Niyogi, K. K. (1999) *Proc. Natl. Acad. Sci. U. S. A.* **96**, 8762–8767
- Crimi, M., Dorra, D., Bosinger, C. S., Giuffra, E., Holzwarth, A. R., and Bassi, R. (2001) *Eur. J. Biochem.* **268**, 260–267
- Formaggio, E., Cinque, G., and Bassi, R. (2001) *J. Mol. Biol.* **314**, 1157–1166
- Nagai, K., and Thogersen, H. C. (1987) *Methods Enzymol.* **153**, 461–481
- Dainese, P., Hoyer-hansen, G., and Bassi, R. (1990) *Photochem. Photobiol.* **51**, 693–703
- Gilmore, A. M., and Yamamoto, H. Y. (1991) *Plant Physiol.* **96**, 635–643
- Connelly, J. P., Müller, M. G., Bassi, R., Croce, R., and Holzwarth, A. R. (1997) *Biochemistry* **36**, 281–287
- Schägger, H., and von Jagow, G. (1987) *Anal. Biochem.* **166**, 368–379
- Hieber, A. D., Bugos, R. C., Verhoeven, A. S., and Yamamoto, H. Y. (2002) *Planta* **214**, 476–483
- Gottesman, S., Halpern, E., and Trisler, P. (1981) *J. Bacteriol.* **148**, 265–273
- Paulsen, H., and Hobe, S. (1992) *Eur. J. Biochem.* **205**, 71–76
- Giuffra, E., Cugini, D., Croce, R., and Bassi, R. (1996) *Eur. J. Biochem.* **238**, 112–120
- Croce, R., Cinque, G., Holzwarth, A. R., and Bassi, R. (2000) *Photosynth. Res.* **64**, 221–231
- Jahns, P., Wehner, A., Paulsen, H., and Hobe, S. (2001) *J. Biol. Chem.* **276**, 22154–22159
- Bergantino, E., Dainese, P., Cerovic, Z., Sechi, S., and Bassi, R. (1995) *J. Biol. Chem.* **270**, 8474–8481
- Croce, R., Breton, J., and Bassi, R. (1996) *Biochemistry* **35**, 11142–11148
- Croce, R., Weiss, S., and Bassi, R. (1999) *J. Biol. Chem.* **274**, 29613–29623
- Frank, H. A., Das, S. K., Bautista, J. A., Bruce, D., Vasil'ev, S., Crimi, M., Croce, R., and Bassi, R. (2001) *Biochemistry* **40**, 1220–1225
- Polivka, T., Zigmantas, D., Sundstrom, V., Formaggio, E., Cinque, G., and Bassi, R. (2002) *Biochemistry* **41**, 439–450
- Bassi, R., Croce, R., Cugini, D., and Sandona, D. (1999) *Proc. Natl. Acad. Sci. U. S. A.* **96**, 10056–10061
- Yamamoto, H. Y., and Higashi, R. M. (1978) *Arch. Biochem. Biophys.* **190**, 514–522
- Yamamoto, H. Y. (1985) *Methods Enzymol.* **110**, 303–312
- Pagano, A., Cinque, G., and Bassi, R. (1998) *J. Biol. Chem.* **273**, 17154–17165
- Yamamoto, H. Y., Nakayama, T. O. M., and Chichester, C. O. (1962) *Arch. Biochem. Biophys.* **97**, 168–173
- Demmig-Adams, B., and Adams, W. W. (1992) *Ann. Rev. Plant Physiol. Plant Mol. Biol.* **43**, 599–626
- Bassi, R., Pineau, B., Dainese, P., and Marquardt, J. (1993) *Eur. J. Biochem.* **212**, 297–303
- Swiatek, M., Kuras, R., Sokolenko, A., Higgs, D., Olive, J., Cinque, G., Muller, B., Eichacker, L. A., Stern, D. B., Bassi, R., Herrmann, R. G., and Wollman, F. A. (2001) *Plant Cell* **13**, 1347–1367
- Dainese, P., and Bassi, R. (1991) *J. Biol. Chem.* **266**, 8136–8142
- Sandona, D., Croce, R., Pagano, A., Crimi, M., and Bassi, R. (1998) *Biochim. Biophys. Acta* **1365**, 207–214
- Walters, R. G., Ruban, A. V., and Horton, P. (1996) *Proc. Natl. Acad. Sci. U. S. A.* **93**, 14204–14209
- Pesaresi, P., Sandona, D., Giuffra, E., and Bassi, R. (1997) *FEBS Lett.* **402**, 151–156
- Dominici, P., Caffarri, S., Armenante, F., Ceoldo, S., Crimi, M., and Bassi, R. (2002) *J. Biol. Chem.* **277**, 22750–22758
- Li, X. P., Björkman, O., Shih, C., Grossman, A. R., Rosenquist, M., Jansson, S., and Niyogi, K. K. (2000) *Nature* **403**, 391–395
- Caffarri, S., Croce, R., Cattivelli, L., and Bassi, R. (2001) *PS2001 Proceedings: 12th International Congress on Photosynthesis*, pp. S31–S34, CSIRO Publishing, Melbourne, Australia
- Giuffra, E., Zucchelli, G., Sandona, D., Croce, R., Cugini, D., Garlaschi, F. M., Bassi, R., and Jennings, R. C. (1997) *Biochemistry* **36**, 12984–12993
- Schmid, V. H. R., Cammarata, K. V., Bruns, B. U., and Schmidt, G. W. (1997) *Proc. Natl. Acad. Sci. U. S. A.* **94**, 7667–7672
- Croce, R., and Bassi, R. (1998) in *Photosynthesis: Mechanisms and Effects* (Garab, G., ed), pp. 421–424, Kluwer Academic Publishers, Dordrecht
- Verhoeven, A. S., Adams, W. W., Demmig-Adams, B., Croce, R., and Bassi, R. (1999) *Plant Physiol.* **120**, 727–737
- Dainese, P., Marquardt, J., Pineau, B., and Bassi, R. (1992) in *Research in Photosynthesis* (Murata, N., ed) Vol. I, pp. 287–290, Kluwer Academic Publishers, Dordrecht
- Pogson, B. J., Niyogi, K. K., Björkman, O., and DellaPenna, D. (1998) *Proc. Natl. Acad. Sci. U. S. A.* **95**, 13324–13329
- Siefermann-Harms, D., and Yamamoto, H. Y. (1974) *Biochim. Biophys. Acta* **144**, 144–150
- Croce, R., Muller, M. G., Bassi, R., and Holzwarth, A. R. (2001) *Biophys. J.* **80**, 901–915
- Remelli, R., Varotto, C., Sandona, D., Croce, R., and Bassi, R. (1999) *J. Biol. Chem.* **274**, 33510–33521
- Kühlbrandt, W., Wang, D. N., and Fujiyoshi, Y. (1994) *Nature* **367**, 614–621
- Jahns, P., and Junge, W. (1990) *Eur. J. Biochem.* **193**, 731–736

D 2

*Mechanistic aspects of the xanthophyll
dynamics in higher plant thylakoids*

This chapter has been published in *Physiologia Plantarum* 119 (3):
347-354. Reproduced with permission

Tomas Morosinotto, Stefano Caffarri, Luca Dall'Osto and
Roberto Bassi

Mechanistic aspects of the xanthophyll dynamics in higher plant thylakoids

Tomas Morosinotto^{a,b}, Stefano Caffarri^{a,b}, Luca Dall'Osto^a and Roberto Bassi^{a,b,*}

^aDipartimento Scientifico e Tecnologico – Università di Verona, Strada Le Grazie, 15-37134 Verona, Italy

^bUniversité Aix-Marseille II, LGBP (Laboratoire de Genetique et Biophysique des Plantes) Faculté des Sciences de Luminy – Département de Biologie – Case 901–163, Avenue de Luminy – 13288 Marseille Cedex 09, France

*Corresponding author, e-mail: bassi@sci.univr.it, bassi@luminy.univ-mrs.fr

Received 16 May 2003; revised 22 May 2003

Plant thylakoids have a highly conserved xanthophyll composition, consisting of β -carotene, lutein, neoxanthin and a pool of violaxanthin that can be converted to antheraxanthin and zeaxanthin in excess light conditions. Recent work has shown that xanthophylls undergo dynamic changes, not only in their composition but also in their distribution among Lhc proteins. Xanthophylls are released from specific binding site in the major trimeric LHCII complex of photosystem II and are subsequently bound to different sites into monomeric Lhcb proteins and dimeric Lhca proteins. In this work we review available evidence from *in vivo* and *in vitro* studies on the structural determinants that control xanthophyll exchange in

Lhc proteins. We conclude that the xanthophyll exchange rate is determined by the structure of individual Lhc gene products and it is specifically controlled by the lumenal pH independently from the activation state of the violaxanthin de-epoxidase enzyme. The xanthophyll exchange induces important modifications in the organization of the antenna system of Photosystem II and, possibly of Photosystem I. Major changes consist into a modulation of the light harvesting efficiency and an increase of the protection from lipid peroxidation. The xanthophyll cycle thus appears to be a signal transduction system for co-ordinated regulation of the photoprotection mechanisms under persistent stress from excess light.

Xanthophyll composition and distribution within Lhc proteins

The pigment composition of higher plants photosynthetic apparatus is extremely well conserved: chloroplast-encoded photosynthetic reaction centre complexes bind β -carotene and Chl *a*, while nuclear-encoded light harvesting proteins bind Chl *a*, Chl *b* and the three xanthophylls lutein, violaxanthin and neoxanthin. β -carotene is also bound to the light harvesting complex of Photosystem I (Lam et al. 1984, Croce et al. 2002b).

Light harvesting polypeptide sequences are also highly conserved (Jansson 1999); nevertheless, each member of the Lhc family has a unique carotenoid composition. Table 1 shows comprehensive data on pigment binding properties of all Lhca1-4 and Lhcb1-6 proteins thus far identified in higher plants, including LHCI polypeptides which have

been recently characterized via *in vitro* reconstitution experiments (Croce et al. 2002b, Castelletti et al. 2003). The conservation of carotenoid composition and distribution across a range of plants suggests a specific role for each xanthophyll species. However, the reason for this diversity is not clear. In fact, all of these xanthophylls possess similar absorption characteristics in the visible region of the spectrum and are capable of quenching ³Chl* and deactivating ROS produced during light harvesting.

Xanthophyll binding sites in Lhc proteins

A molecular model for the LHCII trimeric complex has been proposed by Kühlbrandt et al. (1994). The high

Abbreviations – α -DM, *n*-dodecyl- α -D-maltoside; β -car, β -carotene; Chl, chlorophyll; CP, chlorophyll protein; Lhc, light harvesting protein; Lhca, light harvesting complex of PSI; Lhcb, light harvesting complex of PSII; LHCII, the major light harvesting complex of PSII; Lute, lutein; Neo, neoxanthin; PSI (II), Photosystem I (II); ROS, reactive oxygen species; VDE, violaxanthin de-epoxidase; Viola, violaxanthin; ZEA, zeaxanthin.

degree of homology within the Lhc family suggests conservation in all members of the overall organization. Two carotenoid binding sites, named L1 and L2, are present in all Lhc complexes analysed. In the tridimensional structure of LHCII these sites have been located in correspondence of two transmembrane helices, respectively, helix A and B (Kühlbrandt et al. 1994). Two other binding sites of LHCII, N1 and V1, have not been located by electronic crystallography and are not present in all Lhc. Site N1 has been localized in the domain between the helix C and the helix A/B cross by mutational analysis of Lhcb1 protein (Croce et al. 1999a) and it was proposed to be also present in Lhca1 (Croce et al. 2002b). An additional binding site, named V1, was described in LHCII (Ruban et al. 1999, Caffarri et al. 2001a) and possibly in Lhca3 (Castelletti et al. 2003). This site is peripherally located, as judged from the refraction index (Caffarri et al. 2001a) and its lability upon detergent treatment (Ruban et al. 1999, Caffarri et al. 2001a). Preliminary structural work has located a xanthophyll-binding site in LHCII parallel to helix C, but located peripherally (Lamborghini 2002). This site is likely to correspond to site V1, since such a location is consistent with the properties observed for xanthophylls bound to this site.

Table 1 also reports available data on the occupation of individual carotenoid binding sites in all Lhcb and Lhca proteins. The availability of a comprehensive figure allows identifying features conserved in all Lhc and differences between individual gene products. The most conserved feature is the binding of a lutein molecule in site L1. However, it is interesting to note that in the absence of lutein, binding of other xanthophylls such as violaxanthin or zeaxanthin was observed either in vivo (Pogson et al. 1998) or in vitro (Croce et al. 1999b, Formaggio et al. 2001). The occupancy of site L2 is the most variable: lutein and violaxanthin are found in this site in Lhcb1, Lhcb2, Lhcb3, and Lhca1-4; violaxanthin and neoxanthin, instead, are found in Lhcb4, 5. Violaxanthin is the only ligand in Lhcb6. Site N1 is very specific for neoxanthin in Lhcb1-3. In Lhca1 proteins site N1 binds mostly violaxanthin and lutein (Croce et al. 2002b). Site V1 was only found in LHCII where it loosely

binds violaxanthin and lower proportions of lutein and zeaxanthin (Caffarri et al. 2001a). The presence of site V1 was tentatively proposed for Lhca3, but its occupancy in this case is not yet clear (Castelletti et al. 2003).

Changes in composition and distribution of xanthophylls upon de-epoxidation in vivo

Exposure of plants to excess irradiation leads to the appearance of two additional species of xanthophylls, i.e. antheraxanthin and zeaxanthin, derived from violaxanthin by de-epoxidation of either one or both rings, in a process known as the xanthophyll cycle (Yamamoto et al. 1962). Substrates and products of the reaction are bound to Lhc complexes, although in different amounts. In fact, isolation of individual Lhc complexes following a light stress treatment shows that individual Lhc proteins bind different amount of zeaxanthin. Among Lhc polypeptides the most efficient in binding zeaxanthin were shown to be CP26 and CP24, while zeaxanthin content of CP29 was lower (Verhoeven et al. 1999, Morosinotto et al. 2002). All these polypeptides bind zeaxanthin in the inner site L2. LHCII components, instead, have a low content of zeaxanthin bound to the peripheral site V1 rather than to site L2 (Caffarri et al. 2001a).

Steps of the xanthophyll cycle

The presence of excess proton concentration in the lumen is a signal that the light level absorbed exceeds the capacity of electron transport to NADP⁺. Low pH activates the conversion of violaxanthin to zeaxanthin. A detailed picture of the operation of the xanthophyll cycle is presented below, starting from the establishment of a low luminal pH.

Release of violaxanthin from site V1 of LHCII

As stated above, LHCII has a peripheral carotenoid-binding site named V1 that binds mainly violaxanthin,

Table 1. Pigment binding properties of single Lhc complexes. Pigment binding occupancy of carotenoid binding sites is presented (L, lutein; V, violaxanthin; N, neoxanthin; bc, β -carotene). Data of Lhcb are from *Zea mays* and *Hordeum vulgare*, while for Lhca they are from *Arabidopsis thaliana*. Entries marked with (*) indicates tentative figures of site occupancy.

	Species	Chl	a/b ratio	Car	Lute	Viola	Neo	B-car	L1	L2	N1	V1	References
LHCII	<i>Zea mays</i>	13	1.5	3.8	3.8	0.7	1.0	0	1L	0.9L 0.1V	1N	0.6V 0.2L	Caffarri et al. 2001a
Lhcb1	<i>Zea mays</i>	12	1.4	3.0	1.8	0.2	1.0	0	1L	0.9L 0.1V	1N		Croce et al. 1999b
Lhcb2	<i>H. vulgare</i>	12	1.4	3.0	1.8	0.2	1.0	0	1L	0.9L 0.1V			Caffarri et al. 2001b
Lhcb3	<i>Zea mays</i>	11	1.8	2.6	1.8	0.2	0.6	0	1L	0.9L 0.1V	0.6N		Caffarri et al. 2001b
Lhcb4	<i>Zea mays</i>	8	3.0	2.0	1.0	0.5	0.5	0	1L	0.5V 0.5N			Bassi et al. 1993
Lhcb5	<i>Zea mays</i>	9	2.2	2.0	1.0	0.5	0.5	0	1L	0.5V 0.5N			Bassi et al. 1993
Lhcb6	<i>Zea mays</i>	9	1.2	2.0	1.0	0.1	0	0	1L	1V			Bassi et al. 1993
Lhca1	<i>A. thaliana</i>	10	4.0	3.0	1.8	1.1	0.1	0	1L	0.5L 0.5V	0.3L 0.6V		Croce et al. 2002b
Lhca2*	<i>A. thaliana</i>	10	1.9	2.0	1.5	0.5	0	0	1L	0.5L 0.5V			Castelletti et al. 2003
Lhca3*	<i>A. thaliana</i>	10	6.0	3.0	1.7	0.7	0	0.5	1L	0.5L 0.5bc		0.7V 0.2L	Castelletti et al. 2003
Lhca4	<i>A. thaliana</i>	10	2.3	2.0	1.5	0.5	0	0	1L	0.5L 0.5V			Croce et al. 2002b

but also lutein, under low light conditions (Caffarri et al. 2001a). Xanthophylls in site V1 were shown to be ineffective in energy transfer to Chls and thus they cannot function in light harvesting. Moreover, xanthophyll binding to this site is pH dependent; under acidic conditions the xanthophyll ligand is released (Ruban et al. 1999, Caffarri et al. 2001a). This characteristic of site V1 suggests that its function is to provide a source of available violaxanthin for de-epoxidation by VDE. Quantitative analysis of violaxanthin content in thylakoids of unstressed plants confirmed this picture: LHCII, despite its low violaxanthin binding to site L2 is, in fact, by far the major violaxanthin binding protein due to the peripheral site V1 and its high abundance with respect to other xanthophyll binding proteins (Caffarri et al. 2001a).

Release of violaxanthin from Lhc monomeric complexes

Violaxanthin is also released from Lhcb monomeric complexes CP24, CP26 and CP29. The liberation of violaxanthin from monomeric antennae is important, not only because it provides another source of substrate for VDE, but also because this release provides a population of Lhc complexes with an empty carotenoid binding site, ready for binding the newly synthesized zeaxanthin (see below).

Monomeric antenna complexes have only two carotenoid binding sites: L1 and L2 (Bassi et al. 1999, Croce et al. 2002a). It was previously shown that the L1 site is needed for folding of the pigment-protein complex and that complexes with this site empty are not stable (Formaggio et al. 2001). The compulsory occupancy of site L1 implies that xanthophyll exchange must involve carotenoids of the other binding site, L2. This is confirmed by analysing binding affinities of sites L1 and L2 in different Lhc: in fact, L1 is always occupied by lutein, while violaxanthin is located in site L2 (Bassi et al. 1999, Table 1). The topology of this exchange was recently studied in detail using a system composed of recombinant Lhc proteins in lipid bilayers and recombinant VDE enzyme (Morosinotto et al. 2002). When xanthophylls are bound to a Lhc complex, their spectra undergo a specific shift in wavelength depending on the binding site where they are located (Croce et al. 2000, 2002a). This feature was exploited for the identification of the site involved in releasing violaxanthin and rebinding zeaxanthin. This analysis performed for the different Lhc complexes before and after de-epoxidation *in vitro*, showed that only site L2 was involved in xanthophyll exchange, irrespective of the Lhc gene product analysed (Morosinotto et al. 2002). The finding that only xanthophylls bound to site L2 can be exchanged suggests that the remaining xanthophylls are not exchanged and do not participate in the xanthophyll cycle. This is in agreement with evidence showing the presence of xanthophyll pools being not de-epoxidable (Yamamoto and Bassi 1996). Xanthophylls bound to other sites therefore play different roles as stated above for site L1.

De-epoxidation of violaxanthin to zeaxanthin by VDE

Violaxanthin is de-epoxidated to antheraxanthin and then to zeaxanthin by the luminal enzyme violaxanthin de-epoxidase (VDE, Bugos and Yamamoto 1996). Several studies have shown that VDE activity is dependent on low pH and the purified enzyme was shown to have a pH optimum of 5.2 (Hager 1969, Yamamoto and Higashi 1978). Furthermore, the xanthophyll substrate is dissolved in the thylakoid lipids and VDE must therefore be associated with the membrane in order to come into contact with its substrate. Bratt and co-workers (Bratt et al. 1995) found that VDE is released from the membrane in a pH-dependent process. When raising the pH, VDE is released at pH 6.6 within a very narrow pH range, with a co-operativity of 4 with respect to protons. During the transition from dark to light, the binding of the enzyme to the thylakoid membrane therefore occurs at pH values that allow only low enzyme activity. Although the binding of VDE is needed for de-epoxidation, this process does not appear to be limiting for the reaction rate. The following step for the de-epoxidation of violaxanthin to zeaxanthin appears to be the availability of the substrate. In fact, violaxanthin free in the membrane is available for de-epoxidation by VDE, while violaxanthin bound to Lhc proteins is not (Yamamoto and Bassi 1996). This was confirmed by de-epoxidation experiments performed with the *chlorina f2* mutant of barley that is depleted in Chl *b* and lacks Lhc proteins. In this mutant violaxanthin is free in the membrane. De-epoxidation in *chlorina f2* was shown to be faster and more complete than in the WT barley (Bassi et al. 1993, Peng and Gilmore 2002), thus confirming that the limiting step is the liberation of violaxanthin from Lhcs rather than the activation of VDE.

Binding of zeaxanthin by Lhc proteins

Zeaxanthin synthesized by VDE has a dual location: one fraction is found free in the membrane and another fraction is bound to Lhc complexes. The free moiety has been suggested to be effective in the protection of lipids from peroxidation (Havaux and Niyogi 1999). *In vivo*, the distribution of zeaxanthin among individual Lhc proteins may result from different binding affinities, or from differential accessibility of the binding sites. When affinity was determined *in vitro* using individual Lhc proteins, however, results confirmed that zeaxanthin binding under these conditions closely mirrored the results obtained *in vivo* (Morosinotto et al. 2002). These data clearly show that xanthophyll exchange rate is a property of individual gene products and that the effects of protein steric hindrance in thylakoid membranes, if present, are minor.

Different xanthophyll exchange ability, showed by *in vitro* analysis, suggests a different role of individual Lhc in the operation of the xanthophyll cycle. Individual LHCII components, Lhcb1-3, showed a low ability of xanthophyll exchange in site L2 confirming that its

major role in the xanthophyll cycle is providing readily available violaxanthin from site V1 (Morosinotto et al. 2002). Monomeric antennae instead, particularly CP26 and CP24, showed higher zeaxanthin binding rates. These proteins therefore are probably one of the sites where zeaxanthin plays its function. A possible explanation for differences in zeaxanthin binding between individual Lhcs can be the need for modulation of the photoprotection activity in dependence to the time length of the light stress: CP26 and CP24 may respond faster while CP29 is recruited for energy dissipation only under persistent stress conditions.

Interestingly, some zeaxanthin is bound to the PSI complex under pronounced light stress (Verhoeven et al. 1999). This fraction is located in LHCI antenna complexes, since core complexes do not bind xanthophylls but only β -carotene (Siefertmann-Harms and Ninnemann 1982). A high level of zeaxanthin binding to Lhca1 and Lhca4 was also confirmed by in vitro de-epoxidation experiments. These complexes showed a high efficiency of xanthophyll exchange, lower than that of CP26, but exceeded CP29 and Lhcb1-3 (Morosinotto et al. 2002). These results suggest that PSI responds to environmental stress conditions with xanthophyll conversions similar to those seen in PSII. This is consistent with recent findings that PSI can be an early target for photoinhibition (Tjus et al. 2001).

Changes in Lhc properties upon xanthophyll exchange

The physiological effect of zeaxanthin binding to Lhc proteins was previously proposed to be due to a lower S1 state of zeaxanthin compared to the S1 state of violaxanthin. This difference would have allowed energy transfer from chlorophyll S1 state to zeaxanthin and rapid thermal dissipation (Frank et al. 1994). Recent direct measurements of the S1 state energy level of violaxanthin and zeaxanthin, either in solution or bound to Lhc complexes, showed that instead, S1 transition energy levels of the two xanthophyll species are almost identical (Polivka et al. 1999, 2002). Nevertheless, experimental evidences were recently presented that support the idea that energy transfer from the S1 state of chlorophyll to the S1 state of zeaxanthin is the mechanism for efficient excess energy dissipation (Ma et al. 2003).

The above data suggest that the conversion from violaxanthin to zeaxanthin is not sufficient in itself, but additional requirements are needed for triggering thermal dissipation. Although energetically very similar, energy transfer from Chl to Car S1 states is more efficient with zeaxanthin than with violaxanthin. A possible explanation can be proposed based on the presence of different conformations of Lhc proteins as induced by the binding of zeaxanthin vs. violaxanthin to the allosteric site L2. The Zea binding conformation might have a structural organization favouring energy transfer from Chl to carotenoid S1 state.

The existence of different conformations of Lhc proteins was initially proposed in order to explain the obser-

vation that Lhc proteins have at least two fluorescence decay components in the nanosecond range, while complete equilibration of excitation energy occurs in a few picoseconds (Moya et al. 2001). More recently, two conformations of the Lhcb5 protein (CP26) were separated by biochemical methods, thus implying they are structurally different (Dall'Osto et al. in press). Transition between conformations was shown to be controlled by the occupancy of the allosteric site L2 by either violaxanthin or zeaxanthin (Crimi et al. 2001, Formaggio et al. 2001, Polivka et al. 2002). Interestingly, the Lhc conformations differ for their fluorescence yield, supporting the hypothesis of a conformational switch between states of the antenna system having different light harvesting efficiency.

PsbS pigment binding properties and its role in the xanthophyll cycle

A Lhc-like protein, PsbS, was shown to have a key role in the dissipation of excess energy in higher plants (Li et al. 2000, Külheim et al. 2002). Its pigment binding properties are an interesting issue to be addressed since they have important implications for PsbS function. If PsbS binds chlorophylls as well as carotenoids, it would be able to dissipate the excitation energy directly. If it does not, its function must be a different one, such as, e.g. the regulation of energy dissipation performed by neighbouring proteins.

Early works proposed that both Chls and xanthophylls were bound to PsbS in agreement with its homology with Lhc proteins (Funk et al. 1995). Later works led to the identification of the amino acid residues co-ordinating chlorophylls in Lhc proteins (Kühlbrandt et al. 1994, Bassi et al. 1999) and the finding that only two out of eight are conserved in PsbS. Re-evaluation of pigment binding properties of PsbS showed that pigment binding, if any, is not preserved during isolation from unstressed plants (Dominici et al. 2002, Aspinall-O'Dea et al. 2002). Moreover, recombinant PsbS is unable to refold with pigments in vitro under conditions that lead to the formation of pigment-protein complexes with all other Lhc gene products (Dominici et al. 2002).

Very recently, a pigment free PsbS preparation was shown to bind zeaxanthin in vitro (Aspinall-O'Dea et al. 2002). Spectroscopic characteristics of the reconstituted complex are consistent with the hypothesis that PsbS associated zeaxanthin is responsible for the difference absorption signal at 535 nm appearing in quenched thylakoids (Li et al. 2000, Ruban et al. 2002). This result suggests the possibility that zeaxanthin can be bound by PsbS under light stress conditions and function as a quencher of excess energy.

Can xanthophyll exchange account for NPQ?

Analysis of mutants *npq1* and *npq2* with an altered xanthophyll cycle, has shown that the xanthophyll cycle

plays an important role in the mechanism of photoprotection by excitation energy dissipation known as NPQ (Niyogi et al. 1998). Recently, mutants lacking ascorbate, a cofactor of the de-epoxidase reaction, were analysed and showed reduced NPQ as in the case of *npq1* (Müller-Moule et al. 2002). This observation suggests that quenching ability is correlated to the formation of zeaxanthin, irrespective of the presence of an active VDE enzyme.

Zeaxanthin effect in vivo has also been analysed by evaluating fluorescence yield of mutants. Such experiments have been performed by using *Chlamydomonas reinhardtii npq1* and *npq2* mutants containing either violaxanthin or zeaxanthin, respectively. The zeaxanthin containing strain showed sustained quenching (Govindjee and Seufferheld 2002). Similar results were also obtained with *Arabidopsis thaliana* (Dall'Osto et al. in press), thus confirming the quenching activity of zeaxanthin in vivo.

By comparing the kinetics of NPQ formation in WT vs. *npq1* mutants, it is clear that the quenching process is saturated within about 1 min, when zeaxanthin cannot be formed, while in WT a slower phase of quenching proceeds for several minutes (Niyogi et al. 1998). A residual level of qE, the Δ pH dependent fraction of NPQ, is found in *npq1* plants without zeaxanthin (Niyogi et al. 1998). It should be noticed that since zeaxanthin is a precursor of violaxanthin, the presence of very low zeaxanthin levels in *npq1* cannot be excluded. Zeaxanthin is therefore required for the full expression of NPQ, but it is not the only factor leading to chlorophyll quenching during exposure to excess light. Results with *Arabidopsis* mutants lacking lutein have suggested that initial quenching may be sustained by this xanthophyll species, zeaxanthin role emerging at later times (Pogson et al. 1998). An alternative hypothesis is that lutein is actually responsible for quenching and that zeaxanthin may act in stabilizing the Lhc conformation favouring S1 energy transfer from Chl.

It appears that quenching can be triggered first by a mechanism which is already activated within few seconds (10–20 s) upon exposure to excess light when the amount of zeaxanthin formed, if any, is extremely low. It is possible that zeaxanthin may stabilize a quenching state produced by the earlier, largely zeaxanthin independent process observed in *npq1* or in the presence of the VDE inhibitor DTT.

PsbS was shown to have a key role in initial kinetics of NPQ. In fact in the *npq4* mutant lacking PsbS, establishing of NPQ is slower than in WT, suggesting that PsbS mediates a rapid response to excess light (Li et al. 2000). Lots of evidence is emerging that suggest that PsbS activity is mediated by protonation of some residues. In fact PsbS was shown to bind DCCD, a reagent able to bind protonable residues in hydrophobic environments (Dominici et al. 2002). Other supporting evidence is recent results obtained by complementing *npq4-1* mutants with a mutated PsbS gene encoding for a protein depleted in several acidic residues (glutamate and

aspartate) of lumenal loops. Two acidic residues were shown to be essential for PsbS activity: each single mutant showed about 50% reduction of NPQ with respect to WT and the double mutant had a phenotype very similar to *npq4-1*, where PsbS is absent (Li et al. 2002).

In conclusion, several evidences have emerged confirming a key role of PsbS for photoprotection. At the moment there is no evidence about the molecular mechanism for its functioning in the early phase of stress. In a longer timescale it has been suggested that, by binding zeaxanthin, it can directly quench excess energy. In a shorter timescale there is evidence that it has an important role, modulated by low pH and protonation, but the mechanism of its action is not clear.

The xanthophyll cycle as signal transduction system for overexcitation

Plants experience overexcitation during most of their lifetime and under a variety of stress conditions, such as drought, cold temperatures or sunflecks, that range in time span from seconds to seasons. It is therefore not surprising that different, although concurrent, molecular mechanisms may be involved in photoprotection. This is evident by the finding that even the most drastic mutations, like *npq1* and *npq4*, yet leave a fraction of NPQ still at work.

A key signal for the stress perception is the lowering of lumenal pH. Low pH activates PsbS but also triggers the formation of zeaxanthin (Fig. 1). Zeaxanthin, as discussed before, is not indispensable for NPQ but increases its amplitude. A rapid response was shown to be triggered before activation of the xanthophyll cycle and it causes a quenching of excess energy (indicated as quenching 1 in Fig. 1). PsbS is involved in the rapid response, probably through protonation of lumenal exposed acidic residues (Fig. 1, left). The mechanisms of PsbS function remains to be established. In particular it is not clear if its action is or is not dependent on interactions with chlorophyll binding antenna proteins. In fact, none of the recent reports confirmed early data on chlorophyll binding for PsbS, a necessary condition for direct quenching of energy.

The slower phase of quenching is, instead, zeaxanthin dependent (Fig. 1, right). Newly formed zeaxanthin is initially free in the membrane lipids and can therefore act as a message for amplification of the different photoprotection mechanisms. The prevention of photoinhibitory damage is obtained by synergistically acting on Lhc protein conformation and on PsbS. Zeaxanthin appears to act on both: its binding to Lhc antenna complexes decreases their fluorescence yield, hence their light harvesting function (Formaggio et al. 2001, Moya et al. 2001), promoting an additional quenching effect (quenching 2 in Fig. 1). Zeaxanthin, moreover, was suggested to also bind to PsbS in vitro (Aspinall-O'Dea et al. 2002) and in vivo in conditions of high quenching

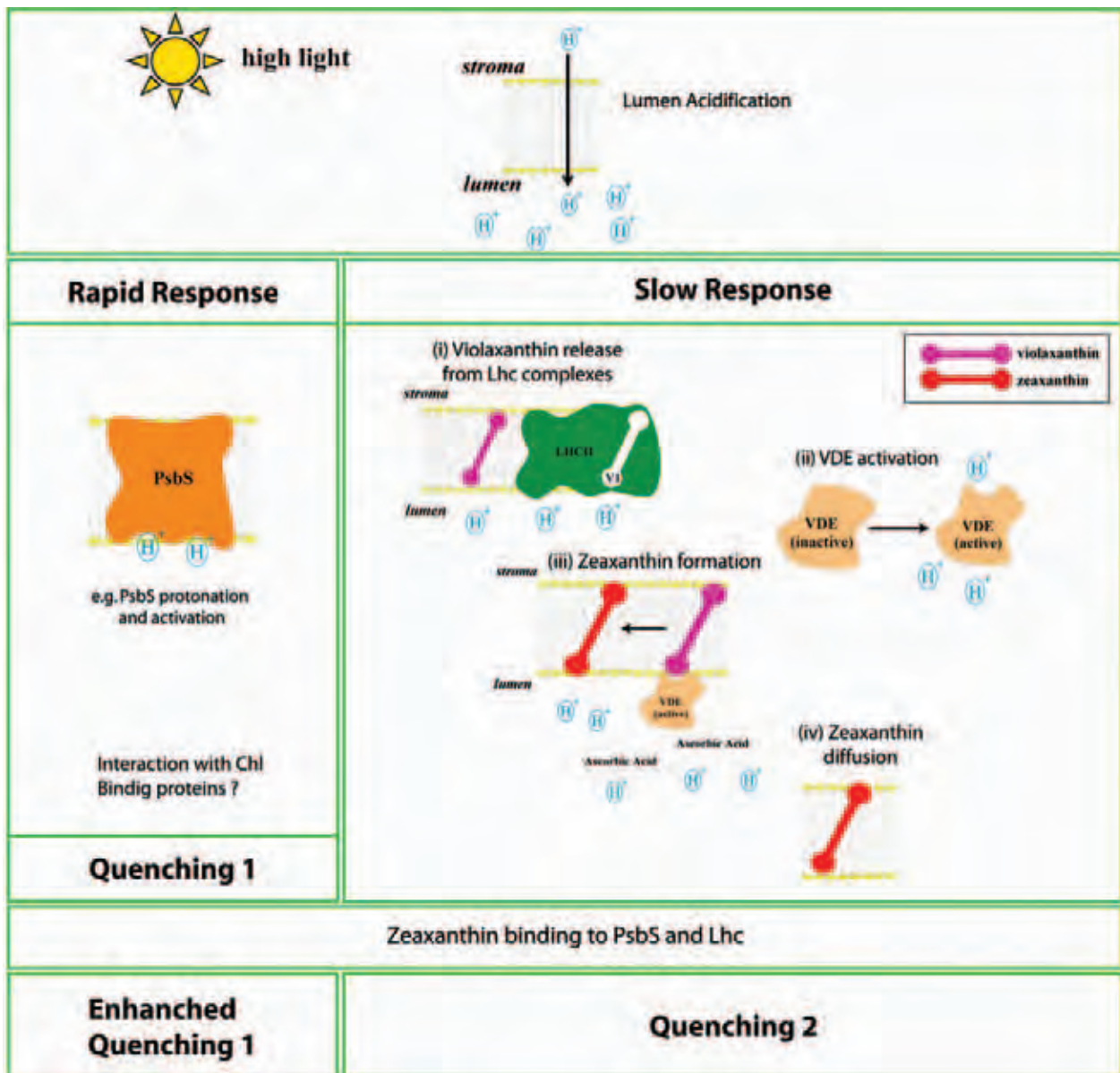


Fig. 1. Representation of the xanthophyll cycle as stress signal transduction system in thylakoids. High light induces activation of rapid excitation energy quenching response triggered by low luminal pH (indicated as quenching 1). The rapid response (left panel) is dependent on PsbS, whose mechanism of action is yet unknown. An alternative way of quenching is dependent on the xanthophyll cycle and its mechanism of action is understood in higher detail as shown in the right panel of the figure. Low pH is also the triggering signal the activation of the xanthophyll cycle activation in several steps: (1), release of violaxanthin from site V1 of LHCII trimers; (2), activation of VDE; (3), zeaxanthin production by VDE in the membrane lipid phase; (4), diffusion of zeaxanthin in the membrane. Zeaxanthin induces sustained quenching (slow response) by binding to PsbS and to the allosteric site L2 of Lhc antenna proteins (enhanced quenching 1 and quenching 2).

(Ruban et al. 2002). This binding can induce sustained quenching (Enhanced quenching 1 in Fig. 1). Sustained accumulation of zeaxanthin and chlorophyll fluorescence quenching are also involved in the overwinter stress resistance. This effect can be obtained either by maintenance of low luminal pH (Gilmore and Björkman 1994) or by a pH independent mechanism (Gilmore and Ball 2000, Matsubara et al. 2002). At the moment it is not clear if pH dependence reflects the involvement of

PsbS in the long term stress resistant state of the photosynthetic apparatus.

The emerging data on the mechanisms of resistance from photooxidation suggest that, although none of these mechanisms are actually inactive in the absence of zeaxanthin, it enhanced the amplitude of the photoprotection responses. In chronic stress conditions a persistent state of chlorophyll fluorescence quenching is obtained upon accumulation of zeaxanthin.

The mode of zeaxanthin production, release in the membrane lipid phase, diffusion to the different components of the photosynthetic apparatus, and modulation of their activity is consistent with the idea that the xanthophyll cycle is in fact a stress signal transduction system. Release of violaxanthin from LHCII trimers plays the role of first messenger while VDE, activated by low luminal pH, is the signal transducer, and zeaxanthin is the second messenger acting as a signal transducer of persisting stress in thylakoids. In fact, it works as an 'allosteric effector' amplifying and stabilizing the operation of the photoprotection mechanisms triggered already in the absence of zeaxanthin (Fig. 1).

Acknowledgements – This work was supported in part by Consiglio Nazionale delle Ricerche Agenzia 2000 and by MIUR Progetto FIRB n. RBAU01ECX.

References

- Aspinall-O'Dea M, Wentworth M, Pascal A, Robert B, Ruban A, Horton P (2002) In vitro reconstitution of the activated zeaxanthin state associated with energy dissipation in plants. *Proc Natl Acad Sci USA* 99: 16331–16335
- Bassi R, Croce R, Cugini D, Sandona D (1999) Mutational analysis of a higher plant antenna protein provides identification of chromophores bound into multiple sites. *Proc Natl Acad Sci USA* 96: 10056–10061
- Bassi R, Pineau B, Dainese P, Marquardt J (1993) Carotenoid-Binding Proteins of Photosystem-II. *Eur J Biochem* 212: 297–303
- Bratt CE, Arvidsson P-O, Carlsson M, Åkerlund H-E (1995) Regulation of violaxanthin de-epoxidase activity by pH and ascorbate concentration. *Photosynth Res* 45: 169–175
- Bugos RC, Yamamoto HY (1996) Molecular cloning of violaxanthin de-epoxidase from romaine lettuce and expression in *Escherichia coli*. *Proc Natl Acad Sci USA* 93: 6320–6325
- Caffarri S, Croce R, Breton J, Bassi R (2001a) The major antenna complex of Photosystem II has a xanthophyll binding site not involved in light harvesting. *J Biol Chem* 276: 35924–35933
- Caffarri S, Croce R, Cattivelli L, Bassi R (2001b) The Lhcb1 2, 3 gene products component the trimeric antenna complex of higher plant Photosystem II, have distinct biochemical, spectroscopic properties. PS2001 Proceedings 12th International Congress on Photosynthesis. CSIRO Publishing, Melbourne, Australia, S31–034
- Castelletti S, Morosinotto T, Robert B, Caffarri S, Bassi R, Croce R (2003) The recombinant Lhca2 and Lhca3 subunits of the Photosystem I antenna system. *Biochemistry* 42: 4226–4234
- Crimi M, Dorra D, Bosinger CS, Giuffra E, Holzwarth AR, Bassi R (2001) Time-resolved fluorescence analysis of the recombinant Photosystem II antenna complex CP29. Effects of zeaxanthin, pH and phosphorylation. *Eur J Biochem* 268: 260–267
- Croce R, Canino G, Ros F, Bassi R (2002a) Chromophore organization in the higher-plant Photosystem II antenna protein CP26. *Biochemistry* 41: 7334–7343
- Croce R, Cinque G, Holzwarth AR, Bassi R (2000) The solet absorption properties of carotenoids and chlorophylls in antenna complexes of higher plants. *Photosynth Res* 64: 221–231
- Croce R, Morosinotto T, Castelletti S, Breton J, Bassi R (2002b) The Lhca antenna complexes of higher plants Photosystem I. *Biochim Biophys Acta* 1556: 29–40
- Croce R, Remelli R, Varotto C, Breton J, Bassi R (1999a) The neoxanthin binding site of the major light harvesting complex (LHC II) from higher plants. *FEBS Lett* 456: 1–6
- Croce R, Weiss S, Bassi R (1999b) Carotenoid-binding sites of the major light-harvesting complex II of higher plants. *J Biol Chem* 274: 29613–29623
- Dall'Osto L, Caffarri S, Bassi R (2003) Isolation of two protein conformations of the antenna protein Lhcb5 with respectively high and low light harvesting efficiency, in press
- Dominici P, Caffarri S, Armenante F, Ceoldo S, Crimi M, Bassi R (2002) Biochemical properties of the PsbS subunit of Photosystem II either purified from chloroplast or recombinant. *J Biol Chem* 277: 22750–22758
- Formaggio E, Cinque G, Bassi R (2001) Functional architecture of the major light-harvesting complex from higher plants. *J Mol Biol* 314: 1157–1166
- Frank HA, Cua A, Chynwat V, Young A, Gosztola D, Wasielewski MR (1994) Photophysics of the carotenoids associated with the xanthophyll cycle in photosynthesis. *Photosynth Res* 41: 389–395
- Funk C, Schröder WP, Napiwotzki A, Tjus SE, Renger G, Andersson B (1995) The PSII-S protein of higher plants: a new type of pigment-binding protein. *Biochemistry* 34: 11133–11141
- Gilmore AM & Ball MC (2000) Protection and storage of chlorophyll in overwintering evergreens. *Proc Natl Acad Sci USA* 97: 11098–11101
- Gilmore AM & Björkman O (1994) Adenine nucleotides and the xanthophyll cycle in leaves. II. Comparison of the effects of CO₂-and temperature-limited photosynthesis on Photosystem II fluorescence quenching, the adenylate energy charge and violaxanthin de-epoxidation in cotton. *Planta* 192: 537–544
- Govindjee, Seufferheld M (2002) Non-photochemical quenching of chlorophyll *a* fluorescence: early history and characterization of two xanthophyll-cycle mutants of *Chlamydomonas reinhardtii*. *Func Plant Biol* 29, 1141–1155
- Hager A (1969) Light dependent decrease of the pH-value in a chloroplast compartment causing the enzymatic interconversion of violaxanthin to zeaxanthin; Relations to photophosphorylation. *Planta* 89: 224–243
- Havaux M & Niyogi KK (1999) The violaxanthin cycle protects plants from photooxidative damage by more than one mechanism. *Proc Natl Acad Sci USA* 96: 8762–8767
- Jansson S (1999) A guide to the Lhc genes and their relatives in *Arabidopsis*. *Trends Plant Sci* 4: 236–240
- Kühlbrandt W, Wang DN, Fujiyoshi Y (1994) Atomic model of plant light-harvesting complex by electron crystallography. *Nature* 367: 614–621
- Külheim C, Agren J, Jansson S (2002) Rapid regulation of light harvesting and plant fitness in the field. *Science* 297: 91–93
- Lam E, Ortiz W, Malkin R (1984) Chlorophyll *a/b* proteins of Photosystem I. *FEBS Lett* 168: 10–14
- Lamborghini M (2002) Three dimensional structure of the light-harvesting chlorophyll *a* and *b* protein complex from plant chloroplasts. PhD Thesis. J. W. Goethe-Universität, Frankfurt am Main, Germany
- Li XP, Björkman O, Shih C, Grossman AR, Rosenquist M, Jansson S, Niyogi KK (2000) A pigment-binding protein essential for regulation of photosynthetic light harvesting. *Nature* 403: 391–395
- Li X-P, Phippard A, Pasari J, Niyogi KK (2002) Structure–function analysis of Photosystem II subunit S (PsbS) in vivo. *Func Plant Biol* 29: 1131–1139
- Ma YZ, Holt NE, Li XP, Niyogi KK, Fleming GR (2003) Evidence for direct carotenoid involvement in the regulation of photosynthetic light harvesting. *Proc Natl Acad Sci USA* 100: 4377–4382
- Matsubara S, Gilmore AM, Ball MC, Anderson JM, Osmond B (2002) Sustained downregulation of Photosystem II in mistletoes during winter depression of photosynthesis. *Func Plant Biol* 29: 1157–1169
- Morosinotto T, Baronio R, Bassi R (2002) Dynamics of chromophore binding to Lhc proteins in vivo and in vitro during operation of the xanthophyll cycle. *J Biol Chem* 277: 36913–36920
- Moya I, Silvestri M, Vallon O, Cinque G, Bassi R (2001) Time-resolved fluorescence analysis of the Photosystem II antenna proteins in detergent micelles and liposomes. *Biochemistry* 40: 12552–12561
- Müller-Moule P, Conklin PL, Niyogi KK (2002) Ascorbate deficiency can limit violaxanthin de-epoxidase activity in vivo. *Plant Physiol* 128: 970–977
- Niyogi KK, Grossman AR, Björkman O (1998) Arabidopsis mutants define a central role for the xanthophyll cycle in the regulation of photosynthetic energy conversion. *Plant Cell* 10: 1121–1134
- Peng CL & Gilmore AM (2002) Comparison of high-light effects with and without methyl viologen indicate barley *chlorina* mutants exhibit contrasting sensitivities depending on the specific nature of the *chlorina* mutation: comparison of wild

- type, chlorophyll-*b*-less *clo f₂* and light-sensitive chlorophyll-*b*-deficient *clo f104* mutants. *Func Plant Biol* 29: 1171–1180
- Pogson BJ, Niyogi KK, Björkman O, DellaPenna D (1998) Altered xanthophyll compositions adversely affect chlorophyll accumulation and nonphotochemical quenching in *Arabidopsis* mutants. *Proc Natl Acad Sci USA* 95: 13324–13329
- Polivka T, Herek JL, Zigmantas D, Åkerlund H-E, Sundström V (1999) Direct observation of the (forbidden) S-1 state in carotenoids. *Proc Natl Acad Sci USA* 96: 4914–4917
- Polivka T, Zigmantas D, Sundstrom V, Formaggio E, Cinque G, Bassi R (2002) Carotenoid S (1) state in a recombinant light-harvesting complex of Photosystem II. *Biochemistry* 41: 439–450
- Ruban AV, Lee PJ, Wentworth M, Young AJ, Horton P (1999) Determination of the stoichiometry and strength of binding of xanthophylls to the Photosystem II light harvesting complexes. *J Biol Chem* 274: 10458–10465
- Ruban AV, Pascal AA, Robert B, Horton P (2002) Activation of zeaxanthin is an obligatory event in the regulation of photosynthetic light harvesting. *J Biol Chem* 277: 7785–7789
- Siefermann-Harms D & Ninnemann H (1982) Pigment organization in the light-harvesting chlorophyll-alpha/beta protein complex of lettuce chloroplasts. Evidence obtained from protection of the chlorophylls against proton attack and from excitation energy transfer. *Photochem Photobiol* 35: 719–731
- Tjus SE, Scheller HV, Andersson B, Moller BL (2001) Active oxygen produced during selective excitation of Photosystem I is damaging not only to Photosystem I, but also to Photosystem II. *Plant Physiol* 125: 2007–2015
- Verhoeven AS, Adams WW, Demmig-Adams B, Croce R, Bassi R (1999) Xanthophyll cycle pigment localization and dynamics during exposure to low temperature and light stress in *Vinca major*. *Plant Physiol* 120: 727–737
- Yamamoto HY & Bassi R (1996) Carotenoids: localization and function. In: Ort DR, Yokum CF (eds) *Oxygenic Photosynthesis: the Light Reactions*. Kluwer Academic Publishers, Dordrecht, pp 539–563
- Yamamoto HY & Higashi RM (1978) Violaxanthin de-epoxidase. Lipid composition and substrate specificity. *Arch Biochem Biophys* 190: 514–522
- Yamamoto HY, Nakayama TOM, Chichester CO (1962) Studies on the light and dark interconversion of leaf xanthophylls. *Arch Biochem Biophys* 97: 168–173

Extracts from:

S. Matsubara, T. Morosinotto, R. Bassi, A. - L. Christian, E. Fischer-Schliebs, U. Lüttge, B. Orthen, A. C. Franco, F. R. Scarano, B. Förster, B. J. Pogson, M. C. Ball, and C. B. Osmond, *Planta* (2003) 217: 868–879

Shizue Matsubara, Maria Naumann, Robin Martin, Caroline Nichol, Uwe Rascher, Tomas Morosinotto, Roberto Bassi, and Barry Osmond *J. Exp. Bot.* In press

Extract 1: Occurrence of the lutein-epoxide cycle in mistletoes of Loranthaceae and Viscaceae

The lutein-epoxide cycle (Lx cycle) is an auxiliary xanthophyll cycle known to operate only in some higher plant species. It occurs in parallel with the common violaxanthin cycle (V cycle) and involves the same epoxidation and de-epoxidation reactions as in the V cycle. In this study, the occurrence of the Lx cycle was investigated in the two major families of mistletoe, Loranthaceae and Viscaceae. In an attempt to find the limiting factor(s) for the occurrence of the Lx cycle, pigment profiles of mistletoes with and without the Lx cycle were compared. The availability of lutein as a substrate for the zeaxanthin epoxidase appeared not to be critical. This was supported by the absence of the Lx cycle in the transgenic *Arabidopsis* plant *lutOE*, in which synthesis of lutein was increased at the expense of V by overexpression of ϵ -cyclase, a key enzyme for lutein synthesis. Furthermore, analysis of pigment distribution within the mistletoe thylakoids excluded the possibility of different localization for the Lx and V cycle pigments. From these findings, together with previous reports on the substrate specificity of the two enzymes in the V cycle, we propose that mutation to zeaxanthin epoxidase could have resulted in altered regulation and/or substrate specificity of the enzyme that gave rise to the parallel operation of two xanthophyll cycles in some plants. The distribution pattern of Lx in the mistletoe phylogeny inferred from 18S rRNA gene sequences also suggested that the occurrence of the Lx cycle is determined genetically. Possible molecular evolutionary processes that may have led to the operation of the Lx cycle in some mistletoes are discussed.

Extract 2: Rethinking photoprotection and photoacclimation: lutein-epoxide in deep shade leaves of a tropical tree legume

Here we show that deeply shaded leaves of the tropical tree legume (*Inga* sp.) with extraordinarily high levels of the α -xanthophyll lutein-epoxide, that are co-located in pigment-protein complexes of the photosynthetic apparatus with the β -xanthophyll violaxanthin, display distinctive time-dependent responses to strong light. Photoprotection (measured as non-photochemical chlorophyll fluorescence quenching) is initiated within the time frame of sun-flecks (minutes), before detectable conversion of violaxanthin to antheraxanthin or zeaxanthin. Photoacclimation to strong light is achieved within hours by simultaneously engaging the reversible violaxanthin cycle and a slowly reversible conversion of lutein-epoxide to lutein. We hypothesize that this lutein occupies sites L2 and V1 in light harvesting

chlorophyll protein complexes of photosystem II, locking-in primary photoprotection during photoacclimation via protein conformational changes that enhance photoprotection through the superior singlet and/or triplet chlorophyll quenching capacity of lutein.

Conclusions and perspectives:

Lutein epoxide cycle appears to be typical of plants adapted to low light conditions. Biochemical studies suggested that lutein epoxide is bound to Lhc complexes and in particular it competes with violaxanthin binding sites. In fact, violaxanthin content in plants having lutein epoxide is lower and thus this second xanthophyll cycle is partially replacing the “usual” one. The reason for its evolution, however, still needs to be elucidated. One possibility to be verified is if the presence of lutein epoxide is able to increase the light harvesting efficiency, thus increasing the adaptability to low light conditions.

Appendix I

Spectroscopic properties of PSI antenna complex

Appendix I. Spectroscopic properties of PSI antenna complex

In this section extracts from spectroscopic analyses of antenna complexes of Photosystem I are presented. First two works were focused on the determination of biophysical parameters of Lhca proteins, with peculiar attention on red forms. The other two, instead, gave interesting results on energy pathways and de-excitation mechanisms in Lhca4. In particular, it was analysed the influence of red forms.

I. The origin of the low energy emission in Lhca complexes: spectroscopic analysis of reconstituted complexes

R. Croce, J. Ihalainen, A. Chojnicka, T. Morosinotto, Frank van Mourik, R. van Grondelle, R. Bassi, and J. Dekker

Submitted

In this work, the spectroscopic properties of Lhca complexes reconstituted in vitro were analysed with different spectroscopic methods: absorption and fluorescence at 4K, site selected fluorescence and fluorescence anisotropy. The aim of the study was the characterisation of red forms and thus particular attention was paid to Lhca3, Lhca4 and Lhca1-4 dimer, the complexes exhibiting the red most emission. The absorption band which originates the red emission was determined and it appear to be located at 704-705, 708-709 and 710 nm for Lhca3 and Lhca4 and Lhca1-4 dimer respectively. Red forms were shown to be characterised by large Stokes shifts and broad bandwidth. The homogeneous and inhomogeneous broadening of the bands were determinate and they are discussed in the frame of excitonic interactions.

II. The room temperature emission band shape of the lowest energy chlorophyll spectral form of LHCI

Robert C. Jennings, Flavio M. Garlaschi, Tomas Morosinotto, Enrico Engelmann, Giuseppe Zucchelli

Published in FEBS Lett. (2003) Jul 17; 547(1-3):107-10, corrigendum in FEBS Lett. 549 (2003)

181

In this work, red forms in LHCI and recombinant Lhca4 were analysed with room temperature fluorescence. In particular, it was measured the pre-equilibration fluorescence deriving from the directly excited pigment states upon selective excitation. This allowed the obtaining of fluorescence band shape of the low energy chlorophyll states, which is characterised by a very large bandwidth (55 nm) and a peculiar asymmetry.

III. Quenching of chlorophyll triplet states by carotenoids in reconstituted Lhca4 subunit of peripheral light-harvesting complex of Photosystem I

Donatella Carbonera, Tomas Morosinotto, Giancarlo Agostani, Roberta Croce and Roberto Bassi
Submitted

In this work, the formation of Chl and Carotenoid triplets in recombinant Lhca4 was analysed by Optically Detected Magnetic Resonance (ODMR). The ability of carotenoid molecules to quench Chl triplets is, in fact, poorly studied in PSI subunits.

The aim of this work aim was to analyse the interaction between red forms and carotenoids: the first result is that, in Lhca4, Chl triplets are quenched by carotenoid molecules, as it was in the case of PSII antennas. Interestingly, it was also shown that red chlorophylls are quenched by carotenoids with an efficiency approaching 100%. In fact, any chlorophyll triplet originating from these chlorophylls have been detected, even at very low temperatures (1.8 K), where energy is concentrated in pigments with the lowest energy levels. In addition, it was shown that one peculiar carotenoid molecule, the one bound to site L2, had the major role in quenching chlorophylls triplets. These data are in good agreement with the mutational analyses showed in section B, where the presence a strong interaction between red chlorophylls and the carotenoid in site L2 was shown. The same measurements were also performed for Lhca4 NH (see B.7), a mutant depleted in red forms. In the mutated complex, the ability of carotenoid to quench the Chl triplets is lowered. Therefore, it appears that the mutation is affecting the chromophores organisation enough to lower the ability of carotenoids to quench the Chl triplets. This is consistent with the hypothesis that the mutation NH is affecting the position of Chl A5, as suggested in B.7. In fact, as it modifies the interaction between Chl A5 and B5, it could affect the distance from carotenoid in site L2, thus influencing the triplets quenching efficiency.

IV. Excitation energy transfer pathways in Lhca4

K.Gibasiewicz, R.Croce, T.Morosinotto, J.Ihalainen, I. van Stokkum, J.Dekker, R. Bassi and R. van Grondelle.

Submitted

In this work, the energy transfer in reconstituted Lhca4 was studied at RT by femtosecond transient absorption spectroscopy. This analysis allowed the observation that two lutein molecules, bound to sites L1 and L2, are characterised by significantly different interactions with nearby chlorophyll *a* molecules. Interestingly, the xanthophyll in site L2 had the highest energy transfer efficiency from the carotenoid toward the chlorophyll (~60-70%). Moreover, about 25% of excited Chls *a* decays extremely fast within ~15 ps and this effect is proposed to be due to the presence of an excitonically coupled dimer of Chls *a* located next to the carotenoid in site L2. This means that the carotenoid in site L2, interacting with red chlorophylls, offers a safe de-excitation channel for Chl singulets. This hypothesis is consistent with the fact that Lhca4 has a fluorescence yield far lower than PSII antenna complexes, which do not have red forms.

These results are in good agreement with the ones presented above on the triplets quenching and could possibly have a physiological significance. In Lhca4, absorbed energy is concentrated in red forms, where both Chlorophyll singulets and triplets are very efficiently quenched by the nearby carotenoid molecule in site L2. It thus appears that the chromophore organisation in Lhca4 is optimised to avoid light induces damages. On the other side, the efficient excitation quenching can lower Lhca4 efficiency in light harvesting and in energy transfer to PSI reaction centre.

Conclusions

Conclusions

In this thesis, the supramolecular organisation of antenna systems and their ability to modulate their biophysical properties were analysed.

The first subject addresses was the association of antenna proteins in PSI-LHCI supercomplexes. The major conclusions obtained has been:

- ✓ One copy per each Lhca polypeptide is bound to PSI core
- ✓ “Gap pigments” composed of Chl a, b and carotenoid molecules are found at the interfaces between Lhca subunits and between antenna and core.
- ✓ The binding of Lhca polypeptides to PSI core is highly cooperative. Interactions between subunits are important for the stability of the whole antenna system
- ✓ The number of Lhca1-4 polypeptides associated to PSI is not dependent on environmental conditions. Other mechanisms are proposed to be important for the regulation of PSI antenna size.

PSI-LHCI is able to largely modulate the absorption properties of its chlorophylls. In particular, some peculiar chlorophylls, called “red forms”, adsorbing at wavelengths longer than 700 nm, are present. In this work, red forms have been deeply studied. Main results obtained are:

- ✓ Red shifted chlorophylls are present in all Lhca polypeptides, although they have different energies. In particular, Lhca1 and 2 have an emission form at 701 nm, Lhca3 at 725 nm and Lhca4 at 735 nm.
- ✓ Red forms are originated in all Lhca complexes, independently from their emission energy, from Chls bound in sites A5/603 and B5/609.
- ✓ An excitonic interaction between two Chl a molecules in sites A5/603 and B5/609 plays a role in shifting chlorophylls to the red.
- ✓ The presence of an asparagine molecule as ligand for Chl A5/603 in Lhca3 and Lhca4 increases the strength of the interaction, allowing the obtaining of emission around 730 nm.

The organisation of antenna system in supercomplexes with reaction centre in PSII was also analysed. The major results have been:

- ✓ A resolution of a 2D map of PSII-LHCII supercomplexes with 17 Å resolution

- ✓ The description of the minimal structural unit of PSII composed by the core complex plus a LHCII trimer, a CP26 and CP29 monomer.
- ✓ The proposal that PSII arrays can have in physiological role in photoprotection, by delocalising excitation energy in multiple subunits.
- ✓ Comparison of PSII supercomplexes with PSI-LHCI showed that gap pigments are not present in PSII. Its antenna system, in fact, is more flexible and prone to regulation in response to environmental conditions

In light stress conditions, zeaxanthin is produced from violaxanthin, in a process called xanthophyll cycle. The xanthophyll dynamics in plant thylakoids and their effect on antenna complexes was also analysed. Main results obtained are:

- ✓ The antenna complexes have a regulatory role in xanthophyll cycle, because they bound violaxanthin protecting it from de-epoxidation. When the lumenal pH is decreased, however, they free violaxanthin and make it available for de-epoxidation by VDE
- ✓ Lhc proteins have a different ability in exchange violaxanthin. They thus generate different pools of violaxanthin with different deepoxydation speeds, that are activated at different times after stress establishment
- ✓ Zeaxanthin, when bound to antenna complexes of PSII, decrease their stability and their fluorescence yield.
- ✓ When bound to antenna complexes of PSI, instead, zeaxanthin induce a reduction of fluorescence yield but the stability of the antenna system is unaffected.